27 July 2007 | S10

Science

AAAS

Brilliant Combination.

Stratagene Mx™ QPCR systems + next generation Brilliant® II reagents = the perfect pair.

Our complete quantitative PCR portfolio features products that include sample preparation, cDNA synthesis, QPCR amplification and detection, and powerful data analysis software to meet today's research needs as well as tomorrow's future applications. Couple our Mx™ line of high performance real-time QPCR systems with our next generation Brilliant® II QPCR reagents and there's no need to look any further than Stratagene for your QPCR research needs.

- **Brilliant® II reagents are designed for earlier Ct detection, improved reproducibility, and dynamic range**
- **Four- or five-color Mx™ QPCR systems with powerful MxPro™ QPCR Software**
- **Complete QPCR portfolio of instruments, reagents, service, and support**

For more information about our Brilliant® II QPCR reagents or Mx™ QPCR systems, please visit www.stratagene.com/MxQPCR.

Stratagene US and Canada
Order: 800-424-5444 x3
Technical Service: 800-894-1304 x2

Stratagene Japan K.K.
Order: 3-5821-8077
Technical Service: 3-5821-8076

Stratagene Europe
Order: 00800-7000-7000
Technical Service: 00800-7400-7400

STRATAGENE
An **Agilent Technologies** Company

Please note that the Mx3000P® QPCR System and the Mx3005P® QPCR System are not offered, sold, and imported in/to Germany.

DNA Methylation Detection *Directly* From Cells

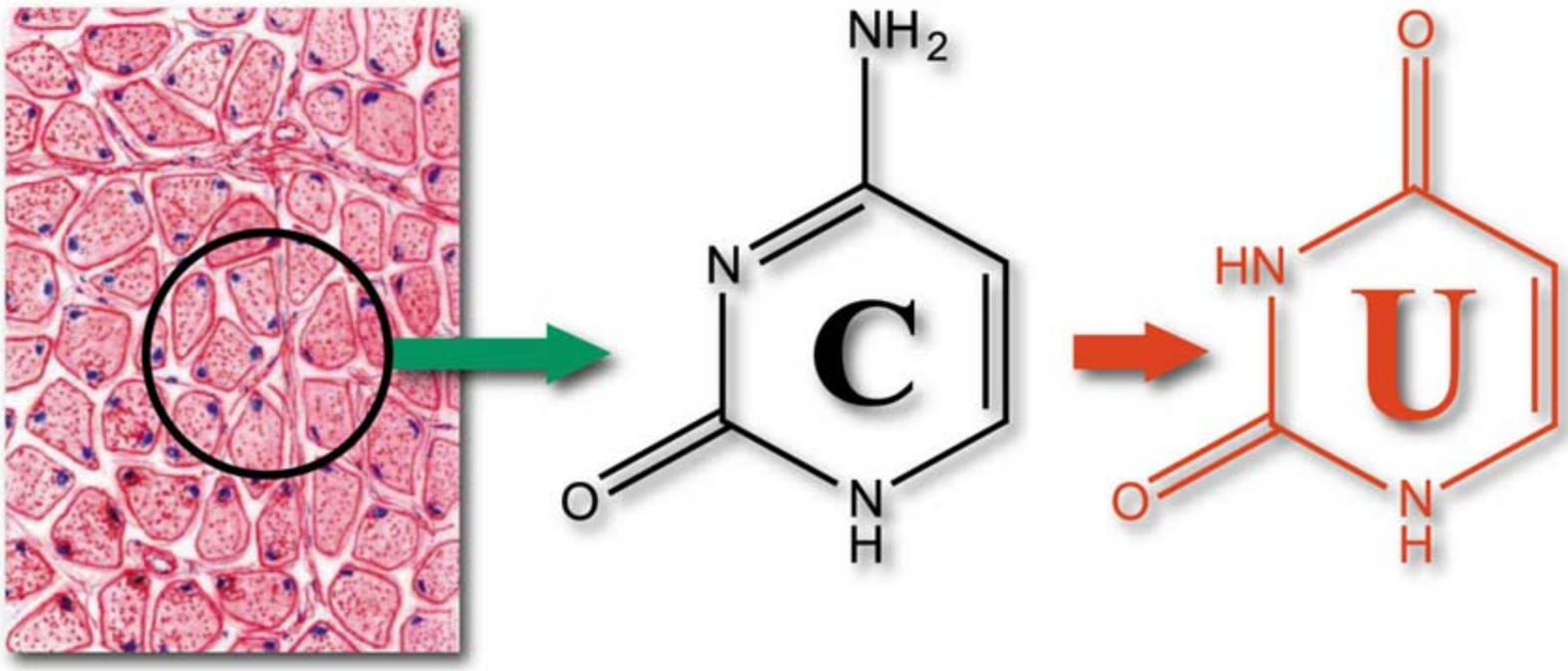

CpGpCpGpCpGp

The EZ DNA Methylation-Direct™ Kit for Complete Bisulfite Conversion of DNA *Directly* From Blood, Tissue, or Cells

- Fastest, most streamlined procedure available for complete conversion of DNA
- Compatible with small sample inputs - as few as 10-20 cells or 50 pg DNA
- Proven, trusted conversion chemistry and purification technology

*Technology is Patent Pending

Free 50 Prep. Kits Are Available While Supplies Last!

50% Off Code SC650*

Cat. No.	Size	Price	
D5020	50 Preps.	$161.00 USD	$80.50* USD
D5021	200 Preps.	$452.00 USD	$226.00* USD
D5022	2x96 Shallow-Well Plates	$362.00 USD	$181.00* USD
D5023	2x96 Deep-Well Plates	$362.00 USD	$181.00* USD

Please use coupon code **SC650** to receive a 50% discount.
Free kit offer and 50% discount valid for U.S. customers only.

Positions in Epigenetics research are available at Zymo Research Corp. See our website for details.

ZYMO RESEARCH
The Beauty of Science is to Make Things Simple

www.zymoresearch.com +1-714-288-9682 INTL 1-888-882-9682 USA

Pure protein is the challenge.
PURE Expertise is the solution.

Imagine having the combined knowledge of hundreds of chromatography experts at your disposal. You'd be able to purify even the most challenging protein and gain the edge in your research. Well now you have it. PURE Expertise is the distillation of 50 years' chromatography experience – available online. Simply put, it's everything you need to gain the best results in protein purification.

Download our purification handbook at **www.gelifesciences.com/pure**

imagination at work

GE Healthcare Bio-Sciences AB, a General Electric Company.
Björkgatan 30, 751 84 Uppsala, Sweden

GE12-07. First printed 07/2007

Volume 317, Issue 5837

COVER

Social scientists and computer scientists meet at the intersection of virtual worlds. These virtual worlds, such as Second Life and World of Warcraft, provide new resources and approaches for research in political science, sociology, and economics. See the Review by Bainbridge on page 472.

Photo: George Joch/courtesy of Argonne National Laboratory

DEPARTMENTS

419 *Science* Online
421 This Week in *Science*
427 Editors' Choice
430 Contact *Science*
433 Random Samples
435 Newsmakers
467 AAAS News & Notes
534 New Products
535 *Science* Careers

EDITORIAL

425 Climate: Game Over
by Donald Kennedy

NEWS OF THE WEEK

A European-Inspired Renaissance for China's Drug Industry? 436
Even Oil Optimists Expect Energy Demand to Outstrip Supply 437
Quake Underscores Shaky Understanding of Ground Forces 438
Aspens Return to Yellowstone, With Help From Some Wolves 438
SCIENCESCOPE 439
Promising Prevention Interventions Perform Poorly in Trials 440
Stung by Controversy, Biomedical Groups Urge Consistent Guidelines 441
Dan Koshland, 1920–2007 441

NEWS FOCUS

Delta Blues, California Style 442
From Crisis to Catastrophe
Digging Into a Desert Mystery 446
Deciphering Ancient Weather Reports, Drip by Drip 448
Order From Chaos, Power From Dissipation in Planetary Flows 449

LETTERS

Retraction *R. M. Roberts, M. Sivaguru, H. Y. Yong* 450
The Shortage of Science Teachers *K. S. Pister*
Explaining Latitudinal Diversity Gradients *C. R. Marshall*
Response *D. Schluter and J. Weir*
Papers Not in the Right Section? *F. Ramus*

BOOKS *ET AL.*

The Politics of Life Itself Biomedicine, Power, and Subjectivity in the Twenty-First Century 454
N. Rose, reviewed by R. M. Herzig
Measuring the World A Novel *D. Kehlmann;* 454
Jaguars and Electric Eels *A. von Humboldt*
Six Impossible Things Before Breakfast 456
The Evolutionary Origin of Belief *L. Wolpert, reviewed by S. Atran*

EDUCATION FORUM

The Two High-School Pillars Supporting College Science 457
P. M. Sadler and R. H. Tai

PERSPECTIVES

Variation and Early Evolution 459
G. Hunt >> Report p. 499
Filling a Void 460
S. L. Brock >> Report p. 490
The Yin-Yang of Sirtuins 461
A. Dillin and J. W. Kelly >> Report p. 516
A Counterion Strategy 462
J. Lacour and D. Linder >> Report p. 496
Necessary Noise 463
J. T. Mettetal and A. van Oudenaarden
>> Report p. 526
Spying on Others Evolves 464
M. Milinski and B. Rockenbach
Pierre-Gilles de Gennes (1932–2007) 466
A. Ajdari

CONTENTS continued >>

Science

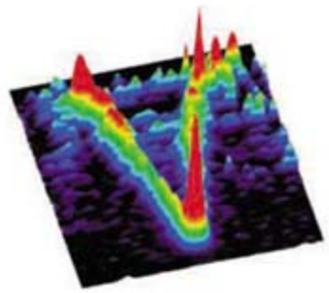

SCIENCE EXPRESS

www.sciencexpress.org

Bilayer ^{3}He: A Simple Two-Dimensional Heavy Fermion System with Quantum Criticality
M. Neumann, J. Nyéki, B. Cowan, J. Saunders
Thermodynamic measurements show that a bilayer of fluid ^{3}He, the simplest Fermi system, surprisingly shows quantum criticality and can be used to study this phenomenon.
10.1126/science.1143607

The Evolution of Selfing in *Arabidopsis thaliana*
C. Tang et al.
An analysis of sex genes shows that at several times throughout its history—including about 1 million years ago—*Arabidopsis* has developed the ability to self-fertilize.
10.1126/science.1143153

Mesoscopic Phase Coherence in a Quantum Spin Fluid
G. Xu et al.
Neutron scattering measurements on a quantum spin fluid reveal the development of mesoscopic quantum phase coherence in a system without classical static magnetic order.
10.1126/science.1143831

MicroRNA Inhibition of Translation Initiation in Vitro by Targeting the Cap-Binding Complex eIF4F
G. Mathonnet et al.
In vitro, microRNAs can act to repress the initial step of protein translation.
10.1126/science.1146067

TECHNICAL COMMENT ABSTRACTS

CHEMISTRY

Comment on "Coherent Control of Retinal Isomerization in Bacteriorhodopsin" 453
M. Joffre
full text at www.sciencemag.org/cgi/content/full/317/5837/453b

Response to Comment on "Coherent Control of Retinal Isomerization in Bacteriorhodopsin"
V. I. Prokhorenko et al.
full text at www.sciencemag.org/cgi/content/full/317/5837/453c

REVIEWS

COMPUTER SCIENCE

Search Technologies for the Internet 468
M. Henzinger

SOCIOLOGY

The Scientific Research Potential of Virtual Worlds 472
W. S. Bainbridge

BREVIA

MEDICINE

AAV Vector Integration Sites in Mouse Hepatocellular Carcinoma 477
A. Donsante et al.
A virus that has shown promise as a vector for human gene therapy causes liver tumors in neonatal mice.

RESEARCH ARTICLES

OCEAN SCIENCE

Free-Drifting Icebergs: Hot Spots of Chemical and Biological Enrichment in the Weddell Sea 478
K. L. Smith Jr. et al.
Trace elements and iron released from free-drifting Antarctic icebergs stimulate local productivity that enhances carbon sequestration in the Southern Ocean.

ECONOMICS

The Product Space Conditions the Development of Nations 482
C. A. Hidalgo, B. Klinger, A.-L. Barabási, R. Hausmann
Network analysis of the products made by rich and poor countries show that movement toward higher-profit products may be restricted for much of the developing world.

REPORTS

PHYSICS

Single-Atom Single-Photon Quantum Interface 488
T. Wilk, S. C. Webster, A. Kuhn, G. Rempe
A sequence of laser pulses targeted on a single atom trapped in a cavity can generate a source of entangled photon pairs.

MATERIALS SCIENCE

Porous Semiconducting Gels and Aerogels from Chalcogenide Clusters 490
S. Bag et al.
The reaction of clusters containing sulfur or selenium with a platinum complex yields highly porous gels that can efficiently absorb heavy metals from water.
>> Perspective p. 460

CHEMISTRY

Stabilization of Labile Carbonyl Addition Intermediates by a Synthetic Receptor 493
T. Iwasawa, R. J. Hooley, J. Rebek Jr.
A synthetic molecular basket stabilizes a short-lived intermediate species in an organic reaction for minutes to hours, allowing it to be probed and identified.

CONTENTS continued >>

What if staying up to date with the latest technology published in journals and patents were as easy as pushing a button?

It is.

With the "Keep Me Posted" alerting feature, SciFinder sends you automatic updates on areas you—and your competitors—are interested in.

You can monitor specific research topics, companies, authors, substances, or sequences, and choose how frequently you receive notifications: daily, monthly, or weekly.

The service isn't just convenient, it's incredibly current. Journal article records often appear in SciFinder before they're even in print. New references, substances, and sequences are added daily. Patents from all the major offices are added within two days of issuance.

As with all SciFinder features, Keep Me Posted is integrated with your workflow. At any point in a search (including the beginning), simply click on the Keep Me Posted button. SciFinder tracks your steps and will generate the appropriate alert—even for complex topics. When you receive a notification, you can follow each reference as you would in a search: find citing or cited articles (with links to the electronic full text), and follow referenced substances and reactions for further information.

Comprehensive, intuitive, seamless—SciFinder doesn't just alert you, it's part of the process. To find out more, call us at 800-753-4227 (North America) or 614-447-3700 (worldwide) or visit www.cas.org/SCIFINDER.

SciFinder®

Part of the process.™

REPORTS *CONTINUED...*

CHEMISTRY

A Powerful Chiral Counterion Strategy for Asymmetric Transition Metal Catalysis 496

G. L. Hamilton, E. J. Kang, M. Mba, F. D. Toste

Pairing an achiral cationic gold complex with a chiral phosphate anion leads to efficient asymmetric catalysis of previously intractable organic reactions. *>> Perspective p. 462*

PALEONTOLOGY

A Cambrian Peak in Morphological Variation Within Trilobite Species 499

M. Webster

In trilobites, the morphology of individual species shows the greatest changes soon after their origin, influencing the course of early evolution in the group. *>> Perspective p. 459*

OCEAN SCIENCE

Four Climate Cycles of Recurring Deep and Surface Water Destabilizations on the Iberian Margin 502

B. Martrat et al.

Alternating penetration of deep ocean waters derived from the two polar regions to low latitudes drove century-to-millennial climate changes for at least the past 400,000 years.

PLANT SCIENCE

Ethylene Modulates Stem Cell Division in the *Arabidopsis thaliana* Root 507

O. Ortega-Martínez, M. Pernas, R. J. Carol, L. Dolan

Stem cell proliferation in a niche within developing roots is limited by the gaseous hormone ethylene.

BIOCHEMISTRY

Crystal Structure of Inhibitor-Bound Human 5-Lipoxygenase–Activating Protein 510

A. D. Ferguson et al.

The structure of a human membrane protein involved in biosynthesis of the inflammation-related leukotrienes may help guide the development of therapeutics.

BIOCHEMISTRY

Spring-Loaded Mechanism of DNA Unwinding by Hepatitis C Virus NS3 Helicase 513

S. Myong, M. M. Bruno, A. M. Pyle, T. Ha

A helicase enzyme unwinds DNA in steps three base pairs long that periodically release the tension resulting from translocation of the helicase's motor domain along the DNA.

MEDICINE

Sirtuin 2 Inhibitors Rescue α-Synuclein–Mediated Toxicity in Models of Parkinson's Disease 516

T. F. Outeiro et al.

An inhibitor of a microtubule deacetylase protects dopamine-containing cells and can rescue *Drosophila* from the toxicity of a protein aggregate associated with Parkinson's disease. *>> Perspective p. 461*

EVOLUTION

The Near Eastern Origin of Cat Domestication 519

C. A. Driscoll et al.

The domestic cat and several of its closely related wild relatives originated in the Fertile Crescent over 100,000 years ago, earlier than had been thought.

MICROBIOLOGY

***Candidatus* Chloracidobacterium thermophilum: An Aerobic Phototrophic Acidobacterium** 523

D. A. Bryant et al.

A distinctive, oxygen-tolerant photosynthetic bacterium has been identified in a metagenomic study of hot-spring communities in Yellowstone National Park.

MICROBIOLOGY

Noise in Gene Expression Determines Cell Fate in *Bacillus subtilis* 526

H. Maamar, A. Raj, D. Dubnau

Bacteria that show more random fluctuations in gene expression are especially likely to switch to an alternative phenotype in which they can take up foreign genetic material.

>> Perspective p. 463

NEUROSCIENCE

Rapid Synthesis and Synaptic Insertion of GluR2 for mGluR-LTD in the Ventral Tegmental Area 530

M. Mameli, B. Balland, R. Luján, C. Lüscher

A decrease in the effectiveness of synapses in a particular brain region is caused by replacement of one glutamate receptor subtype with a less efficient one.

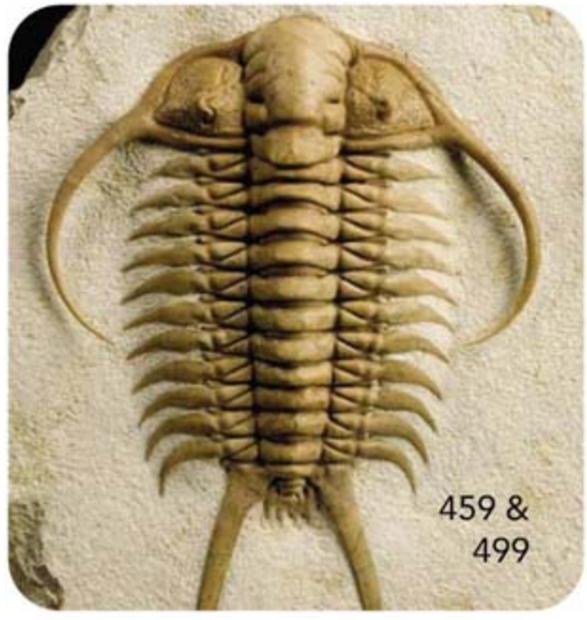

459 & 499

AAAS

ADVANCING SCIENCE, SERVING SOCIETY

SCIENCE (ISSN 0036-8075) is published weekly on Friday, except the last week in December, by the American Association for the Advancement of Science, 1200 New York Avenue, NW, Washington, DC 20005. Periodicals Mail postage (publication No. 484460) paid at Washington, DC, and additional mailing offices. Domestic individual membership and subscription (51 issues): $142 ($74 allocated to subscription). Domestic institutional subscription (51 issues): $710; Foreign postage extra: Mexico, Caribbean (surface mail) $55; other countries (air assist delivery) $85. First class, airmail, student, and emeritus rates on request. Canadian rates with GST available upon request, GST #1254 88122. Publications Mail Agreement Number 1069624. **Printed in the U.S.A.**

Change of address: Allow 4 weeks, giving old and new addresses and 8-digit account number. **Postmaster:** Send change of address to AAAS, P.O. Box 96178, Washington, DC 20090–6178. **Single-copy sales:** $10.00 current issue, $15.00 back issue prepaid includes surface postage; bulk rates on request. **Authorization to photocopy** material for internal or personal use under circumstances not falling within the fair use provisions of the Copyright Act is granted by AAAS to libraries and other users registered with the Copyright Clearance Center (CCC) Transactional Reporting Service, provided that $18.00 per article is paid directly to CCC, 222 Rosewood Drive, Danvers, MA 01923. The identification code for *Science* is 0036-8075. *Science* is indexed in the *Reader's Guide to Periodical Literature* and in several specialized indexes.

CONTENTS continued >>

SCIENCE**NOW**

www.sciencenow.org DAILY NEWS COVERAGE

A Baby Step for Computer Learning
Clever computers can now learn language the way a child does.

The Power to Influence Showers
Researchers link human activity to changes in global precipitation patterns.

Throbbing Oil Demystified
Surface tension and evaporation conspire to make droplets pulse as if alive.

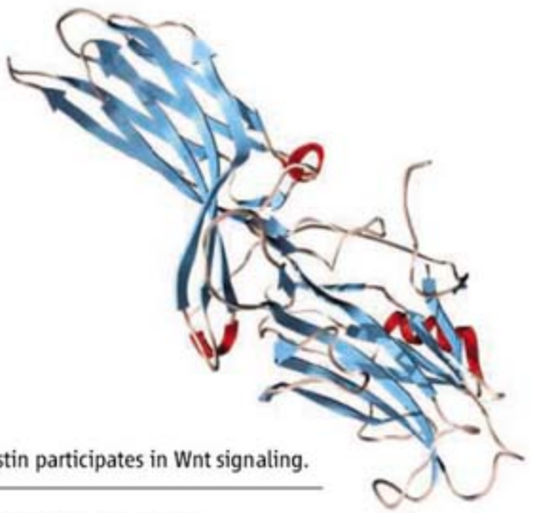

β-arrestin participates in Wnt signaling.

SCIENCE'S **STKE**

www.stke.org SIGNAL TRANSDUCTION KNOWLEDGE ENVIRONMENT

PERSPECTIVE: Molecular Scaffolds Regulate Bidirectional Crosstalk Between Wnt and Classical Seven-Transmembrane Domain Receptor Signaling Pathways
T. Force, K. Woulfe, W. J. Koch, R. Kerkelä
Downstream components interact to allow crosstalk between classical and atypical seven-transmembrane domain receptors.

GLOSSARY
Find out what ELMO, CRABP-II, and fMLP mean in the world of cell signaling.

Grant writing for when the going gets tough.

SCIENCE **CAREERS**

www.sciencecareers.org CAREER RESOURCES FOR SCIENTISTS

GLOBAL: Special Feature—Grant Writing for Tight Times
A. Kotok
As grant approval rates decline, *Science* Careers offers tips to help proposal writers in the United States and Europe.

US: The NIH R01 Toolkit
Science *Careers Editors*
This new guide provides grant writers with lessons for writing a proposal for NIH's main research grant program, the R01.

EUROPE: Getting to the Top of a Big Pile
E. Pain
Science Careers talks to European jury members, who recently reviewed 9000 proposals, about what got some applications to the top.

GLOBAL: *Science* Careers Blog
Science *Careers Editors*
Get your daily career development news and highlights.

SCIENCE**PODCAST**

Listen to the 27 July *Science* Podcast to hear about trouble in the Sacramento–San Joaquin River Delta, the research potential of online virtual worlds, tips for grant writers, and more.
www.sciencemag.org/about/podcast.dtl

CREDIT (SCIENCE CAREERS): CREATIVE COMMONS/JEFF HUTTON

Separate individual or institutional subscriptions to these products may be required for full-text access.

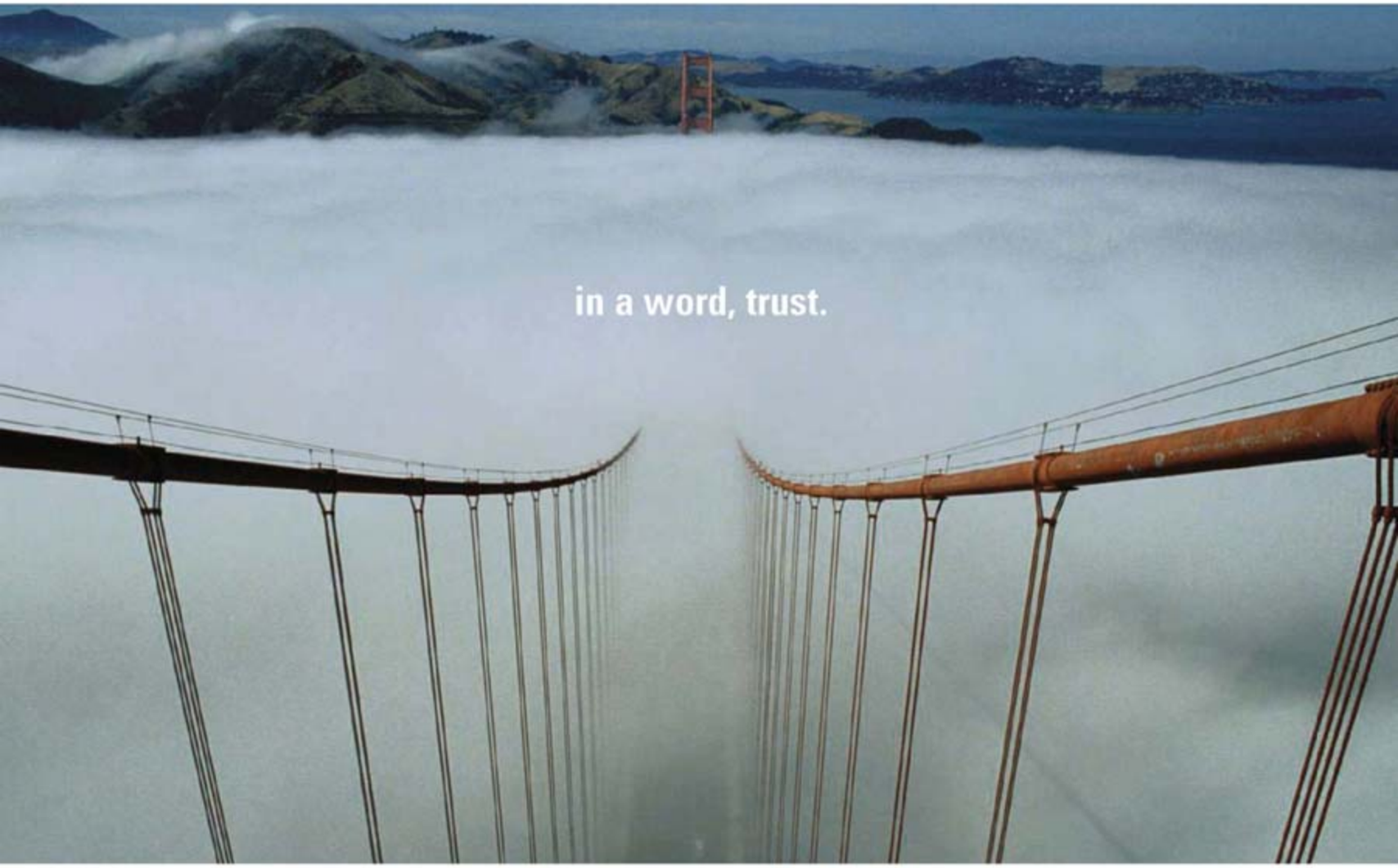

T4 DNA Ligase from New England Biolabs

WHEN YOU NEED LIGASE, TURN TO THE INDUSTRY STANDARD

New England Biolabs is dedicated to providing our customers with guaranteed enzyme performance. Our recombinant T4 DNA Ligase is the most extensively used ligase for cloning experiments. It is available at exceptional value, and an even greater value when purchased in large quantities for high throughput technologies. For cohesive, blunt, simple or complex reactions, make T4 DNA Ligase from NEB your first choice.

- **T4 DNA Ligase*** (R)
  - **Regular Concentration** **M0202S/L**
    For standard cloning reactions
  - **High Concentration** **M0202T/M**
    For large or difficult constructs
- **Quick Ligation™ Kit*** (R) **M2200S/L**
  For ligation of cohesive or blunt-end DNA fragments in 5 minutes at room temperature. See our website for more details.

(R) = Recombinant
*NEB ligase products are BSA-free

Advantages:

- Quality – Highly pure enzyme with no lot-to-lot variation
- Convenience – Choose original T4 DNA Ligase or the Quick Ligation Kit to meet the demands of a variety of reaction conditions
- Flexibility – Active at room temperature or 16°C; reaction times run from 5 minutes to overnight
- Robustness – Active in a variety of reaction buffers

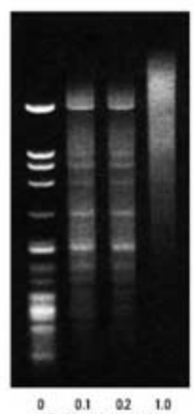

Ligation of blunt-ended HaeIII fragments of Lambda DNA using various amounts of T4 DNA Ligase (400,000 cohesive end units/ml) in a 20 µl reaction volume. Reactions were incubated for 30 minutes at 16°C.

Ligation of HindIII fragments (4-base overhang) of Lambda DNA using 1 cohesive end unit (1µl of 1:400 dilution) of T4 DNA Ligase. Reactions were incubated at 25°C.

For more information and our international distribution network, please visit www.neb.com
New England Biolabs, Inc. is an ISO 9001 certified company

New England Biolabs Inc. 240 County Road, Ipswich, MA 01938 USA 1-800-NEB-LABS Tel. (978) 927-5054 Fax (978) 921-1350 info@neb.com
Canada Tel. (800) 387-1095 info@ca.neb.com • **China** Tel. 010-82378266 beijing@neb-china.com • **Germany** Tel. 0800/246 5227 info@de.neb.com
Japan Tel. +81 (0)3 5669 6191 info@neb-japan.com • **UK** Tel. (0800) 318486 info@uk.neb.com

NEW ENGLAND BioLabs® Inc.
the leader in enzyme technology

<< The Long Lineage of Domestic Cats

Recent genomic information has solved the puzzle about the origin of the domestic cat. **Driscoll *et al.*** (p. 519, published online 28 June) used genomic and mitochondrial markers to piece together the origin of the domestic cat relative to its wild progenitors. The lineage that includes the domestic cat as well as several wild relatives originated much earlier than previously thought, more than 100,000 years ago. Furthermore, it seems that domestication occurred in the Near East in the region of the Fertile Crescent, and not in Africa.

Life Online

Most people begin surfing the Web by going to a search engine, whose function is to index, rank, and categorize Web sites. How these search sites actually find and then evaluate Web sites is a matter of active research and intense corporate competition. **Henzinger** (p. 468) surveys current research into overcoming the difficulties posed by the kinds of queries that Web surfers put to the engines. Some of today's most impressive virtual worlds are the creativity-oriented environment Second Life and the massively multiplayer online role-playing game World of Warcraft. Such online worlds have opened up the possibility of doing scientific research on human interactions—from economics to altruism—at an unprecedented level. **Bainbridge** (p. 472) describes the potential and early progress in this new research arena.

Icebergs and Surface Ocean Productivity

How will the increase in iceberg production from the Antarctic ice sheet, prompted by global warming, affect the surrounding pelagic ecosystem? **Smith *et al.*** (p. 478, published online 21 June) studied two drifting tabular icebergs and the surrounding waters in the northwest Weddell Sea during the austral spring of 2005. Terrigenous material, chlorophyll, krill, and seabirds were more abundant up to as much as 4 kilometers away than they were further from the icebergs. The authors, using a survey of nearby icebergs, calculate that almost 40% of the surface water was influenced by melting, drifting ice, assuming that the effects they measured were representative of icebergs in that general area. Thus, free-drifting icebergs may enhance production and sequestration of organic carbon in areas that otherwise are not as productive.

CREDITS (TOP TO BOTTOM): EWAN MACDONALD; BAG *ET AL.*

Modeling Economic Development

Traditional economics has assumed that countries can always find a combination of goods to sell that put to use their human, physical, and institutional capital. The implication of this view is that the economic growth of a country is mainly a matter of increasing the amount of each form of capital. However, if each of these forms of capital is highly product-specific, the structure of the world of products becomes very important in determining the evolution of a country's productive capabilities. **Hidalgo *et al.*** (p. 482) used network theories and international trade data to build a dynamic model of country growth and development, which may help to explain in part why some countries continue to be poor while others grow economically.

Deterministic Entangled Pairs

A major challenge in quantum information processing and quantum computing is the ability to reliably store and transfer information from one node to another. The entanglement of the qubits, such as those based on photons, is a key feature of achieving such a goal, but has so far relied on probabilistic generation processes. **Wilk *et al.*** (p. 488, published online 21 June) report on the successful implementation of an interface between a stationary qubit (an atom) and a flying qubit (a photon) in a cavity-quantum electrodynamics setup and demonstrate the potential to operate in an almost deterministic way. A sequence of laser pulses targeted on the trapped Rb atom can result in the deterministic generation of entangled photon pairs.

Aerogels Without the Oxygen

The inorganic porous materials used as molecular sieves, ion exchangers, and catalysts have primarily been oxides, but the higher polarizability and "softness" of chalcogenides, such as sulfides and selenides, could improve the ability of such materials to interact with heavy metal ions. **Bag *et al.*** (p. 490; see the Perspective by **Brock**) have prepared a series of gels from the reaction of anionic metal-chalcogenide clusters with Pt(II) salts in water. These gels were then transformed by supercritical drying into mesoporous aerogels that have high surface area and that are semiconductors with compositionally dependent band gaps. These materials can adsorb large quantities of mercury ions from solution as well as nonpolar organic molecules.

Charging Up Gold Catalysts

Asymmetric catalysis has predominantly relied on transition-metal complexes bearing chiral ligands. More recently, chiral anions have been used in metal-free systems to induce asymmetry in acid catalysis or phase-transfer pathways. **Hamilton *et al.*** (p. 496; see the Perspective by

Continued on page 423

BioProcess™ INTERNATIONAL CONFERENCE & EXHIBITION

THE Meeting Place for the Bioprocessing Industry

Conference: October 1-4, 2007• Exhibition: October 1-3, 2007 • Hynes Convention Center Boston, MA

Don't miss your opportunity to attend the most highly respected, well-attended industry event for biopharmaceutical process development and manufacturing.

Accelerate Time to Market.
Implement the Right Technologies.
Learn from the Experts.

Keynote Presentations

Helen N. Winkle
Director, Office of Pharmaceutical Sciences, CDER
FDA

Michael E. Kamarck, Ph.D.
Senior Vice President, Wyeth Biotech Technical Operations and Product Supply
Wyeth Pharmaceuticals

John Ward
Vice President, Global Engineering & Facilities
Biogen Idec

Tobias Massa, Ph.D.
Vice President, Global Regulatory Sciences – CMC
Bristol-Myers Squibb

Markus Gemuend
Senior Vice President, Biochemical Manufacturing
Genentech, Inc.

Barry C. Buckland, Ph.D.
Research Vice President, BioProcess R&D
Merck Research Laboratories

Featuring Four Conference Tracks:

- Production & Economics of Biopharmaceuticals
- Scaling Up from Bench through Commercialization
- Cell Culture & Upstream Processing
- Recovery & Purification

Executive Sponsor

SAFC Biosciences™ Accelerate Success™

Session Sponsor

BD Advanced Bioprocessing

Founding Publication

BioProcess™ INTERNATIONAL

Corporate Sponsors

biogen idec — Transforming Discovery Into Care

GE Healthcare

IrvineScientific Grow With Us™

invitrogen

novasep

sartorius

Register Today

Register Early and Save! Call (800) 390-4078 • Fax: (941) 365-0104 • Email: reg@ibcusa.com

www.IBCLifeSciences.com/BPI/US

Biopharmaceutical Production Series

Organized by

ibc Life Sciences

Continued from page 421

Lacour and Linder) combine these two approaches by pairing cationic gold(I) phosphine complexes with chiral phosphate counterions. A wide range of previously intractable cyclizations of O- and N-substituted allenes proceed in high yield and enantioselectivity. In certain cases, they achieve even higher selectivities by using synergistic combinations of chiral ligands and chiral counterions.

Variable Beginnings

Much work on the fossil record has revealed evolution among related species in a group—examples include horses, ammonites, or humans. What does the fossil record show about evolution within a species, as this is ultimately the building block of evolution? **Webster** (p. 499; see the Perspective by **Hunt**) explores this question by using the excellent fossil record of trilobites, which emerged in the Cambrian. Examination of more than 900 trilobite species shows that their morphological variation was greatest soon after they appeared. Later members of the species show more limited variation. This pattern within species mirrors the larger evolutionary variation shown by trilobites as a whole.

Ethylene Controls Root Meristem Production

In plants, undifferentiated meristem tissue provides stem cells to produce roots and shoots. The root meristem contains a few of these stem cells in a region called the quiescent center. **Ortega-Martínez *et al.*** (p. 507) studied *Arabidopsis* plants with a defect in a gene that controls ethylene biosynthesis and found that it produced more of the gaseous hormone ethylene. The quiescent center cells in these mutants went through more cell divisions than normal, resulting in extra stem cells in the root meristem. Adding exogenous ethylene also increased quiescent cell division, and blocking its synthesis in the mutants prevented extra divisions.

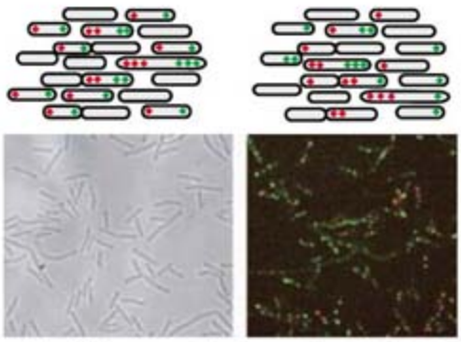

CREDIT: MAAMAR *ET AL.*

Noise, Gene Expression, and Competence

The soil bacterium *Bacillus subtilis* can become "competent"—it can take up genetic material from its surroundings. Competence is regulated by the protein ComK, which controls the genes responsible for DNA uptake. However, cells can only transition to competence in a random fashion during a limited period of time at the beginning of the stationary phase of growth. **Maamar *et al.*** (p. 526, published online 14 June; see the Perspective by **Mettetal and van Oudenaarden**) now find that temporal regulation of *comK* transcription defines the "window of opportunity" during which cells can become competent, and intrinsic noise in gene expression controls the rate at which stochastic transitions to the competent state occur.

Aerobes Far and Wide

Aerobic phototrophic bacteria that utilize bacteriochlorophyll for light harvesting and charge separation were at first thought to be limited to selected, nutrient-rich environments, but similar organisms were later found to be ubiquitously distributed in the upper ocean. The subsequent discovery of proteorhodopsin-containing bacteria indicated that phototrophy is common among Proteobacteria. **Bryant *et al.*** (p. 523) now describe another surprise, an aerobic bacterial phototroph within the phylum *Acidobacteria*.

Potential Parkinson's Intervention

Several neurodegenerative disorders are associated with protein misfolding and are intimately associated with aging. **Outeiro *et al.*** (p. 516, published online 21 June 2007; see the Perspective by **Dillin and Kelly**) identified a compound that can modulate toxicity and aggregation of α-synuclein, a protein associated with Parkinson's disease. The compound exhibited selective inhibitory activity against human sirtuin 2 (SIRT2) deacetylase and possessed efficacy in several Parkinson's disease model systems, increasing the size of intracellular α-synuclein aggregates. The results suggest a cytoprotective role for larger inclusions.

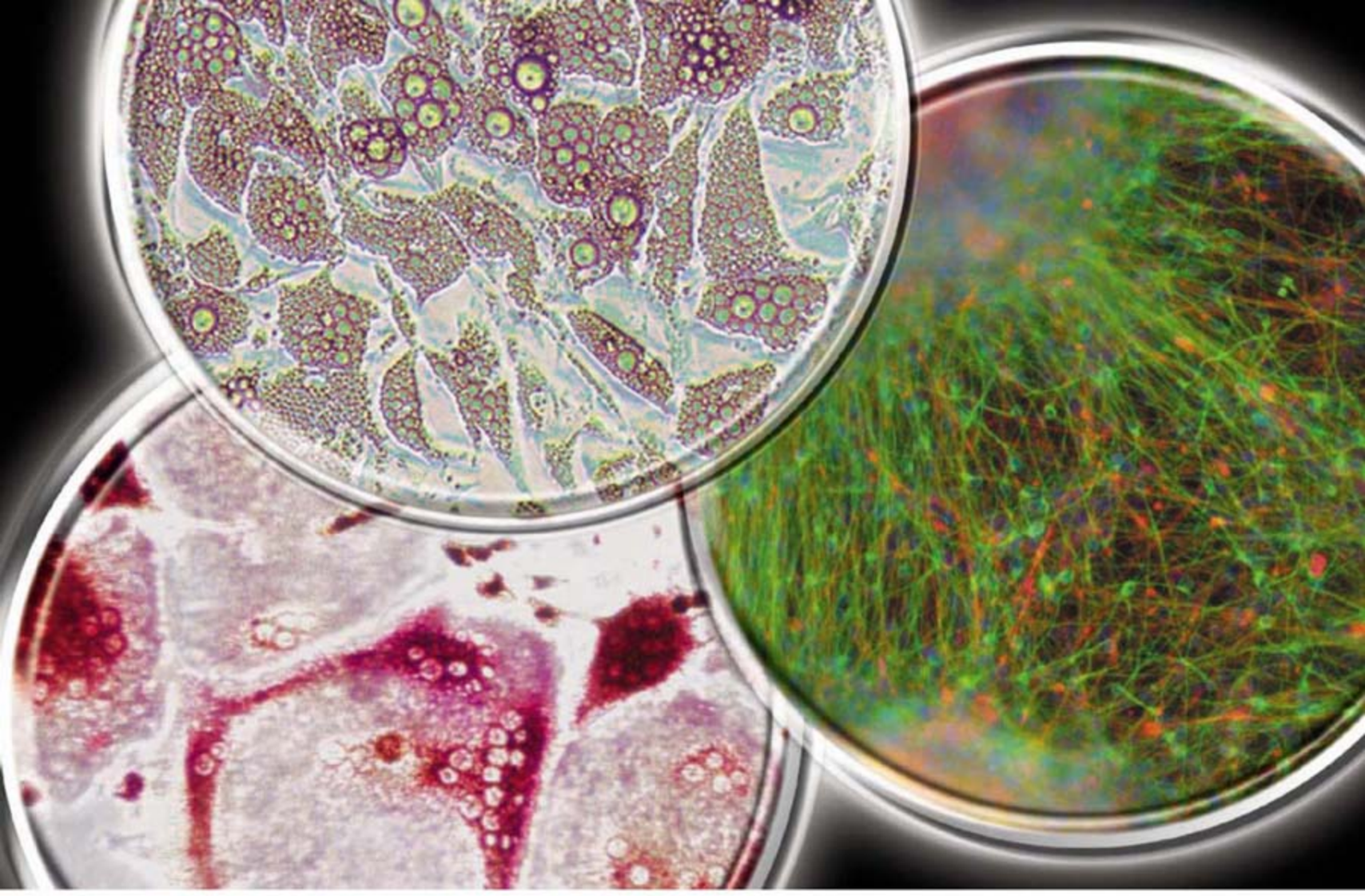

Poietics® Human Stem Cells & Media

In Vivo Relevance. *In Vitro* Results.

As the leader in primary cell culture, Lonza offers a variety of primary stem cells, including:

Human Stem Cells

— New! Poietics® Adipose-Derived Stem Cells purely characterized with relevant stromal and stem markers, and a media kit for growth and expansion

— Multipotent Mesenchymal Stem Cells isolated from bone marrow, and media kits for growth and differentiation of several lineages

Human Bone, Adipose, and Neural Progenitor Cells and Media Kits

— Cryopreserved osteoclast precursors, preadipocytes, and neural progenitors with media kits for growth and differentiation

Human Hematopoietic Progenitor Cells

— Variety of hematopoietic progenitors including CD34+, CD133+, and mononuclear cells isolated from peripheral blood, bone marrow, and umbilical cord blood

Visit our website at www.lonzabioscience.com/poietics to receive a FREE Lonza Cell Mug.

Lonza Walkersville, Inc., 8830 Biggs Ford Road, Walkersville, MD 21793

www.lonza.com

Lonza

Donald Kennedy is Editor-in-Chief of *Science*.

Climate: Game Over

WITH RESPECT TO CLIMATE CHANGE, WE HAVE ABRUPTLY PASSED THE TIPPING POINT IN what until recently has been a tense political controversy. Why? Industry leaders, non-governmental organizations, Al Gore, and public attention have all played a role. At the core, however, it's about the relentless progress of science. As data accumulate, denialists retreat to the safety of the *Wall Street Journal* op-ed page or seek social relaxation with old pals from the tobacco lobby from whom they first learned to "teach the controversy." Meanwhile, political judgments are in, and the game is over. Indeed, on this page last week, a member of Parliament described how the European Union and his British colleagues are moving toward setting hard targets for greenhouse gas reductions.

Now that the scientific consensus is clear, it's time to ask what the U.S. Congress is doing to keep pace with this new reality. The Senate has a recurring strong cap-and-trade bill, sponsored by John McCain (R-AZ) and Joe Lieberman (I-CT). The first time around, it got enough votes to constitute a moral victory for those supporting mitigation, but the next year it missed passage by a wider margin, and no one thinks the votes are there now. Talk of other initiatives abounds, but this area is a two-ring circus: First there's climate, and then there's energy.

You can't really separate these two, but of course there's a committee structure. House Speaker Nancy Pelosi (D-CA) established a new entity to work on climate change issues under the chairmanship of Ed Markey (D-MA), but as a Select Committee, it lacks real authority. Its impotence was a concession to John Dingell (D-MI), the congressman from Ford and Chevy, who heads the powerful Energy and Commerce Committee and wanted no threat to its authority. Dingell later proposed, with Rick Boucher (D-VA), a measure that would have stripped away the right of states (such as California and a dozen others) to set vehicle emissions standards of their own. Speaker Pelosi and Chairman Henry Waxman (D-CA) of the House Oversight and Government Reform Committee, in a startling exercise of leadership, took Big John to the woodshed and killed that effort.

There are so many loci for action that it's hard to keep track of them all. The energy bill completed in the Senate includes corporate average fuel economy (CAFE) standards for the first time in many years. It will have to confront Dingell's House committee, so it's probably time to ponder the old Hill mantra that the House usually wins conferences. Pelosi has pushed the Energy and Commerce Committee to develop an energy bill with fuel efficiency features and research incentives for renewables, and a climate bill with tighter greenhouse gas emissions standards. But it is not clear that much will happen beyond marginal tweaking of the incentive structure for research. What the climate change scientists and the environmental community are looking for is a tough, big-target, emissions reduction plan.

How serious the prospects are for that is suggested by Dingell's response to the notion. He has promised to introduce a bill that amounts to a carbon tax, resembling, if you recall, the Clinton "BTU tax" that failed so miserably. Dingell knows that this is political theater; the tax will go nowhere, and he'll use this to argue that the system just isn't politically ready for proposals that cost consumers money, any more than it's ready for fuel consumption limits on their SUVs.

The bill voted most probable is the one introduced on 10 July by Senators Jeff Bingaman (D-NM) and Arlen Specter (R-PA). It will be a cap-and-trade system setting 2006 emissions levels for 2020 and 1990 levels for 2030. Permits will be distributed (not, alas, auctioned) initially, and emitters may buy additional ones for $12 per ton, increasing by 5% annually. That's insurance: If the going gets tough in the trading system, you can buy yourself out with a modest carbon tax. Some say it doesn't go far enough, but many believe it's a way to get there; if not this year, then the next.

On the main energy and climate front, buckle yourself in and watch the fur fly. Dingell versus Waxman and Pelosi? It's a political junkie's dream.

– Donald Kennedy

10.1126/science.1147817

CREDIT: SCOTT J. FERRELL/GETTY

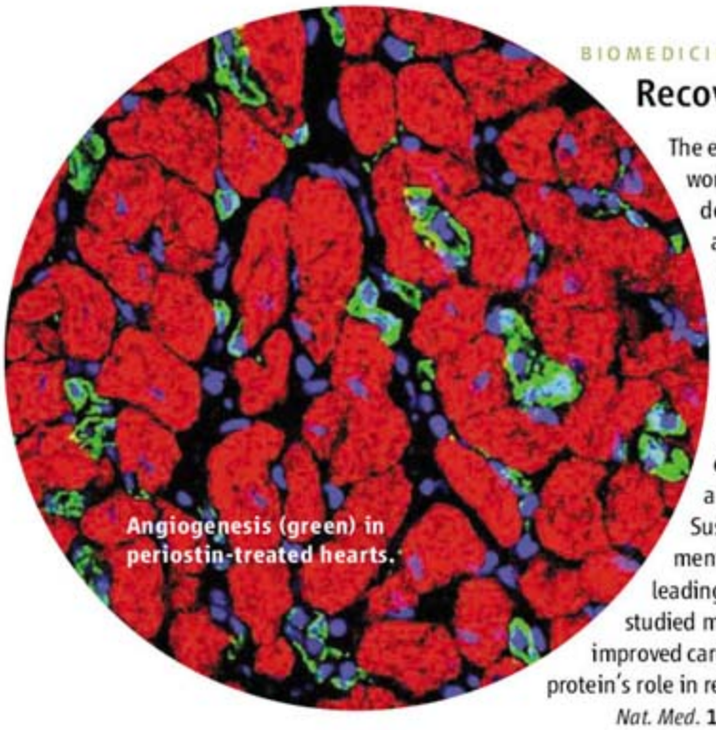

Angiogenesis (green) in periostin-treated hearts.

BIOMEDICINE

Recovering from a Heart Attack

The extracellular matrix (ECM) is increasingly being recognized as a dynamic network of molecules that participates actively in the cellular signaling events that determine an organ's state of health. Most forms of heart failure, for example, are accompanied by alterations in the composition of the ECM. Myocardial infarction (MI) leads to a dramatic increase in the expression of periostin, a 90-kD protein secreted by fibroblasts, yet whether periostin promotes repair of heart damage or contributes to it has been unclear. The answer may be both, as indicated by two research groups who have independently explored periostin function using distinct model systems. In a cell culture study, Kühn *et al.* found that the addition of recombinant periostin to differentiated rat cardiomyocytes caused them to reenter the cell cycle and divide, a process that required integrins as well as phosphatidylinositol 3-kinase. Sustained delivery of recombinant periostin to the heart of rats after experimental MI reduced the extent of heart damage and improved heart function, leading the authors to conclude that the protein enhances heart repair. Oka *et al.* studied mice genetically deficient in periostin. Intriguingly, the mutant mice showed improved cardiac function after MI over the long term, a result the authors attribute to the protein's role in regulating cardiac remodeling and hypertrophy. — PAK

Nat. Med. **13**, 10.1038/nm1619 (2007); *Circ. Res.* 10.1161/CIRCRESAHA.107.149047 (2007).

CREDITS (TOP TO BOTTOM): KÜHN *ET AL.*, *NAT. MED.* **13**, 10.1038/NM1619 (2007); TRAIL *ET AL.*, *GEOCHEM. GEOPHYS. GEOSYST.* **8**, 10.1029/2006GC001449 (2007)

CHEMISTRY

A Light for the Cure

Zeolites are mesoporous minerals used as ion-exchange beds in water purification and softening, and as chemical reaction platforms. Pure silica zeolites have been grown as polycrystalline films on nonporous supports, but the potential utility of these materials depends on their hydrophobicity and porosity, which in turn depends on the presence of grain boundaries. Post-deposition treatments have been used to remove the hydrophilic silanols that form, but typically these approaches either fail to penetrate the pore structure or fail to stand up to the heating required to remove the organic template used during zeolite growth.

Eslava *et al.* show that strong ultraviolet (UV) irradiation during the heating process induces hydrophobicity while also improving the pore structure by creating smaller pores with a narrower distribution. They deposited suspensions of the zeolite silicalite-1 that had been mixed with tetrapropylammonium (TPA) as the organic templating material. UV irradiation during calcination induced methylation by TPA fragments, as well as condensation of polar silanol groups. Film cracking and delamination effects common in other nanocrystalline systems were also suppressed. — MSL

J. Am. Chem. Soc. **129**, 10.1021/ja0723737 (2007).

GEOLOGY

Early Earth Mirrored in Zircon

The oldest minerals on Earth—a few dating as much as 4.4 billion years ago—are igneous zircons that have been eroded and incorporated into comparatively younger 3.8-billion-year-old sedimentary rocks. Several studies have examined the geochemistry of these zircons and inferred conditions on early Earth and the composition of its early crust. Initial results based on the zircon oxygen isotopic compositions and trace element chemistry have implied that liquid water was abundant and that some magmas were cool and water-rich.

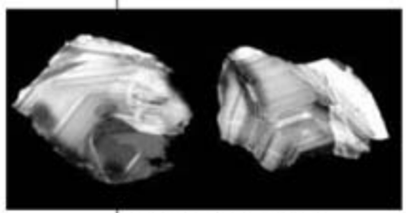

Zircons imaged by cathodoluminescence.

Two related studies provide expanded data and additional constraints. Harrison *et al.* examined the titanium content of zircons, which can be related to the crystallization temperature and thus the water and silica content of a magma. Through a comparative study of zircons in younger granites, they argue that the overall distribution of data in the very old zircons is most consistent with derivation from magmas that formed by remelting of water-rich crust. Trail *et al.* examined the oxygen isotope compositions and confirmed that several grains have high $^{18}O/^{16}O$ ratios, implying derivation of the host magma from water-altered crust or sediments. Together the data imply that early Earth had a vigorous rock cycle involving water, erosion, and burial and heating of sediments, like that operating today. — BH

Geology **35**, 635 (2007); *Geochem. Geophys. Geosyst.* **8**, 10.1029/2006GC001449 (2007).

MOLECULAR BIOLOGY

Promoting Silence

RNA interference (RNAi) can modulate gene expression at the posttranscriptional stage by prompting the degradation of mRNA or blocking its translation into protein. The mRNA is targeted by homologous ~22-nt short interfering (si) RNAs. RNAi can also inhibit gene transcription itself, promoting the formation of silent heterochromatin in yeast, and evidence indicates that siRNAs act via the degradation of low-abundance

Continued on page 429

The shape of Life Science

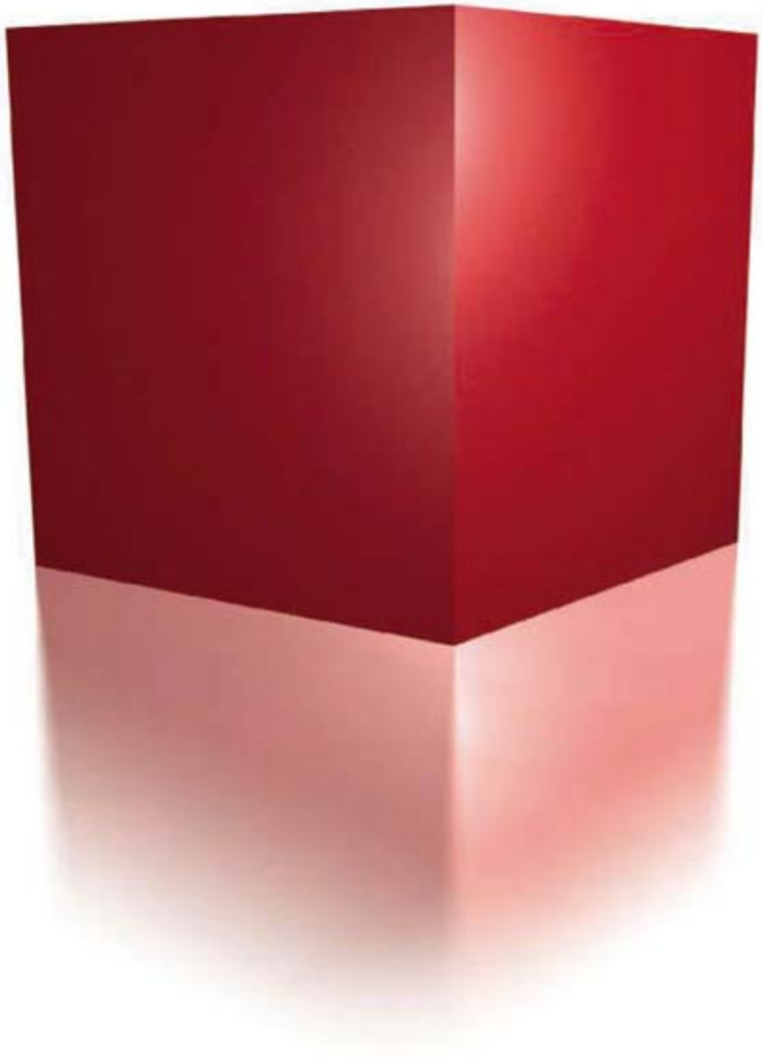

Defined by history, Sigma is at the forefront of life science research and has been for over 60 years.

Outlined by trust, Sigma provides the quality and service expected from a global leader in research and technology.

Shaped by innovation, Sigma Life Science continues our strong tradition — from the original supplier of ATP to a leading solution provider for the revolutionary technology of RNAi.

sigma.com/lifescience

Our Innovation, Your Research

Shaping the Future of Life Science

SIGMA™ Life Science

Continued from page 427

nascent transcripts, rather than on the DNA. In human cells, siRNAs directed against promoter sequences can block gene transcription. Do these siRNAs act on the promoter DNA or, as in yeast, an RNA species? Han *et al.* analyze transcripts from the human EF1a promoter and find a low-abundance sense RNA that initiates ~230 bp upstream of the previously characterized promoter and appears to be a variant EF1a mRNA. Suppression of this variant reduces the ability of promoter-targeted siRNAs to induce transcriptional silencing and to enhance the formation of associated silent chromatin marks. Related results are seen for several other gene promoters in human cells, leading the authors to speculate that these promoter RNAs might function similarly in vivo. — GR

Proc. Natl. Acad. Sci. U.S.A. **104**, 10.1073/pnas.0701635104 (2007).

PHYSICS

Cooler Vibrations

Optical back action can be used to cool micrometer-sized objects such as microresonators and micromirrors to temperatures as low as 1 K. The motivation for such cooling is to be able to access the quantum mechanical oscillations of the thermal vibrations and to use the measurement of these ultrasmall vibrations as exquisite motion sensors for detecting gravity waves as well as for probing possible quantum-mechanical effects in macroscopic systems. Poggio *et al.* show that the cooling can be taken a step further by optimized coupling of an optical cooling setup with the electromechanical motion of a single-crystal silicon cantilever. In their system, 100 nW of laser light is focused onto the paddle of the mass-loaded cantilever, the motion of which is detected in an arm of an interferometer. This interferometric signal is then fed back to induce a piezoelectric mechanical response, resulting in cold damping of the cantilever motion. The net effect is a lowering of the cantilever temperature below 5 mK. — ISO

Phys. Rev. Lett. **99**, 017201 (2007).

BIOCHEMISTRY

A Case of Iron Poisoning

In order to carry out redox reactions on small diatomic gases (such as H_2 and N_2), enzymes enlist the help of metal atoms, often grouping them into clusters and decorating them with non-protein ligands. The [NiFe] hydrogenase offers a case in point; within the Ni-Fe cluster at the active site, the iron atom binds two molecules of cyanide and one of carbon monoxide. Previously, the hydrogenase maturation protein HypF has been shown to transfer a carbamoyl group to a cysteine residue of HypE, which then dehydrates it in situ to generate a thiocyanate (enzyme-SCN).

Watanabe *et al.* have solved the crystal structures of the proteins HypC, HypD, and HypE, which together append the two cyanide moieties to the iron atom—subsequently, a CO is added and the $Fe(CN)_2(CO)$ subassembly is cemented into the large subunit of the hydrogenase before the Ni atom is inserted. They propose that upon binding of HypE to a HypC-HypD complex, a series of thioldisulfide exchanges occurs.

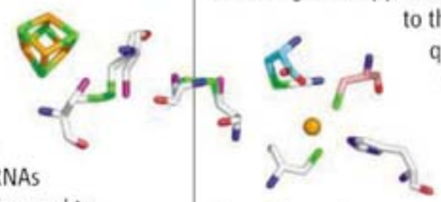

A cysteine relay system (green) adds the first CN (light blue) to the Fe (yellow sphere).

These reactions transfer the CN group from the cysteine of HypE onto the iron atom, which is jointly coordinated by cysteine and histidine residues contributed by HypC and HypD; repeating these steps with a second charged HypE serves to add the second CN ligand. HypD contains its own [4Fe-4S] cluster, which acts catalytically, rather than constitutionally, in facilitating the cysteine redox cascade. — GJC

Mol. Cell **27**, 29 (2007).

CREDIT: WATANABE *ET AL.*, *MOL. CELL* **27**, 29 (2007)

CHEMISTRY

Saddling Up Porphyrins

The stereochemical purity of a polymer or supramolecular assembly can often be set by a comparatively small chiral enrichment of the molecular building blocks or their coordination partners in solution. Toyofuku *et al.* have harnessed this effect to amplify the chiral enrichment of an ensemble of porphyrin complexes. They had previously shown that on complexation with chiral acids, the interconverting saddle-shaped enantiomers of an aryl-substituted porphyrin locked into one favorable diastereomeric conformation, which was conserved when the chiral acids were displaced by the achiral coordinating partner acetic acid. When they instead formed coordination polymers by linking the porphyrins through complexation of tethered pyridyl substituents to Pt ions, they found that the addition of a chiral acid during assembly had a nonlinear amplification effect on the stereochemical outcome. An acid sample of 40% enantiomeric excess was sufficient to induce the highest observed optical purity of the assembly. By adding excess acetic acid and a phosphine ligand, they could then disassemble the polymer and obtain a fully enriched sample of the porphyrin–acetic acid saddles. — JSY

Angew. Chem. Int. Ed. **46**, 10.1002/anie.200701668 (2007).

www.sciencemag.org

Science

1200 New York Avenue, NW
Washington, DC 20005
Editorial: 202-326-6550, FAX 202-289-7562
News: 202-326-6581, FAX 202-371-9227

Bateman House, 82-88 Hills Road
Cambridge, UK CB2 1LQ
+44 (0) 1223 326500, FAX +44 (0) 1223 326501

Subscription Services For change of address, missing issues, new orders and renewals, and payment questions: 866-434-AAAS (2227) or 202-326-6417, FAX 202-842-1065. Mailing addresses: AAAS, P.O. Box 96178, Washington, DC 20090-6178 or AAAS Member Services, 1200 New York Avenue, NW, Washington, DC 20005

Institutional Site Licenses please call 202-326-6755 for any questions or information

Reprints: Author Inquiries 800-635-7181
Commercial Inquiries 803-359-4578

Permissions 202-326-7074, FAX 202-682-0816

Member Benefits Bookstore: AAAS/BarnesandNoble.com bookstore www.aaas.org/bn; Car purchase discount: Subaru VIP Program 202-326-6417; Credit Card: MBNA 800-847-7378; Car Rentals: Hertz 800-654-2200 CDP#343457, Dollar 800-800-4000 #AA1115; AAAS Travels: Betchart Expeditions 800-252-4910; Life Insurance: Seabury & Smith 800-424-9883; Other Benefits: AAAS Member Services 202-326-6417 or www.aaasmember.org.

science_editors@aaas.org	(for general editorial queries)
science_letters@aaas.org	(for queries about letters)
science_reviews@aaas.org	(for returning manuscript reviews)
science_bookrevs@aaas.org	(for book review queries)

Published by the American Association for the Advancement of Science (AAAS), *Science* serves its readers as a forum for the presentation and discussion of important issues related to the advancement of science, including the presentation of minority or conflicting points of view, rather than by publishing only material on which a consensus has been reached. Accordingly, all articles published in *Science*—including editorials, news and comment, and book reviews—are signed and reflect the individual views of the authors and not official points of view adopted by the AAAS or the institutions with which the authors are affiliated.

AAAS was founded in 1848 and incorporated in 1874. Its mission is to advance science and innovation throughout the world for the benefit of all people. The goals of the association are to: foster communication among scientists, engineers and the public; enhance international cooperation in science and its applications; promote the responsible conduct and use of science and technology; foster education in science and technology for everyone; enhance the science and technology workforce and infrastructure; increase public understanding and appreciation of science and technology; and strengthen support for the science and technology enterprise.

Information for Authors

See pages 120 and 121 of the 5 January 2007 issue or access www.sciencemag.org/feature/contribinfo/home.shtml

EDITOR-IN-CHIEF **Donald Kennedy**
EXECUTIVE EDITOR **Monica M. Bradford**
DEPUTY EDITORS **R. Brooks Hanson, Barbara R. Jasny, Katrina L. Kelner**
NEWS EDITOR **Colin Norman**

Editorial supervisory senior editor Phillip D. Szuromi; **senior editor/perspectives** Lisa D. Chong; **senior editors** Gilbert J. Chin, Pamela J. Hines, Paula A. Kiberstis (Boston), Marc S. Lavine (Toronto), Beverly A. Purnell, L. Bryan Ray, Guy Riddihough, H. Jesse Smith, Valda Vinson, David Voss; **associate editors** Jake S. Yeston, Laura M. Zahn; **online editor** Stewart Wills; **associate online editor** Tara S. Marathe; **book review editor** Sherman J. Suter; **associate letters editor** Etta Kavanagh; **editorial manager** Cara Tate; **senior copy editors** Jeffrey E. Cook, Cynthia Howe, Harry Jach, Barbara P. Ordway, Jennifer Sills, Trista Wagoner; **copy editors** Lauren Kmec, Peter Mooreside; **editorial coordinators** Carolyn Kyle, Beverly Shields; **publications assistants** Ramatoulaye Diop, Chris Filiatreau, Joi S. Granger, Jeffrey Hearn, Lisa Johnson, Scott Miller, Jerry Richardson, Brian White, Anita Wynn; **editorial assistants** Maris M. Bish, Emily Guise, Patricia M. Moore, Jennifer A. Seibert; **executive assistant** Sylvia S. Kihara; **administrative support** Maryrose Madrid

News senior correspondent Jean Marx; **deputy news editors** Robert Coontz, Eliot Marshall, Jeffrey Mervis, Leslie Roberts; **contributing editors** Elizabeth Culotta, Polly Shulman; **news writers** Yudhijit Bhattacharjee, Adrian Cho, Jennifer Couzin, David Grimm, Constance Holden, Jocelyn Kaiser, Richard A. Kerr, Eli Kintisch, Andrew Lawler (New England), Greg Miller, Elizabeth Pennisi, Robert F. Service (Pacific NW), Erik Stokstad; **interns** Benjamin Lester, Marissa Cevallos, Veronica Raymond; **contributing correspondents** Barry A. Cipra, Jon Cohen (San Diego, CA), Daniel Ferber, Ann Gibbons, Robert Irion, Mitch Leslie, Charles C. Mann, Evelyn Strauss, Gary Taubes; **copy editors** Rachel Curran, Linda B. Felaco, Melvin Gatling; **administrative support** Scherraine Mack, Fannie Groom; **bureaus** Berkeley, CA: 510-652-0302, FAX 510-652-1867, New England: 207-549-7755, San Diego, CA: 760-942-3252, FAX 760-942-4979, Pacific Northwest: 503-963-1940

Production director James Landry; **senior manager** Wendy K. Shank; **assistant manager** Rebecca Doshi; **senior specialists** Jay Covert, Chris Redwood; **specialist** Steve Forrester; **Preflight director** David M. Tompkins; **manager** Marcus Spiegler; **specialist** Jessie Mudjitaba

Art director Kelly Buckheit Krause; **associate art director** Aaron Morales; **illustrators** Chris Bickel, Katharine Sutliff; **senior art associates** Holly Bishop, Laura Creveling, Preston Huey, Nayomi Kevitiyagala; **associate** Jessica Newfield; **photo editor** Leslie Blizard

***Science* International**

Europe (science@science-int.co.uk) **editorial: international managing editor** Andrew M. Sugden; **senior editor/perspectives** Julia Fahrenkamp-Uppenbrink; **senior editors** Caroline Ash (Geneva: +41 (0) 222 346 3106), Stella M. Hurtley, Ian S. Osborne, Stephen J. Simpson, Peter Stern; **associate editor** Joanne Baker; **editorial support** Deborah Dennison, Rachel Roberts, Alice Whaley; **administrative support** Janet Clements, Jill White; **news: europe news editor** John Travis; **deputy news editor** Daniel Clery; **correspondent** Gretchen Vogel (Berlin: +49 (0) 30 2809 3902, FAX +49 (0) 30 2809 8365); **contributing correspondents** Michael Balter (Paris), Martin Enserink (Amsterdam and Paris), John Bohannon (Vienna); **intern** Krista Zala

Asia Japan Office: Asca Corporation, Eiko Ishioka, Fusako Tamura, 1-8-13, Hirano-cho, Chuo-ku, Osaka-shi, Osaka, 541-0046 Japan; +81 (0) 6 6202 6272, FAX +81 (0) 6 6202 6271; asca@os.gulf.or.jp; **asia news editor** Richard Stone +66 2 662 5818 (rstone@aaas.org); **contributing correspondents** Dennis Normile (Japan: +81 (0) 3 3391 0630, FAX 81 (0) 3 5936 3531; dnormile@gol.com); Hao Xin (China: + 86 (0) 10 6307 4439 or 6307 3676, FAX +86 (0) 10 6307 4358; cindyhao@gmail.com); Pallava Bagla (South Asia: +91 (0) 11 2271 2896; pbagla@vsnl.com)

Africa Robert Koenig (contributing correspondent, rob.koenig@gmail.com)

EXECUTIVE PUBLISHER **Alan I. Leshner**
PUBLISHER **Beth Rosner**

Fulfillment & Membership Services (membership@aaas.org) **director** Marlene Zendell; **manager** Waylon Butler; **systems specialist** Andrew Vargo; **customer service supervisor** Pat Butler; **specialists** Tamara Alfson, Laurie Baker, Latoya Casteel, Vicki Linton; **data entry supervisor** Cynthia Johnson; **specialists** Tomeka Diggs, Tarrika Hill, Erin Layne

Business Operations and Administration director Deborah Rivera-Wienhold; **business manager** Randy Yi; **senior business analyst** Lisa Donovan; **business analyst** Jessica Tierney; **financial analysts** Michael LoBue, Farida Yeasmin; **rights and permissions: administrator** Emilie David; **associate** Elizabeth Sandler; **marketing director** John Meyers; **marketing managers** Darryl Walter, Allison Pritchard; **marketing associates** Julianne Wielga, Mary Ellen Crowley, Catherine Featherston, Alison Chandler, Lauren Lamoureux; **international marketing manager** Wendy Sturley; **marketing executive** Jennifer Reeves; **marketing/member services executive** Linda Rusk; **japan sales** Jason Hannaford; **site license sales director** Tom Ryan; **sales and customer service** Mehan Dossani, Kiki Forsythe, Catherine Holland, Wendy Wise; **electronic media: manager** Lizabeth Harman; **project manager** Trista Snyder; **assistant manager** Lisa Stanford; **senior production specialist** Walter Jones; **production specialists** Nichele Johnston, Kimberly Oster

Advertising director worldwide ad sales Bill Moran

Product (science_advertising@aaas.org); **consumer & sponsorship sales manager** Tina Morra: 202-326-6542 **midwest** Rick Bongiovanni: 330-405-7080, FAX 330-405-7081 • **west coast/w. canada** Teola Young: 650-964-2266 **east coast/e. canada** Christopher Breslin: 443-512-0330, FAX 443-512-0331 • **uk/europe/asia** Michelle Field: +44 (0) 1223-326-524, FAX +44 (0) 1223-325-532 **japan** Mashy Yoshikawa: +81 (0) 33235 5961, FAX +81 (0) 33235 5852; **senior traffic associate** Deiandra Simms

Commercial Editor Sean Sanders: 202-326-6430

Classified (advertise@sciencecareers.org); **u.s.: recruitment sales manager** Ian King: 202-326-6528, FAX 202-289-6742; **inside sales manager: midwest/canada** Daryl Anderson: 202-326-6543; **northeast:** Allison Millar: 202-326-6572; **southeast:** Tina Burks: 202-326-6577; **west:** Nicholas Hintibidze: 202-326-6533; **sales coordinators** Erika Bryant, Rohan Edmonson, Leonard Marshall, Shirley Young; **international: sales manager** Tracy Holmes: +44 (0) 1223 326525, FAX +44 (0) 1223 326532; **sales** Christina Harrison, Alex Palmer; **sales assistant** Louise Moore; **japan:** Jason Hannaford: +81 (0) 52 757 5360, FAX +81 (0) 52 757 5361; **advertising production operations manager** Deborah Tompkins; **senior production specialists** Robert Buck, Amy Hardcastle; **senior traffic associate** Christine Hall; **publications assistant** Mary Lagnaoui

AAAS Board of Directors **retiring president, chair** John P. Holdren; **president** David Baltimore; **president-elect** James J. McCarthy; **treasurer** David E. Shaw; **chief executive officer** Alan I. Leshner; **board** John E. Dowling, Lynn W. Enquist, Susan M. Fitzpatrick, Alice Gast, Linda P. B. Katehi, Cherry A. Murray, Thomas D. Pollard, Kathryn D. Sullivan

AAAS
ADVANCING SCIENCE, SERVING SOCIETY

The shape of Sigma Life Science

Shaped by innovation,

Sigma Life Science continues our strong tradition — from the original supplier of ATP to a leading solution provider for the revolutionary technology of RNAi.

Shape your research with best-in-class technologies from Sigma Life Science.

- World-class RNAi solutions with our MISSION® shRNA and siRNA libraries.
- Genomic DNA amplification for single cell and tissue with our GenomePlex® WGA kits
- Fast and deep protein depletion with our ProteoPrep20® technology
- Rapid multiplex protein expression profiling from our Panorama® Antibody arrays
- Thousands of antibodies and small molecules for gene, protein and cellular research
- Oligos, peptides, and antisera produced under the highest quality systems

sigma.com/lifescience

Our Innovation, Your Research

Shaping the Future of Life Science

SIGMA™ Life Science

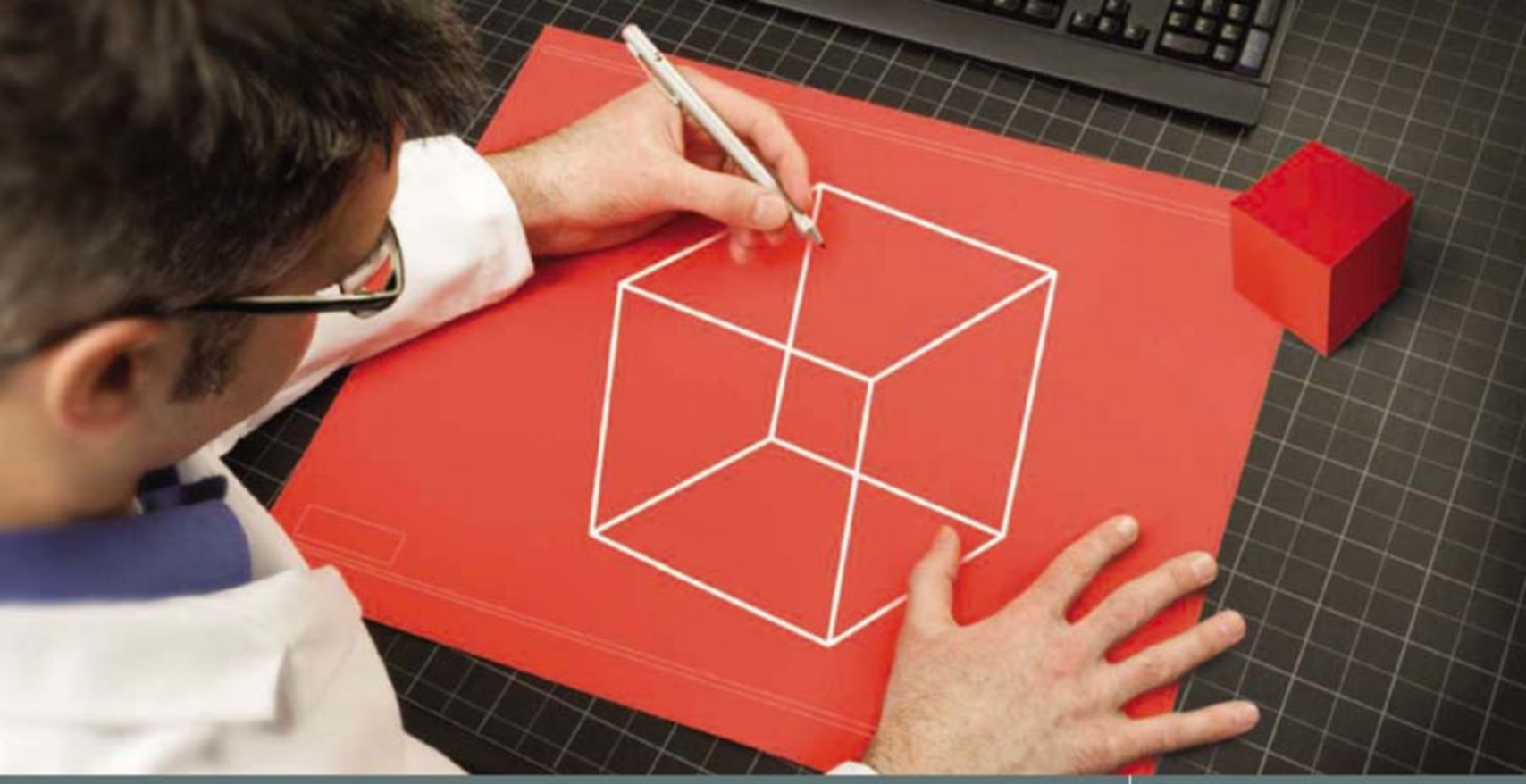

Design!

INNOVATION @ WORK

With MISSION® siRNA – It's About Design!

Sigma and Rosetta Inpharmatics, a recognized leader in Bioinformatics, have partnered to bring you the best siRNA design to improve your RNAi results.

Current studies suggest that the rules used to design gene-specific siRNAs have a direct effect on how well your siRNA will perform in a given RNAi experiment. Using an siRNA designed with a best-in-class algorithm saves time and money, enabling you to focus on downstream applications, not up-front siRNA design work.

The MISSION siRNA Druggable Genome Libraries designed with Rosetta algorithm provide:

- Efficient knockdown for low abundance message
- Improved target specificity
- Flexible gene family sets, pre-arrayed for a range of applications
- Optimum products from highest quality, experienced manufacturing
- Freedom to operate for research use

The MISSION siRNA Performance Guarantee

Sigma guarantees that 2 out of 3 siRNA duplexes per target gene will achieve knockdown efficiencies of greater than or equal to 75%

For more information on MISSION siRNA Druggable Genome Libraries, please visit us on the Web at sigma.com/missionsirna.

Better siRNA Design, Better RNAi Performance

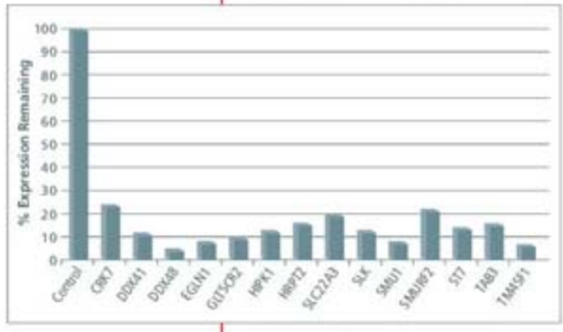

Silencing efficacy of representative MISSION siRNAs designed using the Rosetta algorithm. Target mRNA levels were measured by the QuantiGene® Reagent System from samples harvested 24 hours after transfection into HeLa cells.

POWERED BY ROSETTA INPHARMATICS

Our Innovation, Your Research
Shaping the Future of Life Science

SIGMA Life Science

From Gene to Green

It took a century to go from Mendel's plant-breeding experiments to the genetic code. The Molecular Genetics Explorer can help biology students make the same intellectual journey by connecting changes in an organism's DNA to alterations in its appearance.

NET WATCH

The free virtual lab comes from Brian White and Ethan Bolker of the University of Massachusetts, Boston. Students begin by setting up plant crosses and gene mutations to decipher the inheritance of color in fictional flowers. They then move to the protein level, tinkering with amino acid sequences to see how changes alter a protein's shape and the flower color it produces. The final exercises let users determine the consequences of manipulating DNA. >> intro.bio.umb.edu/MGX/

Rocky Flats Reborn

After a decade of cleanup work by the U.S. Department of Energy at a cost of $7 billion, 1600 hectares of the Rocky Flats nuclear production site outside Denver, Colorado, will become a wildlife refuge boasting deer, elk, and prairie dogs, the government announced on 12 July. The site has been closed since 1989 after being used for almost 40 years by the government to build plutonium triggers for its nuclear weapons, in the process generating 12 tons of waste plutonium. The Environmental Protection Agency says Rocky Flats is now squeaky-clean, but LeRoy Moore of the Rocky Mountain Peace and Justice Center, in Boulder, Colorado, says people could absorb plutonium that has migrated into the newly opened areas.

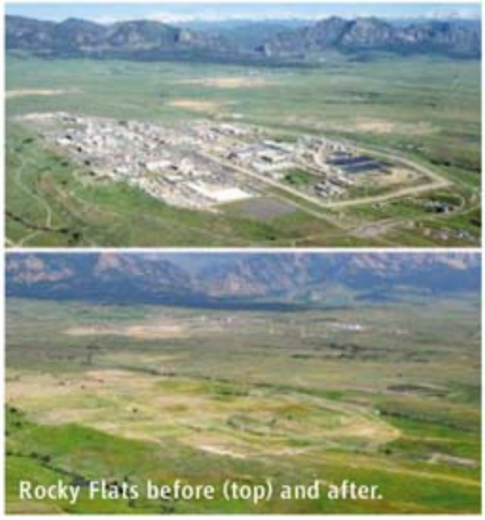

Rocky Flats before (top) and after.

CREDITS (TOP TO BOTTOM): CAROLA RADKE/MUSEUM FÜR NATURKUNDE BERLIN; ESTATE OF PETER MOORE/LICENSED BY VAGA; DEPARTMENT OF ENERGY

Allosaurus

NATURAL HISTORY IN BERLIN

The world's tallest dinosaur skeleton—13.27 meters from toe to head—is again causing visitors to crane their necks in the entry hall of Berlin's Museum für Naturkunde. Reopened after a 2-year renovation, the museum's new main exhibit, called Evolution in Action, draws from a collection of more than 30 million specimens. Located in the former East Berlin, the museum had not seen major renovations since a bomb destroyed one wing at the end of World War II (*Science*, 2 July 2004, p. 35). The dinosaurs have been remounted with outstretched tails, reflecting new calculations about their real-life postures, and each bone can now be removed separately for further study. Museum scientists will be more visible, giving regular tours and talks about their research.

Evolution looks to be a hit in Berlin: Record crowds at the grand opening last week forced a temporary shutdown of the nearby subway station. And Germany's Federal Minister of Education and Research, Annette Schavan, announced her support for a funding boost, raising hopes that the museum will no longer have to scrape along on handouts from the chronically broke city.

Art and Science: Memory Lane

Bell Laboratories engineer Billy Klüver and contemporary art giant Robert Rauschenberg launched a decades-long partnership between artistic and scientific types in 1966 with *9 Evenings: Theater & Engineering*, a series of performance art pieces in New York City. This month, the National Academies in Washington, D.C., showed the first of a new series of documentaries on the novel happenings.

The film relives the first of the 1966 shows. Called *Open Score*, it included a tennis match in which radio transceivers in the rackets caused a gong to sound and lights to go out every time a ball was hit, until the court was in total darkness. The film also highlights some of the technical challenges for the Bell researchers involved, including obtaining an infrared camera for a ghostly dance in the darkness.

Eerie match.

Retired Bell Laboratories technician Harold Hodges calls the work he and his colleagues did for *9 Evenings* "more tinkering" than science. But the events led to the establishment of Experiments in Art and Technology, a worldwide collaboration that continued for decades, at its height claiming 4000 artist and engineer members. One was former Bell Laboratories electrical engineer Per Biorn, who says, "For some of us like me, it was like opening up a window to a whole new world."

EDITED BY YUDHIJIT BHATTACHARJEE

DIGGING FOR PRIDE. The Bosnian government last week promised to spend $140,000 for archaeological work on a hill north of Sarajevo that amateur archaeologist Semir Osmanagic (left) claims is a 12,000-year-old pyramid (*Science*, 22 September 2006, p. 1718). In doing so, Prime Minister Nedzad Brankovic overrode the country's minister of culture, Gavrilo Grahovac, who last month said that the government should stop supporting Osmanagic and instead investigate his tax-free foundation.

The development is "very dispiriting," says Anthony Harding, president of the European Association of Archaeologists, which considers Osmanagic's project to be pseudoscience. "The great majority of people in Bosnia must realize they are being taken for a ride."

Brankovic said the funding will support archaeological "restoration" at the site, particularly of the medieval ruins at the top of the hill. Osmanagic says the region was dominated by a monument-constructing "supercivilization" during the Ice Age. "Why don't we recognize something that is visible to the naked eye?" Brankovic asked reporters after visiting the site. "Why should we disown something that the entire world is interested in?"

TWO CULTURES

HEADY HUMOR. Dean Burnett hopes you'll laugh at his work.

When not doing research on rat memories, the Ph.D. student at Cardiff University in the United Kingdom bills himself as the only neuroscientist turned stand-up comic in South Wales. His routine at the qualifying round of "So You Think You're Funny"—an annual comedy competition at the Edinburgh Festival Fringe—won him a spot at next month's semifinal.

A cadaver launched Burnett's stand-up career. Working as an embalmer at a medical school, he realized that he and the 76-year-old corpse "were wearing exactly the same boxer shorts. I couldn't describe this in a serious context." He sneaks science into his performances. One joke features a guy who refuses to believe in evolution because humans don't have wings.

Another, about opponents of genetically modified foods, makes the point that "being biased against something because of its genes is racism."

"He doesn't baffle people with science," says Jeff Baker, an organizer of the Welsh Comedy Festival, where the 24-year-old performed recently. "But he gives them a more cerebral viewpoint."

AWARDS

SHARING THE GLORY. A research team in Australia and another in the United States have won the 2007 Cosmology Prize from the Gruber Foundation for discovering that the expansion of the universe is accelerating. Saul Perlmutter of the University of California, Berkeley, and his team—the Supernova Cosmology Project—and Brian Schmidt of the Australian National University in Canberra and his group—the High-z Supernova Search Team—arrived at the conclusion, working independently, at about the same time. Perlmutter and Schmidt will split half of the $500,000 prize; the rest will be divvied up among the remaining members of the two teams.

Inside Government >>

KEEPING BUSY. Last week, plant molecular biologist Nina Fedoroff accepted a new job advising U.S. Secretary of State Condoleezza Rice and sold her house in central Pennsylvania in preparation for moving to Washington, D.C. But the 65-year-old chaired professor at Pennsylvania State University and lifelong academic researcher seems to be taking these seismic changes in stride. What's really got her stressed out is her application to renew a grant from the National Science Foundation—on which her fate as an active scientist rests.

"If it gets funded, then I'm in business," says Fedoroff, who's taking a 3-year leave from her faculty position to serve as the State Department's third-ever science and technology adviser. "I think I'll be able to run my lab from Washington. But plant science funding is tight, and if it's rejected, then I'm in trouble."

Starting on 6 August, Fedoroff's job will be to get more outside scientists involved in State Department activities, plug more foreign attachés into the world of science, and lend a hand to government-sponsored research efforts with an international component. Despite receiving no promises of access to Rice—"she's very busy at the moment"—Fedoroff is optimistic about making a difference. "I think there are lots of scientific bridges that can be built across chasms that cannot be crossed because of politics or religion," she says.

The new job wasn't the only big news Fedoroff received last week; she also was chosen for the nation's highest scientific honor, the National Medal of Science. It's the first time in 4 years the list includes women (microbiologist Rita Colwell was also honored). "That's wonderful. I'd like to think it's progress," says Stephanie Pincus, who co-directs a project run by the Society for Women's Health Research to recognize the achievements of women (*Science*, 22 June, p. 1683). But women were once again shut out of the National Medal of Technology, which went to five men. The complete list of awardees can be found at www.ostp.gov.

CREDITS (TOP TO BOTTOM): WWW.BOSNIAPYRAMID.COM; COLIN ROBERTSON; PENN STATE UNIVERSITY

Quake shakes nuclear composure 438

Aspen's best friend 438

DRUG DEVELOPMENT

A European-Inspired Renaissance For China's Drug Industry?

BEIJING—Earlier this month, when the Chinese government executed Zheng Xiaoyu, former commissioner of its State Food and Drug Administration, it sent a strong message that corruption at the watchdog agency would no longer be tolerated. But observers say that China's pharmaceutical industry, replete with firms that churn out copycat drugs—often in violation of patents—and unproven or fake medicine, remains in desperate need of reform. The bottom line, says neuroscientist Lu Bai of the U.S. National Institute of Child Health and Human Development in Bethesda, Maryland, is that Chinese companies must develop their own research capabilities.

Chinese pharma now has a golden opportunity to come up to speed fast. During the past year, three European drug giants have launched major research and development (R&D) facilities on Chinese soil. For local firms, the choice is stark: Adopt a Western approach to drug discovery—from nurturing innovation to demonstrating efficacy by clinical trials and ensuring quality control—or cede the best homegrown scientists, and large chunks of the market, to Western rivals. "Chinese consumers will learn the difference between domestic and foreign drugs and make their choices accordingly," says Lu. Companies that now market unproven medicine with wild claims, he says, "will be wiped out."

Since the Danish company Novo Nordisk opened a research shop in Beijing in 2002, European drug firms have ventured more boldly into Chinese waters than have their U.S. counterparts. The U.S.–based titans Merck and Eli Lilly, for instance, have outsourced some medicinal chemistry R&D to China, and Pfizer in October 2005 set up a small R&D center in Shanghai to provide input into clinical trial design and management.

In contrast to those modest commitments, GlaxoSmithKline (GSK) earlier this month announced plans to recruit 50 to 100 scientists for an R&D center in Shanghai that will have a first-year operating budget of $40 million. GSK poached immunologist Zang Jingwu from the Chinese Academy of Sciences and Shanghai Jiao Tong University to lead GSK R&D China, which will focus on drugs for neurodegenerative diseases such as Alzheimer's disease, Parkinson's disease, and multiple sclerosis. Over time, GSK's entire neurodegenerative drug pipeline—"from target validation to global registration and approval"—will move to China, says Zang, who worked at Baylor College of Medicine in Houston, Texas, before returning to China in 2002. GSK R&D China intends to ramp up to 1000 researchers in a decade, he says.

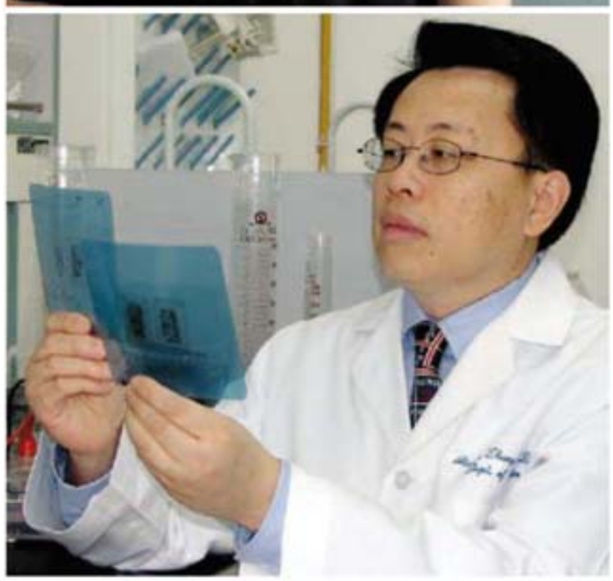

Leading the charge. Two pharmaceutical giants have enlisted expatriate Chinese scientists to head their new R&D labs in Shanghai: AstraZeneca's Zhang Xiaolin (*top*) and GSK's Zang Jingwu.

GSK follows on the heels of AstraZeneca's Innovation Center China, set up in June 2006 to develop drugs for gastric tract and liver cancers that are prevalent in China, and the Novartis Institute for Biomedical Research in Shanghai, which will target infectious causes of cancer (*Science*, 17 November 2006, p. 1064). Unlike GSK R&D China's global aspirations, the AstraZeneca and Novartis facilities will focus primarily on drugs for the domestic market.

The foreign R&D shops will intensify competition for young Chinese stars. "Talents with experience will not be in large supply in the near future," says Zhang Xiaolin, a bioinformatics specialist and cancer researcher brought back from AstraZeneca's research unit in Boston, Massachusetts, last August to head the Chinese center. AstraZeneca plans to pour $100 million over 3 years into the new center, and hire 70 to 80 scientists, primarily locally, by 2009. "I do not believe importing a large talent pool from the West is a viable strategy," explains Zhang, because expatriates often command much higher salaries than homegrown scientists do. "If the salary gap is too big, local morale will be low," which could drive employees into the arms of other companies, Zhang says. To maintain loyalty, he says, AstraZeneca will pay its Chinese staff competitively and give them opportunities to ascend to positions that might otherwise have been filled by overseas hires.

It's not necessarily a bad thing if young scientists flock to foreign labs for higher pay, as their training may ultimately benefit China's industry, says Hu Zhuohan, president of the Ryder Institute of Liver Diseases in Shanghai. He predicts that many scientists who cut ▶

CREDITS (TOP TO BOTTOM): COURTESY OF ASTRAZENECA INNOVATION CENTER CHINA; ZANG JINGWU

California's endangered delta
442

Explaining lines in the sand
446

their teeth in foreign R&D shops will return to Chinese companies or launch their own ventures to control intellectual property rights.

A central challenge for Chinese pharma is a paucity of new ideas. "China does not have its own drugs" according to the definition that a compound has a known structure and a proven efficacy, claims Lu. He and others argue that Chinese drug firms have been content with copying medicines or marketing what would be called "supplements" in the West that are derived from traditional medicine but are of unproven efficacy.

Nevertheless, the stage is set for a transformation. China has stiffened laws to protect intellectual property. "The situation has improved dramatically," says Zhang.

"A Chinese company today cannot risk spending money developing a product if it knows there's a good chance it will be stopped from producing it later," Mark Engel, president of Excel PharmaStudies Inc. in Beijing, told *Burrill Greater China Life Sciences Quarterly*.

Pfizer and Eli Lilly recently won cases in Chinese courts favoring their patents. "The era of copycats will soon be over," predicts Lu, who says that Chinese pharma companies will go "belly up" if they fail to develop their own therapeutics. **–HAO XIN**

OIL RESOURCES

Even Oil Optimists Expect Energy Demand to Outstrip Supply

There are at least a trillion barrels of oil left in the ground to feed the world's appetite for liquid energy, maybe 2 or 3 trillion. Forecasters disagree about when drillers will first fail to deliver all the oil the world wants. Some say that crisis will come in the next decade, some by midcentury. Last week, a federally commissioned report warned that, although the world is not running out of oil, the United States must ambitiously develop additional sources of liquid energy in the next 25 years. Oil alone will not suffice. And a second recent report foresees oil supplies tightening by as early as 2010.

A root problem, everyone agrees, is the rapidly growing demand for energy. Last week's report (www.npc.org) from the federally chartered National Petroleum Council (NPC) starts with the prospect of a 50% to 60% increase in demand for oil by 2030. That's about the percentage by which world production has increased in the past 25 years. But meeting increased demand will be harder this time. The volume of oil required will be 35% greater than what was produced in the previous 25 years; that's more oil than consumed throughout human history up to 2005. And the easiest oil to extract has by now been produced.

The NPC report committee—headed by Lee Raymond, retired chair of Exxon Mobil—compiled forecasts from a dozen energy consulting firms and international oil companies. The forecasts span a range from about 80 million barrels per day in 2030 to about 135 mb/d (see figure). All but one fell short of meeting the expected 50% demand increase. The average of the dozen fell 10 mb/d short of the U.S. Energy Information Administration's forecast for 2030. And the lowest oil company forecast in the study equaled that from the Association for the Study of Peak Oil and Gas, which shows world production peaking by 2015 and then starting to decline by 2020 in a crisis of global proportions.

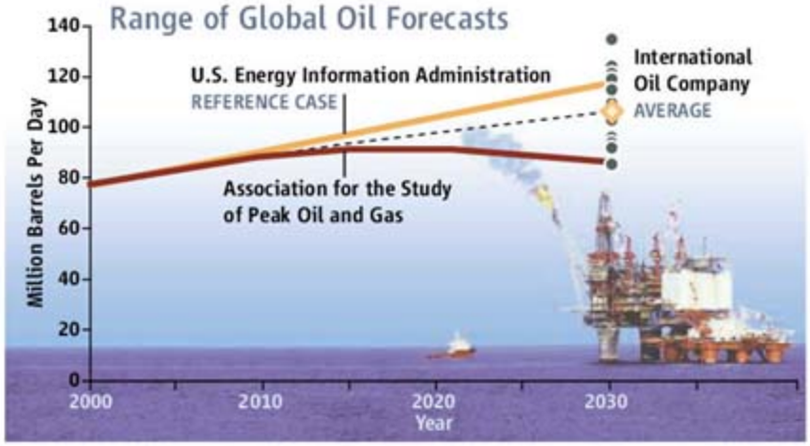

Lower expectations. Oil companies tend to forecast that oil production in 2030 will be below the official U.S. forecast but above pessimists' prediction.

Given such relative pessimism within the oil industry, the NPC committee concluded that "it is a hard truth that the global supply of oil and natural gas from the conventional sources relied upon historically is unlikely to meet projected 50-60 percent growth in demand over the next 25 years." There's probably enough oil in the ground, the NPC says, but there are other, more important constraints: the technical difficulty of extracting what remains, political instability in countries such as Nigeria, reluctance or inability to extract oil faster in places such as Mexico and Venezuela, and the challenge of assembling the required human and financial resources.

Surprisingly, the 40-page executive summary does not mention OPEC (the Organization of the Petroleum Exporting Countries). Energy analyst David Greene of Oak Ridge National Laboratory in Tennessee sees that as "a huge blind spot" for the NPC. Although he agrees that there's lots of oil left in the world, the lion's share lies under OPEC member countries. Organizations such as "the International Energy Agency [IEA], Exxon Mobil, and others have predicted that by 2010 everybody outside of OPEC will find it almost impossible to increase production," he says, because the remaining non-OPEC oil is not abundant enough.

The IEA re-emphasized that conundrum in its Medium-Term Oil Market Report (omrpublic.iea.org/mtomr.htm) released 9 July. Although a spurt of non-OPEC production will bring some relief over the next couple of years, the report says, by 2012 the oil market will be "extremely tight" as planned OPEC and non-OPEC production fail to stay ahead of rising demand. "It is abundantly clear that if the path of demand does not change on its own [by 2011]," says the report, "it may well be driven to change by higher prices." **–RICHARD A. KERR**

CREDITS: NPC STUDY (DATA SOURCE); PHOTOS.COM (IMAGE)

SEISMOLOGY

Quake Underscores Shaky Understanding of Ground Forces

TOKYO—An earthquake that roughed up a nuclear power plant last week has Japan once again debating nuclear safety. The ground shook with unanticipated fury, prompting some seismologists and citizens' groups to claim that many, if not most, of Japan's 55 operating nuclear power plants are disasters waiting to happen. Structural engineers defend current design practices, noting that the main buildings of the nuclear plant, 16 kilometers from the epicenter, were not damaged. But they agree that research is needed to clarify how buildings respond to earthquake forces.

The magnitude-6.6 Niigata Prefecture Chuetsu-Oki Earthquake struck just offshore beneath the Sea of Japan about 455 kilometers northwest of Tokyo on 16 July, killing 10, injuring 1800, and leaving more than 10,000 homeless. The damage—largely confined to older wooden structures known to be vulnerable to earthquakes—would be unremarkable if it did not extend to the Kashiwazaki-Kariwa Nuclear Power Plant.

Safety mechanisms automatically shut down the operating reactors, and the reactor buildings appear to have been undamaged. But plant owner Tokyo Electric Power Co. (TEPCO) has detailed a catalog of woes, including broken piping, buckled pavement, a fire that engulfed a transformer, and leaks of trace amounts of radiation.

Most alarming to experts is that the impact on the nuclear plant may have been greater than what it was nominally designed to withstand. It was once thought that the forces imposed on a structure vary more or less linearly with an earthquake's magnitude and distance from the epicenter. But evidence has accumulated that accelerations can be higher than expected because of local geological conditions. According to data released by TEPCO, designers expected peak ground accelerations of about 270 galileo (gravity's acceleration is 980 galileo); last week, accelerations at the base of one of the reactor buildings hit 680 galileo.

"This clearly shows the insufficiency of the old guidelines for power plants," says Katsuhiko Ishibashi, a seismologist at Kobe University. Guidelines issued last September, although an improvement, do not go far enough in basing design loads on ground accelerations, he says.

Still, the relation between ground accelerations and the loads imposed on buildings "is not fully understood," says Toshimi Kabeyasawa, a structural engineer at the University of Tokyo's Earthquake Research Institute. He notes that during a 1993 earthquake that struck Japan's Hokkaido Island, instruments recorded ground accelerations exceeding the force of gravity, or at least three times the loads that buildings would have been designed to withstand under the latest code. But there was very little damage to structures.

The earthquake design load, defined as a percentage of a building's weight applied horizontally, has not changed significantly since it was set after the 1923 quake that destroyed Tokyo, says Shunsuke Otani, a ▶

ECOLOGY

Aspens Return to Yellowstone, With Help From Some Wolves

To grow a healthy stand of aspen trees, you need a pack of wolves. That's the conclusion of two researchers who have been studying aspens (*Populus tremuloides*) in Yellowstone National Park. The trees, which are long-lived clones that endure for centuries and possibly millennia, had not regenerated in the park for more than a half-century but are now returning in some areas. Their recovery, the researchers say, is not simply because the wolves are hunting the aspens' archenemy, the elk (*Cervus elaphus*); it's also because the wolves have reintroduced the fear factor, making the elk too nervous to linger in an aspen grove and eat. The study adds to other research linking the 1995 return of the park's key predator, *Canis lupus*, to a more biologically diverse and healthier ecosystem. It also lends strength to the notion that the loss of top carnivores leads to degraded environments overall.

"This is exciting because it lends support to a prediction made a decade ago that the aspen in Yellowstone would recommence growing" after the gray wolf was brought back and began to reduce the elk population, says Michael Soulé, an emeritus ecologist at the University of California, Santa Cruz. But that is only part of the story, say ecologist William Ripple and forest hydrologist Robert Beschta of Oregon State University, Corvallis. Their study, which focuses on the aspens in Yellowstone's Lamar Valley, appears in the August issue of *Biological Conservation*.

Trophic cascade. Reintroducing key predators, like the wolf in Yellowstone National Park, can reestablish healthy ecosystems.

CREDIT: PHOTOS.COM

Beschta recalls being "just aghast" when he first saw the Lamar Valley in 1995. "I used a very emphatic, unprintable word," he says. "This valley lies in what is supposed to be the crown jewel of our national parks, and it was being eroded away" as the Lamar River flooded annually, washing away soils that had taken thousands of years to accumulate. The reason: There were hardly any bushes or trees to keep the soil in place. Back at Oregon State, Beschta presented his mystery: Why were the aspens, cottonwoods, and willows in Yellowstone disappearing? Beschta lacked the time to begin such a study, so his colleague, Ripple, and a graduate student, Eric Larsen, took on the job in 1997.

By examining tree rings, Ripple and Larsen found that the park's aspens had stopped regenerating soon after the 1920s—almost exactly the same date that the U.S. government eliminated the gray

Safe enough? Earthquake forces on the Kashiwazaki-Kariwa nuclear plant were greater than nominal design loads; a transformer caught fire, but reactors were undamaged.

CREDIT: 9TH REGIONAL COAST GUARD HEADQUARTERS, KYODO/LANDOV

structural engineer at Chiba University. Nevertheless, buildings are safer thanks to a better understanding of how structures can hold up against horizontal forces. "It is not right to judge structural performance by the acceleration amplitudes of ground motion alone," Otani concludes.

The fact that buildings at Kashiwazaki-Kariwa withstood higher-than-anticipated loads indicates they were designed and constructed well, says Tomotaka Iwata, a geophysicist at Kyoto University's Disaster Prevention Research Institute. "But no one knows just how safe they are," he says. The more immediate issue, Iwata and others say, is the obvious design flaws of the damaged piping systems and secondary structures, which have put Kashiwazaki-Kariwa out of operation for at least a year.

–DENNIS NORMILE

wolf from Yellowstone. "It just boggled my mind to think that wolves could affect a river system," says Beschta. "But the trees were clearly being overbrowsed by elk. To stunt a cottonwood or aspen, all an elk has to do is browse the leader," or the plant's main shoot. Now that wolves were back in the park, Beschta and Ripple teamed up to watch this natural experiment unfold. Would the carnivores' return change the valley's vegetation?

The wolves—which kill an elk every few days—did lower the herbivore's population, as other researchers have documented. And as the elks' numbers dropped, the willows and cottonwoods began to return; the aspens, which elk find especially tasty, are taking longer. "It was only last summer when we stumbled on aspens that are over my head," says Ripple, who is 1.8 meters tall. These clones grew in the riparian parts of the Lamar Valley; aspen clones the scientists measured on nearby upland areas remain stunted and have yet to regenerate. In some places, some trees had recovered, whereas others only a few meters away had not. Why the patchy recovery, when aspens in both locations have suffered equally from overbrowsing?

"We think it's due to what we call 'the ecology of fear,' " says Ripple. "There are just some places now in the riparian zone that are too risky for the elk; a wolf may be lurking nearby." Along the river, the newly thick mix of willows, cottonwoods, and aspens may block an elk's escape route or its view, making the animal too nervous to linger over a long aspen-based lunch.

It's unclear why the aspens in the upland areas are not faring well. One reason is that "they are still getting hammered" by the elk, says Beschta.

That remains a "disappointment," says Soulé. "From a conservation perspective, aspen are a foundation species. When they recover, so do many others, including breeding songbirds."

Still, Beschta and Ripple are optimistic that the upland aspens will return, noting that the degraded Lamar River is also far from recovered. "It's likely just a matter of time," says Beschta. "The park was without wolves for 70 years, an absence that changed its ecosystem. Now, in the presence of wolves, the dynamics are changing again—in ways we can't always predict." Fear may just be the newest factor.

–VIRGINIA MORELL

Virginia Morell is a writer in Ashland, Oregon.

SCIENCESCOPE

Stem Cell Research, China Style

BEIJING—China is hoping to make up lost ground fast on stem cell research. Sources say Beijing plans to spend roughly $1 billion over 10 years to establish an international center for stem cell research and regenerative medicine.

Six U.S.–based Chinese scientists—including Xiangzhong Yang of the University of Connecticut, Storrs, and Ray Wu of Cornell University—proposed the center in a letter to the government last September. Yang argues that China can soon reach the vanguard in stem cell research because the country is not encumbered by religious concerns about cells derived from embryos. "The challenge now is to find the right people," adds Wu. An official at China's Ministry of Science and Technology declined to confirm approval of the center, which has not been made public, but he says details are being worked out and the center would be under the ministry. The center would carry out both basic and clinical research, with the ultimate goal of developing therapies, Yang envisions.

–HAO XIN

U.S.–India Deal Nears

NEW DELHI—India's time in the nuclear doghouse may soon be over. After 2 years of sometimes tortuous negotiations, India and the United States have reached agreement on a landmark nuclear pact. The proposed deal would allow India to purchase equipment and fuel for its civilian nuclear program, ending 3 decades of isolation after India exploded a nuclear device in 1974. Talks hit an impasse last spring over issues such as India's demand to reprocess spent fuel (*Science*, 25 May, p. 1112). But after negotiation last week in Washington, D.C., the two sides released a joint statement noting that "the issue" has been referred to the two governments for "final review."

Details of the agreement remain closely held, but top Indian nuclear scientists say that India has offered to set up a $100 million plant for reprocessing spent fuel provided by the United States and make the plant subject to inspections by the International Atomic Energy Agency (IAEA) to monitor the potential diversion of extracted plutonium. The deal also avoids an automatic nuclear fuel embargo if India were to conduct a future nuclear test, a previous sticking point. If the two governments sign off on the agreement, IAEA and the international Nuclear Suppliers Group will then weigh respective accords on protecting nuclear materials and commerce with India.

–PALLAVA BAGLA

AIDS RESEARCH

Promising Prevention Interventions Perform Poorly in Trials

Adding to a long list of letdowns for AIDS prevention research, two promising approaches to thwarting HIV infection have both failed in their first real-world trials. One intervention attempted to lower people's risk of becoming infected with HIV by treating their existing herpes simplex virus–2 (HSV-2) infections. Several studies have shown that HSV-2 eases entry of HIV. The second approach investigated whether using a latex diaphragm that covers the infection-vulnerable cervix could present a barrier to HIV. Researchers reported disappointing results from the trials this week at the 4th International AIDS Society Conference on HIV Pathogenesis, Treatment and Prevention in Sydney, Australia, 22 to 25 July, where they stressed that the interventions may have failed because trial participants did not use them consistently.

Risky business. Tanzanian women who participated in the HSV-2 treatment study worked in establishments such as this one that put them at high risk of HIV infection.

The HSV-2 study followed 651 Tanzanian women for up to 30 months who at the trial's start were infected with that virus but not HIV. The women worked in places like bars and guesthouses that put them at high risk of becoming infected with HIV. Other epidemiological studies have shown that HSV-2, which causes genital ulcers, triples a person's risk of becoming infected with HIV. Half the participants were assigned to take the HSV-2 drug acyclovir twice a day, whereas the other half received a placebo.

Clinical epidemiologist Deborah Watson-Jones of the London School of Hygiene and Tropical Medicine, the study's lead investigator, reported that they found no difference in HIV acquisition between the two groups. "We were very disappointed," Watson-Jones told *Science* in an interview.

Watson-Jones said many women did not take acyclovir as instructed, which may explain the dispiriting results. Researchers assessed adherence by tallying unused tablets returned at each study visit. Although no one knows precisely how many doses can be missed without undermining effectiveness, only half of the women managed to take the drug 90% of the time.

Biological analyses provide additional evidence that adherence issues clouded the results: The researchers found only a modest decrease in HSV-2 shedding in the vagina and on the cervix in women on acyclovir. "I know of no study that's been published with acyclovir at this dosing that did not have a very substantive effect on HSV-2 itself," says Lawrence Corey, an HSV-2 and HIV researcher at the University of Washington (UW), Seattle, who was not involved with the study. "We're left with [lack of] adherence being the best explanation of why you don't see much of an anti-HIV effect."

In the women who did take 90% or more of the tablets, the study found a trend toward efficacy, but it did not reach statistical significance. "The suggestion of an effect for women who had good adherence is encouraging," says Watson-Jones, but if strict adherence is so critical, "it begs the question of how feasible this is."

Two large, multicountry studies of acyclovir to prevent HIV transmission now under way should have results in the next year, says epidemiologist Connie Celum, a UW epidemiologist who is heading those trials. "I don't think at this point that the Tanzania study disproved the hypothesis that HSV-2 is an important cofactor in acquisition or transmission of HIV," says Celum. "We need to understand the issues around adherence."

The two studies involve 10,000 people in Africa, Latin America, India, and the United States. One trial will have a similar design to the Tanzania study—although it also involves men who have sex with men. The other tests whether people dually infected with HSV-2 and HIV can take acyclovir to lower the risk of transmitting the AIDS virus to their uninfected regular partners. In the first study, which is further along, Celum says they have seen about 90% adherence. She notes that they have much more frequent study visits than in the Tanzania trial, and they also distribute weekly pillboxes to help people remember to take their medication. "There may be tools that really enhance adherence," says Celum.

Adherence issues may also have undermined a trial testing whether a latex diaphragm can protect women from HIV infection. More than 5000 women participated in the trial, held in South Africa and Zimbabwe, which had a control group use condoms alone whereas the experimental group used condoms and the diaphragm. At the end of the 2-year study, HIV infection rates were about 4% per year in both groups, reported epidemiologist Nancy Padian of the University of California, San Francisco. "It's terribly disappointing not to be able to add this to our armamentarium of prevention strategies," said Padian.

Padian and co-workers, who published their results online 13 July in *The Lancet*, noted that the diaphragm group reported using it only 73% of the time; they also reported using condoms much less frequently than the control group. Although this might indicate that the diaphragm compensated for the lack of condom use and did offer some protection from HIV, Padian and co-authors stress that it's equally plausible that the control group overreported its condom use. "This is an area where doing more research on adherence is every bit as important as testing new biological prevention methods," says Padian.

In the *Lancet* report, Padian and co-authors note that of the 25 carefully done HIV-prevention trials to date, all but four have failed. She suspects that some of these apparently failed interventions may actually have had a small protective effect, which was difficult to detect. And she worries that this accumulated failure obscures the fact that many proven prevention interventions exist. "There's still quite a bit we can do with regard to HIV prevention that we know does make a difference," says Padian. "Why aren't we scaling those up?"

–JON COHEN

CREDIT: DEBORAH WATSON-JONES

CONFLICT OF INTEREST

Stung by Controversy, Biomedical Groups Urge Consistent Guidelines

Ever since a scandal broke 3 years ago over drug company consulting by scientists at the National Institutes of Health (NIH), the biomedical community has worried that Congress might clamp down not just on NIH but also on academia. That could be disastrous, say life scientists at universities—many of whom interact with industry to help turn their discoveries into products. Several groups last week suggested their own solution.

The Federation of American Societies for Experimental Biology (FASEB), the largest coalition of biomedical research scientists, called for a national guideline on disclosing and managing academic-industry financial relationships and held a half-day meeting in Washington, D.C., on 17 July to air the issues. Many speakers agreed that conflict-of-interest rules are inconsistent. But some cautioned against adopting a single policy.

Biomedical lobbyists favor taking action because they are concerned that recent controversies could undermine confidence in the research enterprise. A congressional investigation of NIH revealed that some intramural scientists failed to get NIH's approval for outside consulting work. And the recent safety-based recalls of drugs such as Vioxx, along with the failure of some authors of research papers to report financial conflicts, have raised doubts about the objectivity of scientists with industry ties. Drug discovery has gone "from one of the most revered to one of the most reviled industries," said FASEB immediate past president Leo Furcht.

There's been one change already: The House and Senate have each approved a Food and Drug Administration bill that would make it harder for those who give scientific advice to the agency to vote on drug approvals if they have any significant financial conflict. Representative Diana DeGette (D–CO) has also drafted legislation that would require researchers involved in clinical trials to report financial conflicts to the ethics boards that review such trials. Even these modest steps have made some people nervous. "Don't let the pendulum swing too far," cautioned Gail Cassell of Indianapolis, Indiana–based pharmaceutical company Eli Lilly, who fears too-strict rules would exclude "extremely knowledgeable people" as reviewers.

Academic organizations are worried that Congress will require extramural researchers to follow NIH's new ethics policy, which bans all consulting for industry and limits the amount of drug company stock that senior staff members may own. These rules wouldn't make sense for most grantees, NIH Extramural Research chief Norka Ruiz Bravo told the meeting, because grantees are not federal employees and do not get all their support from NIH. Still, she noted, Congress could decide to impose the same rules anyway.

FASEB thinks the answer is to bring more consistency to existing institutional policies, building on guidelines for clinical research that the Association of American Medical Colleges (AAMC) in Washington, D.C., issued to its members in 2001. A survey has since found much variation in responses to the guidelines, said Susan Ehringhaus of AAMC. For example, the threshold for reporting conflicts differs from university to university, and AAMC's advice to include a member of the public on a committee reviewing conflicts is often neglected. Furcht said that FASEB endorses an ongoing effort by AAMC and the Association of American Universities to clarify and strengthen the 2001 AAMC report.

Participants at the FASEB meeting were generally supportive. "As investigators, we would love to have consistency" across institutions, says David Bylund of the University of Nebraska, Omaha. But some university administrators said it would be difficult, partly because public universities have to tailor their policies to state laws. In the meantime, FASEB has unveiled an online "tool kit" to help investigators, institutions, and others navigate conflicts of interest.

–JOCELYN KAISER

Industry Support of Medical School Departments

TYPES OF FUNDING

28%	Research support
20%	Technology transfer funds
14%	Research equipment
14%	Support for students and postdocs

Ties that bind. A recent survey of medical school departments found that a significant fraction had some relationship with industry.

CREDITS (TOP TO BOTTOM): SOURCE: ERIC CAMPBELL/INSTITUTE FOR HEALTH POLICY AT MASSACHUSETTS GENERAL HOSPITAL AND HARVARD MEDICAL SCHOOL; ROBERT HOLMGREN

DAN KOSHLAND, 1920–2007

Daniel E. Koshland Jr., *Science*'s editor-in-chief from 1985 to 1995, died on 23 July, 2 days after suffering a massive stroke.

Koshland, who joined the faculty of the University of California, Berkeley, in 1965, put his stamp on a broad swath of protein chemistry. His fundamental insight that proteins change shape as they interact with other molecules—the "induced fit" theory—changed the way scientists perceived a range of processes, from the catalytic power of enzymes to the action of hormones. He published more than 400 papers, an output that continued unabated in recent years.

He also left his mark on *Science*. He overhauled the peer-review process, establishing a Board of Reviewing Editors; oversaw the internationalization of the journal with the launch of an office in Europe and news bureaus around the world; and increased the number of top-quality papers in the physical sciences. "He had an unmatched talent for recognizing quality," says Executive Editor Monica Bradford.

Don Kennedy, *Science*'s current editor-in-chief, says: "As a grateful successor, I find traces of Dan's thoughtful influence everywhere at *Science*. Dan has been my colleague in planning the Koshland Museum at the National Academy—a jewel that results from a generous gift to honor his late wife Bunny. It is difficult to lose a hero and a friend in the same person."

News of Koshland's death came as this issue of *Science* was going to press. A retrospective will be published in a forthcoming issue, and a page of personal staff remembrances is posted at www.sciencemag.org/sciext/koshland.

Delta Blues, California Style

The hub of California's freshwater system is plagued by crashing fisheries, high demand, invasive species, and pollution—and a major earthquake there could devastate the state's drinking water and agriculture

BYRON, CALIFORNIA—In a makeshift laboratory that was once a refrigerated shipping container, Joan Lindberg, a research biologist at the University of California (UC), Davis, shines a small flashlight into a 2-meter-diameter water tank. Two-centimeter pencil-thin fish known as delta smelt dart away from the light. These small fish, native to the Sacramento–San Joaquin River Delta that flows just beyond these tanks, are bred and farmed out to fisheries biologists throughout the region who are racing to understand their life cycle, feeding habits, and vulnerabilities. It's a race that's now in full sprint, as the population of delta smelt in their native habitat is in free fall.

Historically, millions of the fish swam this delta, which sits just east of San Francisco Bay and is the largest estuary on the West Coast of the United States. But a survey of juvenile smelt conducted in June found only 37, down from 884 found a year earlier. More than 700 smelt were killed this spring by a series of massive pumps nearby that suck a river's worth of water out of the delta and send it south to Los Angeles and San Diego. But the water exports are only one of the smelts' problems, with pollution and invasive species also topping the list of concerns. Now, with the delta smelt teetering on the edge of extinction, Lindberg and her colleagues are looking into ramping up their fish-breeding efforts to try to prevent the fish from going extinct. "We're doing what we feel is prudent to save the wild fish," Lindberg says.

More than a kilometer up the road, a second set of massive pumps sucks out another river's worth of water and sends it primarily to farmers in California's Central Valley. Here, as technicians survey fish caught in a mesh bucket designed to pull fish from the water before it's sent to the pumps, they look intently for smelt and other endangered fish. Today, no delta smelt are among the dozens of striped bass, catfish, and other fry caught. But one was snagged just days earlier, which was enough to send shudders through this farming community. "What comes out of that bucket can determine the economic fate of California's cities and farms," says Jeffrey McCracken, a spokesperson for the U.S. Bureau of Reclamation (BOR), the federal organization that runs the Central Valley Project pumps.

The comment may sound hyperbolic, but it's not. Twenty-five million Californians, nearly two out of every three, depend on the delta for at least some portion of their drinking water. Central Valley farmers, the heart of America's vegetable, fruit, and nut production, are even more dependent, as the delta provides irrigation for about 1 million hectares of farmland. And although water from the delta has flowed to these users for

Sunken landscape. Drained fields have subsided well below the waterways, requiring high levees to keep the water at bay.

CREDIT: CALIFORNIA DEPARTMENT OF WATER RESOURCES/PAUL HAMES

decades, that might not always be the case. In May, citing the U.S. Endangered Species Act and the hundreds of delta smelt killed at the State Water Project pumping facility nearby, a California Superior Court judge ordered the pumps shut down for 10 days, a rare move that fired a shot across the bow of water managers statewide. "This is a very important wake-up call for California," says Lester Snow, head of California's Department of Water Resources.

But the smelt is only the delta's most immediate concern. Several other fish species native to the delta are also in steep decline, also battered by loss of habitat, pollution, and competition from hundreds of invasive species. Rising sea levels prompted by climate change threaten to push salt water from San Francisco Bay much farther inland, possibly even overwhelming the southern delta region where fresh water is drawn for people and irrigation. Finally, the delta is home to a labyrinth of 1770 kilometers of earthen levees designed to channel the delta's water on its way to the bay. Those levees, some 130 years old, sit near six seismic faults that crisscross the region, and it's widely feared that a major quake could produce catastrophic levee failures that would wipe out water supplies for tens of millions of people (see sidebar, p. 444).

"The delta is a mess," says Phillip Isenberg, who chairs the Delta Vision Blue Ribbon Task Force appointed by California Governor Arnold Schwarzenegger last year to come up with potential solutions for the delta. At a congressional field hearing on the delta in Vallejo, California, earlier this month virtually all the participants agreed with Isenberg that the Bay Delta is in crisis and the way it is currently managed is unsustainable. Now, Isenberg says, Californians must make some hard choices concerning competing interests for the water, municipalities, farms, and the environment being among them. "If we do not make these difficult choices, then extinction—whether of a species or a way of life—may be the water policy of California," said Isenberg in written testimony.

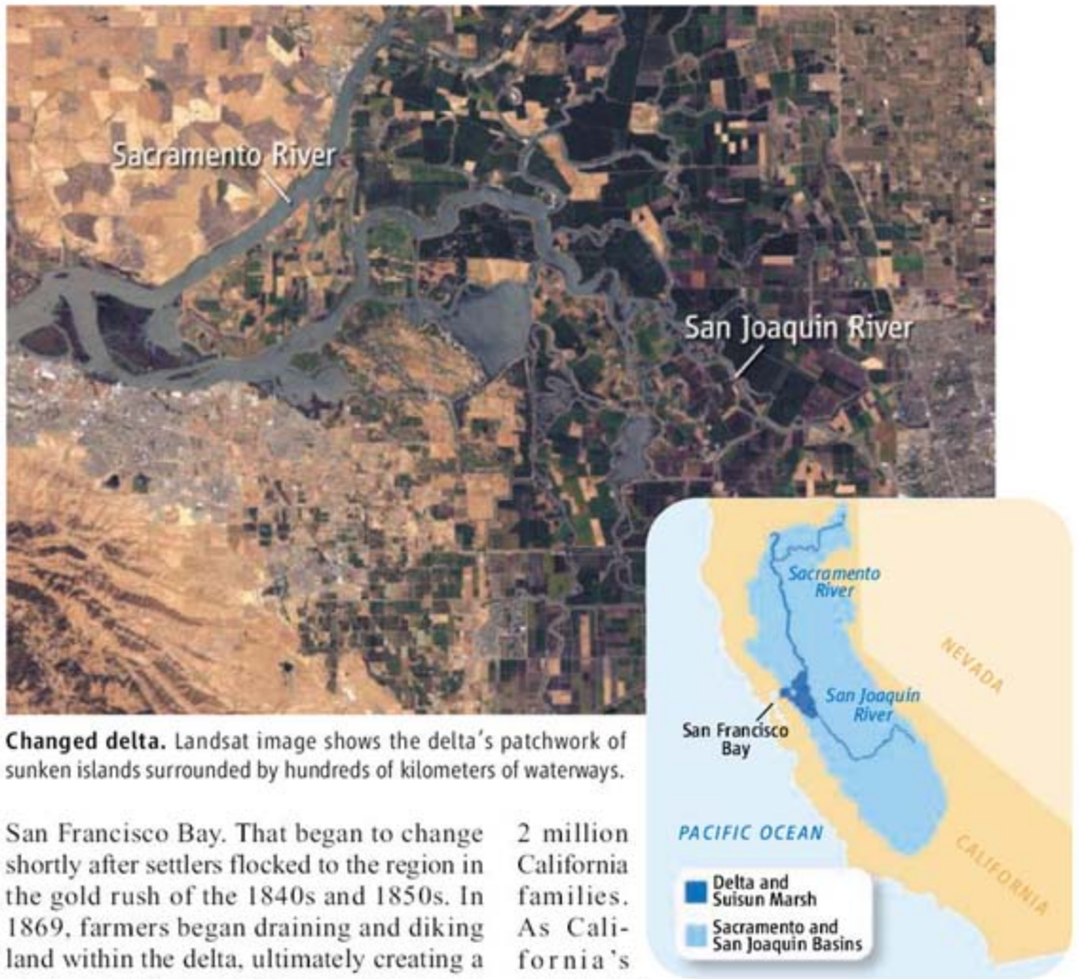

Changed delta. Landsat image shows the delta's patchwork of sunken islands surrounded by hundreds of kilometers of waterways.

Changing tides and rivers

It's a problem that's been brewing for a long time. The Sacramento–San Joaquin River Delta is the hub of California's water system. It's an expansive inland river delta comprising 300,000 hectares of land interlaced with hundreds of kilometers of waterways. Historically, those waterways shifted course seasonally as water draining from the northern Sierra flowed down into neighboring San Francisco Bay. That began to change shortly after settlers flocked to the region in the gold rush of the 1840s and 1850s. In 1869, farmers began draining and diking land within the delta, ultimately creating a patchwork of some 65 "islands." However, unlike natural islands that rise above the surrounding water, the delta's islands are actually vast bowls ringed by levees to keep the water at bay. Over time, this challenge of holding back the tidal waters has steadily increased, as exposure of the former mud flats to the air has oxidized and compacted the peat-rich soils, causing central farmlands within the delta to subside a full 6 to 8 meters below sea level. Delta farmers have responded by building their levees higher, fully engineering some of the breakwaters but simply creating giant mounds of dirt with most of the others.

The levees were only the first of major changes to the delta. With the levees in place, farmers within the delta itself began siphoning off roughly 1 million acre-feet (1.2 billion cubic meters) of water per year, enough to provide the yearly water supply for roughly 2 million California families. As California's population boomed in the early 20th century, other users eyed the delta's abundant water. Beginning in 1951, a series of five massive pumps at the C. W. Jones Pumping Plant began taking out water for Central Valley farmers and nearby communities. Early on, the Central Valley Project typically pulled out around 2 million acre-feet of water per year. But over time, that number has risen to around 3.3 million acre-feet (4 billion cubic meters) of water per year. Meanwhile, withdrawals by the State Water Project, which sends water to southern California, have risen from about 1 million acre-feet (1.2 billion cubic meters) per year in 1968 to 4.2 million acre-feet (5.2 billion cubic meters) per year today. In a dry year, those diversions can amount to about one-third of all the water that would normally flow through the delta into San Francisco Bay. The draw from the pumps is often so great that some river channels through the delta actually flow backward, upstream toward the pumps at a pace too brisk for the smelt and other weak swimmers to escape.

Barely hanging on. The delta smelt, once prolific, is now endangered.

Not everything in the delta is on its way out. More than 200 invasive species now make the delta the most invaded estuary in the world. The invaders, including everything from striped bass to a fast-growing

CREDITS (TOP TO BOTTOM): ROBERT SIMMON/NASA; B. MOOSE PETERSON/U.S. FISH AND WILDLIFE SERVICE

aquatic weed known as *Egeria*, have markedly changed the delta's habitat. Urban development is also on the rise and is expected to add another 130,000 homes in the region over the next decade and more than double the region's population to 7.7 million by 2050. And pollution from urban runoff, sewage, and agricultural chemicals has also been growing steadily.

That combination has challenged fish populations for decades. Of the delta's 29 native fish species, 12 either have been eliminated entirely or are currently threatened with extinction. Today, the delta smelt's plight is forcing the issue, in part because it is seen as an indicator species for the health of the delta in general, much as the northern spotted owl's numbers served as a proxy for the health of old-growth forests in the 1980s and 1990s. But an initial round of crises took shape in the early 1990s, when Chinook salmon and other fish species were found to be in sharp decline. Litigation by environmental groups and requirements under the Endangered Species Act triggered shutdowns of the water project pumps, water supply cutbacks, and widespread complaints that the federal and state agencies were often working at cross purposes with one another.

In hopes of finding a way out, federal and state leaders forged a collaborative research and decision-making process known as CALFED to try to create a common vision for improving the delta. The effort was widely heralded for bringing more than 100 local, state, and federal government agencies that have jurisdiction over some aspect of the delta and its wildlife together with stakeholder groups such as farmers, industry representatives, and environmentalists. But because those stakeholders were unable to agree on major changes to the delta, CALFED leaders focused their efforts on creating a robust science program for studying the delta, initiating numerous habitat restoration projects, and developing a market-based system to pay farmers upstream from the delta to forgo water diversions in order to keep the water in stream for fish.

Although CALFED's science program in particular has largely been viewed as successful in creating a vast knowledge base on which to base ecological decisions, recently the collaborative process has begun breaking down. Ultimately, the delta's problems stem from the fact that there isn't enough water to satisfy all the competing users, Isenberg

Shaky defenses. A break in a levee near Holt in June 2004 sent water pouring into fields and workers scrambling to shore up nearby levees.

FROM CRISIS TO CATASTROPHE

If and when the earth begins to shake along one of six major seismic faults in and around the Sacramento–San Joaquin River Delta, the fate of the small, threatened delta smelt will no longer be the region's biggest problem. The delta is laced with more than 1700 kilometers of earthen levees, many of which would likely breach in a major flood or quake. The results could make the devastation wreaked by Hurricane Katrina look tame by comparison. The system of delta levees, says Jeffrey Mount, a geologist at the University of California, Davis, "is in much worse shape than anybody thought."

In 2005, Mount and his Davis colleague Robert Twiss reported that over the next 50 years there is roughly a two in three chance that a combination of seismic activity and increased flooding from climate change would produce a catastrophic failure of multiple levees in the delta. Those levees surround farmland where the earth has subsided up to 8 meters in many cases. If the levees collapsed due to a quake during a period of low freshwater flows through the delta, water to fill the 2.5 billion cubic meters of space in the island basins would be pulled in from San Francisco Bay and Suisun Marsh at the mouth of the delta, drastically altering the freshwater habitats and likely forcing the shutdown of massive pumps that carry delta water to Central Valley farmers and millions of residents in southern California. According to a new analysis by the California Department of Water Resources, repairs could top $30 billion and take from 1.4 to 6.4 years depending on the extent of the damage. Indirect costs to communities that would lose access to water from the delta could exceed $50 billion.

Last year, California voters passed a bond measure making roughly $1 billion available for delta levee repairs and improvements. Mount calls this "a nice start" that should help bring some of the older levees up to the most basic federal guidelines but adds, "they are sitting on poor foundations and will be unstable in an earthquake." The truth is, Mount says, the economic fate of millions of Californians currently depends on a maze of dirt piles that could easily give way with a little shove from nature. **–R.F.S.**

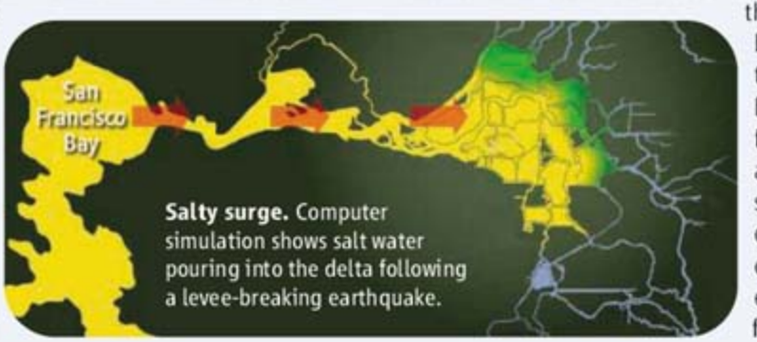

Salty surge. Computer simulation shows salt water pouring into the delta following a levee-breaking earthquake.

CREDITS (TOP TO BOTTOM): AP; CALIFORNIA DEPARTMENT OF WATER RESOURCES

says. And CALFED lacked the political clout to choose winners and losers. "I think it has done all it can do that isn't controversial," says Lois Wolk, a Democratic California State Assembly member from the delta region west of Sacramento who has closely followed delta issues.

A return to the courts

About the only thing that isn't controversial these days is the fact that delta smelt's numbers have plummeted, along with those of the area's other pelagic fish, which spend at least part of their life cycle in the ocean or in brackish estuaries. But just what is causing the crash isn't as obvious. According to the report released in March by a collection of state and federal water agencies known as the Interagency Ecological Program (IEP), the culprits likely include impacts from pollution, invasive species, and water exports. Among the specific concerns, the IEP reported that agricultural pesticides known as pyrethroids have been shown to be acutely toxic to aquatic life, and their use has more than doubled to over 115,000 kilograms per year in the delta, in part to combat noxious aquatic weeds. Of the exotics, one of the most worrisome has been the Asian clam, a filter feeder that consumes phytoplankton. Those phytoplankton are the primary food source for zooplankton, which in turn are a primary food source for the delta smelt.

With the delta smelt's numbers in steep decline, and CALFED's inability to force major changes, environmental groups have returned to the courts. "Litigation has ousted collaboration as the dominant means of solving water issues," says David Nawi, an attorney with Environmental Mediation in Sacramento, California. Last year, a trio of environmental groups challenged the U.S. Fish and Wildlife Service's (USFWS's) 2004 biological opinion, which outlines the agency's strategy for protecting the species. Among other things, they argued that the agency failed to cite the best available science by not using the latest surveys of smelt abundance and not taking climate change into account. On 25 May, a federal judge agreed, tossing out the old biological opinion and forcing a rewrite, which is expected next year. Just what remedies the judge will order in the meantime is scheduled to be decided next month, and court cases on other threatened species and challenges to delta-area development also remain in the works.

According to attorney William Stelle, a veteran of several endangered species battles who is now working on Bay Delta conservation, the recent court decisions are likely to be the beginning of a very eventful year that could decide the fate of the delta for decades to come. In November, Isenberg's Delta Vision task force is scheduled to deliver its recommendations for the region. Another set of stakeholders, meanwhile, is working to create the Bay Delta Conservation Plan to address water-quality and habitat-restoration needs for the ecosystem. Yet another group of academic and nonprofit policy researchers chimed in earlier this year with a report that outlined five viable ways forward for the delta, including managing the estuary for environmental rehabilitation and "armoring" the levees around selected islands to ensure that the fresh water continues to flow through the delta in the event other levees give way.

The list of recommendations will continue next year, when USFWS and BOR are expected to release their revised management plans for the delta smelt, which are likely to govern operations for the next 5 years. And finally, state officials announced this month that they intend to ask voters for a new $5.9 billion bond measure to build two new dams and begin detailed studies of a canal that would remove irrigation and municipal water from higher up the delta and channel it directly to the south delta pumps to avoid sucking fish. California voters overwhelmingly rejected a similar proposal in 1982. But Schwarzenegger recently voiced his support for the plan.

What's not clear yet is how these court decisions, ballot measures, and regional plans are likely to mesh, and whether they'll come in time to save the delta smelt. "The delta smelt will be very lucky if it makes it," says Peter Moyle, a fisheries biologist at UC Davis.

Perhaps, then, it's little surprise that interest in UC Davis's smelt-breeding program is taking off. "It's not something any fish biologist wants to do," Lindberg says. "It would be preferable to restore the natural healthy delta ecosystem. But if the population is nearing extinction, then people are willing to consider the possibility of going down that road."

–ROBERT F. SERVICE

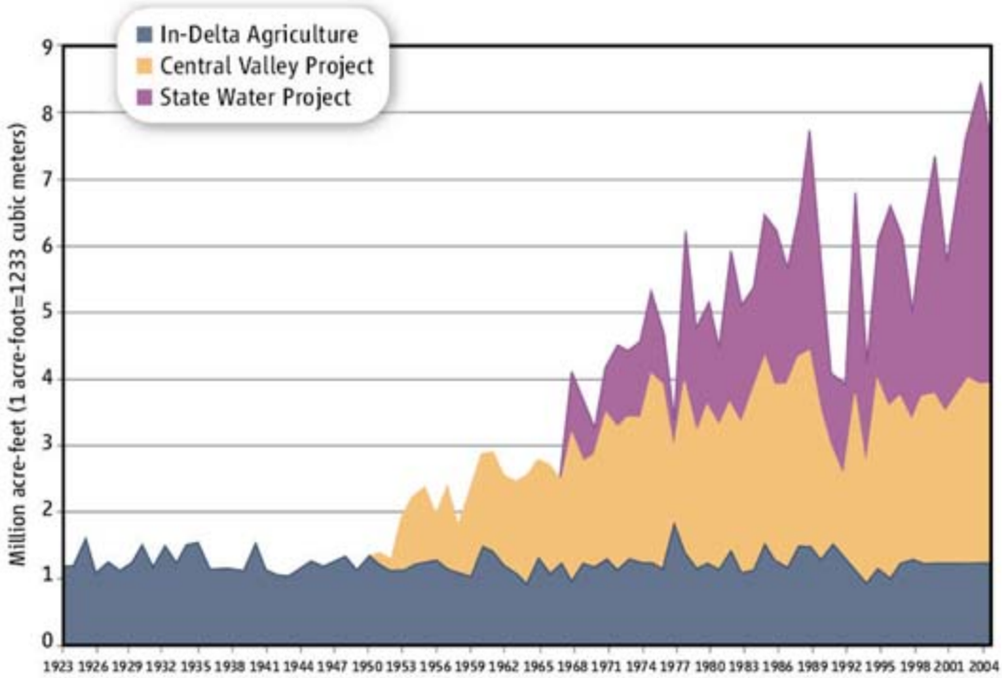

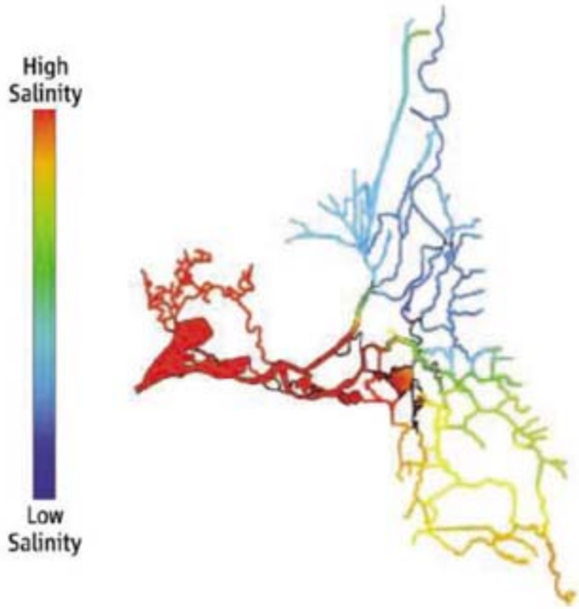

Increased demands. Exports of water outside the delta from two pumping stations (*yellow and purple*) have soared. Low flows into the delta in August 1992 led to saltwater encroachment (*right*).

CREDITS (TOP TO BOTTOM): CALIFORNIA DEPARTMENT OF WATER RESOURCES

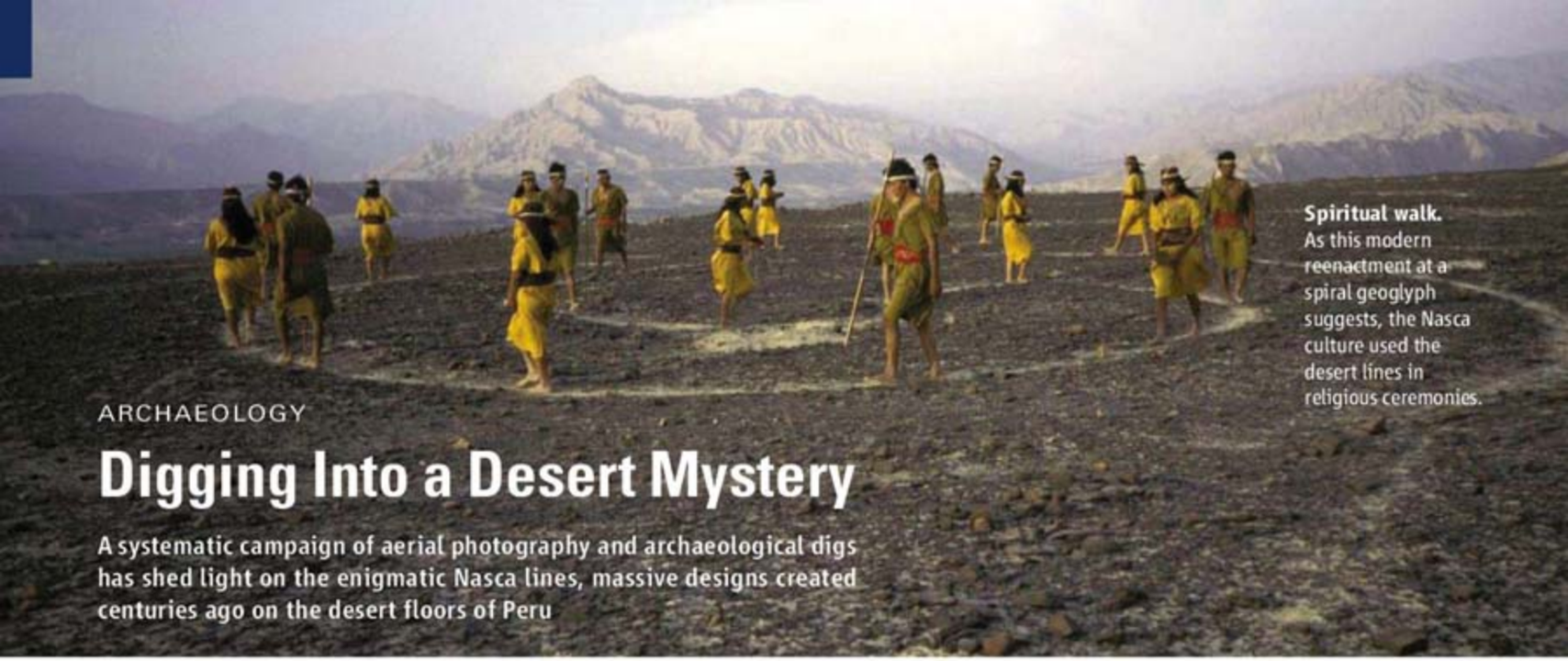

Spiritual walk. As this modern reenactment at a spiral geoglyph suggests, the Nasca culture used the desert lines in religious ceremonies.

ARCHAEOLOGY

Digging Into a Desert Mystery

A systematic campaign of aerial photography and archaeological digs has shed light on the enigmatic Nasca lines, massive designs created centuries ago on the desert floors of Peru

For almost a century, scientists have struggled to explain one of the best known and least understood ceremonial sites in the world. From 500 B.C.E. until approximately 650 C.E., the Nasca and Palpa valleys, 400 kilometers south of Lima, Peru, were home to a sophisticated culture that created massive designs by rearranging stones on the floor of the Atacama Desert. Ranging from spectacular animal and humanoid figures to trapezoids 2 kilometers across, the hundreds of so-called geoglyphs are easily viewed from the air. Some even suggested early on that the locals must have invented hot-air ballooning in order to create the intricate designs. And theories about their purpose have ranged from the somewhat scientific (astronomical charts, water maps) to the mystical (runways for alien spaceships).

Now, a decade-long effort by an international team of researchers is providing some answers. For archaeologists, the glyphs have been forbidding. So large they're nearly geographic features, the designs don't lend themselves to traditional archaeological methods. "Archaeologists are used to going somewhere, digging, and solving a specific historical problem," says Markus Reindel of the German Archaeological Institute (DAI), the project's co-director. "But the geoglyphs are huge objects. They're fascinating, but too much." To get a grip on them, the team employed a battery of high-tech equipment including laser scanners, carbon-dating technology, and even a 2-meter-long robotic helicopter.

At a meeting last month in Bonn, Germany, Reindel, DAI colleagues, and researchers from Peru, Germany, Switzerland, Austria, and elsewhere presented the results of their investigations. The geoglyphs, they reported, unquestionably served a ceremonial function; they were not simply massive pictures on the desert floor. The team members also revealed unprecedented insights into the culture that created the famous Nasca lines—and the reason for its eventual decline. "It's an absolutely first-rate project. They're taking a smart approach to the lines," says University of California, Santa Barbara, anthropologist Katharina Schreiber. "It's the first time a section of the Nasca pampa has been subjected to that intensity of study."

Beyond the Chariots of the Gods

Although the Atacama region is extremely dry, with less than 0.5 millimeter of rainfall annually, between 1800 B.C.E. and 600 C.E., a progression of cultures culminating in the Nasca harnessed what little water there was to create agrarian societies. And beginning about 500 B.C.E., the region's people turned their artistic attention to the stony ground, which has a carpet of dark volcanic rocks atop a layer of lighter sand. Moving the top layer of rocks aside created high-contrast designs. It would have been a simple, if labor-intensive, project.

And the large designs wouldn't have required balloons or extraterrestrial assistance. Scientists over the years have come to the conclusion that a combination of tall posts, upright stones driven into the ground at regular intervals, string, and stakes were probably used to plot rough lines across the desert. The DAI team subscribes to this theory. "Making a geoglyph is easier than it seems," says DAI archaeologist Karsten Lambers.

The Nasca lines first attracted scrutiny from archaeologists in the late 1920s. About a decade later, American Paul Kosok began cataloging the lines while studying ancient irrigation systems. After his death, his German assistant, Maria Reiche, emerged as a charismatic advocate of the theory that the lines were ancient observatories that helped track the sun and stars.

The lines' fame brings with it unusual pressures. Call it the "Erich von Däniken effect," for the Swiss author of the 1968 book *Chariots of the Gods?* who made the lines a centerpiece of his theory that aliens influenced ancient cultures. Von Däniken's book made the Peruvian coast a focus of New Age theorists everywhere. "No archaeologist wanted to follow von Däniken. They'd just get their fingers burned," says Lambers. "When you work on the lines, everybody's watching you, everybody has their opinions."

Peruvian officials and academics have responded by cracking down on research in the area. "Anyone looking in or near the area of the Nasca lines is under extra scrutiny. They're very self-conscious about it," says University of Massachusetts, Amherst, archaeologist Donald Proulx. Archaeologists applying for permits to work in the country must go through a lengthy and expensive review of their credentials and publications.

Beginning in 1997, with funding from the Swiss-Liechtenstein Foundation for Archaeological Research Abroad, a team of archaeologists led by Reindel (then at the University of Bonn) and Johny Isla of the Andean Institute of Archaeological Research in Lima, Peru, overcame the red tape to begin a multipronged attempt to unravel the Nasca's secrets. "It was perfect for Germans; we really like to document things before we analyze. Data collection plays a big role for us," says Reindel.

Working in the Palpa Valley, which is not as well-documented as the Nasca Valley just to the south, the researchers set out to create a detailed survey of everything from settlement sites to geoglyphs. In addition to traditional ground surveys and test excavations, they used a small plane to take high-resolution black-and-white photographs of the designs

CREDIT: DAI

that cover the valley floor—photos good enough to make out individual stones pushed aside to make the geoglyphs.

The project's potential as a test bed for technology attracted the attention of the German Federal Ministry of Education and Research, which began funding the effort in 2002. Soon archaeologists, engineers, computer-imaging experts, and physicists from Germany, Peru, Austria, and Switzerland were visiting the Palpa Valley to test new methods on the desert plain. Experiments included attempts to date the stones based on their underside's last exposure to light and creating detailed aerial maps of specific sites using the robotic helicopter. All the equipment was a challenge to get through Peruvian customs, but the helicopter almost didn't make it at all—Lambers had to get permission from the country's suspicious aviation authority to bring the drone into Peru.

Working with Armin Gruen and his group of photogrammetrists from the Swiss Federal Institute of Technology (ETH) in Zurich, Reindel and Lambers turned the black-and-white photos into a three-dimensional digital model of the valley's topography. Lambers and ETH photogrammetrist Martin Sauerbier then used geographic information systems (GIS) to add layers of other information on elevation and topography to the digital model of the geoglyphs. "With the GIS model, we can calculate visibility index for every point in the terrain," Lambers says.

Far from the glyphs being invisible or incomprehensible to people on the ground, the model suggests that activity on the lines—people walking or conducting ceremonies, for instance—would have been visible far and wide. Spectators standing on neighboring glyphs or at nearby sites would have been able to observe or perhaps participate in valley-wide ceremonies.

Combining the digital efforts with traditional archaeological methods revealed even more. Excavations uncovered platforms and small buildings situated at the ends of large linear geoglyphs. Holes up to 60 centimeters deep situated near the platforms suggest masts or poles several meters tall that served as orientation points in the desert; other, shallower holes might have supported canopylike roofs. Broken pottery and ample evidence of offerings and sacrifices—including guinea pigs, corn, crayfish, and *Spondylus princeps* seashells from thousands of kilometers away—indicate that the sites had a religious function. "It's very clear; the geoglyphs were ritual terrain for water and fertility ceremonies," says Reindel. "They were locations, not pictures."

CREDIT: DAI

A royal surprise

The scientific team also devoted significant attention to the people who created the geoglyphs. Researchers had long assumed that Nasca culture lacked a strict hierarchy, because most of the graves found were fairly modest. Beginning in 1998, however, Reindel and Isla uncovered a royal necropolis while excavating a site called La Muña. Although long since looted, the elaborate grave chambers were as much as 6 meters deep and once filled with pottery and other grave goods. The necropolis was strong evidence that the Nasca had a much more organized class system than previously thought.

Lined up. In addition to massive geometric designs (*above*), Nasca geoglyphs often depicted animals such as birds and monkeys.

The comprehensive look at the Palpa Valley sites—more than 650 settlements were documented—revealed clues to another mystery: What happened to the complex culture that created the lines? Research by Bernard Eitel, a geographer at the University of Heidelberg in Germany, suggests it may have been doomed from the start. About 500 B.C.E., the region's climate began to grow steadily drier. Whereas pre-Nasca peoples lived in the valley basins, grazing their animals on grass and taking water from rivers that flowed down from the highlands, the dawn of the Nasca period around 200 C.E. marked a shift inland. As rivers dried up, the grasslands disappeared, and the desert crept east, people moved toward the mountains, following scarce freshwater supplies. "They moved [farther inland] little by little, because year by year water was difficult to find," Isla says.

In the end, the region's persistent droughts proved to be too much. Carbon dating shows that older settlements were regularly abandoned for new ones in the highlands. By 650 C.E., the culture had essentially dried up.

The German researchers plan to begin publishing their data next year, and they hope to conduct further studies on sites in the highlands to see what interactions the Nasca might have had with cultures on the other side of the Andes. Other archaeologists are already praising the project as a resource. The extensive documentation also "preserves the geoglyphs for future generations of scholars," says Kevin Vaughn of Purdue University in West Lafayette, Indiana.

Preservation is badly needed. As the region's population grows, the centuries-old glyphs are under threat. In 1994, the United Nations Educational, Scientific and Cultural Organization chose the lines as a World Heritage site deserving protection. Modern copies of the ancient glyphs also contaminate the region more and more: Stones that were so easy for the ancients to rearrange are no less tempting for the area's current residents. "People go up to the hills and draw their names, or the name of their girlfriend," Lambers says. Local businesses and even political parties have begun using the slopes as free billboards. Not quite as mysterious as the Nasca lines, but perhaps less likely to be mistaken for alien runways in the future.

–ANDREW CURRY

Andrew Curry is a freelance writer in Berlin.

GEOLOGY

Deciphering Ancient Weather Reports, Drip by Drip

Stalagmites and stalactites are an increasingly valuable trove of high-resolution information on prehistoric climates

When Dominik Fleitmann dissected a few stalagmites from Oman and Yemen, he was in for a surprise. The University of Bern paleoclimatologist had been examining the cave growths for clues to the Persian Gulf's climate over the past 10,000 years. Instead of confirming a hypothesis that monsoon rains abruptly weakened about 5000 years ago, Fleitmann ruled out such a sudden change, observing that monsoons waxed and waned in intensity over decades. The findings, which appeared in *Quaternary Science Reviews* earlier this year (Vol. 26, pp. 170–188), implicate a temperamental climate in the rise and fall of ancient kingdoms in the Gulf whose survival depended on adequate water resources, Fleitmann says.

Scientists have long examined ice cores and marine sediments for clues to past climates. But such records can't reveal much about continental interiors, apart from Antarctica's, and resolution is blurry for changes that occur rapidly, over decades.

Stalagmites and stalactites—deposits of calcium carbonate known as speleothems that form in caves—are beginning to fill crucial gaps. Speleothems are all the rage because of their dazzling precision: Error bars range from a mere year to decades. "Ice cores and cave formations complement each other nicely. [Just as] ice cores are frozen water, I like to see our stalagmites as petrified water," says Fleitmann.

"Speleothems are producing outstanding insights," adds Richard Alley, a glaciologist at Pennsylvania State University in State College.

Speleothems form in limestone caverns over millennia as water seeps through soil and, upon infiltrating a cave, deposits minerals on the ceiling or floor. Since the late 1980s, researchers have dated speleothems using thermal ionization mass spectrometry, which measures the ratio of uranium-234 to thorium-230 and can pinpoint age as far back as 600,000 years, deep into the Pleistocene epoch. Scientists may soon be able to reach even deeper into antiquity thanks to a method for measuring uranium's decay into lead. This dating technique, which several teams are now refining, could extend speleothem climate records by several million years—far beyond ice core climate reconstructions, says Giovanni Zanchetta, a paleoclimatologist at the University of Pisa, Italy. Meanwhile, measuring the ratio of oxygen-18 to oxygen-16 in calcite tells the climate story, as temperature and rainfall control the ratio.

Illustrating the power of speleothems to unravel intricate climate patterns, geologist Xianfeng Wang and colleagues at the University of Minnesota, Twin Cities, and the Instituto do Carste, Brazil, have strong evidence that abrupt global climate shifts are instigated by conditions in the high latitudes. Speleothems from China and Brazil reveal a tight coupling between rainfall patterns in the Northern and Southern hemispheres over the past 90,000 years. When China was wet, Brazil was dry, and vice versa. In a monograph in press at the American Geophysical Union, Wang argues that rainfall patterns on either side of the equator are linked to North Atlantic sea ice, the extent of which is influenced by alterations in the "conveyor belt" that circulates water from the mid- to North Atlantic. "It is wonderful work," says Alley.

Discerning temperature and precipitation patterns over decades could give insights into droughts and floods—phenomena with huge societal impacts. One high-profile event occurred about 9400 years ago, when a natural dam between the Mediterranean Sea and Black Sea broke, creating the Dardanelles. Some scientists contend that precipitous flooding of settlements on the Black Sea coast gave rise to the legend of Noah's flood.

Fleitmann's group will seek to shed new light on the legend by determining whether the flooding was gradual or sudden, according to how quickly oxygen isotope ratios change in a 45,000-year-old stalagmite from the Black Sea coast in Turkey. The scientists will look for altered oxygen ratios as rain originating from a freshwater Black Sea changes to rain from a Black Sea turned brackish after infusion of salt water from the Mediterranean Sea. Analyses of sea sediments have not settled this question. With the stalagmite, Fleitmann says, "we may achieve a much better temporal resolution" that could unmask a sudden shift in oxygen isotopes.

Extracting the fine-grain details of past climates from stalagmites should also help inform future climate scenarios. "Most of us don't care about climate change that occurs over thousands or more years," says Christopher Poulson, a climate modeler at the University of Michigan, Ann Arbor. "We won't be around, our kids and grandkids won't be around, but for abrupt climate change this is a time scale that matters." Scientists hoping to divine how a warming world will look in the coming decades might wish to go spelunking for answers.

–JACOPO PASOTTI

Jacopo Pasotti is a writer in Basel, Switzerland.

Spelunking for clues. Speleothems from this cave in northern Oman revealed a dynamic monsoon 5000 years ago, says Dominik Fleitmann (*inset*, emerging from a cave in Turkey).

CREDITS (TOP TO BOTTOM): MARC LUETSCHER; REMY WENGER

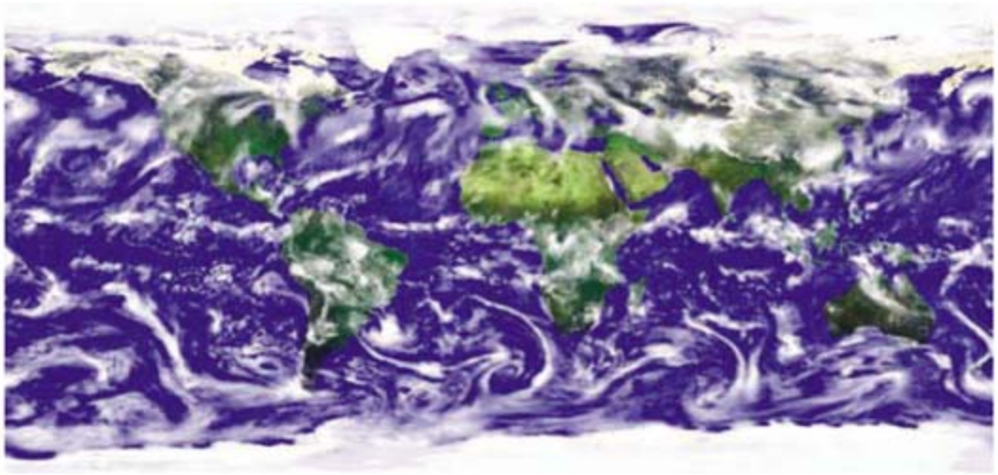

CREDIT: BRIAN F. FARRELL, PETROS J. IOANNOU

Jet squiggles. Rivers of air snaking across mid-latitudes arise—somehow—as a result of turbulence.

METEOROLOGY

Order From Chaos, Power From Dissipation in Planetary Flows

Meteorologists have long believed that almost every narrow, high-speed fluid flow in nature—from Earth's writhing jet streams to Jupiter's banded winds—arises from turbulent churnings. Now comes the hard part: How could that possibly work?

Jets are everywhere. The jet stream brings tornado-laden storms to the U.S. Midwest. A stratospheric jet keeps the ozone hole penned in place over the Antarctic. Another ring of wind in the north wobbles to bring Arctic air deep into North America. But jets "have been neglected for some years, even though they're the most energetic features in the atmosphere," says geophysical fluid dynamicist Peter Rhines of the University of Washington, Seattle. Lately, however, theorists have redoubled their efforts to explain why jets exist. By everyday thinking, they shouldn't.

In the latest theoretical assault on the jet problem, two researchers proposed at a recent meeting* that small-scale turbulence can organize and power up a large-scale jet by sending energy across the chasm between small and large in a single bound. The new approach makes testable predictions about all sorts of jets, from the curiously reversing stratospheric jet over Earth's equator to the 11-year cycle of the sun's circulation. Not all researchers agree that the analysis is as comprehensive as claimed, but "this is a good step," says meteorologist Walter Robinson of the University of Illinois, Urbana-Champaign, "if not the final answer."

Meteorologists have long been able to describe, if not deeply understand, how jets form. The narrow river of wind blowing west to east over Earth's mid-latitudes, for example, draws energy from the warm-to-cold temperature gradient running up from the tropics toward the pole. You might expect the atmosphere's inevitable turbulence to buffet the jet out of existence, but instead—illustrating what Michael McIntyre of the University of Cambridge, U.K., has described as "the exquisitely surprising character" of fluid motion on a rotating sphere—it actually feeds the jet its life-sustaining energy.

However, theorists had trouble explaining just how the orderliness of a narrow, high-speed jet arises from the chaos of turbulence. Lately, some researchers, including Rhines, have come to favor a "cascade" concept for jet formation (*Science*, 26 January, p. 467). In this approach, atmospheric momentum cascades upward from the small scale of individual storms to larger and larger features until the energy is embodied in eddies large enough to power the 1000-kilometer coils of the wriggling mid-latitude jet.

Cascading up to jets does not go far enough for some researchers, however. "It's a more insightful description but not a theory," says meteorologist Brian Farrell of Harvard University. "We haven't had a tool that explains how, out of turbulent flows, can come emergent order. What's been lacking is a predictive theory."

He and Petros Ioannou of the National and Capodistrian University of Athens, Greece, now present what they believe to be a comprehensive, predictive theory in a paper in press at the *Journal of the Atmospheric Sciences*. Farrell and Ioannou's new mathematical tool, which they call stochastic structural stability theory, can be used to calculate how energy moves up from small-scale turbulence to the large-scale atmospheric flow of jets without a continuous cascade to convey it. In effect, the broad-background, west-to-east flow of air organizes random turbulence into jets, says Farrell, even as turbulence tries to change the mean flow. Rhines puts it more metaphorically. According to stochastic analysis, small-scale turbulence randomly beats on the broad west-to-east flow until it "rings like a bell" with the pure tone of a jet's flow. "All of the jets we see on planets—their scales, their structures—naturally fall out" of the calculations, Farrell says. "I think it solves a fairly big chunk of the turbulence problem."

If so, researchers could take a new look at a number of jets. Instead of merely describing the way the stratospheric jet over the tropics reverses direction every 28 months in the so-called quasi-biennial oscillation, they could predict the period of its oscillation. And paleoclimatologists might be able to explain abrupt climate shifts in the geologic past as the effect of "jumping jets." That's Farrell's term for jets inclined to reposition themselves—with their associated climate—suddenly when slowly pushed by changing climate. Using his stochastic analysis, he could predict just what climate change would trigger a jump.

No one is taking stochastic jet formation that far quite yet. Rhines does not believe the process is as random as stochastic structural stability theory assumes. The interaction of large-scale eddies and jets is too tidy a picture to be that wrong, he says. Farrell and Ioannou are "doing very exciting probing of the system," he says, "yet it's not a general theory, it's an exploratory tool."

Meteorologist Maarten Ambaum of the University of Reading, U.K., sees merit in the new tool because "it's a more comprehensive framework than many people have thought about." To develop the approach further, Farrell plans on extending the stochastic analysis from two dimensions to three—an easy next step, he says. And Robinson would like to see model simulations designed to pin down what role random forcing plays in jet formation. Results so far "suggest Brian and Petros are on the right track," says Robinson, so a follow-up effort would be well worthwhile.

–RICHARD A. KERR

* 16th Conference on Atmospheric and Oceanic Fluid Dynamics, 25–29 June, Santa Fe, New Mexico, American Meteorological Society.

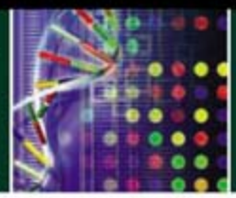

Life itself
454

Specialization trumps order
457

LETTERS

edited by Etta Kavanagh

Retraction

WE WISH TO RETRACT OUR REPORT "*CDX2* GENE EXPRESSION AND TROPHECTODERM LINEAGE specification in mouse embryos" (*1*). Allegations of research misconduct were received by the University of Missouri-Columbia (MU) Provost, and an investigation found that the first author (K.D.) engaged in research misconduct by intentionally falsifying and fabricating digital images in the preparation of Figs. 4I; 4N; 4S; 2G; 3, J to L; S2, V to X; and S6, I to K accompanying the *Science* article. In addition, the original raw image files for the majority of the figures in the paper have not been located (the exceptions being the confocal scanning images in Figs. S1, S3, S4, S5, and S6), raising the possibility that the data they represent may also be suspect. We have decided to withdraw the article in its entirety in view of the fact that the paper was founded at least in part on falsified or fabricated images.

The corresponding author (R.M.R.) takes responsibility for placing excessive trust in his coworker and for not assuring that a complete set of raw data existed at the time the questions first arose about the paper. We deeply regret any scientific misconceptions that have resulted from the publication of this article.

The first author resigned from MU shortly after the allegations of research misconduct were received and could not be found to sign the retraction.

R. MICHAEL ROBERTS,[1] M. SIVAGURU,[2] H. Y. YONG[3]

[1]Division of Animal Sciences, University of Missouri, Columbia, MO 65211, USA. [2]Institute for Genomic Biology, University of Illinois, Urbana-Champaign, IL 61801, USA. [3]BK21 Dental Research Institute, College of Dentistry, Seoul National University, 28 Yongun-dong, Chongno-gu, Seoul 110-749, Korea.

Reference

1. K. Deb, M. Sivaguru, H. Y. Yong, R. M. Roberts, *Science* **311**, 992 (2006).

Editor's Note: Science published an Editorial Expression of Concern (27 October 2006, p. 592) about this paper, which alerted readers to the then-ongoing investigation.

The Shortage of Science Teachers

SCIENCE DESERVES PLAUDITS FOR FOCUSING on the crisis in science education resulting from the lack of properly qualified K–12 teachers in the nation's public schools (News Focus Special: Preparing Teachers, 1 June, pp. 1270–1279). Calling attention to efforts in several states to engage research universities will hopefully begin to address the problem. Unfortunately, the supply side of this issue is only one of several critical, interacting elements of a complex sociopolitical system that is typically controlled or redesigned one element at a time. Focusing only on the supply side is a losing strategy. Let me give examples from California, with which I am most familiar.

If all the graduates of California's public universities who have majored in math in a given year became credentialed teachers in the state, the numbers would still fall short of the projected demand for math teachers in the decade ahead. A second major problem is teacher retention, particularly in hard-to-staff, low-performing schools where "working conditions" are a major factor and where underprepared teachers are predominantly located (*1*). Teacher attrition in the first 1 to 4 years diminishes the importance placed on increasing the number of entrants (*2*). The typical explanation for this phenomenon that a teacher would give is that it stems from the loss of professional status in the teaching profession as a consequence of overemphasis on testing and rigid adherence to standards-based instruction. Teachers no longer enjoy the privilege of controlling delivery of curricula and thus acting as professionals, i.e., exercising judgment in the conduct of their classes.

Finally, teachers with whom I have worked value time above compensation. No university administration expects its faculty to spend the entire day standing in front of a class. Teachers in K–12 need time for collegial activity and professional development to discuss content and pedagogy and, above all, to reduce the sense of isolation that dominates their lives. As an engineering scholar, it is painfully clear to me that the public educational system will never function properly until policy and practice are consonant with a properly designed, controlled, and resourced system. As long as policy-makers continue to tinker with only selected parts of the problem, the "Gathering Storm" will continue to gain energy. If K–12 were an airplane, it never would have taken off.

CREDIT: GETTYIMAGES.COM

KARL S. PISTER

Dean and Roy W. Carlson Professor of Engineering Emeritus, College of Engineering, University of California, Berkeley, Berkeley, CA 94720, USA.

Trilobite evolution

459

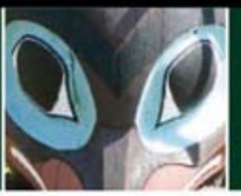

The evolution of spying

464

References

1. The Status of the Teaching Profession 2005 (The Center for the Future of Teaching and Learning, Santa Cruz, CA, 2005), pp. 82–84.
2. California Postsecondary Education Commission, Winter 2006 Request for Proposals, Retention of Math and Science Teachers, footnote, p. 3.

Explaining Latitudinal Diversity Gradients

DIFFERENCES IN MEASURED RATES OF SPECIation and extinction among living species are commonly used to explain latitudinal diversity gradients. The logic is straightforward: the higher the net diversification rate (the difference between the speciation and extinction rate), the greater the number of species. In this vein, J. T. Weir and D. Schluter conclude from their recent study of birds and mammals that decreased extinction rates rather than increased speciation rates account for the higher net diversification rates posited to drive latitudinal diversity gradients ("The latitudinal gradient in recent speciation and extinction rates of birds and mammals," Reports, 16 March, p. 1574).

However, speciation and extinction rates may have little bearing on the cause of latitudinal diversity gradients. Although we have only a poor understanding of what controls species numbers, it is clear that resource availability is of critical importance, and in particular, that the harshness (and reduced area) of the poles limits population numbers. That is, the polar carrying capacity—the number of species that can be supported—is less than that of equatorial regions, and thus we should expect a latitudinal biodiversity gradient. Critically, rates of speciation and extinction do not control carrying capacities, but only reflect rates of species turnover, and the rate at which biotas reapproach their carrying capacities in response to perturbation, or as their carrying capacities shift in response to changing biotic and abiotic influences.

Under this framework, Weir and Schluter's exciting discovery that origination and extinction rates for birds and mammals increase with latitude may have little bearing on the reason that there are latitudinal diversity gradients. Instead, their data suggest that the frequency of extinction and replacement for these animals has been higher at high latitudes than at lower latitudes. This observation implies that ecological disturbance is more frequent, or has greater impact, at higher latitudes, consistent with the greater effects of the Plio-Pleistocene glacial cycles at high latitudes, as Weir and Schluter note.

If we are to explain latitudinal diversity gradients, we need to focus more on the determinants of carrying capacities, and less on the rates at which species turn over, or on how quickly species numbers adjust to

perturbation or to changing carrying capacities.

CHARLES R. MARSHALL

Department of Invertebrate Paleontology, Museum of Comparative Zoology, Harvard University, 26 Oxford Street, Cambridge, MA 02138, USA. E-mail: cmarshal@oeb.harvard.edu

Response

THE STARTING POINT OF OUR STUDY WAS THE previous observation that net diversification rates are higher in the tropics than in the temperate zone (*1*, *2*). This is unexpected if species diversity is at equilibrium, which instead predicts the same average diversification rates everywhere within surviving lineages.

Marshall has not defined "carrying capacity" or its criteria, but his use of the concept suggests an analog to the carrying capacity constant in simple theories of population growth under resource limitation. Yet, although a population carrying capacity might exist on paper, its evidence is typically only that populations are regulated within wide bounds rather than exploding or going extinct (*3*, *4*). Real populations fluctuate according to vagaries of birth and death, and ecologists continue to find clues to the determinants of population size in measurements of these vital rates. Similarly, in the evolutionary process, species diversity is certain to be influenced by the vagaries of past speciation and extinction rates (*5*, *6*). Therefore, measurements of these rates will be useful in understanding present and future species numbers.

The idea has been suggested before that a greater "species carrying capacity" might explain higher species diversity in the tropics compared with the temperate zone (*6*). Unfortunately, the main evidence for a higher species carrying capacity in the tropics is the greater number of species there. At the moment, we are completely unable to explain why, in principle, the numbers of species of birds or plants that can be supported in the temperate zone should not be much greater than the current numbers. Except at the poles, the density of individuals is not much less in the temperate zone than in the tropics (*7*, *8*). What we can record are the frequent disturbances to the temperate zone that have likely knocked back the numbers of species. Our estimates of the impact of these disturbances on species turnover agree with other sources of evidence that point to the influence of extinctions on global patterns of biodiversity (*9*, *10*).

DOLPH SCHLUTER AND JASON WEIR

Biodiversity Research Center and Department of Zoology, University of British Columbia, Vancouver, BC V6T 1Z4, Canada.

Letters to the Editor

Letters (~300 words) discuss material published in *Science* in the previous 3 months or issues of general interest. They can be submitted through the Web (www.submit2science.org) or by regular mail (1200 New York Ave., NW, Washington, DC 20005, USA). Letters are not acknowledged upon receipt, nor are authors generally consulted before publication. Whether published in full or in part, letters are subject to editing for clarity and space.

References

1. M. Cardillo, C. D. L. Orme, I. P. F. Owens, *Ecology* **86**, 2278 (2005).
2. R. E. Ricklefs, *Ecology* **87**, 2468 (2006).
3. A. R. E. Sinclair, J. M. Fryxell, G. Caughley, *Wildlife Ecology, Conservation and Management* (Blackwell, Malden, MA, 2006).
4. W. W. Murdoch, *Ecology* **75**, 271 (1994).
5. R. E. Ricklefs, D. Schluter, Eds., *Ecological Communities: Historical and Geographical Perspectives* (Univ. of Chicago Press, Chicago, 1993).

6. G. G. Mittelbach *et al.*, *Ecol. Lett.* **10**, 315 (2007).
7. D. J. Currie *et al.*, *Ecol. Lett.* **7**, 1121 (2004).
8. B. J. Enquist, K. J. Niklas, *Nature* **410**, 655 (2001).
9. B. A. Hawkins, J. A. F. Diniz, C. A. Jaramillo, S. A. Soeller, *J. Biogr.* **33**, 770 (2006).
10. D. Jablonski, K. Roy, J. W. Valentine, *Science* **314**, 102 (2006).

Papers Not in the Right Section?

THE PAPERS "EVALUATING MONTESSORI EDUcation" (A. Lillard, N. Else-Quest, 29 September 2006, p. 1893) and "Algorithm-guided individualized reading instruction" (C. M. Connor *et al.*, 26 January, p. 464), which appeared in the Education Forum section, seem to be research papers. Since the Education Forum is located in the Commentary section, I assume that the paper has not undergone the same level of peer review as other papers published in *Science*. The Education Forum is supposed to be about science education, but the second paper is on reading instruction. Moreover, it promotes a particular software product, and the authors have declared a possible future conflict of interest. This paper raises the question of why it was published in the Education Forum section rather than being submitted as a Report and scrutinized through *Science*'s normal peer-review process. Education science is most welcome in the pages of *Science*, as long as the work reported fulfills all the scientific standards of the journal.

FRANCK RAMUS

Laboratoire de Sciences Cognitives et Psycholinguistique, Ecole Normale Supérieure, 46 rue d'Ulm, 75230 Paris Cedex 05, France. E-mail: franck.ramus@ens.fr

Editor's Note: As with the other parts of the Commentary section, Education Forums are reviewed at the discretion of the Editor handling the paper.

TECHNICAL COMMENT ABSTRACTS

COMMENT ON "Coherent Control of Retinal Isomerization in Bacteriorhodopsin"

Manuel Joffre

Prokhorenko *et al.* (Research Articles, 1 September 2006, p. 1257) reported that, in the weak-field regime, the efficiency of retinal isomerization in bacteriorhodopsin can be controlled by modulating the spectral phase of the photoexcitation pulse. However, in the linear excitation regime, the signal measured in an experiment involving a time-invariant, stationary process can be shown to be independent of the pulse spectral phase.

Full text at www.sciencemag.org/cgi/content/full/317/5837/453b

RESPONSE TO COMMENT ON "Coherent Control of Retinal Isomerization in Bacteriorhodopsin"

Valentyn I. Prokhorenko, Andrea M. Nagy, Stephen A. Waschuk, Leonid S. Brown, Robert R. Birge, R. J. Dwayne Miller

Joffre attempts to show that the linear response of any quantum system to an external perturbation is phase insensitive, but he uses incorrect mathematical assumptions, misinterprets the time invariance principle, and ignores causality. We argue that the opposite case—an explicit phase dependence for a signal measured in the linear excitation regime—can equally be shown using Joffre's approach and assumptions.

Full text at www.sciencemag.org/cgi/content/full/317/5837/453c

SOCIOLOGY

Reflecting on the Surfaces of Life

Rebecca M. Herzig

Kindergartners taking "cognitive enhancement" drugs. Aged grandmothers giving birth to triplets. Has the breathtaking spread of new biomedical technologies fundamentally altered what it is to be human? This, thankfully, is not the question sociologist Nikolas Rose tackles in *The Politics of Life Itself*. Breaking from the pack of popular and scholarly books on the quandaries posed by emerging biomedical capabilities, his analysis "concerns not what human beings are, but what they think they are: the kinds of human beings they take themselves to be."

Where countless bioethicists, philosophers, and other social critics have fretted over the "posthuman" future signaled by recent developments in neuroscience, genomics, pharmacology, and surgery, Rose (director of the BIOS Centre at the London School of Economics) shrugs off such anxious reflections: "[H]umans have never been 'natural,'" he points out, "and at least since the invention of language we have been augmenting our capacities through intellectual, material, and human technologies." In lieu of positing some epochal break with nature, Rose instead presents a far more intriguing claim: we have never been more biological, never more intimately invested in reshaping our existence as biological organisms. The book centers on these investments, on our increasingly "somatic" self-understandings. The intensely corporeal character of our relationships to ourselves and to our imagined futures, Rose proposes, "forms the milieu within which novel forms of authority are taking shape."

The Politics of Life Itself
Biomedicine, Power, and Subjectivity in the Twenty-First Century

by Nikolas Rose

Princeton University Press, Princeton, NJ, 2007. 367 pp. $65, £38.95. ISBN 9780691121901. Paper, $24.95, £14.95. ISBN 9780691121918.

Of course, authority has always been embodied in one way or another. Governments have long sought to manage not merely the spirit but also the flesh of their subjects—one need only recall the Third Reich's efforts to expunge the most "unfit" from their ranks. Even in more liberal polities, those that emphasize governance by consent rather than governance by force, the management of bodies has been crucial to the development and maintenance of political authority. In 19th-century America, for instance, assessments of white women's physiological frailty helped bolster restrictions on their rights to hold and transfer property, to control their own earnings, and to vote. Political and economic enfranchisement presupposed bodily command and vice versa.

While noting lines of historical continuity, Rose detects in contemporary biomedicine a distinct change, one tied to larger transformations in liberal governance. Increasingly, Rose argues, the "specific vital characteristics of human beings" are the focal point of both individual and institutional control. The proliferation of genetic support groups, dietary consultants, and preventative medications all manifest an ethic of personal health maximization that is by now more or less obligatory: "negative judgments are directed toward those who will not, for whatever reason, adopt an active, informed, positive, and prudent relation to the future." For those of us in the "advanced liberal nations of the West," our hopes and fears concerning the quality of our well-being signal our submission to a new kind of authority—the politics of "life itself."

Rose attributes this field of biopolitics to a convergence of increasingly sophisticated diagnostic and therapeutic tools, increasing financial investment in basic and applied biological research, and increasing ability to visualize and act upon life at the molecular level. Such processes of "technologization," "capitalization," and "molecularization" in turn engage

The reviewer is at the Program in Women and Gender Studies, Pettengill Hall 209, Bates College, Lewiston, ME 04240, USA. E-mail: rherzig@bates.edu

FICTION AND EXPLORATION

The World Measurers

Daniel Kehlmann reveals what a difficult task it is to take the measure of men who themselves feel driven to measure the world. Fortunately, he has chosen the novel as his medium. Taking two contrasting characters, *Measuring the World* weaves the parallel stories of Alexander von Humboldt and Carl Friedrich Gauss between events precipitated by the savants' meeting in Berlin—the occasion that opens and closes the story. The low-born Gauss was famous for exploring the universe of numbers, time, and space. Luckily for him, being a wretchedly poor traveler, his excess of talents mostly allowed him to stay at home. Kehlmann has Gauss reflecting that "to understand the restlessness at the heart of Nature … one didn't need to clamber up mountains or torment oneself in the jungle." Seemingly agreeing with this notion, Kehlmann's Humboldt, scion of nobility, comes to the conclusion that "he could no longer have said which of them had traveled afar and which of them had always stayed at home."

Measuring the World
A Novel

by Daniel Kehlmann

Translated from the German (*1*) by Carol Brown Janeway. Pantheon, New York, 2006. 262 pp. $23, C$30. ISBN 9780375424465. Quercus, London, 2007. £12.99. ISBN 9781847240453.

Jaguars and Electric Eels

by Alexander von Humboldt

Penguin, London, 2007. 112 pp. Paper, £4.99, C$9.99. ISBN 9780141025452. Great Journeys.

Ultimately, Kehlmann's Humboldt remains an enigma, whereas Gauss and Humboldt's companion, Aimé Bonpland, are fully fleshed characters in every sense. In the novel, the irascible Gauss is sufficiently certain of his own worth to berate God for His folly in putting such an intelligent man on an Earth not yet prepared for him. By contrast, Kehlmann portrays Humboldt as a compulsive measurer possessed of an alarming degree of detachment except when confronted by the unavoidably marvelous or frightening. We are told that Bonpland is at a loss when asked what kind of person Humboldt is. Nevertheless, this doesn't stop Kehlmann from using Humboldt as the target in Bonpland's murderous dreams. Kehlmann has him brandishing knives at his mentor during campsite sleepwalking.

I wonder whether Kehlmann's novel of the natural world will be as successful in translation as it has been in German, as over the cen-

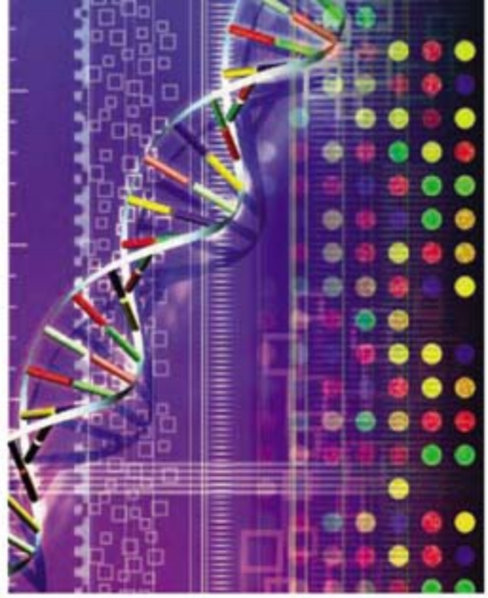

CREDIT: ALFRED PASIEKA/PHOTO RESEARCHERS INC.

broader changes in "marketization, autonomization, and responsibilization," that is to say, in the kinds of state-market relations emerging in places like Australia, Canada, the United States, and the United Kingdom. Rose explicates how these vast processes of global political and economic restructuring are born out through individualized habits: monitoring blood sugar levels, reading self-help books, filling out organ-donation cards. He illuminates how each such practice reveals an intricate entanglement of ethical and economic value: our most tender aspirations are now capillaries of global capital.

Rose shows uncommon restraint in refusing to speculate about the bright or gloomy prospects of such developments. In a refreshingly modest approach, he eschews both breathless anticipation of the possibilities for health and well-being awaiting just around the corner and distressed condemnation of efforts to tamper with human nature. He instead stays firmly focused on a descriptive analysis of the present condition. Drawing on his own well-regarded studies of psychiatry and neuroscience as well as on cutting-edge research by talented social scientists such as Hannah Landecker, Carlos Novas, and Adriana Petryna, Rose synthesizes topics ranging from biological criminology to xenotransplantation in a coherent, thought-provoking frame.

At the center of this frame is the "style of thought," a concept borrowed from Ludwik Fleck. A style of thought, Rose explains, is a particular way of conceiving the world and acting in it. It involves not only specific arrangements of machines, models, customs, and so forth but also membership in a particular "thought community," a group of people disciplined to organize terms, concepts, phenomena, and arguments in a particular way. Rose suggests that contemporary biomedicine demonstrates a new style of thought, one characterized, in part, by an altered relationship to causal depth. Where 19th-century biology (not to mention sociology and psychology) presumed that underlying laws determined the visible characteristics of organisms, contemporary biomedicine effectively flattens the relationship between the surfaces and depths of bodies. No longer dwelling on enigmatic interiors, the contemporary life sciences focus on surface associations—relays of nonhierarchical networks and affiliations. Mind, for instance, is not understood in the mysterious terms of the Freudian unconscious, but simply as "what the brain does." It is this shift away from an "epistemology of depth" that "enables us to be governed in new ways"—to "govern ourselves differently."

The referent of the "us" in such lines is obviously crucial, as Rose readily recognizes. The book's first footnote dismantles any presumption of global inclusiveness carried by words such as we and us and our. As Rose reminds readers, a tiny fraction of the total biomedical resources of the planet are directed to the threats to health facing most of its inhabitants. Médecins Sans Frontières has described this fact as the "10/90 gap," because 90 percent of the world's health problems receive but 10 percent of global expenditures on health research. Elsewhere in his analysis, Rose takes pains to stress similar gaps, noting, for example, that "the ills that afflict most human beings now and in the foreseeable future require no high tech solutions—merely clean water, sufficient food, a living wage, and moderately competent politicians and bureaucrats." Indeed, Rose goes so far as to assert that a "constitutive feature of contemporary biopolitics" is the tension between "the intensifying somatic ethics in the West … and the inequities and injustices of the local and global economic, technological, and biomedical infrastructure required to support such a somatic ethic."

What, then, of this tension and its constitutive role in the politics of life itself? How, ultimately, might we reconcile the disparities of global economic and political restructuring with the trend toward flattening that Rose pinpoints as central to contemporary biomedicine? "Perhaps," Rose proposes at the book's

CREDIT: © ROYAL GEOGRAPHICAL SOCIETY, LONDON/BRIDGEMAN ART LIBRARY

turies English has been well served by stories of explorer-scientists in diaries and fictions. Translation brings obvious and trivial risks, although I enjoyed the thought that Gauss could predict prime numbers asymptomatically.

Kehlmann's words also have to compete directly with Humboldt's personal narrative: particularly now as short extracts from his accounts of his South American journeys are readily available in *Jaguars and Electric Eels* (*2*). Even in such a truncated form, Humboldt gives the reader a far better sense of place than Kehlmann and offers far more enlightenment about the natural world in his accounts of agricultural degradation and altitudinal zonation in South America. Humboldt's own words also provide authentic glimpses of his abundant enthusiasm and curiosity. Perhaps Kehlmann has never been to Venezuela. Even so, considerations of landscape and place lay at the very base of Humboldt's thinking and deserve more care. Kehlmann is generally more sympathetic to the astronomer-mathematician's far less exotic activities. To be fair, the novelist's theme is measurement not synthesis, but this still sells Humboldt short. At least, however, Kehlmann is trying to bring the world of science and discovery to a wider audience.

—Caroline Ash

References and Notes

1. D. Kehlmann, *Die Vermessung der Welt* (Rowohlt, Reinbek bei Hamburg, Germany, 2005).
2. Extract from A. von Humboldt, *Personal Narrative of a Journey to the Equinoctial Regions of the New Continent*, J. Wilson, Ed., Transl. (Penguin, London, 1995).

10.1126/science.1142791

conclusion, "it is not too much to suggest that as the styles of thinking in biology mutate, so then should the styles of thought in those disciplines seeking to understand their social organization and consequences. The critical social sciences also need to understand that the most profound thought is that which remains on the surface." Even as Rose's book offers tremendous insight into our biomedical present, it may be that some of those traditional analyses have something yet to contribute as we confront the unfolding inequities of contemporary vital politics.

10.1126/science.1144402

PSYCHOLOGY

The Nature of Belief

Scott Atran

In explaining why he wrote *Six Impossible Things Before Breakfast*, Lewis Wolpert describes a disturbing encounter with his son's envious belief that father has the advantage in life because he is likely to die sooner and enjoy heaven. In August 2005, while with Muslim mujahedin in Sulawesi, I noticed tears welling up in my traveling companion, Farkhin (who helped bomb the Philippine ambassador's residence in Jakarta and had hosted 9/11 mastermind Khalid Sheikh Mohammed) when he heard of a young man killed in a skirmish with Christian fighters. "Farkhin, you knew the boy?" I asked. "No," he lamented, "but he was only in the Jihad a few weeks; I've been fighting since Afghanistan [late 1980s] and I'm still not a martyr."

In trying to grasp his son's belief as well as the beliefs of people like suicide bombers and today's great clashes among religious and political beliefs, Wolpert draws fresh insight from the biological and evolutionary roots of belief. He surveys a vast domain that begins with children's innate ideas about the differences between how inert objects and animate agents like people interact and ends with the almost miraculous breakaway of scientific beliefs from our intuitive understanding of the world: there are more molecules in a glass of water than glasses of water in the oceans. We find out that other primates lack mental equipment for mind reading. They can't represent or embed another's beliefs in their own thoughts ("John believes that Mary thinks that…"). Thus they can't understand how they or others can have false beliefs or conceive of fiction, God, or scientific truth. And we learn why other animals can't truly imitate or learn a new dance and why homeopathic medicine and psychotherapy involve "beliefs related to witchcraft."

The book's unifying theme is that all belief is ultimately rooted in causal understanding and has its evolutionary origins in the use and manufacture of tools. This lets Wolpert scan the landscape of belief with clarity and direction but leads down the wrong path in key areas. He argues that managing fire "might have been one of the origins of market exchange, and might have led to the advantage of humans knowing about numbers." Yet defining aspects of number, such as the concept of a class of similar classes or of infinite discreteness, relate more to categorization processes and language structure than to causality. We are told "Verbs ranging from 'go' to 'hit' to 'throw' require causal thinking … an essential prerequisite for language development." Now Kanzi, a brilliant bonobo, can use symbolic tokens to reference causal relations between actions and goals; however, Kanzi's strings are usually action-action combinations, such as "chase bite." These strings employ two "predicates" and no subject. No human language allows sentences that have no syntactic arguments and thus cannot express a subject-predicate proposition. Hominid tool play tells us little of testable, scientific interest about linguistic structure, number, or markets.

Six Impossible Things Before Breakfast
The Evolutionary Origins of Belief

by Lewis Wolpert

Faber and Faber, London, 2006. 243 pp., £14.99. ISBN 9780571209200. Norton, New York, 2007. 255 pp. $25.95. ISBN 9780393064490.

But it is Wolpert's speculation on religion that is needlessly awry. He claims religious beliefs "all had their origin in the evolution of causal beliefs, which in turn had its origins in tool use." Gods and prayer act in tandem to promote "optimism and hope" by providing special controlling forces when commonsense expectations fail, catastrophe or chaos leaves life to chance, or death looms. "And since causal beliefs that promote survival are partly programmed by our genes, could that not also be true of some aspects of religious beliefs that promote survival, particularly those that relate to mystical forces, and even, perhaps to the gods themselves?"

Wolpert identifies religion with belief in the supernatural, which is fine by me, but recent work in the cognitive science of religion indicates that there is no genetically privileged "supernatural imagination" or "biologically determined module for making myths." Rather, cognitive production of the supernatural occurs by purposely violating our ordinary and innate ideas about causality. Wolpert acknowledges that "what makes an event magical is that it goes against our natural expectations about causes," just as dragons and other monstrous hybrids violate innate assumptions about essentialized biological categories. But this is not because some extraordinary, parallel faculty of causal reasoning evolved through genetic adaptation.

Religion involves the same causal categories that evolution endowed us with for everyday thinking—including folk mechanics (object boundaries and movements), folk biology (species-like essences and relations), and folk psychology (interactive agents and goal-directed behavior)—and which constrain the ways children learn language. Core religious beliefs minimally violate ordinary notions about how the world is, with all of its inescapable problems, thus enabling cognitively manageable and memorable supernatural worlds that treat existential problems, including death and deception—for example, a world with beings (angels, ghosts, ancestral spirits) that resemble us emotionally, intellectually, and even physically except they can move through solid objects and be immortal.

That "lower blood pressure … has a positive association with religious belief" may be true in settings most familiar to many of us, but it is doubtful for more passionate contexts (e.g., pentecostal or jihadi). And although "one can see how valuable the possible force of prayer is to the more or less helpless individual suffering from severe pain," most prayer—indeed, most religious ceremony—occurs in ritualized social settings that coordinate the congregation's body states (chanting, swaying, displays of submission, etc.) and that arguably promote an emotional consensus that can trump even the most logically compelling and evidence-based beliefs.

If religion is, as Wolpert suggests, a special form of causal belief—immune to logic and evidence—about how things are in the world, then it is true that "science is basically in conflict with religion." But if religion is primarily about what ought to be, including moral framing that convinces people to commit to others beyond the logic and evidence for advancing self-interest, then conflict is not inevitable. Understanding and manipulating causality, though key to science, is only one integral component of religion and other aspects of human brain development, knowledge, and belief that bind us to one another and the world.

10.1126/science.1142653

The reviewer is at the CNRS—Institut Jean Nicod, Ecole Normale Supérieure, 29 rue d'Ulm, 75005 Paris, France. E-mail: satran@umich.edu

TRANSITIONS

The Two High-School Pillars Supporting College Science

Out-of-discipline high-school science courses are not associated with better performance in introductory college biology, chemistry, or physics courses, but high-school math counts.

Philip M. Sadler[1]* and Robert H. Tai[2]

Do students need chemistry in order to understand biology? Is biology the best foundation for beginning science students? How is the study of mathematics associated with the study of science? Whether the sequence of science courses has any cognitive relevance is a matter of dispute among science educators, especially given the emerging interdisciplinary underpinnings of traditional ideas in each field. For example, understanding chemical models requires some knowledge of the physics of electrostatics, and a solid foundation in lipid and protein chemistry can help explain the construction of cellular membranes (*1*–*3*). Meanwhile, the role of mathematics is considered to be less crucial to introductory biology coursework than to physics. One group, often referred to as the "Physics First" movement, promotes a reversal of the traditional biology-chemistry-physics high-school course sequence on the premise that key concepts from physics would better prepare students to study chemistry and even biology (*4*–*6*). To study this theory, we assumed that the benefits of high-school science preparation would extend into college (i.e., a student who has completed high-school physics may perform differently in a college chemistry class than a student who has not taken physics).

In the United States, high-school students can choose the number of years that they study each science subject [none, one year, or a second year, commonly Advanced Placement (AP)] and mathematics (i.e., Algebra II or lower, pre-calculus, calculus, or AP calculus). We analyzed the association between varying amounts of high-school biology, chemistry, physics, and mathematics preparation and performance in introductory college science. Although not an experimental design, this approach does offer the advantage of large participant numbers, while approximating the impact of prior science learning on subsequent science performance. By analyzing the cross-disciplinary benefits of these subjects across high school and college, we sought to bring empirical evidence to a debate that is often fueled by rhetoric.

Sample, Instrument, and Analysis

We randomly selected 77 colleges and universities from a comprehensive list of roughly 1700 4-year institutions. To avoid overrepresenting small, but more numerous, liberal arts colleges, we used a representative stratified random sampling based on college size (<3000, 3000 to 10,000, and >10,000 students). In all, professors for 122 introductory biology, chemistry, and physics courses at 63 of these colleges and universities participated. Only science courses satisfying requirements for science majors in each discipline were surveyed. We excluded from our analysis students who did not attend a U.S. high school, graduate students, and those not in degree programs. Our total sample consisted of 8474 undergraduate students enrolled in one of the three introductory science courses.

We designed three parallel surveys tailored to the disciplines of biology, chemistry, and physics, analogous to a previous pilot study of 2000 college physics students (*7*). We further informed our survey with a series of interviews with college students, high-school teachers, and college professors. We tested for response reliability in a separate analysis involving 113 college chemistry students who completed the chemistry survey twice, 2 weeks apart. The resulting survey included questions on how many high-school courses students had completed in each science subject and mathematics.

Ultimately, the surveys were administered to the sampled students while in class during the Fall semester. Professors reported the final course grade of each student at the end of the term. We converted grades to scores using the following scale: A = 95, A– = 91, B+ = 88, B = 85, and so on. The mean grade was 80.41 (B–) with a standard deviation of 11.43.

We performed three parallel analyses, resulting in three separate yet comparable linear regression models (*8*). The sample sizes were $n = 2650$ for biology, $n = 3561$ for chemistry, and $n = 2263$ for physics. To account for differences among the college science courses (e.g., grading stringency), we used a college-effects model that assigned a variable to each college course (*9*). We chose variables to control for student background differences based on our earlier work (*7*, *10*–*12*), which indicated that we should account for each student's year in college. (Most biology and chemistry students were freshmen, but most physics students were sophomores or juniors). We also accounted for race and gender (tables S3 to S5) (*7*). Recognizing that the quality of teachers and resources available in a high school depends to some degree on the socioeconomic status of the community, we used

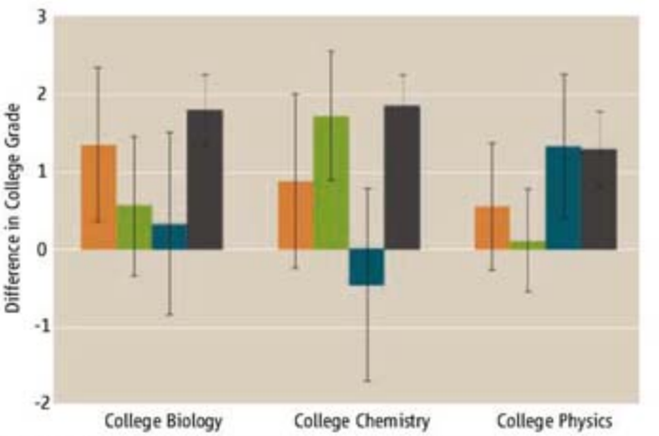

Effect of high-school science and mathematics on college science performance. The more high-school courses a student takes in a given subject, the better the student's college grade in the same subject will be. The average grade-point increase per year of high-school biology (orange), chemistry (green), and physics (blue) is significant for a college course in the same subject but not for a college course in a different subject. Only high-school mathematics (gray) carries significant cross-subject benefit (e.g., students who take high-school calculus average better grades in college science than those who stop at pre-calculus). Grade points are based on a 100-point grade scale. Error bars represent 2 standard errors of the mean.

[1]Department of Science Education, Harvard-Smithsonian Center for Astrophysics, Cambridge, MA 02138, USA. [2]Curry School of Education, University of Virginia, Charlottesville, VA 22904, USA.

*To whom correspondence should be addressed. E-mail: psadler@cfa.harvard.edu

parental education level and the mean education level of the community [retrieved from postal code data (*10*)]. Pre-college academic achievement of students was accounted for in the models by including self-reported standardized test scores. Using a concordance table, we converted ACT scores to SAT equivalents for this analysis (*13*). "Last high school English grade" and "last high school math grade," along with "highest math course taken," provided an estimate of educational achievement outside of science. Using these variables as a baseline model to account for demographic and educational differences, we accounted for the inclusion of the three high-school science predictors [years of biology instruction (ybi), years of chemistry instruction (yci), and years of physics instruction (ypi)]. The completion of high-school courses in each science discipline was entered as a continuous variable (0, 1, or 2 years). For the purposes of this discussion, we focused on the regression coefficients that may be interpreted as grade points on a 100-point final grade scale (see chart on page 457). We based our analytical approach on results from previous research relating to specific disciplines, block scheduling, and content coverage (*10*–*12*).

Results

Multiple linear regression analysis yielded three results: (i) an overall estimate of the outcome variable's variation, (ii) estimated coefficients for predictor variables of the linear model, and (iii) each predictor variable's associated level of statistical significance. The three multiple linear regression models in biology, chemistry, and physics accounted for variances of 32, 31, and 35%, respectively. We found that the three high-school science predictors (ybi, yci, and ypi) were only significant as predictors within their respective disciplines (effect size = 0.13 SD, $P < 0.01$) (see chart). No significant cross-disciplinary effect was found among the three science disciplines.

Years of mathematics instruction (ymi) was a significant predictor of performance across all college science subjects, including introductory college biology, a discipline not traditionally associated with strong mathematics preparation (effect size = 0.14 SD, $P < 0.001$) (see chart and tables S3 and S5).

Discussion

Our research examines correlations and does not offer the proof of causation that an experimental study could. However, the lack of significance in cross-disciplinary coursework supports the claim that cross-disciplinary coursework has a lesser role in preparation for performance than either intradisciplinary or calculus coursework. There may be unexamined variables that offer greater predictive power, such as interest level in a particular field or parental occupation.

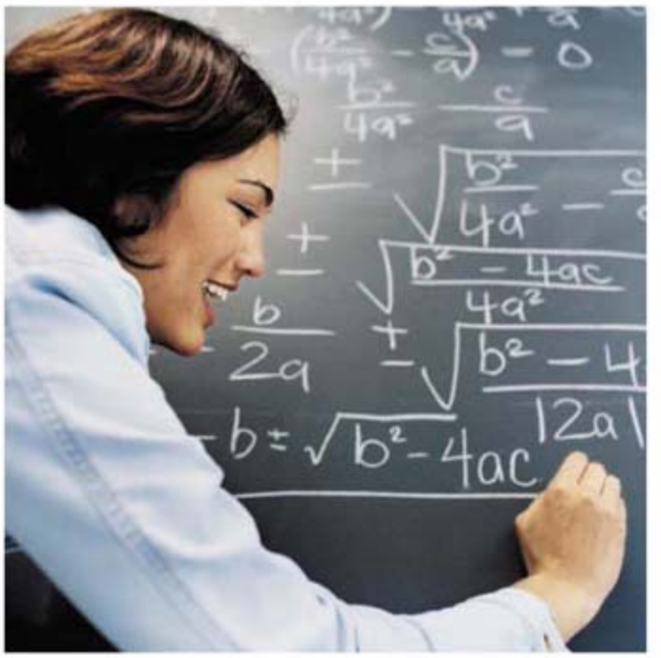

Math class. High-school math prepares students for college science.

Our surveys rely on accurate self-reporting of personal experiences from respondents, which presents an important limitation to consider. The accuracy of self-reports relies on context and relevance. Studies of students' high-school course schedules have found self-reports to be reasonably accurate in comparison with transcript sources (*14*). A review of self-report studies has found that among college students, self-reports on academic backgrounds are also reasonably accurate (*15*). Surveying college science students during their college science classes about their high-school science experiences appears to meet the requirements of context and relevance. We found response reliability to be acceptable for the analysis we undertook in this study (*16*).

We also specifically investigated the ~10% of students in our sample who took high-school AP courses and then enrolled in the corresponding introductory college courses. We were concerned that these AP students in our sample might be biased toward underperformers. However, we found that the mean AP exam score for this group was 2.99, slightly higher (0.15 SD) than the overall mean of 2.81 reported by the College Board.

Our results have some application to the current debate concerning preparation for college science. We found, not surprisingly, that high-school courses in biology, chemistry, and physics prepare students for college courses in the same field. We can also offer some empirical evidence to inform the debate on the reordering of high-school science courses. With regard to the "Physics First" movement, the lack of a relationship between the previous study of physics and later chemistry performance, or the previous study of chemistry and later biology performance, casts doubt on the impact of changing the traditional high-school science sequence. The two pillars supporting college science appear to be study in the same science subject and more advanced study of mathematics in high school. Of course, this finding applies to introductory courses as they are currently taught in college, and the door remains open to develop and teach college courses that could make fuller use of student backgrounds built during high school in other science disciplines.

References and Notes

1. D. Mason, *J. Chem. Educ.* **79**, 1393 (2002).
2. G. Ewald *et al.*, *Phys. Teach.* **43**, 319 (2005).
3. L. Lederman, *Phys. Today* **54**, 11 (2001).
4. M. Bardeen, L. Lederman, *Science* **281**, 178 (1998).
5. L. Lederman, *Educ. Week* **18**, 56. (1999).
6. R. Richards, *Teaching Physics First: Teachers Discuss New Order of Science at Philadelphia Meeting* (American Institute of Physics); www.aip.org/isns/reports/2002/034.html.
7. R. Tai, P. Sadler, *Int. J. Sci. Educ.* **23**, 1017 (2001).
8. As an alternative approach, controls at the course level (enrollment and algebra/calculus-based physics) and institutional level (college or university, public or private, mean SAT/ACT score, and total enrollment) produce similar results.
9. G. Pike, J. Saupe, *Res. Higher Educ.* **43**, 187 (2002).
10. R. Tai *et al.*, *J. Res. Sci. Teach.* **42**, 987 (2005).
11. K. Dexter *et al.*, *The* high-school *J.* **89**, 22 (2006).
12. R. Tai *et al.*, *J. College Sci. Teach.* **35**, 56 (2006).
13. N. J. Dorans, *Correspondences Between ACT and SAT I Scores* (The College Board, New York, 1999).
14. R. Sawyer *et al.*, *College Univ.* **64**, 288 (1989)
15. N. Kuncel *et al.*, *L. L. Rev. Educ. Res.* **75**, 63 (2005).
16. R. Thorndike, *Measurement and Evaluation in Psychology* (Pearson, Upper Saddler River, NJ, 1996).

17. We thank the late Michael Filisky for his leadership on this project carried out under a grant from the Interagency Educational Research Initiative (NSF-REC 0115649). Any opinions, findings and conclusions, or recommendations expressed do not necessarily reflect the views of the NSF, the U.S. Department of Education, or the NIH.

Supporting Online Material

www.sciencemag.org/cgi/content/full/317/5837/457/DC1

10.1126/science.1144214

CREDIT: GETTY IMAGES

PALEONTOLOGY

Variation and Early Evolution

Trilobite fossils provide evidence for elevated morphological variation during the Cambrian Period.

Gene Hunt

Variation is often said to be the raw material for evolution. In the absence of heritable variation, no mechanism—natural selection included—can cause evolutionary change within populations. That variation is necessary for evolution is uncontroversial, but scientists have long wondered if abundant variation might play a more active role in facilitating or channeling evolutionary change (*1*, *2*). Any evolutionary influence of variation would presumably operate continually, but there have been some indications that during the Early Cambrian (542 to 513 million years ago), the link between variation and evolutionary divergence may have been especially strong.

At roughly the same time as the greatest known burst of biological innovation, the Cambrian Explosion of animal body plans, it appears that species may have been unusually variable in their morphology. Although intriguing, the evidence for this increased Cambrian variability has been somewhat equivocal. However, on page 499 of this issue, Webster (*3*) presents the results of a novel analysis of trilobite variability that puts this pattern on much firmer empirical footing. He reports that during the heyday of innovation in the Cambrian, trilobite species were in fact unusually variable, more so than at any other time in their history.

Previous suggestions of elevated Cambrian variability involve a variety of taxa, but special emphasis has been placed on trilobites (*4*, *5*), which have by far the richest fossil record during this interval. One commonly cited example is the number of body segments in the thorax of adult trilobites. Within some Cambrian species, this feature is variable, whereas in post-Cambrian trilobites, the number of segments is almost always fixed within species, and often within higher taxonomic levels such as genera and families (*6*). As interesting as this example is, it applies to only one trait and a small number of trilobite species. More convincing evidence for enhanced variation would require a broader and more systematic survey of characters and traits, but there are formidable obstacles to measuring variation in a meaningful way across very different traits and taxa.

Webster gets around these difficulties by cleverly exploiting a large set of expert observations already in existence. Since the advent of cladistic methods in systematics, specialists generally represent their morphological observations as explicitly defined characters with discretely coded character states. For example, a character might reflect the number of ridges in a defined region of the trilobite head, and there would be different character states corresponding to the presence of one ridge, two ridges, and so on. Systematists not only record the character state attributed to each species in a study but also usually indicate for each character which species were variable. Such coding of species represented by individuals with two or more different character states is called "polymorphic" by systematists.

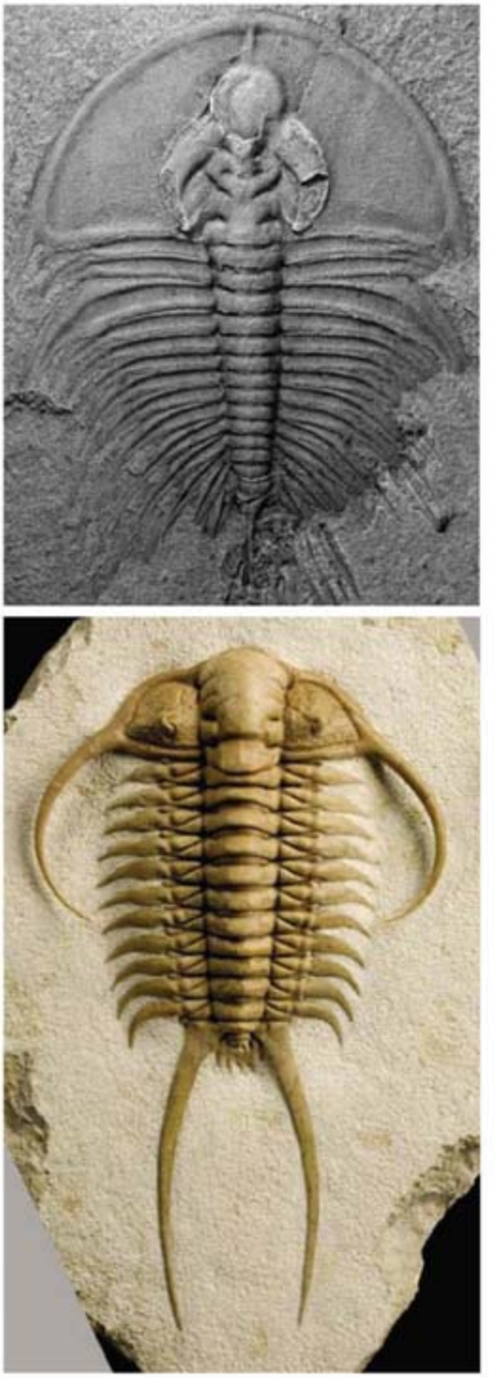

Before and after. (**Top**) An early Cambrian trilobite from an order (Redlichiida) with highly variable species. (**Bottom**) An Ordovician trilobite from an order (Phacopida) with less variable species.

CREDITS (TOP TO BOTTOM): M. WEBSTER, UNIVERSITY OF CHICAGO; C. CLARK, SMITHSONIAN INSTITUTION

By tracking the preponderance of polymorphic versus invariant characters over time, Webster was able to document a dramatic pattern: In the early intervals of trilobite evolution (the Early and Middle Cambrian), polymorphism was much more common than in any subsequent period of trilobite history. Because the elevated polymorphism was not limited to any particular kinds of traits, trilobite species during these early intervals were very likely to have been exceptionally variable in their overall morphology. Moreover, this period of elevated polymorphism occurs at the same time that trilobites were diversifying taxonomically and morphologically, suggesting to Webster that elevated variation may have promoted the radiation of trilobites. Although this large data set of observations is not a random sample of trilobite lineages or traits, a variety of sensitivity analyses suggest that whatever its biases, they do not appear to change markedly over time.

This study, in establishing the reality of increased Cambrian variability for trilobites, implies that evolutionary processes in the distant past may have acted differently, or in a different balance than in more recent periods of time. The cause or causes for these differences likely relate to the proposed explanations for the extravagant evolutionary inventiveness of this period. These explanations fall into two broad categories: genetic and ecological (*7*, *8*). The former suggest that Cambrian genomes were less constrained, or otherwise less apt to generate profoundly novel morphologies, whereas the latter invoke the relative sparseness of early animal ecosystems in allowing large evolutionary jumps to become successfully established.

As Webster notes, either or both of these

The author is in the Department of Paleobiology, National Museum of Natural History, Smithsonian Institution, Washington, DC 20013–7012. E-mail: hunte@si.edu

explanations may account for the greater variability of Cambrian trilobites; more loosely organized genomes might be expected to produce a greater range of morphologies, and less occupied adaptive landscapes might be more permissive of the broad production of variants. Nevertheless, this work highlights the uniqueness of the early Cambrian interval in the evolution of animals and thereby the importance of placing broad evolutionary patterns in a historical and paleontological context.

References

1. G. G. Simpson, *The Major Features of Evolution* (Columbia Univ. Press, New York, 1953).
2. D. Schluter, *Evolution* **50**, 1766 (1996).
3. M. Webster, *Science* **317**, 499 (2007).
4. K. J. McNamara, *Biol. Revi.* **61**, 121 (1986).
5. D. Jablonski, D. J. Bottjer, in *Evolutionary Innovations*, M. H. Nitecki, Ed. (Univ. Chicago Press, Chicago, 1990), pp. 253–288.
6. N. C. Hughes, R. E. Chapman, *Lethaia* **28**, 333 (1995).
7. D. H. Erwin, *Acta Palaeontol. Pol.* **38**, 281 (1994).
8. J. W. Valentine, *Palaios* **10**, 190 (1995).

10.1126/science.1145550

MATERIALS SCIENCE

Filling a Void

Random gel networks formed from chalcogenide clusters and metal ions can selectively remove heavy metal ions from water.

Stephanie L. Brock

Porous inorganic materials are widely used as filters and catalysts—applications that involve the transport of molecules or ions to reactive surfaces. Such materials include zeolites and mesoporous solids (both of which have ordered pore structures), as well as dried gel structures such as aerogels (with a disordered pore structure). The materials vary in the number, size, and distribution of pores, but with few exceptions, they are oxides. This "chemical exclusivity" has severely limited their potential applications. Thus, zeolites efficiently absorb calcium and magnesium ions and are therefore effective water-softening agents, but they are largely ineffective for remediation of heavy metal ions, such as mercury or lead.

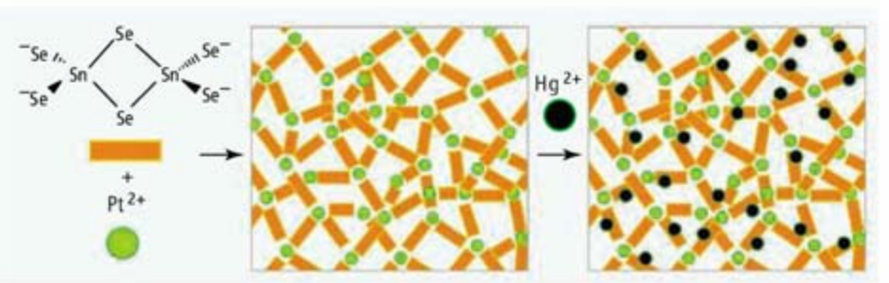

Chalcogel formation and mercury absorption. Bag *et al.* show that chalcogenido molecular ions or clusters such as $Sn_2Se_6^{4-}$ (orange bar) can react with Pt^{2+} (green sphere) in water to form a polymeric cross-linked network. This network can absorb up to ~650 mg of mercury per gram of chalcogel from contaminated solutions.

The problem with oxides is that they prefer to form bonds with small metal ions such as magnesium and zinc. Heavy metals are large and polarizable and cannot be effectively bound by porous oxides. One way to get around this problem involves modifying the surface of the oxide so that it presents a larger, more polarizable binding atom, such as a sulfur group, permitting selective adsorption of heavy metal ions (*1*). On page 490 of this issue, Bag *et al.* report another approach (*2*): They use a sol-gel reaction to construct porous solids that are analogous to oxides but contain the heavier chalcogenides (such as sulfides or selenides) instead of oxide. The resulting chalcogenide aerogels selectively bind heavy metals without requiring modification.

A few methods for making porous chalcogenide aerogels have previously been reported. These methods used either thiolysis chemistry, in which molecular metal precursors are reacted with hydrogen sulfide (*3*), or the oxidative condensation of preformed metal chalcogenide nanoparticles (*4*). The method reported by Bag *et al.* promises additional flexibility because it starts from molecular ions or small clusters of semiconducting metal chalcogenides and uses metal ions as linkers. Both the cluster and the metal ion can be varied to adjust the properties of the resulting material.

This general approach—the linking of chalcogenido clusters with metal ions—has been previously used to prepare mesostructured chalcogenides (*5*-*8*). In these studies, surfactants served as templates, organizing the metal chalcogenide component around the micellar structures, analogous to the synthesis of mesoporous aluminosilicate materials (*9*). However, in contrast to mesoporous aluminosilicates, attempts to remove the surfactant by washing or heating resulted in collapse of the pore structure. The present surfactant-free strategy is simpler, eschewing order completely, yet generating stable porous structures.

Bag *et al.* use a metathesis (or partner-switching) reaction between a metal chalcogenide salt and tetrachloroplatinate in aqueous solution to obtain a solvent-swollen chalcogenide polymer. Wringing out this "sponge" without collapsing the structure can be achieved by drying from a supercritical solvent, producing an aerogel [a term that refers to the fact that the pore solvent has been replaced by air (*10*)].

The chalcogenide aerogels prepared by Bag *et al.* have high surface areas and can be molded into solid monoliths with densities less than 5% that of a corresponding fully dense material. Like any sponge, they are highly absorbent, but because they are composed from polarizable binding groups, they are particularly effective sponges for heavy metal ions. To test this, Bag *et al.* placed the chalcogenide aerogels in a solution consisting of commonly found (and nontoxic) metal ions with low to moderate polarizability, like zinc, along with rarer (but extremely toxic) highly polarizable ions like mercury. The aerogels preferentially adsorbed the heavy ions, removing 99.9% of the mercury but just 40% of the zinc.

The differences between porous chalcogenides and oxides also extend to their optoelectronic properties. Chalcogenide semiconductors tend to be more covalent than oxides, leading to smaller band gaps (the threshold energy for photon absorption) that can be tuned from the ultraviolet to the infrared. In contrast, most oxide semiconductors absorb in the ultraviolet (think of titania, a white paint pigment). Thus, the absorption properties of chalcogenides are better matched to the solar spectrum than those of oxides, making them useful for applications such as photocatalysis (*11*). In the present case, the effective band gap of the

The author is in the Department of Chemistry, Wayne State University, Detroit, MI 48202, USA. E-mail: sbrock@chem.wayne.edu

chalcogels can be varied from 0.2 to 2.0 eV by changing the chemical constituents of the chalcogenide cluster and metal ion linker (*2*).

Whether chalcogenide aerogels will find practical applications remains an unanswered question, although the few studies on these materials have yielded provocative results. In addition to the exceptional sorption properties noted here (*2*), these include the ability to tune the extent of quantum confinement with density (*4*) and to make bulk monoliths of luminescent quantum dots (*12*). It is abundantly clear that our ability to apply sol-gel chemistry to non-oxides, and metal chalcogenides in particular, is far more general than originally thought.

References

1. L. Mercier, T. J. Pinnavaia, *Adv. Mater.* **9**, 500 (1997).
2. S. Bag, P. N. Trikalitis, P. J. Chupas, G. S. Armatas, M. G. Kanatzidis, *Science* **317**, 490 (2007).
3. I. U. Arachchige, K. K. Kalebaila, S. L. Brock, *Comm. Inorg. Chem.* **27**, 103 (2006).
4. J. L. Mohanan, I. U. Arachchige, S. L. Brock, *Science* **307**, 397 (2005).
5. P. N. Trikalitis, K. K. Rangan, T. Bakas, M. G. Kanatzidis, *Nature* **410**, 671 (2001).
6. P. N. Trikalitis, K. K. Rangan, M. G. Kanatzidis, *J. Am. Chem. Soc.* **124**, 2604 (2002).
7. M. J. Maclachlan, N. Coombs, G. A. Ozin, *Nature* **397**, 681 (1999).
8. S. D. Korlann, A. E. Riley, B. L. Kirsch, B. S. Mun, S. H. Tolbert, *J. Am. Chem. Soc.* **127**, 12516 (2005).
9. C. T. Kresge, M. E. Leonowicz, W. J. Roth, J. C. Vartuli, J. S. Beck, *Nature* **359**, 710 (1992).
10. S. S. Kistler, *J. Phys. Chem.* **36**, 52 (1932).
11. N. Zheng, X. Bu, H. Vu, P. Feng, *Angew. Chem. Int. Ed.* **44**, 5299 (2005).
12. I. U. Arachchige, S. L. Brock, *J. Am. Chem. Soc.* **129**, 1840 (2007).

10.1126/science.1146517

MEDICINE

The Yin-Yang of Sirtuins

Two related proteins protect cells from age-associated neurodegenerative disease, but one needs to be activated whereas the other must be inhibited.

Andrew Dillin and Jeffery W. Kelly

The gene encoding SIRT1, a sirtuin histone deacetylase, is widely recognized for its link to aging. SIRT1 activity increases when conditions favor longevity, such as a restricted calorie intake or treatment with the polyphenol resveratrol. Furthermore, increased SIRT1 expression or activity delays the toxic effects induced by α-synuclein (α-Syn), the protein that forms insoluble aggregates in several age-onset pathologies including Parkinson's disease (*1*). Understanding the function of the seven mammalian sirtuins should enhance our ability to promote healthy human aging and to ward off age-onset diseases by manipulating these proteins pharmacologically. On page 516 of this issue, Outeiro and colleagues (*2*) identify an interesting twist related to the family member SIRT2. Surprisingly, inhibition, rather than activation, of SIRT2 protects against α-Syn–related pathology. The study not only identifies SIRT2 as a potential new target for Parkinson's disease intervention, but also bolsters recent work linking age-related cell signaling pathways to protein aggregation processes and age-onset neurodegenerative diseases (*3*, *4*).

SIRT2 is a cytoplasmic nicotinamide adenine dinucleotide (NAD^+)–dependent deacetylase that is prominently expressed in the brain. Outeiro *et al.* discovered that reducing SIRT2 expression by RNA interference, or reducing its activity with small-molecule inhibitors, protects against α-Syn–induced toxicity in three different paradigms: transfected human H4 neuroglioma cells expressing wild-type α-Syn; transfected rat midbrain primary neuronal cells expressing a variant of α-Syn that exhibits increased proteotoxicity; and a fly model (*Drosophila melanogaster*) of Parkinson's disease. Results from the latter two models are particularly exciting because they show diminished neuronal loss in response to reduced SIRT2 activity. The extent of rescue from α-Syn toxicity in H4 cells is comparable to that observed when the cytoplasmic chaperone protein Hsp70 (which assists in protein folding and monitors aggregation) is overexpressed.

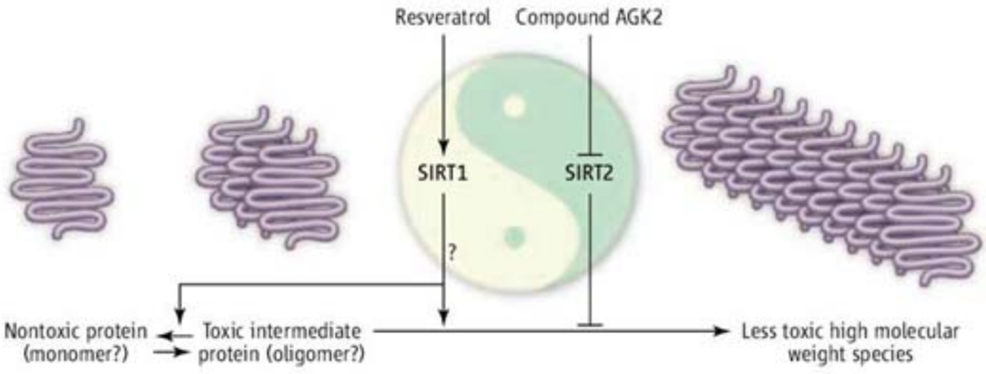

Unity of opposites. Activation of SIRT1 and inhibition of SIRT2 have the same outcome—to block proteotoxicity associated with age-related neurodegenerative diseases. Compounds that act on these sirtuins are therapeutic candidates. Question marks indicate which mechanisms of action are unknown.

How does inactivation of SIRT2 result in a protective effect similar to that seen with activation of SIRT1? The possibility that SIRT2 inhibition simply activates SIRT1 function appears to be ruled out by data presented by Outeiro *et al.* Another explanation is that SIRT1 and SIRT2 may have the same molecular target, but have opposing effects on its activity (see the figure). Alternatively, SIRT1 and SIRT2 may function within independent and opposing signaling pathways to promote cell survival under conditions of proteotoxic stress. We know that SIRT2 inhibition as a means of ameliorating proteotoxicity is at least partially mechanistically distinct from that of SIRT1 activators in worm and mouse models of Huntington's disease (*5*). Only the latter depends on the transcription factor *daf-16/FOXO*. Perturbing cellular signaling pathways that involve *daf-16* protects against proteotoxicity in worm models of Alzheimer's and Huntington's diseases (*3*, *4*). However, *Drosophila* models of Huntington's disease suggest a SIRT2-dependent pathway, based on histone deacetylase inhibitors that arrest progressive neuronal degeneration and reduce lethality (*6*). Thus, the "yin-yang" nature of activating or inhibiting these sirtuins to achieve the same effect is not clear.

It is intriguing that the small molecule inhibitors of SIRT2 identified by Outeiro *et al.*

A. Dillin is at the Salk Institute for Biological Studies, 10010 North Torrey Pines Road, La Jolla, CA 92037, USA. E-mail: dillin@salk.edu J. W. Kelly is at the Skaggs Institute for Chemical Biology and Department of Chemistry, Scripps Research Institute, 10550 North Torrey Pines Road, La Jolla, CA 92037, USA. E-mail: jkelly@scripps.edu

result in accumulation of larger α-Syn aggregates. This result is consistent with recent data on other proteotoxicity disease models wherein large protein aggregates appear to be protective, whereas smaller aggregates correlate with toxicity (*4*, *7*). Thus, modulation of SIRT2 activity may reveal the toxic intermediate(s) in several protein homeostasis–related maladies.

What is the mechanism by which inhibition of SIRT2 protects against α-Syn–mediated toxicity? SIRT2 colocalizes with the microtubule cytoskeleton and primarily deacetylates lysine-40 of α-tubulin (*8*), but it is not so clear how this relates to its protective effect. Other possible cellular roles of SIRT2 may be accountable. For example, histone deacetylases are required for a process associated with autophagy—a cellular self-digestion mechanism—that involves the recruitment of lysosomes to cytoplasmic inclusion bodies (which contain aggregated proteins) located in microtubule organizing regions. This process, which is observed in Huntington's and Parkinson's diseases (*9*), may involve SIRT2. Previous work also implicates transcription factors (p53 and FOXO) and histones (H3 and H4) as sirtuin-regulated targets, indicating that SIRT2 could block the expression of genes that promote protection against proteotoxicity. SIRT2 may also regulate programmed cell death; antiapoptotic effects are observed when cells either express less SIRT2 or are treated with nicotinamide, a sirtuin inhibitor (*10*, *11*).

Aging appears to be the prominent and unifying risk factor in almost all neurodegenerative diseases. Although the function of sirtuins in neuronal protection has been studied in worms, flies, and rodents, their role in protecting neurons in patients with neurodegenerative diseases remains largely uncharted. Nonetheless, sirtuins are promising pharmacological targets to delay and treat human age-related diseases, owing to signaling pathways shared with lower organisms. The recent discovery of many small-molecule sirtuin regulators, particularly SIRT2 inhibitors (*12*), is especially encouraging. Rapidly emerging data from basic and clinical studies of sirtuins and their small-molecule regulators leave optimists with the feeling that new drugs influencing the signaling pathways associated with aging and protein homeostasis could become a reality in the foreseeable future.

References

1. M. Okawara *et al.*, *Biochem. Pharm.* **73**, 550 (2007).
2. T. F. Outeiro *et al.*, *Science* **317**, 516 (2007).
3. J. F. Morely, H. R. Brignull, J. J. Weyers, R. I. Morimoto, *Proc. Natl. Acad. Sci. U.S.A.* **99**, 10417 (2002).
4. E. Cohen, J. Bieschke, R. M. Perciavalle, J. W. Kelly, A. Dillin, *Science* **313**, 1604 (2006)
5. D. Sinclair, *Nat. Genet.* **37**, 339 (2005).
6. J. S. Steffan *et al.*, *Nature* **413**, 739 (2001).
7. M. Arrasate, S. Mitra, E. S. Schweitzer, M. R. Segal, S. Finkbeiner, *Nature* **431**, 805 (2004).
8. B. J. North, B. L. Marshall, M. T. Borra, J. M. Denu, E. Verdin, *Mol. Cell* **11**, 437 (2003).
9. A. Iwata, B. E. Riley, J. A. Johnston, R. R. Kopito, *J. Biol. Chem.* **280**, 40282 (2005).
10. O. Grubisha *et al.*, *J. Biol. Chem.* **281**, 14057 (2006).
11. T. Araki, Y. Sasaki, J. Milbrandt, *Science* **305**, 1010 (2004).
12. C. M. Grozinger, E. D. Chao, H. E. Blackwell, D. Moazed, S. L. Schreiber, *J. Biol. Chem.* **276**, 38837 (2001).

10.1126/science.1146585

CHEMISTRY

A Counterion Strategy

A new way has been found to control the "handedness" of products formed in metal-catalyzed reactions.

Jérôme Lacour and David Linder

Anions and cations (negatively and positively charged atoms or molecules, respectively) play important roles in chemical reactions as reagents, intermediates, and products. They can be chiral molecules, with two non-identical mirror images called enantiomers (*1*). On page 496 of this issue, Hamilton *et al.* show how a chiral anion can help to produce a chiral reaction product consisting almost exclusively of one enantiomer (*2*). This result is important given the increasing demand from academic, agrochemical, and pharmaceutical laboratories for enantiopure (single-enantiomer) molecules.

In solution, ions and their oppositely charged counterions tend to form ion pairs (*3*). Depending on the solvent, the cations and anions within ion pairs may be separated from each other by solvent molecules or may be close together, allowing one partner ion to influence or even control the environment of the other. The latter situation is, however, rare in solution and, prior to the work by Hamilton *et al.*, had not been observed in homogenous metal-catalyzed reactions.

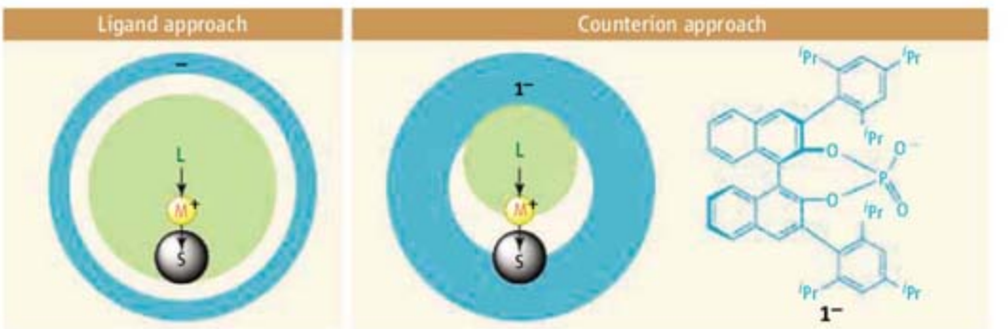

Ligand- versus counterion-mediated enantioselective metal catalysis. Traditionally, product chirality is controlled through the use of enantiopure ligands (L) that are directly bound to the metal ion (M^+)–substrate (S) complex (**left**). In the report of Hamilton *et al.* (**right**), the source of control is an anionic counterion **1**$^-$, it is not directly attached to the metal, but rather controls the selectivity from "afar."

When chiral ions are combined with enantiopure counterions, two different ion pairs can form, which—through the influence of the counterion—can possess rather different chemical and physical properties. If one of the pairs is energetically more stable than the other, it is formed preferentially (*4*). This unbalance has been exploited in the past to achieve high level of asymmetric recognition between chiral cations and anions, leading to efficient processes of resolution, asymmetry induction, and synthesis (*5*).

However, in the field of catalysis, for a long time only cationic counterions—and not anionic ones—were able to control the outcome of reactions and to help produce chiral products as single enantiomers (*6*). This has changed recently with several independent reports in the field of enantioselective organocatalysis (a type of catalysis that uses only organic molecules as catalysts). For example, Leitner and co-workers have used a salt containing an enantiopure borate anion as the solvent in an aza-Baylis-Hillman reaction; the resulting product consisted mostly of one enantiomer, with an ee (enantiomeric excess) of up to 84% (*7*). List and Mayer have

The authors are in the Department of Organic Chemistry, University of Geneva, 1211 Geneva 4, Switzerland. E-mail: jerome.lacour@chiorg.unige.ch

shown that a phosphate anion of type **1** (the same as that used by Hamilton *et al.*; see the figure) can modulate the enantioselective transfer hydrogenation of α,β-unsaturated aldehydes, with an ee of up to 98% (*8*).

However, no chiral-anion–mediated metal catalysis with high enantioselectivity was reported, despite the fact that transition metal–based systems are usually cationic. Most researchers considering the strategy of a metal center surrounded directly by one or more bound enantiopure ligands more efficient (see the figure, left panel); the use of chiral anionic counterions residing in the second coordination sphere of the metal ion (see the figure, right panel) was deemed less effective and predictable.

An opportunity arose in the burgeoning area of homogenous gold catalysis (*9, 10*). Many reactions—including intramolecular nucleophilic additions of alcohols, tosylamines, and carboxylic acids to allenic fragments—are effectively promoted by catalytic amounts of Au(I) ions and phosphine ligands (L). However, highly stereoselective reactions with broad substrate scope have been hard to achieve with the traditional chiral ligand/metal ion strategy (*11*).

Capitalizing on their recent observation that some Au(I)-catalyzed reactions are sensitive to the nature of the anionic counterion (*11*), Hamilton *et al.* hypothesized that an enantiopure counterion of type **1** could be the key to an effective asymmetric transformation of these reactions. Using this approach, they achieved very high level of stereoinduction (ee up to 99%). The protocol can be used for various allenic alcohols and tosylamines. In the case of substrates that lack sterically demanding substituents and for which high enantioselectivity is therefore difficult to achieve, the chiral anion strategy remains efficient (ee 80%); when a chiral phosphine ligand acts in synergy with the anionic counterion, a higher proportion of the major enantiomer is produced (ee 92%). Hamilton *et al.* show that this dual approach of combining chiral ligands and anionic counterions is also effective in the hydroxycarboxylation of allenes, for which the use of either chiral ligands or chiral anions alone fails to succeed.

The work of Hamilton *et al.* may open a new chapter in asymmetric homogenous metal catalysis. There is much to gain from this modular and supramolecular approach, because it may, in some cases, be sufficient to exchange traditional achiral anionic counterions for chiral versions at the last step of the catalyst preparation. However, it remains to be seen how broadly applicable this approach will be. Deep understanding of the mechanisms at play in chiral ion pairing situations may prove to be necessary, possibly requiring the use of modern nuclear magnetic resonance techniques and computational studies (*2, 12, 13*).

References and Notes

1. E. L. Eliel, S. H. Wilen, *Stereochemistry of Organic Compounds* (Wiley, New York, USA, 1994).
2. G. L. Hamilton, E. J. Kang, M. Mba, F. D. Toste, *Science* **317**, 496 (2007).
3. A. Macchioni, *Chem. Rev.* **105**, 2039 (2005).
4. D. Monchaud *et al.*, *Angew. Chem. Int. Ed.* **41**, 2317 (2002).
5. J. Lacour, V. Hebbe-Viton, *Chem. Soc. Rev.* **32**, 373 (2003).
6. K. Maruoka, T. Ooi, *Chem. Rev.* **103**, 3013 (2003).
7. R. Gausepohl *et al.*, *Angew. Chem. Int. Ed.* **45**, 3689 (2006).
8. S. Mayer, B. List, *Angew. Chem. Int. Ed.* **45**, 4193 (2006).
9. A. S. K. Hashmi, G. J. Hutchings, *Angew. Chem. Int. Ed.* **45**, 7896 (2006).
10. E. Jimenez-Nunez, A. M. Echavarren, *Chem. Commun.*, 333 (2007).
11. R. L. LaLonde, B. D. Sherry, E. J. Kang, F. D. Toste, *J. Am. Chem. Soc.* **129**, 2452 (2007).
12. P. S. Pregosin, P. G. A. Kumar, I. Fernandez, *Chem. Rev.* **105**, 2977 (2005).
13. L. N. Appelhans *et al.*, *J. Am. Chem. Soc.* **127**, 16299 (2005).

10.1126/science.1146922

MICROBIOLOGY

Necessary Noise

The randomness of a switch between two alternative bacterial states has been traced to the variable expression of a single protein.

Jerome T. Mettetal and Alexander van Oudenaarden

In the classic view of cellular biology, cells are simply a product of genetic and environmental conditions, and all differences between individual cells can be attributed to one or both of these factors. Recent work, however, suggests that when grown in the same environment, cells from genetically identical populations can exhibit very different behaviors. Even simple attributes, such as the number of proteins produced from a constitutively expressed gene, can vary greatly from cell to cell. In other cases, individual cells will make vastly different phenotypic choices seemingly at random (*1–4*). Why some cells remain in one phenotypic state whereas others switch to a different one, and what the molecular processes are that cause cells to "play dice" when determining their fate, remain open questions.

The authors are in the Department of Physics, Massachusetts Institute of Technology, Cambridge, MA 02139, USA. E-mail: avano@mit.edu

On page 526 in this issue, Maamar *et al.* (*5*) tackle these questions using the soil bacterium *Bacillus subtilis*. They find that the random nature of the phenotypic choice made by these bacteria to remain vegetative (dormant) or become "competent" (able to take up DNA from the environment) can be traced to variable expression of a single protein. Although many organisms exhibit phenotypic variability driven by stochastic gene expression, the *B. subtilis* system is of particular interest because variation ("noise") in protein expression is thought to play a key role in the natural behavior of a population.

Under certain conditions, only some bacteria exit a vegetative state and become competent. The key protein orchestrating this process, ComK, also spurs its own expression by acting as a transcription factor. This autoregulatory positive-feedback loop enables cells to stably reside at either a low or a high level of ComK expression, corresponding to vegetative and competent states respectively. In the vegetative state, cells have too few ComK proteins to activate further *comK* gene expression, ensuring that the concentration of this protein remains low. By contrast, in the competent state, ComK is produced in large quantities, ensuring that the gene remains highly expressed. Further, there is a critical quantity of ComK that separates the two states; cells with a ComK protein concentration above this threshold will become competent (see the figure). It is thought that in vegetative cells, rare fluctuations in protein concentrations can cause cells to cross this threshold.

To determine the source of the fluctuations that drive this transition, Maamar *et al.*, use a fluorescent probe that binds to messenger RNA (mRNA) in situ to measure individual mRNAs produced from the endogenous *comK* gene and from a synthetic gene with an identical upstream promoter region. By measuring correlations in mRNA expression, they

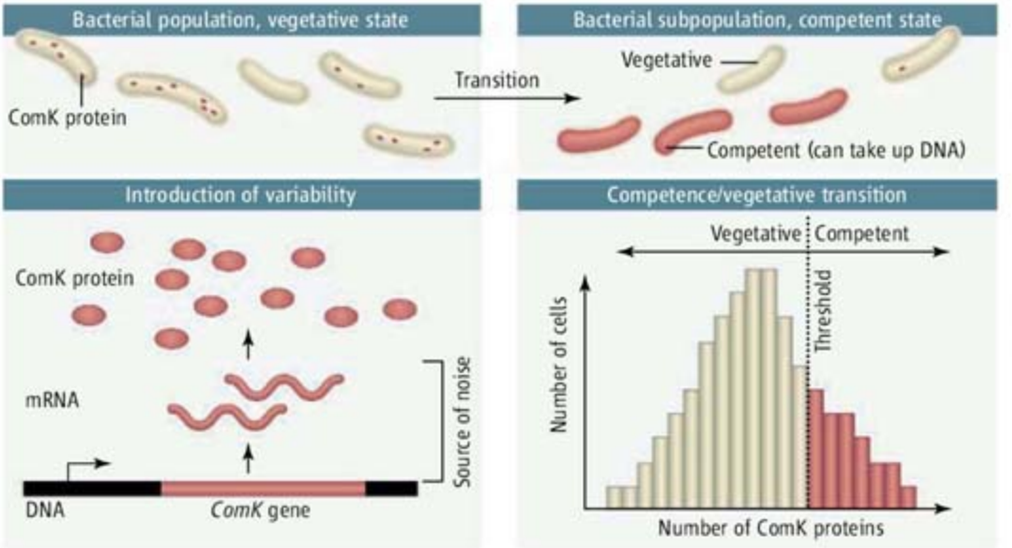

Randomly flipping a cell-fate switch. A population of bacteria can express variable amounts of ComK protein. Only cells that express greater than a threshold concentration of ComK become competent. Cell-to-cell variation in ComK protein expression ("noise") arises from variations in comK mRNA concentration across the cell population.

find that noise in ComK protein expression comes mainly from random production and/or degradation of *comK* mRNA, rather than from external factors (such as variability in ribosome numbers from cell to cell).

To demonstrate that noise in *comK* gene expression is the key factor causing cells to transition to competence, Maamar *et al.* modified a strain (which has an increased basal *comK* mRNA production) by decreasing the rate of translation initiation. This reduces noise (*6*) while keeping the average comK protein concentration fixed. In the modified strain, low noise levels caused cells to transition into the competent state less frequently than wild-type cells. In other words, the reduced-noise strain produces more mRNA, but less protein from each mRNA. This reduces the amount of variability in mRNA expression levels, and thus variability in protein concentration.

In a complementary study, Süel *et al.* (*7*) create a strain in which bacteria cannot complete cell division, causing multiple cells to share cytoplasm. In this strain, cell-to-cell variability is reduced because connected cells share proteins, averaging away differences in protein concentrations between cells. Like Maamar *et al.*, they find that a decrease in cell-to-cell variability leads to a decrease in transitions to the competent state.

Maamar *et al.* and Süel *et al.* provide a comprehensive microscopic view of how stochastic fluctuations in gene expression can cause cells to change their phenotype. An even clearer picture of such cell decision-making might be attained by coupling real-time measurements of mRNA and protein concentrations (*8*, *9*) with switching events in single living cells. There remains the nagging question of why the population only allows a fraction of its cells to become competent. By splitting the population into two phenotypes, *B. subtilis* may use naturally occurring noise to increase population diversity and enhance survival in the face of environmental uncertainty (*10*–*12*). It is possible that evolution has been using a strategy of modifying transcription and translation rates to fine-tune the noise levels (*5*, *6*) of key genes that underlie phenotypic diversity in a population.

References

1. M. Kaern, T. C. Elston, W. J. Blake, J. J. Collins, *Nat. Rev. Genet.* **6**, 451 (2005).
2. M. S. Samoilov, G. Price, A. P. Arkin, *Sci. STKE* **2006**, re17 (2006).
3. N. Maheshri, K. O'Shea E, *Annu. Rev. Biophys. Biomol. Struct.* **36**, 413 (2007).
4. B. B. Kaufmann, A. van Oudenaarden, *Curr. Opin. Genet. Dev.* **17**, 107 (2007).
5. H. Maamar, A. Raj, D. Dubnau, *Science* **317**, 526 (2007); published online 14 June 2007 (10.1126/science.1140818).
6. E. M. Ozbudak, M. Thattai, I. Kurtser, A. D. Grossman, A. van Oudenaarden, *Nat. Genet.* **31**, 69 (2002).
7. G. M. Süel, R. P. Kulkarni, J. Dworkin, J. Garcia-Ojalvo, M. B. Elowitz, *Science* **315**, 1716 (2007).
8. I. Golding, J. Paulsson, S. M. Zawilski, E. C. Cox, *Cell* **123**, 1025 (2005).
9. L. Cai, N. Friedman, X. S. Xie, *Nature* **440**, 358 (2006).
10. M. Thattai, A. van Oudenaarden, *Genetics* **167**, 523 (2004).
11. E. Kussell, S. Leibler, *Science* **309**, 2075 (2005).
12. D. M. Wolf, V. V. Vazirani, A. P. Arkin, *J. Theor. Biol.* **234**, 227 (2005).

10.1126/science.1146747

ECONOMICS

Spying on Others Evolves

Watchful eyes induce altruistic behavior and an "arms race" of signals between observers and the observed.

Manfred Milinski and Bettina Rockenbach

When reputation is at stake, animals as well as humans switch from selfish to altruistic behavior, because only the latter is socially rewarded (*1*, *2*). But how do they assess whether their actions are observed? Recent investigations into human behavior have shown that subtle cues of being watched such as two stylized eye-like shapes on a computer screen background suffice to change behavior (*3*). A picture showing a pair of eyes attached to a cafeteria collection box significantly raises the donated amount compared to a flower symbol; in fact, the eyes were most effective when looking directly at the observer (*4*).

Although just ink on paper, these eye-shaped cues seem to elicit unconscious hard-wired reactions. Indeed, electrophysiological responses recorded from the scalp of normal subjects showed responses to isolated eyes that are even larger than the responses to full faces (*5*). Brain imaging studies in humans have also highlighted a role for the superior temporal sulcus (STS) and amygdala in gaze processing; the STS is likely to be essential for recognizing the eyes, head, and body as stimuli used in social communication, whereas the amygdala is likely to be essential for attaching social and emotional significance to these stimuli (*6*). Interestingly, even birds respond strongly to eye-like shapes, especially when two eyes are staring at them (*7*).

What is the benefit of watching someone? Spying on others seems widespread in animals and humans (*8*). By snooping on one another's social life, animals and humans can work out how to behave when they meet in the future. Recent experiments

M. Milinski is in the Department of Evolutionary Ecology, Max Planck Institute for Evolutionary Biology, D-24306 Plön, Germany. B. Rockenbach is in the Department of Economics, University of Erfurt, D-99089 Erfurt, Germany. E-mail: milinski@mpil-ploen.mpg.de, bettina.rockenbach@uni-erfurt.de

CREDIT: ADAPTED BY P. HUEY/SCIENCE

showed that even fish gain sophisticated information from watching members of the same species (*9*). Some fish can infer the social rank of others by observation alone and use this information to their own advantage in future encounters (*10*). So it comes as no surprise that both humans and animals try to deceive observers by behaving as they want to be seen by others to secure future gains.

For example, the cleaning wrasse fish grooms its client fish in the friendliest way when other clients watch, but without an audience it prefers to bite off pieces of its client's skin (*11*). In a dictator game experiment, only one player (the dictator) is endowed with money and may share it with a second player. Although unidentifiable human "dictators" share almost nothing (*12*), face-to-face identification increases the share rate to 50% (*13*). Consequently, in order to gain accurate information, observers should avoid being recognized: Indeed, some social birds have eyes concealed in dark areas or stripes, ensuring that the observed individual cannot detect being the target (*14*).

Are you being naughty or nice? Totem poles put up in villages in North America several hundred years ago standing vigilant at attention, with ever-watchful eyes. Unlike natural goats, the stylized goat has "human eyes" with white sclera stressing the direction of his gaze.

CREDIT: TONY J. PITCHER/UNIVERSITY OF BRITISH COLUMBIA

This is where humans differ from most animals. We have large white sclera on either side of the dark central iris when looking directly at the observer. This seems to be an honest signal of where we watch (*6*). Obviously there has been a net selective advantage of signaling the direction of our gaze in social interactions. However, having such eyes should be disadvantageous when trying to observe others' "unobserved" behavior, because we should take into account that the observed person turns altruistic as soon as our observing gaze is recognized.

Can we escape being watched? Whenever a person can be recognized by any cue, bad conduct may incur costs. Instead of behaving altruistically, people sometimes avoid having to justify their behavior by masking their faces, for example, at a masked ball, when robbing a bank, etc. Interestingly, the usual way to remove the identity of people on photos is to cover their eyes by a black stripe. Visual cues of faces seem to be of prime importance. Thus, either masking such cues or paying attention to being watched may be socially selected.

Thus, a new dimension arises when issues of reputation are present in human social dilemmas. An "arms race" of hiding signals between observers and observed may result: Observer Alice should take into account that the behavior of Bob (the observed) changes and therefore should conceal her watching; Bob should be very alert to faint signals of being watched by Alice, but he should avoid any sign of having recognized Alice's watching when switching from selfish to altruistic behavior. He should avoid turning his gaze in the direction of the recognized observer. On the other hand, as soon as Alice sees that Bob has recognized that he is being observed, she should eventually not reward the observed altruistic behavior.

An arms race between observing and being observed has implications for the large body of recent research on human altruism. Observed altruistic behavior may often be less the expression of a personal trait than an optimal response to the faint feeling of being observed. Would altruism then function as a potential deceit? For example, what we expect for the efficient interaction between reputation and costly punishment in social dilemmas—where individual and social interests are at odds—might depend on the recognized state of the signaling arms race (*15*). When cues revealing that the observed person has discovered the observation are indeed so subtle that altruism is a successful deceit, the positive effects of reputation can be expected to be present to a much greater extent. However, when the observer can conceal his spying, reputation is subjectively not at stake and thus will not induce altruism.

Does the observer thus really want to see "unobserved" behavior? Yes, but only if the social partner interacts with the observer mostly anonymously and she profits from seeing his "normal" behavior and reacts accordingly. Otherwise she should try her best to generate the impression that her social partners always feel observed so that their "normal" behavior is altruistic. Perhaps this is achieved in some societies by the ever-present watchful eyes of totem poles (see the figure) or a god that "sees through everything." Even actors on billboards, a modern form of ink on paper, may elicit unconscious social reactions in our amygdala and thus influence our behavior.

References

1. R. Bshary, A. S. Grutter, *Nature* **441**, 975 (2006).
2. M. Milinski, D. Semmann, H.-J. Krambeck, J. Marotzke, *Proc. Natl. Acad. Sci. U.S.A.* **103**, 3994 (2006).
3. K. J. Haley, D. M. T. Fessler, *Evol. Hum. Behav.* **26**, 245 (2005).
4. M. Bateson, D. Nettle, G. Roberts, *Biol. Lett.* **2**, 412 (2006).
5. S. Bentin *et al.*, *J. Cogn. Neurosci.* **8**, 551 (1997).
6. N. J. Emery, *Neurosci. Biobehav. Rev.* **24**, 581 (2000).
7. M. Scaife, *Anim. Behav.* **24**, 200 (1976).
8. J. Whitfield, *Nature* **419**, 242 (2002).
9. R. F. Oliveira, P. K. McGregor, C. Latruffe, *Proc. R. Soc. London B* **265**, 1045 (1998).
10. L. Grosenick, T. S. Clement, R. D. Fernald, *Nature* **445**, 429 (2007).
11. R. Bshary, *Proc. R. Soc. London B* **269**, 2087 (2002).
12. E. Hoffman, K. McCabe, V. L. Smith, *Am. Econ. Rev.* **86**, 653 (1996).
13. I. Bohnet, B. S. Frey, *Am. Econ. Rev.* **89**, 335 (1999).
14. L. Gavish, B. Gavish, *Z. Tierpsychol.* **56**, 193 (1981).
15. B. Rockenbach, M. Milinski, *Nature* **444**, 718 (2006).

10.1126/science.1143918

PHYSICS

Pierre-Gilles de Gennes (1932–2007)

Pierre-Gilles de Gennes, one of the greatest physicists of the 20th century, extended the field of condensed-matter physics toward chemistry, biology, and engineering sciences.

Armand Ajdari

Described as the "Isaac Newton of our time" by the Royal Swedish Academy in the citation for his Nobel Prize in Physics in 1991, Pierre-Gilles de Gennes died on 18 May 2007 at the age of 74. Beyond the remarkable lecturer and the advocate of science and scientific research cherished by media and students, Pierre-Gilles de Gennes was above all one of the greatest physicists of the 20th century. The depth and breadth of his scientific achievements are exceptional. In the last year of his life, de Gennes published articles in five different areas, from the motion of dislocations in the quantum regime to the storage of olfactory information in the brain.

De Gennes was born in 1932 to a family of medical doctors. He began his academic career at the Ecole Normale Supérieure in Paris, followed by 4 years at the Commissariat à l'Energie Atomique in Saclay. In his early work, he focused on magnetism, studying the scattering of neutrons in metallic materials close to magnetic transitions, as well as questions regarding spin waves and rare earths. A postdoctoral stay at Berkeley in the group of Charles Kittel followed, before a 2-year stint in the French Navy.

Moving to Orsay in 1961, de Gennes founded an experimental and theoretical effort on superconductors. His work led to important insights into surface superconductivity and into superconductivity without bandgap. Around 1968, de Gennes began to revisit the field of liquid crystals, drawing fruitful formal analogies with superconductors. His insights had a substantial impact on the physical understanding of these materials, which now play an important part in many technologies such as liquid crystal displays.

In 1971, de Gennes was appointed professor at the Collège de France. He then shifted his interest to polymers and to other topics previously categorized as chemistry. Drawing on his creativity, his genius at simplifying problems, and his ability to establish connections with sophisticated formal theories of statistical physics, he demonstrated the power of physics in dealing with these systems. This field is today called soft condensed-matter physics. As he had done previously, de Gennes teamed up with experimentalists at the Collège de France, in Saclay, and in Strasbourg to stimulate his creativity and validate his predictions.

One of his remarkable achievements in that period is the "$n = 0$" theorem, a formal equivalence between the description of magnetic phase transitions and the statistical physics of very long polymer chains, in the exotic limit where the number of components of the magnetization vectors is zero. He also introduced simple tools to explain the properties of polymers without complex computations. The best known is the concept of the "blob" to represent a subsection of a polymer chain short enough to be only weakly affected by external perturbations. This concept proved highly useful for describing, for example, semi-dilute polymer solutions and chains confined or in flows. De Gennes moreover invented the theory of reptation, which describes the complex dynamics of an entangled set of polymer chains through the much simpler representation of a single chain reptating in the "tube" in which it is encaged by the other chains. This theory forms the basis of our current understanding of how molten plastics and polymer solutions flow.

In the 1980s and 1990s, de Gennes continued to study polymers, but also turned his attention to new topics, such as wetting, adhesion, fracture, friction, and granular materials. When he moved to the Institut Curie in 2002, he began to study biological problems, including cellular adhesion, brain function, and chemotaxis of bacteria.

De Gennes often reported his results in short letters that combined simplicity, elegance, and deep insight. These qualities also characterize his major textbooks on superconductors, liquid crystals, and polymers.

Throughout his career, de Gennes was interested in the potential applications of his insights. Many of his results have led to industrial or biomedical innovations impacting our lives, such as improved polymer processes in the plastics industry and the use of DNA gel electrophoresis for genomic studies. De Gennes always maintained links with industrial companies, which provided a stimulus for his own research (triggering, for example, his interest in aquaplaning, enhanced oil recovery, and emulsions). In return, he contributed to the transfer of knowledge from academia to the industrial world.

De Gennes possessed remarkable pedagogical talents. His weekly lectures at the Collège de France were beautiful and attracted both scientists and nonspecialists. He also devoted much energy to modifying and developing the Ecole Supérieure de Physique et Chimie Industrielles (ESPCI), a Parisian Grande Ecole for the training of engineers, which he headed from 1976 to 2002. In particular, he introduced two practices for students traditionally rare in the French system: interactions with faculty or researchers in small groups, and an emphasis on laboratory experiments. De Gennes was an active herald of scientific research, advocating critical observation of nature and hard work as a path to better understanding. He engaged in a genuine "Tour de France" of talks in high schools (more than 150 in the 2 years that followed his Nobel Prize), made frequent appearances in the media, and was much appreciated by the public for his charming and original personality and his graceful explanations of complex phenomena in simple terms.

CREDIT: F. WYART

Above all, his collaborators will remember de Gennes's permanent intellectual appetite, implacable professionalism, and taste for life. All these were served by a unique personality and elegance, displayed in his gestures, in his papers and books, in his lectures, in his drawings, and in his way of relating simply and efficiently to people. Un grand monsieur.

10.1126/science.1146688

The author is at ESPCI, 10 rue Vauquelin, 75005 Paris, France, and at Saint-Gobain, Les Miroirs, 18 av. d'Alsace, 92096 La Défense Cedex, France. E-mail: armand.ajdari@saint-gobain.com

SCIENCE POLICY

AAAS Expands Vital Science Outreach Efforts on Capitol Hill

With issues such as stem cell research, climate change, and alternative fuels increasingly prominent—and urgent—on the U.S. policy agenda, AAAS has moved to expand and strengthen its role as a source of authoritative scientific insight for members of Congress and their staffs.

This year, AAAS CEO Alan I. Leshner testified twice before Congress on the need for a balanced approach to federal research and development funding. AAAS also weighed in on stem cell and science education bills with letters to the U.S. House of Representatives and the Senate, urging the expansion of federally funded embryonic stem cell research and supporting national standards for math and science education.

The AAAS Board issued a statement just before a House committee hearing this spring warning of the diminishing U.S. capacity to use satellites for scientific observation of the Earth. In June, AAAS's Center for Science, Technology and Congress released two briefs on the policy pros and cons of biofuels and coal-to-liquid fuel technology as both houses of Congress consider complex, far-reaching energy bills.

AAAS's constructive relationship with Washington, D.C., policy-makers has a long history. Its Science & Technology Policy Fellowship program, now in its 34th year, has placed about 2000 scientists in temporary policy positions in Congress and in federal agencies, and many have stayed in the policy realm. The R&D Budget and Policy Program is regarded as the gold standard of analysis related to federal funding for science and technology. The 3-year-old Center for Science, Technology and Security Policy regularly holds briefings for congressional staff, with subjects this year ranging from security of U.S. food supplies to the Reliable Replacement Warhead program.

The Center for Science, Technology and Congress has served as a crucial liaison between the scientific community and Congress for over a decade. In recent months, it has been critical in AAAS's effort to expand engagement with elected lawmakers on Capitol Hill.

The repeat invitations to testify before Congress are one indicator of how the Hill has come to rely on AAAS's work. "The way Congress works, they need witnesses on relatively short notice, and we're able to provide a good statement and do the research in a relatively short period of time," said Joanne Padrón Carney, director of the Center for Science, Technology and Congress.

Gary Kline, a veteran legislative staffer now working for Rep. Brian Bilbray (R-Calif.), praised AAAS's reliability. "One of the things I really love about AAAS is that it's a one-stop society, someplace where I can go to find nonbiased information and experts if I need to talk with someone," he said. "They're very easy to work with and they do a great job on their briefings."

The Center launched an online legislative tracker in February to keep up with Congress's work in progress, and recently unveiled a comprehensive chart of the eight different climate change bills working their way through the House and Senate.

The Center itself has doubled in size in the past 2 years, adding senior program associates Erin Heath, who specializes in life sciences policy; Kasey White, who focuses on climate change and environmental science; and program assistant Lina Karaoglanova, who also works with climate issues. White edits the Center's monthly newsletter, *Science and Technology in Congress*, which reaches over 1000 Hill staffers, federal agency officials, and lobbyists.

The newsletter analyzes high-profile topics in Congress such as science education, innovation and economic competitiveness, export controls, and visa regulations. Such issues "affect the conduct of science as a whole" and make them prime targets for AAAS's work, White said.

"AAAS has worked with Congress throughout much of its nearly 160-year history," said Albert H. Teich, director of AAAS Science & Policy Programs, "but it's never before had the kind of influence it does today."

For more information about the Center for Science, Technology and Congress, and for access to its briefings and other resources, see www.aaas.org/spp/cstc.

—Becky Ham

INTERNATIONAL

Brazilian Scientist Sees Hope, Hype in Ethanol

A world thirsty for new energy sources should be cautious about ethanol "hype" because the technology to efficiently produce large amounts of the fuel may be a decade or more away, influential Brazilian scientist José Goldemberg said at AAAS.

José Goldemberg

Goldemberg, a physicist and former secretary of state for Science and Technology in Brazil, said in a 27 June lecture that the United States and other nations have suitable croplands to support ethanol production. The Brazilian program, started in the 1970s, derives fuel from sugarcane and has cut the nation's gasoline consumption by 40%.

But Goldemberg warned that any substantial boost in global ethanol production will require improvements in current technologies, such as more efficient distilleries, as well as breakthroughs in converting cellulose molecules in wood and other biomass into fuel. Researchers are looking to genetically modify cellulose so it can be more easily broken down, he said, and also are trying to genetically engineer microorganisms to do the job.

During his visit to Washington, Goldemberg also spoke at a 25 June Capitol Hill briefing about his nation's small nuclear energy program. In 1991, he said, he was able to convince Fernando Collor de Mello—Brazil's first elected president in more than 25 years—to abandon initial steps toward developing nuclear weapons.

Goldemberg, now at the University of São Paulo, also has served in Brazil as interim secretary of the Environment; minister of Education; and president of the Brazilian Association for the Advancement of Science.

His ethanol seminar was cosponsored by AAAS and the Washington Science Policy Alliance. The Capitol Hill briefing was arranged by AAAS's Center for Science, Technology and Security Policy.

—Earl Lane and Benjamin Somers

Search Technologies for the Internet

Monika Henzinger

About 20% of the world's population uses the Web, and a large majority thereof uses Web search engines to find information. As a result, many Web researchers are devoting much effort to improving the speed and capability of search technology.

A Web search engine consists of two parts: an offline part that gathers Web pages and builds an internal representation of them called an (inverted) index, and an online part that serves user requests by finding all matching documents and ordering or ranking them with the goal of presenting the most relevant documents on top (Fig. 1). To this day, index comprehensiveness and good result ranking are the main challenges faced by Web search engines and are the areas in which Web search engines are competing most fiercely. This article describes these challenges and some solutions, concentrating on the information retrieval aspects of Web searching. It does not discuss the questions arising in the design of the infrastructure needed to support large-scale search engines [see, e.g., (*1*, *2*)].

The first Web search engines became available about 15 years ago. They indexed tens of millions of Web pages and served hundreds of thousands of searches per day. These seemed like large numbers at the time, but since then, Web search engines have had to increase their capacity enormously. Currently, they are indexing tens of billions of Web pages and serving hundreds of millions of Web searches per day. In addition, the quality of the search results has improved noticeably. The first Web search engines used text-only ranking algorithms that had been developed in the field of information retrieval during the preceding 30 years. However, these techniques were designed for searching document collections of well-written, homogeneous articles, such as newspaper archives, that are mostly searched by librarians and other search specialists. In this setting, the comprehensiveness of the results is as important as its relevance. On the Web, the pages are heterogeneous and of varying quality, and the majority of searches are performed by novices. The user looks frequently only at the top 10 results (*3*). Thus, for many queries, the relevance of the top results is more important than the comprehensiveness of the result set. Because the text-only techniques employed by the first search engines were not designed for this setting, the quality of the results was frequently poor.

A substantial improvement in the quality of Web search results was possible through the analysis of the hyperlink structure of the Web (*4*, *5*). Hyperlinks are navigation elements in Web pages. When clicked on, a hyperlink loads into the browser window a different part of the current Web page or a different Web page. Hyperlinks in Web pages serve a similar purpose as do references in scientific articles. In 1955, Garfield showed that an analysis of the structure of

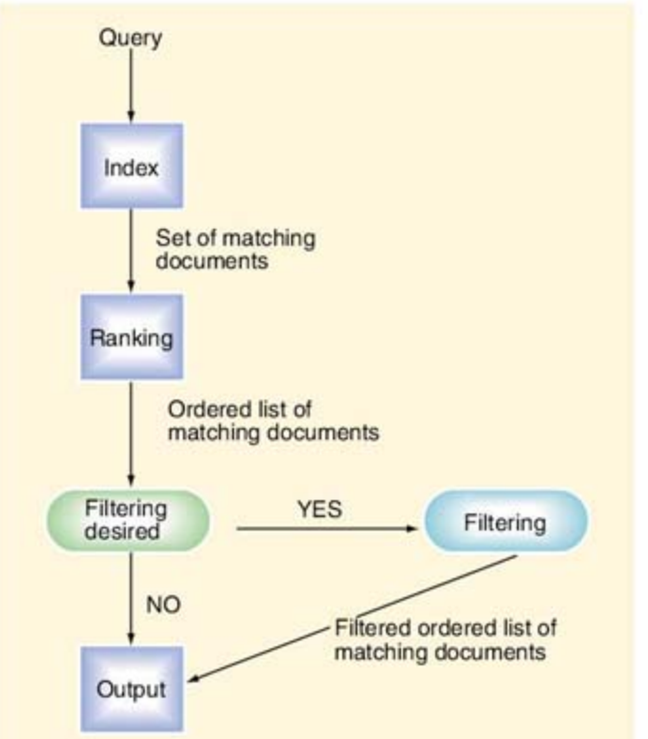

Fig. 1. Steps of a query. The filter can be, for example, a filter for inappropriate content or a language filter.

references can determine the importance of scientific articles and journals (*6*). A similar analysis of the hyperlink structure of the Web gives an estimate for the quality of Web pages. This analysis leads to a query-independent estimate of page quality. To deploy it in a ranking algorithm, it needs to be combined with query-specific signals, such as the frequency of the query terms on the Web page. Google was the first commercial Web search engine to use this kind of hyperlink analysis in its ranking through its PageRank measure (*4*). Mathematically speaking, the PageRank vector contains one entry per Web page and is the Eigenvector of a matrix derived from the hyperlink structure of the Web. If the matrix is seen as a linear transformation of vectors, then the Eigenvector is the vector whose direction is not changed by the transformation. Thus, the PageRank vector can be viewed as an inherent property of the whole Web structure. Informally speaking, hyperlinks are interpreted as recommendations, and PageRank tries to measure how highly recommended a page is. If many hyperlinks point to a page, its PageRank is large. If the pages containing these hyperlinks have high PageRank themselves, that is, are highly recommended, then the PageRank of the page increases even further.

Even though comprehensiveness and result quality of Web search engines have progressed steadily, there is still much room for improvement. Search engines cannot index all Web pages but only the pages that are publicly available and accessible without further "form-filling" actions, like filling in text in boxes or checking buttons on Web pages. By definition, Web pages that are not publicly available are not supposed to be available to the general public. Form filling, however, creates a challenge. Frequently, forms are the only way to access large amounts of information stored in online databases. It is conjectured that this information constitutes a large fraction of the "deep Web," which is the name given to the part of the Web that is not indexed by popular search engines (*7*).

There are many challenges that make ranking difficult. Some of the most important are (i) Many queries are short and underspecified. (ii) Synonyms and homonyms make it difficult to decide whether a page is relevant to a query or not. This classic problem of information retrieval is exacerbated on the Web by homonyms between languages. (iii) Ranking the most authoritative results first is made harder by authors who specifically design their Web pages so as to place them high for certain, mostly commercial searches. This is called search engine spam (not to be confused with e-mail spam). (iv) Users ask for additional features, such as filters for inappropriate content.

Here, I report on some of the ongoing research to address the above questions. I use the term "search engine" to denote a commercial Web search engine and the terms "Web page" or "page" to denote a document publicly accessible on the World Wide Web.

Comprehensiveness

The goal of search engines is to find the most relevant documents for user queries. Because of

Google Switzerland and Ecole Polytechnique Fédérale de Lausanne, 1015 Lausanne, Switzerland. E-mail: monika.henzinger@epfl.ch

the great variety in information needs, search engines must be very comprehensive. One way to achieve this is by indexing as many Web pages as possible. However, the larger the index, the higher is the cost per search for a search engine, because more machines are needed to store and search the index (*8*). Additionally, the more Web pages have already been indexed, the harder it becomes to find pages with new content, that is, content that is not contained in already indexed Web pages. Considering the diminishing returns and increasing cost of larger indices, search engines stop gathering pages after certain criteria regarding the size and coverage of various languages have been met.

A plethora of content is stored in databases rather than in typical Web pages. The pages as well as their URLs (*9*) are created in response to a user filling out a form on the Web. Because search engines are unable to emulate this behavior, such dynamically generated pages cannot be indexed. There has been some research on trying to make form-filling automatic (*10*, *11*), but the problem remains largely unsolved. On the other hand, if the search engine knew the URL, then it could request the page directly. Thus, a search engine simply needs a list of all URLs accessible at a site. Following this idea, Google has proposed an open protocol (*12*), that is, a format for Web sites to disclose a list of all URLs they want indexed by a search engine. This service is available for all Web sites, not only for Web databases. In exchange for disclosing the list, Google reports back to the site which URLs it could not access, along with query and user click statistics for the site. Yahoo and MSN, as well as organizations with large databases, such as Wikipedia and the *New York Times*, have already adopted this protocol.

Result Ranking

Together with comprehensiveness, the quality of the result ranking is crucial for the success of a search engine. One useful signal for ranking is anchor text. Anchor text is the text associated with a hyperlink, usually appearing in blue font. Clicking on it brings the user to the Web page of the associated URL, that is, the page to which the hyperlink points. For ranking purposes, many search engines treat the anchor text as if it were part of the text on the page that it points to. This is useful because anchor text often gives a concise description of the page and can thus match queries that also use a concise keyword description to retrieve the page. Additionally, the home pages of many companies consist of much graphics but few words, thus not giving a strong signal that the page is the official company home page. In such situations, anchor text can often be relied on to identify the homepage.

Handling short or underspecified queries. The average query length has not changed much over the years and is less than three terms. Depending on the type of query, short queries may cause a problem. Queries are roughly classified into these three types (*13*): (i) informational queries, whose goal is to obtain information regarding a topic of interest; (ii) navigational queries, whose goal is to find a specific Web page, such as the home page of a company; and (iii) transactional queries, whose goal is to perform a desired action, such as downloading a certain software package. For navigational and transactional queries, short queries are often sufficient. However, informational queries frequently need more information about the user's topic of interest. A recent study found that many informational queries are not specific enough; it showed that the users' information needs vary greatly even when they use the same query terms (*14*). For example, for the query "trailblazer" one user might want information about the car, whereas another user might want information about the basketball team.

To address this problem, either the user needs to be enticed to be more specific, for example, by refining the search, or user-specific information needs to be taken into account. On the Web, most users are reluctant to do additional work. Thus, the area of automatically exploiting user-specific information so as to personalize result rankings has received considerable attention.

To personalize a search, the search engine needs to know what the specific user is currently looking for (short-term interest). If this is not clearly expressed, then the general interests of the user (long-term interests) may be helpful. Thus, algorithms try to build a model of both the short-term and the long-term user interests. The model can either (i) suggest additional search terms or completely new queries to the user [see, e.g., (*15*)] or (ii) reorder the search results automatically. Recall that the ranking of a search engine usually depends on both query-dependent and query-independent signals. Hence, the reordering can personalize either query-dependent signals, for example, by automatically adding words suggested by the model to the query, or query-independent signals, for example, by using a personalized PageRank.

Data sources for the short-term model are queries issued by the user in the same session or the session history of other users with similar queries. Data sources for the long-term model are search-related user information, such as the user's query and browsing history, and search-independent user information, such as documents and e-mail that the user has read and personalized information that the user provided to the search service. For example, based on the knowledge that the user is a car enthusiast or based on the fact that his or her previous query was for "Chevrolet," the system could automatically add the word "car" to the query "trailblazer." The first studies employing automatically created short-term and long-term models to rerank search results with query-dependent signals found noticeable improvements in search quality (*16*–*18*). More research is under way to explore the full strength of this approach.

Personalizing query-independent signals, specifically PageRank, has also received much attention. This is challenging, because the PageRank computation is time and space intensive. It is time intensive because it requires the solution of a linear system with as many equations and variables as there are Web pages. It is space intensive because it requires storage of a PageRank score for every Web page. Thus, storing a personalized PageRank for every user would be very resource expensive. The current state of the art (*19*) in the personalization of PageRank allows the computation of about 100,000 topic-related PageRanks, which can be arbitrarily combined by a user. See (*20*, *21*) for reviews on the topic.

Handling synonyms and homonyms. Web search engine users have come to expect that their exact query terms appear in the documents of the result set. Thus, search engines are reluctant to return documents that contain synonyms of the query terms but are lacking one of the query terms. At best, they suggest alternate queries that contain synonyms of the original query terms.

An interesting question is what results should be returned in the top 10 for homonyms such as "jaguar." One of the top three dominant search services returns seven results on cars, one on the cat, one on a Macintosh OS X version, and one on a quantum chemistry software package called Jaguar. A second search engine returns four results on cars and four on the animal, one on a sports team, and one on a rock band. The third search service returns six results on cars and four on the animal. This points to a constant discussion in Web searching [see, e.g., (*22*)]: How much diversity should there be in search results? Automatically detecting whether more diversity is needed for a given query is still an open research question.

Some problems with homonyms are due to overlap of words or names of people with names of locations. This has led to interesting research with the goal of detecting the geographic context of a query. Such research addresses two issues: determining the geographic context for queries that do not contain a location but have a geographic context, such as "space needle," and detecting the lack of a geographic context in certain queries with location, such as "denzel washington." Simple lookups in geographic dictionaries, called gazetteers, would fail in both cases. The first problem can be addressed by first retrieving the body text of Web pages that have been clicked on by other users for the same query and/or the body text of the top search results; then using a gazetteer to extract all location names; and finally, based on the frequency and spread of these locations, determining a dominant location. For the query "space needle," "Seattle, Washington," would be by far the most frequent location, and the spread of the remaining locations would not show any particular patterns. Thus, "Seattle" would be selected as the

dominant location. The second problem can be addressed in a similar way. The results for the query "New York Times," for example, would most likely contain the phrase "New York Times" more often than the phrase "New York" by itself, giving a strong signal that "New York Times" is an unbreakable phrase. A lookup in a gazetteer would then indicate that the query does not have a geographic context, because "New York Times" is not a location. With this approach, the geographic context of about 95% of queries can be detected with an accuracy of about 95% (*23*). The next step is to devise algorithms that exploit this information to improve search results.

Fighting search engine spam. Deciding what constitutes search engine spam is often difficult. Some results are obviously search engine spam, such as a page to purchase a quantum chemistry software package that is returned in the top 10 results for the query "jaguar." Others are less clear, for example, when the query "Hilton San Francisco" returns a page of a travel agency that is not affiliated with Hilton Hotels but which allows users to book a hotel room in the San Francisco Hilton.

Search engine spam usually tries to boost the ranking of a specific page while concealing the boosting from the user. Common boosting techniques are content spamming (or keyword stuffing), which tries to manipulate the query-dependent part of the ranking algorithms, and link spamming, which tries to manipulate the query-dependent signal through the anchor text or the query-independent signal through the hyperlink analysis. Hiding techniques are usually very creative. They either attempt to hide the terms used for spamming from the user, such as the famous "white text on white background" approach, or they use cloaking, in which the spammer supplies the search engine with a page that is different from the page that a normal user sees when visiting the same URL. See (*24*) for more details.

Detecting search engine spam is an ongoing research effort. First results indicate that automatic classifiers can be used to identify 82 to 86% of content spam (*25*) and 80 to 81% of link spam (*26*), with very small false positive rates.

Filters for inappropriate content. What is considered inappropriate content differs from culture to culture, and even from person to person. Thus, the first challenge when building a filter for inappropriate content is to find the right definition of what is inappropriate. There seems to be general agreement that filters for children should eliminate pornography, hate sites, and violence-related as well as drug-related material. Such content can often be detected by a classifier that was trained using machine-learning techniques. For training, the filter software is given a large set of "training" documents, which are documents that are annotated either as inappropriate or as not inappropriate; from this, the software builds a model of what features of documents are good indicators of inappropriateness. This model is then used to filter pages with inappropriate content at query time. These and other filters are available at search engines; see, for example, Fig. 2 for Google's filtering options that apply to all searches a user performs (i.e., personalized filter) and Fig. 3 for Google's filtering options for an individual search. In the future, search engines might provide filters for topics, geographic regions, or genres of Web pages.

Future Prospects

To further improve search results, specialized search engines such as Google Scholar, which contain pages only on a certain topic or a certain genre, have been created. Another thrust of current research on result ranking is to analyze user clicks on search results in the aggregate. Researchers are also experimenting with different search interfaces, such as multifaceted searching. Because no search engine indexes the whole Web, comprehensiveness can be improved by combining search results of various search engines. Rank aggregation is the research area that explores different ways of combining ranked lists of search results.

Other interesting research topics are searches of other types of media, such as images, video, and sounds. Current search engines usually exploit textual information associated with the media, such as the text in and surrounding an image, the closed caption of television channels, or user annotations of images, so-called social tagging. The quality of these information sources is variable, which in turn affects the search quality for these media. See (*27*) for more details.

Current search engines do not understand the semantics of queries or Web pages, nor do they apply any form of reasoning. Researchers currently experiment with augmenting search engines with some simple forms of reasoning: They try to extract facts from the Web and store them in databases (*28*). This would allow a search engine to answer questions of the form "List all objects with the following property," such as "Give me all cities in California with more than 1 million inhabitants." Simple deduction rules such as "A is in relation with B, and B is in relation with C, thus A is in relation with C" could then be applied. Other researchers retrieve facts from a manually compiled hierarchy of facts using a theorem prover and attempt to combine them with matches in documents with the goal of answering simple fact-based queries (*29*). Neither approach is used in search engines today, but might be in a future years.

Extracting facts from Web pages is closely related to searching semistructured data, such as XML (Extensible Markup Language) data. These kinds of searches arise frequently in enterprise

Fig. 2. Filtering options of Google applying to all searches of a user.

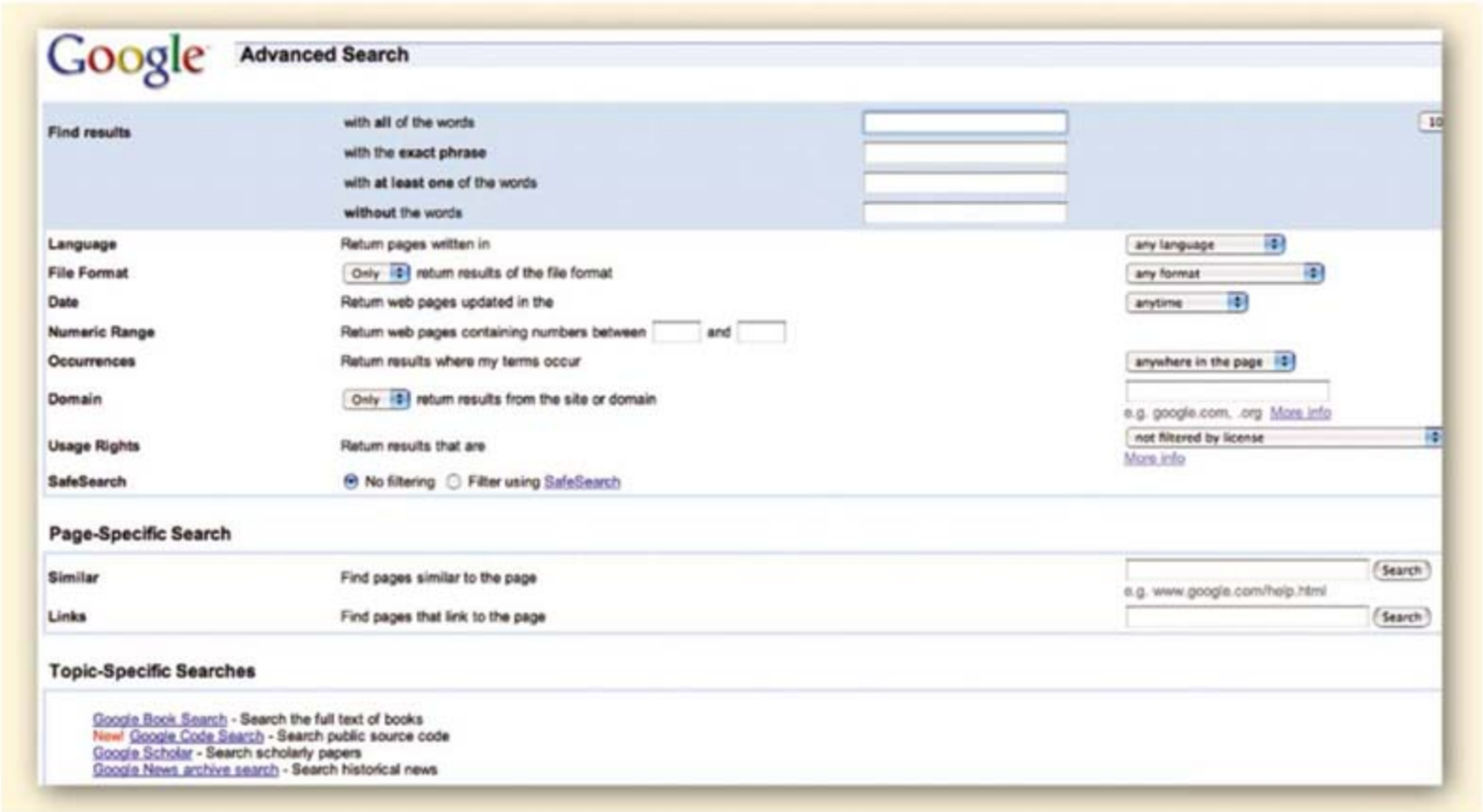

Fig. 3. Filtering options of Google applying to individual searches.

searching (searching the web pages internal to an enterprise) and in the search of digital libraries. Traditionally, databases have been used to search structured data, and search engines have been used for searching unstructured data, such as text. With the arrival of semistructured Web pages, the database and the information retrieval communities have started to explore combining their techniques and research efforts to achieve better retrieval results (*30*, *31*). Thus, a new field of research consisting of the combination of the two areas may be created.

References and Notes

1. S. Ghemawat, H. Gobioff, S.-T. Leung, in *Proceedings of the 16th ACM Symposium on Operation System Principles* (ACM Press, New York, 2003), pp. 29–43.
2. J. Dean, S. Ghemawat, in *Proceedings of the 6th Symp. Operating System Design and Implementation* (Usenix Association, Berkeley, CA, 2004), pp. 137–150.
3. L. Granka, T. Joachims, G. Gay, in *Proceedings of the 27th Annual International ACM SIGIR Conference on Research and Development in Information Retrieval*, K. Järvelin, J. Allan, P. Bruza, M. Sanderson, Eds. (ACM Press, New York, 2004), pp. 478–479.
4. S. Brin, L. Page, *Comput. Netw.* **30**, 107 (1998).
5. J. Kleinberg, *J. ACM* **46**, 604 (1999).
6. E. Garfield, *Science* **122**, 108 (1955).
7. M. K. Bergman, *J. Electronic Pub.* **7**, (2001); www.press.umich.edu/jep/07-01/bergman.html.
8. One obvious way of reducing index size is to omit duplicate and near-duplicate Web pages. According to studies (*32–34*), about 25 to 30% of Web pages can be discarded in this way, making space for other documents.
9. A uniform record locator (URL) is the equivalent of an address for Web pages.
10. W. Wu, A. Doan, C. Yu, in *Proceedings of the 22nd International Conference on Data Engineering*, L. Liu, A. Reuter, K.-Y. Whang, J. Zhang, Eds. (IEEE, Los Alamitos, CA, 2006), p. 44.
11. A. Ntoulas, P. Zerfox, J. Cho, in *Proceedings of the Joint Conference on Digital Libraries* (ACM Press, New York, 2005), pp. 100–109.
12. www.sitemaps.org.
13. A. Z. Broder, *SIGIR Forum* **36**, 3 (2002).
14. J. Teevan, S. Dumais, E. Horvitz, in *Proceedings of the 1st International Workshop on New Technologies for Personalized Information Access (PIA 2005)*, P. Brusilosky, C. Callaway, A. Nürnberger, Eds. Edinburgh, UK, 24 July 2005, DELOS Network of Excellence on Digital Libraries, pp. 84–92.
15. P. Anick, in *Proceedings of the 26th Annual International ACM SIGIR Conference on Research and Development in Information Retrieval*, J. Callan, G. Cormack, C. Clarke, D. Hawking, A. Smeaton, Eds. (ACM Press, New York, 2003), pp. 88–95.
16. X. Shen, B. Tan, C. Zhai, in *Proceedings of the 28th Annual International ACM SIGIR Conference on Research and Development in Information Retrieval*, G. Marchionini, A. Moffat, J. Tait, R. Baeza-Yates, N. Ziviani, Eds. (ACM Press, New York, 2005), pp. 43–50.
17. B. Tan, Z. Shen, C. Zhai, in *Proceedings of the 12th ACM SIGKDD International Conference on Knowledge Discovery and Data Mining*, T. Eliassi-Rad, L. Ungar, M. Craven, D. Gunopulos, Eds. (ACM Press, New York, 2006), pp. 718–723.
18. J. Teevan, S. Dumais, E. Horvitz, in *Proceedings of the 28th Annual International ACM SIGIR Conference on Research and Development in Information Retrieval*, G. Marchionini, A. Moffat, J. Tait, R. Baeza-Yates, N. Ziviani, Eds. (ACM Press, New York, 2005), pp. 449–456.
19. G. Jeh, J. Widom, in *Proceedings of the 12th International World Wide Web Conference* (ACM Press, New York, 2003), pp. 271–279.
20. P. Berkhin, *Internet Math.* **2**, 73 (2005).
21. A. N. Langville, C. D. Meyer, *Internet Math.* **1**, 335 (2005).
22. H. Chen, D. R. Karger, in *Proceedings of the 29th Annual International ACM SIGIR Conference on Research and Development in Information Retrieval*, S. Dumais, E. N. Efthimiadis, D. Hawking, K. Järvelin, Eds. (ACM Press, New York, 2006), pp. 429–436.
23. L. Wang *et al.*, in *Proceedings of the 28th Annual International ACM SIGIR Conference on Research and Development in Information Retrieval*, G. Marchionini, A. Moffat, J. Tait, R. Baeza-Yates, N. Ziviani, Eds. (ACM Press, New York, 2005), pp. 424–431.
24. Z. Gyöngyi, H. Garcia-Molina, *IEEE Comp. Mag.* **38**, 28 (2005).
25. A. Ntoulas, M. Najork, M. Manasse, D. Fetterly, in *Proceedings of the 2006 World Wide Web Conference*, L. Carr, D. De Roure, A. Iyengar, C. A. Goble, M. Dahlin, Eds. (ACM Press, New York, 2006), pp. 83–92.
26. L. Becchetti, C. Castillo, D. Donato, S. Leonardi, R. Baeza-Yates, in *Proceedings of the 2nd International Workshop on Adversarial Information Retrieval on the Web*, B. D. Davison, M. Najork, T. Converse, Eds. (Tech. Rep. LU-CSE-06-027, Department of Computer Science and Engineering, Lehigh University, Bethlehem, PA, 2006), pp. 1–8.
27. M. Sahami, V. Mittal, S. Baluja, H. Rowley, in *Proceedings of the 8th Pacific Rim International Conference on Artificial Intelligence*, C. Zhang, H. W. Guesgen, W.-K. Yeap, Eds. (Springer, New York, 2004), pp. 3–12.
28. O. Etzioni *et al.*, *Artif. Intell.* **165**, 91 (2005).
29. D. Moldovan, C. Clark, S. Harabagiu, S. Maiorano, in *Proceedings of HLT-NAACL 2003, Human Language Techn. Conference of the North American Chapter of the ACL* (ACL Press, Cambridge, MA, 2003), pp. 87–93.
30. S. Amer-Yahia, P. Case, T. Rölleke, J. Shanmugasundaram, G. Weikum, *SIGMOD Record* **34**, 71 (2005).
31. D. Carmel, Y. S. Maarek, M. Mandelbrod, Y. Mass, A. Soffer, in *Proceedings of the 26th Annual International ACM SIGIR Conference on Research and Development in Information Retrieval*, J. Callan, G. Cormack, C. Clarke, D. Hawking, A. Smeaton, Eds. (ACM Press, New York, 2003), pp. 151–158.
32. A. Z. Broder, S. Glassman, M. Manasse, G. Zweig, *Comput. Netw.* **29**, 1157 (1997).
33. D. Fetterly, M. Manasse, M. Najork, in *Proceedings of the 1st Latin American Web Congress (LA-WEB 2003)* (IEEE, Los Alamitos, CA, 2003), pp. 37–45.
34. M. Henzinger, in *Proceedings of the 29th Annual International ACM SIGIR Conference on Research and Development in Information Retrieval*, S. Dumais, E. N. Efthimiadis, D. Hawking, K. Järvelin, Eds. (ACM Press, New York, 2006), pp. 284–291.

10.1126/science.1126557

The Scientific Research Potential of Virtual Worlds

William Sims Bainbridge

Online virtual worlds, electronic environments where people can work and interact in a somewhat realistic manner, have great potential as sites for research in the social, behavioral, and economic sciences, as well as in human-centered computer science. This article uses Second Life and World of Warcraft as two very different examples of current virtual worlds that foreshadow future developments, introducing a number of research methodologies that scientists are now exploring, including formal experimentation, observational ethnography, and quantitative analysis of economic markets or social networks.

Recent sociotechnical developments involving online worldlike environments have made possible new kinds of research in the social and behavioral sciences, raise interesting challenges for computer and information science, and suggest new potential for education across all the sciences (*1*, *2*). We can use the term "virtual world" to describe an electronic environment that visually mimics complex physical spaces, where people can interact with each other and with virtual objects, and where people are represented by animated characters. The diversity of current virtual worlds can be represented by the creativity-oriented environment Second Life (SL) and the massively multiplayer online role-playing game World of Warcraft (WoW). To date, about 6.5 million people have entered SL and WoW reports that it has 8.5 million subscribers, so the impact of this technology is beginning to be felt by society.

The user enters each via a personal computer running special software that connects to one or more servers that pass information back and forth between users over the Internet. Both simulate very large three-dimensional environments filled with virtual objects through which the user may subjectively walk, swim, or fly, and in the case of WoW, with thousands of simple artificial intelligence (AI) characters to interact with. Each user is represented by an avatar and can talk with the others by typing in a chat channel or through optional voice communication (*3*). Both worlds sustain complex internal economies with their own currencies, both enable users to do useful work for each other, and both offer software tools to facilitate social interaction, although some of their specific features are quite different (*4*–*6*) (Fig. 1).

In terms of scientific research methodologies, one can do interviews and ethnographic research in both environments, but other methods would work better in one than the other. SL is especially well designed to mount formal experiments in social psychology or cognitive science, because the researcher can construct a facility comparable to a real-world laboratory and recruit research subjects. WoW may be better for nonintrusive statistical methodologies examining social networks and economic systems, because it naturally generates a vast trove of diverse but standardized data about social and economic interactions. Both allow users to create new software modules to extract data.

The present moment marks a major historical transition. Video games and computer games are in the process of evolving into something much richer, namely virtual worlds, at the same time that electronic games are surpassing the motion picture industry in dollar terms and beginning to cut into television. Already, many families forgo watching TV dramas to quest together in WoW. Previously separate forms of electronic communication are merging in what Americans call ubiquitous computing and Europeans call pervasive computing. The current generation of video game systems—XBox 360, PlayStation 3, and both the Nintendo Wii and the Nintendo DS portable—all connect to the Internet, and games designed for cell phones or Internet-connected pocket computers are proliferating. Researchers are exploring the methods needed to create an entirely new generation of games, called pervasive LARPs (live-action role-playing games), that have players act in the real world while simultaneously interacting over the Internet via wireless mobile connections (*7*–*9*).

During this time of transition, when there is active speculation about the investment opportunities, it is exceedingly difficult to estimate the current economic impact of virtual worlds, let alone project the future. For example, a Web site called *Wowhead* that was merely about WoW recently sold for 1 million dollars, and the game's $15 monthly charge across many subscribers could generate hundreds of millions of dollars per year (*10*). Virtual worlds differ as to whether their internal currency can be exchanged for dollars (SL, yes; WoW, no), so economists face the scientific dilemma of how to count wealth generation inside the games, in addition to the external dollar investments and returns. Exploratory studies by Nick Yee suggest that most players are in fact adults, disproportionately male but with a wide variety of occupations and demographic characteristics (*11*), so virtual worlds are not simply a childish fad. However

Fig. 1. The Stormwind Auction House in WoW. The three figures wearing vests and standing on platforms are the computer-generated auctioneers, whereas the dozen other figures are characters belonging to real human beings participating in auctions involving a thousand or more people. The one waving in the center is the avatar of a scientist who is studying this virtual world and the computer-assisted systems it provides to facilitate social interaction and economic exchange.

Division of Information and Intelligent Systems, National Science Foundation, 4201 Wilson Boulevard, Arlington, VA 22230, USA.

important they may become, a few social scientists and computer scientists have shown that these new realms are already suitable environments for scientific research.

Virtual Laboratory Experiments

For at least a decade, experimentalists in the social and economic sciences have looked to the Internet as a mean of expanding the scope of their research, and virtual worlds may finally turn hopes into opportunities. A scientific agenda for online experiments was already enunciated in 1997, when the National Science Foundation (NSF) sponsored a workshop called NetLab to explore the potential for online experimental laboratories (www.nsf.gov/sbe/ses/soc/asi.jsp). The NetLab report said that the Web could enable experiments to (i) be scaled up from the usual few dozen subjects to hundreds or even thousands; (ii) cross sociocultural boundaries and include research subjects from previously underrepresented groups; (iii) study processes that take place over longer periods of time, including weeks or even months; and (iv) become integrated into the curriculum of undergraduates who do not happen to be in major research universities where such work traditionally takes place.

Over the 10 years since NetLab, a number of workshop participants have employed computer-based experimental methods, and some of these studies attempted to fulfill the vision of research on an expanded scale (*12*–*14*). Several groups have made progress in designing "collaboratories" (*15*, *16*). The effect of these efforts has been increased cooperation between researchers at different universities and improved use of experiments as teaching tools. However, the vision of vastly increased numbers of more diverse respondents interacting over longer periods of time has not been achieved yet.

The scientific motivations for achieving these goals are compelling. Today we understand better than in the past that individual humans, small groups, and large communities are all complex dynamic systems in interaction with each other. Traditional laboratory methods are the best way of testing simple causal theories by manipulating one or more experimental treatments, which are considered the independent variables (*17*, *18*). For statistical reasons, experiments with small numbers of research subjects are limited to detecting very strong effects, which is unlikely to be the case when many different variables influence both the outcomes and each other. To unravel complex causal systems using experimental methods, one needs a very large number of subjects. The background variables of the individuals may have important influences on the connections between the independent and dependent variables, so replication across multiple or diverse populations will be necessary.

Virtual worlds such as SL provide environments and tools that facilitate creating online laboratories that can automatically recruit potentially thousands of research subjects, over a period of months, at low cost (Fig. 2). SL offers scripting and graphics tools that allow anyone to build a virtual laboratory building, functioning equipment to run the experiment, and incentives to motivate participation, such as giving each research subject a virtual helicopter to fly around SL (*19*). It would be quite feasible to have advanced students replicate classic experiments inside SL, adding to our confidence in older results while giving young people valuable skills. Creative scientists may also be able to design experiments that are feasible in virtual worlds but were never possible before. For example, experiments can be done comparing the socioeconomic consequences of alternative government regulations, something next to impossible in society at large (*20*), perhaps taking advantage of the fact that issues of environmental pollution already loom large in WoW quests. A team led by Yasmin Kafai at the University of California, Los Angeles, has already used the children's virtual world *Whyville* in an experimental study of reactions to a measles-like epidemic affecting the avatars (*21*).

Makers of online games are always looking for interesting ways to enhance game play for their subscribers, so they might be willing to incorporate appropriate experiments. This would be especially true if the experiment were novel, if the company were facing stiff competition and were thus open to innovative ideas, and if the scientists had their own funding to cover the additional costs. Consider that players in WoW are split into two opposing factions of many races, called the Alliance and the Horde, engaged in a cold war comparable to the historical NATO/USSR split. In 2006, two years after WoW was originally released, features were intentionally added to two zones to increase conflict between the factions. Eastern Plaguelands gained four towers for the factions to fight over, and in Silithus they compete to collect samples of a valuable mineral. In both cases, much of the benefit is collective, what economists call a public good, given only to members of the winning faction, quite apart from how much the individual player contributed to the victory. Thus, the two zones are effectively field experiments on the question of how individuals can be induced to cooperate in producing public goods (*22*). The evolution of cooperation between individuals is the classic topic for multi-agent–system AI computer simulations in the social sciences, and the fact that virtual worlds combine both AI agents and human-controlled avatars implies that many rigorous experiments on this crucial issue can be conducted in them (*23*–*25*).

Political science uses the experimental method almost exclusively in small laboratory studies that mimic committee deliberations, and none of the social sciences experiment aggressively with social movements, simply because the cost and the ethical issues are daunting. This situation could change online, especially in role-playing games such as WoW, as long as the given experiment harmonized with the mythology of the virtual world. In the days before university committees on research with human subjects, it was not con-

Fig. 2. Three avatars in SL making a door. In a virtual design studio, two scientists are admiring the work of a student intern (center) who is creating a set of displays demonstrating human-centered computing. After the combination lock has been set and made smaller, the door can readily be moved to its final location. Similar methods can be used to construct laboratory facilities and experimental equipment.

sidered unethical for a team of social scientists to join a small social movement in order to study it covertly, thereby seriously affecting its outcome, or to experiment with alternative government programs that had serious consequences for the beneficiaries, but those days are gone (*26*, *27*). Participants in WoW expect the others to be acting aggressively in pursuit of goals defined by the mythos. Thus, a team of agents provocateurs who are researchers in disguise would positively contribute to everybody's dramatic experience, if they promoted a movement that simultaneously supported the mythos and permitted scientifically relevant observations of human behavior. (See the conclusion for a discussion of ethical issues.)

Observational Social and Economic Science

Many scientists and scholars are already conducting research about virtual worlds, and they are beginning to use them as environments to ask general social-scientific questions. Economist Edward Castronova argues that an increasing fraction of human life, economy, and culture will take place in these novel environments, so they need to be studied as important phenomena in their own right (*28*). In a study of social and economic coordination, Castronova has shown that it can be fruitful to compare results from research in different virtual worlds, just as is true for nations on Earth (*29*). There is some evidence that they serve as hatcheries for new cultural movements; for example, facilitating the consolidation of post-Christian religious ideologies (*30*); and are substituting for disintegrating social institutions in the real world (*31*).

It is especially important to study virtual worlds now, because the current period of transformation may not last much longer, and because it may be impossible to reconstruct its key processes and phenomena entirely from historical records that are naturally preserved. Essentially all of the classic one-player electronic games can still be played, either because computer emulators of the old systems have been created or the games have been ported over to new systems. But the same is unlikely to be true for today's virtual worlds, because they depend on the extensive social infrastructure of the companies that support them and on the current population of people who inhabit them.

Virtual worlds are good environments in which to explore wider issues related to emerging technologies, such as intellectual property rights (*32*) and the sociotechnical implications of online misbehavior (*33*–*35*). Research concerning the cultural boundaries of virtual worlds includes studies of the extent to which gender-specific behavioral norms transfer to these nontraditional environments (*36*), comparisons with role-playing games that are not electronic such as *Dungeons and Dragons* (*37*), contrasting the human impact of alternative architectural philosophies (*38*), the emergence of cooperation (*39*), the possibility of addiction to virtual worlds (*40*), and exploration of the different meanings that participants attach to virtual life and death (*41*). To date, much of the research has followed the twin qualitative paradigms of anthropological ethnography and sociological participant observation (*42*), but quantitative approaches using rigorous statistical and computational techniques show very great promise.

WoW is a very conducive environment for quantitative research because it encourages individuals to write "mod" or "add-on" programs, and scientists can use some existing software as research tools or write their own. These range all the way from very simple sequences of character behaviors constructed using macros built into the WoW user interface to long programs written in the Lua language. For example, one widely used program called Auctioneer analyzes prices on the WoW virtual item auction system, and CensusPlus tallies all the players currently online by several characteristics (Fig. 3).

With census data on more than 200,000 WoW characters, a team centered at the Palo Alto Research Center analyzed the factors associated with the upward status mobility of individuals (*43*) and the dynamics of social groups (*44*, *45*). Another team, centered at the University of Illinois, has recently received NSF funding to develop new analytical tools while analyzing data taken directly from computer servers that run another major online role-playing game, augmented with a questionnaire administered to thousands of subscribers (www.nsf.gov/awardsearch/showAward.do?AwardNumber=0628036). In principle, the raw data from a game server record every single interaction between humans, including economic exchanges, the affiliation steps that build groups and networks, every "chat" communication between players, and all action choices that individuals make within the social environment.

Computer and Information Science

Online virtual worlds illustrate well the deficiencies of the Internet (*46*), notably its high latency (slow packet delivery speed) and low bandwidth (amount of information that can be delivered in a given period of time). WoW manages the bandwidth problem by placing all the graphics on the users' computers, but this means that they cannot create their own objects and at best can assemble existing components. This would not work for SL, because the whole point is to empower users to create everything in their virtual world from scratch themselves. The penalty for SL users is a delay whenever the avatar moves to a new location, because all the specifications for the environment must be downloaded from the server, often thousands of miles away.

Latency is a big issue for action-oriented online games (*47*). WoW's user interface includes a latency meter so that the user can decide whether to log off and then back on later in hopes of getting a better connection. Humans can detect latencies of as little as 50 ms, whereas in normal use, Internet latency may be five times that long. Games cover this delay as best they can, typically by restricting players to scripted movements, but this is far from ideal.

Currently, virtual worlds use some variant of client/server architecture, in which a centralized company computer handles interactions among all the players, although WoW does employ a partial peer-to-peer network in distributing its updates. The Nintendo DS portable game system is an example of local peer-to-peer wireless

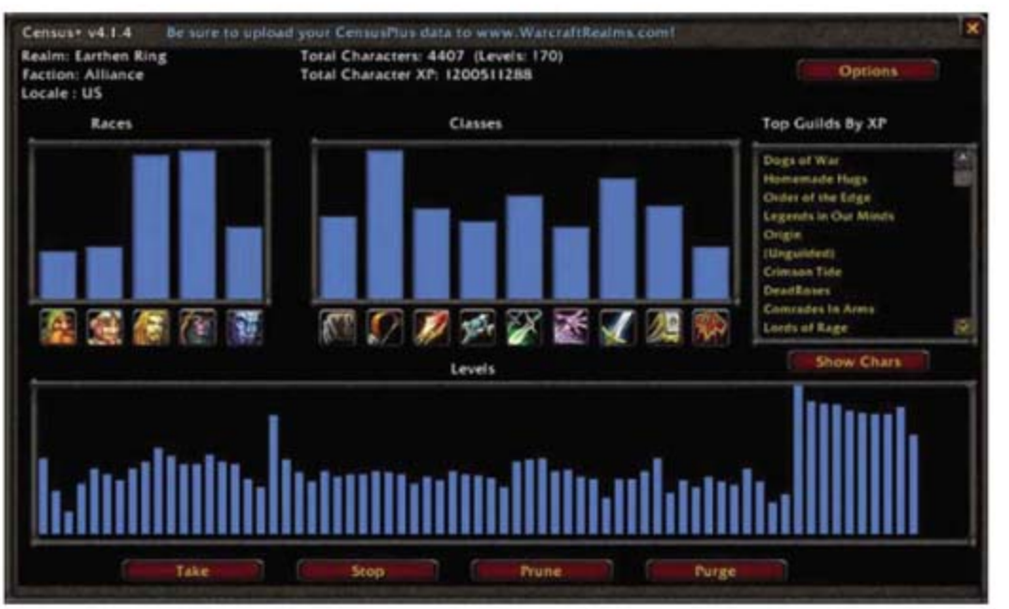

Fig. 3. Example of CensusPlus output from WoW. This display graphs the results of tabulating 4407 active characters for one faction in one of the hundreds of realms of this online game, and exact census numbers are also provided. The bar graph at top left shows the distribution across five "races": dwarves, gnomes, humans, night elves, and Draenei; whereas the other bar graphs show the nine classes (such as warrior or priest) and the distribution across levels of experience.

networking, suggesting the range of alternatives that may be built into a future successor to the Internet.

Virtual worlds are a good proving ground for virtual people, namely AI nonplayer characters (NPCs) like the thousands that inhabit WoW. NPCs can be either friendly (such as merchant characters that serve as portals to the database of virtual objects) or unfriendly (such as the animals that a game player can gain points by killing). Carnivores constantly patrol territory at random and attack the user's avatar if it comes within what players call the "aggro radius" and ethologists of real animals call "reaction distance." The AI system for such an animal is extremely simple, but it often models running away or becoming enraged when it suffers damage. AI representations of humans potentially could be much more complex. Notably, a team led by Mary Lou Maher has been developing conceptual frameworks and detailed methods for giving these agents the motivation to seek novelty and respond creatively (*48*, *49*).

Other fields of computer and information science that may use virtual worlds as laboratories include human/computer interaction (HCI), where "machinima" videos shot in virtual worlds may be used to develop prototypes of a wide range of systems (*50*) and new methods of information visualization (*51*). Today's virtual worlds contrast strongly with the concept of totally immersive virtual reality (VR) that has long been popular with science fiction writers (*52*) but has proven so difficult for computer scientists to achieve in the real world. SL and WoW images are restricted to the screen of an ordinary computer monitor, rather than filling the walls of a VR cave or a binocular head-mounted display. On the one hand, this may suggest that people really do not need visually perfect VR. On the other hand, today's virtual worlds may be preparing millions of people to demand full VR in the future.

Conclusion: Human Challenges

Virtual worlds may help unify some branches of the social sciences and give them greater scientific rigor. Whereas economics and cognitive science have made great strides in recent decades, some other disciplines remain fragmented in myriad competing schools of thought, poised ambiguously between the humanities and the natural sciences. For example, concepts such as "identity" and "self" have been used for nearly a century to describe aspects of human individuality, initially by the psychoanalytic school in psychology and symbolic interactionists in sociology (*53*, *54*). Some contemporary cognitive scientists are skeptical of scholarly conceptions of self (*55*), finding them to be more like literary metaphors distilled from the surrounding folk culture than like rigorously measurable scientific concepts. The cognitive and emotional relationships between a human user and his or her online representation are very actively debated and could become the focus of increasingly rigorous research and a point of convergence for the social sciences (*56*, *57*).

Interestingly, SL and WoW have different orientations. The simulated people in SL are avatars, supposedly expressing the identities of their human owners, just as avatars within Hindu religion personify aspects of the deities. WoW uses the term character, implying that many players may keep a psychological distance from them, considering them toys, puppets, perhaps even friends, but not selves. Avid players tend to run several characters, commonly referring to them as possessions.

Given the great variability across virtual worlds and human participants, the multiplicity of feasible research methodologies would permit a range of overlapping research studies, adjudicating between alternative theoretical propositions and thereby connecting the currently isolated schools of thought. Some studies could examine how humans conceptualize their own avatars or characters, while others could focus on mutual perceptions during social interaction. A third category of studies could look at how humans react to the currently rather simple AIs. A fourth could explore social cognition by designing ever more complex and lifelike AIs, watching their interactions with people, and even modeling them on specific human individuals to better understand the cognitive processes that shape human behavior.

The tremendous research potential of virtual worlds cannot obscure the fact that there are problems as well. A number of organizations hold meetings in SL, from IBM to informal friendship groups, but it is unclear what enhancements are needed to make it a really good environment for serious distributed collaborations of the kinds often undertaken by scientists. Given that university departments hire faculty in a diversity of fields, research collaborations in highly specialized fields often of necessity span institutions, but scientists do not seem to be rushing into SL to find a shared virtual location. What value virtual worlds might add to the existing modes of communication between distant scientific collaborators remains to be seen.

Online research involving human beings may require ethics scrutiny by institutional human subjects review boards, or it may not, depending on the circumstances. Arguably, both SL and WoW are public places, and the fact that both discourage people from using their real names seems to provide anonymity, but these points can be contested. In WoW, for example, some combat arenas and chat channels are accessible only to groups formed by invitation, so these might qualify as private places. Many frequent users of SL craft their avatars to look like themselves and give them portions of their own names. Any avatar is subjectively a second self, so its reputation becomes important to the owner even if its deeds cannot be traced back to the person in the real world.

Academic social scientists are often required to follow NSF's *45 CFR Part 690: Federal Policy for the Protection of Human Subjects*, even if their project does not have federal funding (www.nsf.gov/bfa/dias/policy/docs/45cfr690.pdf). However, people doing research outside the regulatory context of a university or other employer are free to do anything not prohibited by law or the enforced policies of the particular virtual world. Given the low cost and ready accessibility of online virtual worlds, students are already undertaking research projects, from middle school upward, raising a host of ethical issues, starting with the question of whether one can require informed consent from every individual in an online public space. We cannot expect such issues to be resolved in any definitive fashion, because both social norms and the technology are constantly changing, but researchers need to be sensitive to them.

A related human issue concerns the transformation of some kinds of education at pre-college levels, which might harmonize with scientific values more than with traditional values. NSF has supported the development of two virtual worlds devoted to science education: *River City*, where students explore public health issues in a simulated 19th-century town (*58*), and *Quest Atlantis*, where preteens develop fundamental research skills by solving environmental problems (*59*). A number of educational institutions are active in SL, including Ohio University, the University of Texas at Dallas, the University of Cincinnati, Bowling Green State University, the University of North Carolina at Chapel Hill, and Vassar College, often giving students educational experiences in creating content for SL.

Many virtual worlds may foster scientific habits of mind better than traditional schools can, because they constantly require inhabitants to experiment with unfamiliar alternatives, rationally calculate probable outcomes, and develop complex theoretical structures to understand their environment (*60*–*62*). Probably for better, but conceivably for worse, virtual worlds are creating a very new context in which young people are socialized to group norms, learn intellectual skills, and express their individuality (*63*). The "graduates" of SL and WoW may include many future engineers, natural scientists, and social scientists ready to remake the real world in the image of the virtual worlds.

References and Notes

1. R. A. Bartle, *Designing Virtual Worlds* (New Riders, Indianapolis, IN, 2004).
2. C. Ondrejka, *Games Cult.* **1**, 111 (2006).
3. B. Damer, *Avatars: Exploring and Building Virtual Worlds on the Internet* (Peachpit, Berkeley, CA, 1998).
4. C. R. Ondrejka, http://ssrn.com/abstract=614663.
5. M. Lummis, E. Kern, *World of Warcraft: Master Guide* (BradyGames, New York, 2006).
6. M. Lummis, E. Kern, *World of Warcraft: The Burning Crusade* (BradyGames, New York, 2007).
7. M. Bell *et al.*, in *Proceedings of CHI 2006* [Association for Computing Machinery (ACM), New York, 2006], pp. 417–426.

AAV Vector Integration Sites in Mouse Hepatocellular Carcinoma

Anthony Donsante,[1]* Daniel G. Miller,[2]* Yi Li,[3,4] Carole Vogler,[5] Elizabeth M. Brunt,[5] David W. Russell,[3,4]† Mark S. Sands[1,6]†

Adeno-associated viruses (AAVs) are promising vectors for gene therapy. We previously reported a high incidence of hepatocellular carcinoma (HCC) in AAV-treated mice with the lysosomal storage disease mucopolysaccharidosis VII (MPS VII) (*1*). Similar malignant hepatocellular changes were also observed in other mouse models of AAV-mediated gene therapy (*2*, *3*). In each case, the underlying molecular mechanism is unknown.

We examined HCC formation in mice after neonatal intravenous injections of 1.5×10^{11} genome-containing particles of an AAV vector expressing the human β-glucuronidase gene from a β-actin promoter and a cytomegalovirus (CMV) enhancer (AAV-GUSB) (fig. S1). Six of 18 (33%) AAV-treated MPS VII mice developed HCC, compared with 1 of 25 (4%) mice treated with bone marrow transplantation (table S1). Wild-type mice injected with the AAV-GUSB vector or a version lacking the β-actin promoter (fig. S1) also developed HCC at significantly higher rates (56% and 33%, respectively) compared with untreated normal mice (8.3%). No tumors were observed in transgenic mice overexpressing GUSB from the same expression cassette as that in AAV-GUSB.

We attempted to isolate vector-chromosome junctions from six tumors present in six different mice by inverse polymerase chain reaction (PCR). A single, unique amplification product was detected in four samples (Fig. 1A). Each junction was similar to those previously described (*4*, *5*) and contained a portion of the 5′ vector inverted terminal repeat (ITR) with transgene transcription proceeding in a telomeric direction. We compared the copy numbers of junction-specific fragments in tumor tissue and in normal liver. In the three cases where adjacent tissue was available, the junctions were undetectable in normal-appearing liver (<1 copy per 100 genomes). Junction copy numbers ranged from 3 to 27 per 100 diploid genomes in tumor tissue (Fig. 1B). Because murine hepatocytes can be tetraploid or octaploid (*6*) and because tumor samples contain a variety of supporting and inflammatory cells that presumably lack vector proviruses, these values are consistent with a single AAV vector integration event resulting in clonal expansion of transformed cells. However, we cannot exclude the possibility that additional, undetected vector integrations were also present in the tumor samples.

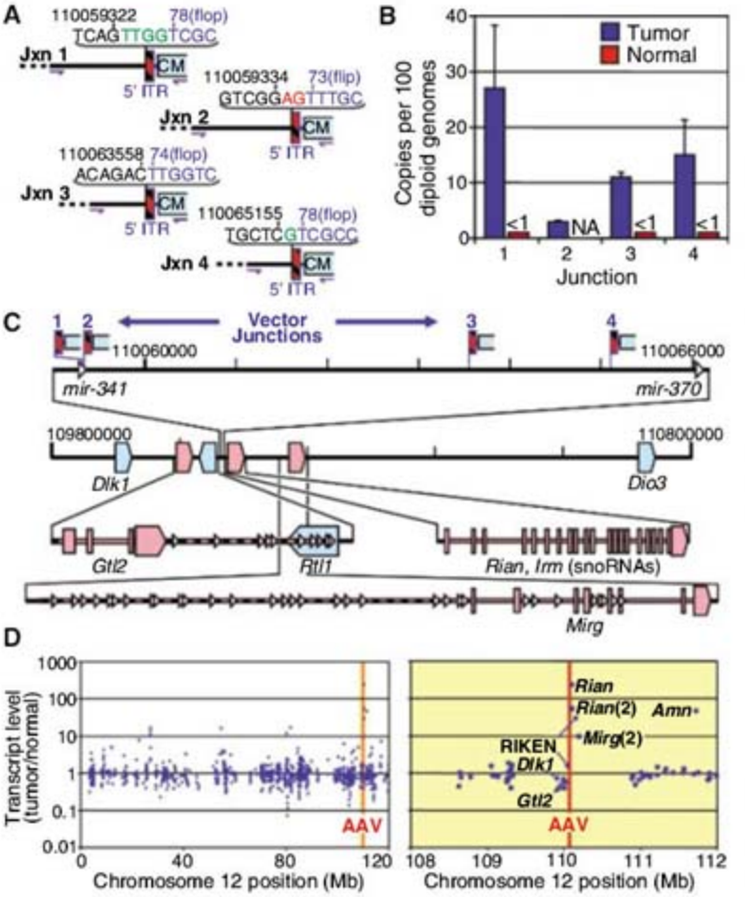

Fig. 1. (**A**) Vector-chromosome junctions are shown with colors indicating sequence origin: black, chromosome 12; blue, AAV; green, microhomologies between AAV and chromosome 12; and red, inserted nucleotides. Chromosomal and AAV ITR (flip or flop orientation) positions are indicated. (**B**) Quantitative PCR for junction copy numbers in tumors and in adjacent, normal tissue [primer sites shown in (A)]. Normal samples were below the limit of detection. NA indicates not available. Error bars represent 1 SD. (**C**) The genomic locus containing the integration sites is shown with relevant portions expanded. Imprinted transcripts expressed from maternal (pink) or paternal (blue) alleles, areas where transcription has not been confirmed (dashed lines), and microRNAs (triangles) are indicated. (**D**) Transcript levels in tumors divided by those from adjacent normal-appearing tissue. Fold differences for mice with junctions 1, 3, and 4 were averaged and plotted versus chromosome 12 positions. Blue dots are assayed transcripts (two overlap for *Rian* and *Mirg*). Red lines are sites of vector integrations.

All four junctions mapped to a 6-kilobase region of chromosome 12 (Fig. 1C). Two of the insertion sites were located just 12 base pairs apart within the mir-341 microRNA transcript. Microarray analysis showed that genes adjacent and telomeric to the AAV vector proviruses were dramatically overexpressed (Fig. 1D), and they were up-regulated in all three tumor samples studied, suggesting that the transcriptional changes were due to provirus insertions.

Thirty-four of the 382 known mouse microRNAs, with thousands of potential target genes, are located within this locus. The highly overexpressed *Rian* and *Mirg* genes contain multiple small nucleolar RNAs (snoRNAs) and microRNAs, respectively, that could have profound effects on host gene expression. The fact that every junction isolated was present at the same locus and resulted in similar changes in expression suggests that these events promote a critical step in tumorigenesis. A similar locus on chromosome 7 was not dysregulated [Supporting Online Material (SOM) text].

Our findings implicate insertional mutagenesis by AAV vectors in the development of hepatocellular carcinoma. Because humans have a syntenic locus on chromosome 14 that has been linked to several cancers (*7*, *8*), these findings raise safety concerns over the clinical use of AAV vectors.

References

1. A. Donsante *et al.*, *Gene Ther.* **8**, 1343 (2001).
2. J. E. Embury *et al.*, *Mol. Ther.* **13**, 583 (2006).
3. P. Bell *et al.*, *Mol. Ther.* **14**, 34 (2006).
4. D. G. Miller *et al.*, *J. Virol.* **79**, 11434 (2005).
5. H. Nakai *et al.*, *J. Virol.* **79**, 3606 (2005).
6. C. J. Epstein, E. A. Gatens, *Nature* **214**, 1050 (1967).
7. T. Kawakami *et al.*, *Hum. Mol. Genet.* **15**, 821 (2006).
8. D. Astuti *et al.*, *Br. J. Cancer* **92**, 1574 (2005).

Supporting Online Material

www.sciencemag.org/cgi/content/full/317/5837/477/DC1
Materials and Methods
SOM Text
Fig. S1
References

19 March 2007; accepted 11 June 2007
10.1126/science.1142658

[1]Department of Internal Medicine, Washington University School of Medicine, Box 8007, 660 South Euclid Avenue, St. Louis, MO 63110, USA. [2]Department of Pediatrics, University of Washington, Seattle, WA 98112, USA. [3]Department of Medicine, University of Washington, Mail Stop 357720, Seattle, WA 98112, USA. [4]Department of Biochemistry, University of Washington, Seattle, WA 98112, USA. [5]Department of Pediatrics, St. Louis University School of Medicine, St. Louis, MO 63104, USA. [6]Department of Genetics, Washington University School of Medicine, St. Louis, MO 63110, USA.

*These authors contributed equally to this study.
†To whom correspondence should be addressed. E-mail: msands@im.wustl.edu (M.S.S.); drussell@u.washington.edu (D.W.R.)

Free-Drifting Icebergs: Hot Spots of Chemical and Biological Enrichment in the Weddell Sea

Kenneth L. Smith Jr.,[1]* Bruce H. Robison,[1] John J. Helly,[2] Ronald S. Kaufmann,[3] Henry A. Ruhl,[1] Timothy J. Shaw,[4] Benjamin S. Twining,[4] Maria Vernet[5]

The proliferation of icebergs from Antarctica over the past decade has raised questions about their potential impact on the surrounding pelagic ecosystem. Two free-drifting icebergs, 0.1 and 30.8 square kilometers in aerial surface area, and the surrounding waters were sampled in the northwest Weddell Sea during austral spring 2005. There was substantial enrichment of terrigenous material, and there were high concentrations of chlorophyll, krill, and seabirds surrounding each iceberg, extending out to a radial distance of ~3.7 kilometers. Extrapolating these results to all icebergs in the same size range, with the use of iceberg population estimates from satellite surveys, indicates that they similarly affect 39% of the surface ocean in this region. These results suggest that free-drifting icebergs can substantially affect the pelagic ecosystem of the Southern Ocean and can serve as areas of enhanced production and sequestration of organic carbon to the deep sea.

Atmospheric warming has been associated with retreating ice shelves and glaciers in the Antarctic over the past decade, particularly around the Antarctic Peninsula (*1*–*4*). The disintegration of ice shelves on both sides of the Antarctic Peninsula during the past 60 years has been attributed to atmospheric warming (*5*, *6*) and has contributed to the increased frequency of icebergs in the Weddell Sea (*7*).

Icebergs are very conspicuous features across the seascape of the Southern Ocean. They range in size from objects that are meters in diameter to large tabular structures that can exceed 300 km in length. In the Southern Ocean during the late 1980s, there were an estimated 200,000 icebergs with linear dimensions in the tens of meters to tens of kilometers (*8*, *9*). Iceberg shapes range from tabular to pinnacle forms, depending on their origin and state of decay by evaporation, melting, wave-induced erosion, and fracturing (*10*) during transit to their final ablation.

Little is known about the impact of free-drifting icebergs on the surrounding pelagic ecosystem. Anecdotal observations suggest that both depletion and enrichment of biological and chemical activity in the pelagic zone can be associated with icebergs. While stationary in a coastal region, a very large (~10,000 km^2) grounded iceberg with an associated faunal community (*11*) created shading and negatively influenced surface primary production (*12*). A smaller, free-drifting iceberg increased concentrations of iron and chlorophyll a in its wake (*13*). The density of acoustically reflective targets, believed to be zooplankton and micronekton, was twice as high under a free-drifting iceberg as compared with that of targets in surrounding open water in the Weddell Sea (*14*). Top predators, such as seabirds and seals, are also commonly associated with icebergs in the Southern Ocean (*15*–*17*).

Given the prevalence of icebergs in the Southern Ocean and the paucity of data concerning their impact on the surrounding ecosystem over their life span of months to years, we sought to address the following null hypothesis: As drifting islands, icebergs impart no significant ($P > 0.05$) chemical and biological characteristics to the surrounding ecosystem when compared with more peripheral waters some distance away.

Icebergs W-86 and A-52. We studied free-drifting icebergs during austral spring 2005 in the northwest (NW) Weddell Sea, an area of abundant icebergs that originate primarily from the ice shelves along the Antarctic Peninsula (Fig. 1A). Two drifting, tabular icebergs, located ~130 km apart and free of pack ice, were sampled along with the surrounding waters. One iceberg, W-86, was studied from 7 to 15 December 2005 as it traversed a total distance of 123 km (Fig. 1B). W-86 was <2 km long, with an aerial

[1]Monterey Bay Aquarium Research Institute (MBARI), 7700 Sandholdt Road, Moss Landing, CA 95039, USA. [2]San Diego Supercomputer Center, University of California, San Diego, La Jolla, CA 92093–0505, USA. [3]Marine Science and Environmental Studies Department, University of San Diego, 5998 Alcalá Park, San Diego, CA 92110, USA. [4]Department of Chemistry and Biochemistry, University of South Carolina, Columbia, SC 29208, USA. [5]Integrative Oceanography Division, Scripps Institution of Oceanography, University of California, San Diego, La Jolla, CA 92093–0218, USA.

*To whom correspondence should be addressed. E-mail: ksmith@mbari.org

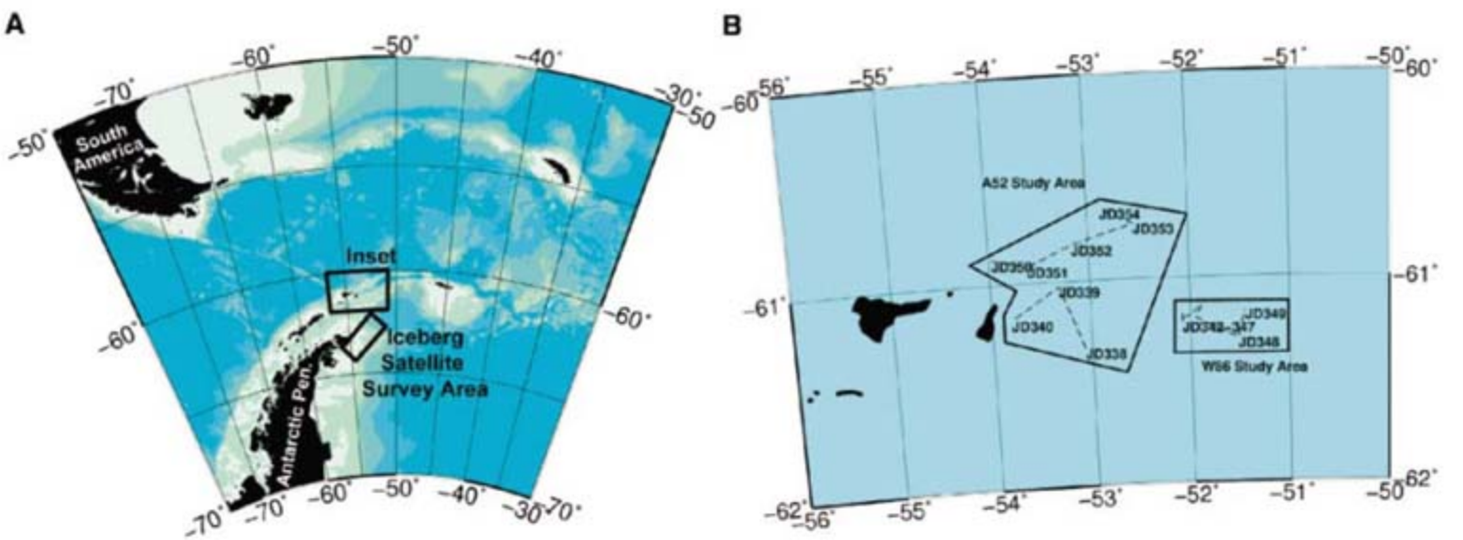

Fig. 1. Northeast extent of the Antarctic Peninsula and South Shetland Island chain, forming the western boundary of the NW Weddell Sea. (**A**) The study region including the shipboard study site [inset depicted in (B)] and the area of the processed SCANSAR-Wideband satellite image for analysis of iceberg number and size. (**B**) Enlarged inset from (A) outlining the study areas for iceberg A-52 to the east of Elephant and Clarence islands and for iceberg W-86 farther to the east. The trajectories of each iceberg, A-52 and W-86, are shown with Julian days (JD) indicated over the course of our study in austral spring 2005.

height of 41 m and a submerged depth of ≥300 m. This iceberg had an estimated aerial surface area of 0.12 km^2. A spiral sampling track was used to encircle the entire iceberg for ship-based surveys of iceberg structure, chlorophyll a, phytoplankton, zooplankton, and micronekton. We used a 10-m^2 opening-closing trawl [multiple opening-closing net and environmental sensing system (MOCNESS)]; a remotely operated vehicle (ROV) with a video camera; an underway flow-through conductivity-temperature-depth (CTD) instrument; a fluorometer; and a large volume pumping system (*18*). Spiral sampling began within 20 m of the iceberg and extended outward beyond 9 km, where the influence of the iceberg was not detectable. Superimposed on this sampling track was a series of CTD-rosette casts and stations where large volumes of water were pumped from depths ≤80 m.

For comparison, we studied a much larger iceberg that was clearly visible as a large feature in satellite images (RADARSAT and QuickSCAT). Iceberg A-52 was first sampled from 3 to 6 December 2005 before its temporary grounding off Clarence Island and was resampled from 16 to 21 December after again becoming free-drifting. The total distance traversed by A-52 over an 18-day period was 531 km (Fig. 1B). A-52 was oblong in shape, with a length of 21 km, an aerial height of 25 to 32 m, and a submerged depth of ≥230 m. The aerial surface area of A-52 was 300.8 km^2 during the first sampling period. However, during the second sampling period, the estimated surface area had decreased by an order of magnitude to 30.8 km^2, after obvious fracturing and ablation. Numerous large waterfalls cascaded from the crest of A-52, suggesting rapid melting across the extensive upper surface. A modified sampling program along the lengths of both sides of A-52, including CTD-rosette casts to 500 m depth, was initiated at parallel distances, extending out from 20 m to 9 km.

Meltwater contributions. Complex surface currents, with a strong diurnal tidal component modulated by inertial currents, imparted irregular spiraling rotations to both icebergs, while A-52 maintained an overall trajectory toward the northeast and W-86 moved primarily east (Fig. 1B) (*19*). Meltwater contributed to highly variable salinity in proximity to both icebergs (Fig. 2, A and B), with lowest salinities most prevalent in surface waters (Fig. 2, C and D). There was enrichment of short-lived ^{224}Ra (half-life = 3.7 days) in the surface waters adjacent to each iceberg. Excess ^{224}Ra (that fraction not supported by ambient parent isotopes) was chosen as an unambiguous terrigenous input. Because the only viable source of excess ^{224}Ra is the decay of ^{228}Th associated with terrigenous particles, the enrichment must indicate local input of ice-rafted detritus into the surrounding surface waters (typically <10 m depth) from meltwater. The sea-surface layer in areas proximal to both icebergs was enriched in excess ^{224}Ra when compared with deeper mixed-layer samples (30 to 80 m depth) that were at or below the detection limit (Fig. 2, E and F), precluding a deep upwelled source of enrichment. Surface enrichments decreased with increasing distance from the icebergs. The highest excess ^{224}Ra enrichment [5.0 disintegrations per minute (dpm) m^{-3}] was observed in water samples collected in brash ice broken off and immediately adjacent to iceberg W-86 (Fig. 2E). These samples also had the highest negative salinity anomaly as compared with samples from the surrounding surface waters, suggesting a meltwater source for the high ^{224}Ra. In contrast, lower excess ^{224}Ra activities were measured between 1 and 5 km from W-86 and from A-52 during the second sampling period (Fig. 2, E and F). We attribute the near "background" activities in some samples collected adjacent to A-52, during the first sampling period, to current-induced upwelling. The trend of decreasing excess ^{224}Ra activity with increasing distance from each iceberg suggests rapid melting and dispersion of the entrained terrigenous material, a potential source of iron to stimulate phytoplankton growth (*20*). Such inputs from free-drifting icebergs likely contribute to the elevated iron concentrations (~1 nM) measured in the Weddell Sea as compared with the extremely low-iron (≤0.1 nM), high-nutrient, low-chlorophyll waters of the Pacific and Indian sectors of the Southern Ocean (*21*).

Surface water concentrations of silicate, phosphate, ammonia, and nitrate revealed no significant pattern with distance from W-86 and A-52 due in part to limited sample sizes (fig. S1).

Phytoplankton community. Phytoplankton biomass, estimated as chlorophyll a integrated between the surface and 10-m depth samples from rosette bottle casts, was diluted in the immediate vicinity (<0.2 km) of iceberg W-86 and increased out to 1.0 km before declining again to significantly lower values ($P < 0.001$) beyond 3.7 km (Fig. 3, A and C, and table S1). A similar pattern, albeit at lower concentrations, was observed around A-52, with higher chlorophyll a concentrations in the immediate vicinity of the iceberg during the first sampling period (Fig. 3, B and D). Moderate concentrations of chlorophyll a occurred <0.25 km from iceberg A-52, with the highest concentrations around 0.5 km and background concentrations beyond 1.0 km. At locations adjacent to both icebergs, underway surface fluorometry measurements also exhibited the highest fluorescence values and variability, which generally decreased with in-

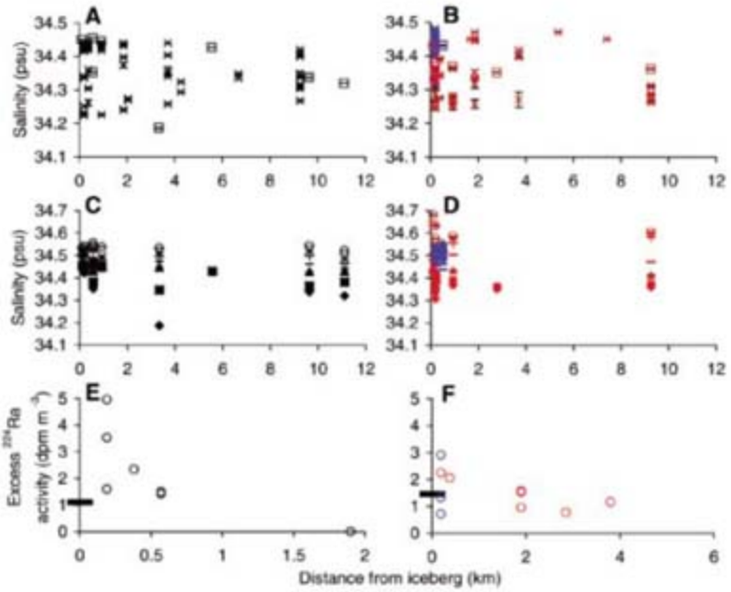

Fig. 2. Surface salinity and excess ^{224}Ra measured with increasing distance from icebergs W-86 and A-52. Black symbols represent measurements around W-86. The first and second sampling periods around A-52 are differentiated by blue and red symbols, respectively. (**A** and **B**) Mean surface salinity (± SE) at meter increments between 0 and 10 m depth determined from CTD casts [open squares; n = 10 measurements (W-86), n = 13 measurements (A-52)] and underway flow system salinity (intake at 5 m depth) determined at 1-min intervals for 5 min [crosses; n = 79 measurements (W-86), n = 100 measurements (A-52)]. The SE of each mean value is generally smaller than the representative symbol. psu, practical salinity units. (**C** and **D**) Mean salinity (± SE) determined from 10 CTD casts at W-86 and 13 casts at A-52 over the following depth intervals: 0 to 10 m (solid diamonds), 11 to 50 m (solid squares), 51 to 100 m (solid triangles), 101 to 200 m (dashes), 201 to 300 m (plus symbols), 301 to 400 m ("×" symbols), and 401 to 500 m (open circles). The SE for each mean value of each depth bin is generally smaller than the size of the representative symbol. (**E** and **F**) Excess ^{224}Ra in surface waters (0 to 10 m depth) with increasing distance from icebergs W-86 and A-52. The first sampling around A-52 (blue symbols) was more variable than the second sampling (red symbols), but the combined trends are similar. For comparison, nearshore sample activities (<10 km from the coastline of the Antarctic Peninsula; n = 7 measurements) are indicated by the black bar on the y axis. Average open ocean (≥100 km from any coastline in the Drake Passage; n = 6 measurements) and mixed-layer samples (30 to 80 m depth proximal to W-86 and A-52; n = 12 measurements) were at or below our detection limit of 0.6 dpm m^{-3}, as was the zero value for W-86 (*18*). [The detection limit was calculated as three (3σ) times our calculated counting error of 0.2 dpm m^{-3}. The error was determined with Poisson statistics on the total counts for each counting interval and propagated based on three counting intervals per sample.]

creasing radial distance (Fig. 3, A and B). The microphytoplankton (>20 μm) composed primarily of diatoms constituted the largest percentage of total chlorophyll a within 1.0 km of W-86 (53%) and A-52 (45%) (Fig. 3, C and D). Beyond a 3-km radius, the microphytoplankton fraction of total chlorophyll a was <24% around both icebergs. The high microphytoplankton biomass associated with W-86 and A-52 is similar to the enhanced biomass encountered in eutrophic areas near the edge of the seasonal pack ice (*22*) or during iron enrichment experiments (*23*, *24*).

Ice-associated community. The submerged sides of W-86 frequently had a reticulated surface, which consisted of indentations (ablation pockets) ~6 to 8 cm across and 1 to 2 cm deep. In the ridges between the indentations were small fragments of volcanic rock that served as attachment surfaces for tufted benthic diatoms, dominated by *Biddulphia aff. punctata*, with associated ciliates and foraminiferans. These diatom communities ranged from the surge-exposure depth of 8 m down to 60 m. Below this depth, there were no obvious signs of epibiota. Juvenile icefish (Channichthyidae) and polychaetes (Polynoidae), associated with pockets and folds in the ice surface, were observed by ROV video but were not collected.

The submerged structural characteristics of A-52 were more diverse than those of W-86, including caves, "subtidal" terraces, scoured areas, and apparent precursor or eroded stages of the reticulated indentations. In one area, a sharp edge led to the suspected underside of the iceberg at 230 m depth. Antarctic krill (*Euphausia superba*) occurred abundantly in association with many substrate forms, including the reticulated surface with attached diatom communities and caves that extended deep into the iceberg's interior. Ctenophores, siphonophores, and chaetognaths were also observed by ROV video in the water adjacent to the ice surface around both icebergs. Extensive expanses of attached diatoms, dominated by *Nitzschia aff. decipiens*, were also present on A-52, aligned as on W-86, between the reticulated indentations in the ice surface (fig. S2). The densest concentrations of these attached algal communities occurred on a flared terrace of the iceberg broadly exposed to downwelling light.

Macrozooplankton and micronekton community. Abundance of macrozooplankton and micronekton, dominated by *E. superba* and the chaetognath *Pseudosagitta gazellae*, was highest within a 3.7-km radius but diminished with increasing distance from both icebergs to much lower background values (Fig. 3, E and F). A Mann-Whitney *U* test revealed a significant decrease ($P < 0.009$) in macrozooplankton and micronekton abundance between the near-field (≤3.7-km radius) and far-field (>3.7-km radius) around A-52 (table S1). Although a similar trend in abundance was associated with W-86, there was no significant difference ($P > 0.05$) between the near- and far-field. The displacement volume of macrozooplankton and micronekton, an estimate of biomass, was highest within 3.7 km of each iceberg, as compared with samples collected >3.7 km away (Fig. 3, G and H). There was a significant decrease ($P < 0.005$) in displacement volume between the near- and far-field surrounding A-52, but no significant difference ($P > 0.05$) in volume was detected between the near- and far-field surrounding W-86 (table S1). Gelatinous zooplankton, especially medusae and siphonophores, were present in higher densities at A-52 than at W-86. In contrast, chaetognaths

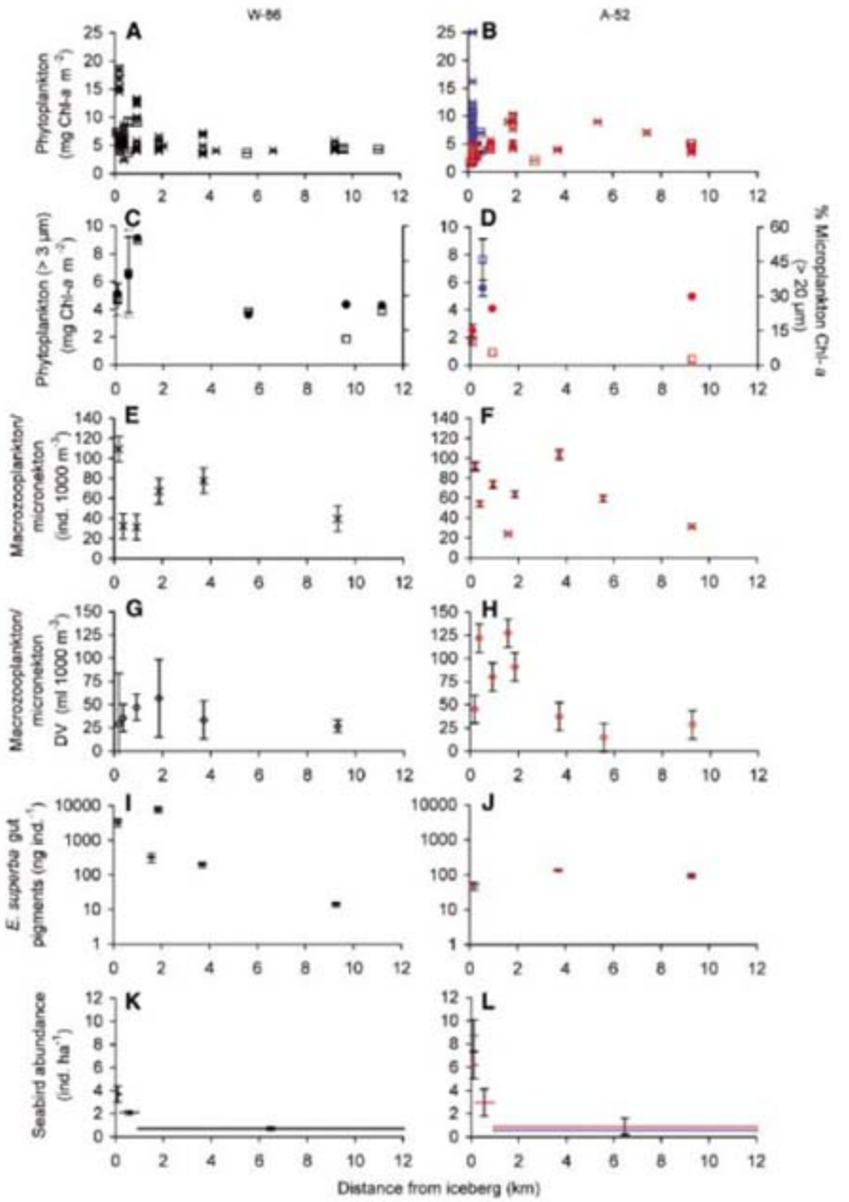

Fig. 3. Pelagic community characteristics as a function of distance from icebergs W-86 and A-52. Black symbols represent measurements around W-86. The first and second sampling periods around A-52 are differentiated by blue and red symbols, respectively. (**A** and **B**) Mean phytoplankton chlorophyll a concentrations (± SE) in filtered size fraction >3 μm integrated from 0 to 10 m depth [open squares; $n = 9$ measurements (W-86), $n = 13$ measurements (A-52)] and chlorophyll a determined from underway fluorometry [crosses; $n = 79$ measurements (W-86), $n = 100$ measurements (A-52)]. SE values of each mean are generally within the bounds of each symbol. (**C** and **D**) Mean chlorophyll a concentration for phytoplankton >3 μm for 0 to 10 m depth (solid circles ± SE) and the percent of that chlorophyll a associated with microphytoplankton >20 μm in size (open squares ± SE). (**E** and **F**) Macrozooplankton and micronekton abundance (mean ± SE) including all taxa. Fauna counted from collections made with a 10-m^2 opening-closing net system with six nets (MOCNESS) towed from ~1100 to 1400 hours (*18*). ind., individuals. (**G** and **H**) Macrozooplankton and micronekton displacement volume (DV) (mean ± SE) for all taxa combined. Fauna were collected as described above, and wet displacement volume was determined shipboard with fresh specimens. (**I** and **J**) Phytopigment analysis of guts from *E. superba*, the dominant macrozooplankton and micronekton species associated with W-86 ($n = 48$ specimens) and A-52 ($n = 39$ specimens). Chlorophyll a is represented by solid circles (mean ± SE) and phaeopigments are represented by "×" symbols (mean ± SE). (**K** and **L**) Pelagic seabird abundance for three aerial zones extending out from each iceberg (mean ± SE).

were more abundant in trawls around W-86 than in trawls near A-52.

In the guts of *E. superba* collected ≤3.7 km from W-86, significantly higher concentrations of phytopigments (chlorophyll a + phaeopigments) were measured, diminishing to lower levels at greater distance ($P < 0.001$; Fig. 3, I and J, and table S1). Consumption of phytoplankton by *E. superba* should contribute to localized export of particulate organic carbon in the form of fecal material (*25*) to greater depths surrounding icebergs. Gut phytopigment concentrations in *E. superba* surrounding W-86 were two orders of magnitude higher than concentrations measured in this species around iceberg A-52. No significant change in gut phytopigment concentration ($P > 0.05$) was detected in *E. superba* with distance from A-52.

Seabird community. Pelagic seabirds were significantly higher in number within 0.9 km of W-86 ($P < 0.001$) and A-52 ($P < 0.001$) in comparison with seabird numbers observed at distances >0.9 km away (Fig. 3, K and L, and table S1). The number of bird species was greater, and community evenness was significantly lower ($P < 0.001$), at locations near W-86 and A-52 as compared with those values measured at positions away from both icebergs. Decreased evenness has previously been associated with the increased dominance of a specific ecological factor, such as resource availability (*26*). Cape petrels (*Daption capense*) were the most numerous bird species, whereas Antarctic fulmars (*Fulmarus glacialoides*) were less abundant and covaried in density with cape petrels. Wilson's storm petrels (*Oceanites oceanicus*) were observed occasionally but were not common.

Bioavailability of terrigenous material. It is clear from our study that icebergs W-86 and A-52 influenced the surrounding pelagic ecosystem, as reflected in elevated concentrations of ^{224}Ra and increased densities of phytoplankton, zooplankton, and pelagic seabirds. As drifting islands, icebergs impart substantial chemical and biological characteristics to the surrounding ecosystem when compared with more peripheral waters some distance away, thus disproving our null hypothesis. We speculate that the release of trace elements, such as iron, stimulates primary production that trophically sustains enhanced populations of krill and predatory seabirds.

We conducted phytoplankton culturing experiments to evaluate the bioavailability of trace metals associated with the iceberg-borne terrigenous material. The growth of the centric diatom *Thalassiosira weissflogii* was compared in media amended with no trace metals, a full complement of trace metals buffered with EDTA, or 10 mg per liter of media of fine terrigenous particles (<63 μm) collected from iceberg fragments adjacent to W-86 (*18*). Diatoms grown in metal-free media amended with iceberg-borne terrigenous material grew at a moderate specific rate of 0.49 per day (a doubling time of 1.4 days), reaching a concentration of 28,000 cells per ml by the end of the 10-day incubation (Fig. 4). In contrast, cells grown in media prepared without metals achieved one cell division before becoming severely metal-limited and slowly senescing for the remainder of the 10-day incubation period. The initial cell division was likely enabled by Fe and other bioactive metals (e.g., Mn, Cu, Zn) stored in the cells before resuspension in the metal-free media. These cultures served as a negative control, demonstrating the limited growth of these cells in trace metal–free media. The highest growth rates for *T. weissflogii* occurred in metal-replete media (Fig. 4) and were similar to those measured by other researchers for this isolate under metal-replete conditions (*27*).

Although isolated from a coastal environment, *T. weissflogii* has been used in numerous studies of Fe availability and uptake, and it is representative of a class of phytoplankton that comprises a critical component of the export production in the Southern Ocean. Previous studies with *T. weissflogii* concluded that the diatom was unable to directly access colloidal or particulate Fe (*28*, *29*), indicating that Fe must dissolve before transport across the cell membrane. Possible mechanisms of dissolution include thermal dissolution (*28*), photoreduction (*30*, *31*), and complexation with siderophores or similar organic ligands (*32*). Each of these mechanisms could occur in the culture flasks of the experiment or naturally in the Southern Ocean.

Population of icebergs. To address how large an "area of influence" was exerted by the two icebergs on the surrounding pelagic zone, we estimated the biological enrichment associated with W-86 and A-52 to be the aerial surface area of each iceberg, depicted as a circle, the radius of which was increased by an additional 3.7 km [the distance beyond which macrozooplankton and micronekton abundance and displacement volume decreased to apparent background levels (Fig. 3, E to H)]. The estimated enrichment area was 47.7 km^2 for W-86 and 577.2 km^2 for A-52. Whether these icebergs have an entrained area of influence or a much larger impact, including a "wake" of enrichment, is yet to be resolved.

Our results show that the estimated area of influence of icebergs W-86 and A-52 was quite extensive. To obtain a broader spatial perspective, we processed the RADARSAT SCANSAR–Wideband satellite image closest in location and time to our study sites (Fig. 1A; image number R15378; 22 Feb 2006). The area processed, 11,265 km^2, contained 962 detectable icebergs free of pack ice, each ≥0.01 km^2 in area (*18*). More than 99% of these icebergs were <0.85 km^2 in area. With an area of 0.12 km^2, W-86 falls within this size range, but A-52 was much larger (fig. S3A). The total area covered by all the icebergs, 50.8 km^2, was only 0.45% of the total area surveyed in the satellite image.

However, our study has shown that there is a zone of biological influence that can extend ~3.7 km in radius from icebergs in the >0.1-km^2 size range. To estimate this expanded zone of biological influence, we assumed that each of the >0.1-km^2 icebergs in the satellite image was circular in area; the radius of each circle was thus calculated and expanded by 3.7 km and then the new area was recalculated (fig. S3B). A total of 89 icebergs fell within this larger size range, and their combined area of influence was 4387 km^2, equaling 39% of the area surveyed in the satellite image. Obviously, this area of influence would increase substantially if the remaining 873 icebergs <0.1 km^2 were included in this analysis. These calculations strongly support the contention that free-drifting icebergs can have a very pronounced impact on the pelagic ecosystem. Furthermore, the proliferation of icebergs associated with global warming should markedly increase their influence on the Southern Ocean ecosystem.

Conclusions. We envision free-drifting icebergs in the Weddell Sea as hot spots of continual micronutrient release that sustain the accompany-

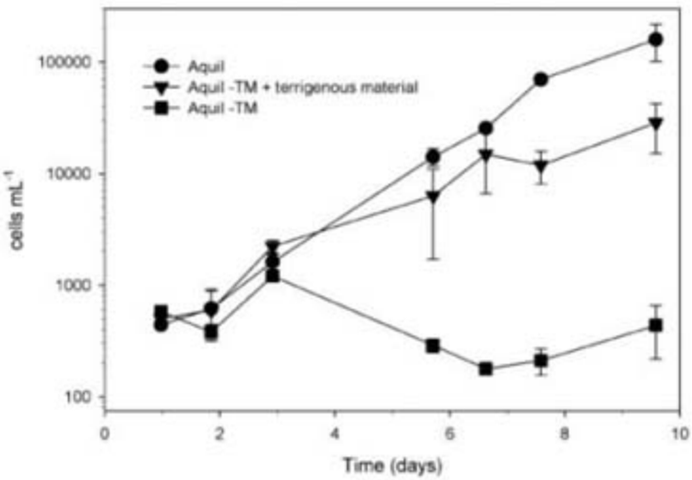

Fig. 4. Cell density of the diatom *T. weissflogii* grown in either metal-replete artificial seawater media (Aquil), media prepared without the addition of any trace metals (Aquil – TM), or media without added metals but amended with 10 mg of washed terrigenous material from iceberg W-86 per liter of media (Aquil – TM + terrigenous material). Cells were grown at 15°C under 300 μmol quanta m^{-2} s^{-1} on a 14:10 light: dark schedule. Cells were preacclimated to metal-deplete media for more than five generations before rinsing and resuspension into each treatment. Cell density was assayed with a Coulter Multisizer II electronic particle counter. Each data point is the mean (± SE) of triplicate cultures.

ing epibiotic and pelagic communities. These icebergs can be compared to estuaries that supply surrounding coastal regions with nutrients. In that respect, icebergs may be thought of as "Lagrangian estuaries," drifting through the Southern Ocean while enriching the surrounding pelagic zone. Our preliminary studies suggest that free-drifting icebergs and their associated communities could serve as areas of increased production and sequestration of organic carbon to the deep sea, a process unaccounted for in current global carbon budgets (*33*).

References and Notes

1. I. Velicogna, J. Wahr, *Science* **311**, 1754 (2006).
2. R. Thomas *et al.*, *Science* **306**, 255 (2004).
3. D. W. J. Thompson, S. Solomon, *Science* **296**, 895 (2002).
4. E. Rignot, S. S. Jacobs, *Science* **296**, 2020 (2002).
5. D. G. Vaughan, G. J. Marshall, W. M. Connolley, J. C. King, R. Mulvaney, *Science* **293**, 1777 (2001).
6. A. J. Cook, A. J. Fox, D. G. Vaughan, J. G. Ferrigno, *Science* **308**, 541 (2005).
7. T. A. Scambos, C. Hulbe, M. Fahnestock, J. Bohlander, *J. Glaciol.* **46**, 516 (2000).
8. R. N. Williams, W. G. Rees, N. W. Young, *Int. J. Remote Sens.* **20**, 3183 (1999).
9. O. Orheim, *Ann. Glaciol.* **11**, 205 (1988).
10. M. Kristensen, *Prog. Phys. Geogr.* **7**, 313 (1983).
11. G. Stone, *Nat. Geog. Mag.*, December 2001, pp. 36–52.
12. K. R. Arrigo, G. L. van Dijken, D. G. Ainley, M. A. Fahnestock, T. Markus, *Geophys. Res. Lett.* **29**, 10.1029/2001GL014160 (2002).
13. H. J. W. de Baar *et al.*, *Nature* **373**, 412 (1995).
14. R. S. Kaufmann *et al.*, *Mar. Biol.* **124**, 387 (1995).
15. D. G. Ainley, E. F. O'Connor, R. J. Boekelheide, *Ornithol. Monogr.* **32**, 1 (1984).
16. C. R. Joiris, *Polar Biol.* **11**, 415 (1991).
17. C. A. Ribic, D. G. Ainley, W. R. Fraser, *Antarct. Sci.* **3**, 181 (1991).
18. Materials and methods are available as supporting material on *Science* Online.
19. Shipboard acoustic doppler current profiler data taken during the cruise were analyzed by T. Chereskin (University of California, San Diego; Scripps Institution of Oceanography) to provide a description of surface currents surrounding icebergs A-52 and W-86.
20. B. M. Loscher, H. J. W. de Baar, J. T. M. de Jong, C. Veth, F. Dehairs, *Deep-Sea Res. II* **44**, 143 (1997).
21. H. J. W. de Baar, J. T. M. de Jong, in *The Biogeochemistry of Iron in Seawater*, D. R. Turner, K. A. Hunter, Eds. (Wiley, New York, 2001), pp. 123–253.
22. W. O. Smith, D. M. Nelson, *Science* **227**, 163 (1985).
23. K. H. Coale *et al.*, *Science* **304**, 408 (2004).
24. P. W. Boyd *et al.*, *Science* **315**, 612 (2007).
25. E. A. Pakhomov, P. W. Froneman, R. Perissinotto, *Deep-Sea Res. II* **49**, 1881 (2002).
26. G. Sugihara, L.-F. Bersier, T. R. Southwood, S. L. Pimm, R. M. May, *Proc. Natl. Acad. Sci. U.S.A.* **100**, 5246 (2003).
27. W. G. Sunda, S. A. Huntsman, *Mar. Chem.* **50**, 189 (1995).
28. M. L. Wells, N. G. Zorkin, A. G. Lewis, *J. Mar. Res.* **41**, 731 (1983).
29. H. W. Rich, F. M. M. Morel, *Limnol. Oceanogr.* **35**, 652 (1990).
30. T. D. Waite, F. M. M. Morel, *J. Colloid Interface Sci.* **102**, 121 (1984).
31. D. A. S. Finden, E. Tipping, G. H. M. Jaworski, C. S. Reynolds, *Nature* **309**, 783 (1984).
32. S. Kraemer, A. Butler, P. Borer, J. Cervini-Silva, *Rev. Mineral. Geochem.* **59**, 53 (2005).
33. I. Marinov, A. Gnanadesiker, J. R. Toggweiler, J. L. Sarmiento, *Nature* **441**, 964 (2006).

34. We thank all the shipboard scientific personnel on the research vessel *Laurence M. Gould* cruise LMG05-14A for excellent support, including R. Wilson, K. Reisenbichler, R. Sherlock, J. Ellena, M. Vardaro, K. Osborn, D. Chakos, J. Derry, L. Ekern, J. Kinsey, C. Koehler, and K. Noble. Captain R. Verret and his crew made sampling around icebergs a reality even under the most difficult conditions. The Raytheon Polar Services support group of S. Suhr-Sliester, J. Spillane, P. Fitzgibbons, K. Pedigo, J. Dolan, E. Roggenstein, and D. Elsberg provided excellent deck and laboratory support. D. Long (Brigham Young University) provided timely QuikSCAT images of the location of iceberg A-52 during our cruise. RADARSAT images of our study area were forwarded to the ship through Palmer Station. This research was supported by NSF grants ANT-0529815, ANT-0650034, and OCE-0327294, and by the David and Lucile Packard Foundation. We thank P. Penhale (NSF, Polar Programs) for having the foresight and courage to fund this speculative project. W. Moore and C. Hexel contributed to the ^{224}Ra analysis and data synthesis. C. Stoker of NASA/Ames Research Center loaned us the ROV, and H. Thomas at MBARI trained us in its operation.

Supporting Online Material

www.sciencemag.org/cgi/content/full/1142834/DC1
Materials and Methods
Figs. S1 to S3
Table S1
References

21 March 2007; accepted 4 June 2007
Published online 21 June 2007;
10.1126/science.1142834
Include this information when citing this paper.

The Product Space Conditions the Development of Nations

C. A. Hidalgo,[1]*† B. Klinger,[2]* A.-L. Barabási,[1] R. Hausmann[2]

Economies grow by upgrading the products they produce and export. The technology, capital, institutions, and skills needed to make newer products are more easily adapted from some products than from others. Here, we study this network of relatedness between products, or "product space," finding that more-sophisticated products are located in a densely connected core whereas less-sophisticated products occupy a less-connected periphery. Empirically, countries move through the product space by developing goods close to those they currently produce. Most countries can reach the core only by traversing empirically infrequent distances, which may help explain why poor countries have trouble developing more competitive exports and fail to converge to the income levels of rich countries.

Does the type of product that a country exports matter for subsequent economic performance? The fathers of development economics held that it does, suggesting that industrialization creates spillover benefits that fuel subsequent growth (*1*–*3*). Yet, lacking formal models, mainstream economic theory has been unable to incorporate these ideas. Instead, two approaches have been used to explain a country's pattern of specialization. The first focuses on the relative proportion between productive factors (i.e., physical capital, labor, land, skills or human capital, infrastructure, and institutions) (*4*). Hence, poor countries specialize in goods intensive in unskilled labor and land, whereas richer countries specialize in goods requiring infrastructure, institutions, and human and physical capital. The second approach emphasizes technological differences (*5*) and has to be complemented with a theory of what underlies them. The varieties and quality ladders models (*6*, *7*) assume that there is always a slightly more advanced product, or just a different one, that countries can move to, disregarding product similarities when thinking about structural transformation and growth.

Think of a product as a tree and the set of all products as a forest. A country is composed of a collection of firms, i.e., of monkeys that live on different trees and exploit those products. The process of growth implies moving from a poorer part of the forest, where trees have little fruit, to better parts of the forest. This implies that monkeys would have to jump distances, that is, redeploy (human, physical, and institutional) capital toward goods that are different from those currently under production. Traditional growth theory assumes there is always a tree within reach; hence, the structure of this forest is unimportant. However, if this forest is heterogeneous, with some dense areas and other more-deserted ones, and if monkeys can jump only limited distances, then monkeys may be unable to move through the forest. If this is the case, the structure of this space and a country's orientation within it become of great importance to the development of countries.

In theory, many possible factors may cause relatedness between products, that is, closeness between trees; such as the intensity of labor, land, and capital (*8*), the level of technological sophistication (*9*, *10*), the inputs or outputs involved in a product's value chain (e.g., cotton, yarn, cloth, and garments) (*11*), or requisite insti-

[1]Center for Complex Network Research and Department of Physics, University of Notre Dame, Notre Dame, IN 46556, USA. [2]Center for International Development, Kennedy School of Government, Harvard University, Cambridge, MA 02139, USA.

*These authors contributed equally to this work.
†To whom correspondence should be addressed. E-mail: chidalgo@nd.edu

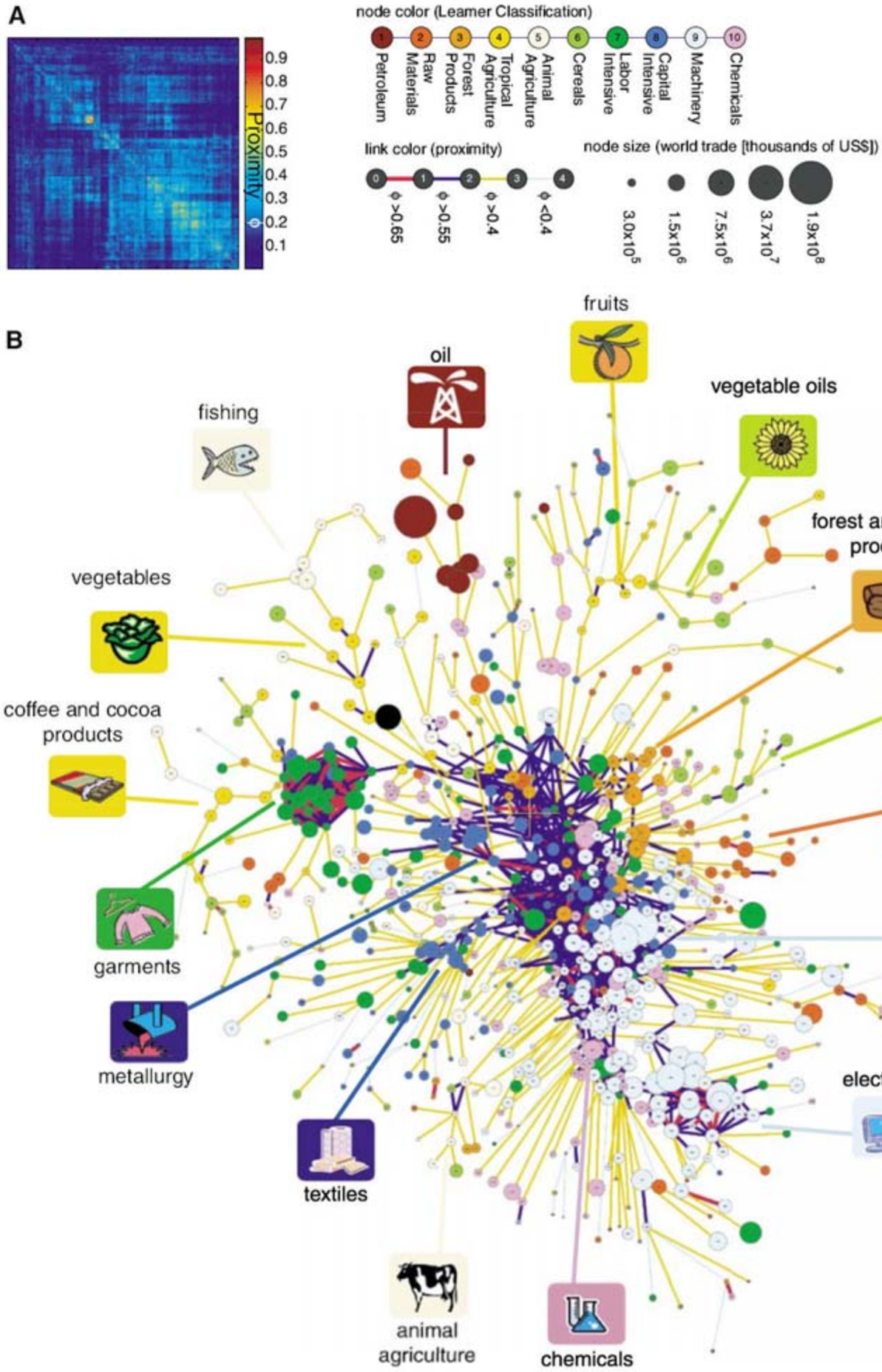

Fig. 1. The product space. (**A**) Hierarchically clustered proximity (ϕ) matrix representing the 775 SITC-4 product classes exported in the 1998–2000 period. (**B**) Network representation of the product space. Links are color coded with their proximity value. The sizes of the nodes are proportional to world trade, and their colors are chosen according to the classification introduced by Leamer.

tutions (*12*, *13*). All of these are a priori notions of what dimension of similarity are most important and assume that factors of production, technological sophistication, or institutional quality exhibit little specificity. Instead, we take an agnostic approach and use an outcomes-based measure, based on the idea that, if two goods are related because they require similar institutions, infrastructure, physical factors, technology, or some combination thereof, they will tend to be produced in tandem, whereas dissimilar goods are less likely to be produced together. We call this measure "proximity," which formalizes the intuitive idea that the ability of a country to produce a product depends on its ability to produce other products. For example, a country with the ability to export apples will probably have most of the conditions suitable to export pears. They would certainly have the soil, climate, packing technologies, and frigorific trucks. In addition, they would have skilled agronomists, phytosanitary laws, and trade agreements that could be easily redeployed to the pear business. If instead we consider a different product such as copper wires or home appliance manufacture, all or most of the capabilities developed for the apple business render useless. We introduce proximity as the concept that captures this intuitive notion.

The concept of proximity. Formally, the proximity ϕ between products i and j is the minimum of the pairwise conditional probabilities of a country exporting a good given that it exports another.

$$\phi_{i,j} = \min\{P(RCAx_i|RCAx_j), P(RCAx_j|RCAx_i)\}$$

Where RCA stands for revealed comparative advantage (*14*)

$$RCA_{c,i} = \frac{x(c,i)}{\sum_i x(c,i)} \Big/ \frac{\sum_c x(c,i)}{\sum_{c,i} x(c,i)}$$

which measures whether a country c exports more of good i, as a share of its total exports, than the "average" country ($RCA > 1$ not $RCA < 1$).

We used international trade data, cleaned and made compatible (*15*) through a National Bureau of Economic Research (NBER) project lead by R. Feenstra (*16*), disaggregated according to the Standardized International Trade Code at the four-digit level (SITC-4), providing for each country the value exported to all other countries for 775 product classes. With these data, we calculated the 775-by-775 matrix of revealed proximities between every pair of products by using the equation above.

A hierarchically clustered version of the matrix is shown (Fig. 1A). A smooth and homogeneous product space would imply uniform values (homogenous coloring), whereas a product-ladder model (*7*) would suggest a matrix with high values (or bright coloring) only along the diagonal. Instead the product space of Fig. 1A appears to be modular (*17*, *18*), with some goods highly connected and others disconnected. Furthermore, as a whole the product space is sparse, with ϕ_{ij} distributed according to a broad distribution (fig. S2) with 5% of its elements equal to zero, 32% of them smaller than 0.1, and 65% of the entries taking values below 0.2. These substantial number of negligible connections call for a network representation (*19*), allowing us to explore the structure of the product space together with the proximity between products of given classifications and participation in world trade. To offer a visualization in which all 775 products are included, we reached all nodes by calculating the maximum spanning tree, which includes the 774 links maximizing the tree's added proximity (fig. S4) and superposed on it all links with a proximity larger than 0.55 (figs. S5 and S6). This set of 1525 links is used to visualize the structure of the full proximity matrix, which is far from homogenous and appears to have a core-periphery structure (Fig. 1B). The core is formed by metal products, machinery, and chemicals, whereas the periphery is formed by the rest of the product classes. The products in the top of the periphery belong to fishing, tropical, and cereal agriculture. To the left there is a strong peripheral cluster formed by garments and another one belonging to textiles, followed by animal agriculture. The bottom of the network shows a large electronics cluster, followed to the right by mining, forest, and paper products.

The network shows clusters of products somewhat related to the classification introduced by

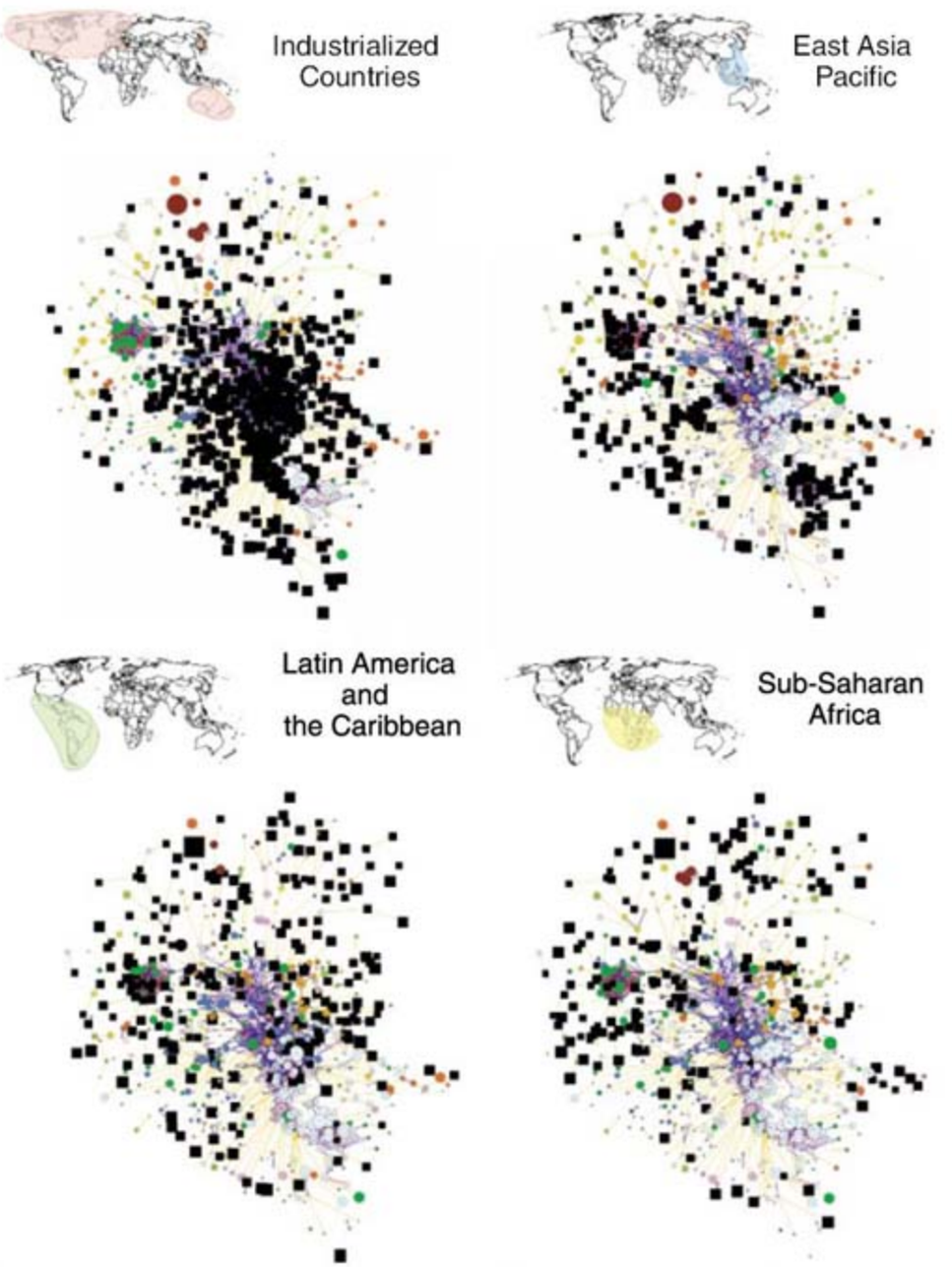

Fig. 2. Localization of the productive structure for different regions of the world. The products for which the region has an $RCA > 1$ are denoted by black squares.

Leamer (*8*), which is based on relative factor intensities (table S1 and fig. S8), that is, the relative amount of capital, labor, land, or skills required to produce each product. Although the classification performed by Leamer was done with a different methodology, the agreement between it and the structure of the product space is striking. Yet it also introduces a more detailed split of some product classes. For example, machinery is naturally split into two clusters, one consisting of vehicles and heavy machinery and another one belonging to electronics. The machinery cluster is interwoven with some capital-intensive metal products but is not tightly connected to similarly classified products such as textiles.

The map obtained can be used to analyze the evolution of a country's productive structure. For this purpose we held the product space fixed and studied the dynamics of production within it, although changes in the product space represent an interesting avenue for future research (*20*).

The pattern of specialization for four regions in the product space is shown in Fig. 2 (*21*). Products exported by a region with $RCA > 1$ are shown with black squares. Industrialized countries occupy the core, composed of machinery, metal products, and chemicals. They also participate in more peripheral products such as textiles, forest products, and animal agriculture. East Asian countries have developed RCA in the garments, electronics, and textile clusters, whereas Latin America and the Caribbean are further out in the periphery in mining, agriculture, and the garments sector. Lastly, sub-Saharan Africa exports few product types, all of which are in the far periphery of the product space. These results indicate that each region has a distinguishable pattern of specialization clearly visible in the product space. Links to the maps for the 132 countries included in the study can be found in the Supporting Online Material (SOM) text.

Next, we show how the structure of the product space affects a country's pattern of specialization. Figure 3A shows how comparative advantages evolved in Malaysia and Colombia between 1980 and 2000 in the electronics and the garments sectors, respectively. Both countries follow a diffusion process in which comparative advantage move preferentially toward products close to existing goods: garments in Colombia and electronics in Malaysia.

Testing diffusion. Beyond this graphical illustration, is it true that countries develop comparative advantage preferentially in nearby goods? We used two different approaches to this question. First, we measured the average proximity of a new potential product j to a country's current productive structure, which we call "density" and define as

$$\omega_j^k = \frac{\sum_i x_i \phi_{ij}}{\sum_i \phi_{ij}}$$

where ω^k_j is the density around good j given the export basket of the kth country and $x_i = 1$ if $RCA_{ki} > 1$ and 0 otherwise. A high density value means that the kth country has many developed products surrounding the jth product. To study the evolution of comparative advantage, we considered "transition products" as those with an $RCA_{c,i} < 0.5$ in 1990 and an $RCA_{c,i} > 1$ in 1995. As a control, we considered "undeveloped products" those that in 1990 and 1995 had an $RCA_{c,i} < 0.5$ and disregarded those cases not fitting any of these two criteria. Figure 3B shows how density is distributed around transition products (yellow) and compares it to densities around undeveloped products (red). Clearly, these distributions are very distinct, with a higher density around transition products than among undeveloped ones [analysis of variance (ANOVA) $P < 10^{-30}$].

At the single product level, we considered the ratio between the average density of all countries in which the jth product was a transition product and the average density of all countries in which the jth product was not developed. Formally, we define the "discovery factor" H_j as

$$H_j = \frac{\sum_{k=1}^{T} \omega^k_j / T}{\sum_{k=T+1}^{N} \omega^k_j / (N-T)}$$

where T is the number of countries in which the jth good was a transition product and N is the total number of countries. Figure 3C shows the frequency distribution of this ratio. For 79% of products, this ratio is greater than 1, indicating that ω_j^k is greater in countries that transitioned into the j^{th} good than in those that did not, often substantially.

An alternative way of illustrating that countries develop *RCA* in goods close to those they

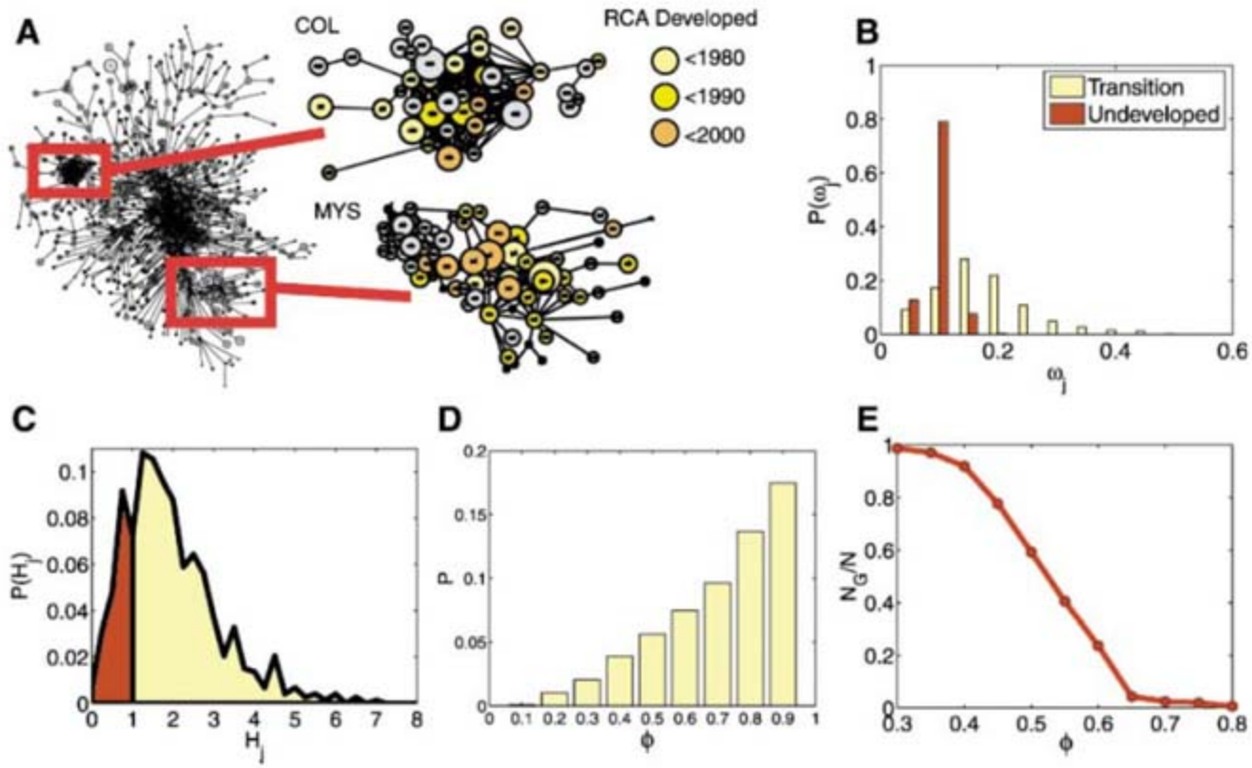

Fig. 3. Empirical evolution of countries. (**A**) Examples of RCA spreading for Colombia (COL) and Malaysia (MYS). The color code shows when this countries first developed $RCA > 1$ for products in the garments sector in Colombia and in the electronics cluster for Malaysia. (**B**) Distribution of density (ω) for transition products and undeveloped products (**C**) Distribution for the relative increase in density for products undergoing a transition with respect to the same products when they remain undeveloped. (**D**) Probability of developing RCA given that the closest connected product is at proximity ϕ. (**E**) Relative size of the largest connected component N_G with respect to the total number of products in the system N as a function of link ϕ.

already had is to calculate the conditional probability of transitioning into a product given that the nearest product with $RCA > 1$ is at a given ϕ. There is a monotonic relationship (Fig. 3D) between the proximity of the nearest developed good and the probability of transitioning into it. Although the probability of moving into a good at $\phi = 0.1$ in the course of 5 years is almost nil, the probability is about 15% if the closest good is at $\phi = 0.8$ (*22*).

Because production shifts to nearby products, we asked whether the product space is sufficiently connected that given enough time, all countries can reach most of it, particularly the richest parts. Lack of connectedness may explain the difficulties faced by countries trying to converge to the income levels of rich countries: they may not be able to undergo structural transformation because proximities are just too low. A simple approach is to calculate the relative size of the largest connected component as a function of ϕ. At $\phi \geq$

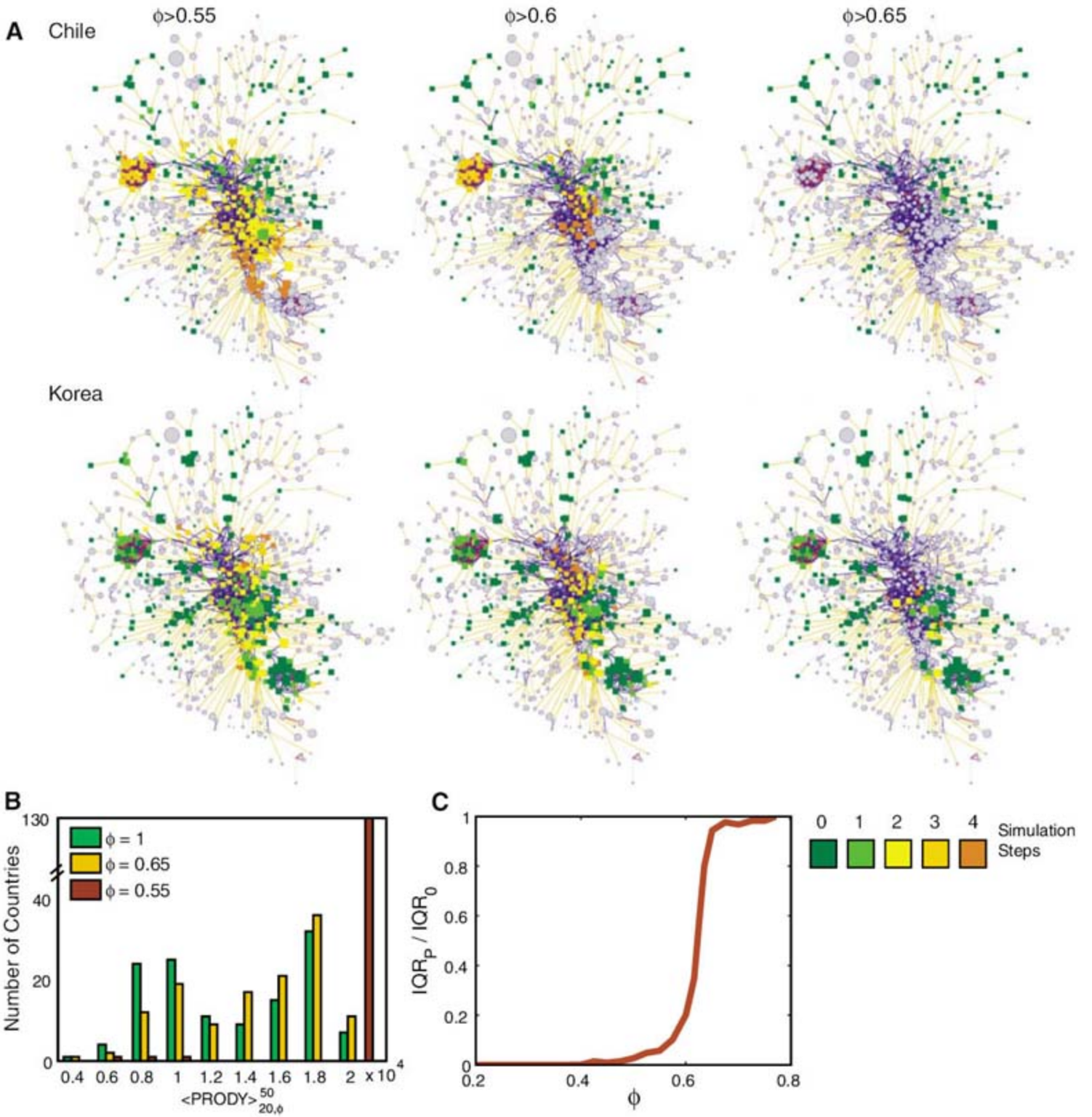

Fig. 4. Simulated diffusion process and inequality. (**A**) Simulated diffusion process for Chile and Korea in which we allowed countries to develop RCA in all products closer than ϕ values of 0.55, 0.6, and 0.65. The number of steps required to develop RCA can be read from the color code on the bottom right corner. (**B**) Distribution for the average PRODY of the best 50 products in a countries basket before and after 20 rounds of diffusion. The original distribution is shown in green, whereas the one associated with the distribution after 20 diffusion rounds with $\phi = 0.65$ is presented in yellow and $\phi = 0.55$ in red. (**C**) IQR of the distribution of the best 50 products after diffusing with a given ϕ normalized by the IQR of the best 50 products in absence of diffusion.

0.6, the largest connected component has a negligible size compared with the total number of products (Fig. 3E), whereas for $\phi \leq 0.3$ the product space is almost fully connected, meaning that there is always a path between two different products.

We studied the impact of the product space structure by simulating how the position of countries evolve when allowed to repeatedly move to products with proximities greater than a certain ϕ_o. If countries diffuse to nearby products and these are sufficiently connected to others, then after several iterations, 20 in our exercise, countries would be able to reach richer parts of the product space. On the other hand, if the product space is disconnected, countries will not be able to find paths to the richer part of the product space, independently of how many steps they are allowed to make.

The results of our simulation for Chile and Korea are presented in Fig. 4A. At a relatively low proximity ($\phi_o = 0.55$), both countries are able to diffuse through to the core of the product space; however, Korea is able to do so much faster, thanks to its positioning in core products. For higher proximities, the question becomes whether a country can spread at all. At $\phi_o = 0.6$, Chile is able to spread slowly throughout the space, whereas Korea is still able to populate the core after four rounds. At $\phi_o = 0.65$, Chile is not able to diffuse, lacking any close-enough products, whereas Korea develops RCA slowly to a few products close to the machinery and electronics cluster.

To generalize this analysis for the whole world, we needed a measure to summarize the position of a country in the product space. We adopted a measure based on Hausmann, Hwang, and Rodrik (*23*), which involves a two-stage process. First, for every product we assigned a value, which is the weighted gross domestic product (GDP) per capita of countries with comparative advantage in that good, called PRODY (*23*). We then averaged the PRODYs of the top N products that a country has access to after M iterations at ϕ_o and denoted it by $< PRODY >^N_{M\phi_o}$. Figure 4B shows the distribution of $< PRODY >^N_{M\phi_o}$ for $N = 50$, $M = 20$, and $\phi_o = 1$ (green), $\phi_o = 0.65$ (yellow), and $\phi = 0.55$ (red). The distribution for $\phi_o = 1$ allows us to characterize the current distribution of countries in the product space, which shows a bimodal distribution, a signature of a world divided into rich and poor countries with few countries occupying the center of the distribution. When we allow countries to diffuse up to $\phi_o = 0.65$, this distribution does not change significantly: it shifts slightly to the right because of the acquisition of a limited number of sophisticated products by some countries. This diffusion process, however, stops after a few rounds, and the world maintains a degree of inequality similar to its current state. Contrarily, when we consider $\phi_o = 0.55$, most countries are able to diffuse and reach the most sophisticated basket in the long run. Only a few countries are left behind, which unsurprisingly make up the poorest end of the income distribution.

To quantify the level of convergence we calculated the interquartile range (IQR) for the $< PRODY >^{50}_{20\phi}$ distribution and normalized this quantity by dividing it with the IQR for the original distribution. Figure 4C shows that the convergence of the system goes through an abrupt transition and that convergence is possible if countries are able to diffuse to products located at a proximity $\phi > 0.65$.

The bimodal distribution of international income levels and a lack of convergence of the poor toward the rich has been explained by using geographic (*24*) and institutional (*12*, *13*) arguments. Here, we introduced another factor to this discussion: the difficulties involved in moving through the product space. The detailed structure of the product space is shown here and, together with the location of the countries and the characteristics of the diffusion process undergone by them, strongly suggests that not all countries face the same opportunities when it comes to development. Poorer countries tend to be located in the periphery, where moving toward new products is harder to achieve. More interestingly, among countries with a similar level of development and seemingly similar levels of production and export sophistication, there is significant variation in the option set implied by their current productive structure, with some on a path to continued structural transformation and growth and others stuck in a dead end.

These findings have important consequences for economic policy, because the incentives to promote structural transformation in the presence of proximate opportunities are quite different from those required when a country hits a dead end. It is quite difficult for production to shift to products far away in the space, and therefore policies to promote large jumps are more challenging. Yet it is precisely these long jumps that generate subsequent structural transformation, convergence, and growth.

References and Notes

1. A. Hirschman, *The Strategy of Economic Development* (Yale Univ. Press, New Haven, CT, 1958).
2. P. Rosenstein-Rodan, *Econ. J.* **53**, 202 (1943).
3. K. Matsuyama, *J. Econ. Theory* **58**, 317 (1992).
4. E. Heckscher, B. Ohlin, *Heckscher-Ohlin Trade Theory*, H. Flam, M. Flanders, Eds. (MIT Press, Cambridge, MA, 1991).
5. P. Romer, *J. Polit. Econ.* **94**, 5 (1986).
6. P. Aghion, P. Howitt, *Econometrica* **60**, 2 (1992).
7. G. Grossman, E. Helpman, *Rev. Econ. Stud.* **58**, 1 (1991).
8. E. Learner, *Sources of Comparative Advantage: Theory and Evidence* (MIT Press, Cambridge, MA, 1984).
9. S. Lall, *Oxf. Dev. Stud.* **28**, 337 (2000).
10. R. Caballero, A. Jaffe, *NBER Macroeconom. Ann.* **8**, 15 (1993).
11. E. Dietzenbacher, M. Lahr, *Input-Output Analysis: Frontiers and Extensions* (Palgrave, New York, 2001).
12. D. Rodrik, A. Subramanian, F. Trebbi, *NBER Work. Pap. 9305* (2002).
13. D. Acemoglu, S. Johnson, J. A. Robinson, *Am. Econ. Rev.* **91**, 1369 (2001).
14. We use the Balassa definition (*25*) of revealed comparative advantage (Materials and Methods).
15. Because one country's exports are another country's imports, national statistics can be reconciled this way, and missing data from nonreporting countries can be completed.
16. R. R. Feenstra, H. D. Lipsey, A. Ma, H. Mo, *NBER Work. Pap. 11040* (2005).
17. E. Ravasz, A. L. Somera, D. A. Mongru, Z. N. Oltvai, A.-L. Barabási, *Science* **297**, 1551 (2002).
18. G. Palla, I. Derenyi, I. Frakas, T. Vicsek, *Nature* **435**, 814 (2005).
19. Good introductions to networks are (*26*, *27*).
20. The network shown here represents the structure of the product space as determined from the 1998–2000 periods. Holding the product space as fixed is a good first approximation, because the dynamics of the network is much slower than the one of countries. The Pearson correlation coefficient (PCC) between the proximity of all links present in this network and the ones obtained from the same network in 1990 and 1985 are 0.69 and 0.66, respectively (SOM text). This indicates that, although the network changes over time, after 15 years the strength of past links still predicts the strength of the current links to a considerable extent.
21. An alternative approach in which the network of trade relationships was studied was undertaken by (*28*–*30*).
22. We repeated the same exercise with the rank of proximity instead of proximity itself in order to assess whether what matters is absolute or relative proximity. We found that absolute distance appears to be what matters most. Although transition probability increases linearly with proximity, they decay with rank as a power law. Moreover, the rank effect is stronger for products in sparser parts of the product space, where transitions are also less frequent. Thus, densely connected products can develop RCA through more paths than sparsely connected ones, indicating the importance of absolute proximity.
23. We follow the methodology developed in Hausmann, Hwang, and Rodrik (*31*), which weighs the GDP per capita of each country exporting that product by the RCA that the country has in that good.
24. J. Gallup, J. Sachs, A. Mellinger, *Int. Reg. Sci. Rev.* **22**, 179 (1999).
25. B. Balassa, *Rev. Econ. Stat.* **68**, 315 (1986).
26. R. A. Barabási, *Rev. Mod. Phys.* **74**, 47 (2002).
27. G. Caldarelli, *Scale-Free Networks: Complex Webs in Nature and Technology* (Oxford Univ. Press, Oxford, 2007).
28. M. A. Serrano, M. Boguña, *Phys. Rev. E* **68**, 015101 (2003).
29. D. Garlaschelli, M. I. Loffredo, *Phys. Rev. Lett.* **93**, 188701 (2004).
30. D. Garlaschelli, T. Di Matteo, T. Aste, G. Caldarelli, M. I. Loffredo, http://arxiv.org/abs/physics/0701030.
31. R. Hausmann, J. Hwang, D. Rodrik, *NBER Work. Pap. 11905* (2006).

32. We would like to thank the following for valuable comments: P. Aghion, L. Alfaro, O. Blanchard, R. Caballero, O. Galor, E. Helpman, A. Khwaja, J. Lahey, R. Lawrence, D. Lederman, L. Pritchett, R. Rigobon, D. Rodrik, A. Rodriguez-Clare, C. Sabel, E. Stein, F. Sturzenegger, and D. Weil. C.A.H. acknowledges support from the Kellogg Institute at Notre Dame. C.A.H. and A.-L.B. acknowledge support from NSF grants ITR DMR-0426737 and IIS-0513650 and from the James McDonald Foundation 220020084.

Supporting Online Material

www.sciencemag.org/cgi/content/full/317/5837/482/DC1
Materials and Methods
SOM Text
Figs. S1 to S18
Table S1
References

2 May 2007; accepted 5 July 2007
10.1126/science.1144581

Single-Atom Single-Photon Quantum Interface

Tatjana Wilk,[1] Simon C. Webster,[1] Axel Kuhn,[2] Gerhard Rempe[1]*

A major challenge for a scalable quantum computing architecture is the faithful transfer of information from one node to another. We report on the realization of an atom-photon quantum interface based on an optical cavity, using it to entangle a single atom with a single photon and then to map the quantum state of the atom onto a second single photon. The latter step disentangles the atom from the light and produces an entangled photon pair. Our scheme is intrinsically deterministic and establishes the basic element required to realize a distributed quantum network with individual atoms at rest as quantum memories and single flying photons as quantum messengers.

Cavity quantum electrodynamics with individually addressable atoms emitting single photons on demand is expected to provide an ideal toolbox for quantum networking and linear optical quantum computing (*1*). First, using a single atom makes it possible to produce single photons (*2*–*5*) with controlled waveform and polarization (*6*). Such light fields with zero multi-photon contribution are a key ingredient of scalable quantum networks (*7*) and quantum repeaters (*8*). Second, the strong atom-cavity coupling achievable in a high-finesse cavity allows the channeling of quantum information stored in atomic states into photons emitted in a well-defined direction. Compared with free-space schemes (*9*–*11*), this boosts the success probability by several orders of magnitude. It allows realizing deterministic protocols in quantum information science, in particular to entangle an atom with a photon, map quantum states between different information carriers such as an atom and a photon, and generate multi-photon entanglement (*12*). Related schemes have been demonstrated with Rydberg atoms passing through a lossless microwave resonator (*13*). Their implementation in a dissipative optical cavity generates the flying photons required for the above-mentioned applications.

We have realized the essential ingredient of an optical quantum network—namely, an atom-photon interface—using a high-finesse optical cavity containing a single ^{87}Rb atom. Strong atom-cavity coupling is achieved and allows for intrinsically deterministic photon emission. The triggered emission of a first photon entangles the internal state of the atom and the polarization state of the photon. In contrast to probabilistic experiments (*9*, *11*), the atomic state is not examined by using a shelving technique and detecting fluorescence photons. Instead, our scheme maps the atomic state onto the state of a second single photon. Such a state mapping is feasible because the atom-cavity system generates single photons very efficiently in a well-defined mode, which can easily be observed. As a result of the state mapping a pair of entangled photons is produced, one emitted after the other into the same mode. The polarization state of the two photons is analyzed by tomography, which also probes the prior entanglement between the atom and the first photon. As a first step toward local control of the memory qubit, we also show rotation of the atomic state between entanglement creation and state mapping. An extension of our scheme should allow stepwise engineering of entangled states with even higher photon number (*12*).

Our scheme (Fig. 1) shows a single ^{87}Rb atom coupled to an optical cavity and prepared in the $|F = 2, m_F = 0\rangle$ state of the $5S_{1/2}$ ground level. With the cavity axis as quantization direction, the cavity supports left- and right-handed circularly polarized σ^+ and σ^- modes. A π-polarized laser (resonant with the transition from $F = 2$ to $F' = 1$ of the excited $5P_{3/2}$ level) together with the cavity (coupling levels $F = 1$ and $F' = 1$) drives a vacuum-stimulated Raman adiabatic passage (*2*, *14*) to the $|F = 1\rangle$ state of the ground level. Two different paths to states $|\pm1\rangle \equiv |F = 1, m_F = \pm1\rangle$ are possible, resulting in the generation of a σ^- or a σ^+ photon, respectively. After photon emission the system is in the entangled state

$$|\Psi_{\text{atom,photon 1}}\rangle = \frac{1}{\sqrt{2}}(|+1,\sigma^-\rangle - |-1,\sigma^+\rangle) \quad (1)$$

where the phase of the superposition is defined by the transition amplitudes from the $|F = 2, m_F = 0\rangle$ state to the $|+1\rangle$ and $|-1\rangle$ states.

To map the atomic state onto a second photon, a π-polarized laser resonant with the transition from $F = 1$ to $F' = 1$, again together with the cavity, drives a second Raman adiabatic passage (Fig. 1B). The population in state $|+1\rangle$ is transferred to $|0\rangle \equiv |F = 1, m_F = 0\rangle$ and a σ^+ photon is emitted, whereas the population in $|-1\rangle$ is also transferred to $|0\rangle$, but a σ^- photon is emitted. The atom-photon entanglement is therefore converted into a polarization entanglement between two photons,

$$|\Psi_{\text{photon 2, photon 1}}\rangle = \frac{1}{\sqrt{2}}(|\sigma^+,\sigma^-\rangle - |\sigma^-,\sigma^+\rangle) \quad (2)$$

while the atom is disentangled from the light.

In the experiment (Fig. 2A), a dilute cloud of laser-cooled ^{87}Rb atoms falls through an optical high-finesse cavity (*6*). The maximum atom-cavity coupling constant for the relevant transitions has a magnitude $g/2\pi = 3.1$ MHz, and the cavity-field decay rate κ and dipole decay rate of the atom γ are $(\kappa, \gamma)/2\pi = (1.25, 3.0)$ MHz. The atom flux through the cavity is so low (about two atoms per millisecond) that the probability of having two atoms during the transit time of 35 μs is negligible. Atoms are illuminated by laser pulses from the side, all polarized linearly along the cavity axis. Preparation of the initial state is achieved by optical pumping with two lasers, one resonant with the transition from $F = 2$ to $F' = 2$, the other coupling levels $F = 1$ and $F' = 2$. Both lasers, applied simultaneously for 2.8 μs, have constant Rabi frequencies of $\Omega/2\pi = 35$ MHz. Failure of the optical pumping does not reduce the measured entanglement fidelity, because an atom in a wrong initial state can only emit a photon in either the first or the second pulse, but not in both. Entangling and mapping laser pulses have a $\sin^2(\pi t/t_P)$ time dependence, with $t_P = 1.1$ μs. The peak Rabi frequency of the entangling pulse is $\Omega/2\pi = 24$ MHz. Because the mapping laser is resonant with the cavity, its peak Rabi frequency is chosen to be lower ($\Omega/2\pi = 9$ MHz) to avoid off-resonant (via $F' = 0$) repeated excitation of the atom. As a result, after detecting a first photon we observe a second photon in the

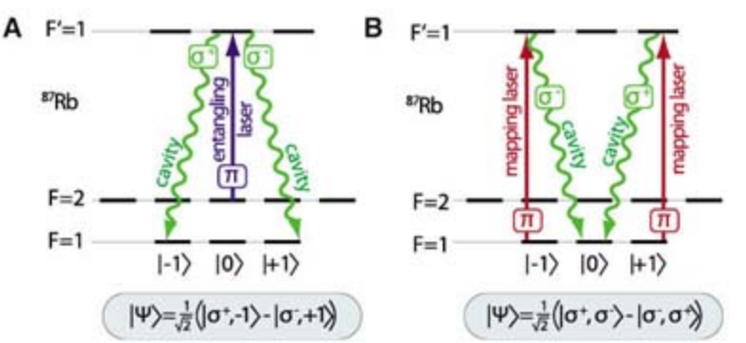

Fig. 1. Entanglement and state mapping. Together with the cavity, laser pulses drive vacuum-stimulated Raman adiabatic passages, first (**A**) creating an entanglement between the atom and the emitted photon, and then (**B**) mapping the atomic state onto the polarization state of a second photon. Entanglement is then shared between two flying photons, with the atom disentangled.

[1]Max-Planck-Institut für Quantenoptik, Hans-Kopfermann-Strasse 1, D-85748 Garching, Germany. [2]Clarendon Laboratory, University of Oxford, Parks Road, Oxford OX1 3PU, UK.

*To whom correspondence should be addressed. E-mail: gerhard.rempe@mpq.mpg.de

same pulse with a probability of only 0.6%. Entangling and mapping pulses are separated from each other by an adjustable time interval, t_S, so detected photons can clearly be assigned to the first or the second laser pulse. Figure 2B displays the pulse sequence and the measured photon arrival-time distribution. From a Hanbury Brown and Twiss measurement, we infer that the efficiency for generating a photon during the entangling (mapping) pulse conditioned on the detection of a photon during the previous entangling pulse is 14.8% (8.8%) (*15*), resulting in a 1.3% success probability for generating an entangled photon pair. This includes the random position of the atom and, hence, the random atom-cavity coupling constant, as well as imperfect state preparation.

Photons emitted from the cavity are circularly polarized, but for technical reasons we rotate them into the linear horizontal/vertical (H/V) basis before sending them through a single-mode optical fiber to the detection area. The detection efficiency for a photon emitted from the cavity is 31%. To perform a full quantum state tomography, the photons are measured in several different bases, selected by using different settings of half- and quarter-wave plates (*16*, *17*). Because the photons are created in the same spatial mode, a nonpolarizing beam splitter (NPBS) is used to direct the photons randomly to one of two measurement setups. This allows each photon to be detected in either the H/V, circular right/left (R/L), or linear diagonal/antidiagonal (D/A) basis.

Photons are produced and detected one after the other. This allows probing of the coherence of the atomic superposition state after the creation of entanglement. Applying a constant magnetic field, B, along the cavity axis shifts the atomic states $|+1\rangle$ and $|-1\rangle$ by an amount $-\Delta$ and $+\Delta$, respectively, with $\Delta = 2\pi \times 0.7$ MHz/G. Our scheme then generates photons with frequencies linked to their polarizations. Specifically, σ^- photons have higher frequencies than σ^+ photons. This has no consequence for the time evolution of the entangled state, Eq. 1, because both parts of the superposition state have the same energy. A frequency-insensitive detection of the first photon with, e.g., right circular polarization $|R\rangle \equiv \frac{1}{\sqrt{2}}(|H\rangle + i|V\rangle)$ after the fiber, however, projects the atomic state into a superposition of $|+1\rangle$ and $|-1\rangle$ with equal amplitudes. The energy difference between the atomic levels then leads to a different time evolution of the two states, resulting in

$$|\psi_{\text{atom}}(t)\rangle = \frac{1}{\sqrt{2}}(e^{i\Delta t}|+1\rangle - ie^{-i\Delta t}|-1\rangle) \quad (3)$$

Subsequent state mapping transfers this state into the photonic state

$$|\psi_{\text{photon 2}}(t)\rangle = \frac{1}{\sqrt{2}}(e^{i\Delta t}|\sigma^+\rangle - ie^{-i\Delta t}|\sigma^-\rangle) \quad (4)$$

which continues rotating until the second photon is detected. The total rotation angle, given by the time difference between the two photon detections, depends on the separation, t_S, between entangling and mapping pulses and the duration of the photon wave packet. Alternatively, for a given time separation, t_S, the time evolution can be controlled by the magnetic-field strength. This state rotation could be suppressed by appropriately delaying the first photon and considering only simultaneous photon-detection events.

To measure the rotation of the atomic state, we observed both photons in the R/L basis, after rotating them from σ^+/σ^- to H/V. We define a contrast $V \equiv P_{|RL\rangle} - P_{|LL\rangle} - P_{|RR\rangle} + P_{|LR\rangle}$, with $P_{|LL\rangle}$ the probability of detecting both photons as left circular polarized (and analogous for $P_{|RR\rangle}$, etc.). For the state given in Eq. 4, one expects a $\cos(2\Delta t_S)$ dependence. Figure 3 shows the measured contrast as a function of the magnetic field for fixed t_S = 2.8 μs. The oscillatory behavior is a manifestation of the phase rotating at twice the Larmor frequency. For increasing field magnitude, the envelope of the oscillation decreases. This is due to the long photon wave packets produced in our scheme (Fig. 2B). As a result, the time interval between two photon detections covers a range of possible values, and thus the superposition state can evolve by differing amounts during this time.

The density matrix of the entangled state given in Eq. 2 is obtained from a full quantum state tomography for $B = 0$ and t_S = 1.3 μs. In this case, no time evolution occurs between the two photon detections. Figure 4A shows the real part of the density matrix reconstructed from the two-photon Stokes parameters, determined by measuring two-photon events in the four detec-

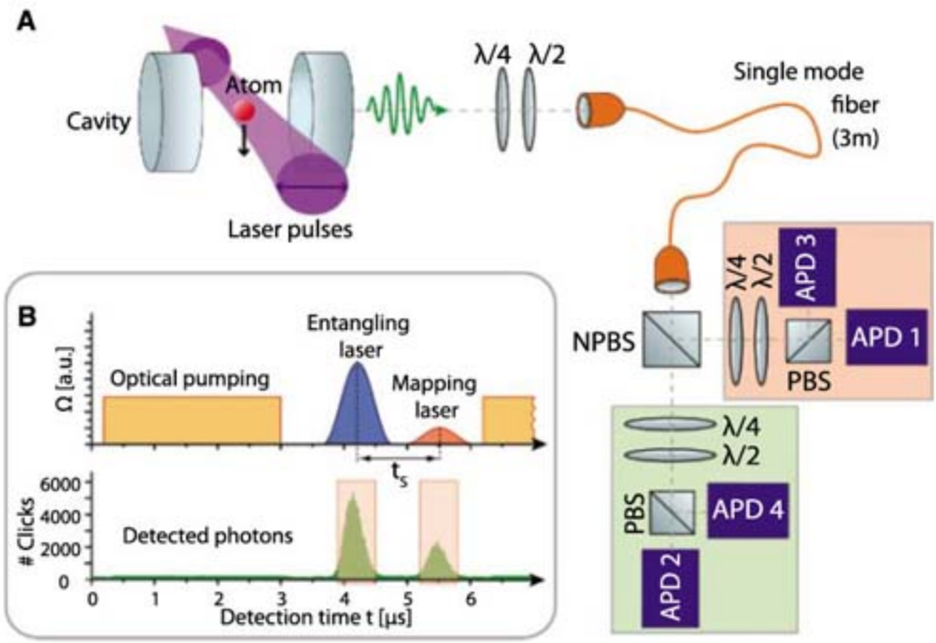

Fig. 2. Scheme of the experiment. (**A**) Laser-cooled atoms traversing the cavity are illuminated with laser pulses. Behind the cavity, the polarization of the emitted σ^+/σ^- photons is rotated to linear horizontal/vertical. Photons are then directed toward two detection setups for measurements in different polarization bases. Detection occurs with avalanche photodiodes (APDs). (**B**) Laser-pulse sequence and photon arrival-time distribution. The photon wave-packets duration is about 300 ns. The displayed time windows are used in the evaluation.

Fig. 3. Atomic state rotation. After detecting the first photon in the R/L basis (behind the fiber), the atom is projected into a superposition state that is time dependent when a magnetic field along the cavity axis is applied (here, t_S = 2.8 μs). Displayed is the contrast, V, as a function of the magnetic field, B. A cosine with a Gaussian envelope fits the data well.

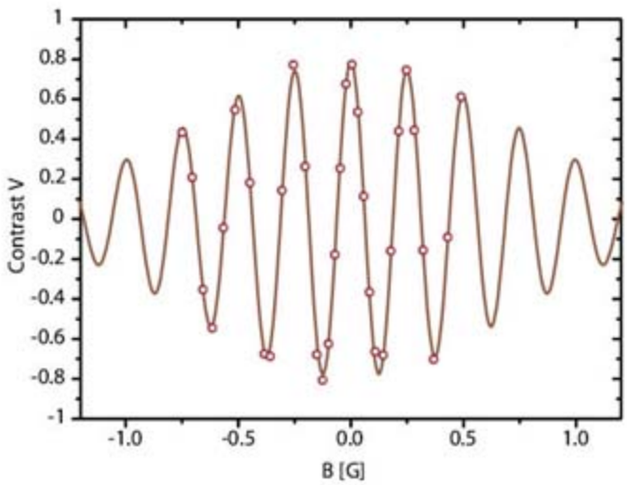

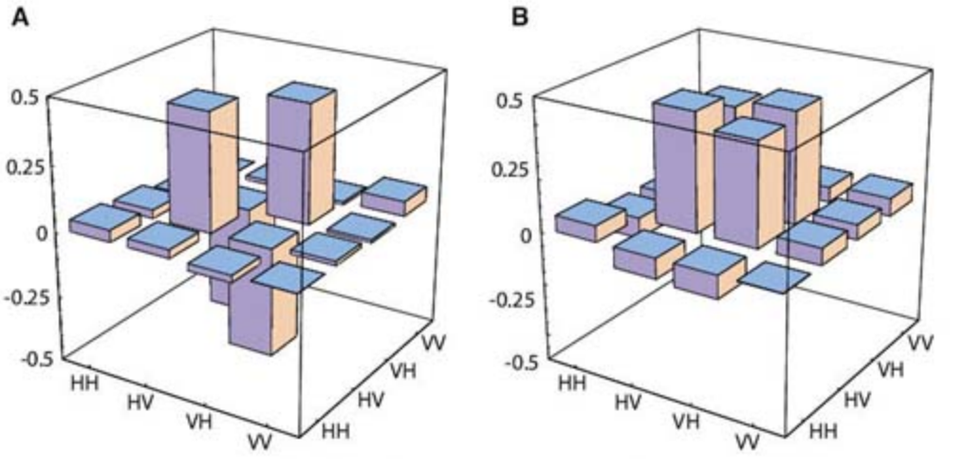

Fig. 4. Quantum state tomography. (**A**) Real part of the reconstructed density matrix for $B = 0$ and $t_S = 1.3$ μs. All imaginary parts (not shown) have a magnitude smaller than 0.03. Fidelity with the $|\Psi^-\rangle$ Bell state is 86.0(4)%. About 2200 entanglement events were collected for each of nine measurement settings. (**B**) For $B = -0.13$ G and $t_S = 2.8$ μs, the atomic superposition state rotates by π. The observed data correspond to a $|\Psi^+\rangle$ Bell state, with fidelity of 82.9(6)%. About 1800 entanglement events were obtained for each of six measurement settings. All imaginary parts (not shown) have a magnitude smaller than 0.05. In (A) and (B), equal detection efficiencies for all detectors were assumed.

tors (*17*). The resulting density matrix has only positive eigenvalues, and hence it represents a physically possible state. Its fidelity with respect to the expected Bell state, $|\Psi^-\rangle$ from Eq. 2, is $F = 86.0(4)\%$, with $0.5 < F \leq 1$ proving entanglement (*18*). From the density matrix, following (*16*), we derive a concurrence of $C = 0.73(7)$, with $0 < C \leq 1$ also proving entanglement. Because of technical imperfections, e.g., of polarizers in the detection setups, the observed fidelity/concurrence sets a lower bound for both the atom-photon and photon-photon entanglement achieved. The same measurements were done for $B = -0.13$ G and $t_S = 2.8$ μs for which the atomic superposition state accumulates a π phase shift (compare to Fig. 3). Therefore, a density matrix corresponding to the Bell state $|\Psi^+\rangle = \frac{1}{\sqrt{2}}(|+1,\sigma^-\rangle + |-1,\sigma^+\rangle)$ is expected. This is indeed observed (Fig. 4B) with a fidelity of $F = 82.9(6)\%$ and a concurrence of $C = 0.72(13)$. The state evolves between the two photon detections as a result of the constant magnetic field.

Future experiments could produce a time-independent $|\Psi^+\rangle$ Bell state by applying a pulsed magnetic field to the atom between entanglement generation and state mapping. Moreover, partial driving of the Raman transition in combination with atomic state manipulation should allow production of highly entangled multiphoton states (*12*). Our technique applied to a quasi-permanently trapped intracavity atom (*3*, *19*) will push the probability of success even further, making the scheme truly deterministic. Two (or more) such systems operated in parallel are perfectly suited for teleportation and entanglement experiments in a quantum network (*20*–*22*) or quantum gate operations in a distributed and, hence, scalable quantum computer (*23*, *24*).

References and Notes

1. E. Knill, R. Laflamme, G. J. Milburn, *Nature* **409**, 46 (2001).
2. A. Kuhn, M. Hennrich, G. Rempe, *Phys. Rev. Lett.* **89**, 067901 (2002).
3. J. McKeever *et al.*, *Science* **303**, 1992 (2004).
4. M. Keller, B. Lange, K. Hayasaka, W. Lange, H. Walther, *Nature* **431**, 1075 (2004).
5. M. Hijlkema *et al.*, *Nat. Phys.* **3**, 253 (2007).
6. T. Wilk, S. C. Webster, H. P. Specht, G. Rempe, A. Kuhn, *Phys. Rev. Lett.* **98**, 063601 (2007).
7. J. I. Cirac, P. Zoller, H. J. Kimble, H. Mabuchi, *Phys. Rev. Lett.* **78**, 3221 (1997).
8. H.-J. Briegel, W. Dür, J. I. Cirac, P. Zoller, *Phys. Rev. Lett.* **81**, 5932 (1998).
9. B. B. Blinov, D. L. Moehring, L.-M. Duan, C. Monroe, *Nature* **428**, 153 (2004).
10. B. Darquié *et al.*, *Science* **309**, 454 (2005).
11. J. Volz *et al.*, *Phys. Rev. Lett.* **96**, 030404 (2006).
12. C. Schön, E. Solano, F. Verstraete, J. I. Cirac, M. M. Wolf, *Phys. Rev. Lett.* **95**, 110503 (2005).
13. J. M. Raimond, M. Brune, S. Haroche, *Rev. Mod. Phys.* **73**, 565 (2001).
14. M. Hennrich, T. Legero, A. Kuhn, G. Rempe, *Phys. Rev. Lett.* **85**, 4872 (2000).
15. M. Hennrich, T. Legero, A. Kuhn, G. Rempe, *N.J. Phys.* **6**, 86 (2004).
16. D. F. V. James, P. G. Kwiat, W. J. Munro, A. G. White, *Phys. Rev. A.* **64**, 052312 (2001).
17. J. B. Altepeter, E. R. Jeffrey, P. G. Kwiat, *Adv. At. Mol. Opt. Phys.* **52**, 105 (2005).
18. C. A. Sackett *et al.*, *Nature* **404**, 256 (2000).
19. S. Nußmann *et al.*, *Nat. Phys.* **1**, 122 (2005).
20. S. Bose, P. L. Knight, M. B. Plenio, V. Vedral, *Phys. Rev. Lett.* **83**, 5158 (1999).
21. L.-M. Duan, H. J. Kimble, *Phys. Rev. Lett.* **90**, 253601 (2003).
22. D. E. Browne, M. B. Plenio, S. F. Huelga, *Phys. Rev. Lett.* **91**, 067901 (2003).
23. Y. L. Lim, A. Beige, L. C. Kwek, *Phys. Rev. Lett.* **95**, 030505 (2005).
24. A. Serafini, S. Mancini, S. Bose, *Phys. Rev. Lett.* **96**, 010503 (2006).

25. We thank J. Bochmann and N. Kiesel for helpful discussions. This work was supported by the Deutsche Forschungsgemeinschaft [Collaborative Research Center 631, Research Unit 635, Munich Center for Advanced Photonics (MAP)] and the European Union [Information Society Technologies (SCALA) and Research Training Network (CONQUEST) programs].

16 April 2007; accepted 7 June 2007
Published online 21 June 2007;
10.1126/science.1143835
Include this information when citing this paper.

Porous Semiconducting Gels and Aerogels from Chalcogenide Clusters

Santanu Bag,[1,2] Pantelis N. Trikalitis,[2]* Peter J. Chupas,[3] Gerasimos S. Armatas,[1,2] Mercouri G. Kanatzidis[1,2,4]†

Inorganic porous materials are being developed for use as molecular sieves, ion exchangers, and catalysts, but most are oxides. We show that various sulfide and selenide clusters, when bound to metal ions, yield gels having porous frameworks. These gels are transformed to aerogels after supercritical drying with carbon dioxide. The aerogels have high internal surface area (up to 327 square meters per gram) and broad pore size distribution, depending on the precursors used. The pores of these sulfide and selenide materials preferentially absorb heavy metals. These materials have narrow energy gaps (between 0.2 and 2.0 electron volts) and low densities, and they may be useful in optoelectronics, as photocatalysts, or in the removal of heavy metals from water.

Inorganic porous materials are at the foundation of broad applications such as molecular sieves, ion exchangers, and catalysts (*1*, *2*). Zeolites and aluminosilicate mesoporous materials constitute the vast majority of this class. Aerogels are another kind of porous inorganic amorphous polymer in which nanosized blocks are interconnected to yield high internal surface area, very low densities, and large open pores (*3*, *4*). Although the sol-gel chemistry of oxide-based materials (e.g., SiO_2, Al_2O_3, TiO_2) and carbon (*5*) is well known, successful attempts to apply this approach to non–oxide-based systems are quite rare, especially for chalcogenides. Such systems would be capable of combining the electronic properties of chalco-

[1]Department of Chemistry, Northwestern University, Evanston, IL 60208, USA. [2]Department of Chemistry, Michigan State University, East Lansing, MI 48824, USA. [3]Advanced Photon Source, Argonne National Laboratory, Argonne, IL 60439, USA. [4]Materials Science Division, Argonne National Laboratory, Argonne, IL 60439, USA.

*Present address: Department of Chemistry, University of Crete, Heraklion 71409, Greece.
†To whom correspondence should be addressed. E-mail: m-kanatzidis@northwestern.edu

genides with internal porosity. Aerogels based on aggregated simple binary nanocrystals (e.g., CdS, CdSe) and on amorphous GeS_2 have been reported (*6*, *7*).

We report on a strategy to create highly porous semiconducting aerogels derived from chalcogenide-based clusters and platinum as the linking metal ion (*8*). A family of chalcogenide gels was prepared in aqueous solution with anionic $[MQ_4]^{4-}$, $[M_2Q_6]^{4-}$, and $[M_4Q_{10}]^{4-}$ (M = Ge, Sn; Q = S, Se) building blocks (Fig. 1A) in the presence of platinum (II) salt, according to the following metathesis reactions:

$$(R_4N)_4[M_4Q_{10}] + 2K_2PtCl_4 \rightarrow Pt_2[M_4Q_{10}] + 4KCl + 4R_4NCl \quad (1)$$

$$K_4[M_2Q_6] + 2K_2PtCl_4 \rightarrow Pt_2[M_2Q_6] + 8KCl \quad (2)$$

$$A_4[MQ_4] + 2K_2PtCl_4 \rightarrow Pt_2[MQ_4] + 4KCl + 4ACl \quad (3)$$

where R= methyl, ethyl; M = Ge, Sn; Q = S, Se; and A = Na, K. In these reactions (e.g., Eq. 1), all chloride ligands of $[PtCl_4]^{2-}$ can be replaced by the Q terminal atoms of chalcogenido clusters, generating materials with a formula of $Pt_2[M_4Q_{10}]$. Energy-dispersive spectroscopy (EDS) revealed that two platinum atoms per complex anion are incorporated in almost every case, giving a charge-balanced formula (Table 1). K^+ or Cl^- ions, used as counterions in the synthesis, were not detected in the product—a result consistent with complete metathesis. This linking/polymerization reaction produced a continuous, extended Pt/M/Q framework of covalently bonded atoms that encapsulates solvent molecules into their pore system during the process of polymerization and finally makes hydrogels (fig. S1, A to C). Because the gels formed are based on all-chalcogenide species, we term these hydrogels "chalcogels" by analogy to the naming of cyanogels (*9*). Table 1 lists the six chalcogels we developed and the Zintl anion incorporated in each case.

After supercritical drying with CO_2, these chalcogels yield highly porous aerogels (Fig. 1, B and C) (*10*). All samples showed consistent Pt/M/Q (M = Ge, Sn; Q = S, Se) ratios very close to those in the starting clusters. However, slight discrepancies were observed for Chalcogel-3 and Chalcogel-6, which might be due to solution equilibrium processes.

Transmission electron microscopy (TEM) images of our aerogel samples revealed empty mesopores with no long-range order (Fig. 2, A to C). Indeed, they appear to be morphologically similar to the silica aerogels where particles are connected to each other, making continuous amorphous (Fig. 2D) networks. The micro- and mesoporosity were confirmed by nitrogen physisorption measurements. The adsorption-desorption isotherms show a type IV adsorption branch with a combination of H1- and H3-type hysteresis loops characteristic of an interconnected mesoporous system (Fig. 3) (*11*). This indicates that the mesopores have cylindrical and slit-shaped geometries. Pore size distribution plots calculated by the Barrett-Joynes-Halenda

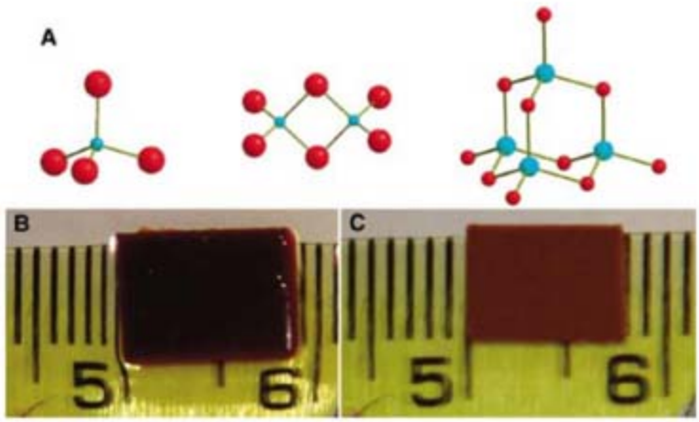

Fig. 1. (**A**) Different building blocks used in chalcogel formation (blue spheres, metal centers; red spheres, chalcogenide atoms). (**B** and **C**) Monolithic hydrogel before (B) and after (C) supercritical drying, showing very little volume loss.

Table 1. Elemental analysis, colors, and optical energy gaps for the chalcogel series.

Chalcogel	Zintl anion	Pt/M/Q ratio*	Empirical formula	Color	Energy gap (eV)
Chalcogel-1	$[Ge_4S_{10}]^{4-}$	2.0:4:9.6	$Pt_{2.0}Ge_4S_{9.6}$	Pinkish brown	2.0
Chalcogel-2	$[Ge_4Se_{10}]^{4-}$	2.0:4:8.7	$Pt_{2.0}Ge_4Se_{8.7}$	Black	1.3
Chalcogel-3	$[Sn_4Se_{10}]^{4-}$	2.1:4:9.7	$Pt_{2.1}Sn_4Se_{9.7}$	Black	1.0
Chalcogel-4	$[Sn_2Se_6]^{4-}$	1.8:2:5.7	$Pt_{1.8}Sn_2Se_{5.7}$	Black	0.8
Chalcogel-5	$[SnSe_4]^{4-}$	2.0:1:4.0	$Pt_{2.0}SnSe_{4.0}$	Black	0.2
Chalcogel-6	$[SnS_4]^{4-}$	1.4:1:4.0	$Pt_{1.4}SnS_{4.0}$	Dark pinkish brown	1.4

*Based on EDS results. Listed values are an average of seven measurements on independently prepared samples.

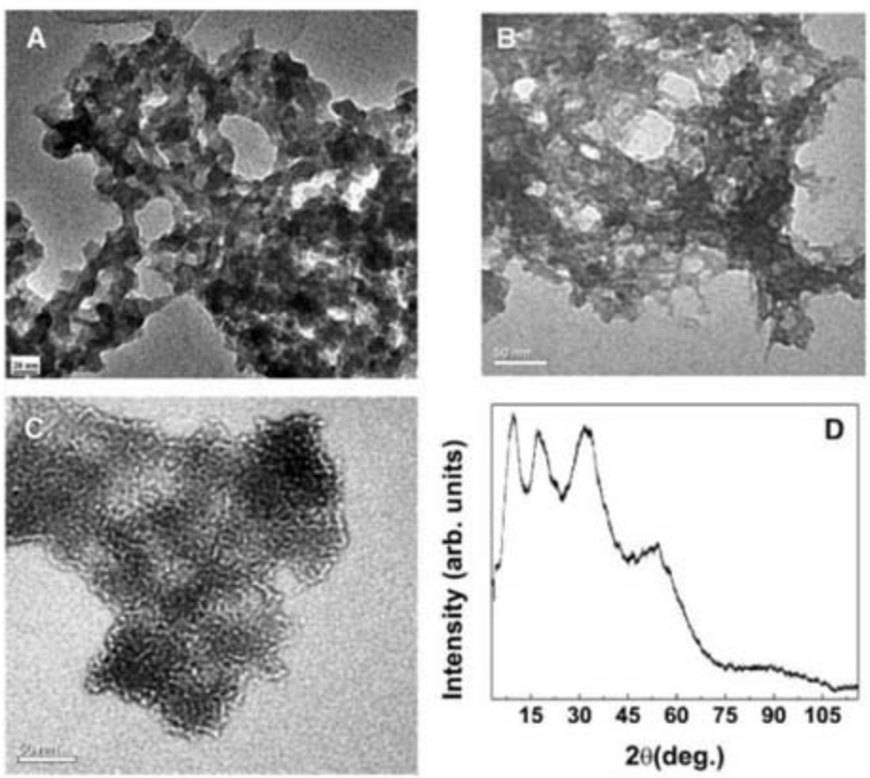

Fig. 2. (**A** and **B**) TEM images of Chalcogel-1 (A) and Chalcogel-2 (B). Pores between the particles in the meso- and macrophase regime are clear from these pictures, although they are not ordered. (**C**) TEM image of Chalcogel-2 shows small pores inside the particle. Large macropores are absent here. (**D**) Wide-angle powder x-ray diffraction data for Chalcogel-1. The amorphous nature of the aerogel and the lack of other crystalline phases are obvious.

(BJH) method (*11*) from the desorption branch suggest the presence of a broad range of pore sizes in the meso region (fig. S1, D and E). Additionally, the absence of saturation in the adsorption isotherm implies the simultaneous presence of macropores (pore diameter >50 nm) in the samples, which would be consistent with the aerogel nature of these chalcogenides.

Brunauer-Emmett-Teller (BET) surface areas obtained from the aerogels range from 108 to 327 m^2/g, depending on the chalcogenido cluster (Table 2). The surface area of 327 m^2/g obtained from $[Ge_4Se_{10}]^{4-}$ in Chalcogel-2 is the highest of the six chalcogels, followed by 323 m^2/g for $[Ge_4S_{10}]^{4-}$ in Chalcogel-1. The smallest cluster, $[SnS_4]^{4-}$ in Chalcogel-6, gave the lowest BET surface area value of 117 m^2/g. Given that the formula weights of these chalcogels are high, on a per-mole basis the surface area values are actually very large. The silica equivalence (*12*) BET surface area of Chalcogel-2 is 1674 m^2/g and that of Chalcogel-3 is 1580 m^2/g (Table 2). Values for silica aerogels range from 100 to 1600 m^2/g and typical values are 600 m^2/g. The bulk density of these chalcogels is very low; for example, Chalcogel-1 showed 0.12 to 0.17 g/cm^3 with a skeletal density of 3.1 g/cm^3.

To probe the local structure of the amorphous aerogels, we used the atomic pair distribution function (PDF) (*13*) technique, which analyzes both diffuse and Bragg scattering by recovering atom-atom correlations in real space in the form of a radial distribution function. A single correlation occurring at 2.36 Å is evident in the PDF of Chalcogel-1 (Fig. 4A), corresponding to the first-neighbor Ge-S and Pt-S bond distances. A clustering of correlations is evident around 3.52 Å, which corresponds to the second-neighbor Ge···Ge, S···S, and Pt···Ge distances. The PDF of Chalcogel-2 is remarkably similar to that of Chalcogel-1, although it exhibits a shift in correlations to longer interatomic distances *r* as a result of the larger atomic radius of Se versus S. Again a single correlation is evident in the PDF of Chalcogel-2 at 2.49 Å (Ge-Se and Pt-Se bond distances), and several appear centered around 3.75 Å. The higher intensity of the first correlation in Chalcogel-2 arises from the larger scattering factor of Se over that of S. Both PDFs show a lack of well-defined features past 6 Å that suggests a lack of long-range translational symmetry. However, a well-defined local structure is evident from the PDF and clearly shows that the adamantane clusters remain intact. The splitting of the correlations (3.52 Å and 3.75 Å) is likely due to subtle distortions, arising from linking of the adamantane clusters, that ultimately disrupt the long-range translational symmetry. The PDF data, together with the complete metathesis chemistry, elemental analysis, and x-ray photoelectron spectroscopy (XPS) (fig. S2), suggest a nonperiodic structure of the type shown in Fig. 4B. Further support for the integrity of the starting clusters in the final aerogels was provided by nuclear magnetic resonance (NMR) (fig. S3), electrospray ionization mass spectroscopy (ESI-MS) (fig. S4), and infrared spectroscopy (fig. S5).

The chalcogels showed a remarkably high capacity for removing heavy metals from contaminated water. For example, starting with water

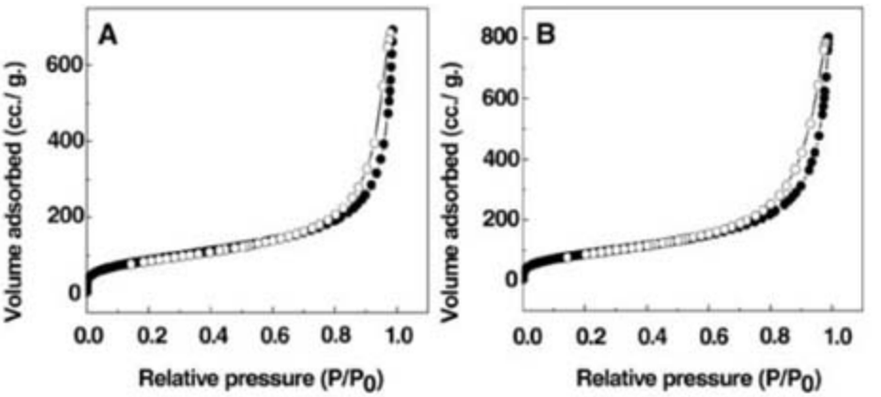

Fig. 3. Nitrogen adsorption-desorption isotherms of (**A**) Chalcogel-1 and (**B**) Chalcogel-2 at 77 K (solid circles, adsorption data; open circles, desorption data). Samples were degassed overnight at 348 K before testing.

Table 2. Nitrogen adsorption-desorption data for the chalcogel series.

Chalcogel	BET surface area (m^2/g)*	Surface area, silica equivalence (m^2/g)	Adsorption total pore volume (cm^3/g)†
Chalcogel-1	276 to 323	1012 to 1184	0.59 to 0.73
Chalcogel-2	282 to 327	1444 to 1674	0.64 to 0.85
Chalcogel-3	196 to 271	1143 to 1580	0.52 to 0.70
Chalcogel-4	225 to 229	1296 to 1319	0.48 to 0.52
Chalcogel-5	210 to 211	1441 to 1448	0.44 to 0.48
Chalcogel-6	108 to 117	467 to 506	0.21 to 0.23

*Three independently prepared samples were measured.
†Single-point adsorption total pore volume was calculated at relative pressure (P/P_0) of 0.97.

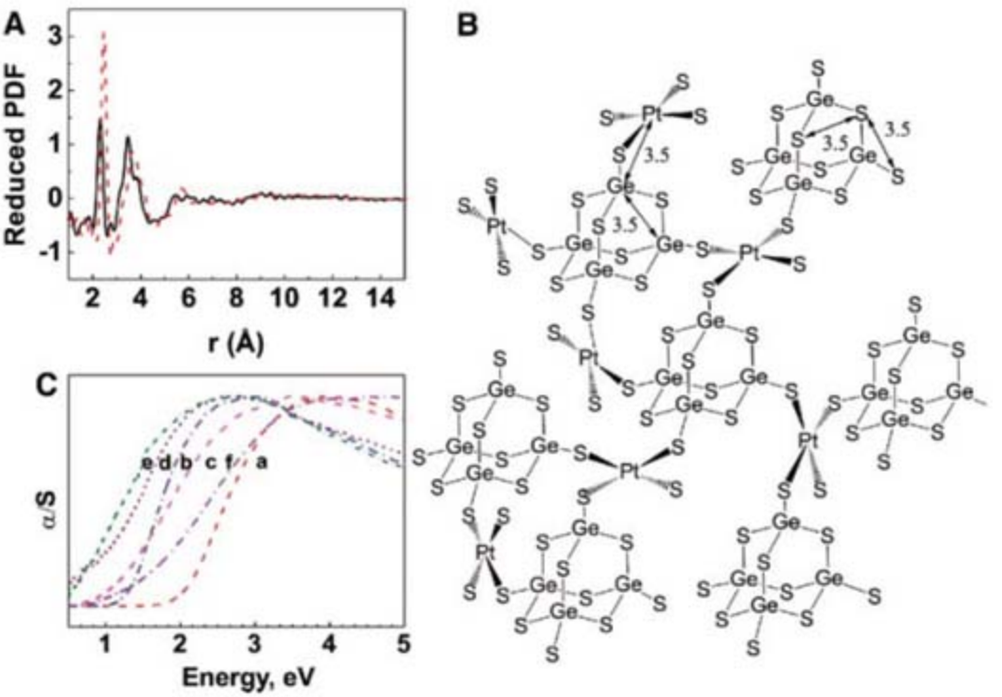

Fig. 4. (**A**) Reduced atomic pair distribution function $G(r)$ of Chalcogel-1 (black line) and Chalcogel-2 (red dashed line) as a function of interatomic distance *r*. (**B**) Interatomic distances (in angstroms) are shown for the $[Ge_4S_{10}]^{4-}$ cluster in the proposed Chalcogel-1 structure. (**C**) Ultraviolet-visible electronic absorption spectra of (a) Chalcogel-1 (red dashed line), (b) Chalcogel-2 (blue dash-dot line), (c) Chalcogel-3 (magenta dashed line), (d) Chalcogel-4 (purple dotted line), (e) Chalcogel-5 (green dashed line), and (f) Chalcogel-6 (violet dash-dot line).

contaminated by 645 parts per million (ppm) Hg^{2+}, 10 mg of Chalcogel-1 removed Hg^{2+} down to concentration levels of ~0.04 ppm (*14*). Whereas mesoporous silicates need to be functionalized with surface-modified thiolate ligands before application toward environmental remediation (*15*), the chalcogels work directly as potential adsorbents for Hg^{2+} (*16*) without prior modification of their surface. The detailed mechanism of metal ion removal is not known.

The chalcogels also efficiently absorb organic hydrophobic aromatic molecules from solution. In contrast to the unmodified silica aerogels—which generally have hydrophilic surfaces and tend to be unstable under a humid atmosphere—the chalcogels present hydrophobic surfaces lined with chalcogen atoms and are immune to high humidity (*17*). Thermal gravimetric analysis indicates that the aerogels are stable to 180°C (fig. S6). As a demonstration of its high affinity for hydrophobic species, Chalcogel-1 absorbed quantitatively all of porphyrin I from a 5.67 μmol/liter ethanolic solution within 24 hours (30 mg of Chalcogel-1 was shaken continuously in 16 ml of the porphyrin solution).

The chalcogels absorb light in the visible and infrared regions, exhibiting sharp energy gaps from 2.0 eV to 0.8 eV (Table 1) as determined by diffuse-reflectance solid-state ultraviolet-visible/near-infrared spectroscopy (Fig. 4C). Only Chalcogel-5 gave a broad absorption with a band gap of 0.2 eV. The optical properties of the highly porous semiconducting aerogels can be tuned by changing the building block. Going from the S to the Se analogs of the adamantane cluster, the energy gap decreases as expected. Also, by changing the group IV metal in the cluster from Ge to Sn, the energy gap is decreased by 0.3 eV. Similarly, the band gap can also be changed by varying the chalcogenide content per metal in the starting clusters. This is well reflected in the observed band gaps of Chalcogel-3, -4, and -5, where the Se content per Sn atom is increased gradually and shows a narrowing of the energy gap.

Given that it is difficult to remove surfactants from mesostructured chalcogenide materials (*18*–*22*), the strategy reported here represents a convenient and general route for making porous materials with chalcogenide-based clusters. Because of the availability of a large number of soluble chalcogenido clusters, together with various linking transition and main-group metal ions, our approach seems to offer a general technique for preparing broad classes of porous chalcogenides.

References and Notes

1. X. He, D. Antonelli, *Angew. Chem. Int. Ed.* **41**, 214 (2002).
2. M. A. Carreon, V. V. Guliants, *Eur. J. Inorg. Chem.* **2005**, 27 (2005).
3. C. J. Brinker, G. W. Scherer, *The Physics and Chemistry of Sol-Gel Processing* (Academic Press, San Diego, CA, 1990).
4. N. Hüsing, U. Schubert, *Angew. Chem. Int. Ed.* **37**, 22 (1998).
5. R. W. Pekala, C. T. Alviso, F. M. Kong, S. S. Hulsey, *J. Non-Cryst. Solids* **145**, 90 (1992).
6. J. L. Mohanan, I. U. Arachchige, S. L. Brock, *Science* **307**, 397 (2005).
7. K. K. Kalebaila, D. G. Georgiev, S. L. Brock, *J. Non-Cryst. Solids* **352**, 232 (2006).
8. See supporting material on *Science* Online.
9. M. Heibel, G. Kumar, C. Wyse, P. Bukovec, A. B. Bocarsly, *Chem. Mater.* **8**, 1504 (1996).
10. S. S. Kistler, *J. Phys. Chem.* **36**, 52 (1932).
11. S. J. Gregg, K. S. W. Sing, *Adsorption, Surface Area and Porosity* (Academic Press, New York, 1982).
12. The molecular formulas were normalized to two sulfur or two selenium atoms to compare well with SiO_2 (e.g., $Pt_2Ge_4S_{10}$ is converted to $Pt_{0.4}Ge_{0.8}S_2$ having formula weight of 220.27) for equivalent surface area calculation.
13. S. J. L. Billinge, M. G. Kanatzidis, *Chem. Commun.* **2004**, 749 (2004).
14. The capacity of Chalcogel-1 to remove Hg^{2+} from aqueous solution is extremely high (645 mg/g or 3.21 mmol/g). This tremendous affinity is also reflected in the calculated distribution coefficient K_d^{Hg} [defined as the amount of adsorbed metal (in micrograms) on 1 g of adsorbing material divided by the metal concentration (in milligrams per milliliter) remaining in the treated water (*8*)]. K_d^{Hg} values varied from 0.92×10^7 ml/g (at 92 ppm Hg^{2+}) to 1.61×10^7 ml/g (at 645 ppm Hg^{2+}).
15. L. Mercier, T. J. Pinnavaia, *Adv. Mater.* **9**, 500 (1997).
16. The specific binding of chalcogels with heavy metals was demonstrated by adding 5 ml each of 89 ppm Zn^{2+} and 92 ppm Hg^{2+} solutions to 10 mg Chalcogel-2 and stirring for 24 hours at room temperature. The final solution contained 52.8 ppm Zn^{2+} and 0.1 ppm Hg^{2+}.
17. The BET surface area remained high after storing the chalcogels for longer times. For example, the surface area of Chalcogel-2 decreased from 327 to 303 m^2/g after 5 weeks and to 265 m^2/g after 3 months.
18. M. J. MacLachlan, N. Coombs, G. A. Ozin, *Nature* **397**, 681 (1999).
19. P. N. Trikalitis, K. K. Rangan, T. Bakas, M. G. Kanatzidis, *Nature* **410**, 671 (2001).
20. P. N. Trikalitis, K. K. Rangan, M. G. Kanatzidis, *J. Am. Chem. Soc.* **124**, 2604 (2002).
21. P. N. Trikalitis, K. K. Rangan, T. Bakas, M. G. Kanatzidis, *J. Am. Chem. Soc.* **124**, 12255 (2002).
22. S. D. Korlann, A. E. Riley, B. L. Kirsch, B. S. Mun, S. H. Tolbert, *J. Am. Chem. Soc.* **127**, 12516 (2005).

23. We thank T. J. Pinnavaia and D. Holmes for use of the nitrogen sorption measurement and NMR handling, respectively. Use of the Advanced Photon Source was supported by the U.S. Department of Energy, Office of Science, Office of Basic Energy Sciences.

Supporting Online Material

www.sciencemag.org/cgi/content/full/317/5837/490/DC1
Materials and Methods
Figs. S1 to S6
References

14 March 2007; accepted 5 June 2007
10.1126/science.1142535

Stabilization of Labile Carbonyl Addition Intermediates by a Synthetic Receptor

Tetsuo Iwasawa, Richard J. Hooley, Julius Rebek Jr.*

Products of unfavorable chemical equilibria are not readily observed because their high energy and increased reactivity result in low concentrations. Biological macromolecules use binding forces to access unfavorable equilibria and stabilize reactive intermediates by isolating them from the medium. In a similar vein, we describe here a synthetic receptor that allows direct observation of labile tetrahedral intermediates: hemiaminals formed in the reaction of an aldehyde carbonyl group with amines. The receptor encapsulates alkyl-substituted primary amines, then orients them toward a covalently tethered aldehyde function. The hemiaminal intermediates appear at high concentration, confined from the bulk solution and observable at ambient temperature by conventional nuclear magnetic resonance spectroscopy.

Chemical reactions often proceed through many intermediate stages between starting materials and products. The reactive intermediates at such stages are generally not observed directly, because their concentrations are vanishingly small, but are treated through steady-state approximations and detected by kinetic or other methods (*1*, *2*). The reaction of carbonyl compounds with nucleophiles invariably involves an addition step that gives an unstable tetrahedral carbon intermediate followed by an elimination step. For example, the reaction of primary amines with aldehydes to give imines (Fig. 1) proceeds through an intermediate hemiaminal (*3*). The process is catalyzed by acids or bases, and the proton transfers involved generate additional transient, charged intermediates. The hemiaminal is, except in very special cases (*4*–*6*), not observed. It is energetically disfavored, because the cost of breaking the carbonyl π bond and the entropic price of bringing the two reactants together are not compensated by the new covalent bonds formed. Accordingly, the unstable hemiaminal dissociates to starting materials or proceeds to imine with loss of water. We tailored a molecular receptor to favor formation of this intermediate and found that the hemiaminal was stabilized for minutes to hours, long

Skaggs Institute for Chemical Biology and Department of Chemistry, Scripps Research Institute, 10550 North Torrey Pines Road, La Jolla, CA 92037, USA.

*To whom correspondence should be addressed. E-mail: jrebek@scripps.edu

enough to characterize by nuclear magnetic resonance (NMR) spectroscopic methods.

We chose as a receptor motif a deep, self-folding cavitand. Cavitands are open-ended structures that recognize and reversibly bind molecules of appropriate size, shape, and chemical complementarity (*7*, *8*). Synthetic receptors such as these are well known to screen unstable species from the external medium and prolong their lifetimes (*9*–*14*). Examples include the isolation of iminium ions (*9*) and siloxanes (*11*) from the surrounding aqueous environment. In these cases, the receptor functions solely as a shield, protecting the kinetically stable but water-sensitive guest from reaction with the outside medium. Enzymes, in contrast, stabilize kinetically labile intermediates by providing functional groups that actively lower the energy of a bound transition state, via hydrogen bonding or other weak intermolecular forces. The cavitand is in several ways reminiscent of an enzyme active site, comprising a hydrophobic cavity, a secondary amide scaffold, and inwardly directed functional groups folded around the substrate. Detection and analysis of reactive intermediates in biological systems is essential for the accurate determination of enzyme mechanism, but the high activity of enzymes has made such observations difficult. X-ray crystallographic analysis of tetrahedral intermediates inside the active site of D-2-deoxyribose-5-phosphate (DRP) aldolase has been possible at cryogenic temperatures or via selective mutation to prevent the enzyme from completing the reaction (*15*, *16*). The system we describe here is similar in action to a mutant DRP aldolase in which only the first half of the amine-catalyzed aldol reaction occurs. The difference is that the stabilization of the kinetically unstable hemiaminal occurs at room temperature in millimolar concentrations; our system does not require cryogenic cooling in order to observe the intermediate. In certain cases, the intermediate hemiaminal species is observable for more than 3 hours.

We prepared cavitand **1** by the condensation of known diamine **2** (*17*) and dialdehyde **3** using air as the oxidant (Fig. 2) (*18*). The cavity of **1** is large enough to surround a single small molecule guest and orient it toward an inwardly directed aldehyde group. The eight benzene rings act as a fixed solvent cage, and the intramolecular hydrogen bonds of the secondary amides help maintain the vase-like conformation (*19*). When isobutyl amine is added to a solution of **1** in mesitylene-d_{12} (a solvent that does not compete for cavitand binding), a complex forms upon mixing. The ^{1}H NMR spectra (Fig. 3 and figs. S2 to S9) show features typical of binding. Separate sets of resonances are observed for free and encapsulated amine (figs. S2 to S9), because the rates of guest exchange in and out of the host capsules are slow on the NMR time scale. In addition, the amine chemical shifts reflect the orientation in the cavity: The resonances of the apolar CH_3 groups of the bound amine guests show large upfield shifts [$\Delta\delta$ = –4 parts per million (ppm)], consistent with their positioning near the bottom of the cavity, where the many aromatic rings create a magnetically shielded environment. Likewise, polar functions of the guests are attracted to the seam of hydrogen bond donors and acceptors at the rim of the cavitand. Within 2 min of mixing, both the surrounded amine **4** and the corresponding hemiacetal **5** are evident in the spectra. The tetrahedral intermediate **5** (with the hemiaminal proton resonance at 4.6 ppm) shows a half-life ($t_{1/2}$) of 30 min and gradually undergoes dehydration to the imine **6**. The different complexes display peaks for both cavitand and guest with different shifts, leading to rather complex spectra. Figure 3 shows the change in three of these peaks over time; benzimidazole proton H_a (Fig. 2) is the most representative cavitand-based signal because it is distant from the other NH peaks, so the changes are easily visible. The most relevant guest peaks are the terminal CH_3 groups of the amine. The arrangement of hydrogen bonds around the rim of the cavity of **1** creates an asymmetric magnetic environment that is stable on the NMR chemical shift time scale. As a result, the amine methyl groups become diastereotopic upon confinement inside the cavity (even before covalent attachment and hemiaminal formation) and so exhibit separate NMR signals. Each complex shows two different doublets for these methyl groups (the signal for one methyl in complex **4** is buried beneath the hemiaminal signal δ = –3.29). The chemical shift of these methyl groups is dependent on their position in the cavitand base; the deepest bound methyls exhibit the most upfield shift. In the noncovalent complex **4** and the hemiaminal **5**, one of the methyls is positioned deeper inside the cavity than the other, and their resonances are separated by 0.2 ppm. In the case of imine product **6**, the methyl groups are less separated, and the two doublets are overlapped and appear similar to a triplet. The splitting of the signal for the C-H bond of the hemiaminal reflects the formation of a new asymmetric center (and hence two diastereomers) and the large (12 Hz) vicinal coupling to the remaining hydrogen of the amine (no coupling is seen to the OH). A view down the C-N bond (**7**) is shown in Fig. 4A. Hemiaminals were also observed within **1** by using isopropylamine, *n*-propylamine, and *n*-butylamine (figs. S6 to S9). In the latter two cases, the initial

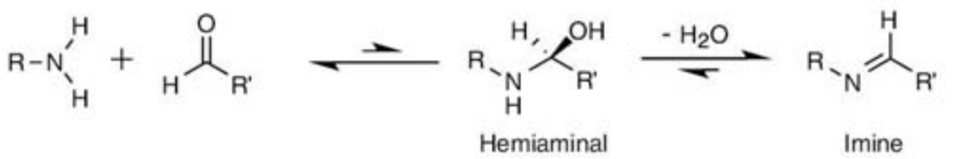

Fig. 1. Mechanism of imine formation from a primary amine and aldehyde. Charged intermediates are not shown.

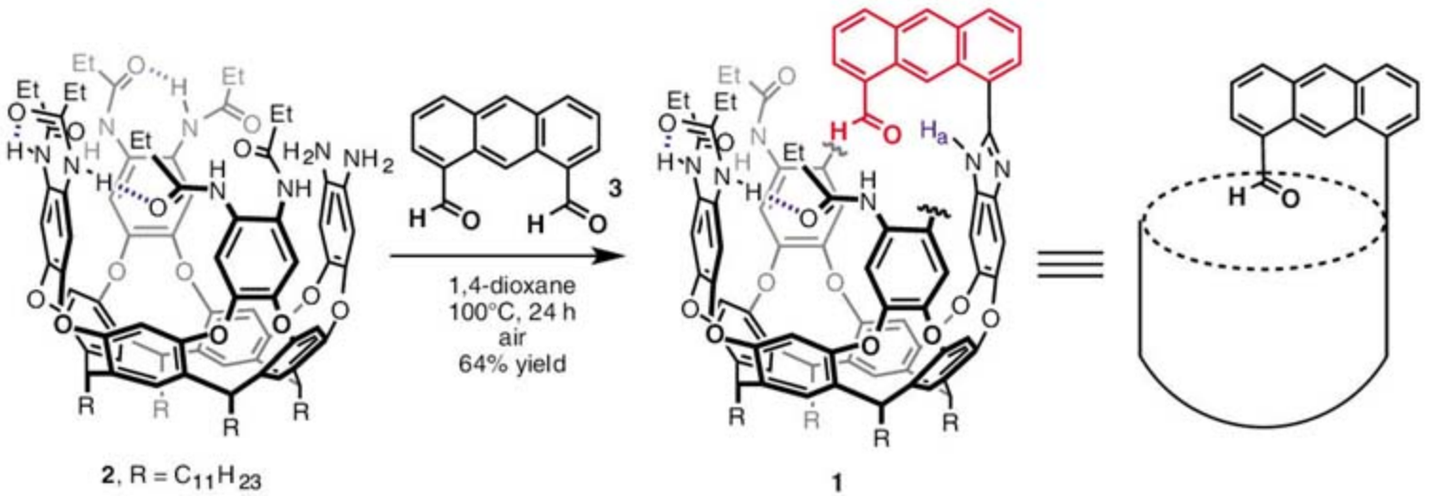

Fig. 2. Synthesis of cavitand **1**. Some peripheral groups were removed for clarity. Et, ethyl group.

noncovalent complexes were too short-lived to observe, and only hemiaminal and imine were seen. The isopropylamine hemiaminal was the longest lived, with a $t_{1/2}$ = 90 min.

Unstabilized hemiaminals have previously been observed very infrequently and only under specialized conditions of highly polar solvents, derivatized starting materials, and high concentrations (*4*–*6*). Our control experiments in the absence of cavitand showed no observable hemiaminal by NMR spectroscopy under the mild conditions used here. On mixing 10 mM *n*-propylamine and 1.5 mM 9-anthraldehyde, we observed only the slow formation of the imine in the NMR spectrum. At these concentrations of amine and receptor **1**, the rate of imine formation is ~50 times faster in the cavitand. In contrast to the steady state behavior that governs the formation of many reactive intermediates, the concentration of the hemiaminal in this case was seen to build up and decline over time (fig. S10). The noncovalent complex persisted at low concentration, and the ratio of hemiaminal to complex was constant after equilibrium was reached. The equilibrium constant for the internal reaction is $K \approx 12.5$.

How does the cavitand stabilize the otherwise elusive hemiaminal intermediates? Previous studies with analogous receptors (lacking the introverted aldehyde functionality) show that the cavitand folds around the amine and isolates it from the bulk solution in an ordered cage of aromatic rings and secondary amide groups (*20*, *21*). When the aldehyde function is positioned over the cavity, it is held close to the guest inside, and the reaction becomes almost intramolecular from an entropic standpoint, lowering the barrier to bond formation. The secondary amides are poised to stabilize the

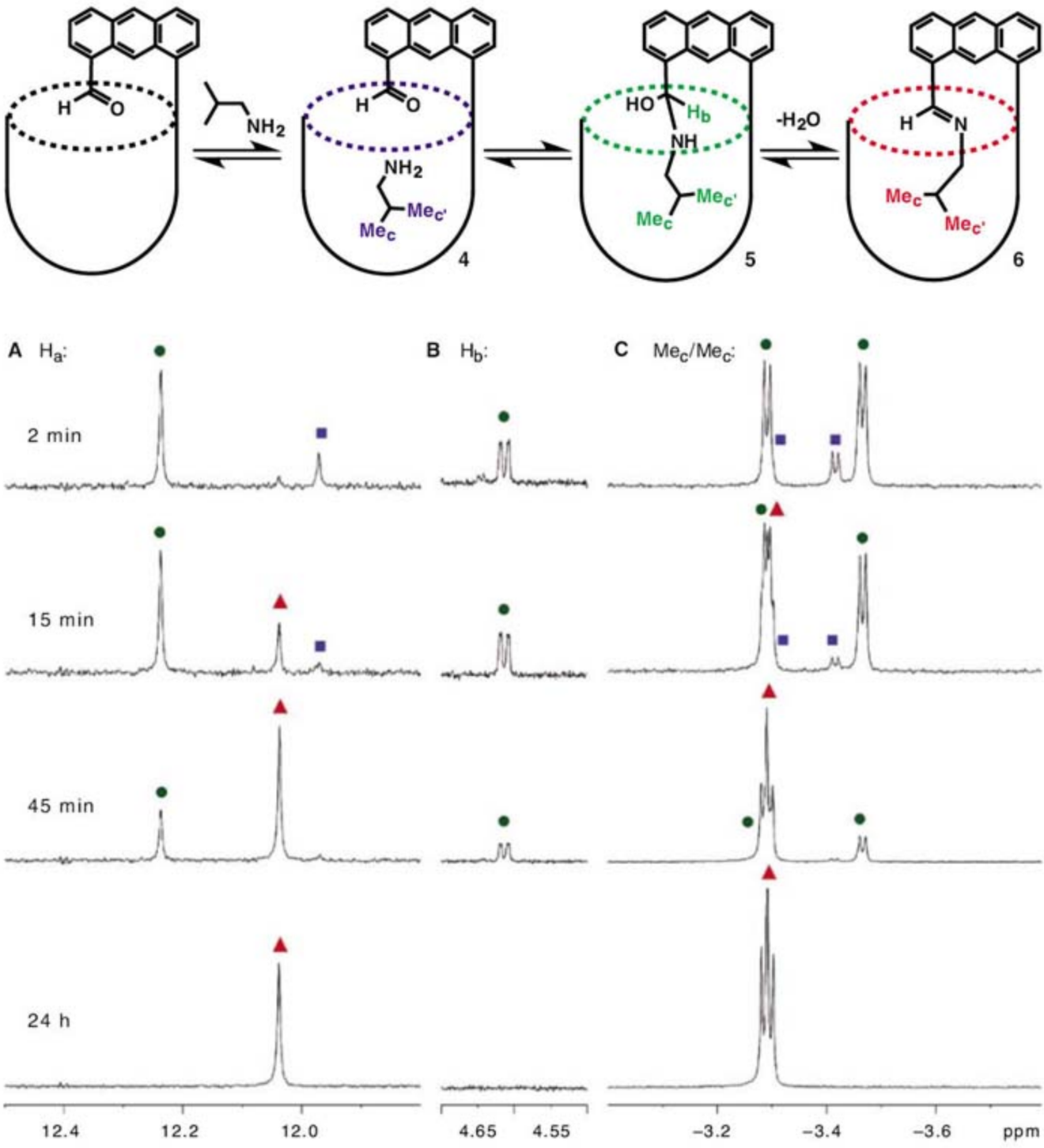

Fig. 3. The reaction in the cavitand. Representation of the reaction process and sections of the ^{1}H NMR spectra obtained upon addition of isobutylamine (10 mM) to a 1.5 mM solution of cavitand **1** in mesitylene-d_{12}. ■ host:guest complex **4**, ● hemiaminal intermediate **5**, and ▲ imine product **6**. (**A**) Downfield region showing benzimidazole proton H_a (Fig. 2); (**B**) mid-field region showing hemiaminal CH_b; (**C**) upfield region showing $Me_{C/C'}$. Me, methyl group.

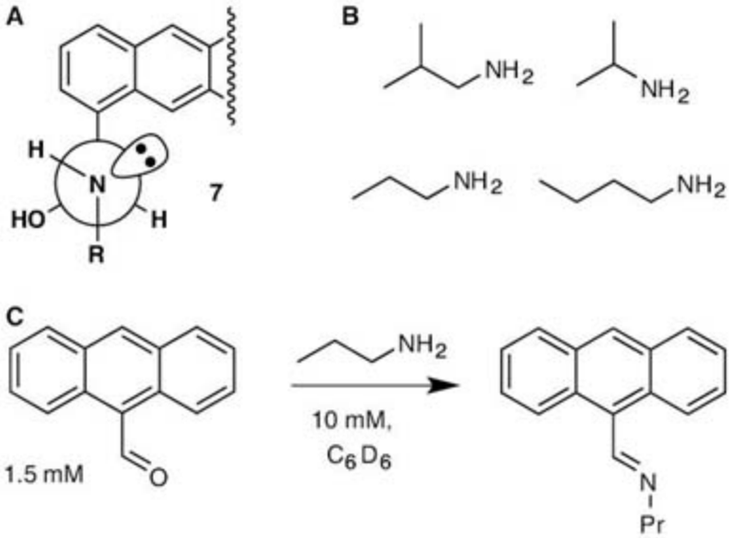

Fig. 4. (**A**) Conformation of the hemiaminal stereocenter inside the complex as viewed down the newly formed N-C bond (one of two possible enantiomers is shown); (**B**) other amines for which hemiaminal formation is observed; (**C**) representation of the cavitand-free control reaction. Pr, propyl group.

tetrahedral intermediates through hydrogen bonding, which also reduces the enthalpic price of the reaction. Accordingly, the cavitand provides a nearly ideal environment for this reaction: The reactants are confined in a limited space and properly oriented, and the desired reactive intermediate is actively stabilized. The stabilization is further enhanced by the binding of the intermediate. In free solution, the dehydration step is self-promoted; in the absence of a better base, a second amine molecule can accelerate the elimination of water. The confinement provided by the cavitand prevents interaction between external base and tetrahedral intermediate, thereby inhibiting progression to the imine.

Are these confining cavities capable of shifting equilibria toward otherwise unstable intermediates (*22*)? Enzyme-catalyzed reactions show enormous rate enhancements through binding to reaction intermediates that structurally resemble transition states. The alteration of equilibria inside enzymes such as triose phosphate isomerase has been proposed (*23*, *24*) but, despite close examination (*25*), has yet to be confirmed. Another proposal relates the magnitude of these effects to the attractive forces between enzyme and substrate, with the greatest effects arising from the formation of covalent bonds (*26*). The evidence presented here supports this view, insofar as the cavitand's functional group arrangement resembles an enzyme active site. Although these cavitands are not catalysts, they show a capacity in stoichiometric quantities to trap reactive intermediates, allowing more direct study of reaction mechanisms.

References and Notes

1. J. Rebek Jr., *Tetrahedron* **35**, 723 (1979).
2. R. I. Masel, *Chemical Kinetics and Catalysis* (Wiley-Interscience, New York, 2001).
3. E. V. Anslyn, D. A. Dougherty, in *Modern Physical Organic Chemistry* (University Science, Sausalito, CA, 2006), ch. 10.
4. D. A. Evans, G. Borg, K. A. Scheidt, *Angew. Chem. Int. Ed.* **41**, 3188 (2002).
5. L. Floriani, E. Marianucci, P. E. Todesco, *J. Chem. Res.* **1984**, 126 (1984).
6. J. A. Chudek, R. Foster, D. Young, *J. Chem. Soc., Perkin Trans. 2* 1285 (1985).
7. D. M. Rudkevich, J. Rebek Jr., *Eur. J. Org. Chem.* **1999**, 1991 (1999).
8. B. W. Purse, P. Ballester, J. Rebek Jr., *J. Am. Chem. Soc.* **125**, 14682 (2003).
9. V. M. Dong, D. Fiedler, B. Carl, R. G. Bergman, K. N. Raymond, *J. Am. Chem. Soc.* **128**, 14464 (2006).
10. M. Ziegler, J. L. Brumaghim, K. N. Raymond, *Angew. Chem. Int. Ed.* **39**, 4119 (2000).
11. M. Yoshizawa, T. Kusukawa, M. Fujita, K. Yamaguchi, *J. Am. Chem. Soc.* **122**, 6311 (2000).
12. T. Iwasawa, E. Mann, J. Rebek Jr., *J. Am. Chem. Soc.* **128**, 9308 (2006).
13. M. Kawano, Y. Kobayashi, T. Ozeki, M. Fujita, *J. Am. Chem. Soc.* **128**, 6558 (2006).
14. D. Fiedler, R. G. Bergman, K. N. Raymond, *Angew. Chem. Int. Ed.* **43**, 6748 (2004).
15. A. Heine *et al.*, *Science* **294**, 369 (2001).
16. E. Lorentzen, B. Siebers, R. Hensel, E. Pohl, *Biochemistry* **44**, 4222 (2005).
17. A. R. Renslo, J. Rebek Jr., *Angew. Chem. Int. Ed.* **39**, 3281 (2000).
18. S. Lin, L. Yang, *Tetrahedron Lett.* **46**, 4315 (2005).
19. T. Gottschalk, B. Jaun, F. Diederich, *Angew. Chem. Int. Ed.* **46**, 260 (2007).
20. R. J. Hooley, J. Rebek Jr., *J. Am. Chem. Soc.* **127**, 11904 (2005).
21. B. W. Purse, A. Gissot, J. Rebek Jr., *J. Am. Chem. Soc.* **127**, 11222 (2005).
22. A. Fersht, *Enzyme Structure and Mechanism* (Freeman, New York, 1984), pp. 47–97.
23. W. J. Albery, J. R. Knowles, *Biochemistry* **15**, 5627 (1976).
24. J. R. Knowles, *Nature* **350**, 121 (1991).
25. S. Rozovsky, A. E. McDermott, *Proc. Natl. Acad. Sci. U.S.A.* **104**, 2080 (2007).
26. X. Zhang, K. N. Houk, *Acc. Chem. Res.* **38**, 379 (2005).
27. We are grateful to the Skaggs Institute and the NIH (grant GM 50174) for financial support. T.I. and R.J.H. are Skaggs Postdoctoral Fellows.

Supporting Online Material

www.sciencemag.org/cgi/content/full/317/5837/493/DC1
Materials and Methods
Figs. S1 to S10
References

2 April 2007; accepted 31 May 2007
10.1126/science.1143272

A Powerful Chiral Counterion Strategy for Asymmetric Transition Metal Catalysis

Gregory L. Hamilton, Eun Joo Kang, Miriam Mba, F. Dean Toste*

Traditionally, transition metal–catalyzed enantioselective transformations rely on chiral ligands tightly bound to the metal to induce asymmetric product distributions. Here we report high enantioselectivities conferred by a chiral counterion in a metal-catalyzed reaction. Two different transformations catalyzed by cationic gold(I) complexes generated products in 90 to 99% enantiomeric excess with the use of chiral binaphthol–derived phosphate anions. Furthermore, we show that the chiral counterion can be combined additively with chiral ligands to enable an asymmetric transformation that cannot be achieved by either method alone. This concept of relaying chiral information via an ion pair should be applicable to a vast number of metal-mediated processes.

The preparation of enantiomerically pure compounds has become a requirement for agrochemical and pharmaceutical synthesis. Such chiral nonracemic compounds are typically accessed from either Nature's "chiral pool," by resolution of a racemate or by means of an enantioselective transformation mediated by a chiral catalyst (*1*). In general, chiral catalysts rely on covalent (dative or nondative) bonds between the reactive site and the chiral moiety. An alternative approach, which takes advantage of the fact that many enantioselective catalysts bear a positive charge, is the induction of asymmetry by interaction of the cationic catalyst with a chiral counteranion associated with the metal in an ion pair. This idea is potentially very powerful because, in principle, the same or a small library of chiral anionic counterions could be used to make a wide range of cationic catalysts enantioselective. The importance of chiral ion pairs is well known in the fields of phase-transfer catalysis (*2*) and organocatalysis (*3*–*6*) and may also be relevant to chiral Brønsted acid catalysis (*7*).

Department of Chemistry, University of California at Berkeley, Berkeley, CA 94720, USA.

*To whom correspondence should be addressed. E-mail: fdtoste@berkeley.edu

Although chiral ions have been successfully applied to the resolution of metal complexes, very few reports have described examining a chiral counterion strategy for metal catalysis (*8*). Support for the concept has been clearly demonstrated; however, the potential has been widely unappreciated because of the low enantioselectivity [0 to 34% ee (enantiomeric excess)] obtained in previous attempts using this method (*9*–*11*). Herein we report a highly enantioselective transition metal–catalyzed reaction mediated by a chiral counterion.

In spite of the recent upsurge of reports documenting reactions catalyzed by homogeneous gold complexes (*12*–*15*), relatively few enantioselective transformations have been discovered (*16*–*22*). Au(I) complexes incorporating chiral phosphines have proven very successful for certain processes but inadequate for others; this deficiency is possibly attributable to the linear coordination geometry of gold, which places the chiral components distant from the substrate. We have previously noted a dramatic effect of the counteranion on the stereoselectivity of cationic Au(I)-catalyzed reactions (*21*). In light of this observation, we envisioned that chiral counterions could provide a particularly advantageous alternative to the traditional chiral ligand approach in the arena of gold chemistry.

Although a number of transition metals catalyze the addition of alcohols across carbon-carbon multiple bonds, to date, only Au(I) complexes have been successful in promoting an asymmetric hydroalkoxylation of allenes (*20*, *23*). Our research efforts, as well as those of others, have found this transformation particularly difficult to achieve with broad substrate scope and high enantioselectivity when using chiral phosphine–ligated catalysts. Only allenol substrates bearing a particular substitution pattern have succumbed to cyclization with high enantioinduction. We therefore saw this reaction as an ideal platform to test the ability of chiral counterions to mediate asymmetric gold reactions.

As expected, for a typical allenol substrate **1**, treatment with a variety of chiral phosphine–substituted gold catalysts in dichloromethane solvent led to poor enantioselectivities (Fig. 1A). In contrast, the catalyst produced in situ from Ph_3PAuCl (in which Ph_3P is triphenylphosphine) and chiral silver phosphate Ag-(*R*)-**6** (*24*, *25*) in dichloromethane solvent furnished a good yield of the hydroalkoxylation product and moderate enantiomeric excess (Fig. 1B). We chose phosphates derived from binaphthol as chiral anions for our investigation because of ease of access and their ready variability (*26*). Moreover, the silver phosphate enables facile generation of the cationic gold(I) catalyst from the phosphinegold (I) chloride driven by precipitation of silver chloride from solution (*27*). Control experiments demonstrated that the reaction is not catalyzed by the phosphoric acid corresponding to protonated **6**, nor is there an appreciable background reaction from either Ph_3PAuCl or the silver phosphate alone. The enantioselectivity of the reaction was improved by utilizing the dinuclear gold complex bearing the bis(diphenylphosphinomethane) ligand (dppm). Examination of other solvents demonstrated that more-polar solvents, such as nitromethane or acetone, gave significantly lower enantiomeric excess values (Fig. 1C). However, the less-polar benzene proved to be the optimal medium, providing the desired product in an exceptional 97% ee. These findings are consistent with an ion-pair model, in which the degree of enantioinduction depends on the proximity of the counteranion to the cationic gold center (*9*).

Knowing the optimized conditions, we explored the scope of the chiral counterion–mediated enantioselective hydroalkoxylation. We found the method could be generally applied to a variety of allenol substrates (Table 1). Different substituents were well tolerated at several positions, including

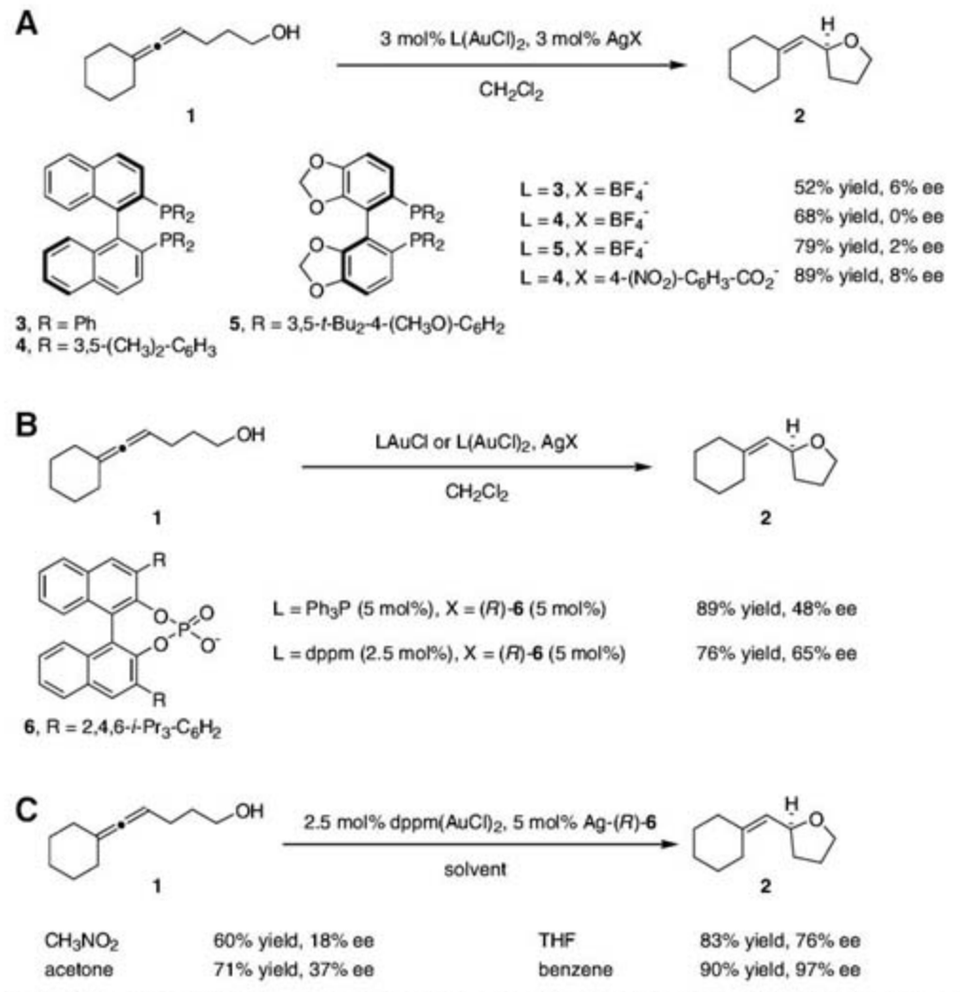

Fig. 1. (**A** and **B**) Comparison of chiral ligands versus chiral counterion for asymmetric hydroalkoxylation. (**C**) Effect of solvent polarity on enantioselectivity.

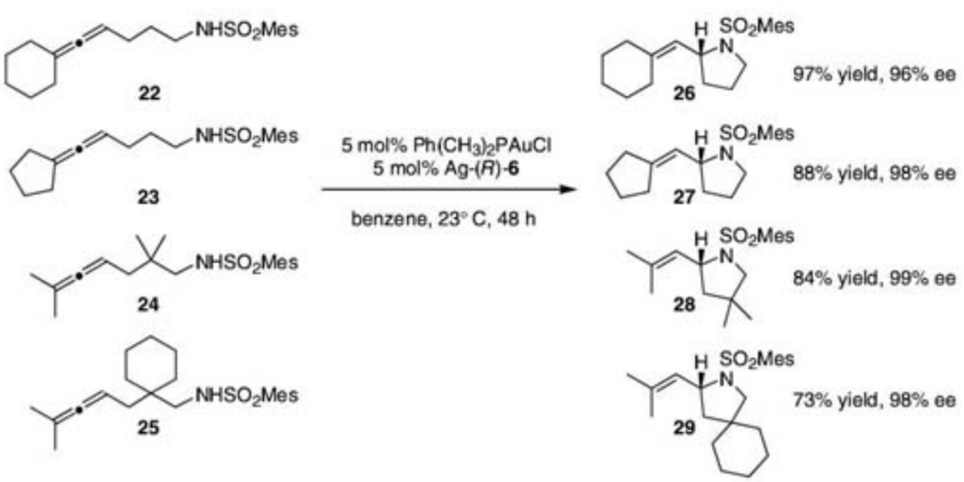

Fig. 2. Counterion-mediated enantioselective hydroamination.

Fig. 3. Hydrocarboxylation using chiral ligand and counterion. The absolute configuration of product enantiomer in excess is noted for each entry.

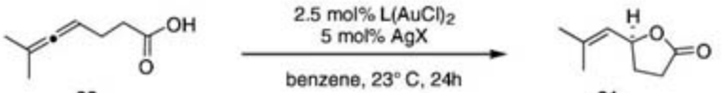

L = (*R*)-**3**, X = 4-(NO_2)-C_6H_3-COO^- — 80% yield, 38% ee (*R*)
L = dppm, X = (*R*)-**6** — 89% yield, 12% ee (*S*)
L = (*R*)-**3**, X = (*R*)-**6** — 91% yield, 3% ee (*R*)
L = (*S*)-**3**, X = (*R*)-**6** — 88% yield, 82% ee (*S*)

Table 1. Scope of asymmetric hydroalkoxylation. Entry 8 was performed using (*S*,*S*)-DIPAMP ligand (**7**); enantiomeric excess from using dppm($AuCl)_2$ is in parentheses. Yields refer to isolated material except for entry 8, which was determined by gas chromatography analysis versus an internal standard.

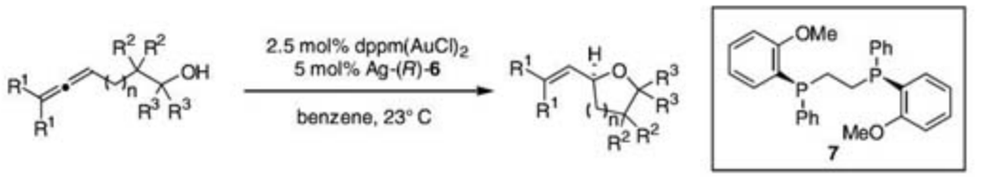

Entry	Substrate	n	R^1	R^2	R^3	Time (h)	Product	% Yield	% ee
1	**1**	1	-$(CH_2)_4$-	H	H	1	**2**	90	97
2	**8**	1	CH_3	H	H	1	**15**	91	95
3	**9**	1	CH_2CH_3	H	H	5	**16**	89	96
4	**10**	1	-$(CH_2)_4$-	H	CH_3	2	**17**	79	99
5	**11**	1	-$(CH_2)_4$-	H	Ph	30	**18**	86	92
6	**12**	1	-$(CH_2)_4$-	CH_3	H	13	**19**	90	90
7	**13**	2	CH_3	H	H	15	**20**	81	90
8	**14**	2	H	H	H	24	**21**	96	92 (80)

the allene terminus (entries 1 to 3) and the α (entries 4 to 5) and β (entry 6) positions of the alcohol. The homologated compound **13** also underwent the reaction to produce tetrahydropyran product **20** with high optical purity.

Even though the achiral ligand system proved successful for a variety of substrates, we were curious to see whether we could combine chiral ligands on gold with the chiral counterion to further improve the enantioselectivity. To study this question, we examined substrate **14**, which lacks any sterically demanding substituents along the backbone or the allene terminus (Table 1, entry 8). This type of unfunctionalized compound is typically very resistant to highly enantioselective transformations, so we were not surprised to find that our standard conditions converted this substrate with slightly reduced enantioselectivity (80% ee). Fortunately, further investigation revealed that combining chiral complex (1*S*,2*S*)-(+)-bis[(2-methoxyphenyl)phenylphosphino]ethane [(*S*,*S*)-DIPAMP]($AuCl)_2$ with Ag-(*S*)-**6** produced the vinyltetrahydropyran product **21** in 92% ee. Pairing the (*S*,*S*)-ligand with the opposite enantiomer of the chiral counterion did not furnish the same improvement in enantioselectivity, indicating that the two combine in a "matched" and "mismatched" fashion. Clearly, the combination of chiral ligands and chiral counterion creates an exceptionally selective system capable of strong enantioinduction for even the most challenging substrates.

Accordingly, we probed the applicability of our chiral counterion strategy to another gold-catalyzed reaction. We considered the intramolecular hydroamination of allenes as a straightforward extension. In the event, we found that a phenyldimethylphosphine-ligated cationic gold complex with the chiral phosphate counterion **6** promoted the desired transformation of allene-sulfonamides with a high level of enantioselectivity (Fig. 2). A number of different substrates performed well under the reaction conditions to give pyrrolidine products in good yield and excellent enantiomeric excess. High enantioselectivity was observed even for compounds **23** and **25**, which gave lower enantiomeric excess values (83% and 70%, respectively) under our previously reported hydroamination conditions in which we used chiral phosphine ligands on gold (*21*). Thus, we have established that the very high enantioinduction from our chiral counterion is not confined to a single reaction, as it offers a useful complementary approach to asymmetric hydroamination of allenes as well.

With these results in hand, we next turned to asymmetric hydrocarboxylation of allenes. Initially, we were disappointed to find that gold complexes incorporating chiral ligands or chiral counterions catalyzed the reaction with poor asymmetric induction (Fig. 3). Nevertheless, we realized this transformation could be an excellent arena in which to test the power of combining chiral ligands and counterions. Despite the extremely low enantioselectivity provided by either component alone, the gold catalyst combining the (*S*)-BINAP [(*S*)-(−)-[2,2′-bis(diphenylphosphino)-1,1′-binaphthyl] ligand [(*S*)-**3**] and (*R*)-**6** counteranion cyclized the allene-carboxylate **30** to lactone **31** in 82% ee. As would be expected, this reaction exhibited a dramatic matched and mismatched pairing effect of the ligand and counterion; the (*R*) enantiomer of the silver phosphate, together with the antipodal (*R*)-BINAP($AuCl)_2$, produced a nearly racemic product. The highly additive effect of counterion and chiral ligand, as demonstrated here, provides more evidence of the enabling power of the counterion strategy for opening previously inaccessible transformations to asymmetric catalysis.

The chiral counterion approach is especially appealing for Au(I) catalysis, given the aforementioned difficulty of transferring chiral information from a ligand disposed 180° from the substrate. We have shown that modification of the counterion can be used to circumvent this problem by introducing an additional source of chirality near the metal center. Our success relative to previous studies may be partially attributed to the choice of chiral anions that have previously demonstrated potential in asymmetric Brønsted acid catalysis; however, in addition to accessing reactivity not available using Brønsted acid catalysts (*12*), the use of chiral anions in metal catalysis benefits from tuning of the ancillary ligands on the metal in a manner that is not possible for H^+. Moreover, this concept does not preclude processes that require a change in the formal oxidation state of the transition metal catalyst, but rather requires that ion-pairing be maintained in the transition state structure of the enantiodetermining step. Therefore, this approach is by no means limited to cationic gold(I) complexes as catalysts or chiral phosphates as counterions. Considering the multitude of reactions catalyzed by ionic complexes of palladium, rhodium, ruthenium, iridium, and other metals, and given the vast possibilities for chiral anionic and cationic species, we envision tremendous potential in the field of chiral counterion–mediated transition metal–catalyzed reactions. This approach should have especially broad applicability, given that the chiral counterion strategy can be combined with existing chiral ligand platforms in a synergistic fashion.

References and Notes

1. J. Mulzer, in *Comprehensive Asymmetric Catalysis*, E. N. Jacobsen, A. Pfaltz, H. Yamamoto, Eds. (Springer, Berlin, 1999), vol. I, chap. 3.
2. M. J. O'Donnell, in *Catalytic Asymmetric Synthesis*, I. Ojima, Ed. (Wiley-VCH, New York, ed. 2, 2000), chap. 10, pp. 727–755.

3. G. Lelais, D. W. C. MacMillan, *Aldrichim Acta* **39**, 79 (2006).
4. M. S. Taylor, E. N. Jacobsen, *Angew. Chem. Int. Ed.* **45**, 1520 (2006).
5. S. Mayer, B. List, *Angew. Chem. Int. Ed.* **45**, 4193 (2006).
6. N. J. A. Martin, B. List, *J. Am. Chem. Soc.* **128**, 13368 (2006).
7. T. Akiyama, J. Itoh, K. Fuchibe, *Adv. Synth. Catal.* **348**, 999 (2006).
8. J. Lacour, V. Hebbe-Viton, *Chem. Soc. Rev.* **32**, 373 (2003).
9. D. B. Llewellyn, D. Adamson, B. A. Arndtsen, *Org. Lett.* **2**, 4165 (2000).
10. D. B. Llewellyn, B. A. Arndtsen, *Tetrahedron Asymmetry* **16**, 1789 (2005).
11. R. Dorta, L. Shimon, D. Milstein, *J. Organomet. Chem.* **689**, 751 (2004).
12. D. J. Gorin, F. D. Toste, *Nature* **446**, 395 (2007).
13. E. Jiménez-Nunez, A. M. Echavarren, *Chem. Commun.* 333 (2007).
14. A. S. K. Hashmi, G. J. Hutchings, *Angew. Chem. Int. Ed.* **45**, 7896 (2006).
15. L. Zhang, J. Sun, S. A. Kozmin, *Adv. Synth. Catal.* **348**, 2271 (2006).
16. Y. Ito, M. Sawamura, T. Hayashi, *J. Am. Chem. Soc.* **108**, 6405 (1986).
17. M. P. Muñoz, J. Adrio, J. C. Carretero, A. M. Echavarren, *Organometallics* **24**, 1293 (2005).
18. C. González-Arellano, A. Corma, M. Iglesias, F. Sanchez, *Chem. Commun.* 3451 (2005).
19. M. J. Johansson, D. J. Gorin, S. T. Staben, F. D. Toste *J. Am. Chem. Soc.* **127**, 18002 (2005).
20. Z. Zhang, R. A. Widenhoefer, *Angew. Chem. Int. Ed.* **46**, 283 (2007).
21. R. L. LaLonde, B. D. Sherry, E. J. Kang, F. D. Toste *J. Am. Chem. Soc.* **129**, 2452 (2007).
22. C. Liu, R. A. Widenhoefer, *Org. Lett.* **9**, 1935 (2007).
23. For a review on transition metal–catalyzed nucleophilic additions to allenes, see (*28*).
24. When viewed with ^{31}P nuclear magnetic resonance, this gold species in solution is seen to have a chemical shift identical to the catalyst bearing the noncoordinating triflate counterion produced from the combination of Ph_3PAuCl and AgOTf (OTf is trifluoromethane sulfonate), which suggests that a similar cationic species is present in either case.
25. Materials and methods are available as supporting online material on *Science* Online.
26. For a review on chiral phosphoric acids, see (*29*).
27. The catalyst can also be generated by protonation of Ph_3PAuCH_3 with phosphoric acid H-(*R*)-**6** to afford the product in the same yield and enantiomeric excess.
28. R. W. Bates, V. Satcharoen, *Chem. Soc. Rev.* **31**, 12 (2002).
29. S. J. Connon, *Angew. Chem. Int. Ed.* **45**, 3909 (2006).

30. We gratefully acknowledge funding from National Institute of General Medical Services support (R01 GM073932), Merck Research Laboratories, Amgen Inc., Bristol-Myers Squibb, Abbott, Pfizer, DuPont, Novartis, and Boehringer-Ingelheim. We thank Takasago for their generous donation of DTBM-SEGPHOS (**5**). G.L.H. is grateful for an NSF predoctoral fellowship. E.J.K. thanks the Korea Research Foundation Grant (MOEHRD; KRF-2006-214-C00044) and M.M. thanks the University of Padua for postdoctoral fellowships.

Supporting Online Material

www.sciencemag.org/cgi/content/full/317/5837/496/DC1
Materials and Methods
References and Notes

16 May 2007; accepted 13 June 2007
10.1126/science.1145229

A Cambrian Peak in Morphological Variation Within Trilobite Species

Mark Webster

Morphological variation within species is a raw material subject to natural selection. However, temporal change in morphological diversity has usually been studied in terms of variation among rather than within species. The distribution of polymorphic traits in cladistic character-taxon matrices reveals that the frequency and extent of morphological variation in 982 trilobite species are greatest early in the evolution of the group: Stratigraphically old and/or phylogenetically basal taxa are significantly more variable than younger and/or more derived taxa. Through its influence on evolutionary tempo, high intraspecific variation may have played a major role in the pronounced Cambrian diversification of trilobites.

Many higher taxa show a markedly asymmetric diversification history, with rapid initial increase in morphological diversity among taxa (disparity) and subsequent decline in or cessation of evolutionary inventiveness (*1*–*4*). Rates of taxonomic diversity increase are also often higher during the early portion of clade evolutionary history (*5*, *6*). Because the potential rate and magnitude of evolutionary change (evolvability) for a species must be to some extent a function of the degree of morphological variation exhibited by that species (*7*, *8*), change in the frequency or nature of intraspecific variation within a clade could profoundly influence its evolutionary dynamics. To the extent that observed phenotypic variation reflects heritable variability (*7*) and therefore evolvability, a clade exhibiting a bottom-heavy diversification history would be predicted to show a temporally declining degree of intraspecific variation among its constituent members, as has been claimed for some animal clades ["Rosa's Rule" (*9*, *10*)].

Here I investigate long-term trends in morphological variation in species using the 270-million-year history (Early Cambrian through Late Permian) of trilobites. Trilobites have a character-rich morphology, abundant fossil record, and high diversity. The diversification history of trilobites was bottom-heavy (fig. S1A): Origination and extinction rates of trilobite genera were generally higher in the Cambrian than later (fig. S1, B and C), although there was rapid diversification within some post-Cambrian clades (*11*). Maximal disparity was achieved during the Early Cambrian [based on among-species variation in thoracic segment number (*12*)] or the Ordovician [based on among-species variation in cranidial outline (*6*, *13*) and qualitative assessment of gross anatomy (*14*)]. Although it has been suggested that the net decline in evolutionary rate corresponded to a general decrease in morphological variability within trilobite species through time (*15*, *16*), the few pertinent studies to date do not provide strong empirical support for unusual variation within Cambrian trilobite species in any aspect of morphology other than number of thoracic segments at maturity [(*12*); see supporting online material (SOM)], and even that trait is variable within only very few species.

I explored temporal patterns in intraspecific variation as represented by character states coded as polymorphic within trilobite species in cladistic analyses. Species coded as polymorphic for a given character are assumed to have exhibited marked variation that spanned two or more states defined by the original authors. Aspects of organismal shape, counts of meristic features (including presence or absence of particular features), and locations and discrete types of particular anatomical structures can all form the basis for characters coded in cladistic analyses, thus maximizing morphological coverage (SOM).

I examined 68 trilobite character-taxon matrices for intraspecific polymorphisms (table S1), but application of stringent criteria to reduce the potential for among-study bias (*17*) resulted in exclusion of some entire matrices, and of particular characters and/or taxa from others (table S1). The final data set consisted of character-taxon matrices from 49 independent studies (tables S1 and S2). Character-state information for a total of 982 species was included (table S2), representing ~5% of all valid trilobite species (*18*). All eight orders of trilobites, plus the problematic burlingiids, were represented. I treated agnostids as trilobites (*19*–*21*), but my general conclusions are not dependent upon their inclusion. All orders were represented by more than 100 species in the analysis, with the exception of the Redlichiida (79 species), the Corynexochida (50 species), and the Asaphida (26 species). With the exception of the Permian, geologic periods were subdivided into two or three temporal bins (typically corresponding to epochs); the stratigraphic age at this finer level of resolution was known for 957

Department of the Geophysical Sciences, University of Chicago, 5734 South Ellis Avenue, Chicago, IL 60637, USA. E-mail: mwebster@geosci.uchicago.edu

of the species. The final data set included representatives from every temporal bin, spanning the entire geologic range of the Trilobita. Most temporal bins included data from 60 or more species (Fig. 1A), although the Late Cambrian, Late Silurian, Late Devonian, Carboniferous, and Permian were each represented by fewer than 40 species. Of the 25 species for which age was known only at the period level of resolution, all were post-Cambrian in age and 24 were coded with no polymorphisms (the polymorphic species being an Ordovician proetid): Their inclusion would therefore have strengthened the temporal trend detected by the present analysis. Some 40,957 positively coded character states, each with the potential for intraspecific polymorphism, were included [excluding missing, inapplicable, and redundant (the same species coded for the same character in multiple studies) characters].

More than 35% of the 982 included trilobite species were polymorphic in at least one positively coded character (table S2). However, these polymorphic species were neither evenly nor randomly distributed through time (Fig. 1, A and B). More than 70% of included Early and Middle Cambrian trilobite species were coded as polymorphic for at least one character. This proportion is significantly higher than in all later temporal bins, where fewer than 40% (and often fewer than 20%) of trilobite species were coded as polymorphic for at least one character. The proportion of species with at least one polymorphism drops sharply between the Middle Cambrian (75%) and Late Cambrian [8% (*22*)], then rises to 40% in the Early Ordovician (coincident with the first sampling of the diverse phacopid and proetid orders), after which there is a progressive decline through the Middle Devonian (1%), interrupted only by a particularly low value (0%) in the Late Silurian. Approximately 37% of included Late Devonian species were coded with at least one polymorphism (all heralding from study 43 in table S1). No polymorphism was recorded in character-state coding among the 23 post-Devonian species. It is unclear whether this pattern is better interpreted as a steplike drop from Early and Middle Cambrian high proportions (<70%) to post–Middle Cambrian low proportions (0 to 40%, averaging 13%), or as a progressive decline through the Paleozoic from the Early and Middle Cambrian (<70%) through the post-Devonian (0%) made noisy by intervals of poor sampling. The proportion of trilobite species polymorphic in at least one character was significantly higher in the Early and Middle Cambrian than in later times.

The most extreme degrees of intraspecific variation were also documented in Early and Middle Cambrian trilobites (Fig. 2, A and B, and fig. S2), when some species were polymorphic in more than 20% of their coded characters. None of the 588 post-Cambrian species exhibited polymorphism in more than 15% of their coded characters (Fig. 2C). The average proportion of characters for which a species was coded as polymorphic falls from 3% in the Early and Middle Cambrian to 0% in post–Middle Cambrian bins.

The phylogenetic distribution of species exhibiting any degree of polymorphism in coded characters is also not uniform (Fig. 3, A and B). A significantly higher proportion of species belonging to the stratigraphically old and/or early diverging (*19*) clades Redlichiida (53%), Ptychopariida (79%), and Agnostida (88%) are polymorphic for at least one character compared to the younger and/or more derived (*19*) Corynexochida (10%), Proetida (17%), Phacopida (7%), Lichida (13%), Asaphida (4%), and Burlingiidae (0%). The temporal decline in intraspecific variation therefore results primarily from differences among trilobite orders. However, there is also support for declining frequency of polymorphic species through time within the long-ranging, well-sampled orders Proetida (Fig. 3, C and D) and Phacopida (Fig. 3, E and F), although the latter showed a return to high proportions in the Late Devonian (attributable to a single study; see above). Any sustained trends within other orders is unclear because of insufficient taxonomic or temporal sampling (figs. S3 and S4), although a significant drop in the proportion of species exhibiting polymorphism following an Early and/or Middle Cambrian peak was seen for the

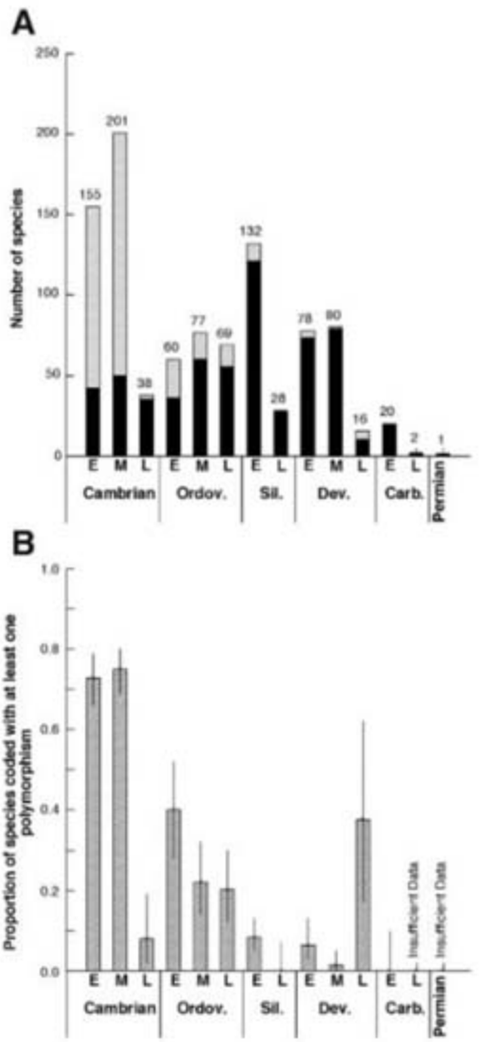

Fig. 1. Temporal pattern of the frequency (**A**) and relative proportion (**B**) of trilobite species coded as polymorphic in at least one character in cladistic analyses. Hatched and solid shading in (A) denotes polymorphic and nonpolymorphic species, respectively. Geologic period abbreviations: Ordov., Ordovician; Sil., Silurian; Dev., Devonian; Carb., Carboniferous; E, early; M, middle; L, late. Error bars indicate two-unit profile likelihood confidence intervals. Data are from table S2.

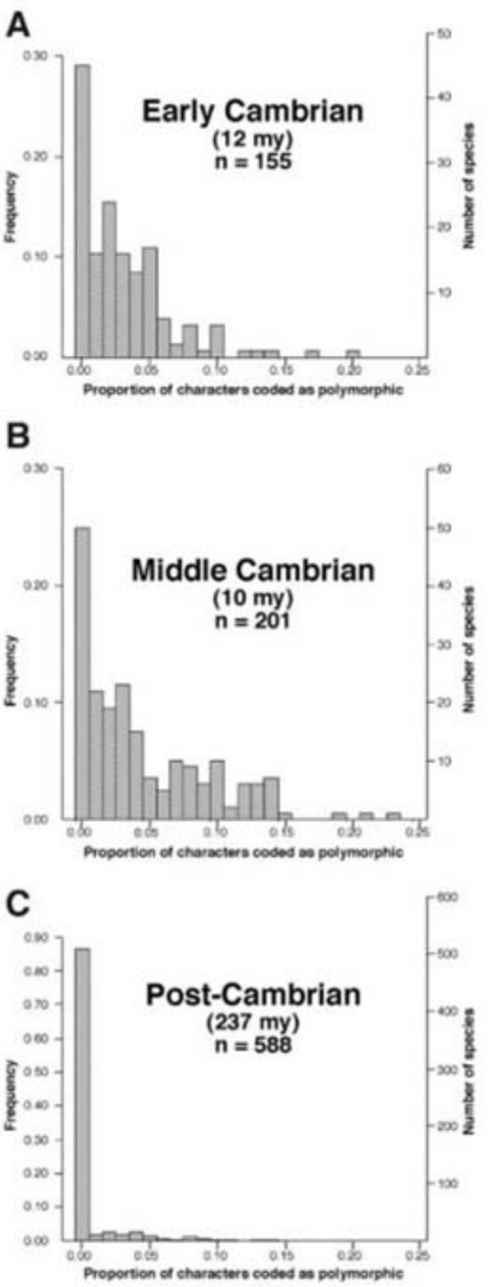

Fig. 2. Frequency distributions for the proportion of characters coded as polymorphic within trilobite species for the Early Cambrian (**A**, median = 2.8%), Middle Cambrian (**B**, median = 3.6%), and post-Cambrian (**C**, median = 0.0%). Approximate duration (in millions of years, my) of each temporal bin is shown; duration for Early Cambrian is based on trilobite-bearing portion only. Frequency distributions at higher temporal resolution are shown in fig. S2. Data are from table S2.

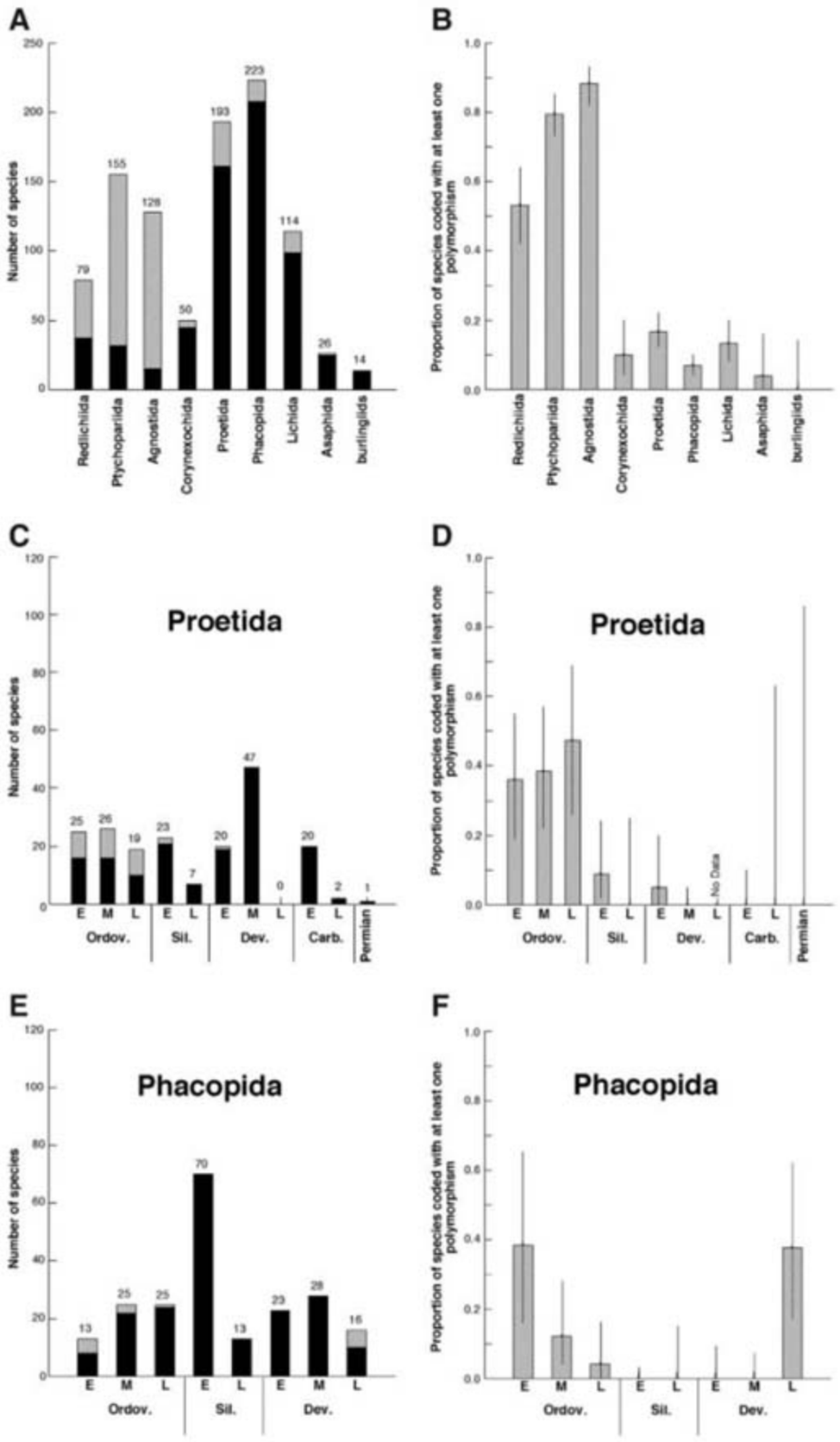

Fig. 3. (**A** and **B**) Differences among trilobite orders in the frequency (A) and relative proportion (B) of species coded as polymorphic in at least one character in cladistic analyses. (**C** and **D**) Temporal pattern of the frequency (C) and relative proportion (D) of proetid trilobite species coded as polymorphic in at least one character in cladistic analyses. (**E** and **F**) Temporal pattern of the frequency (E) and relative proportion (F) of phacopid trilobite species coded as polymorphic in at least one character in cladistic analyses. Hatched and solid shading in (A), (C), and (E) denote polymorphic and nonpolymorphic species, respectively. Error bars indicate two-unit profile likelihood confidence intervals. Data are from table S2. Abbreviations as for Fig. 1.

Ptychopariida [but see (*22*)] and Agnostida. Whether the higher frequency of polymorphic species early in clade history (here detected in the Trilobita as a whole, the Proetida, and arguably the Phacopida, Ptychopariida, and Agnostida) is indicative of a general phenomenon detectable at levels of lesser phylogenetic inclusivity is unknown. The second (Late Devonian) peak among phacopid species suggests that general trends in intraspecific variation are reversible [see also (*23*)].

The nonuniform phylogenetic and temporal distribution of intraspecific variation in trilobites is unlikely to result from a bias in morphological coverage (i.e., the range of characters examined) or in character-state definition, because similar temporal and phylogenetic patterns are detected when analysis is restricted to characters of unequivocal homology across clades and to characters with minimal potential for among-worker differences in coding (figs. S5 and S6). There are fewer trilobite species per genus on average in the Cambrian versus the post-Cambrian (*18*). If this reflects a worker-related bias of "Cambrian lumpers" versus "post-Cambrian splitters," then a higher degree of apparent variation should be expected within Cambrian trilobite species and the results could be construed as artifact. However, similar temporal and phylogenetic patterns are detected based on the work of single researchers (figs. S7 and S8). The post-Cambrian increase in number of species per genus could result from a decline in generic extinction rate (fig. S1C): Genera originating in the Cambrian had shorter average durations than genera originating in the post-Cambrian (*24*), resulting in accrual of lower species-level diversity per genus. Any worker-related bias in generic concept would not affect the results, which involved only species-level data.

The nature of intraspecific variation can influence the rate and direction of adaptive response of a lineage to selective pressure (*8*, *25*, *26*). The high rates of trilobite generic origination in the Early and Middle Cambrian relative to the post-Cambrian (fig. S1B) are consistent with claims that intraspecific variation can also promote speciation and diversification (*27*). However, the Late Cambrian mismatch between high generic diversification rates and the marked decline in intraspecific variation is inconsistent with such claims, suggesting either that other factors play an important role in generic diversification rate or that intraspecific variation is grossly underrepresented in the Late Cambrian sample (*22*).

The nature of the relation between intraspecific variation and morphological diversification is complex because the components of trilobite anatomy were evolutionarily decoupled. Thus, whereas the maxima of intra- and interspecific variation in thoracic segment number coincide during the Early Cambrian (*12*), the Middle Ordovician maximal disparity in cranidial shape was attained later than the Early/Middle Cambrian maximum in frequency of intraspecific variation in characters determining cranidial

outline [fig. S9; although the rate of increase in disparity of cranidial shape was highest in the Early Cambrian and slowed from the Middle Cambrian through Middle Ordovician (figure 5 in (6)]. The role of intraspecific variation in the generation of novelty and therefore of macroevolutionary trends in disparity is unclear: A hypothesis that intraspecific variation is the source of disparity increase predicts that a polymorphism should involve a derived feature, but the data relate only to whether or not a species is polymorphic for a given character, irrespective of whether the character states are derived, primitive, or convergent on another species.

The observed decline in intraspecific variation may have resulted from increasing developmental or ecological constraints. Developmental constraints may stem from increased integration among or regulation of developmental systems, resulting in decreased capacity to generate or accommodate change in those systems without negative effects on viability (*4*, *28*–*33*). Ecological constraints may stem from progressive niche specialization associated with increased diversity and competition: In an ecospace dominated by incumbents, selection pressure could reduce fitness of variant phenotypes even though developmental regulation and integration may remain unchanged (*29*, *34*). Constraint resulting from a decline in developmental flexibility, in success rate for ecological establishment, or in both (*2*, *4*) could lead to loss of phenotypic variation within species and diminishing morphological innovation, which translates into slower response to selection and declining rate of morphological and taxonomic diversification. Further investigation is required to determine the causal mechanisms and whether the post-Middle Cambrian decline in the frequency and extent of intraspecific variation detected here was unique to trilobites or to this time interval. Nevertheless, demonstration of this pattern and its potential correspondence to diversification rate in trilobites suggests that within-species variation may play an important role in shaping clade macroevolutionary history.

References and Notes

1. S. J. Gould, *Wonderful Life: The Burgess Shale and the Nature of History* (Norton, New York, 1989).
2. D. Jablonski, *Palaeontology* **50**, 87 (2007).
3. M. Foote, *Annu. Rev. Ecol. Syst.* **28**, 129 (1997).
4. D. H. Erwin, *Palaeontology* **50**, 57 (2007).
5. S. J. Gould, N. L. Gilinsky, R. Z. German, *Science* **236**, 1437 (1987).
6. M. Foote, *Paleobiology* **19**, 185 (1993).
7. G. P. Wagner, L. Altenberg, *Evolution* **50**, 967 (1996).
8. P. D. Sniegowski, H. A. Murphy, *Curr. Biol.* **16**, R831 (2006).
9. V. Jaanusson, *Fossils and Strata* **4**, 209 (1975).
10. L. Ramsköld, *Trans. R. Soc. Edinb. Earth Sci.* **82**, 143 (1991).
11. J. M. Adrain, R. A. Fortey, S. R. Westrop, *Science* **280**, 1922 (1998).
12. N. C. Hughes, in *Evolving Form and Function: Fossils and Development*, D. E. G. Briggs, Ed. (Peabody Museum of Natural History, Yale Univ., New Haven, CT, 2005), pp. 139–158.
13. M. Foote, *Palaeontology* **34**, 461 (1991).
14. R. A. Fortey, R. M. Owens, in *Evolutionary Trends*, K. J. McNamara, Ed. (Belhaven, London, 1990), pp. 121–142.
15. K. J. McNamara, *Biol. Rev.* **61**, 121 (1986).
16. N. C. Hughes, *Geology* **19**, 913 (1991).
17. Materials and methods are available as supporting material on *Science* Online.
18. J. M. Adrain, *GSA Abstr. Prog.* **38**, 207 (2006).
19. R. A. Fortey, *J. Paleontol.* **75**, 1141 (2001).
20. T. J. Cotton, R. A. Fortey, in *Crustacea and Arthropod Relationships*, S. Koenemann, R. A. Jenner, Eds., vol. 16 of *Crustacean Issues* (Taylor & Francis, Boca Raton, FL, 2005), pp. 95–136.
21. E. B. Naimark, *Paleontol. J.* **40**, 541 (2006).
22. Extremely poor taxonomic representation may bias estimates of Late Cambrian intraspecific variation. Ptychopariid clades underwent a series of pronounced radiations during the Late Cambrian and accounted for most of the trilobite diversity at this time, but are grossly undersampled in the present study (only eight species represented).
23. N. C. Hughes, R. E. Chapman, J. M. Adrain, *Evol. Dev.* **1**, 24 (1999).
24. M. Foote, *Paleobiology* **14**, 258 (1988).
25. D. Schluter, *Evolution* **50**, 1766 (1996).
26. S. Renaud, J.-C. Auffray, J. Michaux, *Evolution* **60**, 1701 (2006).
27. M. J. West-Eberhard, *Developmental Plasticity and Evolution* (Oxford Univ. Press, New York, 2003).
28. R. Riedl, *Order in Living Organisms: A Systems Analysis of Evolution* (Wiley, New York, 1978).
29. J. W. Valentine, *Palaios* **10**, 190 (1995).
30. G. P. Wagner, M. D. Laubichler, *J. Exp. Zool. B Mol. Dev. Evol.* **302B**, 92 (2004).
31. G. E. Budd, *Biol. Rev.* **81**, 609 (2006).
32. E. H. Davidson, D. H. Erwin, *Science* **311**, 796 (2006).
33. Developmental regulation controlling morphogenesis of the features coded in cladistic analyses of trilobites must have lain downstream of the hypothesized kernels of gene-regulatory networks specifying body-plan architecture (*32*). Complex, phylum-defining characters are not seen to vary within species, and their long-term stability renders consideration of their evolution as "population polymorphisms writ large" inappropriate (*31*). The decline in intraspecific variation documented here is therefore unlikely to simply extrapolate into an explanation for the uniqueness of the Cambrian radiation of metazoans.
34. D. H. Erwin, *Acta Palaeontol. Pol.* **38**, 281 (1994).

35. R. Fortey, T. Cotton, S. Westrop, J. Adrain, and G. Edgecombe discussed aspects of character coding and taxonomic sampling in their cladistic analyses. A. R. Palmer assisted in determining the stratigraphic provenance of several species. Comments from D. Jablonski, M. Foote, P. Wagner, P. Crane, B. Sinclair, and two reviewers helped improve the analysis and manuscript. L. Qin translated Chinese literature. Fig. S1 was drafted by M. Foote.

Supporting Online Material

www.sciencemag.org/cgi/content/full/317/5837/499/DC1
Materials and Methods
SOM
Figs. S1 to S9
Tables S1 and S2
References

23 March 2007; accepted 6 June 2007
10.1126/science.1142964

Four Climate Cycles of Recurring Deep and Surface Water Destabilizations on the Iberian Margin

Belen Martrat,[1] Joan O. Grimalt,[1]* Nicholas J. Shackleton,[2]† Lucia de Abreu,[2] Manuel A. Hutterli,[3,4] Thomas F. Stocker[4]

Centennial climate variability over the last ice age exhibits clear bipolar behavior. High-resolution analyses of marine sediment cores from the Iberian margin trace a number of associated changes simultaneously. Proxies of sea surface temperature and water mass distribution, as well as relative biomarker content, demonstrate that this typical north-south coupling was pervasive for the cold phases of climate during the past 420,000 years. Cold episodes after relatively warm and largely ice-free periods occurred when the predominance of deep water formation changed from northern to southern sources. These results reinforce the connection between rapid climate changes at Mediterranean latitudes and century-to-millennial variability in northern and southern polar regions.

The study of abrupt climate change has focused mainly on the last glacial period (*1*–*13*) and has provided important insights about the dynamics of the climate system (*14*, *15*). Synchronization of the $\delta^{18}O$ records from Greenland and Antarctic ice cores has shown that the regions around Antarctica were warming during short-term cooling stages in Greenland (*1*). These high-latitude changes were paralleled by the fine-scale variability of sea surface temperatures (SST) from lower latitudes in their respective hemispheres (*16*, *17*) and were directly linked on a regional scale to the extension and retreat of polar ice (*3*, *4*) and the reorganization of atmospheric (*5*, *6*) and oceanic circulation (*7*–*13*).

A number of paleoarchives have shown that century-to-millennial climate variability also was

[1]Department of Environmental Chemistry, Chemical and Environmental Research Institute of Barcelona, Spanish National Research Council (IIQAB-CSIC), 08034 Barcelona, Spain. [2]Godwin Laboratory for Palaeoclimate Research, Department of Earth Sciences, University of Cambridge, Cambridge, CB2 3EQ, UK. [3]British Antarctic Survey, High Cross, Madingley Road, Cambridge, CB3 0ET, UK. [4]Climate and Environmental Physics, Physics Institute, University of Bern, CH-3012 Bern, Switzerland.

*To whom correspondence should be addressed. E-mail: jgoqam@cid.csic.es
†Deceased.

a robust feature in previous climate cycles (*16*–*25*). However, in these cases, no ice records from the Northern Hemisphere were available for a comprehensive test of the hypothesis that the same dynamics of abrupt climate change existed during previous ice ages. Fortunately, high-resolution marine sediment cores from the Iberian margin contain a record of the different water masses, which came from the northern North Atlantic and Antarctic regions. In these cores, the $\delta^{18}O$ record of benthic foraminifera resembled the Antarctic temperature signal, whereas the $\delta^{18}O$ of planktic foraminifera exhibited changes similar to those found in Greenland ice cores (*7*–*9*). The differences in isotopic composition between surface and deep waters were based on measurements along individual cores and consequently provided a first independent verification of earlier methane interhemispheric phasing for the last climate cycle (*1*).

The Iberian margin is therefore a focal point for comprehensive evaluation of climate variability in both hemispheres over long time periods. We analyzed stable isotopes (n = 1396 samples) and fossil organic compounds synthesized by marine and continental flora (n = 1648 samples) that we found in sediment cores MD01-2443 and MD01-2444; these data allowed us to generate a high-resolution reconstruction of the climatic history of the past 420,000 years (Fig. 1 and Table 1) (*26*–*28*).

Analysis of down-core profiles on their depth scales emphasizes that climatic events recorded in the incremental layers do not vary in shape after application of dating techniques (fig. S1A). The alkenone-derived SST at the Iberian margin is coupled with the $\delta^{18}O$ record of *Globigerina bulloides* (fig. S1B). The specific sedimentation features of the area studied prevent the offset between ages of alkenones and foraminifera from identical sediment depth intervals, further supporting the in-depth evaluation from the nearby northwest African margin (*29*).

None of the climate cycles was an exact reproduction of the others because on the orbital time scale the governing factors of ice-age dynamics have never been identical (*19*, *20*, *30*–*32*) (Fig. 2, A and B). The results show that the rapid SST changes (Fig. 2F) are consistent, for the time span in which they overlap, with Greenland $\delta^{18}O$ profiles (*2*), reconstructions of iceberg discharges at 55°N (*21*), and arboreal pollen in southern Europe (*22*, *23*) (Fig. 2, B to E).

Dansgaard/Oeschger-type variability is recorded all along the Iberian margin over the past four climate cycles (Fig. 2F). For simplification purposes, the warm and cool events are listed and labeled, respectively, as Iberian margin interstadials (IMI) and stadials (IMS), with the

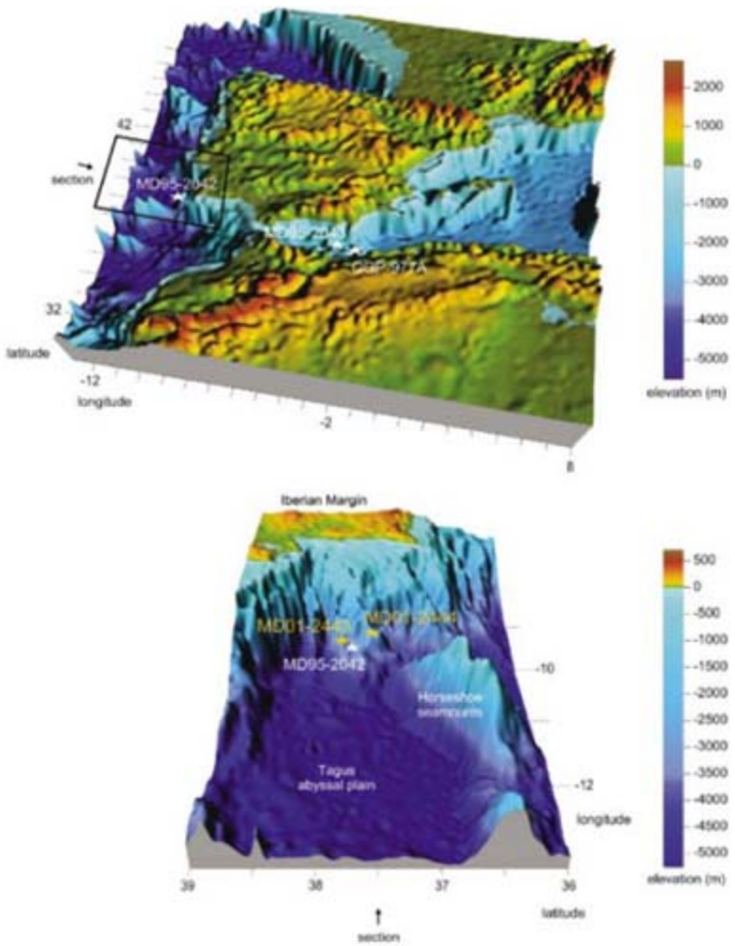

Fig. 1. Maps showing the location of the Iberian margin sediment cores (*28*). The sediment cores studied are MD01-2444 (37°33.68′N, 10°08.53′W, 2637 m below sea level) and MD01-2443 (37°52.85′N, 10°10.57′W, 2925 m below sea level). Existing relevant paleoarchives are MD95-2042 (*7*, *8*, *12*, *13*), MD95-2043 (*10*, *11*), and ODP-977A (*16*), all of which establish the Iberian margin as a sensitive region for recording climatic changes.

Table 1. Summary of the Iberian margin alkenone unsaturation index ($U^{k'}_{37}$)–SST (°C) conditions and time resolution (years) in cores MD01-2444 and MD01-2443 over the past four climate cycles. The average temporal resolution remains comparable at centennial scale throughout the entire period studied. Cores MD01-2444, ODP-977A (*16*), and MD95-2042 (*12*) are in close agreement over the first climate cycle. Correlation coefficients of ODP-977A (*16*) and MD01-2444 $U^{k'}_{37}$-SST (°C) with NGRIP $\delta^{18}O$ (*2*) are r = 0.88 and r = 0.86, respectively. The correlation coefficient of the MD01-2443 benthic profile [(*26*, *27*) and this study] with the Dome C δD record (*18*) is r = 0.92.

SST (°C) $\mu \pm \sigma$ [time resolution (years) $\mu \pm \sigma$]	First climate cycle		Second climate cycle		Third climate cycle		Fourth climate cycle	
	Glacial	Interglacial	Glacial	Interglacial	Glacial	Interglacial	Glacial	Interglacial
MD01-2444, n = 902 samples (this study)	13.8 ± 1.1 [136 ± 83]	17.3 ± 1.9 [275 ± 124]	13.9 ± 2.0 [321 ± 255]					
MD01-2443, n = 764 samples (this study)			14.6 ± 1.3 [590 ± 412]	17.9 ± 1.4 [428 ± 250]	12.6 ± 2.5 [388 ± 144]	16.8 ± 1.8 [333 ± 197]	12.3 ± 2.2 [584 ± 371]	17.2 ± 1.3 [250 ± 149]
ODP-977A, n = 655 samples (*16*)	13.1 ± 1.7 [317 ± 234]	17.9 ± 3.0 [448 ± 522]	14.1 ± 2.2 [370 ± 180]	18.0 ± 2.6 [378 ± 233]				
MD95-2042, n = 299 samples (*12*)	14.5 ± 1.4 [358 ± 199]	17.6 ± 2.2 [923 ± 344]						

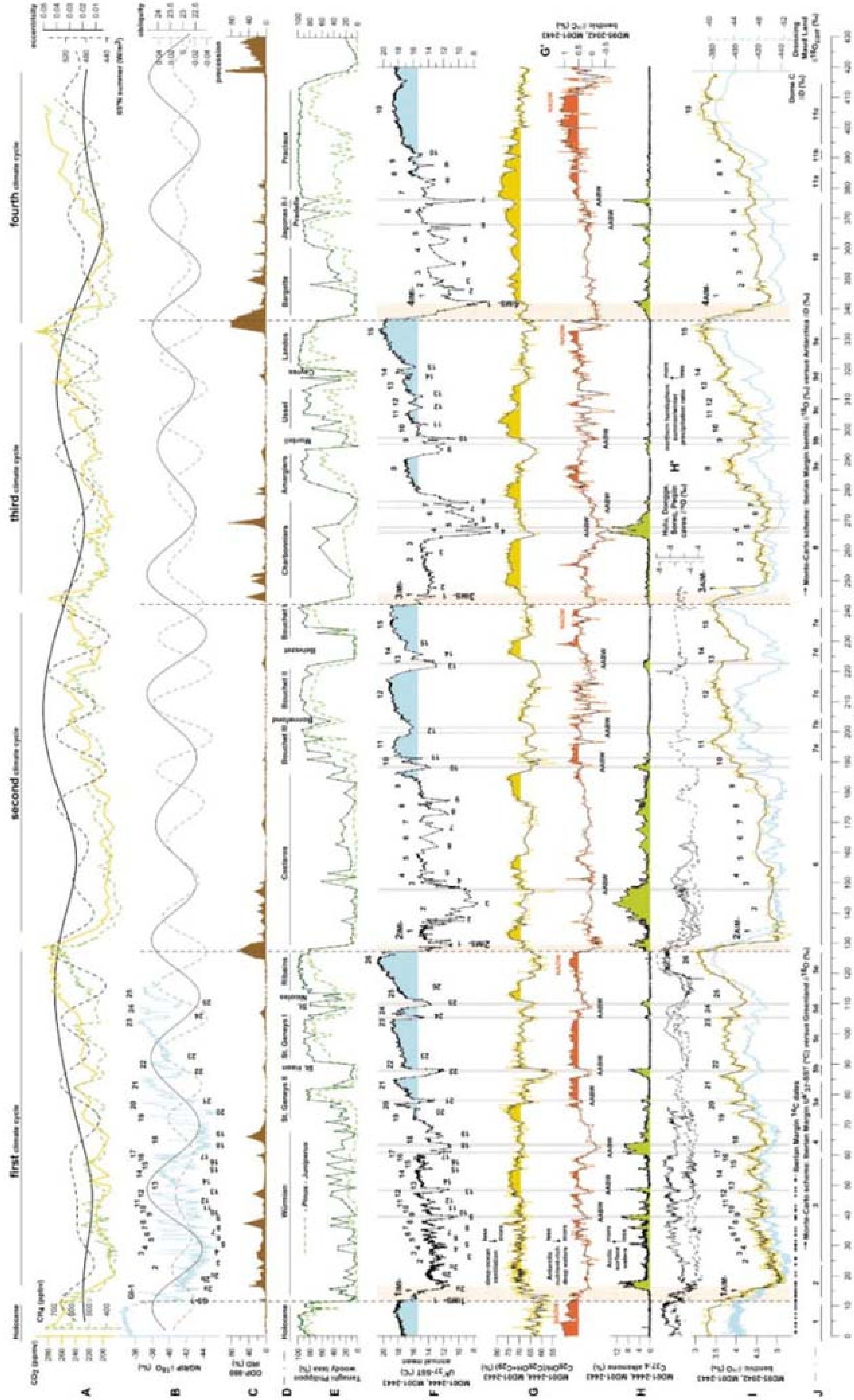
Holocene
first climate cycle
second climate cycle
third climate cycle
fourth climate cycle
age (calendar ky before the present)

Fig. 2. Comparison between the Iberian margin paleoarchive and distance records over the last four interglacial-to-glacial cycles. (**A**) The greenhouse gases CO_2 [solid yellow curve, in parts per million by volume (ppmv)] and CH_4 [dashed green curve, in parts per billion by volume (ppbv)] (*19*, *20*), the eccentricity of the Earth's orbit (solid black curve), and the daily insolation at 65°N during the summer solstice (dashed black curve). These data, along with (**B**) phasing in Earth's obliquity (solid black curve) and precession (dashed gray curve) (*30*) are external triggers of the climate system, although a substantially nonlinear response to these gradual forcings (*31*, *32*) also is evident in the profiles presented here. The North Greenland Ice Core Project (NGRIP) $\delta^{18}O$ profile [per mil (‰)] (*2*) is drawn with the isotopically defined Greenland interstadials (GI) on the top and the subsequent Greenland stadials (GS) on the bottom. (**C**) The ODP-980 relative proportion of detrital lithics ice-rafted debris (IRD) record events when the ice shelves reached a critical extension (*21*). (**D**) The Velay pollen sequence stratigraphy (*23*) applied to (**E**) the Tenaghi Philippon woody taxa; the pollen curve excluding *Pinus* and *Juniperus* is shown by the dashed line, because the ecological requirements of these two genera are not always indicative of temperate climates (*22*). (**F**) $U^{k'}_{37}$-SST in a composite of cores MD01-2444 and MD01-2443 with the IMI on the top and the IMS on the bottom, with the number of the climate cycle to which they belong shown immediately before (values above average are shaded blue). Areas shaded orange show transitions between the climate cycles, and gray areas mark the most prominent bifurcations in climate conditions. (**G**) The relative proportion of *n*-hexacosan-1-ol ($C_{26}OH$) to the sum of *n*-hexacosan-1-ol ($C_{26}OH$) plus *n*-nonacosane (C_{29}) in cores MD01-2444 and MD01-2443 is providing an oxygenation marker of deep sea floor (three-point running average; values above average are shaded orange). (**G'**) Benthic $\delta^{13}C$ in cores MD95-2042 and MD01-2443 [data are from (*7*) and this study; three-point running average)], with alternating influence of NADW (~1 per mil) and AABW (less than 0.5 per mil). (**H**) The percentage of heptatriatetraenone ($C_{37:4}$) to total alkenones is indicative of Arctic surface waters at core locations. (**H'**) $\delta^{18}O$ of stalagmites from Hulu and Dongge caves (solid black curve) and from Soreq and Peqiin caves (dashed black curve) (*6*, *24*, *25*). (**I**) The benthic $\delta^{18}O$ profiles (solid black curve) in cores MD95-2042 and MD01-2443 [data from this study and (*7*, *26*, *27*)] and the Antarctic Dome C δD record (solid blue curve) (*18*) and Dronning Maud Land $\delta^{18}O$ corrected profile (dashed blue curve) (*36*), with a tentative proposal of the Antarctic isotope maxima (AIM) drawn on the top of the benthic profile. Misalignments between the Antarctic ice signal (blue curve) and the Iberian margin benthic record (yellow curve) are due to differences in the age models used, but the resemblance between the signals is unambiguous (Table 1) (*28*). (**J**) Glacial (2 to 4, 6, 8, and 10) and interglacial (1, 5, 7, 9, and 11) marine isotope stages (MISs). It should be emphasized that no ice records from the Northern Hemisphere are available for climate cycles before the last one. Greenland represents the guide for the past 120,000 years (*2*), and Antarctica is the reference for the time preceding that period (*18*). Original data and a comprehensive explanation about age scales are available online (*28*). ky, 1000 years.

number of the climate cycle to which they belong shown immediately before (e.g., 4IMS-7 is the seventh cooling stage of limited duration within the fourth climate cycle). Designation by climate cycles (interglacial followed by a glacial period) is justified on the grounds that attempting rigorous definition of the boundaries of marine isotope stages (MISs) (Fig. 2J) becomes meaningless at the centennial level (*33*).

The climate cycles commence with a rapid warming completing the deglaciation, which lasts just a few centuries (1IMS-1, 1IMS-2a, 2IMS-1, 3IMS-1, and 4IMS-1; Fig. 2F, areas shaded in orange), followed by a gradual cooling over several thousand years, often ending in a final rapid cooling phase. During the initial part of the climate cycles, warm stable periods similar to the Holocene were maintained and oscillations were rare but generally more pronounced than during the ice ages: At least four intense events interrupted the last climate period (1IMS-21, 1IMS-22, 1IMS-24, and 1IMS-25); three severe oscillations punctuated the second cycle (2IMS-11, 2IMS-12, 2IMS-13); just two interrupted the third (3IMS-9 and 3IMS-10); and none occurred during the fourth climate cycle, until sudden entry into a glacial in a single event (4IMS-7).

During fully developed glacials, the frequency of rapid climate variability also differed between climate cycles (Fig. 2F). The Iberian cores register 18 events during the first climate cycle (1IMI and 1IMS events 1 to 18), nine in the second (2IMI and 2IMS events 1 to 9), seven oscillations during the third (3IMI and 3IMS events 1 to 7), and six over the fourth (4IMI and 4IMS events 1 to 6). As a whole, there is a common general trend over the past four climate cycles: Both in variable glacials and in the warm, stable, preceding periods, the pace of climate variability increases as the Pleistocene progresses to the present. The recurring saw-tooth shape of SST fluctuations observed (Fig. 2F) points to a nonlinear threshold behavior of multiple equilibria in the North Atlantic, as referred to in models (*34*, *35*). Whatever mechanisms were responsible, the combination of triggers, amplifiers, and sources of persistence during each climate cycle was never identical, and the abundance, length, and magnitude of the events varied accordingly. For example, the last ice age was characterized by abundant multicentennial shifts, but cold spells were equally or even more severe in the three previous climate cycles (Table 1). The fourth climate cycle was the period with rapid events of the highest amplitude, but with a shorter glacial period.

In this study, we considered different hydrological indicators that permit a better link to other climate archives. First, the relative proportion of tetraunsaturated C_{37} alkenone to total C_{37} alkenones ($C_{37:4}$) is indicative of very cold surface waters at core locations (*16*). Increases in this proxy (Fig. 2H) are in line with weakening of surface Patagonian winds at specific times (*18*) and a decreasing ratio of summer-to-winter precipitation in the eastern Mediterranean and China (*6*, *24*, *25*) (Fig. 2H'). Second, the benthic $\delta^{18}O$ record of cores MD95-2042 (*7*, *8*) and MD01-2443 [see (*26*, *27*) and our data] is consistent with the profiles in Antarctica (*18*, *36*) (Fig. 2I). This correspondence supports the above analogy for the last glacial (*7*–*9*), but our results show that the correlation was maintained over the last four climate cycles. Third, the relative proportion of *n*-hexacosan-1-ol ($C_{26}OH$) to the sum of $C_{26}OH$ plus *n*-nonacosane (C_{29}) is a chemical proxy reflecting oxygenation associated with bottom current intensity, given that both compounds have the same origin (i.e., vascular terrestrial plants) but differed in resistance to degradation by oxygenation of the deep sea floor (*11*) (Fig. 2G). High and low percentages of the $C_{26}OH$ ratio [i.e., $C_{26}OH/(C_{26}OH + C_{29})$] correspond, respectively, to low and high deep-ocean ventilation. Finally, the benthic $\delta^{13}C$ record reflects the influence of both hemispheres (Fig. 2G'). Typical values of North Atlantic deep water (NADW) and Antarctic bottom water (AABW) are about 1.1 and 0.5 per mil, respectively (*37*). This indicator showed depleted values documenting entrances of AABW in the North Atlantic not only during glacials (*9*, *38*), but within the short-term cooling stages of interglacials (*21*). The common trend in changes of SST, $C_{26}OH$ ratio, and benthic $\delta^{13}C$ constitutes a recurring pattern of changes in surface and deep waters measured in the same cores. The observed time sequences of events are therefore independent of the absolute age model of choice (*28*).

Decreases in the $C_{26}OH$ ratio over the deglaciations trace the early arrival of NADW from northern latitudes. During the warmest and largely ice-free portions of the interglacials, the benthic $\delta^{13}C$ record exhibits high values for nutrient-depleted waters arriving from northern locations. Particularly during MIS 1, MIS 5e, and MIS 11c (Fig. 2J), maintenance of low $C_{26}OH$ ratio and high benthic $\delta^{13}C$ indicates conditions of high deep-water ventilation by NADW. For time intervals of 10,000 to 20,000 years after the deglaciation, the relative content of $C_{26}OH$ remained low, whereas benthic $\delta^{13}C$ and $\delta^{18}O$ values stayed high. These climate conditions evolved toward well-defined increases in the $C_{26}OH$ ratio, recording lower oxygenation and a slowdown in the intensity of bottom currents. These periods ended abruptly in harsh drops in SST preceded by steep decreases in both $C_{26}OH$ and benthic $\delta^{13}C$ ratios, indicating a reinvigoration of the deep currents, in this case caused by the inflow of southern-sourced deep waters (AABW). After the swift cold spell within a few centuries, a sharp movement back to warm SST was marked by sudden decreases in

deep water ventilation (increase in C_{26}OH ratio) and a restraint in AABW flow (increase in benthic $\delta^{13}C$).

This pattern was repeatedly observed during numerous prominent SST oscillations over the last climate cycle (1IMS-9, 1IMS-13, 1IMS-18, 1IMS-21, 1IMS-22, 1IMS-24, and 1IMS-25) (Fig. 3). This type of abrupt cooling was also pervasive during the second (2IMS-3, 2IMS-10, 2IMS-12, and 2IMS-13), the third (3IMS-4, 3IMS-5, 3IMS-7, 3IMS-8, 3IMS-9, and 3IMS-10), and the fourth climate cycle (4IMS-6 and 4IMS-7) (Fig. 2, F to I, areas shaded in gray), and it collapsed the entire Mediterranean ecosystem (*16*, *22*) parallel to a massive increase in the size of the northern ice caps (*39*). Vegetational indicators measured along MD01-2443 sediments indicate that the woodland population at the Iberian peninsula was almost nonexistent during some of these intervals, independent of glacial ice (*26*).

During MIS 10, the interhemispheric decoupling was particularly pronounced. Repeated surface temperature shifts occurred at the Iberian margin (4IMI and 4IMS events 1 to 6) and percentages of woody taxa in southern Europe were maintained at high values for almost the entire ice age (up to 78%) (*22*), but the climate variability of southern polar latitudes was almost insignificant (*18*) (Fig. 2, E to I). It is quite likely that each interstadial in northern latitudes had its counterpart in southern latitudes, but the intensity of expression in southern latitudes may vary depending on the power and duration of the event (*34*). This is consistent with the recent observation that, for the last ice age, the duration of the Greenland interstadials is correlated with the warming amplitude in Antarctica (*36*).

The changes observed point to intensification of AABW flow at the Iberian margin preceding the harsh drops in SST that characterize these rapid events (Fig. 3). The results corroborate the North Atlantic determinations of benthic $\delta^{13}C$ (*40*) or $^{231}Pa/^{230}Th$ (*41*), indicating that production of NADW decreased, and in doing so kept pace with the extension of northern polar inland glaciers to the continental shelves; however, this occurred a few centuries before the subsequent generation of icebergs. Climate scenarios that force a change in the ocean circulation with the use of a coupled ocean-atmosphere-sea ice model show that decreases in formation of NADW are capable of triggering large ice surges (*42*).

Computer simulations indicate that the imbalances between northern- and southern-sourced water masses are the primary agent for these abrupt climate oscillations (*43*). Some models propose that the interplay between these two water masses may be driven by changes in AABW (*44*, *45*) and others by NADW (*15*, *46*). However, irrespective of the ultimate origin of these deep water changes, the results presented here show that century-to-millennial variability

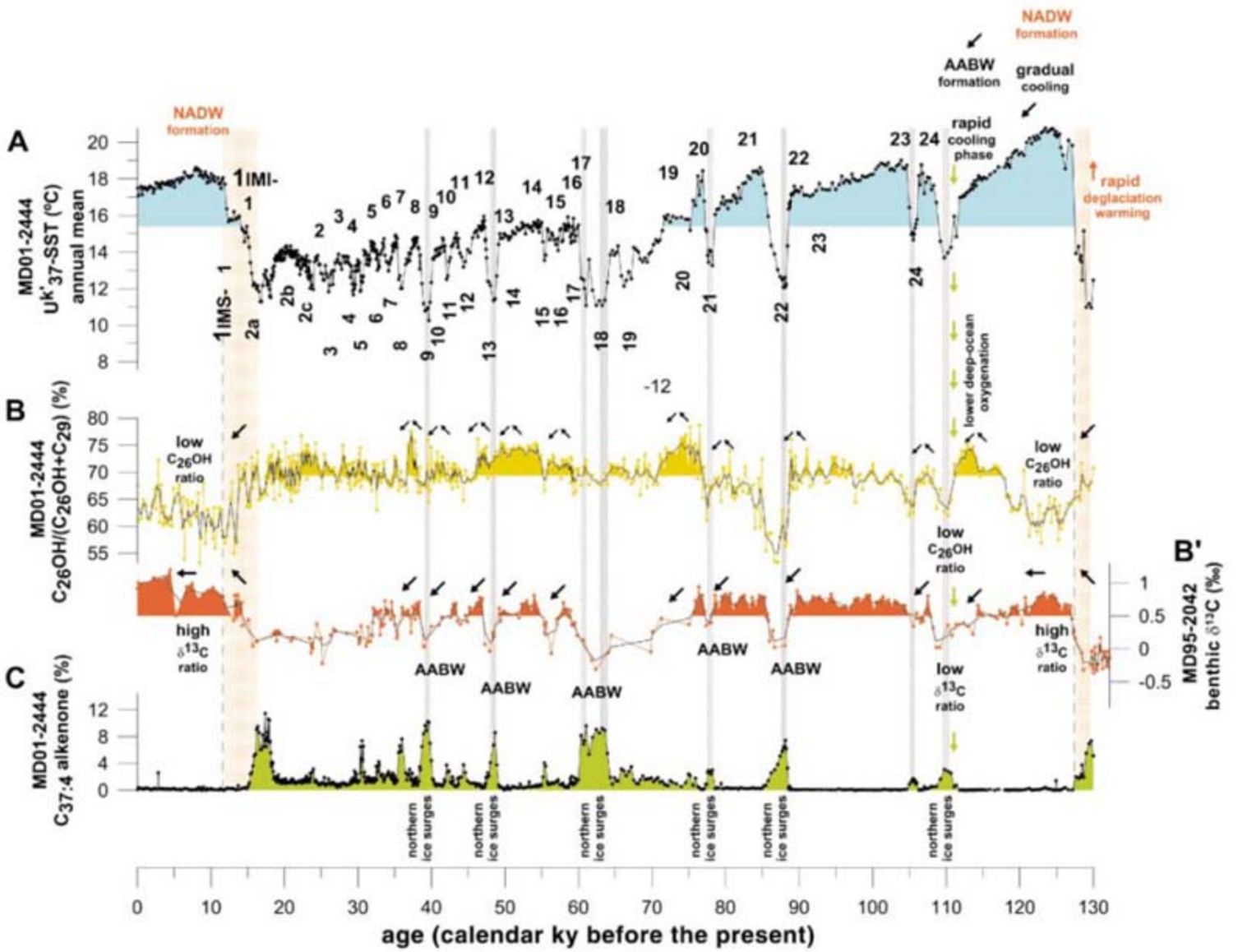

Fig. 3. A more detailed view of the time sequences of events over the last climate cycle. Harsh drops in (**A**) $U^{k'}_{37}$-SST were preceded by steep decreases in both (**B**) C_{26}OH and (**B'**) benthic $\delta^{13}C$ ratios (*7*). Hence, cold episodes after relatively warm and largely ice-free periods occurred when the predominance changed from northern deep waters (NADW) to southern (AABW). These changes occurred a few centuries before the subsequent generation of icebergs, which are traced by increases in (**C**) the percentage of $C_{37:4}$, indicative of very cold surface waters at the Iberian margin (*16*).

characteristic of the last ice age was pervasive during the entire past 420,000 years. In particular, the rapid coolings were preceded by changes in deep waters involving pulses of increasing AABW after retreat of NADW.

The finding that SST shifts become more abundant as climate cycles approach the present calls for a pressing need to understand the mechanisms of rapid climate change. The mean ~1500-year time spacing of the events of the last glacial (*47*) is not observed in previous climate cycles. This is a further indication that a time scale of this nature is not a universal characteristic of the climate system. The marked melting of the ice armadas similar to those reported over the last glacial period can no longer be uniquely associated to the cause of abrupt climate change, given that changes occurred even after relatively warm and largely ice-free periods (e.g., 11MS-21, 11MS-22, 31MS-10, and others; Fig. 2F). Although more continuous freshwater discharge may not leave a notable trace in the marine sediments, it may effectively trigger the gradual deterioration of climate by slowly pushing the ocean circulation in the North Atlantic toward a threshold (*48*).

References and Notes

1. T. Blunier, E. J. Brook, *Science* **291**, 109 (2001).
2. North Greenland Ice Core Project members, *Nature* **431**, 147 (2004).
3. G. C. Bond *et al.*, *Nature* **365**, 143 (1993).
4. S. L. Kanfoush *et al.*, *Science* **288**, 1815 (2000).
5. J. R. M. Allen *et al.*, *Nature* **400**, 740 (1999).
6. Y. J. Wang *et al.*, *Science* **294**, 2345 (2001).
7. N. J. Shackleton, M. A. Hall, E. Vincent, *Paleoceanography* **15**, 565 (2000).
8. N. J. Shackleton, R. G. Fairbanks, T. Chiu, F. Parrenin, *Quat. Sci. Rev.* **23**, 1513 (2004); correction: N. J. Shackleton, *Geophys. Res. Abstr.* **7**, 1607-7962/gra/EGU05-A-05213 (2005).
9. L. C. Skinner, H. Elderfield, *Paleoceanography* **22**, PA1205 (2007).
10. I. Cacho *et al.*, *Paleoceanography* **14**, 698 (1999).
11. I. Cacho, J. O. Grimalt, F. J. Sierro, N. J. Shackleton, M. Canals, *Earth Planet. Sci. Lett.* **183**, 417 (2000).
12. D. Pailler, E. Bard, *Palaeogeogr. Palaeoclimatol. Palaeoecol.* **181**, 431 (2002).
13. E. Bard, F. Rostek, G. Ménot-Combes, *Quat. Res.* **61**, 204 (2004).
14. R. B. Alley *et al.*, *Science* **299**, 2005 (2003).
15. T. F. Stocker, S. J. Johnsen, *Paleoceanography* **18**, PA1087 (2003); correction: T. F. Stocker, S. J. Johnsen, *Paleoceanography* **20**, PA1002 (2005).
16. B. Martrat *et al.*, *Science* **306**, 1762 (2004).
17. K. Pahnke, R. Zahn, *Science* **307**, 1741 (2005).
18. EPICA community members, *Nature* **429**, 623 (2004).
19. M. Delmotte *et al.*, *J. Geophys. Res.* **109**, D12104 (2004).
20. U. Siegenthaler *et al.*, *Science* **310**, 1313 (2005).
21. J. F. McManus, D. W. Oppo, J. L. Cullen, *Science* **283**, 971 (1999).
22. P. C. Tzedakis, J. F. McManus, H. Hooghiemstra, D. W. Oppo, T. A. Wijmstra, *Earth Planet. Sci. Lett.* **212**, 197 (2003).
23. R. Cheddadi *et al.*, *Proc. Natl. Acad. Sci. U.S.A.* **102**, 13939 (2005).
24. M. Bar-Matthews, A. Ayalon, M. Gilmour, A. Matthews, C. J. Hawkesworth, *Geochim. Cosmochim. Acta* **67**, 3181 (2003).
25. D. Yuan *et al.*, *Science* **304**, 575 (2004).
26. P. C. Tzedakis, K. H. Roucoux, L. de Abreu, N. J. Shackleton, *Science* **306**, 2231 (2004).
27. L. de Abreu *et al.*, *Paleoceanography* **20**, PA3009 (2005).
28. Materials and methods are available as supporting material on *Science* Online.
29. G. Mollenhauer *et al.*, *Paleoceanography* **20**, PA1016 (2005).
30. A. L. Berger, *J. Atmos. Sci.* **35**, 2362 (1978).
31. F. Parrenin, D. Paillard, *Earth Planet. Sci. Lett.* **214**, 243 (2003).
32. P. Huybers, W. B. Curry, *Nature* **441**, 329 (2006).
33. L. C. Skinner, N. J. Shackleton, *Quat. Sci. Rev.* **24**, 571 (2005).
34. T. F. Stocker, O. Marchal, *Proc. Natl. Acad. Sci. U.S.A.* **97**, 1362 (2000).
35. M. Siddall *et al.*, *Quat. Sci. Rev.* **25**, 3185 (2006).
36. EPICA community members, *Nature* **444**, 195 (2006).
37. J. F. Adkins, A. P. Ingersoll, C. Pasquero, *Quat. Sci. Rev.* **24**, 581 (2005).
38. J. C. Duplessy *et al.*, *Paleoceanography* **3**, 343 (1988).
39. J. Mangerud *et al.*, *Quat. Sci. Rev.* **23**, 1313 (2004).
40. R. Zahn *et al.*, *Paleoceanography* **12**, 696 (1997).
41. J. F. McManus, R. François, J. M. Gherardi, L. D. Keigwin, S. Brown-Leger, *Nature* **428**, 834 (2004).
42. J. Flückiger, R. Knutti, J. W. C. White, *Paleoceanography* **21**, PA2014 (2006).
43. T. F. Stocker, D. G. Wright, W. S. Broecker, *Paleoceanography* **7**, 529 (1992).
44. J. R. Toggweiler, B. Samuels, *Deep-Sea Res.* **42**, 477 (1995).
45. G. Knorr, G. Lohmann, *Nature* **424**, 532 (2003).
46. R. Knutti, J. Flückiger, T. F. Stocker, A. Timmermann, *Nature* **430**, 851 (2004).
47. G. C. Bond *et al.*, *Science* **278**, 1257 (1997).
48. T. F. Stocker, D. G. Wright, *Nature* **351**, 729 (1991).

49. We thank P. C. Tzedakis for pollen data from Tenaghi Philippon and MD01-2443; J. Schwander for providing the Monte-Carlo wiggle-matching program; J. F. McManus for data of core ODP-980; G. C. Bond for data of core DSDP-609; E. Bard and I. Cacho for biomarker data of cores MD95-2042 and MD95-2043, respectively; North Greenland Ice Core Project members and European Project for Ice Coring in Antarctica (EPICA) community members for data of ice cores; D. Amblas for Fig. 1.; B. H. Oldham for editing the text; I. N. McCave for locating the coring sites; M. A. Hall, B. Luengo, and R. Mas for laboratory assistance; and L. C. Skinner, J. Villanueva, and W. H. Berger for providing useful comments. B.M. thanks the grant I3P-BPG2005 from the Itinerario Integrado de Inserción profesional program of the Spanish National Research Council (CSIC), and L.A. thanks the Portuguese Foundation for Science and Technology (SFRH/BPD/1588/2000). We thank the British ocean sediment core repository (BOSCOR); the International Marine Global Change Studies program (IMAGES), and the Bremen core repository [Ocean Drilling program (ODP)] for supplying sediment samples. This work was supported by the Pole-Ocean-Pole (EVK2-2000-00089) and Patterns of Climate Variability in the North Atlantic (EVR1-2002-000413) projects funded by the European Union.

Supporting Online Material

www.sciencemag.org/cgi/content/full/1139994/DC1
Materials and Methods
Fig. S1
References
Original Data File

16 January 2007; accepted 4 June 2007
Published online 14 June 2007;
10.1126/science.1139994
Include this information when citing this paper.

Ethylene Modulates Stem Cell Division in the *Arabidopsis thaliana* Root

Olga Ortega-Martínez,*† Monica Pernas,*‡ Rachel J. Carol, Liam Dolan§

The construction of multicellular organisms depends on stem cells—cells that can both regenerate and produce daughter cells that undergo differentiation. Here, we show that the gaseous messenger ethylene modulates cell division in the cells of the quiescent center, which act as a source of stem cells in the seedling root. The cells formed through these ethylene-induced divisions express quiescent center-specific genes and can repress differentiation of surrounding initial cells, showing that quiescence is not required for these cells to signal to adjacent stem cells. We propose that ethylene is part of a signaling pathway that modulates cell division in the quiescent center in the stem cell niche during the postembryonic development of the root system.

The bodies of multicellular land plants are derived from populations of dividing cells called meristems, which contain stem cells. Clonal analysis revealed that the ultimate source of cells in the *Arabidopsis thaliana* root meristem is the quiescent center (QC), a group of four cells that divides infrequently and can give rise to cells in all tissue systems of the root (*1*). The QC cells are surrounded by initials that divide to regenerate themselves and produce cells that contribute to the root body and have also been considered to be stem cells (*2*, *3*). Because initials can be replaced by QC cells, the former may be considered to be short-term stem cells, whereas the latter are long-term stem cells. QC cells produce signals that promote division of the abutting initial cells and repress initial cell terminal differentiation (*4*). Together, the QC cells and the surrounding initial cells constitute a stem cell niche (*5*, *6*).

To identify genes that control cell proliferation in the stem cell niche, we screened our collection of root mutants for plants with defective QC cellular organization resulting from deregulated QC cell division. We identified two mutants, E6263 and E4510, in which the cells of the QC divide (Fig. 1, B to F). In the E6263 mutant

Department of Cell and Developmental Biology, John Innes Centre, Norwich NR4 7UH, UK.

*These authors contributed equally to this work.
†Present address: Kristineberg Marine Research Station, Kristineberg 566, 450 34 Fiskebäckskil, Sweden.
‡École Pratique des Hautes Études, 46 rue de Lille, 75007 Paris, France.
§To whom correspondence should be addressed. E-mail: liam.dolan@bbsrc.ac.uk

shown in Fig. 1F, one of the QC cells has divided transversely, resulting in a three-celled QC when viewed in longitudinal section. We determined the time course of the onset of the mutant QC phenotype by quantifying cell divisions for 12 days after germination. QC organization is identical in both wild type and mutants (E6263, E4510) at 2 days. By 4 days after germination, 96% of mutant roots have undergone QC divisions, whereas none was observed in wild type ($n = 21$) (Fig. 1, E and F). By 8 and 12 days, QC divisions had occurred in all mutant plants examined ($n > 20$) (Fig. 1, G to J). Thus, the gene that is defective in the E6263 and E4510 mutants is required normally to repress division in the QC during wild-type development and is usually active during or soon after germination.

We determined by positional cloning that the defective gene in these mutants is At3g51770 (fig. S1). At3g51770 encodes ETHYLENE OVERPRODUCER1 (ETO1), and plants homozygous for loss-of-function *eto1* mutations produce excessive amounts of ethylene (*7*, *8*). ETO1/At3g51770 is a ubiquitin E3 ligase that controls the rates of ethylene synthesis by modulating the levels of aminocyclopropane carboxylic acid synthase 5 (ACS5), a protein that catalyzes the rate-limiting step in ethylene biosynthesis (*8*). *ETO1* is expressed throughout the plant (fig. S1). Mutations in E6263 (hereafter *eto1-11*) and E4510 (hereafter *eto1-12*) result in G→E and G→R at amino acid positions 457 and 786, respectively. Moreover, crosses between plants that are homozygous for the recessive *eto1-11* mutation and the previously characterized recessive *eto1-1* mutation produce mutant F1 offspring with deregulated QC cell divisions, which indicates that mutation of the *ETO1* gene is responsible for the observed QC phenotype.

Our data suggest that ethylene promotes cell division in the QC. An alternative hypothesis is that ETO1 E3-ligase controls QC division by regulating the degradation of other proteins that play no role in ethylene biosynthesis. To distinguish between these alternatives, we determined whether QC division could be controlled by experimentally manipulating ethylene biosynthesis or signaling. If the QC phenotype of *eto1* mutants were the result of ethylene overproduction, the inhibition of ethylene biosynthesis by 2-aminoethoxyvinyl glycine (AVG) should suppress the supernumerary divisions in the QC of the *eto1* mutant. We observed no extra QC cell division in *eto1* mutants grown in media supplemented with 0.5 μM AVG (Fig. 2, A to C). Similarly, if supernumerary cell divisions in the QC of *eto1* mutants were ethylene dependent, it should be possible to phenocopy *eto1* by exposing wild-type plants to ethylene. Growing wild-type plants in the presence of ethylene precursor 1-amino-1-cyclopropane carboxylic acid (ACC) (50 μM) induces QC cell division (Fig. 2D). Furthermore, the *eto2* mutant carries a dominant mutation in an ACC synthase (ACS) gene that results in the overproduction of ethylene (*9*, *10*). In these mutants, the QC cells also undergo supernumerary cell divisions, as they do in *eto1* mutants (Fig. 2E). These data support the conclusion that the overproduction of ethylene is responsible for the supernumerary divisions that occur in the QC divisions in *eto1* roots.

To further verify that ethylene promotes QC cell division, we determined the QC phenotype of plants with defective ethylene signaling. The CONSTITUTIVE TRIPLE RESPONSE1 (CTR1) protein is a negative regulator of the ethylene signal transduction cascade, and loss-of-function mutations in the *CTR1* gene results in constitutive activation of ethylene signaling (*9*). If ethylene were responsible for the stimulation of QC division in the *eto1* mutant, we predict that QC cells should also divide frequently in the *ctr1* mutant. An increased frequency of cell divisions in the QC of *ctr1* mutants results in a cellular organization that is indistinguishable from that observed in *eto1* mutants (Fig. 2, B and F).

We quantified the numbers of extra QC cell divisions induced by ethylene by quantifying the number of QC cells in medial longitudinal sections of roots. Although such numbers underestimate the exact numbers of cell divisions, they allow comparison of the numbers of cell divisions induced in the QC in these different backgrounds and treatments. Treatment of wild-type seedlings with ACC increased the number of extra cells from 0.022 ± 0.003 (SD) to 1.25 ± 0.05 (SD). Similarly, *eto1* [1.35 ± 0.025 (SD)] and *ctr1* [1.50 ± 0.001 (SD)] mutants had more QC cell divisions than wild type [0.022 ± 0.003 (SD)]. These increases correspond to an average of at least one extra cell division per 4-day-old seedling ($n = 50$). These genetic and pharmacological data indicate that ethylene promotes the division of cells in the QC.

To determine the identity of the cells that result from the ethylene-induced division of the QC, we determined the expression of a number of QC-expressed genes in *eto1* mutants and in wild-type plants treated with 50 μM ACC. The QC25 enhancer trap gene is expressed in QC cells of untreated wild-type roots (*11*) (Fig. 3, G and I). Wild-type roots treated with ACC express the QC25 enhancer trap in the supernumerary cells that result from QC division, indicating that the new cells have QC identity (Fig. 3, H and J). SCR is a transcription factor that accumulates

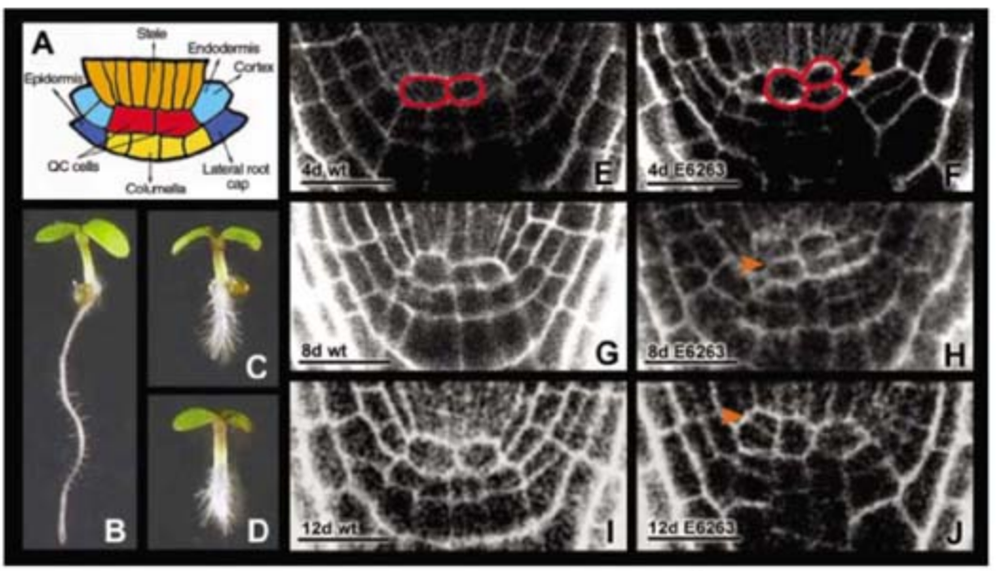

Fig. 1. Identification of mutants in which the QC cells divide. (**A**) Wild-type stem cell niche organization (schematic). (**B**) Wild-type, (**C**) E6263, and (**D**) E4510 root morphologies. Cellular organization of the stem cell niche region (a pair of cells in longitudinal section) in (**E**) 4-day-old, (**G**) 8-day-old, and (**I**) 12-day-old wild-type roots, as revealed by propidium iodide staining. Red lines show the outline of the two QC cells that are visible. Cellular organization in (**F**) 4-day-old, (**H**) 8-day-old, and (**J**) 12-day-old E6263 mutant roots showing supernumerary divisions in the QC (red arrowheads). Scale bars, 25 μm.

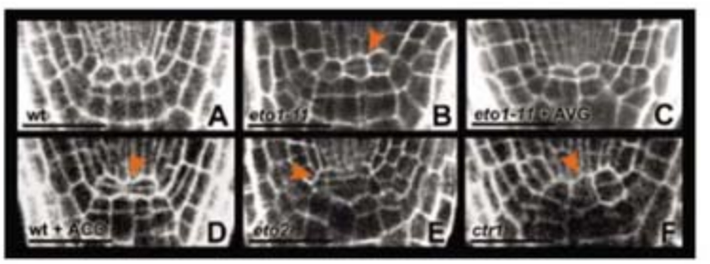

Fig. 2. Ethylene promotes QC cell division. Stem cell niche organization of (**A**) wild-type, (**B**) *eto1-11* mutant, (**C**) *eto1-11* treated with AVG (0.5 μM), (**D**) wild-type treated with ACC (50 μM), (**E**) *eto2* mutant, and (**F**) *ctr1* mutant roots. Red arrowheads, extra cell division in the QC. Scale bars, 50 μm.

in the QC and is required for its development (*12*, *13*) (Fig. 3A). In the *eto1* mutant and in wild-type roots treated with ACC, *SCR* is expressed in cells derived from QC division, which confirms their QC identity (Fig. 3, B and C). Furthermore, we examined the expression of the enhancer trap J0571, which is expressed in the QC of wild type (Fig. 3 D). J0571 is expressed in the QC cells and their derivatives in wild-type plants treated with ACC and in *eto1* mutants, indicating that the cells that form as a result of QC division have QC identity (Fig. 3, E and F). Together these data indicate that, although QC division is controlled by ethylene, the identity of these cells is unaffected by this hormone.

To test whether the extra cells that form in *eto1* mutants function as QC cells, we determined whether they negatively regulated differentiation in the surrounding initial cells (*3*). Ablation of QC cells in wild-type roots results in the precocious differentiation of columella initials, which can be monitored by lugol staining of the starch grains present in columella cells but not columella initials (*3*, *14*). We stained both *eto1* and wild-type roots grown in the presence of ethylene with lugol and found a single layer of unstained cells below the supernumerary cells in the *eto1* and ethylene-treated roots (Fig. 3, H and J). Therefore, the supernumerary cells produced in the QC of *eto1* mutants display both QC identity and QC function.

Because high levels of ethylene induce cell divisions of the QC, we hypothesized that cell division would be repressed in plants that produce less ethylene than wild type and in plants that are ethylene insensitive. The extra divisions that occur in *eto1* mutant roots result in the formation of more columella layers [6.09 ± 0.06 (SD)] than wild type [5.0 ± 0.06 (SD)] (fig. S2). Therefore, we used cell layer number in the columella as a proxy measure of cell division activity in the QC. Plants overexpressing *ETO1* (*CaMV35S::ETO1*) produce less ethylene and have fewer layers [4.16 ± 0.11 (SD)] (Fig. 4C) than wild type (Fig. 4A) (*8*). Similarly, wild-type plants grown in the presence of AVG develop fewer columella layers [3.8 ± 0.11 (SD)] (Fig. 4B). *ethylene insensitive2* (*ein2*) mutant plants insensitive to ethylene because they have a block in ethylene signal transduction also developed fewer cell layers than wild type (*7*, *15*) (Fig. 4D). Together, these data support the conclusion that cell division in cells of the QC is regulated by ethylene.

Auxin regulates the development of the stem cells in the *A. thaliana* root, and ethylene and auxin interact to control developmental processes (*16*–*18*). Therefore, it is possible that the ethylene-induced QC cell divisions observed in *eto1* mutants or in ethylene-treated wild-type roots result from the activation of an auxin-dependent cell division pathway in the QC. No extra divisions were observed in the QC cells of wild-type seedlings that were treated with 0.1 μM of naphthaleneacetic acid compared with untreated controls (fig. S3, E and J). This suggests that auxin itself is not sufficient to induce cell division in the QC of seedling roots. (Further supporting evidence is presented in fig. S3, A to I.)

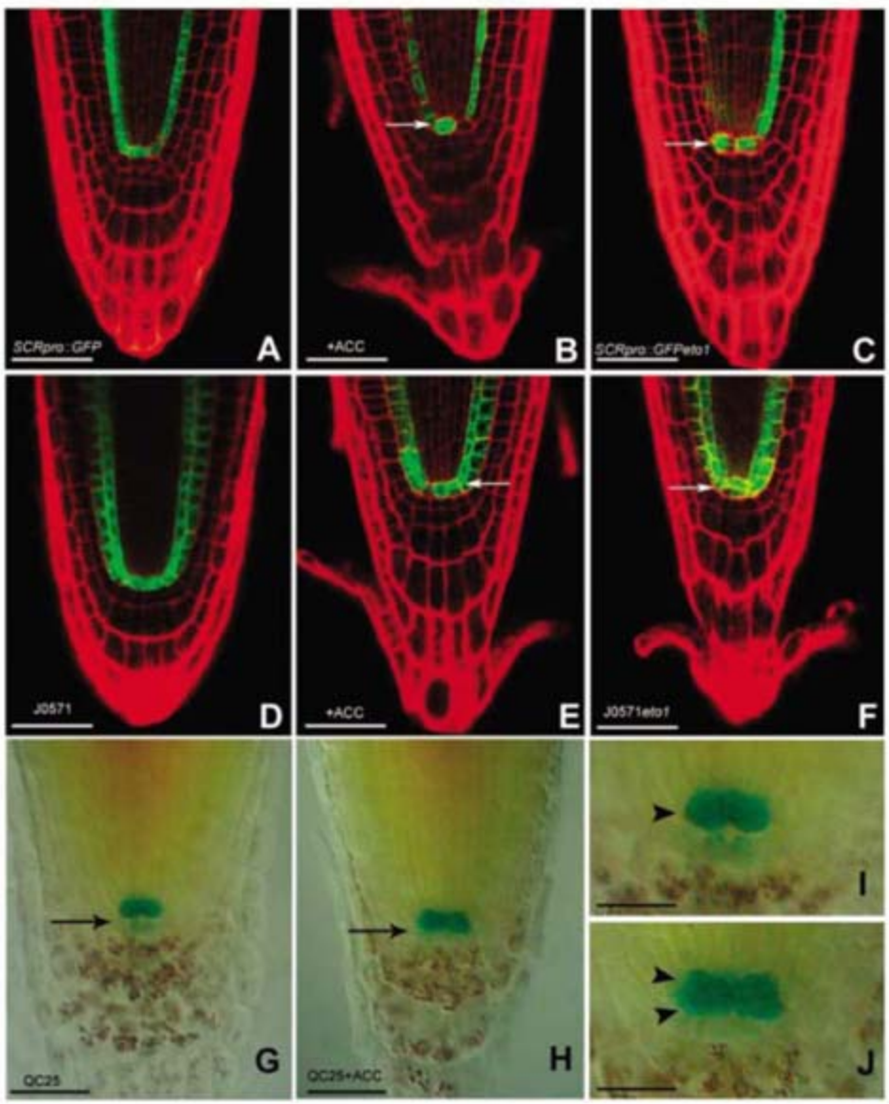

Fig. 3. QC cell identity and function are maintained in *eto1* mutants. *SCRpro::GFP* expression is present in (**A**) the QC cells of wild type, (**B**) the new cells derived from the extra divisions (white arrow) in the QC of ACC-treated wild type, and (**C**) *eto1-11* mutant. The enhancer trap J0571 is expressed in (**D**) the QC cells in wild-type, (**E**) the extra QC cells that develop in wild-type roots treated with ACC (50 μM), and (**F**) *eto1-11* mutant. The QC-25 marker line expresses β-glucuronidase (GUS) activity (blue) in the QC, and lugol staining marks the differentiated columella cells. (**G** and **I**) In wild type, there is a single nonstaining layer of initials (arrow) between the QC and the columella. (I) is a higher-magnification view of (G). (**H** and **J**) The presence of functioning initials is revealed by the absence of lugol staining (arrow) in wild type treated with ACC (50 μM), where there is an increase in the number of blue-stained QC cells (arrowheads). (J) is a higher-magnification view of (H). Scale bars, 50 μm [(G) and (H)], 25 μm [(I) and (J)].

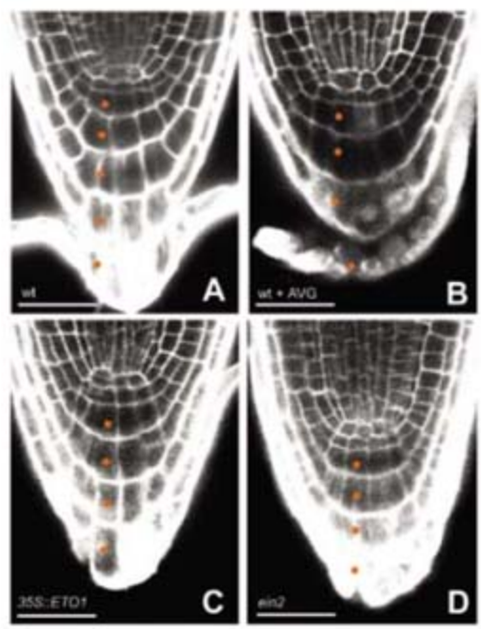

Fig. 4. Ethylene stimulates cell division leading to the formation of additional columella cell layers. (**A**) Phenotype of wild-type root. There is a decrease in the number of columella layers (red dots) in (**B**) wild-type roots that have been treated with AVG, (**C**) plants harboring *35S::ETO1*, and (**D**) *ein2* mutants. Scale bars, 50 μm.

We have shown that ethylene determines the balance between proliferation and quiescence of stem cells in the root. Our data also indicate that mitotic quiescence is not required for the cell-to-cell signaling function carried out by these cells during the root development. Given the role that ethylene plays in the perception and transmission of environmental cues, it is likely that this hormone impacts on aspects of post-embryonic development that are regulated by both endogenous developmental and exogenous environmental signals. This ethylene-mediated integration of endogenous and exogenous signals to control QC division is an attractive molecular framework that explains how the environment modulates stem cell division and activity during the postembryonic stage of the plant life cycle.

References and Notes

1. C. Kidner, V. Sundaresan, K. Roberts, L. Dolan, *Planta* **211**, 191 (2000).
2. M. Wildwater *et al.*, *Cell* **123**, 1337 (2005).
3. C. van den Berg, V. Willemsen, G. Hendriks, P. Weisbeek, B. Scheres, *Nature* **390**, 287 (1997).
4. I. Blilou *et al.*, *Nature* **433**, 39 (2005).
5. J. Xu, B. Scheres, *Plant Cell* **17**, 525 (2005).
6. T. Xie, A. C. Spradling, *Science* **290**, 328 (2000).
7. P. Guzman, J. R. Ecker, *Plant Cell* **2**, 513 (1990).
8. K. L. Wang, H. Yoshida, C. Lurin, J. R. Ecker, *Nature* **428**, 945 (2004).
9. J. J. Kieber, M. Rothenberg, G. Roman, K. A. Feldmann, J. R. Ecker, *Cell* **72**, 427 (1993).
10. H. S. Chae, F. Faure, J. J. Kieber, *Plant Cell* **15**, 545 (2003).
11. M. Aida *et al.*, *Cell* **119**, 109 (2004).
12. L. Di Laurenzio *et al.*, *Cell* **86**, 423 (1996).
13. R. Heidstra, D. Welch, B. Scheres, *Genes Dev.* **18**, 1964 (2004).
14. C. van den Berg, P. Weisbeek, B. Scheres, *Planta* **205**, 483 (1998).
15. J. M. Alonso, T. Hirayama, G. Roman, S. Nourizadeh, J. R. Ecker, *Science* **284**, 2148 (1999).
16. P. M. Chilley *et al.*, *Plant Cell* **18**, 3058 (2006).
17. A. N. Stepanova *et al.*, *Plant Cell* **17**, 2230 (2005).
18. A. Rahman *et al.*, *Plant Physiol.* **130**, 1908 (2002).

19. O.O.M. was supported by a John Innes Foundation studentship. M. Pernas was supported by a postdoctoral fellowship from the Spanish Ministerio de Educacion y Ciencia. R.J.C. and L.D. were supported by the U.K. Biotechnology and Biological Sciences Research Council. We thank J. Ecker and K. Wang (Salk Institute) for providing *eto1*, *eto2*, *eto3*, *ein2*, *ctr1*, and *CaMV::35S ETO1* lines. We thank J. Haseloff, B. Scheres, and P. Benfey for providing lines and P. Linstead for support.

Supporting Online Material

www.sciencemag.org/cgi/content/full/317/5837/507/DC1
Materials and Methods
Figs. S1 to S3
References

4 April 2007; accepted 20 June 2007
10.1126/science.1143409

Crystal Structure of Inhibitor-Bound Human 5-Lipoxygenase–Activating Protein

Andrew D. Ferguson,[1]* Brian M. McKeever,[1,5]* Shihua Xu,[1] Douglas Wisniewski,[2] Douglas K. Miller,[3,6] Ting-Ting Yamin,[3] Robert H. Spencer,[4,7] Lin Chu,[1] Feroze Ujjainwalla,[1] Barry R. Cunningham,[2] Jilly F. Evans,[3,8] Joseph W. Becker[1]†

Leukotrienes are proinflammatory products of arachidonic acid oxidation by 5-lipoxygenase that have been shown to be involved in respiratory and cardiovascular diseases. The integral membrane protein FLAP is essential for leukotriene biosynthesis. We describe the x-ray crystal structures of human FLAP in complex with two leukotriene biosynthesis inhibitors at 4.0 and 4.2 angstrom resolution, respectively. The structures show that inhibitors bind in membrane-embedded pockets of FLAP, which suggests how these inhibitors prevent arachidonic acid from binding to FLAP and subsequently being transferred to 5-lipoxygenase, thereby preventing leukotriene biosynthesis. This structural information provides a platform for the development of therapeutics for respiratory and cardiovascular diseases.

Leukotrienes are lipid mediators of inflammation that are involved in the pathogenesis of respiratory and cardiovascular diseases (*1*, *2*). Cellular activation by immune complexes and other inflammatory stimuli results in an increase of intracellular calcium and the translocation of cytosolic phospholipase A_2 ($cPLA_2$) and 5-lipoxygenase (5-LO) from the cytosol to the nuclear membrane (*3*). In the presence of the 5-lipoxygenase–activating protein (FLAP), arachidonic acid (AA) released from the nuclear membrane by $cPLA_2$ is delivered to 5-LO for conversion to 5-(S)-hydroperoxy-6,8,11,14-eicosatetraenoic acid (5-HpETE) and then leukotriene A_4 (LTA_4) (*4*). Membrane interaction of 5-LO with FLAP is essential for leukotriene biosynthesis (*3*–*5*). FLAP is an integral membrane protein that belongs to the MAPEG (membrane-associated proteins in eicosanoid and glutathione metabolism) superfamily (*6*–*8*). In contrast to other MAPEGs, FLAP has not been shown to have enzymatic activity or to be functionally modulated by glutathione.

The FLAP inhibitor MK-591 inhibits cellular biosynthesis of the neutrophil activator leukotriene B_4 (LTB_4) and the bronchoconstrictive and vasoactive leukotrienes C_4, D_4, and E_4 (LTC_4, LTD_4, and LTE_4, collectively known as cysteinyl leukotrienes) and has been shown to be efficacious in allergen challenge and chronic asthma clinical trials (*9*, *10*). FLAP inhibitors have also been shown to be protective in acute and chronic animal cardiovascular models, and human polymorphisms have been linked to increased risk of myocardial infraction and stroke (*1*, *11*). These studies suggest that, in addition to their therapeutic benefit in respiratory disease, FLAP inhibitors will have an important future role in the prevention and treatment of cardiovascular disease (*1*, *10*, *11*).

FLAP was discovered because it binds MK-886, a leukotriene biosynthesis inhibitor that prevents the binding of AA to FLAP in a concentration-dependent manner (*12*) and that also blocks the association of FLAP with 5-LO at higher concentrations (*13*, *14*). FLAP functions both as a membrane anchor for 5-LO (*3*) and as an AA-binding protein (*12*). How FLAP activates 5-LO is not understood, but it involves a physical interaction between FLAP and 5-LO (*15*). To understand FLAP's role in leukotriene production and how inhibitors regulate its function, we determined the x-ray crystal structure of FLAP in complex with two leukotriene biosynthesis inhibitors.

The crystal structures of FLAP in complex with MK-591 and an iodinated analog of MK-591 (Fig. 1, A and B) (*10*, *13*) were determined at 4.0 Å and 4.2 Å resolution (figs. S1 to S5 and table S1). FLAP contains four transmembrane helices (α1 to α4) that are connected by two elongated cytosolic loops (C1 and C2) and one short lumenal loop (L1) (Fig. 1, C and D). The orientations of the cytosolic and lumenal loops of FLAP are consistent with previous studies on MAPEGs (*16*–*18*). Lumenal helix αL (residues 3 to 8) precedes helix α1 (residues 10 to 37) and is linked to helix α1 by a single residue at the lower leaflet of the membrane (Fig. 1C). Cytosolic loop C1 (residues 38 to 47) connects the first helix to the second (residues 48 to 77), and both protrude from the upper leaflet of the membrane. Helix α2 has a distinctive bend at residue P65 at the midpoint of the membrane. Loop L1 (residues 78 to 80) connects the second to the third helix (residues 81 to 101) which

[1]Department of Medicinal Chemistry, Merck Research Laboratories, Rahway, NJ 07065, USA. [2]Department of Infectious Diseases, Merck Research Laboratories, Rahway, NJ 07065, USA. [3]Department of Cardiovascular Diseases, Merck Research Laboratories, Rahway, NJ 07065, USA. [4]Department of Pain Research, Merck Research Laboratories, West Point, PA 19486, USA. [5]Vitae Pharmaceuticals, Fort Washington, PA 19034, USA. [6]Wyeth Research, Collegeville, PA 19426, USA. [7]Cara Therapeutics, Tarrytown, NY 10591, USA. [8]Amira Pharmaceuticals, San Diego, CA 92121, USA.

*These authors contributed equally to this work.
†To whom correspondence should be addressed. E-mail: joseph_becker@merck.com

is perpendicular to the plane of the bilayer. Loop C2 (residues 102 to 115) connects the third helix to the fourth (residues 116 to 138). Helix α4 begins in the middle of the membrane and continues into the lumen. The C terminus of FLAP is largely disordered beyond residue G140. This region is highly conserved among other FLAP proteins but not in other MAPEGs, suggesting that it may have a role in the biological activity of FLAP. Analysis of sequence similarity indicates that the secondary structure of FLAP is probably shared among other MAPEGs, but FLAP does not display significant structural homology with other protein containing transmembrane helical bundles. Structural comparisons between human FLAP and rat microsomal glutathione *S*-transferase–1 (mGST-1) produces a root mean square deviation of 3.1 Å for 107 aligned residues (fig. S2, A to C). The proposed glutathione binding site in rat microsomal glutathione transferase 1 (*19*) is not conserved in FLAP, and there is no electron density in that region of the molecule, consistent with the lack of evidence that FLAP is modulated by glutathione.

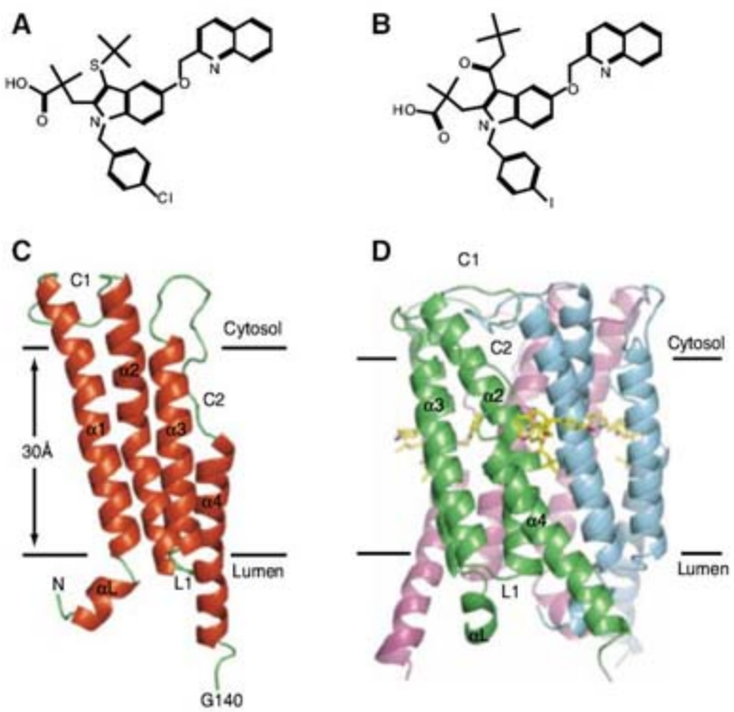

Fig. 1. (**A**) Chemical structures of MK-591 and (**B**) an iodinated analog of MK-591. (**C**) The FLAP monomer viewed parallel to the nuclear membrane with red helices and green loops. The unstructured C terminus of FLAP (residues 141 to 161) extends beyond G140. (**D**) The FLAP trimer with monomers colored green, cyan, and magenta. The view is given parallel to the nuclear membrane. Bound inhibitor molecules are shown as stick models with yellow carbon atoms, blue nitrogen atoms, red oxygen atoms, and purple iodine atoms.

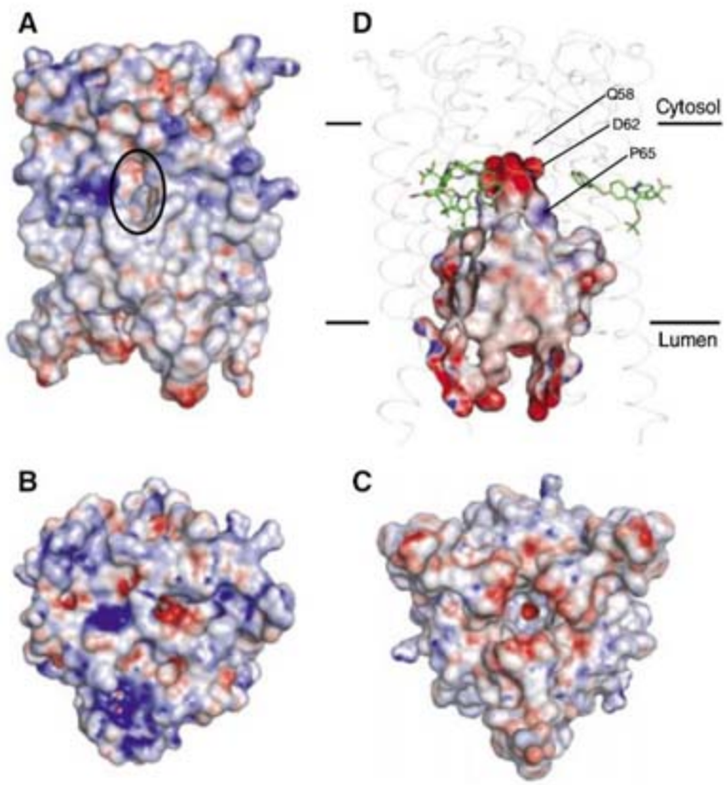

Fig. 2. Electrostatic surface of FLAP. The view is given (**A**) parallel to the nuclear membrane, (**B**) from the cytosol, and (**C**) from the lumen. One of the three surface grooves has been circled. The cytosolic and lumenal ends of the trimer are positively charged and negatively charged, respectively. (**D**) Central pocket of FLAP as calculated by CASTp (Computed Atlas of Surface Topography of proteins) (*28*). Bound inhibitor molecules are shown as stick models with green carbon atoms, blue nitrogen atoms, red oxygen atoms, and purple iodine atoms, and the trimer is shown as a white coil. The front of this pocket has been removed for clarity. The lumenal entrance to this pocket is formed by negatively charged helices. The negatively charged constriction within the membrane is formed by residues Q58 and D62. The surfaces are colored by electrostatic potential with blue and red corresponding to +40 kT and −40 kT.

FLAP crystallizes as a homotrimer (Fig. 1D), consistent with previous studies on MAPEGs (*19*–*21*). The trimer has a flattened cytosolic top (Figs. 1D and 2B) and a slightly pointed lumenal base (Figs. 1D and 2C). Electron density and temperature factors indicate that the cytosolic loops are flexible. The three-fold axis of the trimer is perpendicular to the plane of the membrane, and it resembles a cylinder 60 Å high and 36 Å wide.

There are extensive intersubunit contacts, with each monomer burying ~4900 Å^2. On both sides of the membrane and within the bilayer, cytosolic loops C1 and C2, lumenal helix αL, and helices α1, α2, and α4 form an elaborate network of intermolecular contacts. Unexpectedly, helix α3 and the lumenal loop do not form any intersubunit contacts within the membrane. There are also three polar interactions (N23-T66, Q58-Q58 and Q58-D62) between adjacent monomers near the three-fold axis. Hydrophobic residues line the membrane-embedded portion of the intersubunit interfaces and form extensive nonpolar contacts. There is also nonprotein electron density in the lipid-exposed regions that most likely represents bound detergent or lipid molecules.

Three ~750 Å^3 grooves are located between adjacent monomers on the lipid-exposed surface of the trimer (Fig. 2A). Within these grooves, there is clear connected nonprotein electron density and peaks in anomalous difference maps that are consistent with three bound inhibitor molecules (figs. S3 to S5). Inhibitors intercalate between monomers in the surface grooves and form van der Waals interactions with residues V20, V21, G24, F25, and A27 from helix α1; Y112 and I113 from cytosolic loop C2; A63 from helix α2; and I119, L120, and F123 from helix α4 of the adjacent monomer (Fig. 3, A and B). A limited number of weak polar interactions are also formed with residue N23 from helix α1, D62, and T66 from helix α2, and K116 from helix α4 of the neighboring subunit (Fig. 3, A and B).

Given the resolution of our electron density maps and the unexpected location of the inhibitor binding site, we performed direct mutagenesis to confirm the location of the site by measuring the binding of radiolabeled iodinated analog of MK-591 to mutant forms of FLAP. Mutating residues close (≤4 Å) to the inhibitor cause a dramatic decrease in binding affinity (Fig. 3A and table S2). Unexpectedly, several directed mutations increase inhibitor binding affinity (V20A, I113A, K116A, and Δ1-10). The insensitivity of mutations distant from the bound

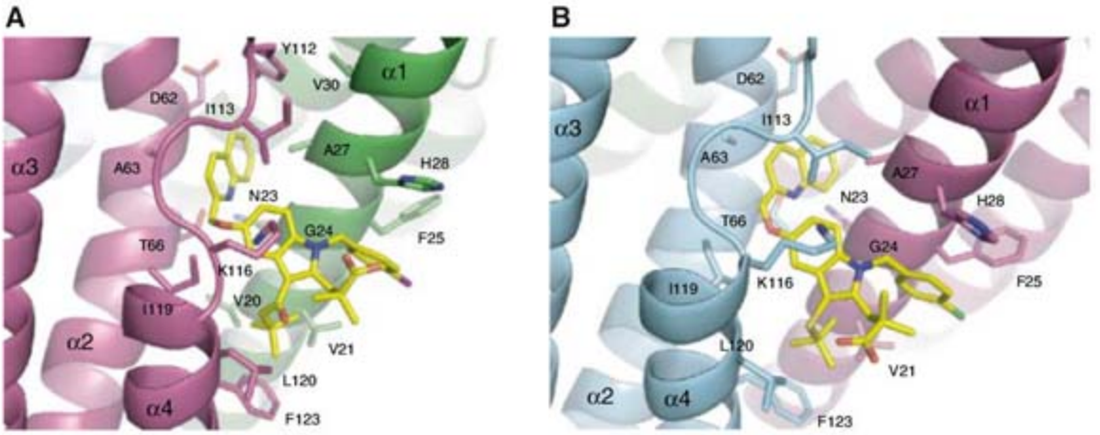

Fig. 3. The inhibitor binding site of FLAP in complex with (**A**) the iodinated analog of MK-591 and (**B**) MK-591. Monomers are colored green, cyan, and magenta. All side chains within these inhibitors are shown as sticks. Inhibitor molecules are shown as stick models with yellow carbon atoms, blue nitrogens, red oxygens, purple iodines, green chlorines, and orange sulfurs.

inhibitor (>4 Å) suggests that the observed loss in binding affinity is a direct result of mutating proximal residues and not due to aberrant folding. Collectively, these data support our identification of the inhibitor binding site.

Previous studies defined regions of FLAP that are important for binding of inhibitors (table S3) (*22*–*24*). When viewed in the context of the FLAP structure, most of the loss-of-function deletions are at the cytosolic surface. Jointly removing the cytosolic portions of helices α1 and α2 and cytosolic loop C1 would substantially alter the FLAP structure, providing a likely explanation for the observed loss in inhibitor binding. In contrast, the mutations that do not significantly affect activity involve removing a short cytosolic piece of helix α1 and/or cytosolic loop C1 or three residues from cytosolic loop C2. These mutations would cause a minimal structural perturbation and would not affect inhibitor binding.

Perhaps the most unexpected feature of the FLAP structure is an internal ~3,200 $Å^3$ pocket at the bottom of the trimer and open to the lumen (Fig. 2, C and D). The entrance to this pocket has an internal diameter of ~6 Å and is formed by the lumenal helices and loops that define three distinct entry crevices on the lumenal surface of the trimer (Fig. 2, C and D). The pocket extends to about the middle of the membrane, where it is constricted by a symmetric ring of P65 residues (minimum radius of ~0.5 Å) (*25*), which coincides with the bend in helix α2. Proline-induced distortions in transmembrane helices are known to be involved in transmembrane signal transduction and solute transport by acting as molecular hinges (*26*). An additional symmetric ring, formed by residues Q58 and D62 from helix α2, sits above this point. The asymmetric distribution of the electrostatic potential of this pocket is striking: Its lumenal entrance and membrane-embedded constriction point are negatively charged, whereas the interior lining is largely hydrophobic (Fig. 2, C and D).

By combining the structure presented here with previous data, we can propose a model to explain the selective transfer of AA to 5-LO by FLAP and how FLAP inhibitors prevent this process. Cellular activation initiates the calcium-dependent translocation of $cPLA_2$ and 5-LO from the cytosol to the nuclear membrane. The N terminus of 5-LO contains a calcium-binding domain that presumably anchors it to the nuclear membrane adjacent to FLAP. It is reasonable to assume that the C-terminal catalytic domain of 5-LO binds to the cytosolic loops of FLAP. Previous FLAP mutagenesis studies show partial overlap between the AA and inhibitor binding sites of FLAP (*22*–*24*). Our structure shows that the inhibitor binding sites are located within nuclear membrane, which provides an appropriate environment for the lateral diffusion of AA molecules to FLAP. This event may be coupled to structural changes in FLAP, specifically the relative conformation of helix α2, the constriction formed by the symmetrical ring of P65 residues, and the negatively charged symmetrical ring of Q58 and D62 residues. We hypothesize that one 5-LO molecule binds to each FLAP trimer and that AA molecules are sequentially transferred to 5-LO. When loaded with AA, 5-LO converts AA to HpETE and then to LTA_4, which can be either converted to LTB_4 by leukotriene A_4 hydrolase, exported from cells for transcellular metabolism, or released back into the nuclear membrane for conversion to LTC_4 by leukotriene C_4 synthase (*2*, *4*, *5*). The lateral transfer of LTA_4 from FLAP to leukotriene C_4 synthase within the nuclear membrane is consistent with recent observations showing that these MAPEGs form a macromolecular complex (*27*).

Leukotrienes have an established pathological role in allergic and respiratory diseases. Animal and human genetic evidence suggests they may also have an important role in atherosclerosis, myocardial infarction, and stroke. The structure of FLAP provides a tool for the development of novel therapies for respiratory and cardiovascular diseases and for the design of focused experiments to probe the cell biology of FLAP and its role in leukotriene biosynthesis.

References and Notes

1. C. D. Funk, *Nat. Rev. Drug Discov.* **4**, 664 (2005).
2. C. D. Funk, *Science* **294**, 1871 (2001).
3. J. Woods *et al.*, *J. Exp. Med.* **178**, 1935 (1993).
4. O. Radmark, B. Samuelsson, *Biochem. Biophys. Res. Commun.* **338**, 102 (2005).
5. G. Folco, R. C. Murphy, *Pharmacol. Rev.* **58**, 375 (2006).
6. A. Bresell *et al.*, *FEBS J.* **272**, 1688 (2005).
7. R. A. Dixon *et al.*, *Nature* **343**, 282 (1990).
8. D. K. Miller *et al.*, *Nature* **343**, 278 (1990).
9. Z. Diamant *et al.*, *J. Allergy Clin. Immunol.* **95**, 42 (1995).
10. R. Young, *Eur. J. Med. Chem.* **34**, 671 (1999).
11. A. Helgadottir *et al.*, *Nat. Genet.* **36**, 233 (2004).
12. J. Mancini *et al.*, *FEBS Lett.* **318**, 277 (1993).
13. R. Young, J. Gillard, J. Hutchinson, S. Leger, P. Prasit, *J. Lipid Mediat.* **6**, 233 (1993).
14. C. Rouzer, A. Ford-Hutchinson, H. Morton, J. Gillard, *J. Biol. Chem.* **265**, 1436 (1990).
15. H. Plante, S. Picard, J. Mancini, P. Borgeat, *Biochem. J.* **393**, 211 (2006).
16. B. K. Lam, J. F. Penrose, K. Xu, M. H. Baldasaro, K. F. Austen, *J. Biol. Chem.* **272**, 13923 (1997).
17. C. Andersson, R. Weinander, G. Lundqvist, J. W. DePierre, R. Morgenstern, *Biochim. Biophys. Acta* **1204**, 298 (1994).
18. R. Weinander *et al.*, *J. Biol. Chem.* **272**, 8871 (1997).
19. P. Holm *et al.*, *J. Mol. Biol.* **360**, 934 (2006).
20. I. Schmidt-Krey *et al.*, *Structure* **12**, 2009 (2004).
21. S. Thoren *et al.*, *J. Biol. Chem.* **278**, 22199 (2003).
22. P. Vickers *et al.*, *J. Lipid Mediat.* **6**, 31 (1993).
23. J. Mancini, M. Coppolino, J. Klassen, S. Charleson, P. Vickers, *Life Sci.* **54**, 137 (1994).
24. P. Vickers *et al.*, *Mol. Pharmacol.* **42**, 94 (1992).
25. O. Smart, J. Neduvelil, X. Wang, B. Wallace, M. Sansom, *J. Mol. Graph.* **14**, 354 (1996).
26. F. Cordes, J. Bright, M. Sansom, *J. Mol. Biol.* **323**, 951 (2002).
27. A. Mandal *et al.*, *Proc. Natl. Acad. Sci. U.S.A.* **101**, 6587 (2004).
28. T. Binkowski, L. Adamian, J. Liang, *J. Mol. Biol.* **332**, 505 (2003).

29. We thank K. Bateman, T. LeRiche, and D. Zink for mass spectrometry data; J. Badger for assistance with Rigaku software; C. Vonrhein for useful discussions and assistance using Global Phasing software; and M. Abramovitz, J. A. Mancini, J. Menke, R. T. Mosley, M. Ouellet, and S. M. Soisson for useful discussions and critical review of the manuscript. Coordinates and structure factors have been deposited in the Protein Data Bank under the accession codes 2Q7M and 2Q7R.

Supporting Online Material

www.sciencemag.org/cgi/content/full/1144346/DC1
Materials and Methods
Figs. S1 to S5
Tables S1 to S3
References

27 April 2007; accepted 15 June 2007
Published online 28 June 2007;
10.1126/science.1144346
Include this information when citing this paper.

Spring-Loaded Mechanism of DNA Unwinding by Hepatitis C Virus NS3 Helicase

Sua Myong,[1,2]* Michael M. Bruno,[3,4] Anna M. Pyle,[3,4] Taekjip Ha[1,2,4]

NS3, an essential helicase for replication of hepatitis C virus, is a model enzyme for investigating helicase function. Using single-molecule fluorescence analysis, we showed that NS3 unwinds DNA in discrete steps of about three base pairs (bp). Dwell time analysis indicated that about three hidden steps are required before a 3-bp step is taken. Taking into account the available structural data, we propose a spring-loaded mechanism in which several steps of one nucleotide per adenosine triphosphate molecule accumulate tension on the protein-DNA complex, which is relieved periodically via a burst of 3-bp unwinding. NS3 appears to shelter the displaced strand during unwinding, and, upon encountering a barrier or after unwinding >18 bp, it snaps or slips backward rapidly and repeats unwinding many times in succession. Such repetitive unwinding behavior over a short stretch of duplex may help to keep secondary structures resolved during viral genome replication.

In hepatitis C virus (HCV), nonstructural protein 3 (NS3) is an essential component of the viral replication complex that works with the polymerase NS5B and other protein cofactors (such as NS4A, NS5A, and NS2) to ensure effective copying of the virus. The NS3 protein is a bifunctional enzyme that contains both protease and helicase domains (*1*–*3*) and is unusual in that it can unwind both DNA and RNA substrates (*4*, *5*). Unwinding of the highly structured RNA genome of HCV is likely to be the major role for the NS3 helicase; however, it remains possible that activity toward host DNA substrates plays a role in viral function. Indeed, NS3 rapidly binds DNA and unwinds it processively (*6*). Given these facts and the availability of crystallographic data on NS3-DNA complexes (*7*–*9*), we sought to elucidate the elementary steps and kinetic mechanisms involved with NS3 unwinding of DNA.

In a previous ensemble study, NS3 was observed to unwind RNA with a physical and kinetic size of ~18 base pairs (bp) (*10*). More recently, single-molecule mechanical studies under assisting force confirmed the periodic nature of RNA unwinding by NS3, but displayed rapid steps of ~3 to 4 bp that were interrupted by long pauses approximately every 11 bp (*11*). These large apparent steps by NS3 contrast with structural studies of other helicases, which suggest that the elemental step for helicase activity is the unwinding of a single base pair, and that this is linked to individual adenosine triphosphate (ATP) hydrolysis events (*12*, *13*). Nonetheless, there are no functional data supporting the existence of unwinding steps of a single base pair each, nor any information on how they might correlate with the larger steps that appear to be involved in the mechanical function of helicase enzymes (*14*).

We used single-molecule fluorescence resonance energy transfer (FRET) to resolve the individual steps of DNA separation catalyzed by NS3 in the absence of applied force. Our standard substrate, PD1, is a partial-duplex DNA (18 bp) with a 3′ single-stranded DNA (ssDNA) tail 20 nucleotides (nt) in length. The donor (Cy3) and acceptor (Cy5) fluorophores are attached to the junction through aminodeoxythymidine without interrupting the DNA backbone. The DNA is tethered to a polymer-passivated quartz surface via biotin at the 3′ tail terminus (Fig. 1A). After incubation of this assembly with full-length NS3 protein (25 nM) for 15 min, 4 mM ATP solution is flowed into the cell to initiate DNA unwinding. The flow of ATP also serves to remove unbound protein in solution and thereby allows us to monitor unwinding by prebound NS3 (*15*).

After addition of ATP, we observed a FRET decrease that is caused by the increase in the time-averaged (time resolution, 30 ms) interfluorophore distance as the DNA is unwound. The measurements taken at 37°C indicate a rapid FRET decrease that appears to involve intermediate steps (fig. S1). When the temperature was lowered to 30°C to slow the reaction, FRET values decreased with a discrete pattern marked by apparent plateaus corresponding to six steps for unwinding of the 18-bp duplex (Fig. 1, B to E). The same experiment was then performed with an otherwise identical substrate, PD2, in which the fluorophores were relocated 9 bp away from the junction, such that FRET signal is sensitive only to the final 9-bp unwinding (Fig. 1F). Plateaus were also observed in that case, although they occurred with larger FRET increments corresponding to three unwinding steps for unwinding 9 bp (Fig. 1, G to J). Both sets of data are consistent with a 3-bp unwinding step size. The data also indicate that the two strands do not spontaneously separate when only a few base pairs remain (i.e., via thermal duplex fraying). At the end of each experiment, the displacement of acceptor-labeled strands was confirmed by a direct excitation with a red laser.

To quantify the stepping behavior, we used an automated step-finding algorithm (*16*) (fig. S2), which yielded the average FRET values for each plateau and its dwell time (Fig. 2, A and D). We then built transition density plots (*17*), which represent the two-dimensional histogram for pairs of FRET values before (FRET enter) and after (FRET exit) each transition. Six and three well-isolated peaks emerged for 18-bp and 9-bp unwinding, respectively (about 75 molecules each) (Fig. 2, B and E). The highest FRET peak region (Fig. 2B) appears to be in broader distribution than other peak regions, possibly as a result of the NS3 binding and fluctuating or partially melting the junction and thus slightly separating the two dyes. This analysis shows that there are well-defined FRET states that are visited sequentially during unwinding and that they are each separated by about 3 bp. Similar evidence for 3-bp unwinding steps was found for unwinding an 18-bp duplex of unrelated sequence (fig. S3).

If 3 bp is the elementary step size of unwinding—for example, due to the hydrolysis of a single ATP—the dwell time histogram of the steps would follow a single-exponential decay. In contrast, we obtained nonexponential dwell time histograms that displayed a rising phase followed by a decay (Fig. 2, C and F). If we assume that each 3-bp step requires n hidden irreversible Poissonian steps with identical rate k, the data can be fit with the gamma distribution, $t^{n-1}\exp(-kt)$. The fits gave $n = 2.84$ for 18-bp unwinding and $n = 2.72$ for 9-bp unwinding. The k values were 0.78 s^{-1} and 0.89 s^{-1}, respectively. These rates are similar to the unwinding rate estimated from an earlier bulk solution study of an 18-bp duplex of unmodified DNA (0.66 s^{-1} bp^{-1}) (*6*). Dwell time histograms built for individual steps gave similar n and k values for each step (fig. S4). Overall, our data suggest that each 3-bp step is composed of three hidden steps of 1 bp, presumably due to hydrolysis of one ATP each. The emerging model here is that, after three successive ATP hydrolysis events, there occurs an abrupt 3-bp separation.

The helicase domain of NS3 (NS3h), belonging to superfamily 2 (SF2), has three domains. Domain 1 and domain 2 have RecA-like folds, and there is an ATP-binding pocket between the domains. In the crystal structure of NS3h bound to deoxyuridine octamer $(dU)_8$, domains 1 and 2 make contacts exclusively to the phosphate-ribose backbone of $(dU)_8$ with no contact to the bases (*9*). Nonetheless, bases are well resolved in the structure and there is enough room for duplex formation on the 5′ side, with only a minor change in the relative position of domain 3.

[1]Physics Department, University of Illinois, 1110 West Green Street, Urbana, IL 61801, USA. [2]Institute for Genomic Biology, University of Illinois, 1206 West Gregory Drive, Urbana, IL 61801, USA. [3]Molecular Biophysics and Biochemistry, Yale University, 266 Whitney Avenue, Room 334A, Bass Building, New Haven, CT 06511, USA. [4]Howard Hughes Medical Institute.

*To whom correspondence should be addressed. E-mail: smyong@uiuc.edu

The structure, obtained in the absence of ATP, shows that two highly conserved threonines (Thr^{269} and Thr^{411}) bind to two phosphates that are located 3 nt apart. Mutation of either of these NS3 threonines abolishes unwinding activity (*18*). By contrast, the Vasa helicase and eIF4AIII structures, determined with adenylyl-imidodiphosphate and 5′-adenylyl-β-γ-imidodiphosphate bound, respectively (*19*, *20*), suggest that domains 1 and 2 will close upon ATP binding and that this would bring the equivalent two threonine residues 2 nt apart (fig. S5, A to C). This change in the distance between threonine contacts may represent the structural basis for a 1-nt movement: Each ATP binding and product release event is expected to result in the 1-nt movement of domains 1 and 2 in the 3′ to 5′ direction.

Domain 3 presents a tryptophan (Trp^{501}) that is critical for activity. The importance of an aromatic residue at this position is demonstrated by the fact that it can be substituted with phenylalanine, whereas alanine disrupts unwinding (*18*). The Trp^{501} stacks against the base at the 3′ end of $(dU)_8$ (fig. S5A), which might keep the relative positions of domain 3 and DNA fixed while domains 1 and 2 translocate. This effect would lead to the buildup of tension on both the protein and the DNA, which we propose is released after 3-nt translocation by a sudden movement of domain 3, with concomitant 3-bp unwinding of the DNA (fig. S9).

SF1 helicases such as Rep, UvrD, and PcrA are structurally analogous to SF2 helicases with

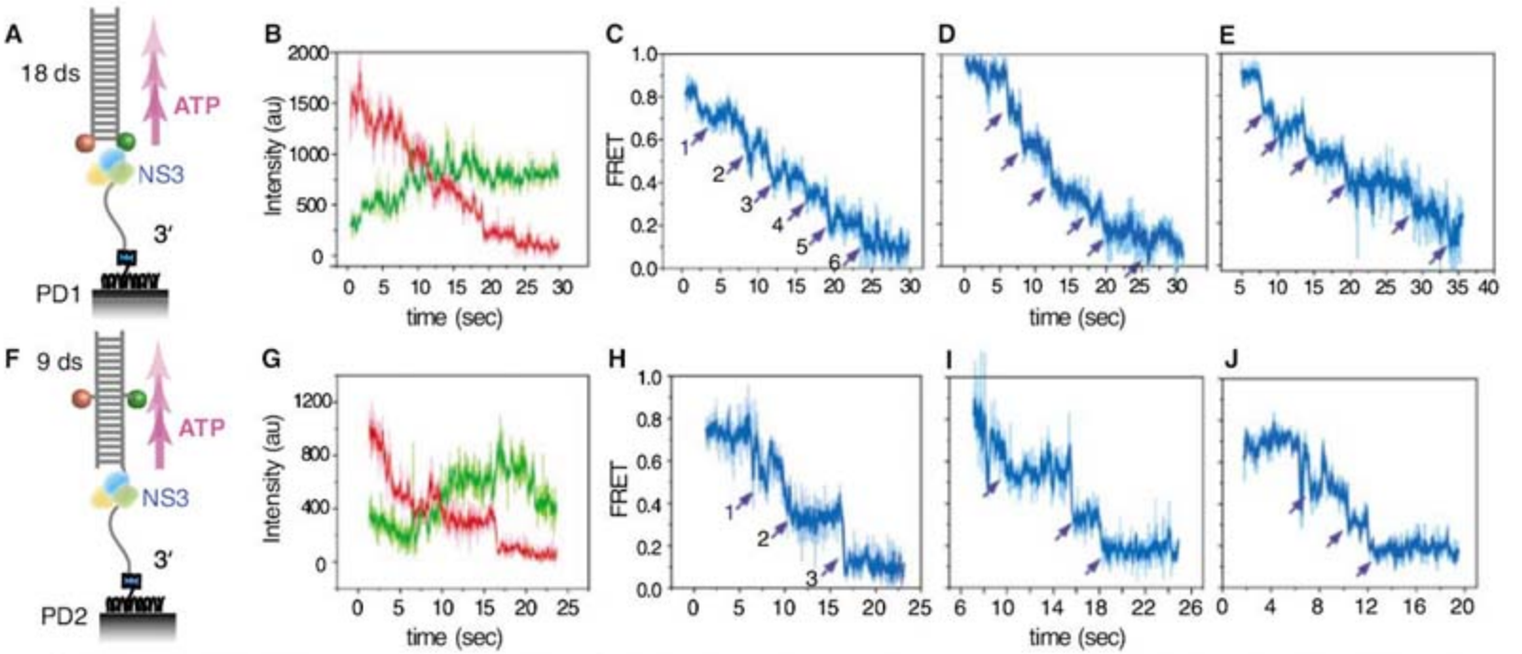

Fig. 1. NS3 unwinds DNA in 3-bp steps. (**A**) PD1, a DNA with 18 double strands (ds) and 20 single strands (ss), was labeled with donor (Cy3) and acceptor (Cy5) at the ds-ss junction and was tethered to a polyethylene glycol surface by 3′ biotin. (**B**) Cy3 (green) and Cy5 (red) intensities monitored during unwinding of a single PD1 molecule (raw time traces in light color, three-point averaged traces in dark color). (**C**) Calculated FRET efficiency versus time for the molecule shown in (B). (**D** and **E**) Two more examples of FRET traces of PD1. (**F**) PD2 is the same construct as in (A) but prepared with dyes in the middle of duplex. (**G** to **J**) Plots analogous to those in (B) to (E) for PD2.

Fig. 2. Each 3-bp step consists of three hidden steps. (**A**) A step-finding algorithm was used to quantify FRET values (orange arrows) and dwell times (blue arrows, Δt) at each step for a single molecule of PD1. (**B**) FRET values obtained from 75 molecules of PD1 were combined to make a total density plot. (**C**) Gamma distribution fitting of the collected dwell times at each plateau pause duration for PD1 yielded approximately three irreversible steps (n values) within the 3-bp step, indicating a strong possibility of one nucleotide as an elementary step size. (**D** to **F**) Plots analogous to those in (A) to (C) for PD2.

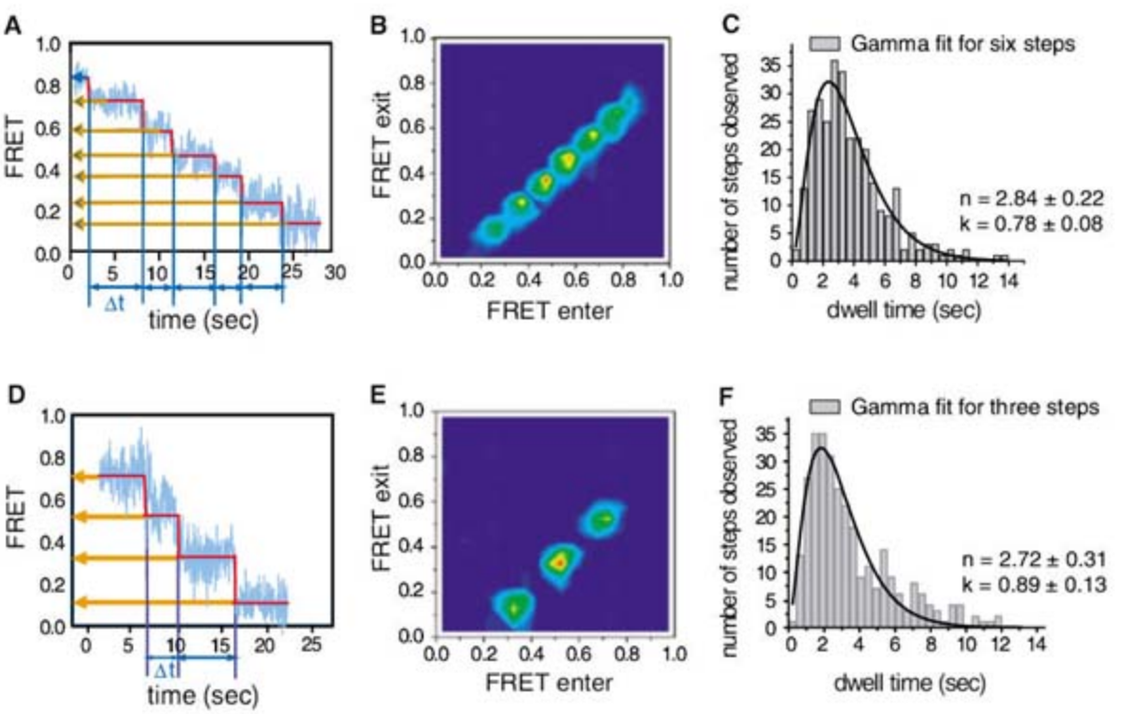

superimposable domain arrangement and catalytic site (*21*, *22*). The available crystal structures of these three SF1 helicases all have well-conserved threonine pairs and an aromatic gatekeeper residue, phenylalanine, at the analogous locations to NS3 (fig. S5, D and E). ATP-bound UvrD has the two threonines 2 nt apart, whereas Rep with no ATP shows the threonines 3 nt apart, again supporting the 1-nt movement coupled to one ATP consumption (*23*).

To observe the unwinding behavior when the duplex end is challenged with a presence of physical blockade, we next examined unwinding of an inverted configuration where the duplex end was tethered to the surface via biotin-streptavidin (Fig. 3A). In this construct we swapped the dye positions so that the donor was attached to the displaced strand and the acceptor on the tracking strand. At 37°C, the same stepwise behavior was observed but the unwinding could not be completed, perhaps because of steric hindrance by the biotin-streptavidin blockade. Some molecules (25%) showed the displaced strand (donor attached strand) remaining in contact with the enzyme for long periods (fig. S6A) after unwinding, whereas many others (75%) displayed a repetitive FRET pattern as shown in Fig. 3B. In most cases, the peaks were asymmetric with an abrupt FRET increase followed by a gradual FRET decrease. We interpret this characteristic pattern as repeated trials of helicase unwinding followed by rapid rezipping/reannealing of the duplex. Because the unwinding reaction initiated after washing out free protein, such repetition likely arises from one unit rather than the successive binding of different molecules. Could it be that the enzyme bears a secondary binding site that enables it to snap back to restart the next round of unwinding?

We therefore designed a substrate such that the whereabouts of the acceptor-labeled 5′ end of the displaced strand could be monitored via FRET from the donor at the duplex end (Fig. 3C). In this experiment, we observed a repeating pattern in the shape of an asymmetric sawtooth where each peak involved a gradual rising phase of FRET followed by an abrupt decrease (Fig. 3D), indicating that the 5′ region of the displaced strand is brought close to the duplex end as DNA is unwound. This effect can arise from the enzyme maintaining contact with the 5′ region of the displaced strand or from the displaced strand becoming compact because of the flexibility of ssDNA. We prefer the former scenario because of its consistency with the larger FRET changes per step seen for PD2 than for PD1 (Fig. 1). A protein contact with the 5′ region of the displaced strand would lead to a looping of the strand, giving rise to a larger distance change per step if the fluorophores are attached to the middle of the duplex (fig. S7). In this view, the abrupt decrease in FRET may be attributed to NS3 losing its grip on the tracking strand and snapping or slipping back near the junction while maintaining contact with the 5′ region of the displaced strand.

On the basis of our findings, we propose the following model for NS3 unwinding of DNA (fig. S9). Domains 1 and 2 of NS3 move along the tracking strand (3′ to 5′) one nucleotide at a time, consuming one ATP, where ATP binding and ADP release induce closing and opening of the two domains, respectively. The third domain of the protein lags behind by anchoring itself to the DNA until three such steps take place. At the third step, the spring-loaded domain 3 moves forward in a burst motion, unzipping 3 bp as a consequence. The displaced strand is likely to be sheltered by the enzyme instead of being released free. NS3 continues unwinding in 3-bp steps up to about 18 bp unless it encounters an apparent barrier (movie S1). Unwinding performed with duplexes 24 bp or longer showed evidence of repetitive unwinding even when the duplex ends were not blocked (fig. S8), which suggests that NS3 is not highly efficient in going much beyond 18 bp; this is consistent with the reported drop in processivity that is observed every 18 bp in RNA unwinding in bulk solution (*10*).

The HCV genome is a ~10,000-nt single-stranded RNA that is copied upon binding of the NS3-NS4A-NS5B replicative complex to highly structured terminal untranslated regions (UTRs). Sequence and structural analysis suggests that the UTRs are complex structures comprising short stems and loops (*24*). The ability of NS3 to maintain contact with displaced strands may provide an advantage by allowing it to stay in a local region to keep RNA stems unwound, because reforming of the secondary structure could hinder viral replication. The repetitive unwinding behavior of NS3 is reminiscent of the repeated translocation observed in Rep (*25*).

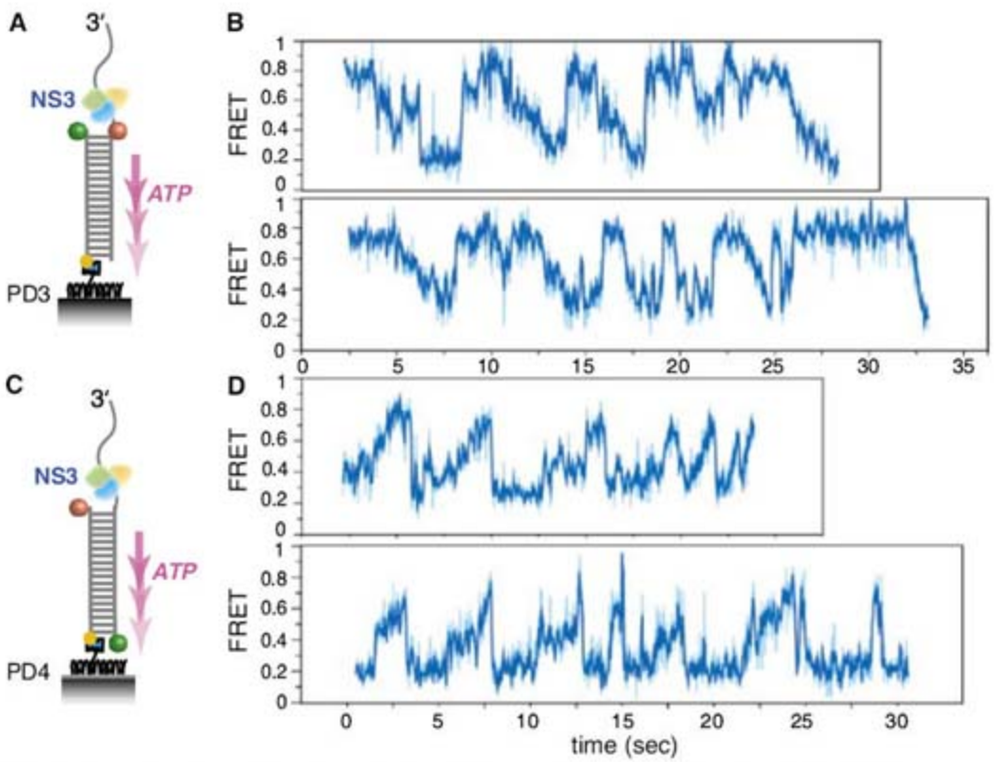

Fig. 3. Repetitive unwinding of a short duplex stretch. (**A**) PD3, a partial duplex with 18 double strands and a tail of 30 single strands, was labeled with cy3 and cy5 at the ds-ss junction and blocked at the duplex end via biotin-streptavidin. (**B**) A majority of molecules (75%) showed a repetitive unwinding pattern where the enzyme appeared to snap or slip back to near the junction upon encountering a blockade. (**C**) PD4, a partial duplex with 18 double strands and a tail of 20 single strands, was labeled with cy5 at the ds-ss junction and cy3 at the duplex end. (**D**) The repetitive cycles of gradual FRET increase followed by rapid FRET decrease indicate that the displaced strand is brought close to the duplex end by NS3, then snaps or slips back to the junction rapidly after encountering the blockade.

References and Notes

1. A. M. Di Bisceglie, *Hepatology* **26**, 34S (1997).
2. L. B. Seeff, *Hepatology* **28**, 1710 (1998).
3. D. Lavanchy, *J. Hepatol.* **31** (suppl. 1), 146 (1999).
4. D. W. Kim, Y. Gwack, J. H. Han, J. Choe, *Biochem. Biophys. Res. Commun.* **215**, 160 (1995).
5. C. L. Tai, W. K. Chi, D. S. Chen, L. H. Hwang, *J. Virol.* **70**, 8477 (1996).
6. P. S. Pang, E. Jankowsky, P. J. Planet, A. M. Pyle, *EMBO J.* **21**, 1168 (2002).
7. H. P. Yao, D. J. Xia, L. H. Zhang, K. Z. Liu, *Zhejiang Da Xue Xue Bao Yi Xue Ban* **31**, 2 (2002).
8. L. W. Kang *et al.*, *Acta Crystallogr. D* **54**, 121 (1998).
9. J. L. Kim *et al.*, *Structure* **6**, 89 (1998).
10. V. Serebrov, A. M. Pyle, *Nature* **430**, 476 (2004).
11. S. Dumont *et al.*, *Nature* **439**, 105 (2006).
12. J. Y. Lee, W. Yang, *Cell* **127**, 1349 (2006).
13. M. S. Dillingham, D. B. Wigley, M. R. Webb, *Biochemistry* **39**, 205 (2000).
14. A. J. Ali, T. M. Lohman, *Science* **275**, 377 (1997).
15. See supporting material on *Science* Online.
16. J. W. Kerssemakers *et al.*, *Nature* **442**, 709 (2006).
17. C. Joo *et al.*, *Cell* **126**, 515 (2006).
18. C. Lin, J. L. Kim, *J. Virol.* **73**, 8798 (1999).
19. T. Sengoku, O. Nureki, A. Nakamura, S. Kobayashi, S. Yokoyama, *Cell* **125**, 287 (2006).

20. C. B. F. Andersen *et al.*, *Science* **313**, 1968 (2006); published online 23 August 2006 (10.1126/science.1131981).
21. K. J. Marians, *Structure* **5**, 1129 (1997).
22. S. Korolev, N. Yao, T. M. Lohman, P. C. Weber, G. Waksman, *Protein Sci.* **7**, 605 (1998).
23. E. J. Tomko, C. J. Fischer, A. Niedziela-Majka, T. M. Lohman, *Mol. Cell* **26**, 335 (2007).
24. M. Houghton, A. Weiner, J. Han, G. Kuo, Q. L. Choo, *Hepatology* **14**, 381 (1991).
25. S. Myong, I. Rasnik, C. Joo, T. M. Lohman, T. Ha, *Nature* **437**, 1321 (2005).
26. We thank C. Joo for help in manuscript preparation. Supported by NIH grants R01-GM060620 and R01-GM065367. T.H. and A.M.P. are investigators with the Howard Hughes Medical Institute.

Supporting Online Material
www.sciencemag.org/cgi/content/full/317/5837/513/DC1
Materials and Methods
Figs. S1 to S9
Movie S1

23 April 2007; accepted 26 June 2007
10.1126/science.1144130

Sirtuin 2 Inhibitors Rescue α-Synuclein–Mediated Toxicity in Models of Parkinson's Disease

Tiago Fleming Outeiro,[1,2] Eirene Kontopoulos,[3*] Stephen M. Altmann,[2*] Irina Kufareva,[4] Katherine E. Strathearn,[5] Allison M. Amore,[2] Catherine B. Volk,[5] Michele M. Maxwell,[2] Jean-Christophe Rochet,[5] Pamela J. McLean,[1,2] Anne B. Young,[2] Ruben Abagyan,[4] Mel B. Feany,[3] Bradley T. Hyman,[1,2] Aleksey G. Kazantsev[2†]

The sirtuins are members of the histone deacetylase family of proteins that participate in a variety of cellular functions and play a role in aging. We identified a potent inhibitor of sirtuin 2 (SIRT2) and found that inhibition of SIRT2 rescued α-synuclein toxicity and modified inclusion morphology in a cellular model of Parkinson's disease. Genetic inhibition of SIRT2 via small interfering RNA similarly rescued α-synuclein toxicity. Furthermore, the inhibitors protected against dopaminergic cell death both in vitro and in a *Drosophila* model of Parkinson's disease. The results suggest a link between neurodegeneration and aging.

Aging is a major risk factor for the development of several neurodegenerative diseases, including Parkinson's disease (PD). Although the molecular basis of aging is yet to be determined, biological pathways involved in aging may provide targets for therapeutic intervention in neurodegeneration. PD causes loss of dopaminergic neurons and development of Lewy bodies containing α-synuclein (α-Syn) in the substantia nigra (*1*). Allele multiplication and mutations link α-Syn to familial forms of PD (*2*).

Silent information regulator 2 (Sir2), a nicotinamide adenine dinucleotide–dependent histone deacetylase (HDAC) in yeast, participates in numerous cell functions including cell protection and cell cycle regulation (*3*). The sirtuins are evolutionarily conserved, and seven distinct sirtuin proteins, SIRT1 to SIRT7, have been identified in humans. The mammalian ortholog of yeast Sir2, SIRT1, is up-regulated under conditions of caloric restriction and resveratrol treatment and is predicted to have a role in cell survival (*4*). Human SIRT2 is involved in cell cycle regulation via the deacetylation of α-tubulin (*5*). However, the identification of p53 and histones H3 and H4 as additional substrates for SIRT2 suggests a broader regulatory role in the cell (*6*, *7*). Small-molecule inhibitors targeting HDACs ameliorate several models of neurodegeneration (*8*).

Compound B2 is associated with an increase in intracellular α-Syn inclusion size from numerous small aggregates to larger inclusions (*9*). B2 activity was examined in a panel of cell-free enzymatic assays including HDAC I and II; SIRT1, 2, and 3; caspase 1 and 6; β-site amyloid precursor protein cleaving enzyme–1 (BACE1); calpain; cathepsin H, L, and S; and molecular chaperones Hsp70 and Hsp27. The only activity detected was a weak [median inhibitory concentration (IC_{50}) = 35 μM], but consistent, selective inhibition of SIRT2 (Fig. 1, A and B, and fig. S1). To determine the relevance of SIRT2 inhibition, we used a targeted knockdown approach. Human neuroglioma cells (H4) were cotransfected with α-Syn expression constructs and synthetic small interfering RNA (siRNA) against either SIRT2 or SIRT3 for 24 hours and were then assessed for cytotoxicity. Rescue of α-Syn–mediated toxicity was observed only in cells receiving the SIRT2

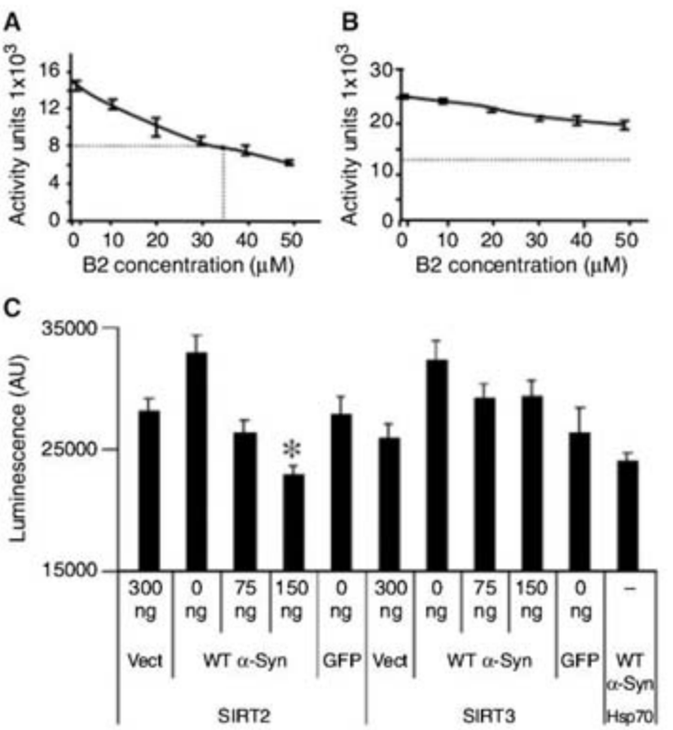

Fig. 1. Inhibition of SIRT2 modulates α-Syn toxicity. (**A** and **B**) B2 biochemical activity profiles against SIRT2 (A) and SIRT3 (B) in an in vitro deacetylation biochemical assay containing recombinant SIRT proteins. (**C**) α-Syn-mediated toxicity can be rescued with SIRT2 siRNA and Hsp70 overexpression but not with SIRT3 siRNA in vitro (*t* test, $n = 3$, $^*P < 0.005$).

[1]Alzheimer's Research Unit, MGH, Harvard Medical School, CNY 114, 16th Street, Charlestown, MA 02129, USA. [2]MassGeneral Institute for Neurodegenerative Disease, MGH, Harvard Medical School, CNY 114, 16th Street, Charlestown, MA 02129, USA. [3]Harvard Medical School and Brigham and Women's Hospital, Department of Pathology, Brigham and Women's Hospital, Harvard Medical School, Harvard New Research Building, Room 630, 77 Louis Pasteur Avenue, Boston, MA 02115, USA. [4]Department of Molecular Biology, Scripps Research Institute, 10550 North Torrey Pines Road, La Jolla, CA 92037, USA. [5]Department of Medicinal Chemistry and Molecular Pharmacology, Purdue University, 575 Stadium Mall Drive, West Lafayette, IN 47907, USA.

*These authors contributed equally to this work.
†To whom correspondence should be addressed. E-mail: akazantsev@partners.org

siRNA (Fig. 1C). A comparable rescue of α-Syn–mediated toxicity was achieved with Hsp70 overexpression (Fig. 1C).

Next, we designed a library of 200 structural analogs of B2 and other previously identified aggregation modifiers. Screening the library by means of SIRT2 (Fig. 2A) and SIRT3 (Fig. 2B) fluorometric assays revealed a promising lead series scaffold, AGK (fig. S1A). Inhibition profiles against human SIRT1, 2, and 3 were generated (figs. S2 and S3). The most potent inhibitor, AGK2 (Fig. 2C), had a calculated IC_{50} for SIRT2 of 3.5 μM, representing a factor of 10 increase in potency over B2 (Fig. 2D). By contrast, a slight inhibition of SIRT1 and 3 was observed only at concentrations over 40 μM (Fig. 2, E and F), indicating that AGK2 was a potent and selective inhibitor of SIRT2. Additional selective lower-potency SIRT2 inhibitors were identified (figs. S2 and S3).

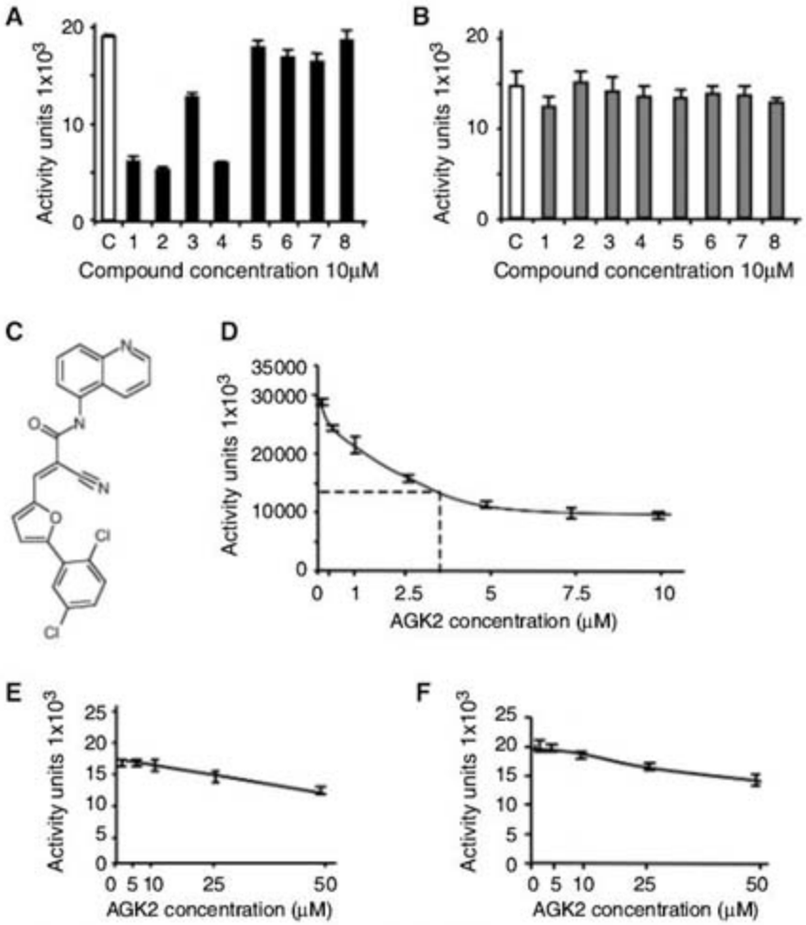

Fig. 2. Identification of a potent and selective SIRT2 inhibitor. (**A** and **B**) Effect of eight representative compounds (out of 200) from a focused B2 library against SIRT2 (A) and SIRT3 (B) activity identifies compound 2 (AGK2) as the most potent against SIRT2. A single-dose (10 μM) primary screen was conducted for each compound, using an in vitro SIRT2 biochemical assay. C is DMSO control. (**C** and **D**) Structure (C) and dose-response profile (D) of AGK2 in a SIRT2 enzymatic assay. (**E** and **F**) Dose-response inhibition profiles of AGK2 in SIRT1 (E) and SIRT3 (F) in an in vitro enzymatic assay.

SIRT2 preferentially deacetylates α-tubulin at Lys^{40} in both purified tubulin heterodimers and taxol-stabilized microtubules (*5*). To determine whether AGK2 could inhibit the deacetylation activity of SIRT2 against a native substrate, we used tubulin heterodimers purified from bovine brain. Treatment with AGK2 led to an increase in acetylated tubulin relative to an inactive control, AGK7, and the known SIRT2 inhibitor sirtinol (Fig. 3A). Only one other compound from a different structural scaffold, AK-1, resulted in increased acetylation in this assay, indicating its stringent specificity (fig. S3D).

To determine whether AGK2 inhibited SIRT2 activity in human cells, we transfected HeLa cells with a SIRT2-myc expression construct. Immunoprecipitated SIRT2 was then used in the enzyme assay, with or without AGK2. As anticipated, AGK2 was effective in inhibiting the activity of SIRT2-myc; hence, the activity of AGK2 was not limited to recombinant SIRT2 but was also effective against SIRT2 that had been folded and processed by the intracellular machinery (Fig. 3B). A comparable assay using immunoprecipitated SIRT3 showed no inhibition by AGK2.

We next examined insoluble, polymerized microtubules and soluble α-tubulin after treatment of HeLa cells with either AGK2 or AGK3, a less potent structural analog of AGK2, for 3 hours. A dose-dependent increase in acetylated

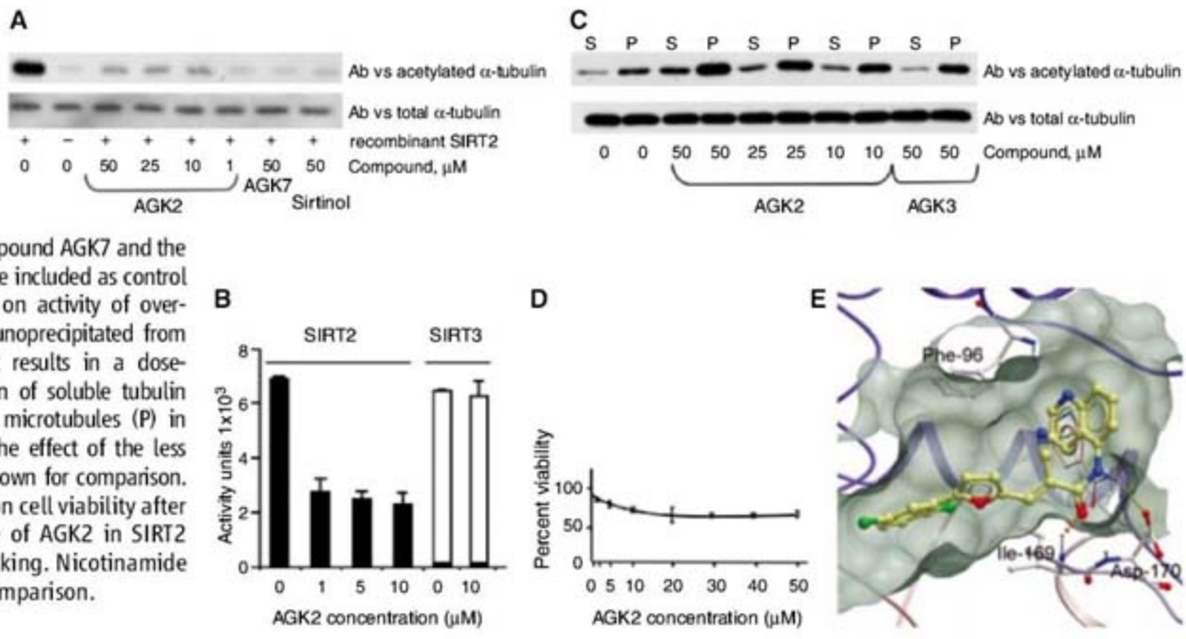

Fig. 3. Validation of AGK2-mediated inhibition of SIRT2. (**A**) The ability of AGK2 to inhibit deacetylation of α-tubulin by SIRT2 was assessed via immunoblot using antibodies (Ab) to acetylated (top lanes) and total (bottom lanes) α-tubulin. The inactive compound AGK7 and the known SIRT2 inhibitor sirtinol were included as control compounds. (**B**) Effect of AGK2 on activity of overexpressed SIRT2 and SIRT3 immunoprecipitated from HeLa cells. (**C**) AGK2 treatment results in a dose-dependent increase in acetylation of soluble tubulin monomers (S) and polymerized microtubules (P) in fractionated HeLa cell extracts. The effect of the less potent SIRT2 inhibitor AGK3 is shown for comparison. (**D**) AGK2 has a minimal effect on cell viability after 72 hours. (**E**) Low-energy pose of AGK2 in SIRT2 generated by virtual ligand docking. Nicotinamide position is shown in wire for comparison.

tubulin was observed in both fractions of AGK2-treated cells relative to untreated or AGK3-treated cells (Fig. 3C). Thus, AGK2 could enter cells and act on endogenous SIRT2 in its native environment. By contrast, AK-1 did not increase acetylated tubulin in live cells, which suggests that its lower potency was insufficient to produce a detectable effect in this particular assay. Incubation of HeLa cells with AGK2 for 72 hours resulted in only minimal toxicity at the higher compound concentrations (Fig. 3D).

To elucidate the structural mechanism of SIRT2 inhibition by AGK2 and AK-1, we developed models of human SIRT2 in several different conformations (*10*). Comparative analysis of the low-energy ligand conformations confirmed that the preferred site for ligand binding is the "C-pocket" (*11*). This hydrogen-bonding pattern mimics the effect of nicotinamide, a known inhibitor of sirtuins (*11*). Examples of the top-scoring poses for AGK2 and AK-1 are shown in Fig. 3E and fig. S4C, respectively.

For pharmacological validation of SIRT2 as a target in a PD functional assay, we transfected H4 cells with α-Syn or a control empty vector and treated them for 24 hours with AGK2, AK-1, AGK7, or dimethyl sulfoxide (DMSO). AGK2 reduced α-Syn–mediated toxicity in a dose-dependent manner, whereas the less potent AK-1 reduced α-Syn–mediated toxicity to a lesser extent and without clear dose dependency. By contrast, the inactive AGK7 had no effect (Fig. 4A).

To rule out other explanations for the alleviation of α-Syn toxicity, we examined levels of α-Syn as well as chaperones Hsp70 and Hsp27, which are known to rescue α-Syn–mediated toxicity (*12*, *13*), after AGK2 treatment. We detected no change in α-Syn, Hsp70, or Hsp27 in the presence of AGK2. As a positive control, cells were treated with the Hsp90 inhibitor geldanamycin, which induces Hsp70 and prevents α-Syn–mediated toxicity in H4 cells (*14*).

To assess the effect of SIRT2 inhibition on α-Syn aggregation, we cotransfected H4 cells with α-Syn and synphilin-1, an established paradigm that leads to inclusion formation in H4 cells (*15*). After transfection, cells were treated with AGK2, AK-1, or AGK7 for 24 hours. When compared to DMSO-treated cells (Fig. 4C), the inactive AGK7 failed to affect α-Syn aggregation (Fig. 4D), whereas AGK2 and AK-1 promoted the formation of enlarged inclusions (Fig. 4, E and F), although AK-1 did so to a lesser extent.

To determine whether AGK2 and AK-1 protected dopaminergic neurons from α-Syn–induced toxicity, we examined α-SynA53T–dependent dopaminergic cell death in primary midbrain cultures. We focused our efforts on the α-SynA53T ($Ala^{53} \rightarrow Thr$) mutant because it is more toxic than wild-type α-Syn in this assay (*16*). Primary midbrain cultures were transduced with lentivirus encoding α-SynA53T with or without compounds B2, AK-1, or AGK2. Untransduced cells were treated with DMSO (0.2%, v/v) to control for nonspecific toxicity. Cultures infected with A53T lentivirus had fewer tyrosine hydroxylase (TH)–positive neurons relative to cultures infected with A53T virus in the presence of B2, AK-1, or AGK2, which were similar to control, untransduced levels (Fig. 4G). Thus, B2, AK-1, or AGK2 rescued α-SynA53T–mediated dopaminergic cell death in this alternative model.

To validate the protective effects of AK-1 and AGK2 against α-Syn–mediated toxicity in vivo, we used a *Drosophila* model of PD (*17*) where α-Syn, under the control of the upstream activating sequence for the yeast transcription factor GAL4, is directed to the fly brain via the *elav-GAL4* pan-neuronal driver. Transgenic flies were fed DMSO or increasing doses of AK-1 or AGK2 for the first 20 days of adult life. As expected, DMSO-fed flies exhibited a marked loss of TH-positive neurons in the dorsomedial cluster, the region that is sensitive to α-Syn–induced toxicity (*17*, *18*). By contrast,

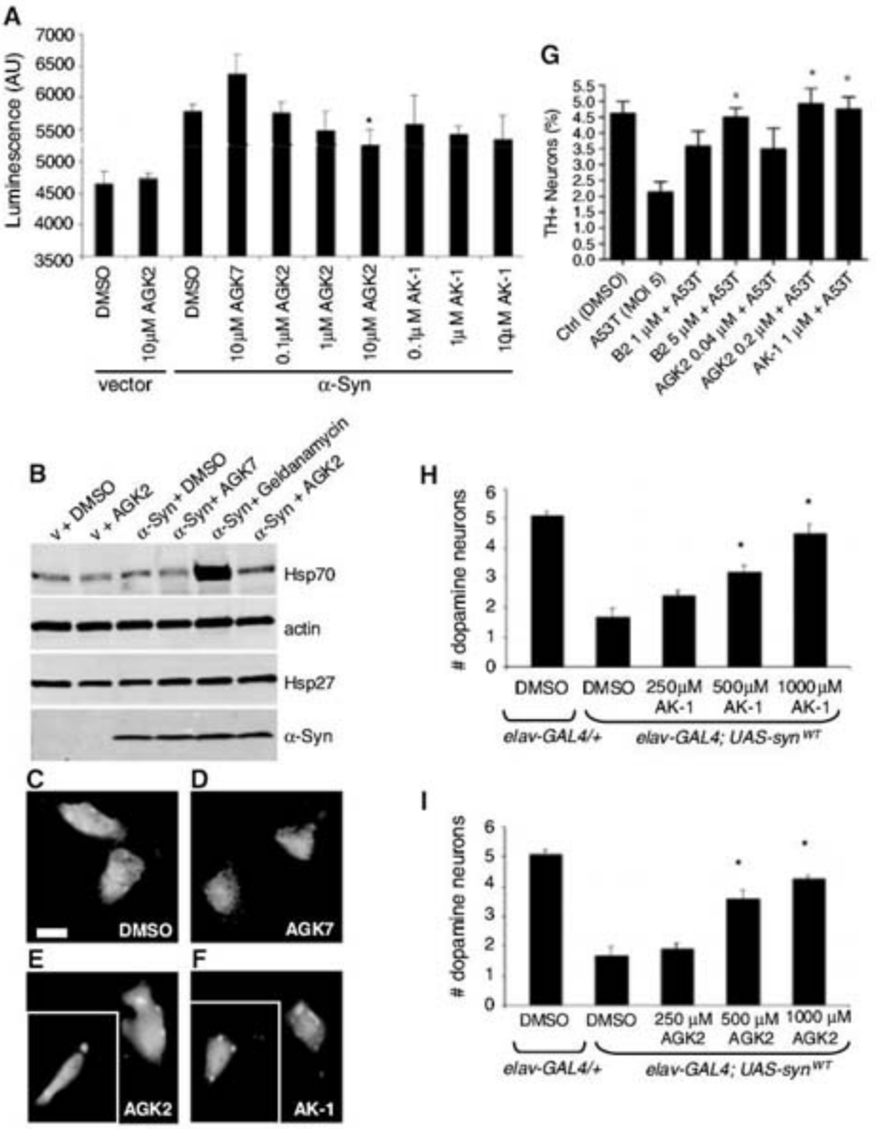

Fig. 4. SIRT2 inhibitors rescue α-Syn–mediated toxicity and modify aggregation in models of PD. (**A**) AGK2 reduces α-Syn–mediated toxicity in a dose-dependent manner as measured via release of adenylate kinase into cell culture media (paired *t* test, $n = 3$, $^*P < 0.05$). The inactive compound AGK7 had no effect, and the less potent AK-1 is not dose-dependent. (**B**) AGK2 has no effect on Hsp70 or Hsp27 expression, whereas geldanamycin induces Hsp70 expression. V = empty vector. (**C** to **F**) α-Syn inclusions remain unaltered in DMSO (C) and the inactive compound AGK7 (D) but decrease in number and increase in size after treatment with AGK2 (E) or AK-1 (F) for 24 hours. Scale bar, 20 μm. (**G**) Primary midbrain cultures were transduced with α-SynA53T encoding lentivirus (multiplicity of infection = 5) in the presence of vehicle (DMSO) or increasing concentrations of B2, AGK2, or AK-1. Control cells were untransduced but treated with DMSO. Dopaminergic cell death was evaluated with antibodies to MAP2 and TH; viability is expressed as the percentage of MAP2-immunopositive cells that were also TH-immunopositive. Data are means ± SEM, $N > 3$, $^*P < 0.01$, one-way analysis of variance with Dunnett's multiple-comparison post hoc test (versus α-SynA53T alone). (**H** and **I**) Administration of AK-1 (H) or AGK2 (I) rescues α-Syn–mediated toxicity of dorsomedial dopamine neurons in 20-day-old wild-type transgenic flies in a dose-dependent manner ($^*P < 0.01$). Animals were fed 250, 500, or 1000 μM AK-1 or AGK2 for 20 days.

transgenic flies fed increasing doses of either AK-1 or AGK2 had a striking dose-dependent rescue of dorsomedial neurons (Fig. 4, H and I). No change occurred in steady-state levels of α-Syn after administration of the SIRT2 inhibitors (fig. S5).

Rescue via inclusion enlargement, and the concomitant reduction in total surface area of inclusions, agrees with a cytoprotective role of aggregates (*19*) and suggests a mechanistic basis for the effect of SIRT2 inhibition—that it reduces aberrant interactions of aggregates with cellular proteins. Conceivably, coalescence of misfolded proteins into larger inclusions may lower the concentration of toxic, submicroscopic α-Syn oligomers, thereby leading to the rescue of proteasome dysfunction. Indeed, the formation of large β-amyloid aggregates is protective against proteotoxicity in *Caenorhabditis elegans* (*20*).

The exact mechanism whereby SIRT2 inhibition affects α-Syn aggregation remains uncertain. Increased α-tubulin acetylation is associated with microtubule stabilization, and α-Syn has been reported to interact with α-tubulin as well as the microtubule-binding proteins MABP1 and tau (*21*, *22*). One possibility is that the increase in acetylated α-tubulin resulting from SIRT2 inhibition may stimulate aggregation of α-Syn through its affinity to microtubules. Moreover, microtubule stabilization itself could be an important factor contributing to neuroprotection. A neuroprotective role for another microtubule deacetylase, HDAC6, was recently proposed, although the protective mechanism is unclear (*23*–*25*).

Our data are consistent with the recent observation that α-Syn–dependent inhibition of histone acetylation is associated with increased neurotoxicity (*4*). Thus, SIRT2 targeting may be therapeutically beneficial in other diseases where aggregation of misfolded proteins is central to disease pathogenesis.

References and Notes

1. M. G. Spillantini *et al.*, *Nature* **388**, 839 (1997).
2. A. B. Singleton *et al.*, *Science* **302**, 841 (2003).
3. G. Blander, L. Guarente, *Annu. Rev. Biochem.* **73**, 417 (2004).
4. E. Kontopoulos, J. D. Parvin, M. B. Feany, *Hum. Mol. Genet.* **15**, 3012 (2006).
5. B. J. North, B. L. Marshall, M. T. Borra, J. M. Denu, E. Verdin, *Mol. Cell* **11**, 437 (2003).
6. B. Heltweg *et al.*, *Cancer Res.* **66**, 4368 (2006).
7. A. Vaquero *et al.*, *Genes Dev.* **20**, 1256 (2006).
8. B. Langley, J. M. Gensert, M. F. Beal, R. R. Ratan, *Curr. Drug Targets CNS Neurol. Disord.* **4**, 41 (2005).
9. R. A. Bodner *et al.*, *Proc. Natl. Acad. Sci. U.S.A.* **103**, 4246 (2006).
10. R. Abagyan, M. Totrov, D. Kuznetsov, *J. Comput. Chem.* **15**, 488 (1994).
11. J. L. Avalos, K. M. Bever, C. Wolberger, *Mol. Cell* **17**, 855 (2005).
12. J. Klucken, Y. Shin, E. Masliah, B. T. Hyman, P. J. McLean, *J. Biol. Chem.* **279**, 25497 (2004).
13. T. F. Outeiro *et al.*, *Biochem. Biophys. Res. Commun.* **351**, 631 (2006).
14. P. J. McLean *et al.*, *J. Neurochem.* **83**, 846 (2002).
15. P. J. McLean, H. Kawamata, B. T. Hyman, *Neuroscience* **104**, 901 (2001).
16. W. Zhou, M. S. Hurlbert, J. Schaack, K. N. Prasad, C. R. Freed, *Brain Res.* **866**, 33 (2000).
17. M. B. Feany, W. W. Bender, *Nature* **404**, 394 (2000).
18. P. K. Auluck, H. Y. E. Chan, J. Q. Trojanowski, V. M.-Y. Lee, N. M. Bonini, *Science* **295**, 865 (2002); published online 20 December 2001 (10.1126/science.1067389).
19. M. Tanaka *et al.*, *J. Biol. Chem.* **279**, 4625 (2004).
20. E. Cohen, J. Bieschke, R. M. Perciavalle, J. W. Kelly, A. Dillin, *Science* **313**, 1604 (2006); published online 9 August 2006 (10.1126/science.1124646).
21. P. H. Jensen *et al.*, *J. Biol. Chem.* **275**, 21500 (2000).
22. M. A. Alim *et al.*, *J. Alzheimers Dis.* **6**, 435 (2004).
23. Y. Kawaguchi *et al.*, *Cell* **115**, 727 (2003).
24. A. Iwata, B. E. Riley, J. A. Johnston, R. R. Kopito, *J. Biol. Chem.* **280**, 40282 (2005).
25. J. P. Dompierre *et al.*, *J. Neurosci.* **27**, 3571 (2007).

26. Supported by a Tosteson postdoctoral fellowship award from Massachusetts Biomedical Research Corporation (T.F.O.), NIH grant 5P50-NS38372A-06 (B.T.H.), NIH grant R01-NS049221 (J.-C.R.), and a gift from Discovery of Novel Neurodegenerative Disease Therapeutics, MassGeneral Institute for Neurodegenerative Disease.

Supporting Online Material

www.sciencemag.org/cgi/content/full/1143780/DC1
Materials and Methods
Figs. S1 to S5
References

13 April 2007; accepted 8 June 2007
Published online 21 June 2007;
10.1126/science.1143780
Include this information when citing this paper.

The Near Eastern Origin of Cat Domestication

Carlos A. Driscoll,[1,2]* Marilyn Menotti-Raymond,[1] Alfred L. Roca,[3] Karsten Hupe,[4] Warren E. Johnson,[1] Eli Geffen,[5] Eric H. Harley,[6] Miguel Delibes,[7] Dominique Pontier,[8] Andrew C. Kitchener,[9,10] Nobuyuki Yamaguchi,[2] Stephen J. O'Brien,[1]* David W. Macdonald[2]*

The world's domestic cats carry patterns of sequence variation in their genome that reflect a history of domestication and breed development. A genetic assessment of 979 domestic cats and their wild progenitors—*Felis silvestris silvestris* (European wildcat), *F. s. lybica* (Near Eastern wildcat), *F. s. ornata* (central Asian wildcat), *F. s. cafra* (southern African wildcat), and *F. s. bieti* (Chinese desert cat)—indicated that each wild group represents a distinctive subspecies of *Felis silvestris*. Further analysis revealed that cats were domesticated in the Near East, probably coincident with agricultural village development in the Fertile Crescent. Domestic cats derive from at least five founders from across this region, whose descendants were transported across the world by human assistance.

The domestic cat may be the world's most numerous pet, yet little is certain of the cat's origin (*1*–*9*). Archaeological remains and anthropological clues suggest that, unlike species domesticated for agriculture (e.g., cow, pig, and sheep) or transport (horse and donkey), the cat probably began its association with humans as a commensal, feeding on the rodent pests that infested the grain stores of the first farmers (*1*). The earliest evidence of cat-human association involves their co-occurrence in Cyprus deposits determined to be 9500 years old (*6*). Domestic cats are generally considered to have descended from the Old World wildcats, but they differ from these hypothesized progenitors in behavior, tameness, and coat color diversity (*9*, *10*). Further, domestic cats appear to lack neotenous characteristics typical of other domesticated species (*11*).

Felis silvestris, from which domestic cats were derived, is classified as a polytypic wild species composed of three or more distinct interfertile subspecies: *F. s. silvestris* in Europe, *F. s. lybica* in Africa and the Near East, *F. s. ornata* in the Middle East and central Asia (*1*, *2*, *12*–*15*), and possibly the Chinese desert cat, *F. s. bieti* (Fig. 1A, inset). The domestic cat is sometimes considered an additional subspecies, *F. s. catus*, possibly derived from wildcats in the Middle East or Egypt (*1*, *12*, *14*, *15*). The imprecise subspecific status of *F. silvestris* populations and of the relationship of the domestic cat within this assemblage stems from morphological similarities among these groups (*1*, *13*). A feral domestic cat with a "wild-type" mackerel tabby pattern is difficult to distinguish visually from a "true" wildcat (*15*, *16*), which is further confounded by ongoing admixture (*16*–*19*). Moreover, the relationship between *F. silvestris* and the Chinese desert cat—which may be a

[1]Laboratory of Genomic Diversity, National Cancer Institute, Frederick, MD 21702, USA. [2]Wildlife Conservation Research Unit, Department of Zoology, University of Oxford, Oxford OX1 3PS, UK. [3]Laboratory of Genomic Diversity, SAIC-Frederick Inc., NCI-Frederick, Frederick, MD 21702, USA. [4]JagdEinrichtungsBüro, Am Sahlbach 9a, 37170 Fürstenhagen, Germany. [5]Department of Zoology, Tel Aviv University, Tel Aviv 69978, Israel. [6]Division of Chemical Pathology, University of Cape Town, Observatory 7925, Cape Town, South Africa. [7]Department of Applied Biology, Estación Biológica de Doñana, CSIC, Avda Maria Luisa s/n Pabellón del Perú, 41013 Sevilla, Spain. [8]UMR-CNRS 5558 Biométrie et Biologie Evolutive, Université Claude Bernard Lyon I, 43 boulevard du 11 novembre 1918, 69622 Villeurbanne, France. [9]Department of Natural Sciences, National Museums Scotland, Chambers Street, Edinburgh EH1 1JF, UK. [10]Institute of Geography, School of Geosciences, University of Edinburgh, Drummond Street, Edinburgh EH8 9XP, UK.

*To whom correspondence should be addressed. E-mail: obrien@ncifcrf.gov; driscoll@ncifcrf.gov; david.macdonald@zoology.oxford.ac.uk

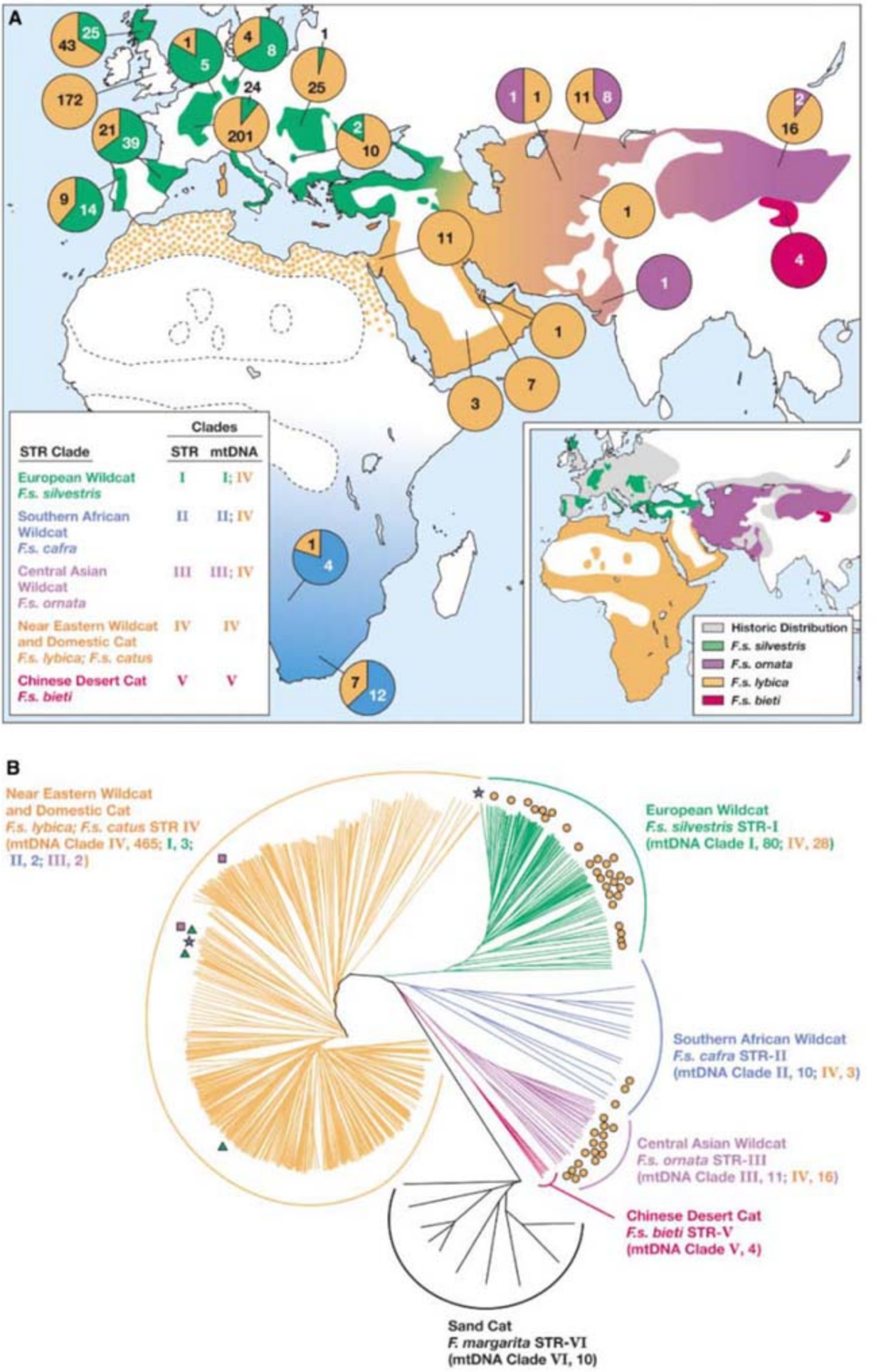

Fig. 1. (**A**) Current range of *F. silvestris* and areas of sample collection. Colored regions reflect the location of capture of individuals carrying different STR clade genotypes (defined at lower left). mtDNA haplotype frequencies are indicated in pie charts specifying the number of specimens carrying mtDNA haplotypes for each clade. Central Asian denotes Asian cats east of the Caspian Sea. Near Eastern denotes cats in Israel, Saudi Arabia, Bahrain, and the United Arab Emirates. European denotes specimens collected west of the Caspian Sea. Domestic cats (*F. s. catus*) are distributed worldwide and overwhelmingly carry clade IV mtDNA haplotypes (beige). Inset: Current and historical range of *F. silvestris* subspecies on the basis of traditional morphology-based taxonomy (*2*, *12*, *13*). The Chinese desert cat is referred to throughout as a wildcat subspecies, *F. silvestris bieti* (*9*, *12*), as supported by data presented here. (**B**) Phenogram of 851 domestic and wild specimens created on the basis of STRs, *Dps* genetic distance, and minimum evolution (neighbor-joining) algorithm. Color groups correspond to geographic locales specified in (A). Symbols indicate cytonuclear-discordant individuals that contain a STR composite clade of the indicated cluster but carry mtDNA of an alternative locale (see text); in parentheses are the numbers of cats in each STR clade that carry various mtDNA clade haplotypes.

separate *Felis* species, *Felis bieti*, or a wildcat subspecies, *F. silvestris bieti* (*9*, *12*)—is uncertain. The sand cat *F. margarita*, a distinct species of *Felis* that ranges across North Africa and the Middle East, is the closest outgroup of the *F. silvestris/bieti* complex on the basis of morphological and molecular data (*12*, *13*, *20*).

To investigate the relationships among domestic cats, their indigenous wild progenitors, and related species of the genus *Felis*, we collected tissue from 979 individuals (fig. S1; see table S1 for breakdown of number of cats tested for different genetic markers) including putative wildcats and feral domestic cats on three continents ($N = 629$), fancy-breed domestic cats ($N = 112$), sand cats (*F. margarita*, $N = 11$), and Chinese desert cats (*F. s. bieti*, $N = 5$). We extracted DNA and genotyped 851 cats for 36 short tandem repeat (STR) or microsatellite domestic cat loci (*21*) variable in *F. silvestris*, *F. s. bieti*, *F. margarita*, and domestic cats, and sequenced 2604 base pairs (bp) of mitochondrial DNA (mtDNA) genes *ND5* and *ND6* from 742 cats.

Neighbor-joining phylogenetic analyses for STR genotypes with kinship coefficient (*Dkf*) and proportion of shared alleles (*Dps*) genetic distance estimators provided concordant topologies that specified six clusters (Fig. 1B; referred to here as "clades" as also specified by mtDNA phylogenetic analyses; see below) corresponding to the following subspecies designations: (i) *F. s. silvestris*, wildcats from Europe (STR clade I, green in Fig. 1); (ii) *F. s. ornata*, wildcats from central Asia east of the Caspian Sea (STR clade III, purple); (iii) *F. s. lybica*, wildcats from the Near East (STR clade IV, beige); (iv) *F. s. cafra*, wildcats from southern Africa (STR clade II, blue); (v) *F. s. bieti*, Chinese desert cats (STR clade V, red); and (vi) *F. margarita*, sand cat (STR clade VI, black). *Felis cafra* was first named in 1822 and renamed as *F. lybica cafra* subspecies in 1944 on the basis of a description of a wildcat specimen captured in "Kaffraria" (*9*), an area from whence our southern African wildcat samples derive.

The composite STR genotypes of all known domestic house cats, fancy-breed cats, and feral domestic cats occurring in the wild populations all fell within a large monophyletic group (clade IV) that also included wildcats from the Near East. The phylogenetic tree suggests that domestication occurred in the Near East, where STR clade IV wildcats live today. This inference was further explored by examining mtDNA variation, STR variation, and ongoing admixture hybridization in the study areas (*17*–*19*).

Phylogenetic analysis of *ND5* and *ND6* sequence reveals 245 parsimony-informative sites specifying 176 distinct mtDNA genotypes (Fig. 2A, fig. S2, and table S2). The mtDNA haplotypes were analyzed with Bayesian Markov chain Monte Carlo (MCMC), maximum parsimony, maximum likelihood, and distance-based methods (*22*, *23*). All methods resulted in identical topologies for the principal groupings corresponding to both geographic origins and STR clade designations. The consensus mtDNA gene tree (Fig. 2A), rooted with *F. margarita*, shows *F. s. bieti* basal to *F. silvestris*, as inferred from morphology. However, the short branch lengths and relatively weak bootstrap support for the node separating *F. s. bieti* from *F. silvestris* (27 to 68% bootstrap) indicates a close genetic relationship between these two taxa, which supports the grouping of *F. s. bieti* and *F. silvestris* as a single species, *F. silvestris*.

The *F. silvestris* mtDNA haplotypes fall into specific geographic locales (Fig. 2A). A basal lineage [clade I, *F. s. silvestris* (European wildcat), green] is found in European populations from Scotland and Portugal in the west to Hungary and Serbia in the east and is sister to *F. silvestris* from Asia and Africa and to domestic cats. An early/basal European versus Africa-Asia divergence supported by recent morphological studies of fossil specimens of wildcats (*15*, *24*) may reflect a postglacial repopulation of Europe from Iberian founders, as previously suggested (*9*, *15*, *24*). The basal position of an Iberian wildcat, Fsi-257, within mtDNA clade I also supports an Iberian refugium (Fig. 2A).

Beyond Europe, mtDNA clades II, III, and IV correspond with geography and STR analysis (Fig. 2A). Within mtDNA clade IV, we identified five principal lineages of mtDNA haplotypes (A to E, Fig. 2A) with no obvious phylo-geographic association among these lineages. Domestication appears to have occurred within the Near Eastern region where clade IV wildcats are currently extant (beige, Fig. 2A), because clade IV wildcats and domestic cats are monophyletic.

Because of hybridization between wildcats and feral domestic cats, domestic cat mtDNA haplotypes (clade IV in Fig. 2A) are commonly found in European, African, and central Asian populations along with indigenous wildcat haplotypes (Fig. 1A). The observed genetic admixture may be explained by the presence of feral domestic cats or by hybridization between wildcats and domestic cats. Hybrid individuals carrying one mtDNA-clade genotype but a different STR-clade genotype can be identified. Such cytonuclear-discordant individuals were common in our data set (Figs. 1B and 2A). Of cats sampled for both STR and mtDNA genotypes, seven of the 472 cats in STR clade IV were discordant, with a wildcat mtDNA type (Fig. 1B). However, among 108 putative European wildcats (on the basis of STR genotype; Fig. 1B), 28 carried the clade IV (domestic) mtDNA type, as did 3 of 13 southern African (STR clade II) wildcats. The wildcats in central Asia (STR clade III) included the highest frequency of discordant individuals (mtDNA clades III and IV; Fig. 1B), perhaps as a result of incomplete lineage sorting or recent gene flow between adjacent populations (Fig. 2A).

We implemented the Bayesian population genetic analysis program STRUCTURE, which assesses population subdivision (*25*) and characterizes genomic evidence of recent hybridization. STRUCTURE analyses of the 851 STR genotypes placed cats into discrete population clusters corresponding to European, African, and central Asian wildcats and identified a subdivision of domestic cats from different regions (Fig. 2B). Interestingly, we identified a discrete population of wild and domestic cats from the Near East (brown group in Fig. 2B) distinct from the other *F. silvestris* subspecies, as well as three subgroupings of domestic cats. These 15 individuals had concordant mtDNA and STR phylogenies identical to those of domestic cats and were collected in remote deserts of Israel, United Arab Emirates, Bahrain, or Saudi Arabia. These data suggest that these Near Eastern wildcats may represent the ancestral founder population of domestic cats, supporting a domestication origin in the Near East.

Identification of hybrids (STRUCTURE $Q < 0.8$) revealed that some (~22%) of the identified cytonuclear-discordant cats in Figs. 1B and 2A showed evidence of recent hybridization. For this reason, we removed 81 hybrid cats defined by STRUCTURE and generated new phylogenies combining the STR genotypes of cats grouped within the distinct populations (Fig. 2C). This analysis reaffirms the recognition of the major *F. silvestris* subspecies groups illustrated in Fig. 1A and the distinctiveness of Near Eastern wildcats as the closest group to all domestic cats. The results also suggest a close affinity between *F. s. bieti* (Chinese desert cat) and the Asian wildcats, plus paraphyly of other *F. silvestris* subspecies with respect to *F. s. bieti*, in support of the recognition of *F. s. bieti* as a subspecies of *F. silvestris* (Fig. 2C).

The coalescence-based age of mtDNA ancestral nodes for domestic cats (clade IV) and all *F. silvestris* mtDNA lineages was estimated with the linearized tree method (*26*). After fulfilling the requirement for molecular clock rate homogeneity across all lineages (table S4), we constructed a neighbor-joining algorithm on the basis of the linearized tree with Kimura two-parameter distances. We adopted a sequence divergence rate specific for *ND5* and *ND6* genes of 2.24 bp per million years (*27*). This rate would predict one new variant, on average (range: 0 to 2), in the most recent 17,000-year period of domestic cat ancestry (*28*). Indeed, 90% of the domestic cats within the five lineages (A to E in Fig. 2A) share haplotypes that are 0 to 3 bp apart, reflecting modest mutation accumulation within lineages. By contrast, the estimated coalescent date on the basis of the mtDNA data for all *F. silvestris* (including *F. s. bieti*) subspecies is 230,000 years ago, whereas the estimated age for the ancestor of *F. s. lybica* and domestic cats is 131,000 years. Other methods of date estimation suggested a range from 107,000 to 155,000 years (*28*). These estimates are all greater by an order of magnitude than the age implied by archaeological evidence for cat domestication (*6*). The persistence of five well-supported mtDNA lineages dating back 100,000 years before any

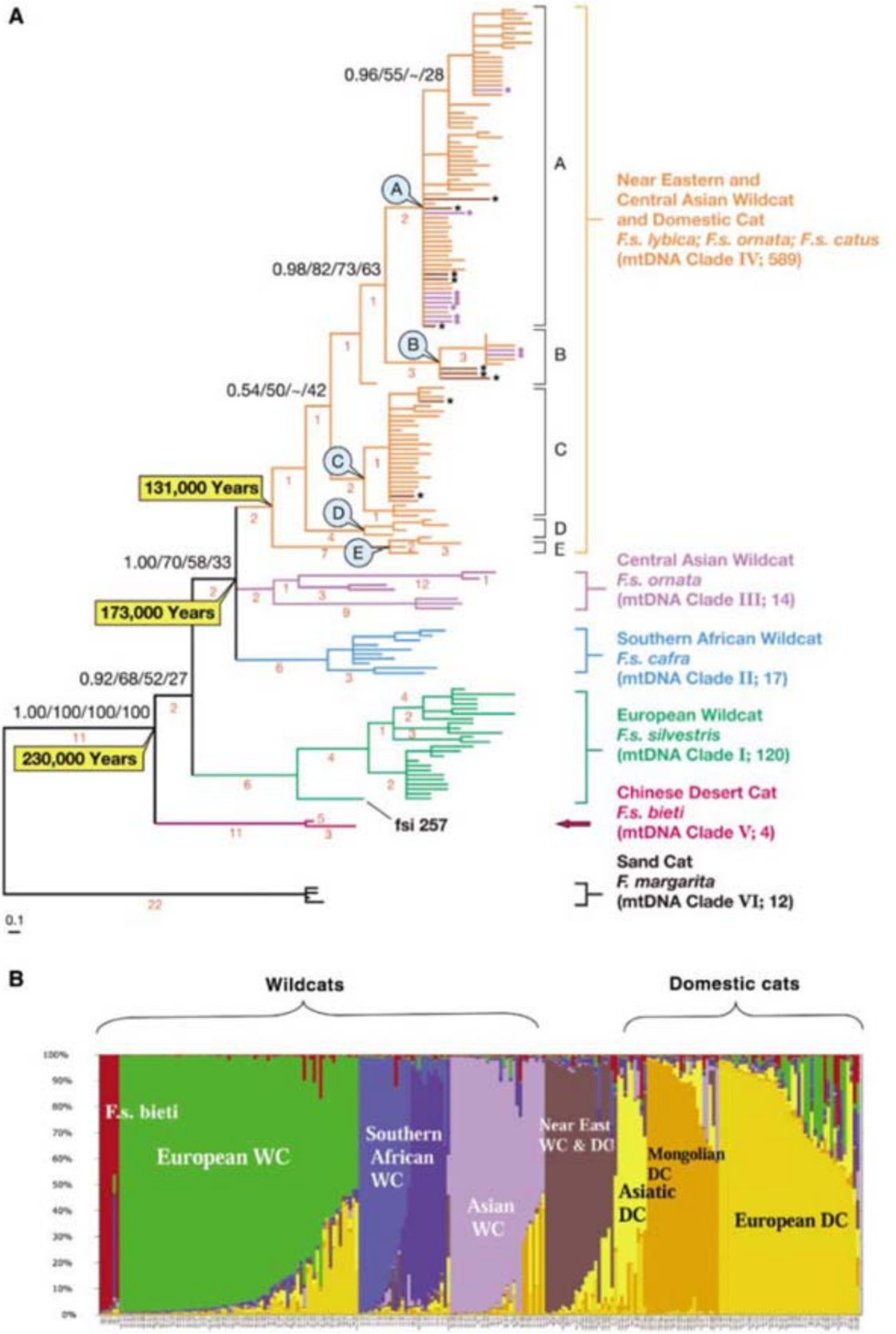

Fig. 2. (**A**) Phylogenetic tree of mitochondrial DNA sequence [minimum evolution (neighbor-joining) phylogram of 2604 bp of the *ND5* and *ND6* genes] of 176 haplotypes discerned from 742 cats sampled across the range of the domestic cat, European wildcat, Near Eastern wildcat, central Asian wildcat, southern African wildcat, Chinese desert cat, and sand cat. Trees created from Bayesian, maximum likelihood, and maximum parsimony methods result in identical topologies for principal clade groupings. Confidence/bootstrap values (from left to right: Bayes/maximum parsimony/maximum likelihood/minimum evolution) are based on 1000 iterations and are adjacent to nodes. The number of single-nucleotide differences is indicated in red below the corresponding branch. Clade designations and numbers of individuals are indicated in parentheses after the corresponding common name and taxonomic trinomial. A through E designate lineages within mtDNA clade IV. Confidence/bootstrap values for these nodes are as follows: A, 1.00/87/71/54; B, 1.00/82/80/80; C, 0.97/63/59/42; D, 1.00/98/99/88; E, 1.00/100/100/82. Purple and brown tree limbs within mtDNA clade IV reflect individuals from two locales that bear cytonuclear-discordant mtDNA versus STR genotypes (see text). Clade IV individuals bearing mtDNA haplotypes are found among domestic cats; in wild potentially admixed populations in Europe, Asia, or Africa (see Fig. 1A); and in Near Eastern wildcats (see text). (**B**) STRUCTURE-based populations resolved 851 cats into several wildcat groups, three domestic cat groups, and one group (brown) that included both domestic cats and Near Eastern wildcats. The *y* axis represents *Q*-value, the percent representation of resolved populations (colors) within each individual (listed on *x* axis). (**C**) Phylogenetic relationships among *F. silvestris* groups as defined by composite STR genotypes based on 36 STR loci. Tree is rooted at sand cat. Bootstrap values at corresponding nodes are based on 1000 iterations with the following measures (from left to right): $Dps = 1 - (ps)/Dkf = 1 - (kf)/Dps = -\ln(ps)/Dkf = -\ln(kf)$. All methods resulted in identical topologies. Individuals were clustered into representative populations based on STRUCTURE *Q*-value of 0.80 or greater with the same loci (see text). All known domestic cats cluster into domestic-Asia, domestic-Europe, or Near Eastern wildcats, regardless of provenance, and these groups also cluster together.

archaeological record of domestication would suggest that domestic cats originated from at least five matrilineal mtDNA haplotypes.

The variation described here is important for the conservation and management of free-ranging wildcat populations (*16*, *29*). In table S6 we present a full list of population-specific (private) STR alleles as well as mtDNA population-specific site genotypes suitable for assessment of a wildcat's population, subspecies of origin, and distinction from domestic cats. The domestication of wild species to complement human civilization stands as one of the more successful "biological experiments" ever undertaken. For cats, the process began more than 9000 years ago when the earliest

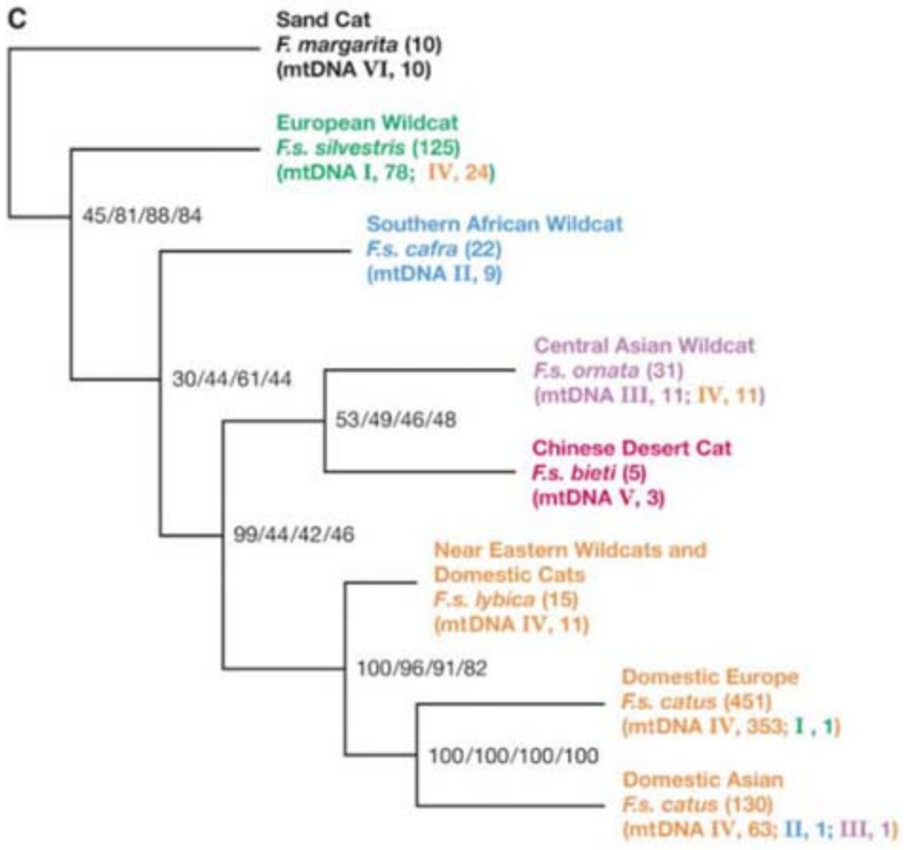

farmers of the Fertile Crescent domesticated grains and cereals as well as livestock (*1*, *3*, *4*, *30*–*32*). In parallel, the endemic wildcats of the region may have adapted by both regulating the rodents in the grain stores and abandoning their aggressive wild-born behaviors. The archaeological imprints left in the genomes of living cats here weigh into inferences about the timing, steps, and provenance of domestication—a dynamic exercise depicted in art, in history, and in human cultural development since recorded evidence began.

References and Notes

1. J. A. Clutton-Brock, *Natural History of Domesticated Mammals* (Cambridge Univ. Press, Cambridge, 1999).
2. A. Kitchener, *The Natural History of the Wild Cats* (Comstock Associates, Ithaca, NY, 1991).
3. G. Stephens, T. Yamazaki, *Legacy of the Cat: The Ultimate Illustrated Guide* (Chronicle, San Francisco, 2001).
4. S. Budiansky, *The Covenant of the Wild: Why Animals Chose Domestication* (Yale Univ. Press, New Haven, CT, 1999).
5. J. M. Legay, *C. R. Acad. Sci. III* **303**, 709 (1986).
6. J.-D. Vigne, J. Guilaine, K. Debue, L. Haye, P. Gérard, *Science* **304**, 259 (2004).
7. M. D. Donalson, *The Domestic Cat in Roman Civilization* (Mellen, New York, 1999).
8. B. Kurten, *Acta Zool. Fenn.* **111**, 3 (1965).
9. R. I. Pocock, *Catalogue of the Genus* Felis (British Museum–Natural History, London, 1951).
10. C. M. Vella, L. M. Shelton, J. J. McGonagle, T. W. Stanglein, *Robinson's Genetics for Cat Breeders & Veterinarians* (Elsevier Science, Edinburgh, 2003).
11. D. W. Macdonald *et al.*, *Adv. Ethol.* **28**, 1 (1987).
12. K. Nowell, P. Jackson, *Status Survey and Conservation Action Plan, Wild Cats* (International Union for Conservation of Nature and Natural Resources, Gland, Switzerland, 1996).
13. M. E. Sunquist, F. Sunquist, *Wild Cats of the World* (Univ. of Chicago Press, Chicago, 2002).
14. R. I. Pocock, *Proc. Zool. Soc. London* **1907**, 656 (1907).
15. E. Randi, B. Ragni, *J. Mammal.* **72**, 79 (1991).
16. D. W. Macdonald, M. J. Daniels, C. Driscoll, A. C. Kitchener, N. Yamaguchi, *The Scottish Wildcat: Analyses for Conservation and an Action Plan* (Wildlife Conservation Research Unit, Oxford, 2004).
17. M. Beaumont *et al.*, *Mol. Ecol.* **10**, 319 (2001).
18. E. Randi *et al.*, *Mol. Biol. Evol.* **18**, 1679 (2001).
19. R. Lecis *et al.*, *Mol. Ecol.* **15**, 119 (2006).
20. W. E. Johnson *et al.*, *Science* **311**, 73 (2006).
21. M. Menotti-Raymond *et al.*, *Cytogenet. Genome Res.* **102**, 272 (2003).
22. D. L. Swofford, *Phylogenetic Analysis Using Parsimony (PAUP)* (Natural History Survey, Champaign, IL, 1985).
23. J. P. Huelsenbeck, F. Ronquist, *Bioinformatics* **17**, 754 (2001).
24. N. Yamaguchi *et al.*, *Anim. Conserv.* **7**, 339 (2004).
25. J. K. Pritchard, P. Donnelly, *Theor. Popul. Biol.* **60**, 227 (2001).
26. N. Takezaki *et al.*, *Mol. Biol. Evol.* **12**, 828 (1995).
27. J. V. Lopez, M. Culver, J. C. Stephens, W. E. Johnson, S. J. O'Brien, *Mol. Biol. Evol.* **14**, 277 (1997).
28. See supporting material on *Science* Online.
29. S. J. O'Brien, W. E. Johnson, *Annu. Rev. Genomics Hum. Genet.* **6**, 407 (2005).
30. K. Tanno, G. Willcox, *Science* **311**, 1886 (2006).
31. G. Willcox, in *13th IWGP Symposium*, R. Buxo, S. Jacomet, F. Bitmann, Eds. (Springer, Girona, Spain, 2005), pp. 534–541.
32. P. L. Morrell, M. T. Clegg, *Proc. Natl. Acad. Sci. U.S.A.* **104**, 3289 (2007).

33. We thank M. W. Smith, A. Schmidt-Kuntzel, C. O'hUigen, and B. Gold for discussions and J. Bruksch, A. Brandt, S. Rosendale, and F. Hussain for technical assistance. We appreciate the efforts of all of our collaborators listed in fig. S1 who provided biological specimens used in this study. All tissues were collected in full compliance with federal fish and wildlife permits [Convention on International Trade in Endangered Species of Wild Fauna and Flora (CITES)] issued to the National Cancer Institute (NCI; principal officer, S.J.O.) by the Fish and Wildlife Service, U.S. Department of the Interior. Supported by NCI grant N01-CO-12400 and the Intramural Research Program of the NCI Center for Cancer Research. Sequences have been deposited in GenBank with accession numbers EF587016 to EF587179.

Supporting Online Material

www.sciencemag.org/cgi/content/full/1139518/DC1
SOM Text
Tables S1 to S6
Figs. S1 and S2
References

4 January 2007; accepted 18 June 2007
Published online 28 June 2007;
10.1126/science.1139518
Include this information when citing this paper.

Candidatus Chloracidobacterium thermophilum: An Aerobic Phototrophic Acidobacterium

Donald A. Bryant,[1]* Amaya M. Garcia Costas,[1] Julia A. Maresca,[1]† Aline Gomez Maqueo Chew,[1]‡ Christian G. Klatt,[2] Mary M. Bateson,[2] Luke J. Tallon,[3] Jessica Hostetler,[3] William C. Nelson,[3] John F. Heidelberg,[3,4] David M. Ward[2]

Only five bacterial phyla with members capable of chlorophyll (Chl)–based phototrophy are presently known. Metagenomic data from the phototrophic microbial mats of alkaline siliceous hot springs in Yellowstone National Park revealed the existence of a distinctive bacteriochlorophyll (BChl)–synthesizing, phototrophic bacterium. A highly enriched culture of this bacterium grew photoheterotrophically, synthesized BChls a and c under oxic conditions, and had chlorosomes and type 1 reaction centers. "*Candidatus* Chloracidobacterium thermophilum" is a BChl-producing member of the poorly characterized phylum *Acidobacteria*.

Sequencing environmental DNA is a powerful approach for predicting the physiological and metabolic potential of microbial ecosystems. Metagenomic analyses have provided insights into the properties of uncultured microorganisms that have escaped detection in field studies (*1*–*6*). We used metagenomic data from the microbial mat communities

of Octopus and Mushroom Springs in Yellowstone National Park (Yellowstone NP) (*5*–*7*) to search for previously unrecognized BChl/Chl-synthesizing phototrophs (chlorophototrophs).

Only five bacterial phyla contain chlorophototrophs: *Cyanobacteria*, *Chlorobi*, *Proteobacteria*, *Chloroflexi*, and *Firmicutes* (*8*, *9*). In chlorophototrophs, light energy is transduced into chemical potential energy by reaction centers, photo-oxidoreductases that form two families of BChl/Chl-containing, pigment-protein complexes (*10*). Type 1 reaction centers include cyanobacterial Photosystem I and the homodimeric reaction centers of *Chlorobi* and heliobacteria (*Firmicutes*). Type 2 reaction centers include cyanobacterial Photosystem II and the reaction centers of *Proteobacteria* and *Chloroflexi*. Although their subunits are not discernibly similar in sequence, the two reaction-center types probably share a common evolutionary origin because their electron-transfer domains have similar structures and cofactor arrangements (*11*).

16*S* ribosomal RNA (rRNA) surveys of the Yellowstone NP phototrophic mat communities suggested the presence of green sulfur bacteria (*12*). Metagenomic data obtained from these mats (*5*–*7*, *9*) were queried with the tblastn algorithm and the amino acid sequence of PscA, the BChl a–binding apoprotein of a homodimeric, P840-binding, type 1 reaction center from *Chlorobium tepidum* (*9*, *13*). Two incomplete sequences that encode (B)Chl-binding apoproteins of type 1 reaction centers were recovered. Phylogenetic analyses suggested that one sequence (OS GSB PscA) belonged to a green sulfur bacterium that grouped with PscA from *Chloroherpeton thalassium* (Fig. 1A). The second sequence, labeled Cab. thermophilum PscA, was only very distantly related to other PscA sequences and other type 1 reaction-center proteins (Fig. 1A and figs. S1 to S3); this suggested the existence of a previously unrecognized chlorophototroph in the mat community. Plasmids encoding this gene were recovered and sequenced (*9*), and the data revealed a probable operon, 5′*pscAB-fmoA* (Fig. 1B). *pscB* encodes the apoprotein of an 8Fe-8S ferredoxin of a type 1 reaction center (*13*), and *fmoA* encodes the BChl a–binding, Fenna-Matthews-Olson protein (Fig. 1B and figs. S4 and S5) (*14*). The *pscA* gene predicted a protein of 865 amino acids that was larger than the apoproteins of other type 1 reaction centers. Most of the size difference was caused by an insertion of ~165 amino acids into a periplasmic loop between transmembrane α helices VII and VIII (Fig. 1C and fig. S1). Many of the genes flanking the *pscAB-fmoA* operon predicted proteins that were most similar to those of *Acidobacterium* sp. Ellin345 or *Solibacter usitatus* Ellin6076, two soil bacteria belonging to the poorly characterized phylum *Acidobacteria*, whose genomes were recently sequenced. Thus, we hypothesized that the unknown phototroph might belong to the phylum *Acidobacteria*.

Analyses of metagenomic sequence data and end-reads from a bacterial artificial chromosome (BAC) library predicted that the *pscAB-fmoA*, *recA*, and rRNA genes were encoded on a single BAC insert (*9*). We confirmed this prediction by sequencing the 271,846–base pair (bp) insert (fig. S6; GenBank accession number EF531339). The 16*S* rRNA sequence derived from this BAC clone was identical to a partial sequence assembled from the metagenome and was nearly identical (differences at 2 of 1348 shared positions) to that from an acidobacterium denoted GFP1 [see 16*S* rRNA tree in figure 1 of (*15*); or see (*16*)] (fig. S7). The 16*S* rRNA of GFP1 was recovered from Green Finger Pool in the Lower Geyser Basin of Yellowstone NP, a site ~5 km from Octopus Spring. These data unequivocally establish that the divergent *pscAB-fmoA* genes are derived from a GFP1-like organism belonging to the phylum *Acidobacteria*.

To gain insights into the physiology and metabolism of this GFP1-like organism, we computer-annotated and analyzed the binned sequence assemblies putatively derived from the GFP1-like acidobacterium (*9*). The binned sequences contained several genes for BChl (*bchG*, *bchK*, *bchR*, *bchU*, *bchY*, and *acsF*) and carotenoid (*crtB*, *crtP*, and *crtH*) biosynthesis (figs. S6 to S10). A *csmA* gene, the product of

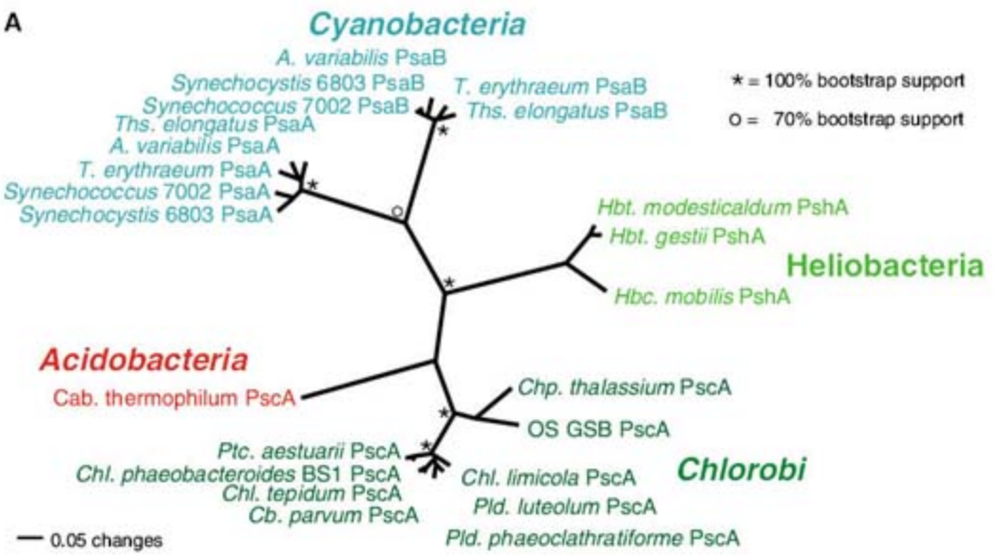

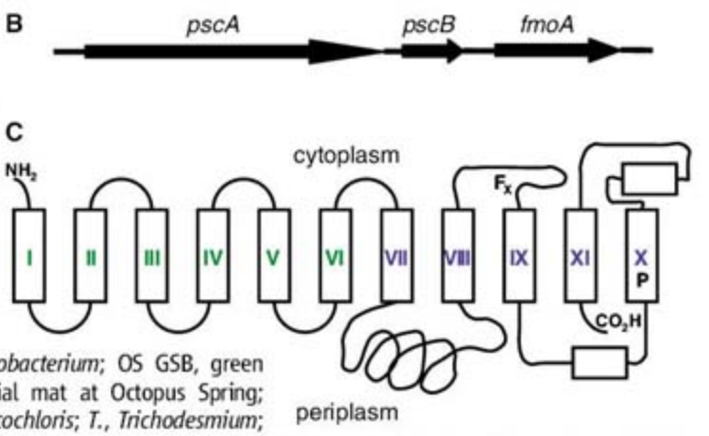

Fig. 1. (**A**) Unrooted neighbor-joining tree of protein sequences for type 1 reaction centers from *Cyanobacteria*, *Chlorobi*, heliobacteria, and a divergent PscA-like sequence (Cab. thermophilum) obtained from the mat metagenome of Octopus and Mushroom Springs, Yellowstone NP. *A.*, *Anabaena*; Cab., Chloracidobacterium; *Cb.*, *Chlorobaculum*; *Chl.*, *Chlorobium*; *Chp.*, *Chloroherpeton*; *Hbc.*, *Heliobacillus*; *Hbt.*, *Heliobacterium*; OS GSB, green sulfur bacterium from microbial mat at Octopus Spring; *Pld.*, *Pelodictyon*; *Ptc.*, *Prosthecochloris*; *T.*, *Trichodesmium*; *Ths.*, *Thermosynechococcus*. Nodes marked with a "*" have 100% bootstrap support; the node separating the PsaA and PsaB clades is marked with a "**o**" and has 70% bootstrap support. (**B**) Organization of the *pscA*, *pscB*, and *fmoA* genes in Cab. thermophilum. (**C**) Diagram showing the organization of the 11 predicted transmembrane α helices of Cab. thermophilum PscA. "F_X" denotes the positions of two cysteine residues that are predicted to be ligands to the intersubunit [4Fe-4S] cluster F_X, and "P" indicates the approximate position of the conserved histidine residue predicted to form a ligand to one of the two predicted BChl a molecules of the reaction-center special pair. Green Roman numerals I to VI indicate the antenna domain, and blue Roman numerals VII to XI indicate the electron-transfer domain.

[1]Department of Biochemistry and Molecular Biology, The Pennsylvania State University, University Park, PA 16802, USA. [2]Department of Land Resources and Environmental Sciences, Montana State University, Post Office Box 173120, Bozeman, MT 59717–3120, USA. [3]The Institute for Genomic Research, 9712 Medical Center Drive, Rockville, MD 20850, USA. [4]Department of Biology, University of Southern California, Wrigley Marine Science Center, Post Office Box 5069, Avalon, CA 90704, USA.

*To whom correspondence should be addressed. E-mail: dab14@psu.edu

†Present address: Department of Civil and Environmental Engineering, Massachusetts Institute of Technology, Cambridge, MA 02139, USA.

‡Present address: Department of Microbiology, Ohio State University, Columbus, OH 43210, USA.

which forms the baseplate of chlorosomes, the light-harvesting antenna complexes in *Chlorobi* and *Chloroflexi* (*17*), was also found. The presence of genes encoding subunits of a nicotinamide adenine dinucleotide, reduced (NADH): quinone oxidoreductase, the quinol:cytochrome c oxidoreductase, and cytochrome oxidase implied that the acidobacterium might respire aerobically. The data collectively predicted that the mat acidobacterium is probably an aerobic photoheterotroph that synthesizes BChl a, methylated BChl c, chlorosomes, FmoA, and type 1 reaction centers. The organism seemed physiologically most similar to aerobic anoxygenic phototrophs or to facultatively photo(auto/hetero)trophic organisms like *Roseiflexus* and *Chloroflexus* spp. (*8*).

Allewalt *et al.* (*18*) described the establishment of uni-cyanobacterial enrichments for thermophilic *Synechococcus* spp. from Octopus Spring (Fig. 2A). The presence of a closely related acidobacterium in an oxic enrichment was indicated by specific polymerase chain reaction (PCR) amplification of genes for acidobacterial *pscA*, *fmoA*, *csmA*, *acsF*, *bchU*, *recA*, and 16*S* rRNA (*9*) (table S1). By serially culturing this enrichment culture in a modified cyanobacterial growth medium containing ammonium, a mixture of carbon sources, and the Photosystem II inhibitor atrazine (*9*), we eliminated *Synechococcus* sp. strain JA-2-3B'a (2-13). The resulting brownish-orange culture contained only the acidobacterium and *Anoxybacillus* sp. (Fig. 2A). The latter could be isolated on Luria-Bertani plates, did not synthesize BChl (Fig. 2A), and did not possess any genes for BChl biosynthesis or formation of a light-harvesting apparatus. The absorption spectrum of the enrichment culture shows a maximum at 743 to 745 nm that is characteristic of BChl c aggregates in chlorosomes (Fig. 2B). Using a method for the isolation of chlorosomes from green sulfur bacteria (*9*), we isolated chlorosomes that were morphologically similar to those of *C. tepidum* (*17*) (Fig. 3). Serial culturing of the *Anoxybacillus* sp.–acidobacterium enrichment in the dark resulted in the simultaneous loss of the 746-nm absorbance (Fig. 2B) and acidobacterial 16*S* rRNA (Fig. 2C). This experiment definitively establishes that the acidobacterium grows photoheterotrophically. The enrichment did not grow with bicarbonate as the sole carbon source.

High-performance liquid chromatography (HPLC) analyses of pigments extracted from cells from the *Anoxybacillus* sp.–acidobacterium enrichment verified the presence of both BChl c and BChl a (Fig. 4). The complex pattern of BChl c homologs, appearing in groupings of four (fig. S13), was consistent with methylation of both the C-8^2 and C-12^1 carbons, as occurs in *C. tepidum* and other *Chlorobi* strains (*19*). The elution profile also indicated that BChl c was esterified by several alcohol species. Only trace amounts of farnesylated BChl c were detected, and the major BChl c homologs were more hydrophobic than farnesylated BChl c, the esterifying alcohol most commonly found in green sulfur bacteria (Fig. 4). The major BChl c homologs were slightly more hydrophobic than the BChl c homologs produced by *Chloroflexus aurantiacus* Y-400-fl (Fig. 4). However, *Chloroflexus* spp. do not methylate BChl c at the C-8^2 or C-12^1 positions, and their BChl c is typically esterified with multiple alcohols including phytol, geranylgeraniol, and stearol (*8*, *19*).

16*S* rRNA analyses, including the present study, indicate that the acidobacterial chlorophototroph grows at temperatures from ~50° to 66°C at Mushroom Spring, Octopus Spring, and Green Finger Pool (*15*, *20*). 16*S* rRNA sequences closely related to that of this acidobacterium have also been recovered from Mammoth Hot Springs in Yellowstone NP and from hot springs in Tibet and Thailand (*21*, *22*). Therefore, acidobacterial chlorophototrophs may be members of microbial mat communities associated with thermal features worldwide. Because strains of *Acidobacteria* are also widely distributed in soils and other environments (*15*, *23*), it will be interesting to determine whether phototrophy is widespread in this poorly characterized phylum. Analyses of the genomes of two acidobacteria, *S. usitatus* Ellin6076 and *Acidobacterium* sp. Ellin345, demonstrate that these organisms do not have this capability (*24*).

In this study we applied metagenomics to discover a previously unknown chlorophototroph, and we used enrichment techniques and biochemical methods to verify that this organism is a bacillus (Fig. 2, D and E) that synthesizes BChls

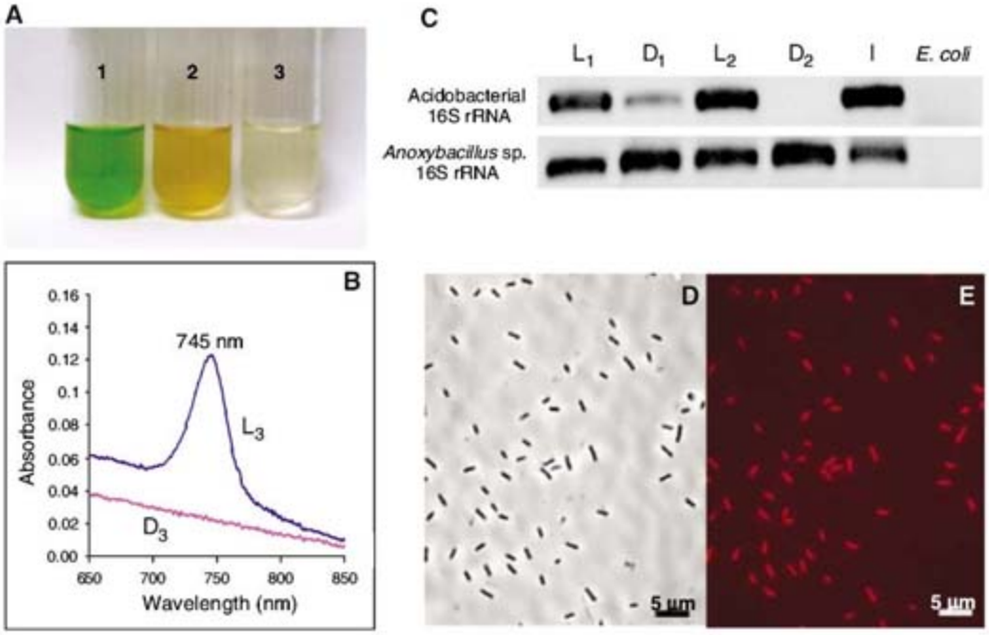

Fig. 2. (**A**) Cultures containing (1) *Synechococcus* sp. strain JA-2-3B'a (2-13), Cab. Thermophilum, and *Anoxybacillus* sp.; (2) Cab. thermophilum and *Anoxybacillus* sp.; and (3) *Anoxybacillus* sp. (**B**) Absorption spectra of an enrichment culture containing Cab. thermophilum and *Anoxybacillus* sp. after serial culturing three times in the light (L_3) or in the dark (D_3). The 745-nm absorption due to aggregated BChl c is only observed in the light-grown cells. Note the change from 746 to 745 nm to match the number in the figure. (**C**) PCR amplification with the use of primers (*9*) (table S1) specific for Cab. thermophilum (top) and *Anoxybacillus* sp. (bottom) and DNA templates isolated from an initial light-grown inoculum (I), and serial cultures 1 and 2 grown for two periods of 5 days exclusively in the light (L_1, L_2) or in the dark (D_1, D_2). *Escherichia coli* DNA was tested as a negative control with both primer sets. For additional details, see (*9*). (**D**) Light micrograph of a 5-day-old enrichment culture containing Cab. thermophilum and *Anoxybacillus* sp. grown in the light. (**E**) Fluorescence micrograph of the field of cells in (D). Cells were treated with 1-hexanol to disrupt the BChl c aggregates and to enhance BChl c fluorescence (*9*).

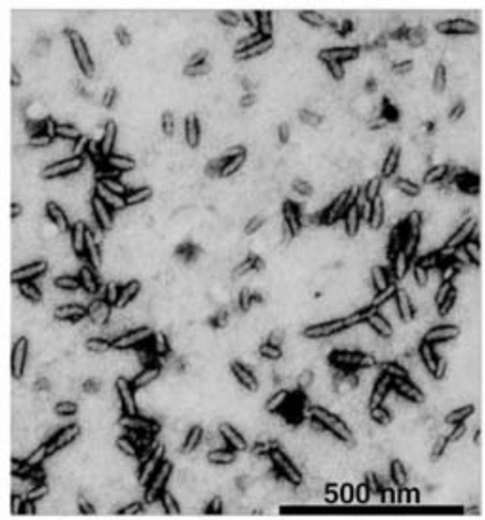

Fig. 3. Transmission electron micrograph of isolated chlorosomes from an enrichment culture containing Cab. thermophilum and *Anoxybacillus* sp. after negative staining with 1% (w/v) uranyl acetate.

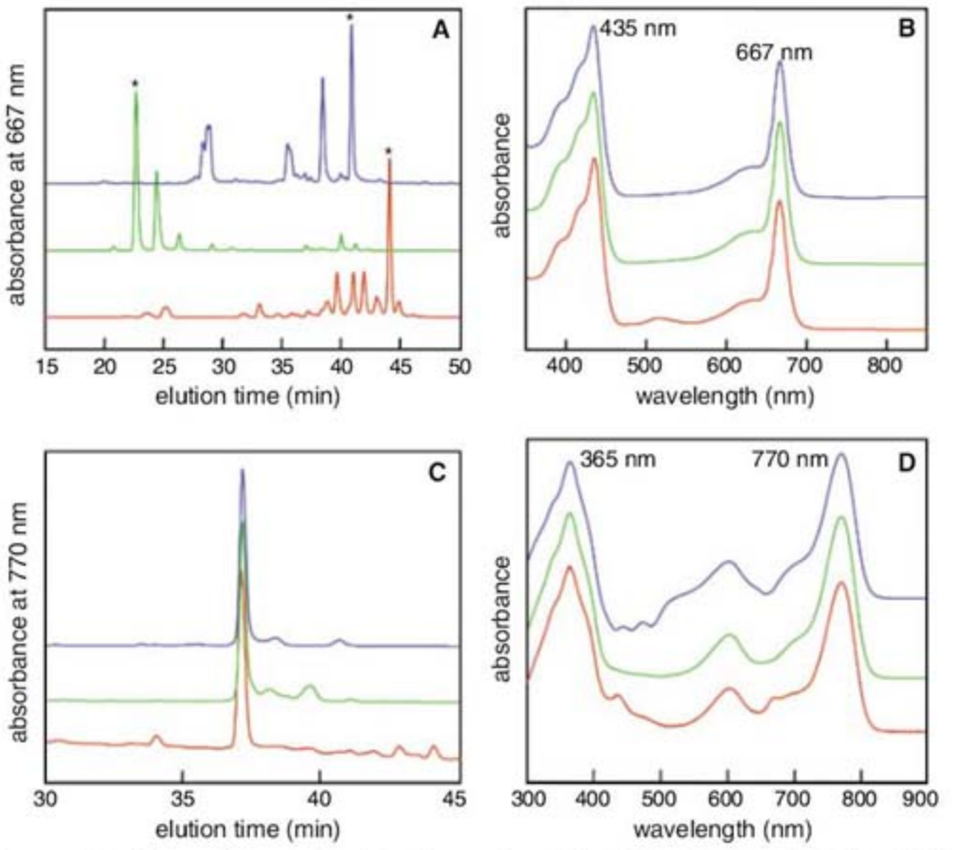

Fig. 4. HPLC elution profiles monitored at 667 nm for BChl c (**A**) and 770 nm for BChl a (**C**) for pigments extracted from a light-grown culture containing Cab. thermophilum and *Anoxybacillus* sp. (red line); *Chlorobium tepidum* (green line); and *Chloroflexus aurantiacus* strain Y-400-fl (blue line). The spectra of the BChl c peaks indicated by stars in (A) are shown in (**B**); the spectra of the BChl a peaks eluting at 37 min in (C) are shown in (**D**). All other peaks in (A) also had the absorption spectrum of BChl c.

a and c and produces chlorosomes under oxic conditions. Although chlorosomes are also found in some *Chloroflexi*, the new chlorophototroph is the only described organism outside the phylum *Chlorobi* that produces FmoA. Growth of this acidobacterium is strongly stimulated by light under photoheterotrophic conditions, but additional studies will be required to establish whether the organism is capable of autotrophic growth. Because no chlorophototroph with these properties has yet been described, we propose the name "*Candidatus* Chloracidobacterium thermophilum," gen. nov., sp. nov., for this BChl-synthesizing, phototrophic member of the phylum *Acidobacteria*.

References and Notes

1. J. C. Venter *et al.*, *Science* **304**, 66 (2004).
2. G. W. Tyson *et al.*, *Nature* **428**, 37 (2004).
3. S. G. Tringe *et al.*, *Science* **308**, 554 (2005).
4. E. F. DeLong, *Nat. Rev. Microbiol.* **3**, 459 (2005).
5. A. S. Steunou *et al.*, *Proc. Natl. Acad. Sci. U.S.A.* **103**, 2398 (2006).
6. D. M. Ward *et al.*, *Heredity* 10.1038/sj.hdy.6801011 (6 June 2007).
7. www.tigr.org/tdb/ENVMGX/YNPHS/
8. D. A. Bryant, N.-U. Frigaard, *Trends Microbiol.* **14**, 488 (2006).
9. Supporting material is available on *Science* Online.
10. J. H. Golbeck, *Proc. Natl. Acad. Sci. U.S.A.* **90**, 1642 (1993).
11. W.-D. Schubert *et al.*, *J. Mol. Biol.* **280**, 297 (1998).
12. D. M. Ward, M. J. Ferris, S. C. Nold, M. M. Bateson, *Microbiol. Mol. Biol. Rev.* **62**, 1353 (1998).
13. G. Hauska, T. Schoedl, H. Remigy, G. Tsiotis, *Biochim. Biophys. Acta* **1507**, 260 (2001).
14. A. Camara-Artigas, R. E. Blankenship, J. P. Allen, *Photosynth. Res.* **75**, 49 (2003).
15. S. M. Barns, S. L. Takala, C. R. Kuske, *Appl. Environ. Microbiol.* **65**, 1731 (1999).
16. http://greengenes.lbl.gov/Download/Taxonomic_Outlines/
17. N.-U. Frigaard, D. A. Bryant, in *Complex Intracellular Structures in Prokaryotes*, J. M. Shively, Ed. (Springer, Berlin, 2006), pp. 79–114.
18. J. P. Allewalt *et al.*, *Appl. Environ. Microbiol.* **72**, 544 (2006).
19. A. Gomez Maqueo Chew, D. A. Bryant, *Annu. Rev. Microbiol.* 10.1146/annurev.micro.61.080706.093242 (5 June 2007).
20. D. M. Ward *et al.*, *Philos. Trans. R. Soc. London B Biol. Sci.* **361**, 1997 (2006).
21. P. Kanokratana, S. Chanapan, K. Pootanakit, L. Eurwilaichitr, *J. Basic Microbiol.* **44**, 430 (2004).
22. L. C. Yim, J. Hongmei, J. C. Aitchison, S. B. Pointing, *FEMS Microbiol. Lett.* **57**, 80 (2006).
23. A. Quaiser *et al.*, *Mol. Microbiol.* **50**, 563 (2003).
24. http://genome.jgi-psf.org

25. This work was supported by NSF grant MCB-0523100 and U.S. Department of Energy grant DE-FG02-94ER20137 (to D.A.B.). The metagenomics database used in this work was created under the auspices of grant EF-0328698 from the Frontiers in Integrative Biology Program of the NSF (to D.M.W.), who also acknowledges support from the NASA Exobiology Program (NAG5-8824). D.A.B. thanks S. Schuster, J. Eisen, R. Blankenship, R. Casterholz, and S. Giovannoni for helpful discussions and comments on the manuscript. D.A.B. and D.M.W. also gratefully acknowledge the Thermal Biology Institute of Montana State University (NASA NAG5-8807) for support and hospitality while D.A.B. was a visiting fellow in summer 2005, when this work was initiated. We thank M. Melendrez and Q. Tao for preparation of the BAC library. The *pscAB-fmoA*, *recA*, and rRNA genes were encoded on a single BAC clone, M60-018 J19: GenBank accession number EF531339. *Roseiflexus* sp. isolate, strain RS1: GenBank accession number AAQU00000000. *Synechococcus* sp. OS-A and OS-B' genome sequences: GenBank accession numbers CP000239 and CP000240.

Supporting Online Material

www.sciencemag.org/cgi/content/full/317/5837/523/DC1
Methods
SOM Text
Figs. S1 to S13
Table S1
References

30 March 2007; accepted 27 June 2007
10.1126/science.1143236

Noise in Gene Expression Determines Cell Fate in *Bacillus subtilis*

Hédia Maamar,† Arjun Raj,*† David Dubnau‡

Random cell-to-cell variations in gene expression within an isogenic population can lead to transitions between alternative states of gene expression. Little is known about how these variations (noise) in natural systems affect such transitions. In *Bacillus subtilis*, noise in ComK, the protein that regulates competence for DNA uptake, is thought to cause cells to transition to the competent state in which genes encoding DNA uptake proteins are expressed. We demonstrate that noise in *comK* expression selects cells for competence and that experimental reduction of this noise decreases the number of competent cells. We also show that transitions are limited temporally by a reduction in *comK* transcription. These results illustrate how such stochastic transitions are regulated in a natural system and suggest that noise characteristics are subject to evolutionary forces.

Variability in gene expression within a population of genetically identical cells enables those cells to maintain a diversity of phenotypes, potentially enhancing fitness (*1*, *2*). When the underlying gene network contains regulatory positive feedback loops, indi-

vidual cells can exist in different states; some cells may, for example, live in the "off" expression state of a particular gene, whereas others are in the "on" expression state (this is an example of bistable gene expression). These stochastic fluctuations in gene expression, commonly referred to as noise, have been proposed to cause transitions between these states (*3*–*7*). We apply recently developed theories of noise (*8*, *9*) to examine how noise influences these transitions in a natural system.

An example of bistable expression with associated stochastic transitions (*10*–*16*) involves the ability of the soil bacterium *Bacillus subtilis* to develop "competence" for DNA uptake as it enters stationary growth phase, potentially allowing bacteria to increase their fitness by incorporating new genetic material. The genes needed for competence are transcribed only in the presence of ComK, the master regulator of competence. *comK* expression is subject to positive autoregulation effected by the cooperative binding of ComK to its own promoter (Fig. 1A) (*17*–*19*), resulting in bistability (*5*). In one state, the positive autoregulatory loop is not activated and *comK* expression is low, and in the other state, the loop is activated because the level of ComK has exceeded a critical threshold and *comK* expression is high (*13*, *14*).

The capacity for bistability is subject to temporal regulation. While the cells are growing exponentially, the level of ComK is kept low (i) through the action of the MecA-ClpC-ClpP protease complex, which actively degrades the ComK protein, and (ii) by transcriptional repressors such as Rok, AbrB, and CodY, precluding transitions to the competent state. Upon reaching stationary phase, the accumulation of an extracellular peptide causes an increase in the expression of the ComS protein (*20*) (the time of the onset of stationary phase is denoted as T_0) (Fig. 1B). ComS competes with ComK for binding to the MecA-ClpC-ClpP complex (*21*), effectively lowering the rate of ComK degradation and allowing random fluctuations in the level of ComK to occasionally cause transitions to the competent state. Cells continue to randomly transition to competence for 2 hours, by which time (T_2) transitions have ceased to occur (*16*) and the 15% of the cells that have become competent remain so until diluted into fresh growth medium (Fig. 1C and movie S1). In this report, we ask why cells only transition to competence for a limited duration of time and investigate the source of the fluctuations that actuate the ComK feedback loop in a minority of cells.

To understand why cells only transition to the competent state for ~2 hours during stationary phase, we examined the dynamics of *comK* expression in noncompetent cells. Because the level of ComK in noncompetent cells is very low, we used fluorescence in situ hybridization (FISH) to count individual *comK* mRNA molecules in single cells (*22*–*24*). We achieved this level of sensitivity by using six fluorescently labeled single-stranded DNA probes, complementary to different regions of the *comK* mRNA (Fig. 2A, left). The hybridization of many fluorophores to individual mRNA molecules resulted in spots that are visible through a fluorescence microscope (Fig. 2, B and C).

During late exponential and early stationary phase in the wild-type (WT) strain, the mean number of *comK* mRNA molecules increased from 0.7 to 1 molecules per cell at T_0, at which point transitions to competence begin to occur. Thereafter, the average number of *comK* transcripts per noncompetent cell declined to 0.3 molecules per cell at T_2 (Fig. 2, D and E).

We postulated that in early stationary phase, when the average mRNA level is elevated, the probability of transition is high because of the increased likelihood of randomly generating enough ComK to activate the positive feedback loop. Later in stationary phase, when the average is low, the probability of such an accumulation is much smaller. To test this possibility, we counted the number of *comK* mRNA molecules in a strain that cannot synthesize Rok, the transcriptional repressor of *comK*. Inactivation of *rok* does not change the temporal pattern of competence expression but markedly increases the fraction of competent cells (*14*). The average number of *comK* mRNA molecules per noncompetent cell in this strain was twice as large as that in the WT strain at T_0 (Fig. 2D), in accordance with the larger number of competent cells observed in the *rok* strain (*14*, *25*).

It is possible that the increased rate of transition to competence observed at T_0 is not caused by the increased basal rate of *comK* transcription but is rather the cause of the increased transcription rate, because of positive feedback at the *comK* promoter. This possibility was eliminated by measuring the *comK* promoter activity in a strain lacking a functional *comK* gene but instead having the *comK* promoter drive a sequence consisting of a 50–base pair (bp) motif repeated 32 times (*comK-M2*). The corresponding mRNA was detected with a single-stranded DNA probe complementary to the 50-bp sequence (Fig. 2A, right). We found that the number of these mRNAs in a strain lacking an active *comK* gene was similar to that in the WT strain (Fig. 2E), indicating that positive feedback does not play a role in *comK* expression in noncompetent cells. To further verify that the *comK-M2* construct had similar expression properties to those of the endogenous *comK* mRNA, we integrated the construct in the WT strain and simultaneously measured the abundance of transcripts from both the endogenous *comK* gene and the *comK-M2* gene, using differently colored fluorophores to label the two mRNAs. The mean and variance of the numbers of the two transcripts were almost identical (fig. S1).

To verify that the observed decrease in *comK* transcripts during stationary phase could account for a decrease in the rate of transition to competence, we constructed a simple stochastic model of

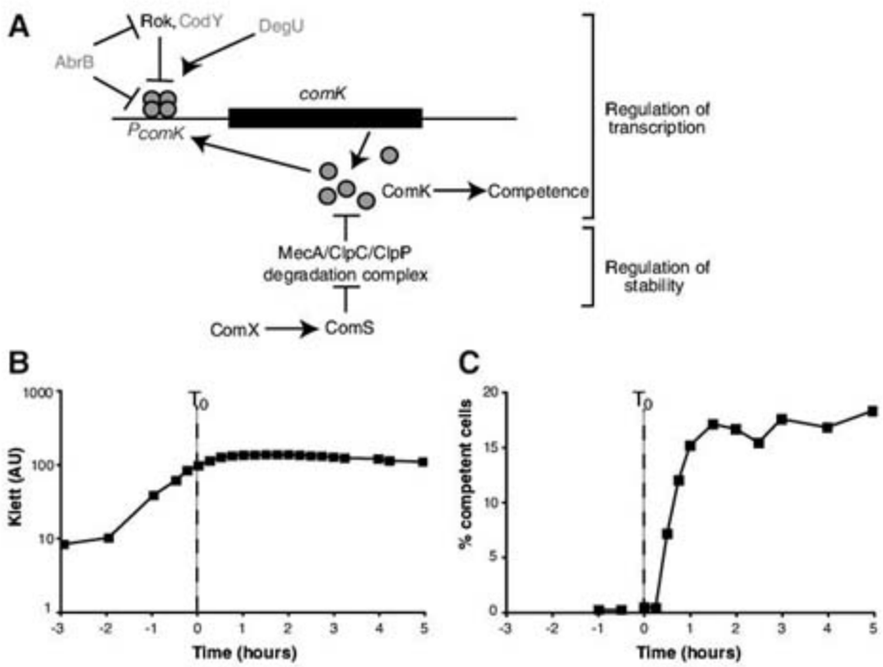

Fig. 1. The regulation of competence in *B. subtilis*. (**A**) The *comK* regulatory network. Arrows and perpendiculars represent positive and negative regulation, respectively. For simplicity, factors shown in gray were not considered in our modeling. (**B**) The kinetics of growth in competence medium [in absorbance units (AU) measured in a Klett colorimeter]. (**C**) Competence development, determined microscopically with strains carrying a *comK-cfp** fusion. The dashed lines in (B) and (C) represent T_0.

Public Health Research Institute Center, New Jersey Medical School, 225 Warren Street, Newark, NJ 07103, USA.

*Present address: Department of Physics, Massachusetts Institute of Technology, 77 Massachusetts Avenue, Cambridge, MA 02139, USA.

†These authors contributed equally to this work.

‡To whom correspondence should be addressed. E-mail: dubnauda@umdnj.edu

the *comK* positive feedback loop containing the salient features of the competence network, most notably the positive feedback loop [see the supporting online material (SOM)]. The model confirmed the plausibility of our conclusion that a relatively small decrease in *comK* transcription can effectively end transitions to the competent state (fig. S4).

Together, these data suggest that temporal regulation of transcription controls the frequency of transitions to the competent state and that the decline in transcription of *comK* during stationary phase effectively defines a "window of opportunity," which explains why cells are only able to transition to competence for a limited amount of time.

Because the cells are genetically identical and grown in a well-stirred medium, the determination of which cells are selected for competence is likely due to random cell-to-cell variations in proteins involved in competence regulation. Given its critical role in the regulation of competence, we examined the role that noise in *comK* plays in selecting cells for competence. Cell-to-cell variations in the numbers of *comK* mRNAs can come from two sources (*26*, *27*): (i) intrinsically random events of transcription and mRNA decay (intrinsic noise) and (ii) cell-to-cell variations in regulators, polymerases, and other global factors (extrinsic noise). To gauge the relative contributions of these two types of noise to the fluctuations leading to competence, we used an approach derived from Elowitz *et al.* (*26*): counting the numbers of both endogenous *comK* mRNA and *comK-M2* mRNA in individual cells (Fig. 3, B and C). Because any extrinsic variations should affect both genes simultaneously, correlated variations between the mRNA numbers indicate that the variations are primarily extrinsic, whereas uncorrelated variations indicate an intrinsically stochastic origin for the fluctuations in mRNA numbers (Fig. 3A). In early stationary phase when most of the transitions occur, the numbers of mRNA molecules from the two species were largely uncorrelated (correlation coefficient $r = 0.15$ at T_0) (Fig. 3, D and E). This finding indicates that intrinsically random fluctuations in *comK* mRNA production and degradation are likely to be a significant source of variations in ComK protein, leading to the initiation of competence (*28*).

To test the hypothesis that intrinsic noise is responsible for transitions to the competent state, we changed the noise in ComK protein production by altering the transcriptional and translational efficiency of *comK*. Recent studies have shown that intrinsic variations in protein expression are inversely related to the rate of transcription but are unaffected by the rate of translation (*8*, *9*) (see SOM). Thus, increasing the rate of transcription of a gene while reducing the rate of translation by an equivalent amount would reduce noise in gene expression, despite having the same mean expression level. This reduction in noise should lead to fewer transitions to the

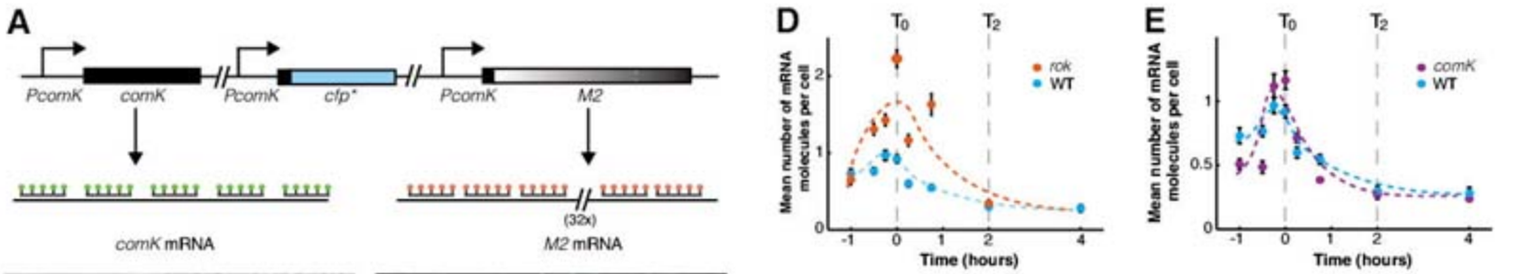

Fig. 2. Detection of single RNA molecules (*comK* and *comK-M2*) by FISH. (**A**) Schematic diagram depicting the endogenous *comK* (left), *comK-cfp** (middle), and *comK-M2* (right) reporters, all controlled by the *comK* promoter (PcomK). Multiple specific fluorescent probes bind to each mRNA molecule [*comK* (green) or *comK-M2* (red)], yielding distinct fluorescent signals. The *comK-cfp** construct identifies competent cells. *comK-cfp** designates an in-frame fusion of CFP to *comK*, and M2 designates the RNA with 32 repeat sequences. (**B**) Differential interference contrast (DIC) images and (**C**) pseudo-colored fluorescence images taken at T_0 for the WT strain, in which the *comK* mRNA was hybridized to six FISH probes [C6–tetramethyl rhodamine (C6-TMR)] that bind to the *comK* open reading frame. Dots correspond to individual mRNA molecules. Scale bars, 4 μm. (**D** and **E**) Kinetics of the population means of mRNA molecules per noncompetent cell before and after T_0 for the WT (blue circles, BD4379), the *rok* (red circles, BD4380), and the *comK* (purple circles, BD4382) strains. The WT and the *rok* strains (D) were hybridized to C6-TMR to detect *comK* mRNA molecules. The *comK* strain (E) was hybridized to a probe (PM2-Alexa 594) that binds to the M2 probe-binding sequence. Error bars were obtained by bootstrapping.

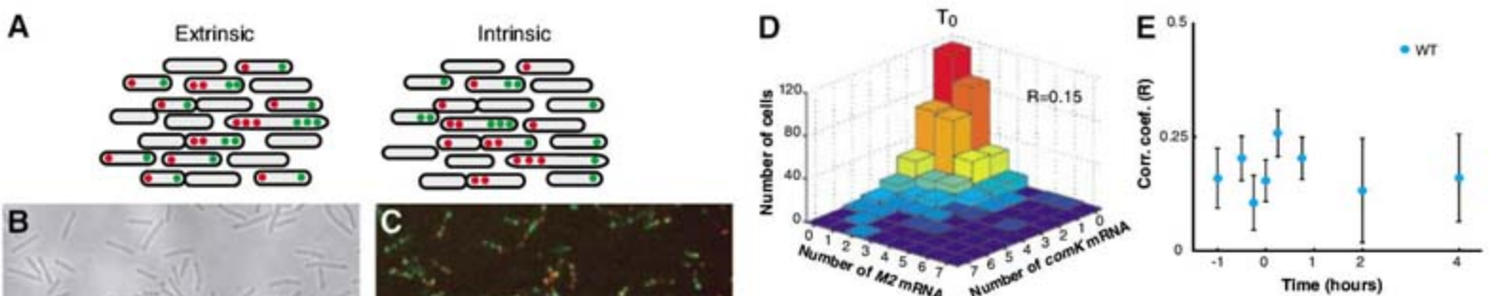

Fig. 3. Noise in *comK* transcription is mainly intrinsic. (**A**) Intrinsic and extrinsic noise were measured by detecting the mRNA from two coexpressed genes (*comK* and *comK-M2*) controlled by the comK promoter (*26*). Uncorrelated gene expression in individual cells is indicative of intrinsic noise. (**B**) DIC images and (**C**) pseudo-colored merged fluorescence images taken at T_0 showing hybridization to *comK-M2* (red) and *comK* (green) mRNA with the PM2-Alexa 594 and C6-TMR probes, respectively. Scale bars, 4 μm. (**D**) Distribution of *comK* and *comK-M2* mRNA molecules for the WT strain (BD4379) at T_0, showing weak correlations between production of the two mRNA molecules ($r = 0.15$). (**E**) Correlation coefficients throughout growth for the same strain. Error bars indicate SE.

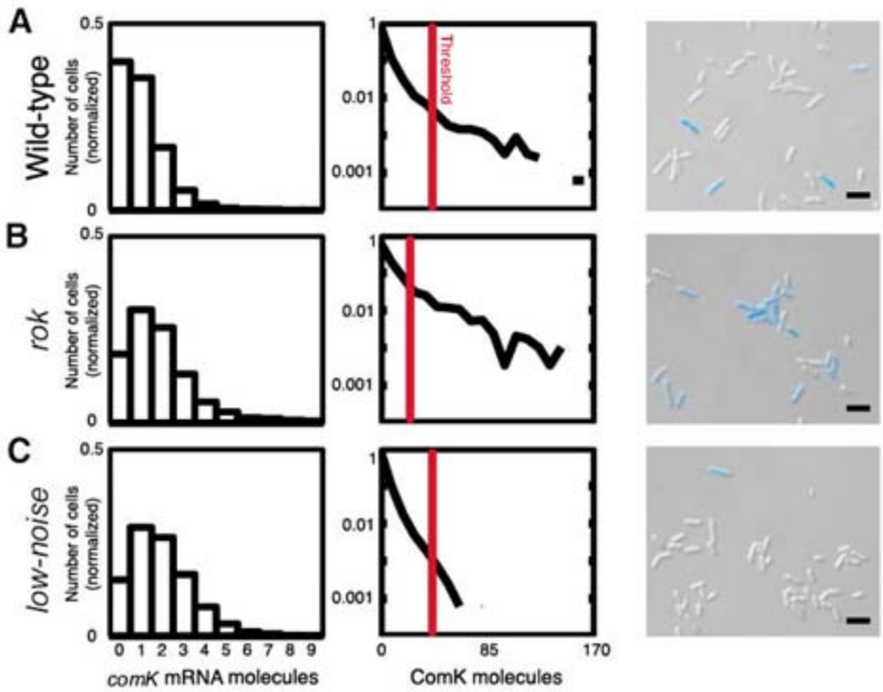

Fig. 4. Noise reduction in *comK* expression lowers the percentage of competent cells. The leftmost column depicts *comK* mRNA distributions predicted by the model for the WT (**A**), *rok* (**B**), and low-noise (**C**) strains at T_0. The middle column shows ComK protein distributions at T_0 assuming a high rate of translation in the WT and *rok* strains [(A) and (B)] and a lowered rate of translation in the low-noise strain (C). The vertical red lines show the predicted threshold beyond which the positive autoregulatory loop of *comK* would be activated, resulting in competence [the threshold in the *rok* strain changes because of increased gene expression (see SOM)]. The rightmost column shows CFP fluorescence images from the three strains, taken at T_2 and overlaid on DIC images. All three strains expressed the *comK-cfp** fusion, thus fluorescing when competent. The lowest panel in the column shows a microscopic field for the low-noise strain selected to show one competent cell, although the frequency of such cells was less than 1%. Scale bars, 4 μm.

competent state, because large fluctuations triggering activation of the positive feedback loop would become less likely (*29*).

To test this prediction, we used the *rok* strain, which exhibits a twofold increase in *comK* mRNA transcription over the WT strain at T_0 (Fig. 4, panels in leftmost column) (*25*, *30*), thus decreasing the noise in ComK protein levels. To adjust the mean ComK protein level in the *rok* strain to approximate that of the WT strain, we changed the ATG initiation codon of *comK* to GTG, thereby reducing its translational efficiency (*9*). We verified that the mean ComK levels in the low-noise and WT strains were similar by quantifying the amount of basal ComK–cyan fluorescent protein (CFP) fluorescence in bulk culture at $T_{-0.5}$ and T_0. Despite the slightly higher mean fluorescence in the low-noise strain, the number of its competent cells at T_2 was dramatically lower than that in the WT strain, with fewer than 1% of cells being competent as compared with 15% in the WT strain (Fig. 4, panels in rightmost column). These experiments show that intrinsic noise in *comK* expression is responsible for the transitions to competence and that reducing noise can substantially alter the rate at which those transitions occur.

This result suggests that the noise characteristics of particular genes may be subject to evolutionary pressures. Indeed, the fact that the *comK* gene is weakly transcribed (*12*) while having a "strong" Shine-Dalgarno sequence (GGAGG–7 bp–ATG) is suggestive. For a desired final percentage of competent cells, there must be a set fraction of cells with the level of ComK above a particular threshold, achievable either by having a basal ComK distribution with a low mean and a large variance or by having a higher mean with a lower variance. Because of the metabolic cost of maintaining a larger mean number of proteins, it is plausible that cells would opt for the former option rather than the latter, as appears to be the case for *comK*.

The temporal regulation of *comK* transcription during stationary phase defines when transitions to the competent state may occur (the window of opportunity), and intrinsic noise in *comK* expression defines the rate at which cells become competent. Our results imply that noise properties are subject to evolutionary forces and suggest how cells might alter those rates to increase fitness. Because noise has been implicated in a variety of cellular behaviors, such knowledge can help both in the understanding of natural regulatory networks (*7*, *31*) and in the synthesis of artificial networks (*4*, *32*).

References and Notes

1. J. M. Raser, E. K. O'Shea, *Science* **304**, 1811 (2004).
2. M. Kaern, T. C. Elston, W. J. Blake, J. J. Collins, *Nat. Rev. Genet.* **6**, 451 (2005).
3. E. M. Ozbudak, M. Thattai, H. N. Lim, B. I. Shraiman, A. van Oudenaarden, *Nature* **427**, 737 (2004).
4. T. S. Gardner, C. R. Cantor, J. J. Collins, *Nature* **403**, 339 (2000).
5. F. J. Isaacs, J. Hasty, C. R. Cantor, J. J. Collins, *Proc. Natl. Acad. Sci. U.S.A.* **100**, 7714 (2003).
6. A. Becskei, B. Seraphin, L. Serrano, *EMBO J.* **20**, 2528 (2001).
7. M. Acar, A. Becskei, A. van Oudenaarden, *Nature* **435**, 228 (2005).
8. M. Thattai, A. van Oudenaarden, *Proc. Natl. Acad. Sci. U.S.A.* **98**, 8614 (2001).
9. E. M. Ozbudak, M. Thattai, I. Kurtser, A. D. Grossman, A. van Oudenaarden, *Nat. Genet.* **31**, 69 (2002).
10. D. Dubnau, R. Losick, *Mol. Microbiol.* **61**, 564 (2006).
11. W. K. Smits, O. P. Kuipers, J. W. Veening, *Nat. Rev. Microbiol.* **4**, 259 (2006).
12. G. M. Suel, J. Garcia-Ojalvo, L. M. Liberman, M. B. Elowitz, *Nature* **440**, 545 (2006).
13. W. K. Smits *et al.*, *Mol. Microbiol.* **56**, 604 (2005).
14. H. Maamar, D. Dubnau, *Mol. Microbiol.* **56**, 615 (2005).
15. G. M. Suel, R. P. Kulkarni, J. Dworkin, J. Garcia-Ojalvo, M. B. Elowitz, *Science* **315**, 1716 (2007).
16. M. Leisner, K. Stingl, J. O. Radler, B. Maier, *Mol. Microbiol.* **63**, 1806 (2007).
17. D. van Sinderen, G. Venema, *J. Bacteriol.* **176**, 5762 (1994).
18. D. van Sinderen *et al.*, *Mol. Microbiol.* **15**, 455 (1995).
19. L. W. Hamoen, A. F. Van Werkhoven, J. J. E. Bijlsma, D. Dubnau, G. Venema, *Genes Dev.* **12**, 1539 (1998).
20. J. Hahn, L. Kong, D. Dubnau, *J. Bacteriol.* **176**, 5753 (1994).
21. P. Prepiak, D. Dubnau, *Mol. Cell* **26**, 639 (2007).
22. A. J. Rodriguez, S. M. Shenoy, R. H. Singer, J. Condeelis, *J. Cell Biol.* **175**, 67 (2006).
23. A. Raj, C. S. Peskin, D. Tranchina, D. Y. Vargas, S. Tyagi, *PLoS Biol.* **4**, e309 (2006).
24. A. M. Femino, F. S. Fay, K. Fogarty, R. H. Singer, *Science* **280**, 585 (1998).
25. T. T. Hoa, P. Tortosa, M. Albano, D. Dubnau, *Mol. Microbiol.* **43**, 15 (2002).
26. M. B. Elowitz, A. J. Levine, E. D. Siggia, P. S. Swain, *Science* **297**, 1183 (2002).
27. P. S. Swain, M. B. Elowitz, E. D. Siggia, *Proc. Natl. Acad. Sci. U.S.A.* **99**, 12795 (2002).
28. It is conceivable that fluctuations in the posttranslational control of ComK levels could introduce some extrinsic variations in ComK, but the fact that *comS* is transcribed equally in competent and noncompetent cells (*20*) argues against this possibility. It is also possible that the small extrinsic component of the noise in transcription could be magnified at the protein level if the ComK protein degradation rate was extremely low; however, stochastic simulations show that this is very unlikely in our case (fig. S7; see SOM for further discussion).
29. We verified this intuitive picture by using computer simulations of the complete model referred to previously (fig. S5).
30. M. Albano *et al.*, *J. Bacteriol.* **187**, 2010 (2005).
31. N. Q. Balaban, J. Merrin, R. Chait, L. Kowalik, S. Leibler, *Science* **305**, 1622 (2004).
32. M. B. Elowitz, S. Leibler, *Nature* **403**, 335 (2000).

33. We acknowledge the assistance of S. Tyagi, S. Marras, and D. Gold for the gift of the repeat sequence plasmid, for the use of their spectrophotometer and microscope, and for the preparation of fluorescent probes. We also acknowledge D. Rudner for the gift of the codon-optimized CFP and C. S. Peskin for valuable discussions. We also thank S. Tyagi, A. van Oudenaarden, J. Gore, J. Tsang, M. B. Elowitz, G. M. Suel, and P. Mehta for comments on the manuscript, as well as an anonymous reviewer for insightful comments. This work was supported by NIH grant GM 57720. A.R. was supported by NIH grant GM 070357 and by NSF postdoctoral fellowship DMS-0603392.

Supporting Online Material

www.sciencemag.org/cgi/content/full/1140818/DC1
Materials and Methods
SOM Text
Figs. S1 to S7
Tables S1 to S3
References
Movie S1

5 February 2007; accepted 6 June 2007
Published online 14 June 2007;
10.1126/science.1140818
Include this information when citing this paper.

Rapid Synthesis and Synaptic Insertion of GluR2 for mGluR-LTD in the Ventral Tegmental Area

Manuel Mameli,[1] Bénédicte Balland,[1] Rafael Luján,[2] Christian Lüscher[1,3]*

The activation of metabotropic glutamate receptors (mGluRs) leads to long-term depression (mGluR-LTD) at many synapses of the brain. The induction of mGluR-LTD is well characterized, whereas the mechanisms underlying its expression remain largely elusive. mGluR-LTD in the ventral tegmental area (VTA) efficiently reverses cocaine-induced strengthening of excitatory inputs onto dopamine neurons. We show that mGluR-LTD is expressed by an exchange of GluR2-lacking AMPA receptors for GluR2-containing receptors with a lower single-channel conductance. The synaptic insertion of GluR2 depends on de novo protein synthesis via rapid messenger RNA translation of GluR2. Regulated synthesis of GluR2 in the VTA is therefore required to reverse cocaine-induced synaptic plasticity.

In the VTA, synaptic induction of mGluR-LTD requires burst firing [e.g., several repetitions of five stimuli at 66 Hz (*1*)]. mGluR-LTD can also be chemically induced by bath application of the selective mGluR group I agonist 3,4-dihydroxyphenylglycol (DHPG), which occludes the mGluR-LTD induced by synaptic activity (*2*). mGluR-LTD may therefore be mediated by mGluR1 or mGluR5, which in other parts of the brain induce LTD through heterotrimeric GTP-binding proteins (G proteins) of the pertussis toxin–insensitive G_q family (*3*).

We examined the expression of mGluR-LTD at excitatory synapses onto dopamine (DA) neurons of the VTA by monitoring excitatory postsynaptic currents (EPSCs) mediated by α-amino-3-hydroxy-5-methylisoxazole-4-propionic acid receptors (AMPAR) (fig. S1) and evoked by extracellular stimulation (*4*). Cocaine and other addictive drugs fundamentally change the efficacy (*5*–*7*) and the quality (*1*) of transmission

[1]Department of Basic Neuroscience, Medical Faculty, University of Geneva, CH-1211 Geneva, Switzerland. [2]Department Ciencias Médicas, Facultad de Medicina–Centro Regional de Investigaciones Biomedicas, Universidad de Castilla–La Mancha, 02006 Albacete, Spain. [3]Clinic of Neurology, Department of Clinical Neuroscience, Geneva University Hospital, CH-1211 Geneva, Switzerland.

*To whom correspondence should be addressed. E-mail: Christian.Luscher@medecine.unige.ch

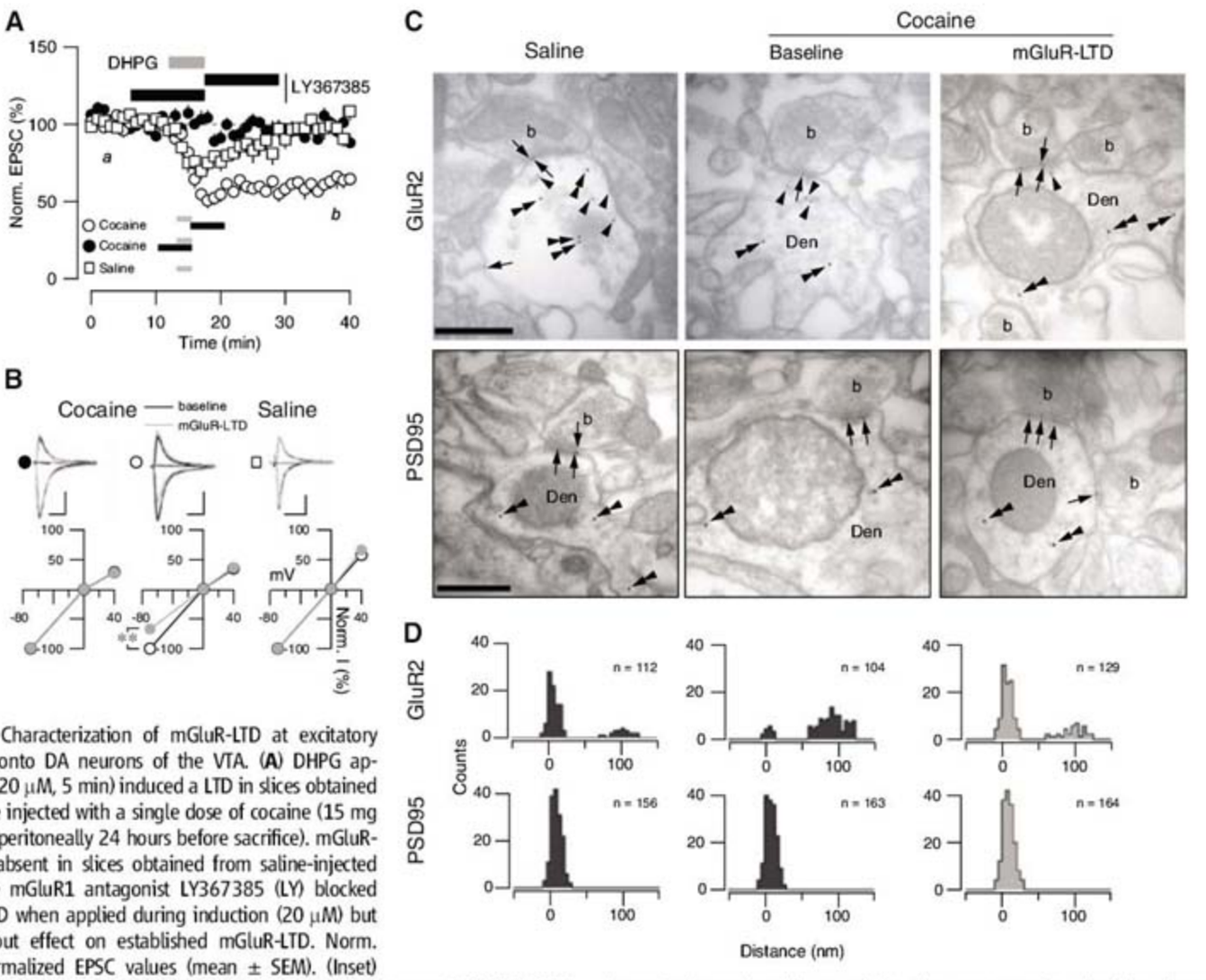

Fig. 1. Characterization of mGluR-LTD at excitatory synapses onto DA neurons of the VTA. (**A**) DHPG application (20 μM, 5 min) induced a LTD in slices obtained from mice injected with a single dose of cocaine (15 mg kg^{-1} intraperitoneally 24 hours before sacrifice). mGluR-LTD was absent in slices obtained from saline-injected mice. The mGluR1 antagonist LY367385 (LY) blocked mGluR-LTD when applied during induction (20 μM) but was without effect on established mGluR-LTD. Norm. EPSC, normalized EPSC values (mean ± SEM). (Inset) Gray bars, DHPG; black bars, LY. (**B**) Overlay of averaged traces of AMPAR-EPSCs recorded at −70, 0, and +40 mV before (black line) and after (gray line) DHPG application with corresponding *I-V* plots from representative cells in (A) at time points a and b. Scale bars indicate 5 ms (horizontal axis) and 50 pA (vertical axis). (**C**) Examples of postembedding immunoreactivity for tyrosine hydroxylase (TH) (double arrowheads), GluR2, and PSD95. Immunoparticles for GluR2 were found beneath (arrowheads) or within the postsynaptic densities (arrows) of asymmetrical synapses established by dendritic shafts (Den) of TH-positive neurons and axon terminals (b). As a control, PSD95 (arrows) always appeared in the postsynaptic densities. Scale bars, 0.5 μm. (**D**) Histograms compiling distances of GluR2 and PSD95 from the synapse (*n* particles in 60 identified synapses analyzed blindly from three hemislices of three mice for each condition).

at this synapse. Twenty-four hours after a single injection of cocaine, the AMPA/*N*-methyl-D-aspartate (NMDA) ratio of evoked EPSCs (eEPSC) is increased, and the AMPA-EPSCs become rectifying. This suggests that new AMPARs are inserted into the synapse, of which a substantial fraction is devoid of the subunit GluR2. mGluR-LTD can reverse cocaine-induced synaptic plasticity (*1*), but the mechanisms underlying this process remain unclear.

To identify the mechanisms underlying mGluR-LTD in the VTA, we applied DHPG and recorded EPSCs in DA neurons. DHPG induced LTD in slices obtained from cocaine-injected mice but not in slices obtained from mice that were injected with saline (Fig. 1A) [46.9 ± 4.1% (mean ± SEM) compared with 3.76 ± 1.4%, n = 11 cells, $P < 0.01$]. This effect was blocked by the mGluR1 antagonist LY367385 (Fig. 1A, solid circles) (3.1 ± 2.7%, n = 7), but only when applied during the induction protocol; the same drug was ineffective when applied after mGluR-LTD was established (Fig. 1A, open circles). The current-voltage (*I-V*) relationship of the EPSCs was rectifying in slices from cocaine-treated mice and became linear after the induction of mGluR-LTD (*1*). In contrast, *I-V* curves plotted in slices from saline-treated mice were linear and did not change with DHPG treatment (Fig. 1B). Thus, activation of mGluR1 reverses cocaine-induced potentiation and leads to a reduction in the contribution of GluR2-lacking AMPARs to the EPSC, as expected (fig. S1) (*1*).

The redistribution of GluR2 was confirmed with postembedding immunogold labeling at the electron microscopy (EM) level. In slices from saline-treated mice, the majority of GluR2 labeling was observed at the synapse, along with a small cytoplasmic pool associated with intracellular membrane compartments. In slices from cocaine-exposed mice, the number of cytoplasmic GluR2 particles increased at the expense of synaptic labeling. Furthermore, DHPG treatment of slices from cocaine-exposed mice led to the reappearance of a predominantly synaptic pool. As a control, labeling of postsynaptic density (PSD95) was observed at synaptic locations in all three conditions (Fig. 1, C and D). Taken together, the electrophysiological and the EM observations demonstrate that, after cocaine exposure, GluR2 is redistributed toward intracellular compartments and that the induction of mGluR-LTD may restore basal conditions.

These results raise the possibility that LTD is expressed by the replacement of GluR2-lacking AMPARs with GluR2-containing AMPARs, which have a smaller single-channel conductance (γ) (*8–10*). We applied nonstationary fluctuation analysis (NSFA) to eEPSC and found that γ was significantly higher in slices from cocaine-treated mice compared with those from saline-treated controls (Fig. 2, A and B, and fig. S2). In slices from cocaine-treated mice, DHPG led to a significant relative decrease of γ (Fig. 2, C and D) (42.6 ± 6.9% versus 5 ± 10% in saline controls, n from 6 to 8, $P < 0.01$), yielding values similar to γ measured in saline controls where mGluR-LTD was absent (fig. S2). Importantly, the average number of receptors open at the peak (N) remained constant during mGluR-LTD (relative change for cocaine –4.4 ± 9.2%, for saline 1.2 ± 4.8%, n from 6 to 8). Thus, mGluR-LTD in the VTA is caused by a replacement of GluR2-lacking AMPARs with GluR2-containing AMPARs so that the total number of AMPARs remains constant.

Such an exchange could occur through lateral redistribution with an extrasynaptic pool or may involve the internalization of receptors. In the latter case, interfering with the endocytotic machinery should block mGluR-LTD. We therefore loaded the cells with a dominant negative peptide composed of 15 amino acids (D15) (*11*) that mimics the interaction site of dynamin with amphiphysin, two essential components for the internalization of clathrin-coated vesicles. D15 efficiently blocked the expression of mGluR-LTD without affecting baseline transmission in control conditions (Fig. 2C and fig. S2) (3.57 ± 2.1%, n = 7; for control, 48.6 ± 2.6%, n = 6; $P < 0.01$). This is in contrast to previous reports in the hippocampus where a significant run-up was observed (*11*) and argues against a rapid constitutive recycling of AMPARs. To specifically interfere with the mobile pool of GluR2-containing receptors, we loaded cells with the active EVKI peptide that disrupts the interaction of GluR2 with PICK1 (*12*). This manipulation blocked the expression of mGluR-LTD (Fig. 2F) (13.1 ± 1.7%, n = 9, versus inactive pep2-SVKE control 47.1 ± 1.6%, n = 9, $P < 0.05$).

mGluR-LTD was blocked by an mGluR1 antagonist (Fig. 1, A and B). mGluR1 via Gq activates many pathways, including the extracellular signal–regulated kinase (ERK) (*13*) and phosphoinositide 3-kinase-Akt-mammalian tar-

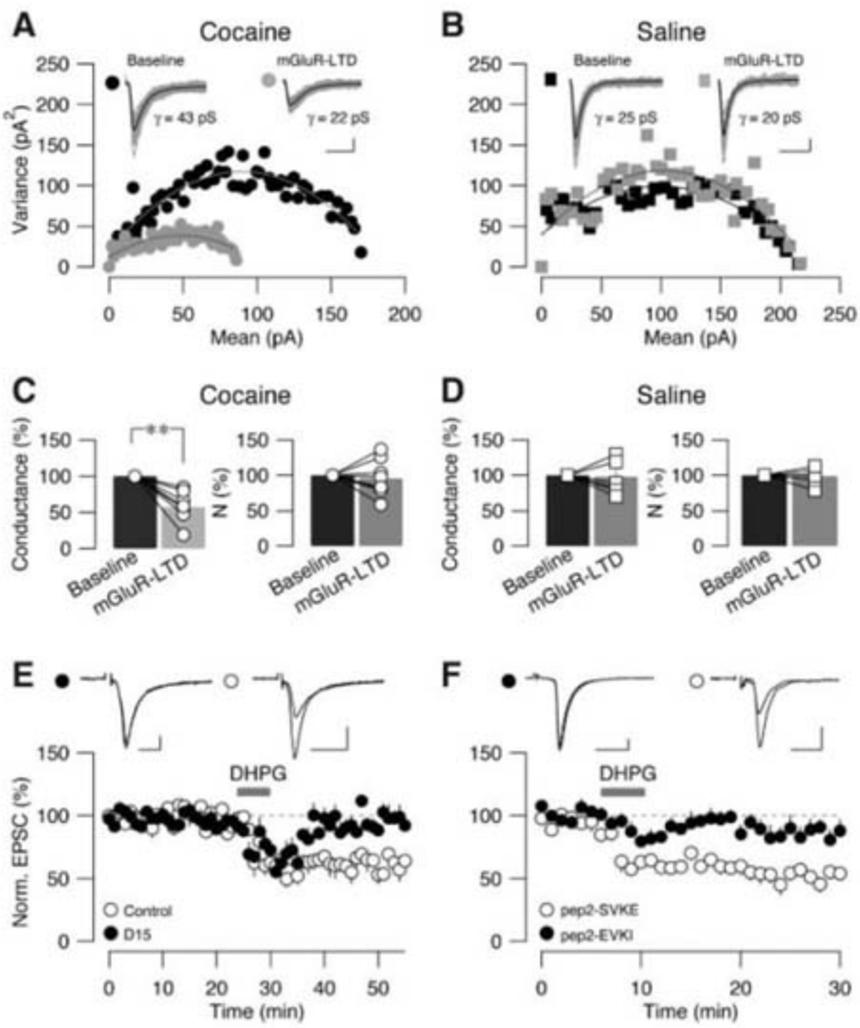

Fig. 2. mGluR-LTD expression involved the exchange of high-conductive AMPARs for low-conductive AMPARs. (**A** and **B**) Examples of *I-V* relationship before and after DHPG application in mice injected with cocaine (A) or saline (B). (Insets) Overlay of 20 consecutive traces. γ was estimated from the initial slope of the parabolic fit. (**C** and **D**) Relative changes in γ and number of channels (N) open at the peak of the response. (**E**). Disruption of the protein-protein interaction between dynamin-amphiphysin with a dominant negative peptide (D15, 1.5 mM) prevented mGluR-LTD. Averaged traces recorded before and after mGluR-LTD induction with and without D15 in the patch pipette. (**F**). Dialysis of DA neurons with the dominant negative peptide pep2-EVKI (100 μM) blocked mGluR-LTD, whereas its inactive form (pep2-SVKE, 100 μM) was without effect. Scale bars for (A), (B), (E), and (F) indicate 5 ms and 50 pA.

get of rapamycin (mTOR) (*14*). Although the ERK inhibitor U0126 was inefficient in blocking mGluR-LTD (Fig. 3A) (36.4 ± 1.1%; for control, 41.1 ± 3.7%; n from 4 to 8; $P > 0.05$), we observed a block of the depression (6.45 ± 1.3%; for control, 46.5 ± 1.3%; n from 5 to 9; $P < 0.01$) with rapamycin (10- to 20-min preincubation), strongly implicating mTOR signaling in expression (Fig. 3B).

The involvement of mTOR in mGluR-LTD in the VTA suggests that this form of plasticity requires local translation. To directly test this possibility, we assessed the sensitivity of mGluR-LTD to two translational inhibitors. When cycloheximide (C-hex), which blocks translational elongation through an effect on the 60*S* ribosomal complex, was applied to the bath, we observed a significant reduction of the mGluR-LTD (Fig. 3C) (18.5 ± 2%, $n = 10$, $P < 0.05$). The residual depression during mGluR-LTD in C-hex was indistinguishable from that in interleaved experiments in which only C-hex was applied (13.2 ± 1.1%, $n = 5$, $P > 0.05$). To control for this nonspecific effect of C-hex, we obtained a within-cell control by applying DHPG first with and a second time without C-hex. We observed an almost-complete block of the depression in the presence of the translation inhibitor, whereas mGluR-LTD was restored after its washout (Fig. 3D, 13.1 ± 3.2% after first DHPG application; 45.3 ± 1.6% after washout of C-hex, $n = 8$, $P < 0.01$). Anisomycin, which inhibits translation via the 80*S* ribosomal complex, had no effect on baseline transmission but blocked mGluR-LTD, whether DHPG (Fig. 3E) (1.4 ± 2%, $n = 14$, $P < 0.01$) or brief trains of synaptic stimulation (Fig. 3F) (0.2 ± 2.1%, $n = 7$, $P < 0.01$) was used as induction protocol.

If mGluR-LTD depends on rapid translation, what is the protein that needs to be synthesized? One possibility is that GluR2-lacking AMPARs are removed from the synapse by a protein synthesized during mGluR-LTD. Alternatively, the synthesis of AMPARs that contain GluR2 may displace GluR2-lacking AMPARs, in which case GluR2 would be rapidly synthesized during LTD induction. The dendrites of many neurons contain mRNA for AMPAR subunits, and the machinery to integrate them into the membrane is also present (*15*, *16*). We therefore tested for synthesis and insertion of endogenous GluR2 by specifically interfering with the mRNA of GluR2. We chose two approaches, antisense oligonucleotide and small interfering RNA (siRNA), against a unique sequence in the N-terminal region of GluR2 (positions 1575 to 1595) (*17*). In both cases, the goal was not to deplete the endogenous protein but to rapidly and selectively prevent GluR2 mRNA from being translated. We filled the patch pipette with antisense oligonucleotide or siRNA and allowed free diffusion for 20 min while monitoring baseline synaptic transmission. With both interventions, baseline transmission was unaffected, whereas mGluR-LTD was abolished (Fig. 4, A to C) (for antisense oligonucleotide, 3.3 ± 1.2%; for siRNA-GluR2, 4.6 ± 1.6%; and for 66 Hz and siRNA-GluR2, 2 ± 3.1%; n from 8 to 18). As controls, we loaded the cells with scrambled versions of the oligonucleotide and siRNA, which did not block mGluR-LTD (for antisense oligonucleotide, 37.4 ± 1.7%; for siRNA-GluR2, 33.5 ± 5.1%; and for 66 Hz

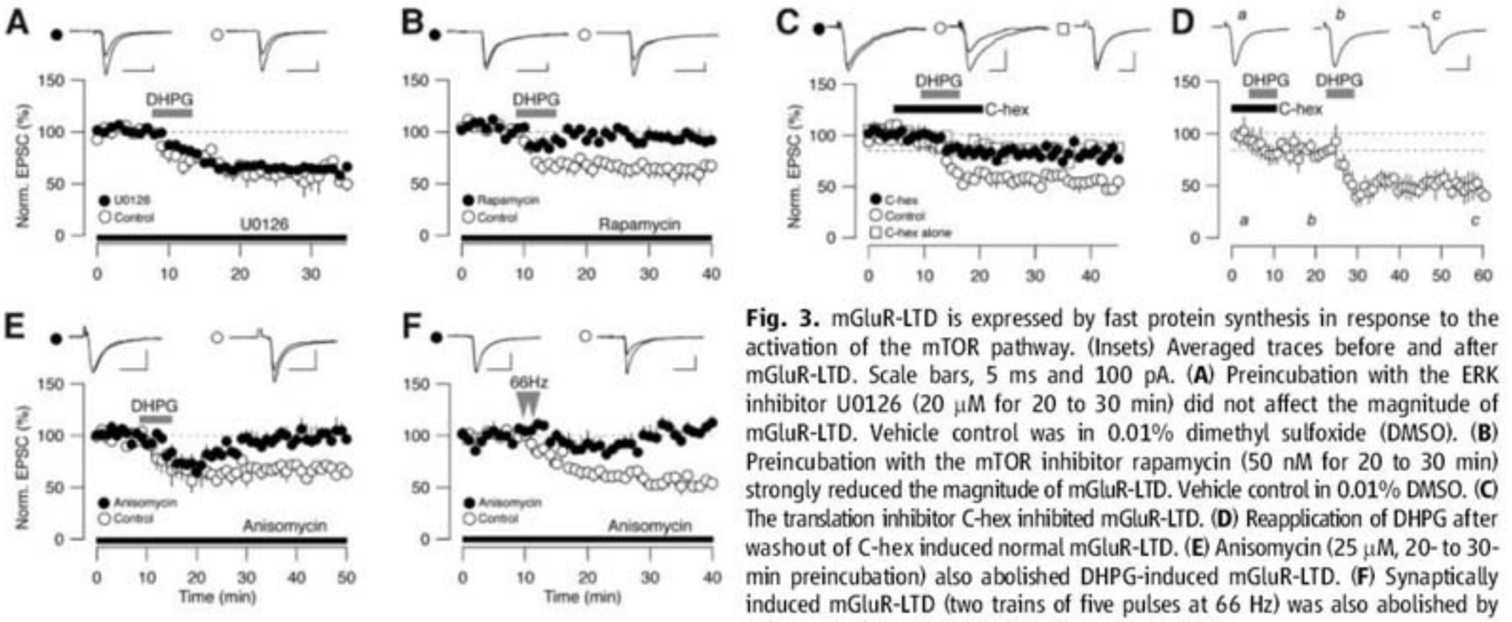

Fig. 3. mGluR-LTD is expressed by fast protein synthesis in response to the activation of the mTOR pathway. (Insets) Averaged traces before and after mGluR-LTD. Scale bars, 5 ms and 100 pA. (**A**) Preincubation with the ERK inhibitor U0126 (20 μM for 20 to 30 min) did not affect the magnitude of mGluR-LTD. Vehicle control was in 0.01% dimethyl sulfoxide (DMSO). (**B**) Preincubation with the mTOR inhibitor rapamycin (50 nM for 20 to 30 min) strongly reduced the magnitude of mGluR-LTD. Vehicle control in 0.01% DMSO. (**C**) The translation inhibitor C-hex inhibited mGluR-LTD. (**D**) Reapplication of DHPG after washout of C-hex induced normal mGluR-LTD. (**E**) Anisomycin (25 μM, 20- to 30-min preincubation) also abolished DHPG-induced mGluR-LTD. (**F**) Synaptically induced mGluR-LTD (two trains of five pulses at 66 Hz) was also abolished by anisomycin (25 μM, 20- to 30-min preincubation).

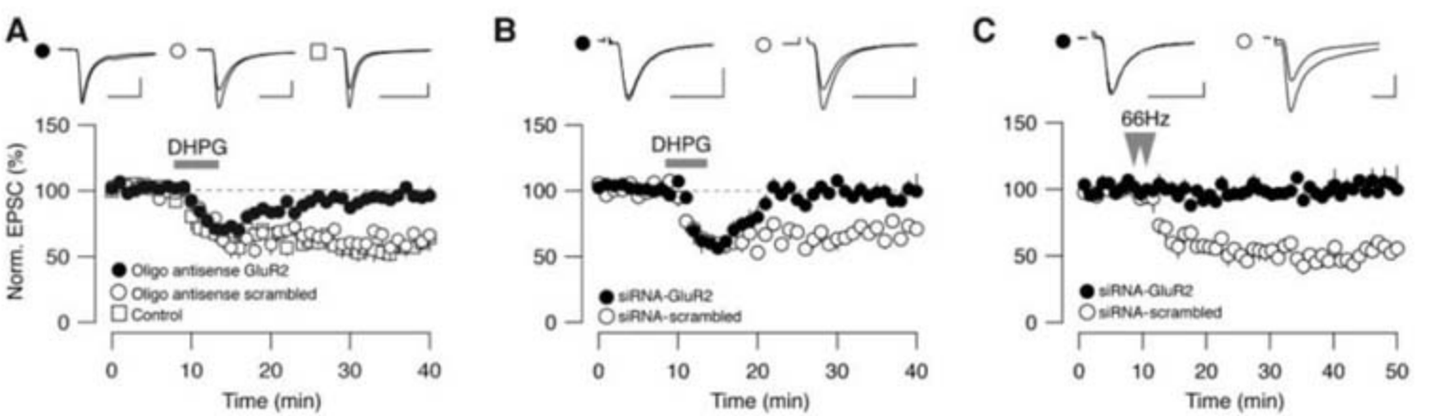

Fig. 4. Specific targeting of GluR2-mRNA abolished mGluR-LTD. (Insets) Averaged traces before and after mGluR-LTD. Scale bars, 5 ms and 50 pA. (**A**) Antisense oligonucleotide against the N-terminal sequence of GluR2-mRNA (250 μM, positions 1575 to 1595) dialyzed intracellularly blocked mGluR-LTD. (**B**) Double-stranded siRNA (30 nM) targeting GluR2-mRNA abolished mGluR-LTD. (**C**) Synaptically induced mGluR-LTD was also abolished by the GluR2-siRNA.

and siRNA-GluR2, 49.3 ± 3.3%; n from 5 to 7; $P < 0.01$ against corresponding active siRNA).

Our results define two unexpected features of mGluR-LTD in the VTA. First, we found that mGluR-LTD in the VTA is not due to the simple removal of AMPARs from the synapse; rather, AMPARs that lack the GluR2 subunit are selectively endocytosed and immediately replaced by AMPARs that contain GluR2. Second, we found that de novo synthesis of GluR2 is required for LTD.

Protein synthesis is involved in many forms of synaptic plasticity, typically during the maintenance phase several hours after induction (*18*). However, forms of synaptic plasticity that rely on local protein synthesis on a much faster time scale have been described (*19, 20*) and components of the translation machinery, such as polyribosomes and mRNA are present in dendrites (*15, 16*). However in most cases, the identity of the proteins synthesized on demand remains unknown. Unbiased strategies to fill this gap, such as cDNA microarrays in dendritic fractions, have revealed mRNA of several genes, including ribosomal proteins, transcription factors, or components of the induction cascade for plasticity (*21, 22*). mGluRs can initiate such synthesis in expression system. DHPG drives the translation of recombinant GluR2 mRNA into receptor subunits, which are then detected in the cell membrane (*23, 24*).

In the VTA, GluR2 seems to be both (i) synthesized in response to the induction of plasticity and (ii) directly involved in the expression of plasticity. Thus, as in other systems, LTD does lead to AMPAR withdrawal, but in the VTA these receptors are replaced by newly synthesized AMPARs so that the total number of AMPARs at synapses remains constant. Thus, synapses express LTD because the conductance of the newly synthesized GluR2-containing AMPARs is smaller than that of GluR2-lacking AMPARs that were present before LTD.

Our data are reminiscent of a form of synaptic plasticity observed in stellate cells of the cerebellum that is associated with a loss of rectification (*25, 26*); however, in that case, GluR2-containing receptors are present at extrasynaptic sites and incorporated through lateral movement (*25*). In contrast, in the VTA, GluR2 appears to be a protein that needs to be synthesized in order for synapses to express mGluR-LTD. This does not exclude the possibility that other proteins must also be synthesized, for example to form functional heteromeric AMPARs.

Our results may be of physiological and pharmacological relevance in the context of drug addiction. Several studies implicate synaptic plasticity in DA neurons of the VTA as core components of drug addiction (*27*). Analogous to pain sensitization or ischemia (*10*), the Ca^{2+} permeability of the AMPARs could play an important role in the pathological process. Activation of mGluR1 may restore Ca^{2+}-impermeable transmission, and regulated synthesis of GluR2 may be an important requirement to reverse cocaine-induced synaptic plasticity.

References and Notes

1. C. Bellone, C. Lüscher, *Nat. Neurosci.* **9**, 636 (2006).
2. C. Bellone, C. Lüscher, *Eur. J. Neurosci.* **21**, 1280 (2005).
3. J. Harnisch *et al.*, *J. Neurosci.* **24**, 9119 (2004).
4. Materials and methods are available on *Science* Online.
5. M. A. Ungless, J. L. Whistler, R. C. Malenka, A. Bonci, *Nature* **411**, 583 (2001).
6. D. Saal, Y. Dong, A. Bonci, R. C. Malenka, *Neuron* **37**, 577 (2003).
7. Q. S. Liu, L. Pu, M. M. Poo, *Nature* **437**, 1027 (2005).
8. S. Cull-Candy, L. Kelly, M. Farrant, *Curr. Opin. Neurobiol.* **16**, 288 (2006).
9. R. Dingledine, K. Borges, D. Bowie, S. F. Traynelis, *Pharmacol. Rev.* **51**, 7 (1999).
10. S. J. Liu, R. S. Zukin, *Trends Neurosci.* **30**, 126 (2007).
11. C. Lüscher *et al.*, *Neuron* **24**, 649 (1999).
12. M. J. Xiao *et al.*, *Neuron* **28**, 873 (2000).
13. S. M. Gallagher, C. A. Daly, M. F. Bear, K. M. Huber, *J. Neurosci.* **24**, 4859 (2004).
14. L. Hou, E. Klann, *J. Neurosci.* **24**, 6352 (2004).
15. O. Steward, T. M. Reeves, *J. Neurosci.* **8**, 176 (1988).
16. L. E. Ostroff, J. C. Fiala, B. Allwardt, K. M. Harris, *Neuron* **35**, 535 (2002).
17. K. Ogura *et al.*, *J. Neurosci.* **19**, 9050 (1999).
18. P. V. Nguyen, T. Abel, E. R. Kandel, *Science* **265**, 1104 (1994).
19. H. Kang, E. M. Schuman, *Science* **273**, 1402 (1996).
20. K. M. Huber, M. S. Kayser, M. F. Bear, *Science* **288**, 1254 (2000).
21. O. Steward, E. M. Schuman, *Annu. Rev. Neurosci.* **24**, 299 (2001).
22. J. Eberwine, B. Belt, J. E. Kacharmina, K. Miyashiro, *Neurochem. Res.* **27**, 1065 (2002).
23. J. E. Kacharmina, C. Job, P. Crino, J. Eberwine, *Proc. Natl. Acad. Sci. U.S.A.* **97**, 11545 (2000).
24. M. Ju *et al.*, *Nat. Neurosci.* **7**, 244 (2004).
25. S. Q. Liu, S. G. Cull-Candy, *J. Neurosci.* **22**, 3881 (2002).
26. S. Q. Liu, S. G. Cull-Candy, *Nature* **405**, 454 (2000).
27. M. A. Ungless Jr., S. J. Nestler, *Trends Neurosci.* **29**, 638 (2006).
28. Animal procedures were approved by the animal welfare committee of the University of Geneva. Supported by grants from the Swiss National Science Foundation, the European commission (EMBO/AFP), and National Institute on Drug Abuse (all to C.L.) and from the Spanish Ministry of Education and Science and the Junta de Comunidades de Castilla-La Mancha (to R.L.). We thank M. Frerking, M. Serafin, C. F. Valenzuela, M. Carta, C. Bellone, M. Jemseek, and the whole Lüscher lab for comments.

Supporting Online Material

www.sciencemag.org/cgi/content/full/317/5837/530/DC1

Materials and Methods

Figs. S1 and S2

9 March 2007; accepted 26 June 2007
10.1126/science.1142365

Matrix Deposition Device

The ImagePrep sample preparation device is for automated matrix deposition onto tissue slices for analysis with the matrix-assisted laser desorption ionization (MALDI) Molecular Imager. The Molecular Imager allows color-coded visualization of the distribution of peptide or small protein biomarkers, or of drugs and their major metabolites, for the direct analysis of molecular distribution in tissue sections. The ImagePrep device provides reproducible sample preparations for MALDI imaging in an automated, push-button process. Another advantage of ImagePrep is the combination of excellent spectral quality at high image resolution of 50 microns.

Bruker Daltonics For information 978-667-9580 www.bdal.com

Imaging Platform

The Hoefer ULTima imaging platform provides a versatile, easy-to-use, and readily upgradeable gel documentation system with superior dynamic range for applications in proteomics and genomics. The ULTima's image positioning system features patented optics to enable simple, accurate positioning with no loss of optical resolution and no need to open the cabinet or manually adjust a fragile gel. The slant-correction feature permits optical rotation of the sample by ± 5° for optimum lane detection, without touching the gel. The versatile system offers true multi-fluorophore capabilities and sensitivity, performing fast chemiluminescent imaging and faint-band fluorescent detection. The filter changer accommodates up to five filters, and an optional epi-illumination module enables excitation of fluorophores within the visible/near infrared range.

Hoefer For information 415-550-3472 www.hoeferinc.com

Ultrafiltration Cartridge

The BioPak C disposable ultrafiltration cartridge is designed to minimize alkaline phosphatase (ALP) released by bacteria that may be present in immunoassay and clinical analyzer feed water used to prepare buffers, make blanks, and rinse tubing and probes. CLSI Clinical Laboratory Reagent Water can degrade quickly when standing in tubing and reservoirs during downtime, increasing bacterial counts and releasing ALP. This can interfere with some biochemical assays, resulting in inconsistent blanks and the need for more frequent decontamination and calibration. When attached to any Millipore AFS or Elix clinical water purification system as a final purification step, the Millipore BioPak C filter delivers ALP-free water with bacteria levels lower than 10 cfu/mL.

Millipore For information 800-548-7853 www.millipore.com

Microfocus X-Ray Source

The FR-E+ SuperBright is a microfocus x-ray source of comparable brightness to second-generation synchrotron beams, producing intensities of 1.6×10^{11} x-rays/mm^2/sec. The FR-E+ SuperBright microfocus rotating anode x-ray generator is the most intense home laboratory x-ray available for macromolecular crystallography, according to the manufacturer.

Rigaku For information 281-362-2300 www.rigaku.com

Rechargeable Lithium-Ion Battery

A patented system lets designers add a rechargeable lithium-ion battery for back-up power as an OEM component of virtually any type of electronic and electromechanical equipment. The Intelligent Battery and Power System serves as a complete AC/DC power supply and provides clean, regulated DC, from a variety sources, including from lithium-ion battery packs, an AC wall outlet, or any external DC source, such as solar and wind power. The batteries take over seamlessly if the external power is interrupted, and recharge automatically when the power is restored.

OceanServer Technology For information 508-678-0550 www.ocean-server.com

Vibration Isolation Workstation

The MK26 is an ultra-low-natural-frequency vibration isolation workstation. The workstation makes use of the Minus K stiff spring and negative-stiffness mechanism to achieve a low net vertical stiffness without affecting the static load supporting capability. Horizontal isolation is provided by beam columns connected in series with the vertical-motion isolator. Adjusted to a 0.5 Hz natural frequency, the workstation achieves 93% isolation efficiency at 2 Hz, 99% at 5 Hz, and 99.7% at 10 Hz. The MK26 can be configured for a wide variety of locations where disturbances due to external vibrations can adversely affect the operation of sensitive equipment. Customization options include guard rails, padded armrests, overhead equipment shelves, monitor stands, non-isolated shelves for supporting equipment off the tabletop, oversized keyboard shelves, retractable casters, Faraday cages to protect sensitive operations from electromagnetic interference, tabletop enclosures to protect against harsh manufacturing environments, and electrical accessories such as outlet strips for lighting.

Kinetic Systems For information 617-522-8700 www.kineticsystems.com

Literature

Optimizing Electroporation Parameters for Effective Gene Silencing in Jurkat Cells is an application note that describes the use of electroporation for the transfection of Jurkat cells with small-interfering RNA (siRNA). The protocol describes how to determine the best electroporation conditions (voltage and pulse duration) and the optimum concentration of siRNA to achieve a high transfection rate and minimum cell damage, which can result in a silencing efficiency of 85%. The experiments featured the Eppendorf Multiporator and Eppendorf hypo-osmolar electroporation buffer. The Multiporator applies electronically regulated microsecond pulses for a high cell survival rate, which in combination with the hypo-osmolar buffer achieves a high transfection yield.

Eppendorf For information 800-645-3050 www.eppendorf.com

Newly offered instrumentation, apparatus, and laboratory materials of interest to researchers in all disciplines in academic, industrial, and government organizations are featured in this space. Emphasis is given to purpose, chief characteristics, and availability of products and materials. Endorsement by *Science* or AAAS of any products or materials mentioned is not implied. Additional information may be obtained from the manufacturer or supplier.

POSITIONS OPEN

DIRECTOR
Center for Bioprocessing R and D

The South Dakota School of Mines and Technology (SDSMT) invites applications for the Director for the State supported 2010 Center for Bioprocessing Research and Development **(website: http://www.sdbor.edu/administration/research/index.htm).** The candidate should have a strong background in engineering or biological sciences with experience in a field related to bioprocessing and a Ph.D. degree (preferred) or a Master's degree and five to ten years of experience. A highly qualified candidate with a B.S. degree and extensive experience will also be considered. The successful candidate will actively participate in at least one of the research focus areas (pretreatment, conversion, separation, extremophiles). Preference will be given to candidates with established records of excellence in industrial processing, business management, research management, entrepreneurship, and grantsmanship.

Please apply online and view complete job description at **website: http://sdmines.sdsmt.edu/sdsmt/employment.** Review of applications will continue until the position is filled. For questions regarding the position contact **e-mail: cbrd_dir_search@sdsmt.edu.** For information regarding Rapid City and SDSMT visit **website: http://www.rapidcity.com and www.sdsmt.edu.**

SDSMT is an Equal Employment Opportunity/Affirmative Action/ADA Employer and Provider.

FACULTY OPPORTUNITIES
Pediatric Neurology and Multiple Sclerosis

The Department of Neurology at the University of Wisconsin is seeking fellowship-trained Board-eligible/Board-certified junior faculty to develop academic programs including research, clinical care, and education in pediatric neurology and multiple sclerosis. The positions include resources for clinical and basic research, expectation of collaborative clinical and translational research with colleagues, and participation in tertiary clinical care in a referral network including Wisconsin and adjoining states. The research environment includes the diverse neuroscience faculty of the University of Wisconsin, its Center for Neuroscience, and a new Clinical and Translational Research Institute. Primary clinical facilities include the University of Wisconsin Hospital and Clinics and the new American Family Children's Hospital.

The successful candidate will have demonstrated training and preparation for a successful academic career combining excellence in clinical service, research, and teaching.

Please send letter of interest and curriculum vitae and arrange for references to be sent electronically to **e-mail: applications@neurology.wisc.edu.**

Unless confidentiality is requested in writing, information regarding the applicants must be released upon request. Wisconsin Caregiver law applies. *UW-Madison is an Affirmative Action/Equal Opportunity Employer.*

YALE UNIVERSITY
Department of Chemistry

The Department of Chemistry at Yale University invites applications for tenure-track positions at the **ASSISTANT PROFESSOR** level to commence 1 July 2008. We seek creative **TEACHER-SCHOLARS** who show promise for developing outstanding research programs in inorganic chemistry or organic chemistry, broadly defined to include both materials chemistry and chemical biology. Applicants should send their curriculum vitae and a statement of research plans, and arrange for the submission of three letters of recommendation. All materials should be received by 15 October 2007. Send applications to: **Chair, Junior Faculty Search Committee, P.O. Box 208107, Yale University, New Haven, CT 06520-8107.** *Yale University is an Equal Opportunity/Affirmative Action Employer, and applications from women and underrepresented minority group members are especially encouraged.*

POSITIONS OPEN

FACULTY POSITIONS
Human Molecular Genetics Program, Children's Memorial Research Center and Northwestern University
Chicago, Illinois

Applications are solicited for **ASSISTANT PROFESSOR** level positions in the Human Molecular Genetics Program at Children's Memorial Research Center (CMRC). We seek Ph.D. and M.D./Ph.D. candidates with outstanding graduate and postdoctoral training, a strong publication record, the potential to attract external funding, and a commitment to develop an interactive research program. New laboratory space and state-of-the-art equipment are in place. Startup packages will be generous and successful applicants will be eligible for tenure-track faculty positions in the Department of Pediatrics, Feinberg School of Medicine, Northwestern University. Candidates with research interests in all areas of human genetics will be considered, including human genetic disease and models thereof, gene structure and function, regulation of gene expression, chromatin structure and modification, and bioinformatic approaches to human genome analysis.

Please send curriculum vitae, a statement of research interests, contact information of three references, and PDF files of most relevant publications care of: **Chris Pomeroy, Human Molecular Genetics Program, Children's Memorial Research Center, 2430 N. Halsted Street, Chicago, IL 60614 U.S.A. E-mail: c-pomeroy@northwestern.edu.**

Review of applications will continue until positions are filled.

Northwestern University is an Affirmative Action/Equal Opportunity Employer. Hiring is contingent upon eligibility to work in the United States. Women and minority candidates are strongly encouraged to apply.

The Department of Pathology and Anatomical Sciences at the University of Missouri School of Medicine is seeking a junior-level **ANATOMIST** for a tenure-track position. We are seeking candidates with strong research programs whose interests complement those of current faculty in the integrative anatomy group **(website: http://anatomy.missouri.edu).** The University of Missouri provides a collegial environment with substantial opportunities for intellectual creativity and diverse research. The position also includes a commitment to education, including graduate students, medical students, nursing and health care professions students, and undergraduate students. Applicants should be committed to excellence in scholarship, research, and teaching. The position requires a Ph.D. or M.D., or equivalent professional training and expertise. Preference will be given to individuals with sufficient experience to satisfy criteria for appointment as **ASSISTANT PROFESSOR** on the tenure track, and who have experience teaching a laboratory-based anatomy course. Applications will be accepted until the position is filled.

Interested individuals should submit a letter of interest, current curriculum vitae, a statement of current and future research plans, and a list of at least three references by September 1, 2007, to:

Douglas C. Anthony, M.D., Ph.D.
Professor and Chair
Department of Pathology and Anatomical Sciences
M263 Medical Sciences Building
University of Missouri School of Medicine
One Hospital Drive
Columbia, MO 65212

Or electronically (preferred) to **e-mail: greshammk@health.missouri.edu.**

The University of Missouri is an Equal Opportunity Employer/Affirmative Action and welcomes applications from members of underrepresented groups. For ADA accommodations, please contact our ***ADA coordinator*** *at* ***telephone: 573-884-7278 (V/TTY).***

Positions @ NIH

THE NATIONAL INSTITUTES OF HEALTH

OFFICE OF PORTFOLIO ANALYSIS AND STRATEGIC INITATIVES
DIRECTOR, DIVISION OF STRATEGIC COORDINATION

The Office of the Director, National Institutes of Health (NIH) in Bethesda, Maryland, is seeking a Director of the Division of Strategic Coordination (DSC) within the Office of Portfolio Analysis and Strategic Initiatives (OPASI). If you are an exceptional candidate with an M.D. and/or Ph.D., we encourage your application.

The OPASI's primary objective is to develop: a transparent process of planning and priority-setting characterized by a defined scope of review with broad input from the scientific community and the public; valid and reliable information resources and tools, including uniform disease coding and accurate, current and comprehensive information on burden of disease; an institutionalized process of regularly scheduled evaluations based on current best practices; the ability to weigh scientific opportunity against public health urgency; a method of assessing outcomes to enhance accountability; and a system for identifying areas of scientific and health improvement opportunities and supporting regular trans-NIH scientific planning and initiatives.

As the DSC Director, you will be responsible for integrating information and developing recommendations to inform the priority-setting and decision-making processes of the NIH in formulating NIH-wide strategic initiatives. These initiatives will address exceptional scientific opportunities and emerging public health needs (akin to the Roadmap, Obesity, and Neuroscience Blueprint initiatives). You will also be responsible for providing the NIH Director with the information needed to allocate resources effectively for trans-NIH efforts.

Salary is commensurate with experience and includes a full benefits package. A detailed vacancy announcement with the mandatory qualifications and application procedures can be obtained on **USAJOBS at www.usajobs.gov (announcement number OD-07-172844-T42) and the NIH Web Site at http://www.jobs.nih.gov**. Questions on the application procedures may be addressed to **Brian Harper on 301-594-5332**. Applications must be received by midnight eastern standard time on **August 10, 2007.**

OFFICE OF PORTFOLIO ANALYSIS AND STRATEGIC INITATIVES
DIRECTOR, DIVISION OF EVALUATION AND SYSTEMIC ASSESSMENTS

The Office of the Director, National Institutes of Health (NIH) in Bethesda, Maryland, is seeking a Director of the Division of Evaluation and Systemic Assessments (DESA) within the Office of Portfolio Analysis and Strategic Initiatives (OPASI). If you are an exceptional candidate with an M.D. and/or Ph.D. and the vision and ability to integrate evaluation systems and programs across multiple disciplines and organizations, we encourage your application.

The OPASI's primary objective is to develop: a transparent process of planning and priority-setting characterized by a defined scope of review with broad input from the scientific community and the public; valid and reliable information resources and tools, including uniform disease coding and accurate, current and comprehensive information on burden of disease; an institutionalized process of regularly scheduled evaluations based on current best practices; the ability to weigh scientific opportunity against public health urgency; a method of assessing outcomes to enhance accountability; and a system for identifying areas of scientific and health improvement opportunities and supporting regular trans-NIH scientific planning and initiatives.

As the DESA Director, you will be responsible for planning, conducting, supporting, and coordinating, specific program evaluations and projects of NIH Institutes and Centers such as the Roadmap, Obesity, and Neuroscience Blueprint initiatives. In addition, you will serve as the liaison for conducting governmentally required assessments according to the Government Performance and Results Act (GPRA) and OMB Program Assessment Rating Tool (PART). You will also serve as a member of the OPASI Steering Committee involved in oversight of institution-wide planning and analysis.

Salary is commensurate with experience and includes a full benefits package. A detailed vacancy announcement with the mandatory qualifications and application procedures can be obtained on **USAJOBS at www.usajobs.gov (announcement number OD-07-172847-T42) and the NIH Web Site at http://www.jobs.nih.gov**. Questions on the application procedures may be addressed to **Brian Harper on 301-594-5332**. Applications must be received by midnight eastern standard time on **August 10, 2007**.

WWW.NIH.GOV

OFFICE OF PORTFOLIO ANALYSIS AND STRATEGIC INITATIVES
DIRECTOR, DIVISION OF RESOURCE DEVELOPMENT AND ANALYSIS

The Office of the Director, National Institutes of Health (NIH) in Bethesda, Maryland, is seeking a Director of the Division of Resource Development and Analysis (DRDA) within the Office of Portfolio Analysis and Strategic Initiatives (OPASI). If you are an exceptional candidate with an M.D. and/or Ph.D., we encourage your application.

The OPASI's primary objective is to develop: a transparent process of planning and priority-setting characterized by a defined scope of review with broad input from the scientific community and the public; valid and reliable information resources and tools, including uniform disease coding and accurate, current and comprehensive information on burden of disease; an institutionalized process of regularly scheduled evaluations based on current best practices; the ability to weigh scientific opportunity against public health urgency; a method of assessing outcomes to enhance accountability; and a system for identifying areas of scientific and health improvement opportunities and supporting regular trans-NIH scientific planning and initiatives.

As the DRDA Director, you will be responsible for employing resources (databases, analytic tools, and methodologies) and developing specifications for new resources, when needed, in order to conduct assessments based on NIH-owned and other databases in support of portfolio analyses and priority setting in scientific areas of interest across NIH.

Salary is commensurate with experience and includes a full benefits package. A detailed vacancy announcement with the mandatory qualifications and application procedures can be obtained on **USAJOBS at www..usajobs.gov (OD-07-172841-T42) and the NIH Web Site at http://www.jobs.nih.gov**. Questions on the application procedures may be addressed to **Brian Harper on 301-594-5332**. Applications must be received by midnight eastern standard time on **August 10, 2007**.

NIEHS
National Institute of Environmental Health Sciences
National Institutes of Health

Director, Division of Extramural Research and Training (DERT)

Research Triangle Park, North Carolina

The National Institute of Environmental Health Sciences of the National Institutes of Health is seeking an exceptional candidate to fill the position of Director, Division of Extramural Research and Training. The incumbent of this position will direct the Institute's Extramural Research Program, which is organized into seven branches and centers and is composed of 56 FTEs. DERT is responsible for approximately 755 research grants for a total of $388 million. This dynamic and diverse grants portfolio covers a variety of scientific disciplines in support of research and research training in environmental health. The Division of Extramural Research and Training supports research that spans the entire spectrum, from basic mechanistic research to clinical studies. The Division supports translational research on the role of the environment in children's health, breast cancer, Parkinson's and other neurodegenerative diseases, respiratory diseases including asthma and reproductive health, to name just a few. Additionally, the Division is actively engaged in developing the next generation of environmental scientists through our training and career development programs, and the Director should be someone committed to this objective. The opportunity may be available for the incumbent to have his or her own intramural research program depending on scientific accomplishments and interests.

The position of Director, DERT, is one of the top five senior level positions reporting directly to the Director, NIEHS. The Director, DERT also serves as a principal advisor to the Institute Director on scientific affairs affecting the extramural community; develops and recommends procedures and policy for the execution of the research program; determines effectiveness of current programs and recommends new research programs in order to meet national environmental health needs. The incumbent is also expected to lead the staff and develop collaborations and relationships with other Federal agencies and also with advocacy groups and industry.

Candidates must have either an M.D., Ph.D. or equivalent degree in a discipline relevant to environmental health science. Candidates should be accomplished researchers in environmental health science, as evidenced by a publication record. Applicants should be aware of current trends, research directions and needs in environmental health sciences and be conversant with the policy implications of the research. Candidates should have a proven track record of administrative experience and scientific program development. Familiarity with NIH procedures and programs is helpful. Salary will be commensurate with level of experience.

Please forward questions regarding the position to:

Dr. Stephanie London, Search Committee Chair
National Institute of Environmental Health Sciences
111 Alexander Drive, P.O. Box 12233, Maildrop A3-05
Research Triangle Park, NC 27709
919-541-5772
London2@niehs.nih.gov

Interested persons should submit a curriculum vitae, a statement regarding reasons for interest in the position and unique qualifications by **August 24, 2007** to:

Ms. Stephanie Jones (Vacancy HHS/NIH-2007-DERT-01)
Office of Human Resources
National Institute of Environmental Health Sciences
P.O. Box 12233, Maildrop NH-01,
Research Triangle Park, NC 27709
Jones17@mail.nih.gov

http://www.niehs.nih.gov/dert/

DHHS and NIH are Equal Opportunity Employers

This position is subject to a background investigation.

(osi)™ pharmaceuticals

Shaping Medicine, Changing Lives

Position yourself on the cutting-edge at OSI Pharmaceuticals. We turn research opportunities into breakthrough medical treatments and offer a stimulating, collaborative environment where scientists can build rewarding careers. Discover your potential with an opening at ***our state-of-the-art Farmingdale, NY*** *research facility.*

EMT Research Leader

Lead EMT research efforts to further understand the central targets/pathways that drive the epithelial-to-mesenchymal transition in human cancers, identify novel drug targets and provide a basis for rational clinical use of agents that inhibit EMT or mesenchymal cell survival. A Ph.D. with 10+ years of experience and an international reputation in the field required. Extensive publication record on EMT in Oncology and demonstrated ability to both lead and work collaboratively are essential. Familiarity with clinical drug development practices in oncology a plus. **Ref# FA00142**

Research Project Leader (Molecular Targeted Therapies)

Lead cancer biology drug discovery efforts along with multi-departmental project teams to generate novel small molecules for treatment of cancer. Requires a Ph.D. with 8-15 years experience including strong oncology drug discovery and project leadership background. Knowledge of cancer cell signal transduction and experience in a biopharmaceutical company environment are essential. Expertise in molecular targeted therapies, biochemistry, cell biology and *in vitro* pharmacology and an understanding of PK/PD/efficacy relationships a must. Excellent communication skills required. **Ref# FA00143**

OSI offers a competitive benefits package including 401K, vacation, stock and much more. **Interested candidates, please apply online at http://careers.osip.com. (Ref # FA00142 & FA00143).** EOE M/F/D/V.

Faculty Position in Center for Molecular Chaperone/ Radiobiology and Cancer Virology

The Medical College of Georgia (MCG), Georgia's premier Health Sciences University, is recruiting an assistant or associate professor level faculty. Candidates should have a proven track record of productive research and preference will be given to those with funded projects. The chosen candidate will receive a competitive startup package. Areas of expertise should be investigating the role of molecular chaperones in protein misfolding diseases such as neurodegeneration and myopathies, cancer, protein trafficking, signal transduction, nuclear receptors assembly and function, as well as other related fields focusing on basic or translational research. Applicants will join a group of scientists investigating the role of molecular chaperones in animal models (mice, yeast, zebrafish) of human disease such as neurodegenerative disease, cancer, myopathies, viral immunology and inflammation. Excellent core facilities include Electron Microscopy, Transgenic and Knockout Mouse, Transgenic Zebrafish, Molecular Biology, Flow Cytometry, Proteomics and Genomics, Mass Spectrometry, Small Animal Behavioral Core, Imaging facilities, and a Human Brain lab.

Additional information is available at **www.mcg.edu** or from the Chair of the search committee **Dr. Nahid Mivechi**. Applications with a statement of research interests, curriculum vitae, and names and contact information for three references should be sent to: **Nahid Mivechi, PhD, MCG, Center for Molecular Chaperone/Radiobiology and Cancer Virology, 1410 Laney Walker Blvd. CN-3153, Augusta, GA 30912 (nmivechi@mcg.edu)**. Review of applications will begin on **September 1, 2007**.

MCG is an EEO/AA/Equal Access Employer.

SYRACUSE UNIVERSITY BIOMEDICAL AND CHEMICAL ENGINEERING

The L. C. Smith College of Engineering and Computer Science at Syracuse University invites applications for two tenure-track faculty positions in the Department of Biomedical and Chemical Engineering. Syracuse University is focusing strategically on the area of Biomaterials with cluster hiring across multiple colleges and departments, including these two junior faculty positions. Applicants should have a Ph.D. and academic and/or industrial experience indicating promise of an exceptional future in engineering research in the biomaterials area, including tissue engineering, controlled drug release, smart medical devices, biodegradable polymers, biointerfaces, computational or imaging techniques, and/or biocompatibility. In addition to collaboration with faculty in other schools and colleges, the Institute for Sensory Research and the Center of Excellence in Environmental and Energy Systems within Syracuse University, collaborative research opportunities extend to the adjacent campuses of the SUNY Upstate Medical University and the SUNY College of Environmental Science and Forestry. The Department offers B.S. (ABET-accredited), M.S. and Ph.D. degrees in both chemical engineering and bioengineering and the successful applicant will be able to teach in these programs. The greater Syracuse region is growing industry-academic opportunities in the biotechnology realm as evidenced by planned construction of a life sciences building at Syracuse University (see **http://lifesciences.syr.edu/main.html**), the new Syracuse Biotechnology Research Center (see **http://www.upstate.edu/biocenter/**), and the recent creation of MedTech (see **http://medtech.org/**) a regional organization to foster commercialization of biomedical technologies.

Applicants should submit a curriculum vitae, and statements of research and teaching interests to: **Dr. Jeremy Gilbert, Search Chair, Department of Biomedical & Chemical Engineering, 121 Link Hall, Syracuse University, Syracuse, NY 13244-1240**. At least three letters of reference should be sent to the same address. Application materials should be submitted electronically to www.sujobopps.com. Review of applications will begin **July 1, 2007** and will continue until the positions are filled.

Syracuse University is an Equal Opportunity/Affirmative Action Employer with a strong commitment to equality of opportunity and a diverse work force.

Oklahoma University Cancer Institute Director, Center for Basic and Translational Cancer Research

The OU Cancer Institute (OUCI) at the University of Oklahoma Health Sciences Center (OUHSC) is seeking qualified candidates for the position of Director of the newly created OUCI Center for Basic and Translational Cancer Research. Applicants are expected to have a successful track record of sustained, collaborative, peer-reviewed funding and publications, and to maintain an active research program, with preference given to NCI funding. The successful candidate will have the opportunity, authority and resources to develop and oversee basic and translational cancer research within the OUCI, especially in developmental therapeutics and translational research. This is a Deputy Director leadership position within the OUCI, with the responsibility of working closely with the Director to ensure that the Center supports the overall mission and goals of the OUCI. Substantial resources will be available to recruit faculty and build cancer research programs within the Center.

The OUCI is the only academic Cancer Center in Oklahoma, has received a P20 Cancer Center Planning Grant from the NCI, and participates in a P20 Clinical and Translational Science Award (CTSA) from the NIH. Five year investments in the OUCI total $210 million. Of this amount, $120 million is dedicated to funding a new cancer treatment and research facility. The additional $90 million is dedicated to creating endowed chairs to recruit cancer research faculty and providing support for program and infrastructure development.

Applications/nominations should include a current curriculum vitae and personal statement. Electronic submission of applications is preferred. All applications and inquiries will be confidential. Direct correspondence and inquiries to: **Robert Roswell, MD, Search Committee Chair, Senior Associate Dean, College of Medicine, University of Oklahoma Health Sciences Center, PO Box 26901, Oklahoma City, OK 73190; robert-roswell@ouhsc.edu; (405) 271-2307.**

The University of Oklahoma is an Equal Opportunity/ Affirmative Action Employer.

Pfizer

Working for a healthier world™

Research Technology Center, Cambridge

When does collaboration become a cure?

Imagine what you can achieve at a biotech start-up with unrivaled global resources. Imagine applying innovative science to identify and validate novel drug discovery targets. Imagine a biotech company atmosphere within one of the world's largest pharmaceutical organizations.

At Pfizer Research Technology Center (RTC) in Cambridge, MA, we apply innovative science to identify and validate novel drug discovery targets for Pfizer R&D and use creative scientific approaches to increase the diversity of potential drugs which may bind to these targets.

Surrounded by more than 300 biotechnology companies and world-leading research hospitals and academic institutions, a key element in the success of the RTC is the growing and dynamic portfolio of partnerships with these innovators. With them, we're applying cutting-edge techniques and technologies with broad utility across different therapeutic areas - developing a deep knowledge of new drug discovery targets, identifying novel chemical structures, and understanding mechanisms of toxicology.

At the RTC, we're balancing the strength of Pfizer R&D with the nimble feel of a small biotech, and creating an exciting and team-based scientific environment for over 150 colleagues with a wide range of scientific skills and experience. Collaboration and cooperation are the norm here. And the unique working environment is allowing science to leap forward into the future and bring to market what are miracles for many.

Now you can be a vital member of Pfizer Research Technology Center, a research center unlike any in the world, and use your talents to change the world.

Join Pfizer RTC and collaborate to find cures. We are currently hiring the following disciplines:

ADME Biology
Biochemistry
Biophysics
Cell Biology
Computational Biology
Computational Chemistry
Enzymology
Genomics
LCMS
Mathematical Modeling
Molecular Profiling
Protein Sciences/Protein Engineering
Proteomics
Synthetic/Medicinal Chemistry
Systems Biology
Text Mining

To apply now and learn more about our people, our pipeline, and our plans for the future, visit **www.pfizercambridge.com**

We're proud to be an equal opportunity employer and welcome applications from people with different experiences, backgrounds and ethnic origins.

VANDERBILT UNIVERSITY
SCHOOL OF MEDICINE

CHAIR
Department of
Molecular Physiology and Biophysics

Vanderbilt University School of Medicine is conducting a search for Chair, Department of Molecular Physiology and Biophysics. The department has a rich history of research in the areas of metabolism and cell signaling, and is consistently ranked among the very best of Physiology Departments. The department has accomplished, well funded faculty working in diverse areas including neuroscience, human genetics, diabetes, biophysics, cell signaling, and gene regulation. This is an exciting opportunity for a productive investigator to lead expansion of a distinguished department to an even greater level of excellence. The successful candidate will possess an outstanding record of published research, a commitment to education, with demonstrated vision, energy, and leadership capacity. She/he will have an appreciation of diverse areas of research and a strong record of productive collaboration.

Interested candidates should send *curriculum vitae*, bibliography, and a list of five professional references. The search committee will begin the review of applications on **September 1, 2007** and continue until the position is filled. Applications may be sent either electronically (**marlene.jayne@vanderbilt.edu**) or by mail to:

Michael R. Waterman, Ph.D
Chair, Molecular Physiology and Biophysics
Search Committee
c/o Marlene Jayne, BIOCH, 607 Light Hall
Vanderbilt University School of Medicine
Nashville, TN 37232-0146

PROJECT MANAGER

NIH Supported Interdisciplinary Research Consortium
SysCODE: Systems-based Consortium for Organ Design and Engineering

Brigham & Women's Hospital, Children's Hospital Boston, Harvard Medical School, Harvard University, M.I.T., Boston University, Vanderbilt University

This newly funded NIH Road Map Interdisciplinary Research Consortium will enjoin 23 exceptional scientists from the above institutions in a $24M, five year, NIH funded initiative to build artificial organ parts from stem cells. The Consortium will apply contemporary tools of developmental biology, genomics and proteomics, computational science, and tissue engineering to deduce molecular blueprints for the fabrication of teeth, pancreatic islets and heart valves. The anticipated start date is September, 2007.

The requisite skill set for this position includes: Ph.D. or M.B.A. degree, significant experience in scientific research administration, operations and financial management, superb organizational and team building skills, and a commitment to working with a group of highly motivated scientists. In direct collaboration with the Consortium Director, this individual will help lead the overall scientific efforts of the Consortium, including fiscal oversight of ten linked grants, training grant management and helping to define the Consortium agenda. The successful applicant will reside in the Genetics Division, Department of Medicine at Brigham & Women's Hospital and Harvard Medical School, and will enjoy an outstanding salary and benefits. Send cover letter outlining qualifications and CV electronically by **August 15, 2007** to **Richard Maas, M.D., Ph.D.**, Consortium Director, at: **SysCODE@genetics.med.harvard.edu**.

BWH is an Equal Opportunity Employer.

Yale University
Faculty Position
in
Ecology and
Evolutionary Biology

The Department of Ecology and Evolutionary Biology at Yale University invites applications for a faculty position at either the tenured or tenure track in the field of ecology. We are particularly interested in candidates whose research unites theory and empirical work in ways that shed new light on basic questions. A record of outstanding achievement and a promising research program are more important than the specific research area.

Interested candidates should submit their CV, three relevant reprints or manuscripts, brief research and teaching statements, and the names and addresses of four potential evaluators by **15 September 2007**. The search will remain open until the position is filled. Send materials to: **Department of Ecology and Evolutionary Biology, Yale University, P.O. Box 208106, New Haven, CT 06520-8106 USA, Attn: Francine Horowitz**.

The Department is described at:
www.eeb.yale.edu

Yale University is an Equal Opportunity/ Affirmative Action Employer. Men and women of diverse racial/ethnic backgrounds and cultures are encouraged to apply.

Wheaton College
For Christ and His Kingdom

Health Epidemiologist

The Applied Health Science Department of Wheaton College is searching for a full-time, tenure track faculty member with expertise in chronic diseases and physical activity epidemiology at the Assistant or Associate Professor level. The successful candidate will be expected to teach *Concepts and Principles of Epidemiology* and *Wellness* and conduct health related epidemiologic research with undergraduate students. Special consideration will be given to candidates who have expertise in Urban Public Health. Doctoral degree required.

Application deadline is October 31, 2007

The appointment will begin July 1, 2008

Applicants should send curriculum vita and description of their teaching philosophy and research interests to: Dr. David Ianuzzo, Chair; Applied Health Science Department; Wheaton College; 501 College Avenue; Wheaton, IL 60187 or email **david.ianuzzo@wheaton.edu**. Additional application materials will be sent to eligible candidates.

Wheaton College is an evangelical protestant Christian liberal arts college whose faculty members affirm a Statement of Faith and the moral and lifestyle expectations of our Community Covenant. Wheaton College complies with federal and state guidelines for nondiscrimination in employment; women and minorities are encouraged to apply.

FACULTY POSITIONS IN PLANT-RELATED MICROBIOLOGY

The Institute of Plant and Microbial Biology, Academia Sinica, Taipei is enthusiastically inviting applications for faculty positions in the research areas of microbiology with preference for plant-microbe interactions and plant-related microbiology. These positions are at the levels of Assistant Research Fellow, Associate Research Fellow, or Full Research Fellow (equivalent to Assistant Professor, Associate Professor, or Full Professor in universities). Excellent facilities and starter grants will be provided for these positions. For details of the Institute and Academia Sinica, please visit the website at **http://ipmb.sinica.edu.tw/**. Applicants are expected to have a Ph.D. degree plus postdoctoral training. Chinese language skills are NOT required and international scientists are encouraged to apply. The application folder should include curriculum vitae, a statement of research accomplishments, and future research plans. The application folder and at least three letters of recommendation should be sent to Dr. Na-Sheng Lin, Chair of Search Committee, Institute of Plant and Microbial Biology, Academia Sinica, Academia Rd, Nankang, Taipei, Taiwan 11529. e-mail: **nslin2@sinica.edu.tw**. FAX: (+886)2-2782-1605. The review of applications will start on Sept. 20, 2007 until the positions are filled.

U.S. Department of Energy
Associate Director
Office of Science for
Biological and Environmental Research
Announcement # SES-SC-HQ-014 (kd)

The U.S. Department of Energy's (DOE's) Office of Science is seeking qualified candidates to lead its Biological and Environmental Research (BER) Program. With an annual budget of more than $500 million, the BER Program is the nation's leading program devoted to applications of biology to bio-energy production and use and to environmental remediation. The BER Program supports major research programs in genomics, proteomics, systems biology, and environmental remediation. The Program is also one of the nation's leading contributors to understanding the effects of greenhouse gas emissions, aerosols, and atmospheric particulates on global climate change.

The Director of Biological and Environmental Research is responsible for all strategic program planning in the BER Program; budget formulation and execution; management of the BER office including a federal workforce of more than 30 technical and administrative staff; program integration with other Office of Science activities and with the DOE technology offices; and interagency integration. The position is within the ranks of the U.S. government's Senior Executive Service (SES); members of the SES serve in key positions just below the top Presidential appointees. For more information on the program please go to **http://www.sc.doe.gov/ober/**.

For further information about this position and the instructions on how to apply and submit an application, please go to the following website: **http://jobsearch.usajobs.opm.gov/getjob.asp?JobID=58520806&AVSDM=2007%2D06%2D06+13%3A44%3A02&Logo=0&q=SES-SC-HQ-014+(kd)&FedEmp=N&sort=rv&vw=d&brd=3876&ss=0&FedPub=Y&SUBMIT1.x=47&SUBMIT1.y=18**. To be considered for this position you must apply online. It is important that you follow the instructions as stated on the announcement **SES-SC-HQ-014 (kd)** located at the website above.

PURDUE
UNIVERSITY

FACULTY POSITIONS IN ECOLOGY, BIOLOGY, and SOCIAL SCIENCE of NATURAL RESOURCES

Purdue University seeks to complement existing strengths in ecology, biology, climate change, and social science by filling 4 tenure-track, academic-year positions at the rank of Assistant Professor in the areas of Forest Ecology (FE), Ecological Impacts of Climate Change (EICC), Fisheries Biology (FB), and Human Dimensions of Natural Resources (HDNR). Abundant opportunities for collaborative and interdisciplinary activities exist within a vibrant academic atmosphere facilitated by the Purdue Climate Change Research Center, the Purdue Interdisciplinary Center for Ecological Sustainability, the Hardwood Tree Improvement and Regeneration Center, and the newly created Discovery Park Center for the Environment.

The successful candidates will be expected to teach and develop dynamic, externally funded research programs within the following focal areas:

- **FE** – ecological processes in temperate forests, predicting the strength and context-dependence of species interactions across multiple scales; identifying the importance of feedbacks from individual interactions to ecosystem dynamics, and linking pattern with process to understand species coexistence.
- **EICC** – impacts of climate change on the ecology of terrestrial and/or aquatic populations or communities at landscape to global scales.
- **FB** – applied issues related to the conservation and management of aquatic resources.
- **HDNR** – critical examination of the human dimensions of forestry, fisheries, and/or wildlife with an emphasis on quantitative techniques.

Qualifications: A Ph.D. and evidence of significant research accomplishments. Screening of applications will begin October 1 for the FE position, and November 1 for the EICC, FB, and HDNR positions and continue until the positions are filled. Details on application procedures and complete descriptions of the positions are available at: **http://www.fnr.purdue.edu**. Please direct questions or inquiries to: **mbrown4@purdue.edu**.

Purdue University is an Equal Access/Equal Opportunity/Affirmative Action Employer fully committed to achieving a diverse workforce.

Research Scientist

An experienced doctoral level scientist is sought as an active team member for a research project to identify genes and mechanisms that modify susceptibility to prion infection or that are involved in prion replication. This non-tenure track faculty position is supported by a NINDS Program Project led by **George Carlson**, Director of **McLaughlin Research Institute**. Emphasis will be placed on exploiting a newly developed CNS stem cell culture system that can be infected with prions. Interaction with co-investigators at larger research centers in Seattle (**L.E. Hood**) and San Francisco (**S.B. Prusiner** and **S.J. DeArmond**) is required. Successful applicants will have a solid background in molecular genetics or CNS stem cell biology and will be expected to participate in experimental design, data evaluation, laboratory management, and preparation of publications and grant applications, as well as bench work. Salary is commensurate with experience.

McLaughlin Research Institute is a small, non-profit research organization located near **Montana's** Rocky Mountain front. Opportunities for outdoor recreation abound. Great Falls offers a pleasant environment, good public schools, and low housing costs.

Applications, including names and contact information for three to five individuals who may serve as references, should be sent to:

George A. Carlson, Ph.D.
Director, McLaughlin Research Institute
1520 23rd Street South
Great Falls, MT 59405

An Equal Opportunity/Affirmative Action Employer.

UNIVERSITY of CALIFORNIA
SAN DIEGO
MEDICAL CENTER
MOORES CANCER CENTER

Senior Investigator in Cancer Prevention and Control Rebecca and John Moores UCSD Cancer Center

The Rebecca and John Moores UCSD Comprehensive Cancer Center is seeking a faculty leader for its Cancer Prevention and Control (CP&C) Program (see **http://cancer.ucsd.edu**). The Comprehensive Cancer Center is part of the highly ranked UCSD School of Medicine.

The position includes a faculty appointment with tenure in an appropriate Department in the School of Medicine. The CP&C program has 15 peer-review-funded principal investigators. The future leader will be expected to be able to develop successful collaborations with cancer center members from other Cancer Center programs. The CP&C program houses the large WHEL biological specimens repository.

The Moores UCSD Cancer Center is a matrix center. This faculty position will be located in the department within the School of Medicine department that best suits the skills of the successful applicant. The position will be housed in the new Moores Cancer Center building within the 23,000 sf assigned to population science research. This includes a Clinical Research facility and a Healing Foods kitchen which will be available for use of the successful candidate.

The position will require a doctorate in a relevant research field and a track record of grant support with quality peer reviewed publications as well as other professional recognition of accomplishment. Good collaboration skills, teaching experience and a demonstrated ability to coordinate a research program will be an advantage. Salary will be commensurate with experience. Review of application will begin **June 30, 2007**, and will continue until the position is filled. Interested applicants should send the curriculum vitae to: **Dr John P. Pierce, Chair, Cancer Prevention and Control Search Committee, Moores UCSD Cancer Center, 3855 Health Sciences Drive, La Jolla, California 92093-0901; Email: jppierce@ucsd.edu**

UCSD is an Equal Opportunity Employer.

Faculty Position in Neuroscience Texas A&M University

The Department of Biology at Texas A&M University (TAMU) invites applications for a faculty position in neuroscience at the **FULL PROFESSOR** level. We are interested in outstanding neuroscientists with well-funded, internationally recognized research programs. We especially invite applications from researchers who will interact with, and enhance, an existing or emerging area in behavioral biology, neural plasticity, developmental neurobiology, genetics and functional genomics, sensory neurobiology, circadian biology, computational biology, and structural biology.

We seek applications from individuals who will lead efforts to strengthen interdisciplinary/translational research and training associated with Texas A&M University's Interdisciplinary Life Science Building (**http://ilsb.tamu.edu**), its newly formed Texas Institute for Genomic Medicine (**http://www.tigm-knockouts.org**), and its emerging Graduate Program in Neuroscience. More information about our department can be found at **www.bio.tamu.edu**. For full consideration, applicants should send a letter of intent, *curriculum vitae*, statement on research and teaching, and three letters of recommendation (preferably in electronic form by email) by **September 15, 2007** to:

Biology Neuroscience Search Committee
Attn: Mark J. Zoran, Committee Chair
Department of Biology
Texas A&M University
3258 TAMU
College Station, TX 77843-3258
Email: zoran@mail.bio.tamu.edu

Texas A&M University is an Equal Opportunity Employer and has a policy of being responsive to the needs of dual-career couples.

Dave Jensen
Industry Recruiter

Science Careers Forum

- How can you write a resume that stands out in a crowd?
- What do you need to transition from academia to industry?
- Should you do a postdoc in academia or in industry?

Let ScienceCareers.org help you answer these questions. ScienceCcareers.org has partnered with moderator Dave Jensen and four well-respected advisers who, along with your peers, will field career-related questions.

Visit ScienceCareers.org and start an online dialogue.

ScienceCareers.org
We know science AAAS

U.S. Department of Energy
Office of Science
Deputy for Programs
Announcement #SES-SC-HQ-013 (kd)

The U.S. Department of Energy's (DOE) Office of Science is seeking highly qualified candidates with outstanding scientific achievements to fill the Deputy for Programs position. The Office of Science is the single largest supporter of basic research in the physical sciences in the United States, with a 2007 budget of $3.8 billion. It oversees the Nation's research programs in high-energy and nuclear physics, basic and fusion energy sciences, and biological, environmental and computational sciences. The Office of Science is the Federal Government's largest single funder of materials and chemical sciences, and it supports unique and vital parts of U.S. research in climate change, geophysics, genomics, life sciences, and science education. The Office of Science also manages 10 world-class laboratories and oversees the construction and operation of some of the Nation's most advanced R&D user facilities, located at national laboratories and universities. These include particle and nuclear physics accelerators, synchrotron light sources, nanoscale science research centers, neutron scattering facilities, bio-energy research centers, supercomputers and high-speed computer networks. More information on the Office of Science can be found at **http://science.doe.gov**.

The Deputy for Programs provides scientific and management oversight of the six program offices by ensuring program activities are strategically conceived and executed; formulating and defending the Office of Science budget request; establishing policies, plans, and procedures related to the management of the program offices; ensuring the research portfolio is integrated across the program offices with other DOE program offices and other Federal agencies; and representing the organization and make commitments for the Department in discussions and meetings with high-level government and private sector officials. The position is within the ranks of the U.S. government's Senior Executive Service (SES); members of the SES serve in key positions just below the top Presidential appointees.

To apply for this position, please see the announcement and application instructions at **http://jobsearch.usajobs.opm.gov/ses.asp** under the vacancy announcement of **#SES-SC-HQ-013 (kd)**. Qualified candidates are asked to submit their online applications by **August 29, 2007**.

Postdoctoral Fellowships in Cell and Molecular Biology

Fellowships for the National Research Service Award Program of the National Institute of Diabetes and Digestive Kidney Diseases (NIDDK), National Institutes of Health (NIH) at Stony Brook University, are available in cell and molecular biology of metabolic diseases for candidates with Ph.D., D.Sc., M.D., or equivalent (within five years of Ph.D. for non-clinical applicants). Stipend levels are competitive. This institutional postdoctoral training program is interdisciplinary, interdepartmental, and interinstitutional by design, supported by regional interaction with Brookhaven National Laboratory and Cold Spring Harbor Laboratory. The program benefits from 25+ NIH-supported trainers with state-of-the-art research programs in areas of cell signaling relevant to diabetes, endocrine, and metabolic diseases.

Current research/mentor opportunities include:

Wadie Bahou: Proteases and endothelial cell pathology; **Deborah Brown:** Lipids rafts and caveolae; **Weiliam Chen:** Bioengineering of bioactive wound healing matrices; **Richard Clark:** Structure-function of non-enzymatic glycated fibronectin that adversely affect cell migration; **Ira Cohen:** Molecular and cellular cardiovascular research; **Howard Crawford:** Matrix metalloproteinases in pancreatic cancer; **Michael Frohman:** Phospholipase D and membrane vesicular trafficking; **Bruce Futcher:** Microarray analysis of transcriptional control in yeast; **Marie Gelato:** Pathogenesis of the insulin resistance and hyperlipidemia in HIV disease; **Robert Haltiwanger:** O-glycosylation and Notch function; **Jamie Konopka:** G protein- coupled receptors signaling in yeast; **Irwin Kurland:** Hepatic insulin action and role of the pentose shunt; **William Lennarz:** Congenital disorders of glycosylation in humans; **Richard Lin:** G protein signaling and insulin resistance; **Craig Malbon:** GPCRs, scaffold proteins, and Wnt-Frizzled signaling; **Mirjana Maletic-Savatic:** Neural stem cell fate and function; biomarkers of human neurological disorders; **Stuart McLaughlin:** Biophysics of signal transduction; **Margaret McNurlan:** Insulin action in muscle; **Todd Miller:** Signal transduction by tyrosine kinases; **Yingtian Pan:** Cystoscopic optical coherence tomography in human disease; **Jeffrey Pessin:** Insulin signaling and regulation of glucose transport; **Nicole Sampson:** Biosynthesis of steroids in innate defense mechanisms; **Suzanne Scarlata:** Activation of PLC by G proteins; **Steve Smith:** Structural studies of membrane channels and receptors; **Ken Takemaru:** Role of beta- catenin antagonist Chibby in atherosclerosis; **Fayanne Thorngate:** Apolipoprotein E, atherosclerosis, and signaling; **Stella Tsirka:** Neuronal-microglial interactions in the mammalian brain; **Hsien-yu Wang:** G proteins and development.

Only U.S. citizens or permanent residents (within five years of Ph.D. for non-clinical applicants) are eligible for these NIH-supported fellowships.

Applicants should send a C.V., brief letter of research interest, and names of three references to:
Dr. Craig C. Malbon, Director-DMDRC, Pharmacology, Stony Brook University
SUNY, Stony Brook, NY 11794-8651
Fax: (631) 444-7696. For more information or to apply online visit:
www.stonybrook.edu/cjo
Equal Opportunity/Affirmative Action Employer.

STONY BROOK

ASU

DIRECTOR
Department of Animal Care and Technologies

ASU is part of a very fast growing biomedical movement in Phoenix that seeks to link basic scientists at the university with clinical scientists and clinicians in the surrounding hospitals and medical institutions. These linkages have resulted in new research ventures, and new education programs including a new medical school curriculum, a product of the Arizona College of Medicine-Phoenix, in partnership with Arizona State University. Animal research will play a key role in these research and education developments, and in the enhancement of bioscience and biotechnology in this fast growing state. The Department of Animal Care and Technologies at ASU occupies, operates in, and manages a total of 72,000 square feet of animal use facilities, provides care to 25 different species, and currently serves 74 investigators with multiple active protocols.

JOB DESCRIPTION: Under administrative direction, the Director performs work of considerable responsibility in planning, directing and controlling the Department of Animal Care and Technologies in facilitating animal research and assuring compliance with all current federal, state and university animal welfare regulations. The Director reports to the Associate Vice President for Research Administration.

DUTIES AND RESPONSIBILITIES: Directs animal procurement, use and husbandry, and formulates university policy for animal care and use. Collaborates with faculty regarding animal research, support services, and instructional infrastructure for contemporary biomedical science. Ensures compliance with university policy and governmental animal welfare regulations for continued AAALAC International accreditation. Supervises animal care personnel. Provides fiscal program management including preparation of the annual budget and maintenance of the cost recovery program. Leads the development of new animal facilities and renovation/ improvements of existing animal facilities. Develops funding proposals to private, state and federal agencies to support upkeep, modernization and expansion of animal care facilities.

DESIRED QUALIFICATIONS: Demonstrated experience of: management principles and techniques including those dealing with personnel; budgetary practices and procedures. Demonstrated experience in: grant funding; governmental regulations and contemporary practices in animal care; developing modern animal care facilities in animal research using a broad range of traditional animal models used in biomedical research, and nontraditional species. Ability to communicate and implement policies and procedure within a diverse population. Effective written and oral communication.

MINIMUM QUALIFICATIONS: Doctoral (Ph.D. or DVM) degree in a relevant discipline and five years of experience in animal research, including three years of experience in an administrative/supervisory capacity of an academic or research institute animal care program; OR, Any equivalent combination of education and/ or experience from which comparable knowledge, skills and abilities have been achieved

GENERAL INFORMATION: The Director of the Animal Care and Technologies program serves as a voting member of the University Institutional Animal Care and Use Committee (IACUC) and works closely with the Chair for that committee, the University Veterinarian, and the animal use advisory committee regarding animal procurement, use and husbandry. The Director works closely with the university administration including department chairs, deans and center directors. The Director should be visionary and play a strong role in helping implement the design imperatives of the New American University model www.asu.edu/president/newamericanuniversity

TO APPLY: Submit (1) a cover letter, (2) a resume or curriculum vitae, (3) a statement of professional vision, and (4) the names, addresses, phone numbers and email addresses of 3 professional references. Please be sure that applications include all requested information: **Arizona State University, Office of the Vice President for Research and Economic Affairs, Box 872703, Tempe, AZ 85287-2703**. Close date: **September 15, 2007**.

Arizona State University is an Affirmative Action/ Equal Opportunity Employer and Educator.

XX INTERNATIONAL CONGRESS OF GENETICS, BERLIN, 2008

BERLIN, GERMANY, JULY 12 – 17, 2008

GENETICS – UNDERSTANDING LIVING SYSTEMS

Registration NOW open

Abstract Submission Deadline
January 15, 2008

Deadline for Early Registration Fee
January 15, 2008

Early Exhibitor Deadline
January 18, 2008

Genetics reveals the structure, function and evolution of living systems.

Genomics revolutionized genetic research. Now, complete annotated genome sequences are available for the human, our closest relative, the chimpanzee, and for many other model organisms. Multiple genomes have been compared and scrutinized for past and ongoing processes of variation, adaptation and speciation. Traces of the foregoing RNA world show it to be far more influential than previously suspected. Comprehensive maps of genome variation and polymorphism paint a rich picture of our population and evolutionary history and illustrate new strategies that will explain genetic, epigenetic and environmental contributions to disease risk. Transcriptomes comprehensively documenting gene expression and proteomic data sets are being built into functional networks and systems. Bioinformatics and modeling of genomic data attempt to predict and explain the functional architecture of genomes across the diversity of organisms.

The Congress in Berlin will present the latest genetic and genomic insights in ten plenary lectures and 54 concurrent symposia. 280 of the world's most prominent geneticists will speak.

For more information on the scientific program and associated activities, please visit:
http://www.geneticsberlin2008.com

Scientific Topics:
(selection)

- Ageing and longevity
- Biodiversity
- Clocks and rhythms
- Computational genetics and systems biology
- Development of multicellular organisms
- Epigenetics and chromatin
- Evolutionary genomics, adaptation, speciation
- Human evolution
- Human genetics and human disease
- Metagenomics
- Neurogenetics
- RNA world
- Stem cells
- Synthetic biology

Congress President:
Rudi Balling (HZI Braunschweig, Germany)

Co-Chairs International Program Committee:
Charles Langley (UC Davis, USA)
Rudi Balling (HZI Braunschweig, Germany)

Honorary Presidents:
Rudolf Jaenisch
Christiane Nüsslein-Volhard
Tomoko Otah

Congress Secretary General:
Alfred Nordheim (Tuebingen University, Germany)

Plenary Lecturers:
(confirmed)
Richard Axel
Elizabeth Blackburn
Rudolf Jaenisch
Eric Lander
Svante Pääbo
Phillip Sharp

International Genetics Federation (IGF)

BERLIN 2008 XX INTERNATIONAL CONGRESS OF GENETICS

German Genetics Society (GfG)

In partnership with nature genetics

PRIZES

Novartis is delighted to congratulate the winners of the

2007 Novartis Immunology Prizes

The prizes are awarded for outstanding achievements to the understanding of immunology and major immunological discoveries that lead to therapeutic applications in such fields as transplantation, haematopoiesis, cancer immunology, immunity to infectious diseases, rheumatology, dermatology and asthma.

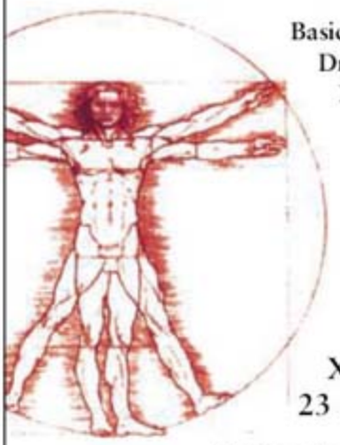

Basic Immunology Prize

Dr. Frederick W. Alt and **Dr. Klaus Rajewsky**, Harvard Medical School, Boston, USA and **Dr. Fritz Melchers**, Biozentrum, Basel, Switzerland, for their discovery of novel and fundamental mechanisms of B lymphocyte physiology at the genetic, developmental and cell-receptor levels.

Clinical Immunology Prize

Dr. John T. Schiller and **Dr. R. Lowry**, National Institutes of Health, Bethesda, Maryland, USA and **Dr. Ian H. Frazer**, University of Queensland, Australia, for their discoveries that enabled the development of the human papilloma virus vaccine.

The 2007 Novartis Immunology Prizes will be awarded at the XIIIth International Congress of Immunology in Rio de Janeiro on 23 August 2007.

Reviews by the Novartis Prize Awardees will be published in the *European Journal of Immunology*.

Jury: Andrew McMichael (Chair), Jean-François Bach, Max D. Cooper, Tasuku Honjo, Philippa Marrack, Randall Morris, Hidde Ploegh, David H. Sachs, Jan de Vries.

NOVARTIS

CONFERENCE

SCIENTIFIC CONFERENCES
HINXTON CAMBRIDGE UK

wellcome trust

FUNCTIONAL GENOMICS & SYSTEMS BIOLOGY

10 - 14 OCTOBER 2007

A new Wellcome Trust/Cold Spring Harbor Laboratory Conference to be held at the Wellcome Trust Conference Centre on the Wellcome Trust Genome Campus, Hinxton, Cambridge, UK

Abstract and registration deadline **10 August 2007**

To Register please visit **www.wellcome.ac.uk/conferences**

Topics Include

Transcriptome and proteome analysis, RNAi and mutagenesis studies, Single cell level analysis, Gene regulation networks and pathway analysis, New high throughput technologies and their applications, Computational data analysis, interpretation and resourses, Cell and molecular level simulations, Functional genomics of disease.

The Wellcome Trust Conference Centre is operated through two companies: Hinxton Hall Limited, a charity registered in England (no. 1048066) and a company registered in England (no. 3062160); and Wellcome Trust Trading Limited, a non-charitable company registered in England (no. 3227027), controlled by the Wellcome Trust. The registered offices of both companies are at 215 Euston Road, London NW1 2BE, UK.

Enjoying the dog days of summer on Cold Spring Harbor

Cold Spring Harbor Laboratory
2007 Late Summer and Fall Meetings

Yeast Cell Biology
August 15 - 19
Kerry Bloom, Peter Pryciak, Lois Weisman

Eukaryotic mRNA Processing
August 22 - 26
Douglas Black, Timothy Nilsen, Joan Steitz

Mechanisms of Eukaryotic Transcription
August 29 - September 2
Barbara Graves, Steven Hahn, Jerry Workman

Eukaryotic DNA Replication
September 5 - 9
Stephen Bell, Joachim Li

Microbial Pathogenesis and Host Response
September 15 - 19
Brendan Cormack, Theresa Koehler, James Slauch

Cell Death
September 26 - 30
J. Marie Hardwick, Jurg Tschopp, Junying Yuan

Neurobiology of *Drosophila*
October 3 - 7
Alex Kolodkin, Amita Sehgal

Clinical Cardiovascular Genomics
October 10 - 14
David Ginsburg, Elizabeth Nabel, Edward Rubin

Genome Informatics
November 1 - 5 abstracts due: August 1
Michele Clamp, Tim Hubbard, Jason Swedlow

In Vivo Barriers to Gene Delivery
November 15 - 18 abstracts due: August 31
Nori Kasahara, Stephen Russell, Jim Wilson

Molecular & Immunological Approaches to Vaccine Design
November 29 - December 2 abstracts due: Sept. 14
Peter Beverley, Kathrin Jansen, Susan Swain

Rat Genomics & Models
December 6 - 9 abstracts due: October 5
Timothy Aitman, Norbert Hubner, Anne Kwitek, James Shull

CSHL Meetings & Courses Program, Cold Spring Harbor, New York http://meetings.cshl.edu

POSITIONS OPEN

ASSISTANT/ASSOCIATE/FULL PROFESSOR (Inhalation Toxicology and Cardiology/Tenure-Track) Comparative Biomedical Sciences

Biomedical Department with a well-equipped inhalation research facility seeks a **FACULTY** person in inhalation toxicology and cardiology. Required qualifications: Ph.D. or equivalent degree in biological/biomedical sciences or related field; postdoctoral experience; research background in inhalation toxicology and cardiology; significant extramural funding; ability to teach in professional and graduate program. Responsibilities: maintains an extramurally funded research program; contributes to the graduate and professional program; expands collaborative usage of inhalation research facility. Salary and rank will be commensurate with qualifications. *An offer of employment is contingent on a satisfactory pre-employment background check.* Application deadline is August 24, 2007, or until candidate is selected.

Submit letter of application and resume (including e-mail address) to:

Dr. Arthur Penn
Department of Comparative Biomedical Sciences
School of Veterinary Medicine
Louisiana State University
Reference: #027599
Baton Rouge, LA 70803
Telephone: 225-578-9889
E-mail: apenn@vetmed.lsu.edu

LSU is an Equal Opportunity/Equal Access Employer.

LABORATORY MANAGER (Job Number 38464) Laser Ablation-Inductively Coupled Plasma Mass Spectrometry Arizona LaserChron Center

The University of Arizona seeks a highly motivated scientist to serve as Manager of the Arizona LaserChron Center, which is a multi-user facility that focuses on U-Th-Pb geochronology by laser ablation-multicollector inductively coupled plasma mass spectrometry (ICPMS). Responsibilities would include: (1) directing installation of a new multicollector ICPMS and Excimer laser, (2) developing new analytical techniques and applications using an existing multicollector ICPMS (GVI Isoprobe) and Excimer laser (DUV193), (3) performing minor maintenance and overseeing major repairs of these instruments, (4) supervising visits of research scientists, and (5) conducting independent research. The position is full-time and permanent. Applicants should have a M.S. or Ph.D. in earth science or chemistry, and have demonstrated experience with ICPMS instrumentation. Applications will be reviewed beginning 15 August 2007, and will continue until the position is filled. Applications should be submitted at **website: https://www.uacareertrack.com** for job number 38464. For additional information, please visit the Arizona LaserChron Center **website: http://www.geo.arizona.edu/alc** and contact **George Gehrels (e-mail: ggehrels@e-mail.arizona.edu)** or **Joaquin Ruiz (e-mail: jruiz@e-mail.arizona.edu).** *The University of Arizona is an Equal Opportunity, Affirmative Action Organization.*

FACULTY
Geological, Environmental, and Marine Sciences

Rider University's Geological, Environmental, and Marine Sciences Department invites applications for a tenure-track faculty position at the rank of **ASSISTANT or ASSOCIATE PROFESSOR,** commensurate with experience and research credentials, beginning in September 2008. Preferred areas of specialization could include, but are not limited to, atmospheric/climatologic sciences, fluvial/lacustrine processes, or marine/estuarine environments.

For more information on this position and for application instructions, please visit our **website: http://www.rider.edu/hr,** employment opportunities, position #208102. *Affirmative Action/Equal Opportunity Employer.*

POSITIONS OPEN

University of Massachusetts Medical School
UMASS

POSTDOCTORAL POSITION
Small Animal Imaging and Biomarker Development

The University of Massachusetts Medical School has an immediate opening for a Postdoctoral Scientist with interest and aptitude in small animal imaging to assume daily responsibility for a microPET/SPECT/CT and an optical camera. As a member of the Laboratory for Biomarker Development, the successful candidate will join a multidisciplinary team emphasizing bench and bedside research in molecular imaging of cancer, infections, and other diseases and will be encouraged to conduct independent research. Preference will be given to those holding a Doctorate in disciplines useful in the development of biomarkers such as radiopharmaceutical and fluorescent chemistry. The Laboratory is well funded through multiyear NIH grants. Salaries will be consistent with NIH guidelines.

Please respond with resume, names, and addresses of three references and a short statement of career goals to: **D. J. Hnatowich, Ph.D., Professor, Nuclear Medicine, Department of Radiology, University of Massachusetts Medical School, Worcester, MA 01655. E-mail: donald.hnatowich@umassmed.edu.**

MICROBIOLOGY FACULTY POSITIONS

The Department of Immunology/Microbiology at Rush University Medical Center seeks two outstanding investigators for tenure-track positions at the **ASSISTANT or ASSOCIATE PROFESSOR** levels. The successful applicants will be expected to develop strong independent research programs in microbial or viral pathogenesis and to participate in both medical and graduate student teaching. The Department currently has strong research programs in the areas of innate immunity and molecular virology and pathogenesis. Applicants must have a Ph.D., D.Sc., or M.D. degree with postdoctoral experience and a quality publication record. Competitive salary and startup funds are available. Applicants at the Associate Professor level should have a record of substantial productivity and sustained extramural funding. Please submit curriculum vitae, a two-page summary of research interests, and the names of three references electronically to: **Sonia Raigoza, Immunology/Microbiology Search Committee, Rush University Medical Center, 1735 West Harrison Street, Chicago, IL 60612. E-mail: sonia_raigoza@rush.edu.** *Rush University Medical Center is an Equal Opportunity/Affirmative Action Employer.*

POSTDOCTORAL RESEARCH FELLOWSHIPS
Emory Chemical Biology Discovery Center

We are looking for bright, independent, energetic Postdoctoral scientists at all levels to join our team of biomedical investigators, synthetic chemists, and cheminformaticists, who work together to create novel small organic molecules that target disease-related proteins and processes. Successful candidates will learn how to form bridges between basic research and early stage therapeutic development. Background in biochemistry, pharmacology, cell physiology, or cellular imaging, an advanced degree, excellent writing and communication skills, and a track record of publications are essential. Send a letter of intent, curriculum vitae, PDFs of no more than three papers, and names and contact information of three references to **Haian Fu** or **Ray Dingledine** at **e-mail: discovery@pharm.emory.edu** at the **Department of Pharmacology, Emory University School of Medicine, 1510 Clifton Road, Atlanta, GA 30322.** *Affirmative Action/Equal Opportunity Employer.*

POSITIONS OPEN

TENURE-TRACK FACULTY POSITION
Department of Pediatrics/Center for Molecular Medicine and Genetics
Wayne State University School of Medicine

A tenure-track position for an outstanding **PHYSICIAN-SCIENTIST** (M.D. or M.D.-Ph.D. degrees) at the **ASSISTANT, ASSOCIATE, or FULL PROFESSOR** level is available as a joint appointment between the Department of Pediatrics and the Center for Molecular Medicine and Genetics **(website: http://www.genetics.wayne.edu).** The appointee would be housed in the Laboratories of the Center, which recently underwent a $20 million renovation of its Laboratory and core research facilities. The candidate would join an active faculty conducting basic and translational research. An attractive startup package is available. The Department of Pediatrics is housed in the 235-bed Children's Hospital of Michigan **(website: http://chmkids.org)** and includes 170 faculty, 100 residents, and 50 fellows. There are also significant clinical research opportunities through the Children's Research Center of Michigan **(website: http://www.med.wayne.edu/crcm/),** which currently manages $6.7 million in NIH funding. We are recruiting a candidate who has areas of ongoing research in translational genetics or genomics, including inborn errors of metabolism, mitochondrial disorders, or treatment of genetic disorders. The Division of Genetic and Metabolic Disorders within the Department of Pediatrics is responsible for the management of all patients diagnosed with an inborn error of metabolism in the state of Michigan, offering an opportunity to develop novel treatment or research protocols for these patients. There are extensive opportunities for collaboration and excellent opportunities to develop translational research with industry, government, and other academic institutions. Wayne State University is Michigan's only research university located in an urban setting. Applications will be reviewed upon receipt and review continued until the position has been filled.

Applications should include a letter of application, curriculum vitae, and the names and addresses of at least three references and be sent to: **Ms. Mary Anne Housey, Center for Molecular Medicine and Genetics, Wayne State University School of Medicine, Room 3127 Scott Hall, 540 E. Canfield Avenue, Detroit, MI 48201** or by **e-mail: mhousey@genetics.wayne.edu.**

WSU, an Equal Opportunity/Affirmative Action Employer.

CALL for POSTDOCTORAL FELLOWSHIP APPLICATIONS
Cornelia de Lange Syndrome Foundation, U.S.A.

The Cornelia de Lange Syndrome (CdLS) Foundation announces a Postdoctoral Fellowship to support basic or clinical research on CdLS to start July 1, 2008. CdLS is caused by genetic changes affecting the NIPBL, Smc1 or Smc3 proteins involved in sister chromatid cohesion, gene expression, and DNA repair. The Fellowship provides $60,000/year for two years to cover salary/benefits for a researcher who has a Ph.D. or M.D. but does not hold a tenure-track faculty position. Applications on topics ranging from molecular functions of the sister chromatid cohesion apparatus in model organisms to therapeutic treatments for CdLS will be considered. The Fellow will present his/her work at the CdLS Foundation's national meetings.

For details and requirements, go to **website: http://www.cdlsusa.org/research/index.shtml.** Applications are due November 15, 2007.

POSTDOCTORAL POSITION at the University of Montana. **MOLECULAR BIOCHEMIST** to study transcription-induced hypermutation in human cell lines. Expertise in genetic engineering and cell culture techniques required. Position available this August. Send curriculum vitae to **e-mail: barbara.wright@mso.umt.edu.** *Affirmative Action/Equal Opportunity Employer.*

POSITIONS OPEN

RESEARCH MOLECULAR BIOLOGIST
United States Department of Agriculture (USDA)
Agricultural Research Service (ARS)

The Eastern Regional Research Center (ERRC), Agricultural Research Service (ARS) has a challenging position available for a temporary **POSTDOCTORAL** full-time **MOLECULAR BIOLOGIST.** The individual will serve as a scientist in the prestigious Microbial Food Safety Research Unit, which is located on an attractive 27-acre campus just outside of Philadelphia, in Wyndmoor, Montgomery County, Pennsylvania. Employees enjoy a flexible work schedule and have access to public transportation. Research facilities include sophisticated and well-equipped laboratories, pilot plants, a computer unit, and library. The scientist will be responsible for conducting research aimed at identifying molecular markers for lag phase duration (LPD), thus leading to more mechanistic models and greater certainty predicting the LPD of foodborne pathogens directly in foods. Candidates must have knowledge of molecular biology, food sampling methodology, statistical methods, and computer techniques. *Please see the following website concerning citizenship requirements.* **Website: http://www.afm.ars.usda.gov./hrd/jobs/visa/countries.htm.** Salary commensurate with experience, GS-11: $55,829 to $72,579. For information on the position, contact **Dr. John B. Luchansky** at **telephone: 215-233-6620, e-mail: john.luchansky@ars.usda.gov** or **Dr. Vijay K. Juneja** at **telephone: 215-233-6500, e-mail: vijay.juneja@ars.usda.gov.** For more detailed information on announcement number RA-07-046L visit **website: http://www.ars.usda.gov** on the internet. *USDA is an Equal Opportunity Provider and Employer.*

COLUMBIA UNIVERSITY MEDICAL CENTER
Pathology

A position at the level of **ASSOCIATE RESEARCH SCIENTIST** is available immediately to investigate the cellular biology of infection of cells by varicella zoster virus (VZV) and the role of serotonin in the development and function of enteric neurons. The Laboratory maintains three NIH-funded research projects focusing on the enteric nervous system (ENS). In addition to the studies in which enteric neurons are employed to investigate VZV entry, latency, and reactivation, the projects study the development of the ENS and the molecular and cellular mechanisms that underlie its control of gastrointestinal behavior. A Doctorate background with molecular and cellular biology techniques is required. Work will include cell and organ culture, gene transfer, in situ hybridization, quantitative PCR analyses, immunocytochemistry and microscopic imaging. Evidence should be presented of prior accomplishment and the ability to supervise the work of others. Send curriculum vitae to: **Dr. M. Gershon, Columbia University Medical Center; 630 West 168th Street, MC #32; New York, NY 10032.**

Columbia University takes Affirmative Action toward Equal Employment Opportunity.

The University of Hawaii's (UH) John A. Burns School of Medicine is recruiting for two full-time, **TENURE-TRACK POSITIONS** in pharmacology and physiology. For a full description of the pharmacology position, please visit the Work at UH **website: http://workatuh.hawaii.edu/zoom_job.php?7673.** For inquiries on the pharmacology position, please contact the **Search Committee Chair, Dr. Vivek R. Nerurkar, telephone: 808-692-1665** or **e-mail: pharma@hawaii.edu.** For a full description of the physiology position (#84851), please visit the Work at UH **website: http://workatuh.hawaii.edu/zoom_job.php?4649.** For inquires on the physiology position, please contact **Dr. Steve Ward, telephone: 808-956-5189** or **e-mail: wward@hawaii.edu.**

POSITIONS OPEN

ASSISTANT PROFESSOR/ASSISTANT SCIENTIST or ASSOCIATE PROFESSOR/ASSOCIATE SCIENTIST, Plant Science, Washington State University, Institute of Biological Chemistry. Applications are invited for a full-time, permanent, nine-month, tenure-track (25 percent Academic Programs, 75 percent Agricultural Research Center) position to begin in 2008 at the Pullman, Washington campus. Applicants must have a Ph.D. or equivalent, as well as at least one year of postdoctoral experience by start date. Candidates should demonstrate quality and quantity of research accomplished in a fundamental area of modern plant science; expertise in using biochemical, biophysical, or structural biology approaches to investigate biological problems, a coherent research plan that incorporates these approaches, and excellent oral and written communication skills. At Associate level there must be a record of mentoring skills; demonstration of ability to establish an independent research program, and an emerging national and international reputation. The candidate will also be expected to participate in teaching graduate-level courses in an area of modern plant biology. The Institute **(website: http://www.ibc.wsu.edu/)** provides a supportive research environment with more than 120 scientists, excellent equipment and facilities, and ready access to specialized techniques in biochemistry, cell biology, proteomics, metabolomics, and genomics. For more details see **website: http://www.hrs.wsu.edu/employment/FAPvacancies.asp (search #4758).** Candidates should submit curriculum vitae, a statement of research interests, and a description of future research plans as a PDF file to **e-mail: millerhm@wsu.edu.** In addition, applicants should arrange for three letters of reference, preferably as PDF files, to be sent to: **Dr. Michael L. Kahn, Search Committee Chair, Institute of Biological Chemistry, Washington State University, P.O. Box 646340, Pullman, WA 99164-6340 (telephone: 509-335-8383; e-mail: millerhm@wsu.edu; fax: 509-335-7643).** Review of applications will begin September 15, 2007. *Equal Employment Opportunity/Affirmative Action/ADA.*

POSTDOCTORAL POSITIONS
Bacterial Pathogenesis

Two positions available immediately. One is to investigate immune cell interactions with pathogenic bacteria, with focus on intracellular trafficking and sensing by macrophages and dendritic cells. The second is to investigate the mechanisms underlying cellular interactions by bacterial toxins, with focus on mechanisms underlying toxin binding, entry, and intracellular trafficking. Experience in molecular cell biology or biochemistry required, and molecular genetics or immunology desired. To submit an electronic application (curriculum vitae, statement of research interests, and names of three references), please contact **Dr. Steven Blanke, Department of Microbiology, University of Illinois, Urbana, Illinois** at **e-mail: sblanke@life.uiuc.edu.**

POSTDOCTORAL POSITIONS available immediately at the University of Rochester to investigate molecular mechanisms in acute myeloid leukemia and myelodysplastic syndrome using the mouse as a model system. Our Laboratory focuses on the zinc finger oncoprotein EVI1, and has developed a number of genetic models to investigate its function. Please send curriculum vitae and names of three references to **Archibald S. Perkins, M.D., Ph.D.,** at **e-mail: archibald_perkins@urmc.rochester.edu.**

HARVARD MEDICAL SCHOOL

POSTDOCTORAL POSITIONS to study the role of heat shock proteins in cancer and immunology. Requirements: Ph.D. or M.D., expertise in transcriptional regulation, immunology, or cancer research. Contact **Dr. Stuart Calderwood, Beth Isreal Deaconess Medical Center, Harvard Medical School, telephone: 617-632-0628; e-mail: calderwood.stuart@gmail.com.**

POSITIONS OPEN

The BROOKDALE UNIVERSITY HOSPITAL and MEDICAL CENTER
Division of Hematology/Oncology
Affiliate of the State University of New York Health Sciences at Downstate

We are seeking an **ASSOCIATE RESEARCH SCIENTIST** to continue the ongoing research of myelofibrosis. Applicant must have a Ph.D. degree and expertise in molecular biology. Competitive salaries/benefits. Please forward resumes to **e-mail: jcwang5@aol.com,** or to: **The Brookdale University Hospital and Medical Center, 1 Brookdale Plaza, CHC 131, Brooklyn, NY 11212. Attn: Jen C. Wang, M.D., Director of Research.**

POSTDOCTORAL FELLOW

Postdoctoral position available at the Chicago Medical School of Rosalind Franklin University to investigate cell and molecular biology of muscle fiber type development, particularly focusing on mechanisms of calcium release, signal transduction, and gene regulation. Experience in protein expression systems, mutagenesis, proteomics, cell culture, immunoprecipitation, and calcium imaging is desired. Send curriculum vitae to **Joseph DiMario, Ph.D.** at **e-mail: joseph.dimario@rosalindfranklin.edu.** *Equal Employment Opportunity/Affirmative Action.*

POSTDOCTORAL POSITIONS at Texas A&M University to exploit yeast models of human bone marrow failure and leukemia, and to discover drugs to treat same. High-quality publications in yeast cell biology and/or genetics required. These NIH-funded positions come with excellent benefits and a salary that is commensurate with experience. To apply, please visit **website: http://greatjobs.tamu.edu** and click on November 27, 2007, or November 27, 2005. *Texas A&M University is an Equal Opportunity Employer.*

POSTDOCTORAL POSITION to investigate gene networks regulating myeloid differentiation and leukemogenesis. Prior experience in quantitative real time polymerase chain reaction and microarray analyses required. Expertise in flow cytometry will be helpful. Send curriculum vitae and names of three references to: **Dr. Daniel Johnson, Hillman Cancer Center, Room 2.18c, University of Pittsburgh, 5117 Centre Avenue, Pittsburgh, PA 15213. E-mail: johnsond@pitt.edu.**

Venable L.L.P.'s Washington, D.C. office seeks a **TECHNICAL ADVISOR** for the intellectual property group. Four-year Bachelor's degree required, advanced science degree, Ph.D. in life sciences, strongly preferred. Send resume to: **Maria Krupinsky, Recruiting Manager, 2 Hopkins Place, Suite 1800, Baltimore, MD 21201** or **e-mail: mtkrupinsky@venable.com.** *Equal Opportunity Employer-Minorities/Females/Persons with Disabilities/Veterans.*

MARKETPLACE

New Products, Services, and Solutions

Experiment reproduced, discovery verified

Amplify Difficult Targets Every Time

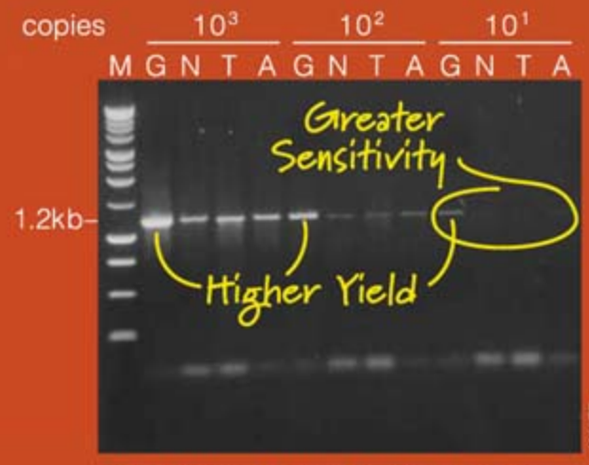

GoTaq® Green Master Mix (G) outperforms standard *Taq* DNA Polymerase (competitors N, T and A) under standard conditions.

Whether you are performing standard PCR, RT-PCR, or quantitative PCR get reproducible results, high yield and great sensitivity. Promega GoTaq® DNA Polymerase is one of a comprehensive line of superior amplification products. Experience the robust performance of GoTaq with your toughest targets.

Qualify for a FREE SAMPLE of GoTaq.
Visit www.promega.com/amplification

TODAY COULD BE THE DAY.

Promega

Powerful, Multi-modal Imaging

Now so easy everyone is lining up to do it!

Novel
KODAK X-SIGHT Imaging Agents & Antibody Conjugates
NOW AVAILABLE

Ventral position imaging shows two optical signals generating metastatic lesions located in the cranial region of the mouse.

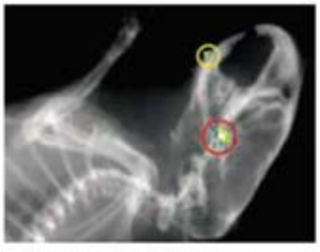

Subsequent lateral position imaging clearly separates the two lesions to specific jaw and skull locations.

Images Courtesy Dr. Bohumil Bednar, Merck Co., Inc.

Kodak Molecular Imaging Systems

The KODAK In-Vivo Imaging System FX Pro combines high-sensitivity Optical Molecular Imaging and high resolution digital X-ray to deliver precise anatomical localization of molecular and cellular biomarkers.

New full precision automation makes complex multi-modal imaging protocols easy and repeatable.

- Automated excitation and emission filters for outstanding fluorescent imaging sensitivity and flexibility from 390nm to 830nm
- 10x optical zoom and auto-focus lens for precise and repeatable results
- Automated imaging chamber enables remote switching between optical, X-ray or radioisotopic imaging without moving the subject

Whether you're performing multi-wavelength fluorescence, luminescence, X-ray, radioisotopic or a combination of these imaging modalities, the In-Vivo FX Pro fully automates the process for an entirely new level of sensitivity, throughput, repeatability, and ease-of-use.

Find out more

1-877-747-4357, exp. code 7
www.carestreamhealth.com/go/invivo4
www.carestreamhealth.com/go/X-Sight

Carestream HEALTH